

Crystal specific constraints on subvolcanic processes preceding eruptions at Mt Taranaki, New Zealand

Sarah Alicia Martin

A thesis submitted in partial fulfilment of the requirements for the degree of Masters of Science with Honours in Geology, Victoria University of Wellington, August 2012

ABSTRACT

Andesitic magmas are the product of a complex interplay of processes including fractional crystallisation, crystal accumulation, magma mixing and crustal assimilation. Recent studies have suggested that andesitic rocks are in many cases a complex mixture of a crystal cargo and melts with more silicic compositions than andesite. *In situ* glass- and mineral-specific geochemical techniques are therefore key to unravelling the processes and timescales over which andesitic magmas are produced, assembled and transported to the surface. To this end, this thesis presents a detailed *in situ* glass- and mineral-specific study of six Holocene eruptions (Kaupokonui, Maketawa, Inglewood a and b, and Korito) at Mt Taranaki to investigate the petrogenetic processes responsible for producing these sub-plinian eruptions at this long-lived (130 000 yr) andesitic volcano. Mt Taranaki is an andesitic stratovolcano located on the west coast of New Zealand's North Island and as such it is distinct from the main subduction related volcanism. Crystal-specific major and trace element data were combined with textural analysis and quantitative modelling of intensive magmatic parameters and crystal residence times to identify distinct mineral populations and constrain the magmatic histories of the crystal populations.

Least-squares mixing modelling of glass and phenocryst compositions demonstrates that the andesitic compositions of bulk rock Mt Taranaki eruptives results from mixing of a dacitic-rhyolitic melt and a complex crystal cargo (plagioclase, pyroxene, amphibole) that crystallised from multiple melts under a wide range of crustal conditions. Magma mixing of compositionally similar end members that mix efficiently also occurred beneath Mt Taranaki, and as such only produced prominent disequilibrium textures in a small proportion of the minerals in the crystal cargo. The chemistry of the earliest crystallising amphibole indicates crystallisation from an andesitic-dacitic melt at depths of ca. 20-25 km, within the lower crust. Magmas then ascended through the crust relatively slowly via a complex magmatic plumbing system. However, most of the crystal cargo formed by decompression-driven crystallisation at depth so 6-10 km, as is indicated by the dominance of oscillatory zoning and the equilibrium obtained between mineral rims and the host glasses.

Taranaki magmas recharge on timescales of 1000-2000 yrs. The eruptions investigated here provide a snapshot of the end of one cycle and the beginning of another. The younger Kaupokonui and Maketawa eruptions (ca. 2890 - <1950 yr BP) are the least evolved magmas, record a stronger mixing signal in the crystal cargo, and are volumetrically smaller than the earlier Inglewood a and b and Korito eruptions (ca. 4150-3580 yr BP). The Kaupokonui and Maketawa eruptions may reflect arrival of a new pulse of magma from the lower crust, or that these are early eruptions within a recharge sequence, which have not had as much time to further differentiate and evolve as the earlier Inglewood a and b and Korito eruptions that represent the end of a magma recharge cycle. One of the six investigated eruptions was identified to come from Fantham's Peak on the basis of its distinctive glass and mineral chemistry and petrology. Glass trace element data indicate that this eruption's magmatic system was distinct from that of the other main vent Holocene eruptions investigated in this study.

Crystal residence times were investigated using Fe-Mg interdiffusion in clinopyroxene and indicate that magma bodies stall in upper crustal storage chambers for timescales of a few months to years. The younger eruptions of the least evolved magmas with the strongest mixing signal return the shortest residence times, which may indicate that magma mixing events occurring a few months before eruption may have been the trigger for these eruptions at Mt Taranaki. Amphibole geospeedometry for these eruptives reveal rapid magma transport from depths of 6-10 km to the surface on timescales of < 1 week.

ACKNOWLEDGEMENTS

Firstly, thank you to my supervisor, Prof. Joel Baker for his time and patience throughout this thesis and for believing in me in the first place. Also thank you Dr. Marc-Alban Millet for being my unofficial secondary supervisor. Your encouragement and feedback were greatly appreciated, as well as your help in the lab.

Dan Morgan is thanked for his invaluable help with diffusion modelling and Kate Saunders for help at the beginning of this project.

The following people are thanked for their assistance during this project: Richard Wysoczanski, Sophie Barton, Alex McCoy-West and Nicole Semple for their help with fieldwork, I would have been lost and lonely without you; John Creech for his patience in setting up the EMPA techniques and answering my frantic messages even when he was off the clock; Stewart Bush for preparing thin sections; Monica Handler for help in the Geochemistry Lab; Colin Wilson, Brent Alloway, Julie Vry and Richard Wysoczanski for helpful conversations that got me thinking 'outside the box'; Colin Wilson, Alexa Van Eaton, Aidan Allan, Jess Orsman and Melissa Rotella for editing various parts of this thesis, which no doubt greatly improved its quality.

Thank you to my office mates over the years, Sophie, Chelsea, Kate, Chris, Melissa and Kirsty for the productive (and often unproductive) chats and encouragement and to Alexa, Julene and Netty, who have tried to keep me sane over the last few months. Your encouragements, distractions and the constant supply of sugar and coffee are very much appreciated.

To Jess, Sophie and Chelsea, it was a pleasure sharing this experience with you. Thank you for your friendship, the coffee breaks and sympathetic ears. Also, Lucy who now knows far more geochemistry than any philosopher should.

A big thanks to everyone who offered feedback and support, particularly Simon, James, Aidan and Kylie.

To my parents, David and Anne and brothers, Matthew, Michael and Daniel, thank you for the moral and financial support. You will no longer have to feign interest in geochemical techniques and magmatic processes over dinner.

Finally, to George, I could not have done this without you. Your constant love and support has been what has kept me going through out this.

TABLE OF CONTENTS		page
<u>Front matter</u>		i
0.1	Title page	i
0.2	Abstract	ii
0.3	Acknowledgements	iii
0.4	Table of contents	iv
0.5	List of tables	ix
0.6	List of figures	x
 <u>Chapter 1 Introduction</u>		1
1.1	Introduction	2
1.1.1	Andesite magmatism and implications for continental crust generation	2
1.1.2	Hazard assessment	3
1.2	Subduction zone magmatism	4
1.3	Andesite petrogenesis	6
1.4	Crystal forensics	9
1.5	Constraining timescales of magmatic processes	11
1.6	Geological background	12
1.6.1	Regional tectonic setting	12
1.6.2	Taupo Volcanic Zone	12
1.6.3	Taranaki setting	13
1.6.3.1	Taranaki Basin	13
1.6.3.2	Miocene volcanism	14
1.6.3.3	Taranaki Volcanic Lineament	14
1.6.4	Mount Taranaki	16
1.6.4.1	History of Taranaki volcanism	16
1.6.4.2	Petrology	17
1.7	Objectives and structure of this thesis	19
 <u>Chapter 2 Fieldwork and Samples</u>		22
2.1	Fieldwork methods	23
2.2	Site locations	24
2.2.1	Site 3 and 4 – Opunake Road	24
2.2.2	Site 5 - Opunake Road	24

2.2.3	Site 6 – Pembroke Road	25
2.2.4	Site 7 – Pembroke Road	26
2.3	Samples	28
 <u>Chapter 3 Methods</u>		 30
3.1	Major element analysis	31
3.1.1	Sample preparation	31
3.1.2	Electron microprobe analyses	31
3.1.2.1	JEOL 733 Superprobe electron probe micro-analyser	32
3.1.2.2	JEOL JXA-8230 electron probe micro-analyser	32
3.1.2.3	Comparison of EMPA data	35
3.2	Trace element analysis	39
3.2.1	Glass trace element analysis	39
3.2.1.1	Sample preparation	39
3.2.1.2	Mass spectrometry	40
3.2.2	Laser ablation ICP-MS mineral trace element analysis	45
3.3	Thermobarometry	49
3.3.1	Amphibole thermobarometry	49
3.3.1.1	Model	49
3.3.1.2	Method	50
3.3.2	Clinopyroxene-melt thermometry	54
3.3.2.1	Model	54
3.3.2.2	Method	55
3.3.2.3	Equilibrium	57
3.3.2.4	Other clinopyroxene thermometers	61
3.3.3	Plagioclase-melt thermometry	61
3.3.3.1	Model	61
3.3.3.2	Method	62
3.3.3.3	Equilibrium	62
3.3.3.4	Other plagioclase-melt thermometers	63
3.3.4	Comparison of results from different thermometers	65
3.4	Diffusion modelling	67
3.4.1	Introduction to diffusion modelling theory	67
3.4.1.1	Diffusion in minerals	67
3.4.1.2	Diffusion mechanisms	68

3.4.1.3	Diffusion equations	69
3.4.2	Fe-Mg interdiffusion in clinopyroxene	70
3.4.2.1	Model parameters	70
3.4.2.2	Model conditions	72
3.4.3	Method	74
3.4.3.1	Minimum resolution of the model	78
3.4.4	Sources of error	79
3.4.4.1	Diffusion coefficient	80
3.4.4.2	Sectioning effects	81
3.4.4.3	Image parameters	82
<u>Chapter 4 Results</u>		84
4.1	Petrology	85
4.1.1	Plagioclase	85
4.1.2	Clinopyroxene	88
4.1.2.1	Patchy cores and oscillatory rims	88
4.1.2.2	Dark rim	90
4.1.3	Amphibole	90
4.1.4	Fe-Ti oxides	92
4.1.5	Orthopyroxene	92
4.2	Major element chemistry	93
4.2.1	Glass major element chemistry	93
4.2.2	Melt inclusion major element chemistry	95
4.2.3	Mineral major element chemistry	95
4.2.3.1	Plagioclase	95
4.2.3.2	Clinopyroxene	98
4.2.3.3	Orthopyroxene	98
4.2.3.4	Amphibole	100
4.2.3.5	Fe-Ti oxides	100
4.3	Trace element chemistry	103
4.3.1	Glass trace element chemistry	103
4.3.2	Mineral trace element chemistry	106
4.3.2.1	Plagioclase	106
4.3.2.2	Clinopyroxene	109
4.3.2.3	Amphibole	112
4.4	Thermobarometry	115
4.4.1	Thermometry	115

4.4.2	Amphibole thermobarometry	116
Chapter 5 Discussion		120
5.1	Glass chemistry	121
5.1.1	Comparison with published glass studies	121
5.1.2	Comparison with whole rock geochemistry	122
5.1.3	The relationship between glass and mineral phases	126
5.2	Mineral chemistry	128
5.2.1	Plagioclase	128
5.2.1.1	Patchy/sieved textured crystals	129
5.2.1.2	Oscillatory zoned crystals	131
5.2.1.3	Calculated plagioclase equilibrium melt Compositions	133
5.2.2	Clinopyroxene	138
5.2.2.1	Clinopyroxene textures	139
5.2.2.2	Clinopyroxene chemistry	139
5.2.2.3	Inglewood a, Inglewood b and Korito processes	142
5.2.2.4	Kaupokonui, SM-6C and Maketawa processes	143
5.2.3	Amphibole	144
5.2.3.1	Physical conditions of amphibole crystallisation	145
5.2.3.2	Melt differentiation	151
5.2.3.3	Amphibole model	151
5.2.4	Fe-Ti oxides	152
5.2.4.1	SM-6C	154
5.2.5	Relationship between mineral phases	154
5.2.5.1	Crystal cores	155
5.2.5.2	Zoning and rims	155
5.3	Temporal variability	159
5.4	Timescales of magmatic processes	163
5.4.1	Clinopyroxene residence times	163
5.4.1.1	Magma storage	163
5.4.1.2	Mixing	164
5.4.2	Comparisons with other studies	166
5.4.2.1	Previous work using Fe-Ti diffusion in oxides	168
5.4.3	Relationship between the older three samples	171
5.5	Andesite petrogenesis at Mt Taranaki	172

<u>Chapter 6 Conclusions and Future work</u>	178
6.1 Conclusions	179
6.2 Suggestions for future work	180
<u>References</u>	182
<u>Appendix 1 Sample List</u>	A.2
<u>Appendix 2 Major Element Data</u>	A.4
<u>Appendix 3 Trace Element Data</u>	A.210
<u>Appendix 4 Diffusion Modelling Images and Profiles</u>	A.250

<u>Chapter 1: Introduction</u>		
Table 1.1	Summary of the stratigraphic groups for Mt Taranaki lava and selected tephra units	17
<u>Chapter 3: Methods</u>		
Table 3.1	JEOL 733 Superprobe Electron Probe Micro-Analyser standard data precision and accuracy	33
Table 3.2	Analytical conditions during analytical sessions with the JEOL JXA-8230 EMPA.	34
Table 3.3	JEOL JXA-8230 EMPA precision and accuracy of major element mineral analyses	36
Table 3.4	ICP-MS instrumental and analysis conditions	42
Table 3.5	Precision and accuracy of solution ICP-MS data	43
Table 3.6	Reproducibility of duplicate samples analysed by solution ICP-MS	44
Table 3.7	LA-ICP-MS instrumental and analytical conditions for in situ clinopyroxene, amphibole and plagioclase trace element analyses	47
Table 3.8	Precision and accuracy of LA-ICP-MS data based on multiple repeat analyses of BHVO-2G	48
Table 3.9	Amphibole analyses used for thermobarometry	52
Table 3.10	Temperature (°C) calculated using clinopyroxene-melt thermometry using variable pressure and water content inputs.	56
Table 3.11	Melt inclusion/glass and clinopyroxene pairs used for thermometry and the associated results	59
Table 3.12	Melt and plagioclase pairs used for thermometry and the associated results	64
Table 3.13	Summary of mineral thermometry results	66
<u>Chapter 4: Results</u>		
Table 4.1	Summary of the petrographic variation observed within Taranaki eruptives investigated in this study. Mineral proportions estimated visually under a petrographic microscope.	85
<u>Chapter 5: Discussion</u>		
Table 5.1	Least squares mixing modelling results for selected samples.	124
Table 5.2	Plagioclase-melt partition coefficients used in this study.	133

Table 5.3	The starting composition, partition coefficients (k_D) and the fractionating assemblage used to model fractional crystallisation in this study.	136
Table 5.4	Clinopyroxene-melt (andesite to dacite) partition coefficients used in this study.	142
Table 5.5	Amphibole-melt (andesite-dacite) partition coefficients used in this study.	151
Table 5.6	Summary of previous studies applying diffusion modelling to volcanic systems	167

List of Illustrations

page

<u>Chapter 1: Introduction</u>		
Figure 1.1	Schematic cross section of a subduction zone	4
Figure 1.2	Primitive mantle normalised multi-element diagram	6
Figure 1.3	Map illustrating the distribution of selected North Island Miocene-Present volcanism	15
Figure 1.4	N-MORB normalised multi-element diagram of selected Taranaki lavas	18
<u>Chapter 2: Fieldwork and Samples</u>		
Figure 2.1	Map of the field area for this study showing sample locations	24
Figure 2.2	Annotated photograph of Site 6 with sampled tephra units identified	25
Figure 2.3	Annotated photograph of Site 7 with sampled tephra units identified	27
Figure 2.4	Stratigraphic locations of the samples investigated in this study	29
<u>Chapter 3: Methods</u>		
Figure 3.1	Comparison between the JEOL 733 Superprobe and JEOL JXA-8230 Electron Probe Micro-Analysers	39
Figure 3.2	Comparison of two clinopyroxene-liquid barometers from Putirka (2008)	56
Figure 3.3	Predicted clinopyroxene components based on the melt composition vs the observed clinopyroxene components	58
Figure 3.4	Schematic representation of the history of a crystal and how diffusion modelling of crystal zoning represents magmatic events	68
Figure 3.5	Schematic representation of the different types of diffusion mechanisms in minerals. Figure taken from Watson & Baxter (2007).	69
Figure 3.6	Nature of an erf curve and how it can be used for diffusion modelling	71
Figure 3.7	Examples of how diffusion profiles are obtained from BSE images.	75
Figure 3.8	Graphs illustrating the relationship between greyscale and selected major elements	77
Figure 3.9	Graph illustrating the power function relationship between magnification of BSE image and minimum temporal resolution of the diffusion model as determined by EQ 3.20	79
Figure 3.10	Schematic representation of the effect of oblique sectioning on the 2-dimensional view of the crystal.	82

Figure 3.11	Calculated diffusion ages on the same zone in the same crystal using variable image parameters	83
<u>Chapter 4: Results</u>		
Figure 4.1	Backscattered electron images of representative plagioclase crystals	86
Figure 4.2	Backscattered electron images of representative clinopyroxene crystals.	89
Figure 4.3	Backscattered electron images of representative amphibole crystals.	91
Figure 4.4	Backscattered electron images of titanomagnetite	92
Figure 4.5	Backscattered electron images of orthopyroxene crystals.	93
Figure 4.6	Major element glass analyses	94
Figure 4.7	Total alkali-silica diagram of glass and melt inclusion data	96
Figure 4.8	Histograms of plagioclase anorthite content	97
Figure 4.9	Histograms of clinopyroxene Mg#	99
Figure 4.10	Histograms of amphibole Mg# and Al ₂ O ₃	101
Figure 4.11	Bivariate diagrams of Fe-Ti oxide major element chemistry	102
Figure 4.12	Representative glass trace element data plotted versus SiO ₂	104
Figure 4.13	REE and multi-element diagrams of glass trace element chemistry	105
Figure 4.14	Selected trace elements versus anorthite content of plagioclase	107
Figure 4.15	Multi-element diagrams of plagioclase trace element chemistry	108
Figure 4.16	Selected trace elements versus Mg# of clinopyroxene	110
Figure 4.17	Multi-element diagrams of clinopyroxene trace element chemistry	111
Figure 4.18	Selected trace elements plotted versus Mg# of amphibole	113
Figure 4.19	Multi-element diagrams of amphibole trace element chemistry	114
Figure 4.20	Summary of thermobarometry models	115
Figure 4.21	Amphibole thermobarometry results	117
Figure 4.22	Amphibole hygrometry results	118
Figure 4.23	Amphibole oxybarometry results	119
<u>Chapter 5: Discussion</u>		
Figure 5.1	Comparison of glass data from this study and selected published data using selected major elements.	122
Figure 5.2	Total alkalis-silica plot of Taranaki eruptives. Whole rock data as compared with glass data from this study.	123
Figure 5.3	Examples of plagioclase crystals with sieved/patchy core and mantle from Kaupokonui	130

Figure 5.4	An example of a plagioclase transect showing the anti-correlation between MgO and anorthite content indicating that the Sr and Ba trace element composition of plagioclase crystals have not been modified by diffusion.	134
Figure 5.5	Trace element concentrations of plagioclase equilibrium melt.	137
Figure 5.6	Mg# vs Al ₂ O ₃ content of clinopyroxene cores, rims and zoning in each of the samples investigated in this study.	140
Figure 5.7	Mg# and Al ₂ O ₃ plotted against a representative trace element (Sc)	141
Figure 5.8	Selected trace element ratios vs Ce of melt various zones within clinopyroxene crystallised from.	143
Figure 5.9	Graphs of amphibole crystallisation pressure versus Ce and Sr concentrations of the melt in equilibrium with the amphibole.	146
Figure 5.10	Amphibole thermobarometry	148
Figure 5.11	Selected trace elements concentrations of amphibole equilibrium melt.	150
Figure 5.12	Selected major element chemistry of Fe-Ti oxides.	153
Figure 5.13	Trace element concentrations of melt in equilibrium with the plagioclase, clinopyroxene and amphibole. With the modelled fractional crystallisation shown	157
Figure 5.14	Summary of the mineral textures observed in the Taranaki eruptives and the associated interpretation.	158
Figure 5.15	Multi-element diagrams of mineral trace element analyses for samples Inglewood a and b and Korito.	160
Figure 5.16	Probability density functions showing the results of diffusion modelling for the rims of each sample.	164
Figure 5.17	Probability density functions of representative samples showing the results of diffusion modelling zones that are not the outermost rim	165
Figure 5.18	Schematic diagram of the sub-volcanic system at Mt Taranaki	173

CHAPTER 1: **INTRODUCTION**

1.1 INTRODUCTION

1.1.1 ANDESITE MAGMATISM AND IMPLICATIONS FOR CONTINENTAL CRUST GENERATION

The origin of andesitic (intermediate) volcanism is a contentious and important problem in the Earth Sciences. The bulk continental crust, which covers *ca.* 40% of Earth's surface area, has an intermediate composition (55-65 wt% SiO₂) with a similar geochemistry to that of andesite (Figure 1.2) (Rudnick, 1995; Rudnick & Gao, 2003; Hawkesworth & Kemp, 2006). Convergent margins where andesites are most commonly erupted, are thus considered to be the site of continental crust growth (e.g. Kay, 1980; Tatsumi & Eggins, 1995; Taylor & McLennan, 1995; Plank, 2005). However, primary arc magmas are typically mantle-derived basalts that are geochemically distinct from the continental crust (45-55 wt% SiO₂) (Kay, 1980; Anderson, 1982; Rudnick, 1995; Tatsumi & Eggins, 1995; Taylor & McLennan, 1995; Plank, 2005). Thus investigating the generation of andesitic melts aids in the understanding of generation of the continental crust.

Intermediate magmas such as andesites are thought to form through various processes including: 1) crystallisation of mafic magmas within the crust or upper mantle (e.g. Sisson & Grove, 1993; Grove et al., 1997; 2003; Annen & Sparks, 2002; Prouteau & Scaillet, 2003; Larocque & Canil, 2010); 2) partial melting of older crustal rocks by intrusion or underplating of mantle-derived basaltic magma (e.g. Hildreth & Moorbath, 1988; Petford & Atherton, 1996; Petford & Gallagher, 2001; Annen & Sparks, 2002); 3) Mixing between basaltic and silicic magmas (e.g. Eichelberger, 1978; Heiken & Eichelberger, 1980; Tatsumi & Takahashi, 2006).

In reality, a likely scenario is some combination of these processes where crystallisation of hydrous basalt produces silicic melt in the lower crust and the heat supplied by this basalt enables partial melting of lower crustal rocks (Annen et al., 2006). These two melt types mix and are further modified during ascent of the crust by processes such as fractional crystallisation, crustal assimilation and magma mixing.

Detailed petrological and geochemical investigation of intermediate arc magmas can constrain the processes which generate andesitic magmas. This thesis study aims to add to this discussion by investigating the processes that generated recent andesitic magmas at Mt Taranaki, New Zealand.

1.1.2 HAZARD ASSESSMENT

Andesitic magmatism is also a significant hazard around the world as this type of volcanism is widespread and often explosive. The deadliness and unpredictability of andesite volcanism has been illustrated multiple times during the 20th century by events such the 1902 eruption at Mt Pelee which killed 29 000 people (Witham, 2005). The renewal of volcanic activity at Mt St. Helens was closely monitored, yet even so, 57 people died when it suddenly erupted explosively in 1980 (Foxworthy & Hill, 1982).

Mt Taranaki (New Zealand) is an andesitic stratovolcano that last erupted in AD 1854 (Platz, 2007). The tephrostratigraphic record shows that sub-plinian eruptions ($0.1-2 \text{ km}^3$) occurred on average every 232 yr, with smaller eruptions occurring every *ca.* 16 yr (Alloway et al., 1995; Turner, 2008). The probability of another Taranaki eruption occurring in the next 50 yr is estimated as 0.37-0.59 (Turner, 2008; Turner et al., 2009).

This study aims to contribute to the understanding of past hazardous events at Taranaki by looking at the timescales of pre-eruptive magma processes and storage in the past *ca.* 4000 yr. This will yield models for the pre-eruptive timescales that are of direct value in assessing the time scales between future unrest and possible eruption at Mt Taranaki. In particular, the information on magma depths and rise rates should be directly relevant to interpreting geophysical signals from future events.

1.2 SUBDUCTION ZONE MAGMATISM

Andesite magmatism typically occurs at convergent plate boundaries, where one tectonic plate is subducted beneath another. The interaction between the down going slab and associated sediment package with the overlying mantle wedge produces magma within the mantle wedge (e.g. Kay, 1980; Gill, 1981; McCulloch & Gamble, 1991; Elliot et al., 1997; Hawkesworth et al., 1997; Kogiso et al., 2009; Kimura et al., 2010) (Figure 1.1).

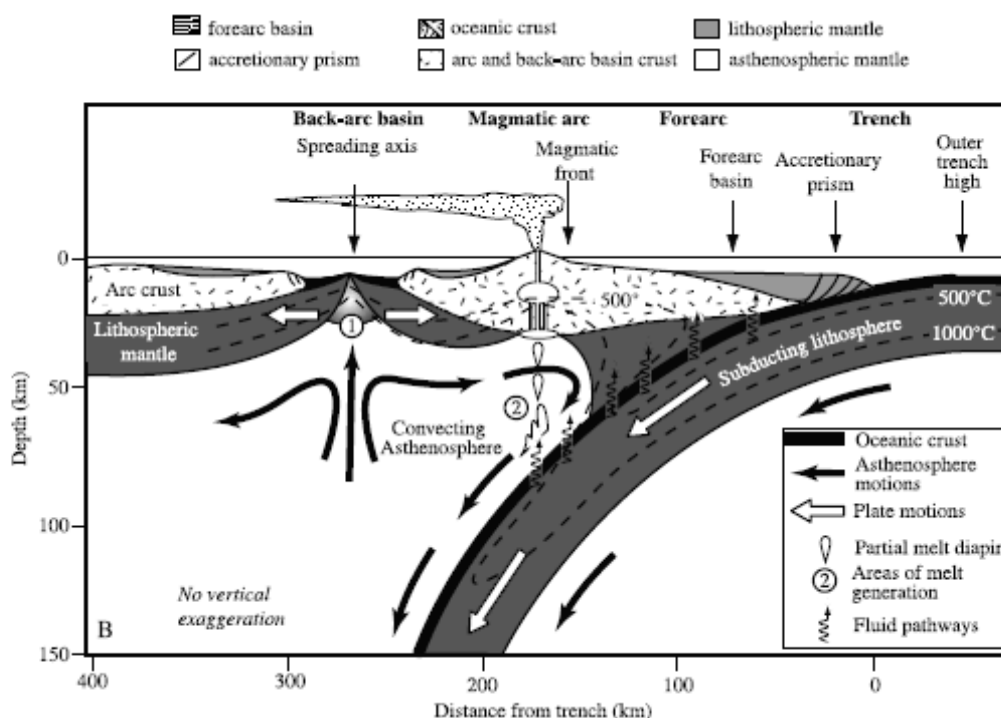


Figure 1.1 Schematic cross section of a subduction zone. Figure taken from Stern (2002).

As the oceanic plate and sediment package are subducted, these components undergo dehydration reactions as a result of prograde metamorphism (e.g. Gill, 1981; Tatsumi & Eggins, 1995; Schmidt & Poli, 1998; Hermann et al., 2006; Kimura et al., 2010). This release of fluids metasomatises the overlying mantle wedge, lowers the solidus of the peridotite by several hundred degrees and induces partial melting (e.g. Gill, 1981; Plank & Langmuir, 1988; Schmidt & Poli, 1998; Kessel et al., 2005). These fluids also carry a trace element cargo that imparts a distinct chemistry to subduction derived magma. It is generally accepted that in most subduction

zones, the down going slab does not itself partially melt because temperatures are not sufficiently high (e.g. Peacock et al., 1994). The exception to this may be adakites which have been interpreted to form by melting of a garnet source or direct melting of the subducted slab when the slab is relatively young (< 25 Ma) and hot (Defant & Drummond, 1990; Martin et al., 2005). It is currently unclear whether the sediment melts, as petrological and geochemical studies such as Johnson & Plank (1999), Elliot et al. (1997) and Hawkesworth et al. (1997) require melting in order to transport fluid immobile elements such as Be and Th, which are observed in significant concentrations in arc lavas, to the mantle wedge. Thermal models, however, predict temperatures that are in general too low for sediment melting (e.g. Peacock et al., 1994). Either way, the result is mass transfer from the sediment to the mantle wedge, resulting in some of the enrichment in large ion lithophile elements (LILEs) and Th (Gill, 1981).

Primary magmas derived from the mantle wedge are generally basaltic with a distinctive trace element geochemistry showing depletion in high field strength elements (HFSEs) (e.g. Ta, Nb, Zr, Hf, Ti) and enrichment in LILEs (e.g. Cs, Rb, K, Ba, Pb, Sr) (e.g. Pearce & Cann, 1973; Gill, 1981; Hawkesworth et al., 1997; Figure 1.2). Much of the enrichment in LILEs occurs because many of these are fluid mobile and so are transported by the aqueous fluids from the subducted slab and associated sediment into the mantle wedge. The origin of HFSE depletion is more controversial with two hypotheses proposed. (1) The mantle wedge may be depleted due to a previous melting event at the back arc that produced back arc basalts. This would have the effect of depleting the mantle wedge of incompatible elements and those elements that are fluid immobile would not be replenished by subduction processes, resulting in an overall depletion of HFSEs in arc magmas (McCulloch & Gamble, 1991; Woodhead et al., 1993). (2) Melting within the mantle wedge could occur in the presence of Ti-rich accessory minerals (e.g. rutile) which retain HFSEs, resulting in an HFSE depletion in arc magmas (e.g. Green, 1981; Stern, 2002). The subduction zone signature would become more pronounced with time as the mantle wedge becomes progressively more altered by slab-derived fluids (Murphy, 2007).

The volcanic front where arc volcanism typically occurs is globally located *ca.* 100 km above the top surface of the down going slab (Gill, 1981). This is thought to be controlled by

the flow and thermal regime of the mantle wedge (Kogiso et al., 2009), where the dehydration reactions occur (Tatsumi & Eggins, 1995) and where the permeability of the mantle increases (Mibe et al., 1999). The volcanic front forms where the wet peridotite of the mantle wedge becomes hot enough to melt (Kushiro, 1983).

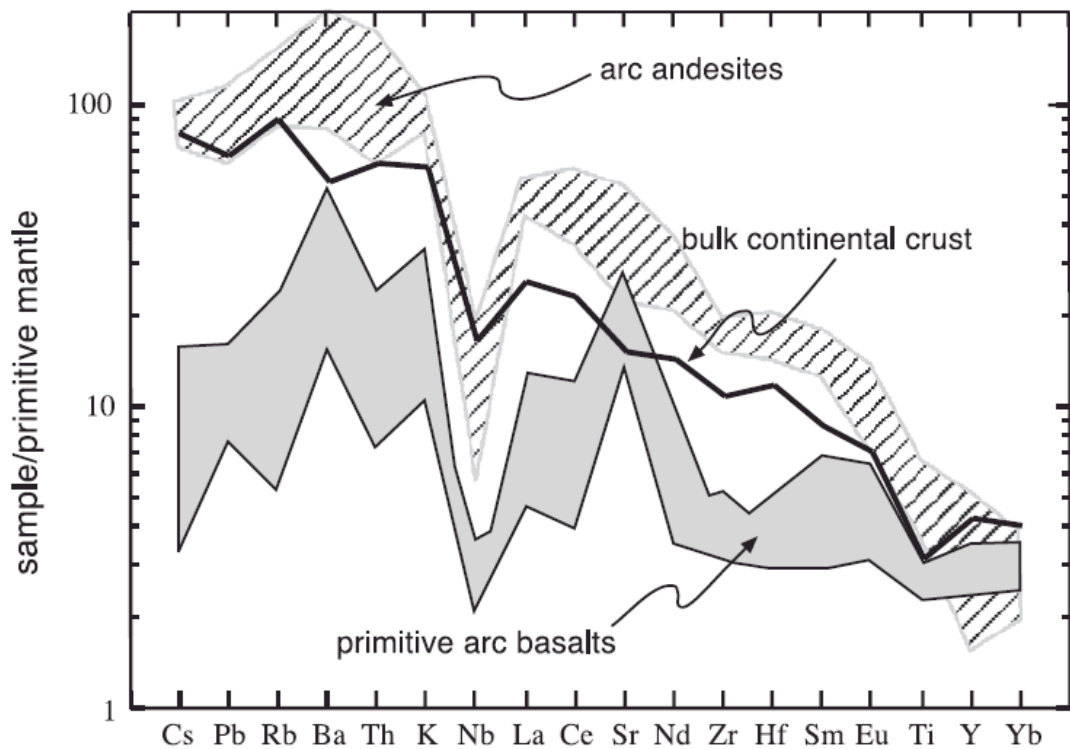


Figure 1.2 Primitive mantle normalised multi-element diagram illustrating the relative enrichment in LILEs and depletion in HFSEs of primitive arc basalts typical of subduction related magmas. Also note the broad similarities in composition between arc andesites and bulk continental crust. Figure taken from Davidson et al. (2005).

1.3 ANDESITE PETROGENESIS

The dominant magma type erupted at convergent margins is andesitic in composition so there is much interest in determining how these form given that primary, mantle wedge-derived magmas are generally basaltic in composition (Gill, 1981; Tatsumi & Eggins, 1995). These primary magmas must travel through the crust, and undergo intracrustal processes and density filtering (Annen et al., 2006). Magma differentiation may occur at depth by partial melting of mafic source rocks or incomplete crystallisation of basalt with further modification occurring in upper

crustal magma chambers (Hildreth & Moorbath, 1988-MASH; Annen et al., 2006-Deep Crustal Hot Zone; Reubi & Blundy, 2009). Alternatively, differentiation may occur at shallow crustal levels by fractional crystallisation and/or crustal assimilation (e.g. Grove & Kinzler, 1986; Pichavant et al., 2002). To account for the complexity and diversity observed at andesite volcanoes, a range of processes have been proposed including fractional crystallisation, crustal assimilation, mafic recharge and magma mixing (DePaolo, 1981; Hildreth & Moorbath, 1988; Murphy et al., 2000; Annen et al., 2006). It is difficult to explain the features of andesites by any single mechanism and in most cases these different processes are interdependent (Gill, 1981).

Assimilation of crustal material is expected to some degree whenever basaltic magma is stored in the continental crust (Hildreth & Moorbath, 1988). Geochemical variability has been attributed to this process at a number of volcanic centres (e.g. Andes of Central Chile, Hildreth & Moorbath, 1988; San Vincenzo Italy, Ferrara et al., 1989; Mt Ruapehu, New Zealand, Graham & Hackett, 1987, Price et al., 1999, 2005). This can occur as either bulk assimilation where crustal rocks are incorporated and subsequently melt, or selective assimilation where partial melts extracted from the country rock are incorporated (Streck, 2008). Crustal assimilation can occur simultaneously with fractional crystallisation (AFC) as this latter process provides the necessary heat for assimilation (DePaolo, 1981; Bohrson & Spera, 2001).

Fractional crystallisation has long been considered key in the formation of silicic magmas as the continued growth and removal of crystals from the melt evolves the composition of the magma along the liquid line of descent to more silicic compositions (Grove & Kinzler, 1986). The crystallising phases form a crystal mush, from which a high silica melt may be extracted (Hildreth, 2004; Bachmann & Bergantz, 2004). Alternatively, this can be remobilised by mafic recharge where the injection of a hotter magma reheats and partially melts the crystalline body (e.g. Sparks et al., 1977; Murphy et al., 2000; Bachmann et al., 2002; Dungan & Davidson, 2004; Fowler & Spera, 2010). The hotter, more mafic magma mixes with the silicic magma and remobilised crystal mush (Murphy et al., 2000; Dungan & Davidson, 2004). This interaction has

often been proposed to trigger eruptions on a timescale of days to months after the mafic recharge event (Sparks et al., 1977; Martin et al., 2008; Kent et al., 2010).

The mixing/mingling of different magma bodies, which may or may not be genetically related, is a common process. Disequilibrium features include: sieved mineral textures; disequilibrium mineral assemblages or those that crystallise over an implausibly wide range of temperatures (e.g. quartz and magnesian olivine, Ca-plagioclase and Na-plagioclase); disequilibrium between glass and mineral compositions; heterogeneous glass; Si-rich melt inclusions in andesitic eruptive products; and the presence of mafic enclaves. These have been interpreted as evidence for magma mixing (e.g. Anderson, 1976; Sparks et al., 1977; Sakuyama, 1979; Pallister et al., 1992; Murphy et al., 2000).

With micro-analytical analysis, it is now apparent that andesitic magmas are not generally intermediate in composition when the individual components of the eruptives are analysed, but are comprised of a liquid and a crystal cargo, which are not necessarily cogenetic (e.g. Eichelberger, 1975; Reubi & Blundy, 2009). Andesitic magmas typically have a dacitic-rhyolitic melt which is leveraged to intermediate whole-rock compositions by their more mafic crystal cargo (e.g. Eichelberger, 1975; Davidson et al., 2005; Annen et al., 2006; Reubi & Blundy, 2009). In fact, despite the dominance of andesitic magmas, there is an 'andesite gap' in melt compositions (Reubi & Blundy, 2009). This suggests, that while a range of compositions are created at depth, those with an intermediate composition (59-66 wt% SiO₂) are less likely to be erupted due to the large compositional changes over this range that occur with a small change in temperature (Reubi & Blundy, 2009). The abundance of andesites erupted at the surface is therefore a product of magma mixing between silicic and mafic end member magmas at shallow crustal depths (Anderson, 1976; Eichelberger, 1978; Reubi & Blundy, 2009). The mixture of these two products is preferentially erupted as the combination of the two minimises the physical barriers to eruption (Kent et al., 2010). Basaltic magmas are dense and rhyolitic magmas are viscous, both of which hinder eruption. When these factors combine, the resulting magma is less dense and less viscous and therefore can erupt (Kent et al., 2010).

1.4 CRYSTAL FORENSICS

Due to the complexity observed in andesites, in situ crystal specific studies are required to unravel the processes which formed these magmas. These studies make it possible for us to track magmatic processes such as crystallisation, crustal assimilation, magma mixing, decompression and convection (Berlo et al., 2007; Ginibre et al., 2007; Jerram & Martin, 2008). Whole rock analyses average out and hide complexities, as they do not correspond to liquid compositions, or liquid lines of descent, resulting in whole rock data that is an overly simplistic interpretation of petrogenetic processes (Stewart et al., 1996; Streck et al., 2005; Davidson et al., 2005; 2007a; Eichelberger et al., 2006; Berlo et al., 2007; Jerram & Martin, 2008; Reubi & Blundy, 2009).

Crystals represent an archive of magmatic conditions as crystal texture and zoning both record changes in the physical and chemical conditions in the magma (Ginibre et al., 2002a). The progressive zones from core to rim within a crystal represent a time sequence, therefore the changing composition represents changing conditions through time (Davidson et al., 2007b). Dissolution surfaces and major compositional changes correspond to periods where the crystal was partially dissolved and no growth occurred (Davidson et al., 2007b).

Textural analysis can be combined with micro-geochemical techniques to further resolve magmatic processes. Micron scale major element analyses can be obtained by electron microprobe traverses, and trace element analyses at spot sizes of *ca.* 20-35 μm by laser ablation inductively coupled plasma mass spectrometry. The crystal composition is dependent on the crystallising conditions, and thus the host magma at the time of crystallisation (Ginibre et al., 2007). The major element composition can vary as a function of pressure, temperature, melt composition and water content (e.g. Ginibre et al., 2002a). Trace element analyses may further constrain which of these processes is occurring, as many trace elements are primarily sensitive to changes in melt composition (e.g. Cr in clinopyroxene - Streck et al., 2002). Therefore, a change in major element chemistry, without a corresponding change in trace element chemistry,

can indicate variation in the physical processes in the magma chamber - such as a decompression or degassing – rather than a compositional change (Ginibre et al., 2007).

Andesitic magmas typically contain multiple populations of crystals that have different histories (Jerram & Martin, 2008). These have been broadly classified into phenocrysts, antecrysts and xenocrysts based on the relationship of a crystal to the host melt (Jerram & Martin, 2008; Streck, 2008). Phenocrysts grow in situ from a magma and constrain the evolution of the erupted magma. Antecrysts are crystals which grew from a melt genetically related to that erupted and preserve information about the magmatic system as a whole. These crystals are older, and may have crystallised from the host melt prior to a mixing event for example. Xenocrysts, which are not genetically related to the host magma, indicate interaction of the magmatic system with foreign material such as wall rocks. An individual crystal may fall into all of these categories depending on the zone of interest. Differentiating between these various crystal-melt relationships is challenging and generally requires the use of micro-analytical geochemical techniques in conjunction with textural analysis. This is highlighted by cases where phenocrysts and the crystals within xenoliths are texturally and chemically similar (e.g. Price et al., 2005).

Volcanic glass represents the composition of the residual melt and can be used to investigate the relationship of the crystal cargo to the magma in which it is found (Streck, 2008). Glass analyses provide further constraints on the processes and history of the magma chamber and indicate the degree of chemical heterogeneity within the erupted melt body. Furthermore, melt inclusion analyses can provide information on the co-existing melt at the time of melt inclusion closure, assuming no post-entrapment modification and therefore can provide a relative time series of magma composition.

1.5 CONSTRAINING TIMESCALES OF MAGMATIC PROCESSES

Quantifying the timescales of magmatic processes aids in our understanding of andesite petrogenesis and the evaluation of volcanic hazards (Turner & Costa, 2007). Uranium-series isotopes have traditionally been used to constrain the timescales of magmatic systems by dating bulk samples or mineral separates (e.g. Cooper et al., 2001; Cooper & Reid, 2003; Turner et al., 2003; Hawkesworth et al., 2004). This gave an average age of a crystal that can be misleading, especially where crystal cores are significantly older than rims. Recent advances in understanding of diffusion in solid silicates have enabled the *in situ* determination of timescales on a variety of mineral phases. This enables a chronology to be linked to the textural and chemical features of individual minerals and the processes these elucidate (Hawkesworth et al., 2004; Turner & Costa, 2007). Further, multiple ages can be obtained from a number of crystals to provide a statistically robust model, and/or investigate different crystal populations and compare the processes affecting them (Chakraborty, 2008). Numerous zones within a single crystal can also be modelled enabling multiple events recorded within crystal zoning to be studied.

Diffusion modelling quantifies the time a mineral zone remained at magmatic temperatures and so dates the time between a magmatic process and eruption. Mineral zoning begins to re-equilibrate immediately after formation, but this process is infinitely slow at surface temperatures (Morgan et al., 2004). Measuring the degree of compositional ‘smoothing’ that has occurred can therefore be used to quantify the time between the event that formed the mineral zoning and eruption (Morgan et al., 2004). As diffusion effectively terminates once the rock is erupted, the timescales of these processes can be measured independent of sample age even when they are orders of magnitude smaller than the age of the sample (Morgan et al., 2004; Chakraborty, 2008). All timescales of geological interest can be investigated using diffusion modelling as different elements diffuse at different rates within different minerals (Chakraborty, 2008; Costa et al., 2008).

A range of different processes have been investigated using diffusion modelling of various mineral-element pairs. For example, Morgan & Blake (2006) calculated that magma differentiation occurred on a timescale of 100 000 yr before the Bishop Tuff eruption based on Ba and Sr zoning in sanidine. Timescales of the order of days to weeks have been calculated for mafic recharge events, which are interpreted to be the eruption triggering process, using a range of element and mineral species (e.g. Fe-Mg in olivine-Martin et al., 2008; Ti in titanomagnetite-Turner et al., 2008; Mg in plagioclase-Kent et al., 2010).

1.6 GEOLOGICAL BACKGROUND

1.6.1 REGIONAL TECTONIC SETTING

New Zealand sits astride the plate boundary between the Pacific and Australian plates, which are converging obliquely at a rate of 42 mm/yr at the latitude of Taranaki (De Mets et al., 1994). Offshore of the North Island, the Pacific Plate is being subducted to the west beneath the Australian Plate at the Hikurangi Trough. The subducted Pacific lithosphere initially dips shallowly at around 20° and gradually increases to a dip of 55° at 100 km depth under the central North Island (Anderson & Webb, 1994). The slab continues to dip more steeply to a depth of around 200 km beyond which it is near vertical (Anderson & Webb, 1994; Reyners et al., 2006). Beneath the Taranaki region, the Wadati-Benioff zone is around 250 km deep (Adams & Ware, 1977; Anderson & Webb, 1994; Reyners et al., 2006). Very deep earthquakes at 600 km depth suggest that there is also a small detached piece of the slab at this depth beneath Taranaki (Boddington et al., 2004). There is also evidence that the subducted slab is segmented by lateral tears trending in a northwest direction (Reyners, 1983).

1.6.2 TAUPO VOLCANIC ZONE

The Taupo Volcanic Zone (TVZ) in the central North Island is the main expression of subduction-related volcanism in the North Island (Fig. 1.3A). It is a region of active rifting, characterised by extremely high heat flow of $\sim 700 \text{ mW/m}^2$ (e.g. Stern, 1985; Stern et al., 1987; Bibby et al., 1995; Wallace et al. 2004). The brittle upper crust is around 16 km thick; below

this is either low velocity mantle (Stratford & Stern, 2004) or extensively intruded or underplated lower crust (Harrison & White, 2004). This is one of the most productive magmatic systems on Earth, erupting an average of $0.28 \text{ m}^3 \text{ s}^{-1}$ of magma in the last 340 Kyr and is overwhelmingly rhyolitic in composition (Houghton et al., 1995; Wilson et al., 1995). Basaltic volcanism is evenly distributed throughout the TVZ, however rhyolitic volcanism is confined to the central portion and andesitic to dacitic volcanism is dominant only in the northern and southern segments of the TVZ (Wilson et al., 1995). The Tongariro Volcanic Centre (TgVC) is located at the southern end of the TVZ and includes the active cones of Ruapehu and Mt Ngauruhoe (Figure 1.3A). These volcanoes are dominated by medium-K, plagioclase and two-pyroxene andesites (Graham & Hackett, 1987). While the TgVC has the largest and most active andesitic volcanoes associated with this arc, volcanism in Taranaki has been present for *ca.* 2 Ma in a back arc setting *sensu lato* (e.g. Price et al., 1992, 1999, 2005). This distinct tectonic location can provide important insights into cross arc variation and the behaviour of subduction related volcanism in general.

1.6.3 TARANAKI SETTING

1.6.3.1 Taranaki Basin

Mt Taranaki, also known as Egmont Volcano, is an andesitic stratovolcano located on the western side of New Zealand's North Island within the Taranaki Basin (Figure 1.3). This basin opened during the Mid-Late Cretaceous as a result of rifting associated with the break-up of the paleo-Pacific margin of Gondwana and the opening of the Tasman Sea (King & Thrasher, 1996; Muir et al., 2000). The tectonically active region of the Taranaki Basin is bound to the west by the Cape Egmont Fault Zone and to the east by the Taranaki Fault - a crustal scale fault that is thought to be a major terrane boundary (King & Thrasher, 1996; Stagpoole & Nicol, 2008; Giba et al., 2010). The crust in the Taranaki Basin is 25-35 km thick, thickening from west to east (Stern & Davey, 1987; 1990). The basement is comprised of plutonic rocks of the Median Tectonic Zone, dominated by subduction-related calc-alkaline diorites and granites (Challis et

al., 1994; Mortimer et al., 1997; Rattenbury et al., 1998). The basement has been overlain by *ca.* 6 km of Cretaceous to Cenozoic sediment (King & Thrasher, 1996; Kamp et al., 2004).

The brittle-ductile transition is shallow at 10 km depth below Mt Taranaki and is thought to be due to the high geothermal gradient associated with this volcanism via mid-crustal intrusion and/or crustal underplating (Allis et al., 1995; Sherburn & White, 2005). The andesitic roots of Taranaki Quaternary volcanoes intrude this crust at least as far as the basement rock on the basis of 3-dimensional gravity and magnetic anomalies (Locke et al., 1993; 1994; Locke & Cassidy, 1997). A structure 5 km in diameter and extending to a depth of at least 10 km under Mt Taranaki is interpreted as the roots of the volcano and is also likely to be the focus of future magmatic intrusions (Sherburn et al., 2006).

1.6.3.2 Miocene Volcanism

The Mohakatino Volcanic Centre (Figure 1.3A) is a region of andesitic volcanism in the northern Taranaki Basin that was active during Miocene times (~18-7 Ma) (King & Thrasher, 1996). There is an overall NNE trend and volcanism generally becomes progressively younger towards the south (Stagpoole and Funnel, 2001; Mortimer et al., 2010). These andesitic volcanoes are thought to have a subduction-related origin, and are the southernmost expression of Miocene arc volcanism associated with the contemporaneous Pacific-Australian plate boundary. The Mohakatino Volcanic Centre is interpreted to be a part of the same volcanic arc as the Coromandel Volcanic Zone, Colville Ridge and Lau Islands that were active from 17-5 Ma (Herzer, 1995; Mortimer et al., 2010). The Coromandel Volcanic Zone and the Mohakatino Volcanics are thought to be the southern, continental propagation of the oceanic arc (Herzer, 1995).

1.6.3.3 Taranaki Volcanic Lineament

Mt Taranaki defines the youngest focus of a northwest to southeast trending lineament of Quaternary volcanic centres, along which volcanism has migrated southeast with time over *ca.* 1-2 Ma (Neall et al., 1986). The other three volcanic edifices in this progression are Paritutu and

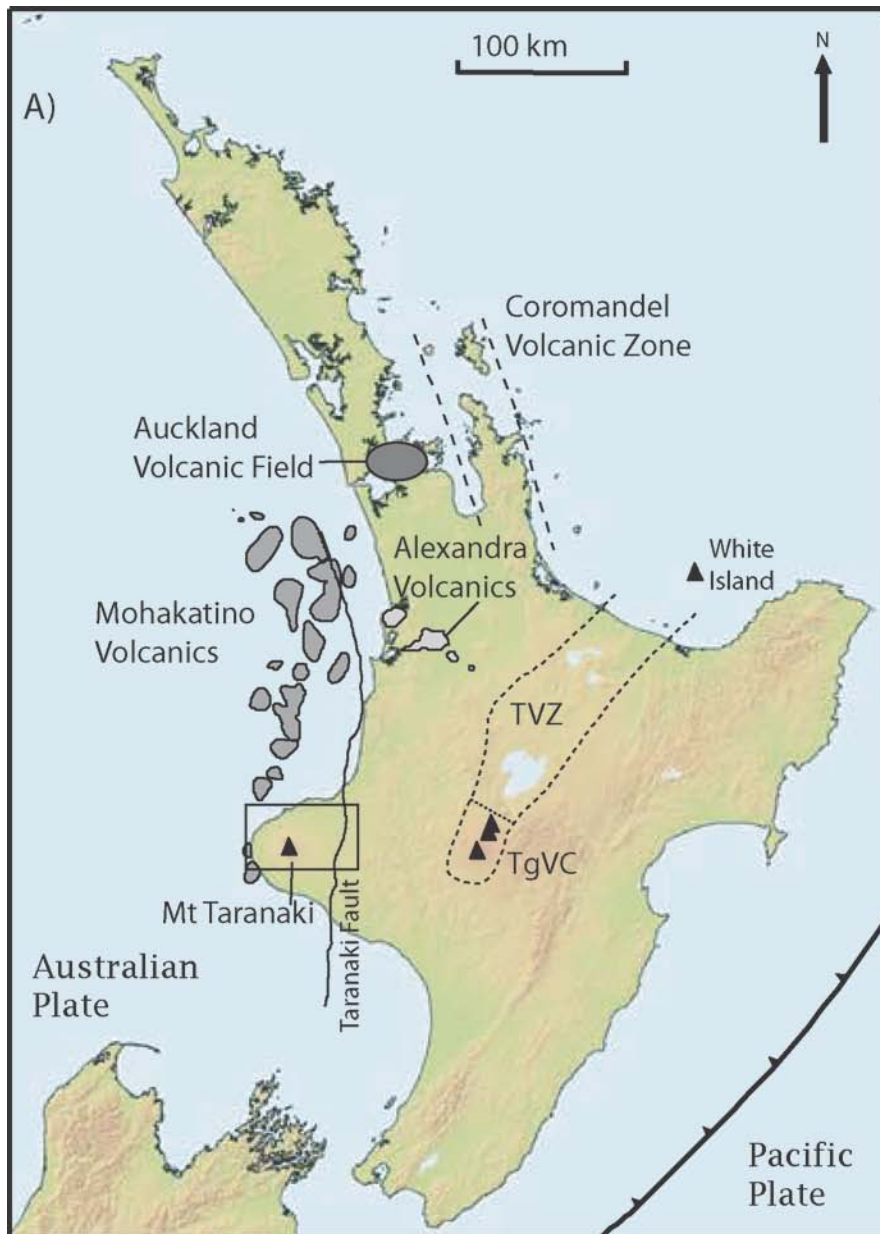


Figure 1.3 A) Map illustrating the distribution of selected North Island Miocene-Recent volcanism. Figure is based on diagrams from King & Thrasher (1996), Stagpoole & Funnel (2001) and Allan (2008). B) Map showing the location of Quaternary volcanism on the Taranaki Peninsula. Backgrounds courtesy of GeographX.

the Sugar Loaf Islands (1.74 Ma), Kaitake (0.5 Ma) and Pouakai (0.25 Ma) (Figure 1.3B) (Neall, 1979). These are comprised of hornblende andesite and minor dacite (Neall, 1979; Neall et al., 1986; Locke et al., 1994). The older volcanoes are all extinct and either highly altered by hydrothermal activity and weathering, or covered in dense bush, or both. The presence of this volcanic lineament could be related to: 1) edge effects of mantle flow; or 2) tears in the subducting slab (Price et al., 1992). There may be thermal up-welling of the asthenosphere around the edge of the slab inducing a low degree of melting in a previously metasomatised mantle wedge (Price et al., 1992). The tears in the subducting slab are roughly parallel to this lineament and could localise fluid and/or melt loss from the slab forming linear zones of magma generation that are expressed as lines of volcanism (Reyners, 1983; Price et al., 1992, 1999).

1.6.4 MT TARANAKI

1.6.4.1 History of Taranaki Volcanism

Volcanic activity has occurred at Mt Taranaki for at least 130 Kyr and the most recent eruption occurred in AD 1854. During this period, Mt Taranaki has undergone a minimum of 13 sector collapses and subsequent cone building phases, with five of these occurring in the last 30 Kyr (Zernack et al., 2009). The most recent sector collapse occurred 7000 yr ago and these collapses have constructed a substantial ring plain. Much of the Holocene evolution of Mt Taranaki has been described by Neall et al. (1986).

The present cone is mostly comprised of material < 10 000 yr old. It consists of detrital fragments of the remnants of older cones overlain by the younger lava flows of the most recent cone. Fanthams Peak is a parasitic cone on the southern slopes of Mt Taranaki that has been active for ca. 7000 yr. Downey et al. (1994) grouped the lava flows of the current cone into four categories on the basis of field relationships and paleomagnetic data (Table 1.1). These can be correlated with the tephro-stratigraphic record (e.g. Stewart et al., 1996). Until recently the youngest eruptive event was believed to be the Tahurangi Ash, which occurred in AD 1755 (Neall et al., 1986). It is now thought that two dome collapse events occurred in AD 1800 and 1854 (Platz, 2007).

There is an average eruption periodicity of around 232-330 yr for sub-plinian eruptions (Alloway et al., 1995; Turner, 2008). There are also more frequent, smaller scale eruptions (dome- and block and ash-forming events) that tephro-stratigraphic evidence suggests generally occurs on a decadal basis (Turner, 2008; Turner et al., 2009.).

Stratigraphic group	Age (BP)	Correlative tephras
Summit	> 0.7 ka	Newall Ash and lapilli (AD 1604); Burrell Lapilli (AD 1655); Tahurangi Ash (AD 1755)
Staircase	0.7-2 ka	Kaupokonui Tephra (1.4 ka BP)
Fanthams Peak	7-< 1 ka	Manganui Tephra (3.3 ka BP)
Warwicks Castle	8-3 ka	Korito Tephra (4.1 ka BP); Inglewood Tephras (3.6 ka BP); Maketawa Tephra (2.9 ka BP)

Table 1.1 Summary of the stratigraphic groupings for Mt Taranaki lava and selected tephra units. After Price et al. (1999) using data from Neall et al. (1986), Downey et al. (1994), Alloway et al. (1995) and Stewart et al. (1996).

1.6.4.2 Petrology & Geochemistry

Mt. Taranaki eruptives are classified as high-K basalts, basaltic andesites and andesites based on whole rock data (Neall et al., 1986; Price et al., 1992; Stewart et al., 1996; Price et al., 1999, 2005). The mineral assemblage typically consists of plagioclase, clinopyroxene, hornblende and titanomagnetite with minor amounts of olivine, orthopyroxene and ilmenite (Gow, 1968; Neall et al., 1986; Stewart et al., 1996). Fanthams Peak eruptives are similar to those of the main vent but are generally more basaltic (basalt-basaltic andesite whole rock compositions) and contain a larger proportion of olivine and less amphibole (<5%) (Price et al., 1992). Glass specific analyses show that the composition of the melt phase immediately prior to eruption is considerably more silicic than the whole rock data suggests and that these are andesitic, dacitic and rhyolitic in composition (Price et al., 2005; Platz et al., 2007a). Trace element chemistry is typical of subduction related magmas exhibiting enrichment in LILE and depletion of HFSE (Figure 1.4; Price et al., 1992, 1999, 2005). The magmas are also relatively evolved with very low concentrations of Ni and Cr (Price et al., 1992, 1999; Stewart et al., 1996). $^{87}\text{Sr}/^{86}\text{Sr}$ and $^{143}\text{Nd}/^{144}\text{Nd}$ isotope data from Price et al. (1992, 1999) define narrow ranges ($^{87}\text{Sr}/^{86}\text{Sr} = 0.70378\text{-}0.70504$; $^{143}\text{Nd}/^{144}\text{Nd} = 0.51276\text{-}0.51281$) and suggest limited involvement of continental crustal material.

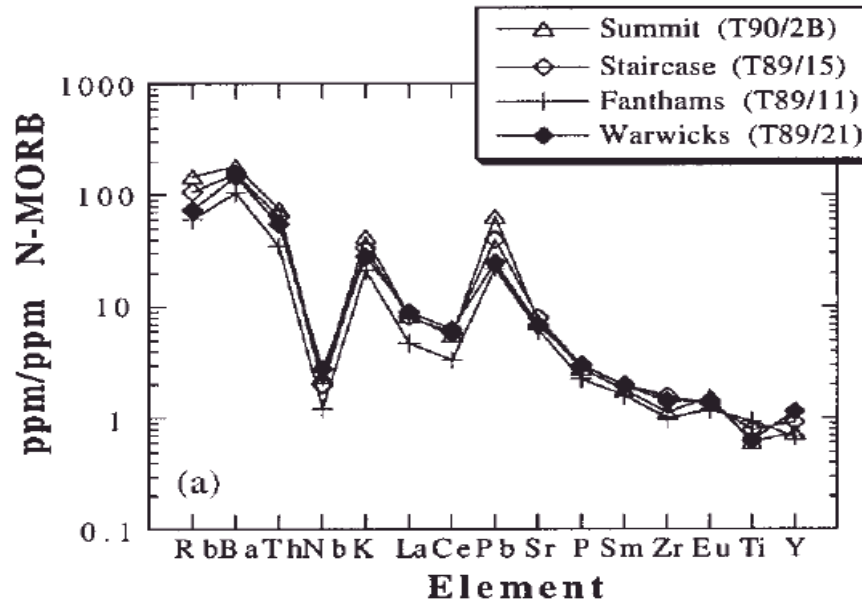


Figure 1.4 N-MORB normalised multi-element diagram of selected Taranaki lavas to illustrate the ‘subduction signature’ typical of Taranaki lavas. Figure taken from Price et al. (1999).

The primary magmas associated with Taranaki eruptives are thought to be hydrous, high-Mg basalts, which are relatively under-saturated with respect to SiO_2 and were formed by low degrees of partial melting of a relatively depleted, metasomatised mantle wedge (Price et al., 1992, 1999; Stewart et al., 1996). The high-Mg basalts evolved to high-Al basalts and basaltic andesites by fractionation of mafic minerals, inferred to be now represented by pyroxenite and amphibolite cumulates at the base of the crust (Stewart et al., 1996; Price et al., 1999). Assimilation and fractional crystallisation processes further modified the magma compositions (Price et al., 1992, 1999, 2005), with slight compositional and physical differences between magma batches (Price et al., 2005; Turner et al., 2008). These magma batches are inferred to have mixed at upper crustal depths on a timescale of days to weeks prior to the onset of an eruption (Turner et al., 2008). The physical similarities (i.e. temperature and viscosity) between the different magmas enable efficient mixing to occur (Turner et al., 2008).

Temporal variability

Taranaki eruptives have become increasingly enriched in SiO_2 and K_2O over the past *ca.* 115 000 yr (Price et al., 1999). This temporal variation may be related to changes at the magma source such as declining degrees of partial melting, changing fluid flux and/or mantle source

heterogeneity (Price et al., 1999). Alternatively, partial anatexis of the amphibolitic cumulates in the lower crust may occur due to a rising geothermal gradient (Stewart et al., 1996; Price et al., 1999). This would produce a high-K melt that would then interact with the high-Al basalt producing progressively more K-rich magmas with time (Stewart et al., 1996; Price et al., 1999).

Cross arc variation

Taranaki has been used in conjunction with the TgVC, especially Ruapehu, to examine cross arc variation (e.g. Price et al., 1992, 1999, 2005). These studies show that Taranaki overlies a more depleted mantle wedge that has undergone a lower degree of partial melting than the TgVC as indicated by higher abundances of LILE and HFSE in the Taranaki eruptives (Price et al., 1992, 1999). The fluids involved at each volcanic centre are geochemically different as there is a declining influence of sediment at deeper levels of the subduction system and subduction is deeper below Mt Taranaki (Price et al., 1999). The nature of the crust at the two centres has further differentiated the magma suites by influencing the degree of interaction and the material magmas have interacted with (Price et al., 1992, 1999, 2005). Taranaki eruptives have less involvement with the crust than the andesites of the TgVC on the basis of lower $\delta^{18}\text{O}$ values, a lack of correlation between SiO_2 and $^{87}\text{Sr}/^{86}\text{Sr}$ as well as less radiogenic Pb isotopes when compared with Ruapehu (Price et al., 1992, 1999).

1.7 OBJECTIVES AND STRUCTURE OF THIS THESIS

The overall objective of this thesis is to improve understanding of explosive andesitic eruptions through investigations of the shallow crustal processes responsible for producing recent sub-plinian eruptions at Mt Taranaki. This objective is pursued through a series of mineral-specific and micro-analytical studies including:

- (a) petrography and characterisation of the mineral phases present in Taranaki eruptives;

- (b) detailed in situ major and trace element analyses of these minerals using electron microprobe (EMPA) and laser ablation inductively coupled plasma mass spectrometry (LA-ICP-MS) analyses;
- (c) major and trace element analyses of glass separates using EMPA and solution ICP-MS;
- (d) calculation of pre-eruptive conditions including magmatic temperature, pressure, water content and oxygen fugacity calculated using amphibole geothermobarometry, clinopyroxene-melt thermometry and plagioclase-melt thermometry; and
- (e) magmatic residence times of clinopyroxene crystals from diffusion modelling.

Specifically this study aims to:

- (a) Compare and contrast whole-rock and glass chemistry as a guide to fractionation pathways within Taranaki.
- (b) Use crystal chemistry and texture to constrain the magmatic systems and the processes operating within them.
- (c) Investigate the evolution of the Taranaki magmatic system by exploring the temporal variability in the eruptive products across six samples, representing a *ca.* 2700 year period of eruptions from ~1400 to 4100 years before present (B.P.).
- (d) Quantify the timescales of the shallow crustal processes that may trigger eruptions.

This thesis is comprised of six chapters and four appendices with the following structure:

Chapter 1: *Introduction* - An overview of andesitic magmatism including the importance of understanding these systems, how these magmas form and how they are modified by crustal processes as well as a summary of some of the techniques that can be used to resolve these processes. A background of the Taranaki region and volcanism including a summary of previous geochemical studies is also given.

Chapter 2: *Fieldwork* – A chapter showing the locations and details of sample collection.

Chapter 3: *Methods* - A description of the methods used to collect the geochemical data for this thesis including an evaluation of the data quality and the standards used. The thermobarometry and diffusion modelling techniques applied in this study are also described and evaluated.

Chapter 4: *Results* – Presents the key geochemical and modelling results from this study.

Chapter 5: *Discussion* – An interpretation of the results, relating them to various magmatic processes and comparing this work with previous studies on Mt Taranaki as well as key global examples of andesitic magmatism.

Chapter 6: *Conclusions* – A summary of the key findings of this research and suggestions for future work.

Appendices 1-4: A list of the samples, geochemical data and diffusion modelling profiles used in this study.

CHAPTER 2:
FIELDWORK AND
SAMPLES

2.1 FIELDWORK METHODS

Tephra samples were collected in February 2008 from road cuttings on the eastern slopes of Mt Taranaki. The prevailing westerly winds carry eruptive products to the east and therefore this is the location of the most comprehensive tephrostratigraphic record. Field sites were selected to best represent the recent stratigraphic record and avoid areas of reworking.

Four sites were selected that collectively covered the tephrostratigraphic record of Mt Taranaki using the work of Alloway et al. (1995). In total 152 samples were collected from these sites, covering the time period of < 2000 to 23 000 yr B.P. with the last 10 000 yr sampled continuously.

At each site, the section was cleared off with a spade so the weathered surface was removed. The sites were then measured and photographed. Every layer was sampled and described including those thought to be paleosols. Sampling began at the top of each section, working down through the stratigraphy. Where necessary, multiple sections of an outcrop were sampled to cover the entire tephrostratigraphic sequence present at an outcrop.

2.2 SITE LOCATIONS

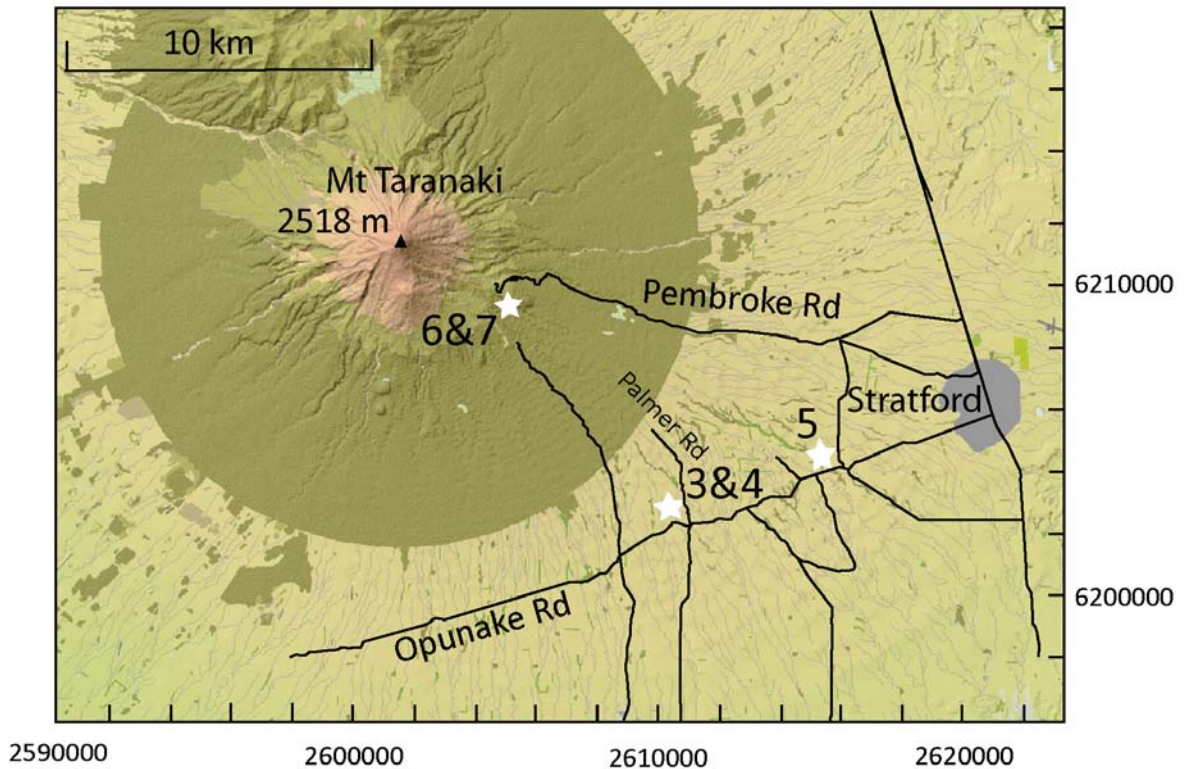


Figure 2.1 Map of the field area for this study showing the location of sampling sites. Main roads and those roads referred to in the text are also shown. Co-ordinates are New Zealand Map Grid (NZMG).

2.2.1 SITE 3 AND 4—OPUNAKE ROAD

Sites 3 and 4 are a north facing road cutting located on Opunake Road west of the intersection with Palmer Road (NZMG E2605134 N6202446) (Figure 2.1). The outcrop was approximately 20 metres in length and had a maximum height of around five metres. Sampling took place in six sections to cover the entire timespan represented in this outcrop. In total, 57 samples were collected covering the Maketawa to the Kaponga Tephra. Areas of this outcrop showed evidence for reworking, particularly towards the base. The six sections were carefully selected to avoid these areas where possible. Stratigraphy is unclear for the bottom three sections and may be affected by reworking.

2.2.2 SITE 5 – OPUNAKE RD

Site 5 is a north facing road cutting located on Opunake Road opposite Cardiff Walkway Carpark (NZMG E2615707 N6204236). This road cutting is largely covered in scrub therefore in order to sample as much of the tephrostratigraphy at this site as possible six sections of 0.5 to

2 m in height were sampled over a length of *ca.* 20 m. The easternmost of these sections are located 2 m east of location 7 from Alloway et al. (1995). Sampling began at the eastern end of the outcrop and progressed up the road, with each section stratigraphically above the previous, with sampling beginning at the top of each section. In total, 53 samples were taken spanning from the Poto c to Kaihouru tephra units with some possible breaks within this sequence.

2.2.3 SITE 6 – PEMBROKE RD

Site 6 is a north facing road cutting on Pembroke Road within Egmont National Park (NZMG E2605134 N6210266) where 13 samples were collected. This section is *ca.* 1.5 m in height and covers the youngest samples collected for this study (Kaupokonui Tephra to the Manganui Tephra; Figure 2.2).

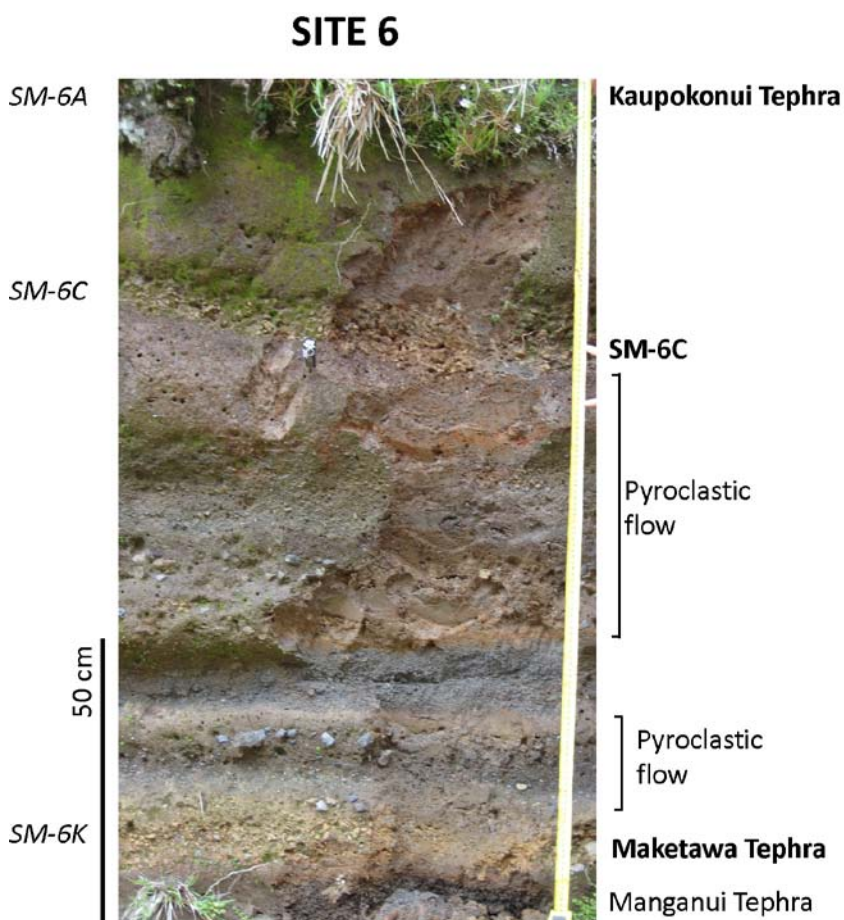


Figure 2.2 Annotated photograph of Site 6. Samples investigated in this study are identified by the sample ID (*italics*) and the corresponding tephra unit (**bold**). Other tephra units and key features are also highlighted. Note the Kaupokonui tephra (unit *SM-6A*) is obscured by vegetation in this image.

2.2.4 SITE 7 – PEMBROKE RD

Site 7 is a south facing road cutting on Pembroke Road within Egmont National Park across the road from Site 6 (NZMG E2605134 N6210266). Much of this section overlaps that of Site 6, but this site extends to encompass older units. Sampling began at the Maketawa Tephra, rather than the top of this section to slightly overlap this site with Site 6 to ensure a continuous record. Twenty-one samples were collected from this site encompassing from the Maketawa Tephra to the Korito Tephra. Samples were collected where the tephrostratigraphy was clearest within this site and as a result, three sections were sampled, progressing down hill (Figure 2.3).

SITE 7

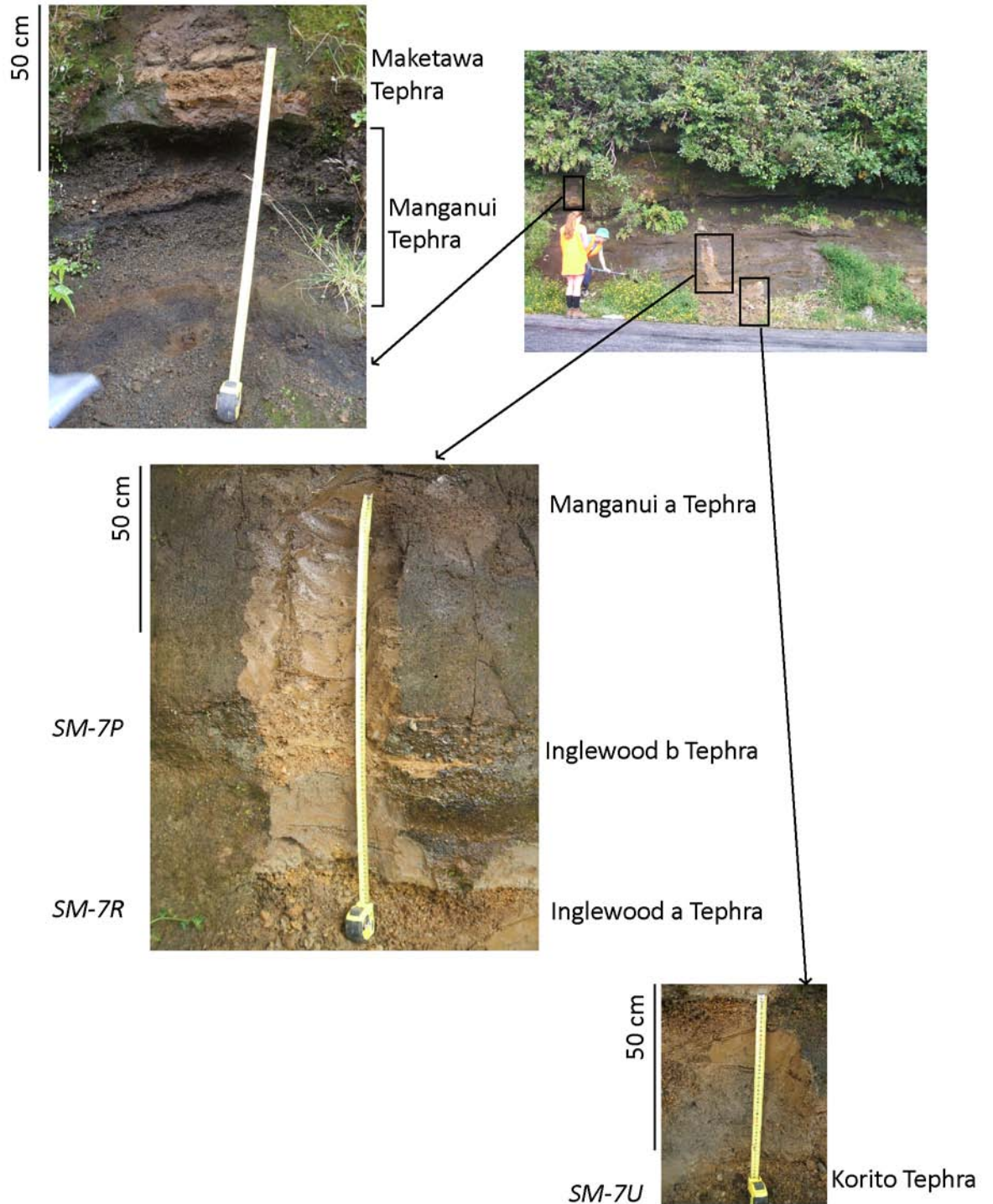


Figure 2.3 Annotated photographs of Site 7. The tephra units identified in this sample are identified. Samples worked on for this study are also labelled with the sample ID (*italics*).

2.3 SAMPLES

In total 152 samples were collected, of which six samples from Sites 6 and 7 were selected for this study as identified in Figure 2.4. These six samples are the youngest pumiceous samples collected and are considered to characterise Holocene sub-plinian eruptions from Mt Taranaki. Younger samples have better age constraints and are less likely to be affected by secondary processes such as reworking of material and weathering. Pumiceous samples were used as these represent the magma composition at the time of eruption. Glass and mineral phases are also easier to work with in pumice as there is ample glass available for analysis and mineral phases can be easily separated without fragmenting the crystals.

Tephra units were identified and correlated to the existing tephrostratigraphic record using the tephrochronology of Alloway et al. (1995) and Turner et al. (2008) (Figure 2.4). Age constraints for these samples are based on the stratigraphic position of the tephra units in relation to radiocarbon dates of peats and woods from Neall (1979), Neall & Alloway (1986), Hogg et al. (1987), Lowe (1988), McGlone et al. (1988) and Alloway (1989).

Sample SM-6C was unable to be correlated with a named unit from these workers. The only named unit stratigraphically between the Maketawa and Kaupokonui Tephra is the Curtis Ridge Episode from Turner et al. (2008) (Figure 2.4). The low lithic proportion of SM-6C (~20%) compared with that of the Curtis Ridge Episode (60% grading to 30% of Unit 1; all of Unit 2) indicates that these are different units. Comparison of the mineral textures and chemistry for SM-6C from this study and the Curtis Ridge Episode from Turner et al. (2008) further indicate that these are different units. For example, the Turner et al. (2008) describe clinopyroxene crystals as having a patchy textured core and oscillatory zoned rim. This is a common feature of Taranaki clinopyroxene, but is notably absent from SM-6C. Confirmation that these units are not the same would require the comparison of glass chemical data, which is not available for the Curtis Ridge Episode. SM-6C directly overlies a series of pyroclastic flow deposits (Figure 2.2), therefore this may be the unnamed pumiceous fall deposit identified by Turner et al. (2008) (Figure 2.4).

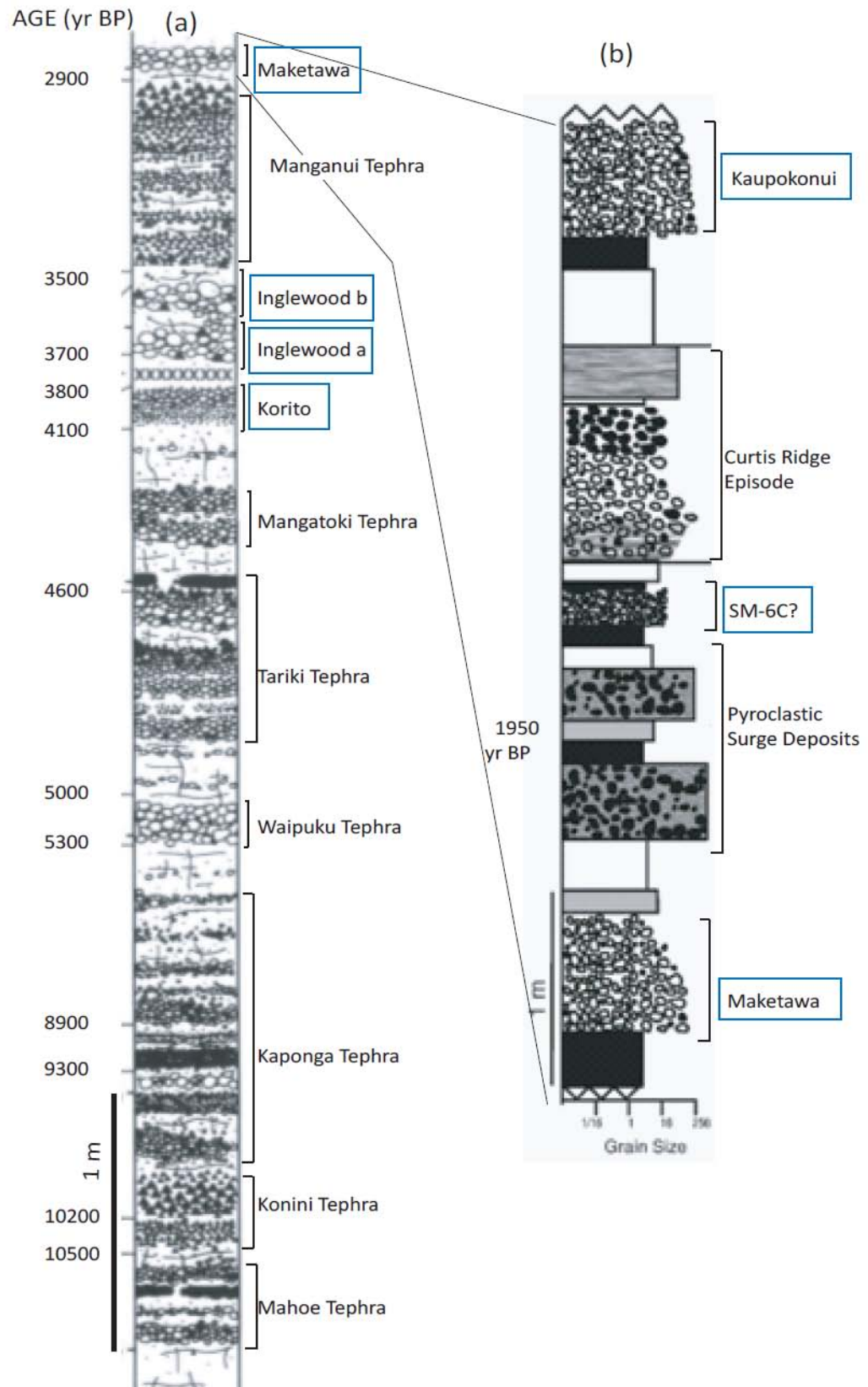


Figure 2.4 The stratigraphic locations of the samples investigated in this study. (a) after Alloway et al. (1995); (b) after Turner et al. (2008).

CHAPTER 3: **METHODS**

3.1 MAJOR ELEMENT ANALYSIS

3.1.1 SAMPLE PREPARATION

Six samples were prepared for in situ geochemical analyses of mineral phases and glass. Initially all samples were rinsed with water to remove external contaminants and soaked in an ultrasonic tank for up to 20 cycles until the water remained clear. Clean samples were then dried in an oven at 25-40 °C for 1-3 days. Pumice clasts 2-3 cm in size from the six samples of interest were mounted in epoxy resin blocks and sequentially with 400, 600, 2000 and 4000 grit silicon carbide paper followed by 3 and 1 µm diamond suspension. Remaining pumice clasts were crushed in a mortar and pestle or, for more delicate clasts, crushed with a pestle in multiple sealed plastic bags to minimise crystal breakage. Glass was separated from the crystals using the hydrodynamic settling method. The resulting crystal concentrate was dried in a 40 °C oven for 12-48 hr and sieved into > 1 mm, 1 mm-500 µm, 500-250 µm and < 250 µm fractions. Clinopyroxene crystals were handpicked from the most crystal-rich fractions under a binocular microscope and mounted on their b-axis (exposing the (010) plane) in epoxy resin blocks to view zone boundaries dipping as closely as possible to vertical (Morgan et al., 2004). Crystals were exposed half way through using 600 and 2000 grit silicon carbide paper, and subsequently polished on 3, 1 and 0.25 µm diamond suspension and finally with colloidal silica to eliminate scratches. Each mount was covered in a 25 nm carbon coat prior to electron microprobe analysis (EMPA) analysis and imaging.

3.1.2 ELECTRON MICROPROBE ANALYSES

Major element mineral and glass analyses were obtained at Victoria University of Wellington's (VUW) Geochemistry Laboratory in Wellington, New Zealand, using two different instruments. The differences between these instruments and compatibility of data are addressed in the following sections.

3.1.2.1 JEOL 733 Superprobe Electron Probe Micro-Analyser

Glass, clinopyroxene, amphibole and plagioclase analyses of samples SM-6C, SM-6K and SM-7P were determined using a JEOL 733 Superprobe equipped with three wavelength dispersive spectrometers. Major element concentrations were determined using the ZAF correction method. An accelerating voltage of 15 kV, beam current of 12 nA and a focused beam were employed for mineral analyses. For glass, an accelerating voltage of 15 kV, beam current of 8 nA and a 10 μm defocused beam were used. Count times were 30 s with 10 s of background for each element except Na and K, which were analysed first and with shorter count times of 10 s and 5 s background to minimise alkali loss. Instrumental calibration was carried out daily using synthetic standards for Al, Cr, Fe, Mg, Mn, and Ti and natural samples for Cl (sodalite), K (orthoclase), Na (jadeite), Si and Ca (wollastonite). Secondary standards were run at the start and end of each day to monitor spectrometer drift during the analysis and evaluate machine precision and accuracy. The secondary standards used were basaltic glass VG-A99 (USNM 113498/1) for volcanic glass and plagioclase, Kakanui augite (USNM 122142) for clinopyroxene and hornblende P.S.U. 4-190 for amphibole analyses. The precision and accuracy of these measurements are listed in Table A2.1. All standard values were accurate to $\leq 7\%$ except for MnO, Cr₂O₃ and Cl which are always present at levels $< 0.5\text{ wt } \%$ in these standards resulting in significantly higher errors.

Backscattered electron (BSE) imaging of clinopyroxene crystals for diffusion modelling was carried out on this instrument at an accelerating voltage of 15 kV and beam current of 12 nA. The magnification and contrast settings were optimised for each image to highlight mineral zoning.

3.1.2.2 JEOL JXA-8230 Electron Probe Micro-Analyser

Glass, clinopyroxene, amphibole, plagioclase and Fe-Ti oxide analyses for all samples were determined on a JEOL JXA-8230 Electron Probe Micro-Analyser with five wavelength dispersive spectrometers (WDS), two containing large crystals to measure minor elements present at relatively low concentrations. Mineral phases were analysed under a static electron

Table 3.1 JEOL 733 Superprobe Electron Probe Micro-Analyser standard data precision and accuracy. Recommended values: VG-A99-Jarosweich et al. (1980); Kakanui Augite-Klugel et al. (2005); Hornblende 4-190-Ingamells (1983)

VG-A99 Basaltic Glass (USNM 113498/1)					
	Mean¹	Recommended values	2 SD	% 2 SD² (precision)	% Difference³ (accuracy)
SiO₂ (wt %)	50.72	50.94	0.93	1.8	-0.4
TiO₂	4.14	4.06	0.24	5.9	1.9
Al₂O₃	12.63	12.49	0.30	2.4	1.1
FeO	13.31	13.3	0.43	3.2	0.1
MnO	0.25	0.15	0.08	32.5	66.0
MgO	5.24	5.08	0.21	4.1	3.2
CaO	9.16	9.3	0.21	2.3	-1.5
Na₂O	2.73	2.66	0.10	3.6	2.7
K₂O	0.84	0.82	0.04	5.1	2.3
TOTAL	98.81	98.80			
n	59				
Kakanui augite (USNM 122142)					
	Mean¹	Recommended values	2 SD	% 2 SD² (precision)	% Difference³ (accuracy)
SiO₂	50.69	50.39	0.82	1.6	0.6
TiO₂	0.85	0.78	0.06	7.1	9.5
Al₂O₃	8.76	8.72	0.39	4.5	0.5
Cr₂O₃	0.21	0.15	0.07	31.2	39.3
FeO	6.38	6.31	0.14	2.2	1.1
MnO	0.17	0.14	0.05	26.7	22.6
MgO	16.72	16.45	0.29	1.8	1.6
CaO	15.97	15.89	0.24	1.5	0.5
Na₂O	1.36	1.25	0.05	3.7	8.7
TOTAL	101.07	100.08			
n	39				
Hornblende 4-190					
	Mean¹	Recommended values	2 SD	% 2 SD² (precision)	% Difference³ (accuracy)
SiO₂	40.04	39.54	1.49	3.7	1.3
TiO₂	2.69	2.88	0.14	5.2	-6.5
Al₂O₃	10.58	10.00	0.32	3.0	5.8
FeO	26.00	26.15	0.68	2.6	-0.6
MnO	0.47	0.41	0.09	19.8	14.5
MgO	4.58	4.38	0.03	0.6	4.6
CaO	10.74	10.79	0.15	1.4	-0.5
Na₂O	2.09	2.02	0.01	0.4	3.3
K₂O	1.47	1.47	0.04	3.0	0.2
Cl	0.19	0.18	0.05	28.2	7.4
Total	98.85	97.82			
n	20				

¹Mean of n analyses

²% 2 sd = (2 sd/mean) x 100

³% difference = ((mean-recommended)/recommended) x 100

beam of 15 kV accelerating voltage and a current of 12 nA, whilst glass analyses used a 10 µm defocused beam with an accelerating voltage of 15 kV and beam current of 8 nA. Each element had a count time of 30 s and a background count time of 15 s per analysis. Alkali monitoring detected no measureable Na or K loss using these count times. Table 3.2 shows the conditions for each analysis type. Calibrations were carried out daily on well characterised reference materials (primary standards), listed in Table 3.2. The primary standard chosen for each set of analyses was compositionally similar to the phase being analysed in order to minimise matrix effects. Where element concentrations in the standard materials were not sufficient to produce accurate calibrations (< 0.5 wt %), oxides were used for calibration. These same primary standards were analysed as secondary standards immediately after instrument calibration and after every 10-20 sample analyses. This allowed monitoring of any instrumental drift and correction for variation in analytical conditions. Mineral and glass analyses were corrected to this secondary standard. If secondary standard values were inaccurate, the calibration was redone.

Table 3.2: Analytical conditions during analytical sessions with the JEOL JXA-8230 EMPA. Crystal used in noted in brackets.

Glass: Primary/Secondary Standard-VG-A99; Additional Standard-VG568				
Channel 1	Channel 2	Channel 3	Channel 4	Channel 5
Ti (PET)	Si (TAP)	Na (TAP)	K (PET)	Ca (PET)
Mn* (LIF)	Mg (TAP)	Al (TAP)	Fe (LIF)	
Clinopyroxene: Primary/Secondary Standard-Kakanui augite; Additional Standard-PX-1				
Channel 1	Channel 2	Channel 3	Channel 4	Channel 5
Mn* (LIF)	Si (TAP)	Mg (TAP)	Ca (PET)	Fe (LIF)
	Al (TAP)	Na (TAP)		Ti (PET)
Amphibole: Primary/Secondary Standard-Hornblende 4-190; Additional Standard- Engles amphibole				
Channel 1	Channel 2	Channel 3	Channel 4	Channel 5
Ti (PET)	Na (TAP)	Si (TAP)	Fe (LIF)	K (PET)
	Mg (TAP)	Al (TAP)	Ca (PET)	Mn* (PET)
Plagioclase: Primary/Secondary Standard-Plagioclase NMNH 96189; Additional Standard- Or-1A				
Channel 1	Channel 2	Channel 3	Channel 4	Channel 5
Sr* (PET)	Na (TAP)	Si (TAP)	Ca (PET)	K# (PET)
Sr* (PET)	Mg* (TAP)	Al (TAP)	Fe* (LIF)	Ti* (PET)
Oxides: Primary/Secondary Standard-Ilmenite NMNH 96189; Additional Standard- Magnetite NMNH 96189				
Channel 1	Channel 2	Channel 3	Channel 4	Channel 5
Ca ⁺ (PET)	Mg* (TAP)	Si ⁺ (TAP)	Fe (LIF)	Mn (LIF)
Ti (PET)		Al* (TAP)		Cr* (PET)

Unless otherwise stated calibration for each element was on the primary standard.

* element standardized on oxide

element standardized on Or-1

+ element standardized on Wollastonite.

This procedure also gives an indication of analytical precision and accuracy and enables correction for instrument drift and any changes in analytical conditions. However, it underestimates true analytical error by neglecting to account for the matrix effects of slight compositional differences between standards and sample mineral analyses. To better quantify these uncertainties, additional reference materials were analysed with a similar composition to the sample and primary/secondary standards. These additional standards, specified in Tables 3.2 and 3.3, were analysed immediately after instrument calibration. These showed reduced precision and accuracy compared to the primary/secondary standard. For elements present in moderate to high concentrations in the primary/secondary standards (≥ 0.5 wt %) the precision was typically $< \pm 5\%$ and always $< \pm 7\%$, and accuracy for these elements was always $< 5\%$ (except for TiO_2 in Kakanui augite). The additional standards have precisions of $< \pm 15\%$ except for MnO in Engles amphibole and Na_2O in orthoclase. The accuracy for these additional standards is $\leq 11\%$ except for Na_2O in orthoclase. Errors increase significantly when concentrations are < 0.5 wt% with precisions typically ± 20 - 30% up to ± 300 - 400% for K_2O and SrO in plagioclase and accuracy around ± 16 - 75% . These elements (except K_2O) were analysed using LA-ICP-MS to a much greater precision and accuracy. In most cases (except for glass) the errors for sample analyses are much closer to those of the primary/secondary standards because these are closer in composition than the additional standards.

Backscattered electron imaging was again carried out using an accelerating voltage of 15 kV and a current of 12 nA.

3.1.2.3 Comparison of EMPA data

The majority of major element data used in this study were obtained from the JEOL JXA - 8230 EMPA. The data between the two instruments is comparable as the precision and accuracy of elements in concentrations of > 0.5 wt% is < 5 - 7% for both instruments (Figure 3.1). However, at lower concentrations the JEOL JXA-8230 has significantly lower errors. The standardising procedure is also much more robust for this instrument as standardising was

Table 3.3 Continued

AMPHIBOLE									
Hornblende 4-190					Engels Amphibole				
Mean ¹	Recommended values ²	2 SD	% 2 SD ³ (precision)	% Difference ⁴ (accuracy)	Mean ¹	Recommended values ²	2 SD	% 2 SD ³ (precision)	% Difference ⁴ (accuracy)
SiO ₂	39.74	0.36	0.9	0.5	41.29	42.14	0.50	1.2	-2.0
TiO ₂	2.83	0.12	4.3	-1.9	0.84	0.94	0.04	4.6	-10.1
Al ₂ O ₃	10.03	0.52	5.2	0.3	12.42	12.09	0.68	5.5	2.7
FeO	26.44	0.64	2.4	1.1	18.91	19.05	0.50	2.6	-0.7
MnO	0.33	0.00	1.5	-18.8	0.57	0.63	0.11	19.1	-9.8
MgO	4.40	0.22	5.0	0.4	9.09	8.67	0.15	1.7	4.9
CaO	10.69	0.36	3.3	-1.0	11.45	11.56	0.15	1.3	-0.9
Na ₂ O	2.05	0.10	4.8	1.6	1.56	1.63	0.25	16.0	-4.1
K ₂ O	1.46	0.03	2.3	-1.0	0.94	0.91	0.02	1.9	2.9
Total	97.95	1.47	97.63		97.07	97.62			
n	20				3				
PLAGIOCLASE									
Plagioclase (Labradorite) Lake Country (NMNH 96189)					Or-1A				
Mean ¹	Recommended values ²	2 SD	% 2 SD ³ (precision)	% Difference ⁴ (accuracy)	Mean ¹	Recommended values ²	2 SD	% 2 SD ³ (precision)	% Difference ⁴ (accuracy)
SiO ₂	51.31	1.05	2.1	0.1	63.57	64.39	1.47	2.3	-1.3
TiO ₂	0.03	0.01	21.0	-37.0	0.00	-	0.01	127.6	-
Al ₂ O ₃	30.70	1.11	3.6	-0.7	19.23	18.19	0.87	4.5	5.7
FeO	0.45	0.05	10.0	-2.2	0.02	0.03	0.04	229.5	-44.0
MgO	0.14	0.02	11.0	-2.4	0.00	-	0.01	239.0	-
SrO	0.00	0.00	493.8	-	0.01	0.04	0.04	407.3	-74.1
CaO	13.52	0.94	7.0	-0.9	0.38	-	0.99	263.4	-
Na ₂ O	3.43	0.22	6.4	-0.7	0.91	1.14	0.27	30.1	-20.4
K ₂ O	0.32	0.18	329.6	75.0	14.57	14.92	0.98	6.7	-2.4
Total	99.89	100.08			98.68	98.71			
n	228				30				

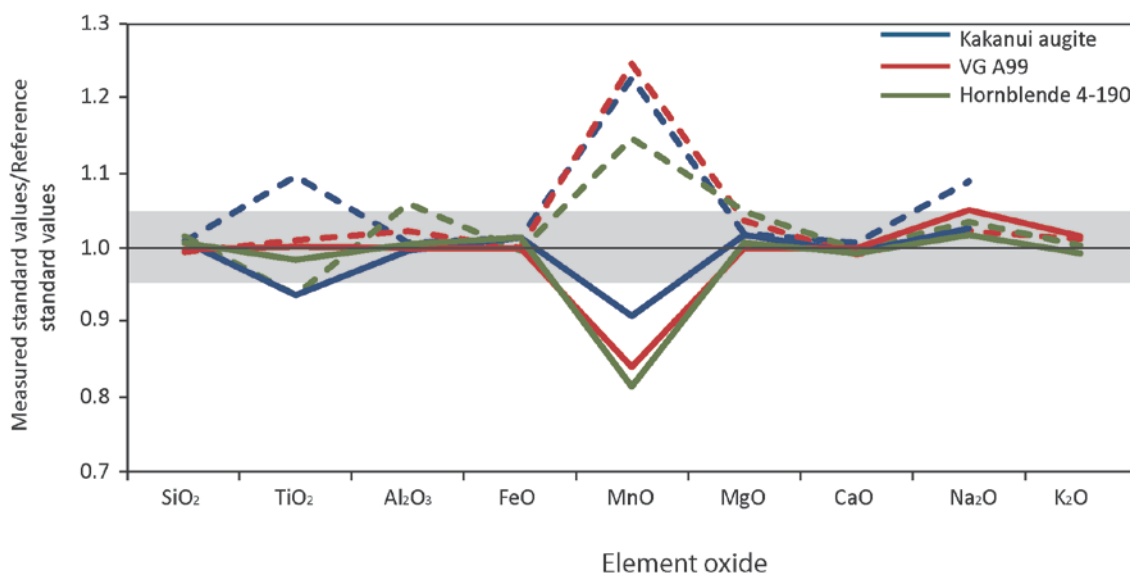
Table 3.3 Continued

	OXIDES									
	Ilmenite, Ilmenite Mountains, USSR (NMNH 96189)				Magnetite					
	Mean ¹	Recommended values ²	2 SD	% 2 SD ³ (precision)	% Difference ⁴ (accuracy)	Mean ¹	Recommended values ²	2 SD	% 2 SD ³ (precision)	% Difference ⁴ (accuracy)
SiO ₂	0.01	-	0.00	2.7	-	0.04	-	0.02	43.5	-
TiO ₂	45.93	45.70	0.90	2.0	0.5	0.19	0.16	0.07	35.2	20.5
Al ₂ O ₃	0.02	-	0.01	38.8	-	0.05	-	0.01	31.2	-
Cr ₂ O ₃	0.09	-	0.05	55.0	-	0.26	0.25	0.07	26.3	3.0
FeO	46.80	46.54	0.20	0.4	0.6	93.57	90.94	0.66	0.7	2.9
MnO	4.86	4.77	0.30	6.3	1.8	0.07	<0.01	0.00	3.2	-
MgO	0.30	0.31	0.00	0.2	-2.3	0.11	0.05	0.04	33.0	116.2
Total	98.00	97.32				94.29	91.40			
n	81					51				

¹Mean of nm analyses²Recommended values: VG-A99, VG568, Plagioclase, Ilmenite, Magnetite-Jarosweich et al. (1980); Kakanui Augite-Klugel et al. (2005); Hornblende 4-190-Ingamells (1983); Engels Amphibole-Ingamells (1980); Or-1A, Px-1-Ingamells (1980); Goldlich et al. (1967).³% 2 sd = (2 sd/mean) x 100⁴% difference = ((mean-recommended)/recommended) x 1

performed on mineral standards of a similar composition to the unknown rather than oxides and two standards were run to more completely assess the errors involved in these analyses.

Figure 3.1 A graphical comparison between the JEOL 733 Superprobe (dashed line) and JEOL JXA-8230 (solid line) Electron Probe Micro-Analysers evaluated by comparing how closely the average measured values of standards reproduces the reference values. Grey area represents $\pm 5\%$ accuracy.



3.2 TRACE ELEMENT ANALYSIS

3.2.1 GLASS TRACE ELEMENT ANALYSIS

3.2.1.1 Sample Preparation

Glass trace element chemistry was obtained by solution inductively coupled plasma mass spectrometry (ICP-MS). Crushed pumice, which was earlier separated from crystals, was rinsed in methanol to separate the glass fraction for each sample. These were then dried at 40° C in an oven and inspected under a binocular microscope to check the purity of the glass was satisfactory. The samples were then rinsed three times in > 18.2 MΩ ultra clean water (MQ H₂O) and again dried at 40° C in an oven.

A total of 12 analyses were carried out: three samples were run in duplicate, three samples were run once and BHVO-2 and BCR-2 basaltic rock standards were run as primary and secondary standards, respectively. A blank was also analysed to check that the digestion process did not

introduce any contamination. Care was taken at each step to ensure that no material was lost during digestion, as this would invalidate the dilution factors. Savillex[®] teflon beakers (23 mL) were acid cleaned in 6M AR grade HCl, 6M AR grade HNO₃, 7M sub-boiled (sb) HNO₃ and Seastar (ss) 1mL 7M HNO₃ with 0.2 mL ss HF. Beakers were capped and heated at 120° C on a hotplate during each acid step for at least 24 hr. Between cleaning steps, beakers were rinsed thoroughly three times with MQ H₂O. Glass digestion was carried out using the following steps: 1) between 50 and 80 mg of glass from each sample was weighed into acid cleaned beakers using a high precision balance (± 0.0001 g). 2) approximately 0.2 mL of ss 16M HNO₃ and 1 mL of concentrated ss HF were added to the glass and capped and left on a hotplate at 120° C for two days. 3) samples were then evaporated at 120° C for ca. 5 hr until they were incipiently dry (dry, but not yet cracking). 4) 1 mL of 16M ss HNO₃ was added, left uncapped on the hotplate overnight to nitrify the sample, and then capped on the hotplate in 5 mL of 6M ss HCl for 3 hr until it was fully in solution. 5) the sample was then uncapped and dried overnight. 6) approximately 1 mL of 16M ss HNO₃ was then added to each sample for nitrification and immediately evaporated. Step 6 was repeated followed by the addition of 9 mL of 1M HNO₃ to the samples, which were then capped and put on the hotplate until analysis.

Thirty 10mL centrifuge tubes were rinsed three times with MQ H₂O, soaked in dilute ss HNO₃ for three weeks and rinsed three more times in MQ H₂O. These were then weighed using the high precision balance so that the mass of samples transferred to the centrifuge tube could be determined. Each sample solution was transferred to centrifuge tubes, weighed and centrifuged at 2000 rpm for 5 min. These were inspected for sedimentation to ensure all material had been digested. 60 μ L of each sample was transferred into another centrifuge tube and diluted with 6 mL 1% HNO₃ and reweighed. Sample weights recorded at each of these steps were used to precisely calculate the dilution factors.

3.2.1.2 Mass Spectrometry

Trace element concentrations of glass were analysed using the Agilent 7500CS ICP-MS at VUW, Wellington, New Zealand. Each analysis comprised 90 s of background measurement

whilst aspirating 1% ss HNO₃, a total count time of 180 s and then 180 s of washout involving 30 s of MQ H₂O and 150 s of 1% HNO₃. Analyses were bracketed by the primary standard (BHVO-2) and regular analyses of the secondary standard (BCR-2). ICP-MS tuning was carried out on a Agilent 1 ppb tuning solution which contains Li, Co, Y, Ce and Tl to maximise signal stability resulting in RSD values of < 4% for all monitored elements and oxide interferences as determined by CeO⁺/Ce⁺ of < 1.5%. This tuning resulted in RSD values of < 4% for all monitored elements when running BHVO-2. Analysis conditions are shown in Table 3.4.

CaO values from the ICP-MS analysis were compared with CaO values obtained from EMPA analysis as an internal calibration to correct for instrument drift and sample loss. After background counts were subtracted, the trace element concentrations were calculated by:

$$C_{sample}^{CaO,ICP-MS} = C_{std}^{CaO} \times \left(\frac{CPS_{sample}^{Ca}}{CPS_{std}^{Ca}} \right) \quad \text{EQ 3.1}$$

$$C_{sample}^{x,ICP-MS} = C_{std}^x \times \left(\frac{C_{sample}^{CaO,EMPA}}{C_{sample}^{CaO,ICP-MS}} \right) \times \left(\frac{CPS_{sample}^x}{CPS_{std}^x} \right) \quad \text{EQ 3.2}$$

$C_{sample}^{CaO,ICP-MS}$ $C_{sample}^{CaO,EMPA}$ = concentration of Ca determined by ICP-MS or EMPA

C_{std}^{CaO} = reference CaO concentration of the primary standard BHVO-2

CPS_{sample}^{Ca} , CPS_{std}^{Ca} = counts per second obtained on ⁴³Ca during the analysis of the dilution of the sample or standard

$C_{sample}^{x,ICP-MS}$ = concentration of element x determined by ICP-MS

C_{std}^x = reference concentration of element x in the standard BHVO-2 from the Georem database (<http://georem.mpch-mainz.gwdg.de/>)

CPS_{sample}^x , CPS_{std}^x = counts per second obtained on an isotope of element x in the dilution of the sample or standard

Table 3.4 ICP-MS instrumental and analysis conditions

ICP-MS	
ICP-MS system	Agilent 7500CS
Acquisition mode	Peak hopping
Detection mode	Pulse and analogue
Standards and Calibration	
Calibration standard	BHVO-2
Secondary standard	BCR-2
Internal standard	⁴³ Ca
Method	
Background acquisition	90 s
Sample/standard acquisition	180 s
Washout time	180 s
Measured isotopes and integration times	10 ms: ⁷ Li, ⁴³ Ca, ⁴⁵ Sc, ⁵¹ V, ⁵³ Cr, ⁵⁹ Co, ⁶⁰ Ni, ⁶³ Cu, ⁶⁶ Zn, ⁷¹ Ga, ⁸⁵ Rb, ⁸⁶ Sr, ⁸⁹ Y, ⁹⁰ Zr, ⁹¹ Zr, ⁹³ Nb, ⁹⁵ Mo, ¹³³ Cs, ¹³⁷ Ba, ¹³⁹ La, ¹⁴⁰ Ce, ¹⁴¹ Pr, ¹⁴⁶ Nd, ¹⁴⁷ Sm, ¹⁵¹ Eu, ¹⁵³ Eu, ¹⁵⁷ Gd, ¹⁵⁹ Tb, ¹⁶³ Dy, ¹⁶⁵ Ho, ¹⁶⁶ Er, ¹⁶⁹ Tm, ¹⁷² Yb, ¹⁷⁵ Lu, ¹⁷⁸ Hf, ¹⁸¹ Ta, ¹⁸² W, ²⁰⁸ Pb, ²³² Th, ²³⁸ U
Tuning	
Tuning standard	Agilent 1 ppb solution (Li, Co, Y, Ce, Tl)
Monitored isotopes during tuning	⁷ Li, ⁵⁹ Co, ⁸⁹ Y, ¹⁴⁰ Ce, ²⁰⁵ Tl (RSD < 4% for each isotope)
Calibration standard	BHVO-2
Monitored isotopes during tuning	⁷ Li, ²⁵ Mg, ⁴³ Ca, ⁴⁷ Ti, ⁵¹ V, ⁵³ Cr, ⁶⁰ Ni, ⁸⁶ Sr, ⁹⁰ Zr, ¹³⁷ Ba, ¹⁴⁰ Ce, ²⁰⁸ Pb
Background	⁴³ Ca typically < 5000 cps always < 7000 cps (ca. < 1% BHVO-2 signal, < 10% sample signal)
Oxides	CeO ⁺ /Ce ⁺ : 1 ppb solution < 1.5%
Carrier gas (Ar)	1.11 L/min
Makeup gas (Ar)	0 L/min
RF power	1500 W
RF matching	1.74 V
Sample depth (z)	7 mm

The precision and accuracy of glass trace element analyses were determined by twice analysing BCR-2 as a secondary standard during the analyses (Table 3.5). Most elements have a precision < 5% except Cr, Zn, Sr (< 10%) and Cu (22%). The BCR-2 analyses have an accuracy of < 10% for most elements except Mo, Pb and U (< 20%) and Cr, Cu (< 30%). The reproducibility of the analyses were assessed by running duplicates of three of the six samples, which also show that most elements reproducible to $\pm 5\%$ (exceptions to this are ⁴⁵Sc, ⁶⁶Zn, ²⁰⁸Pb, ²³²Th; Table 3.6).

Table 3.5 Precision and accuracy of ICP-MS trace element data

CaO=7.12	average BCR-2 a	average BCR-2 b	Mean	recommended values ¹	2 SD	%2 SD ² (precision)	% difference ³ (accuracy)
TiO₂ (wt%)	2.16	2.17	2.17	2.26	0.02	0.70	-4.04
MgO	3.50	3.55	3.52	3.59	0.07	2.06	-1.91
CaO	7.12	7.12	7.12	7.12	0.00	0.00	0.00
ppm							
Li	9.64	9.71	9.67	9	0.09	0.94	7.48
Sc	31.8	32.7	32.3	33	1.25	3.88	-2.27
V	398	399	398	416	1.30	0.33	-4.24
Cr	12.6	13.2	12.9	18	0.78	6.05	-28.29
Co	35.7	35.9	35.8	37	0.29	0.82	-3.20
Ni	4.05	8.44	6.25	18	6.21	99.43	-65.29
Cu	13.6	15.9	14.7	21	3.27	22.17	-29.86
Zn	124	131	127	127	10.24	8.05	0.15
Ga	21.5	22.1	21.8	23	0.90	4.13	-5.15
Rb	45.8	46.5	46.2	46.9	1.06	2.29	-1.55
Sr	326	340	333	340	19.58	5.87	-1.97
Y	35.0	35.6	35.3	37	0.91	2.57	-4.67
⁹⁰Zr	175	179	177	184	5.31	3.00	-3.82
⁹¹Zr	174	178	176	184	6.00	3.41	-4.31
Nb	11.6	11.9	11.8	12.6	0.39	3.34	-6.52
Mo	282	287	285	250	7.25	2.55	13.91
Cs	1.15	1.14	1.14	1.1	0.00	0.16	4.05
Ba	668	684	676	677	22.78	3.37	-0.17
La	24.5	24.9	24.7	24.9	0.57	2.33	-0.71
Ce	50.5	51.1	50.8	52.9	0.90	1.76	-4.02
Pr	6.71	6.78	6.74	6.7	0.09	1.34	0.67
Nd	28.5	28.8	28.6	28.7	0.42	1.47	-0.31
Sm	6.50	6.47	6.49	6.58	0.03	0.50	-1.43
¹⁵¹Eu	2.00	1.99	2.00	1.96	0.00	0.08	1.81
¹⁵³Eu	2.06	2.06	2.06	1.96	0.00	0.24	5.18
Gd	6.85	6.78	6.82	6.75	0.10	1.40	1.00
Tb	1.03	1.03	1.03	1.07	0.01	0.70	-3.90
Dy	6.36	6.35	6.35	6.41	0.02	0.31	-0.86
Ho	1.28	1.28	1.28	1.28	0.01	0.39	0.24
Er	3.61	3.58	3.60	3.66	0.05	1.26	-1.71
Tm	0.506	0.518	0.512	0.54	0.02	3.28	-5.17
Yb	3.30	3.31	3.31	3.38	0.02	0.55	-2.17
Lu	0.480	0.486	0.483	0.503	0.01	1.64	-3.98
Hf	4.56	4.55	4.55	4.9	0.02	0.47	-7.06
Ta	0.739	0.746	0.742	0.74	0.01	1.33	0.32
W	0.330	0.326	0.328	-	0.01	1.66	-
Pb	12.9	13.2	13.1	11	0.44	3.38	18.89
Th	5.64	5.47	5.55	5.7	0.23	4.13	-2.55
U	1.48	1.51	1.49	1.69	0.04	2.95	-11.58

¹Recommended values: Georem preferred values²% 2 sd = (2 sd/mean) x 100³% difference = ((mean-recommended)/recommended) x 100

Table 3.6 Reproducibility of duplicate sample analyses

wt%	6a-1	6a-2	% difference ¹	6c-1	6c-2	% difference ¹	7r-1	7r-2	% difference ¹
	6a			6c			7r		
TiO ₂	0.392	0.405	-3.3	0.900	0.882	2.0	0.219	0.215	2.1
MgO	0.852	0.896	-4.9	1.743	1.700	2.6	0.263	0.260	0.9
CaO	2.72	2.72	0.0	5.09	5.09	0.0	1.41	1.41	0.0
ppm									
Li	29.9	30.0	-0.4	30.4	29.7	2.1	21.0	20.2	4.1
Sc	3.10	3.46	-10.3	9.72	9.19	5.7	0.981	1.13	-13.3
V	55.4	56.9	-2.6	129	127	2.0	12.3	12.2	0.2
Cr	BDL ¹	BDL ¹	-	BDL ¹	BDL ¹	-	BDL ¹	BDL ¹	-
Co	5.01	5.17	-3.1	10.6	10.3	2.4	1.11	1.12	-0.4
Ni	BDL ¹	BDL ¹	-	BDL ¹	BDL ¹	-	BDL ¹	BDL ¹	-
Cu	77.7	74.4	4.4	150	145	3.1	14.1	15.5	-8.6
Zn	56.1	45.9	22.2	78.9	82.1	-3.9	27.1	28.8	-5.9
Ga	17.1	17.4	-1.9	27.0	26.3	2.5	11.6	11.3	2.7
Rb	107	108	-1.1	103	100	2.1	69.8	64.0	9.0
Sr	320	327	-1.9	537	526	2.2	176	176	-0.2
Y	14.3	14.9	-3.5	27.3	26.3	3.7	12.3	12.0	2.4
⁹⁰ Zr	187	191	-1.9	259	251	3.4	154	152	1.6
⁹¹ Zr	187	195	-4.1	259	252	3.1	157	154	2.3
Nb	6.16	6.24	-1.3	10.1	9.81	2.7	4.84	4.77	1.5
Mo	2.34	2.45	-4.3	2.86	2.89	-1.0	1.82	1.77	3.0
Cs	6.69	6.59	1.5	6.41	6.35	0.9	4.49	4.40	2.2
Ba	1162	1180	-1.5	1296	1279	1.3	760	743	2.3
La	21.6	21.6	0.0	26.1	25.7	1.6	14.6	14.3	1.8
Ce	40.5	41.0	-1.1	55.7	54.5	2.2	29.3	28.8	1.6
Pr	4.56	4.55	0.2	6.91	6.71	3.0	3.33	3.30	0.7
Nd	16.6	16.7	-0.8	28.2	27.1	3.9	12.6	12.4	1.4
Sm	3.05	3.04	0.4	5.97	5.83	2.4	2.37	2.36	0.7
¹⁵¹ Eu	0.877	0.869	0.9	1.652	1.607	2.8	0.622	0.624	-0.3
¹⁵³ Eu	1.00	0.976	2.8	1.76	1.74	1.0	0.701	0.688	1.9
Gd	2.88	2.91	-1.2	5.70	5.74	-0.6	2.19	2.20	-0.3
Tb	0.395	0.393	0.5	0.811	0.808	0.3	0.314	0.319	-1.5
Dy	2.36	2.34	1.0	4.79	4.85	-1.3	1.91	1.95	-2.0
Ho	0.484	0.484	0.1	0.962	0.983	-2.2	0.397	0.405	-2.0
Er	1.52	1.46	4.5	2.82	2.89	-2.3	1.22	1.23	-0.9
Tm	0.232	0.234	-0.8	0.404	0.424	-4.6	0.192	0.194	-1.1
Yb	1.65	1.59	3.8	2.82	2.87	-1.6	1.43	1.43	-0.2
Lu	0.257	0.249	3.1	0.427	0.431	-0.7	0.222	0.224	-1.1
Hf	4.69	4.60	2.0	6.78	6.78	0.1	3.81	3.89	-2.0
Ta	0.434	0.429	1.2	0.647	0.659	-1.8	0.327	0.332	-1.4
W	1.10	1.09	1.3	1.22	1.25	-1.9	0.650	0.661	-1.6
Pb	33.5	30.4	10.0	40.3	41.9	-3.8	23.2	23.7	-2.5
Th	11.8	10.8	9.4	13.1	13.7	-4.5	7.98	8.26	-3.4
U	2.99	2.90	2.9	3.04	3.13	-2.7	2.01	2.04	-1.1

¹% difference = ((sample 1-sample 2)/sample 2) x 100

²BDL= below detection limit

3.2.2 LASER ABLATION ICP-MS MINERAL TRACE ELEMENT ANALYSIS

In situ trace element analyses of plagioclase, clinopyroxene and amphibole crystals were carried out at VUW using a New Wave deep ultraviolet (193 nm) solid state laser ablation system coupled to an Agilent 7500CS ICP-MS. The circular mounts were halved using a slow diamond saw and the carbon coat necessary for EPMA analysis was removed from each epoxy block using AR grade methanol. The mounts were rinsed in MQ H₂O and dried overnight at 40° C in an oven.

Individual spots ranging in diameter from 20 to 35 µm were analysed. Each analysis was preceded by 60 s of background acquisition and had a dwell time of 60 s, followed by 20-30 s of washout time. Helium was used as the ablation gas. Tuning was carried out on BCR-2G where gas flow and torch conditions were optimised to obtain RSD values of < 10% for monitored elements (Li, Ca, Y, La, Ce, Pb) in most cases and a ThO⁺/Th⁺ ratio of < 1.5% to minimise oxide interferences. Pulse/analogue (P/A) factors were measured daily prior to analysis for elements that may be present in sufficient concentrations (> 1 000 000 cps) that analysis mode would switch from pulse to analogue. Details of analytical conditions are given in Table 3.7.

Primary standards were measured after every 5-10 sample spot analyses to monitor drift in machine conditions and immediately after changing samples. The primary standards used were those which best matched the composition of the mineral being analysed to minimise matrix effects. BCR-2G was used as a standard for clinopyroxene and amphibole analyses and NIST612 was used for plagioclase. Internal standardisation was carried out using a minor isotope (⁴³Ca) of an element measured previously by EMPA as this corrects for machine drift and the specific analytical conditions for that day. All data have been individually screened to ensure that data associated with inclusions were excluded and only the phase of interest was assessed. After background corrections the concentration of each element at each point is determined by the relationships:

$$C_{sample}^{CaO, ICP-MS} = C_{std}^{CaO} \times \left(\frac{CPS_{sample}^{Ca}}{CPS_{std}^{Ca}} \right)$$

$$C_{sample}^{x, ICP-MS} = C_{std}^x \times \left(\frac{C_{sample}^{CaO, EMPA}}{C_{sample}^{CaO, ICP-MS}} \right) \times \left(\frac{CPS_{sample}^x}{CPS_{std}^x} \right)$$

$C_{sample}^{CaO, ICP-MS}$ $C_{sample}^{CaO, EMPA}$ = concentration of Ca determined by LA-ICP-MS or EMPA

C_{std}^{CaO} = reference CaO concentration of the primary standard (BCR-2 or NIST 612)

CPS_{sample}^{Ca} , CPS_{std}^{Ca} = counts per second obtained on ^{43}Ca whilst ablating the sample or standard

$C_{sample}^{x, ICP-MS}$ = concentration of element x determined by LA-ICP-MS

C_{std}^x = reference concentration of element x in the standard (BCR-2 or NIST 612)

CPS_{sample}^x , CPS_{std}^x = counts per second obtained on an isotope of element x whilst ablating the sample or standard

BHVO-2G was run as a secondary standard for the clinopyroxene and amphibole analyses (Table 3.8). The precision of these analyses is typically < 15 % for those elements with atomic weights < 166 and 15-30% for heavier elements. B and Cs were less reproducible, with %2 SD values of 60 and 51 respectively. Most elements are within ± 15 % of the reference values except for Ni (18 %), Pb and Cr (21-22 %) and Cu (32 %) probably due to poorly constrained reference values or a low abundance in the standard (Pb). No secondary standards were analysed for the plagioclase method. However, a detailed study was undertaken at VUW by Allan et al. (2008) which quantified the precision and accuracy of the LA-ICP-MS method used here, finding that the mean (n = 91) abundances of 29 elements analysed in the rhyolitic glass standard ATHO-G were within ca. $\pm 5\%$ of the certified values from Jochum et al. (2006). Cs was ca. 15-20% lower than reference values and Mg higher by ca. 15%

Table 3.7 LA-ICP-MS instrumental and analytical conditions for in situ clinopyroxene, amphibole and plagioclase trace element analyses

	Clinopyroxene and amphibole	Plagioclase
LA-ICP-MS		
Laser ablation system	New Wave 193 nm (deep UV) solid state	New Wave 193 nm (deep UV) solid state
Ablation mode	Static spot analyses	Static spot analyses
Spot size	20, 25 or 35 μm	20, 25 or 35 μm
Repetition rate	5 Hz	5 Hz
Laser power	65%	65%
ICP-MS		
ICP-MS system	Agilent 7500CS octopole	Agilent 7500CS octopole
Acquisition mode	Peak hopping	Peak hopping
Detection mode	Pulse and analogue	Pulse and analogue
Standards and Calibration		
Calibration standard	BCR-2G	NIST612
Secondary standard	BHVO-2G	-
Internal standard	^{43}Ca	^{43}Ca
Method		
Background acquisition	60 s	60 s
Sample/standard acquisition	60 s	60 s
Washout time	15-30 s	25-30 s
Measured isotopes and integration times	10 ms: ^7Li , ^{11}B , ^{24}Mg , ^{29}Si , ^{43}Ca , ^{45}Sc , ^{47}Ti , ^{51}V , ^{53}Cr , ^{55}Mn , ^{60}Ni , ^{63}Cu , ^{66}Zn , ^{85}Rb , ^{88}Sr , ^{89}Y , ^{90}Zr , ^{93}Nb , ^{133}Cs , ^{137}Ba , ^{139}La , ^{140}Ce , ^{141}Pr , ^{146}Nd , ^{147}Sm , ^{153}Eu , ^{157}Gd , ^{159}Tb , ^{163}Dy , ^{165}Ho , ^{166}Er , ^{169}Tm , ^{172}Yb , ^{175}Lu , ^{178}Hf , ^{181}Ta , ^{208}Pb , ^{232}Th , ^{238}U	10 ms: ^{29}Si , ^{43}Ca , ^{88}Sr , ^{137}Ba , ^{138}Ba 20 ms: ^7Li , ^{24}Mg , ^{25}Mg , ^{139}La , ^{140}Ce 50 ms: ^{85}Rb , ^{89}Y , ^{133}Cs , ^{141}Pr , ^{146}Nd , ^{147}Sm , ^{153}Eu , ^{157}Gd , ^{208}Pb
Tuning		
Tuning standard	BCR-2G	NIST612
Ablation mode	Rastering $2\mu\text{m/s}$ beneath a 35 or 50 μm spot	Rastering $2\mu\text{m/s}$ beneath a 50 μm spot
Monitored isotopes during tuning	^7Li , ^{43}Ca , ^{89}Y , ^{138}Ba , ^{140}Ce , ^{208}Pb (RSD for each isotope typically <10%)	^7Li , ^{24}Mg , ^{25}Mg , ^{29}Si , ^{43}Ca , ^{85}Rb , ^{88}Sr , ^{89}Y , ^{137}Ba , ^{138}Ba , ^{208}Pb (RSD for each isotope typically <10%)
Background	^{43}Ca typically <200 cps, always <400 cps (ca. 1% of BCR-2G and sample signal)	^{43}Ca typically <200 cps, always <400 cps (ca. 1% of NIST612 and 10% sample signal)
Oxides	$\text{ThO}^+/\text{Th}^+ < 1\%$	$\text{ThO}^+/\text{Th}^+ < 1\%$
Carrier gas (Ar)	0.85-0.9 L/min	0.85-0.89 L/min
Ablation gas (He)	80-90.5%	80-89%
RF power	1500 W	1500 W
RF matching	1.69-1.78 V	1.76 V
Sample depth (z)	3.5-4 mm	3.5 mm

Table 3.8 Precision and accuracy of LA-ICP-MS trace element data based on repeated analyses of BHVO-2G

	A	B	C	D	E	F	G	H	I	J	Mean	Recommended ¹ values	2 SD	% 2 SD ² (precision)	% difference ³ (accuracy)
CaO=11.4															
SiO ₂ (wt%)	51.9	51.9	51.4	51.5	51.4	51.0	52.8	51.7	50.6	52.1	51.6	49.3	1.2	2.4	4.7
TiO ₂	2.75	2.77	2.80	2.77	2.84	2.74	2.85	2.73	2.60	2.75	2.76	2.79	0.1	5.0	-1.1
MnO	0.178	0.182	0.178	0.172	0.170	0.175	0.183	0.174	0.176	0.175	0.176	0.17	0.0	4.7	3.7
MgO	7.45	7.32	7.49	7.37	7.51	7.32	7.78	7.54	7.41	7.52	7.47	7.13	0.3	3.6	4.8
Li (ppm)	4.61	4.91	4.96	4.28	4.77	4.39	4.63	4.72	4.53	4.76	4.66	4.4	0.4	9.3	5.8
B	4.87	5.57	7.86	5.58	2.24	5.55	3.52	5.38	3.71	4.25	4.85	-	3.1	63.1	-
Sc	29.6	30.2	30.9	29.4	31.1	30.0	30.4	29.4	28.9	29.7	30.0	33	1.4	4.6	-9.2
V	335	343	330	340	349	329	353	336	343	343	340	308	15.6	4.6	10.4
Cr	388	382	370	357	376	313	345	343	349	326	355	293	49.2	13.8	21.1
Ni	133	133	137	136	140	136	156	127	128	141	137	116	16.1	11.8	17.9
Cu	168	170	166	165	161	170	176	156	181	169	168	127	14.1	8.4	32.3
Zn	107	110	114	106	114	104	119	100	105	104	108	102	11.7	10.9	6.1
Rb	9.73	10.5	9.73	9.70	10.7	10.2	11.4	9.27	10.1	10.4	10.2	9.2	1.2	12.0	10.6
Sr	436	446	440	413	451	430	458	416	452	428	437	396	30.2	6.9	10.4
Y	24.9	25.9	25.6	24.3	26.5	25.7	27.1	24.0	27.4	24.7	25.6	26	2.3	8.9	-1.5
Zr	173	180	173	166	178	164	187	161	177	172	173	170	16.0	9.3	1.8
Nb	19.9	20.7	19.3	19.3	21.0	20.3	22.0	19.9	19.9	20.5	20.3	18.3	1.7	8.2	10.9
Cs	0.057	0.126	0.079	0.119	0.078	0.133	0.125	0.098	0.072	0.092	0.098	0.1	0.1	53.8	-2.1
Ba	146	143	134	132	134	142	147	140	137	136	139	131	10.4	7.5	6.2
La	16.5	15.7	15.0	14.8	15.2	15.2	17.0	14.4	15.5	15.1	15.4	15.2	1.6	10.2	1.5
Ce	41.1	40.6	37.5	39.6	41.2	38.9	44.0	38.3	39.6	39.2	40.0	37.6	3.7	9.2	6.4
Pr	5.88	5.52	4.94	5.42	5.35	5.57	5.75	5.27	5.32	5.59	5.46	5.35	0.5	9.8	2.1
Nd	24.8	25.9	24.2	25.5	27.5	25.8	28.1	24.9	25.6	26.1	25.8	24.5	2.4	9.2	5.5
Sm	6.58	6.11	6.22	5.99	6.71	7.00	6.43	5.87	6.48	5.92	6.33	6.1	0.7	11.7	3.8
Eu	2.31	2.19	2.04	2.24	1.92	2.45	2.44	2.26	2.04	2.21	2.21	2.07	0.3	15.6	6.8
Gd	6.66	6.48	6.09	6.70	5.96	6.39	6.23	6.18	5.76	6.92	6.34	6.16	0.7	11.4	2.9
Tb	0.923	0.899	0.855	0.933	0.993	1.007	0.839	0.849	0.802	0.948	0.905	0.92	0.1	15.0	-1.7
Dy	5.40	5.64	5.16	5.71	5.36	5.90	6.48	5.38	5.47	5.68	5.62	5.28	0.7	13.3	6.4
Ho	1.050	0.859	0.915	1.011	0.909	0.889	0.926	0.999	0.875	0.877	0.931	0.98	0.1	14.2	-5.0
Er	2.57	2.46	2.50	2.37	2.00	2.98	3.03	2.75	2.60	2.83	2.61	2.56	0.6	23.6	1.9
Tm	0.460	0.381	0.341	0.347	0.336	0.289	0.339	0.348	0.372	0.471	0.368	0.34	0.1	30.8	8.4
Yb	2.18	1.97	2.16	2.09	1.86	2.71	2.11	2.16	2.16	1.93	2.13	2.01	0.5	21.7	6.1
Lu	0.293	0.293	0.305	0.238	0.318	0.264	0.233	0.265	0.294	0.267	0.277	0.279	0.1	20.3	-0.7
Hf	4.67	4.01	4.34	3.96	4.39	4.39	3.80	4.58	3.61	4.14	4.19	4.32	0.7	16.4	-3.0
Ta	1.12	1.28	1.12	1.12	1.19	1.32	1.45	1.34	1.38	1.29	1.26	1.15	0.2	18.8	9.6
Pb	2.37	2.26	2.02	1.89	1.91	1.96	2.05	2.41	2.00	1.84	2.07	1.7	0.4	19.6	21.8
Th	1.02	1.19	1.22	1.11	1.16	1.26	1.33	1.20	1.13	1.12	1.17	1.22	0.2	15.0	-3.7
U	0.499	0.391	0.386	0.404	0.422	0.434	0.523	0.416	0.463	0.432	0.437	0.403	0.1	20.7	8.4

¹Recommended values: Geotem preferred values

²% 2 sd = (2 sd/mean) x 100

³% difference = ((mean-recommended)/recommended) x 100

3.3 THERMOBAROMETRY

Estimating the physical conditions of a magmatic system can provide important insights into the behaviour and state of these systems during their evolution and immediately prior to eruption. Accurate thermometry is particularly important in this study due to the strong temperature dependence of the diffusion modelling applied in this study. Thermometry was carried out using phenocryst rims and coexisting glass to constrain the pre-eruptive magmatic conditions. In addition, amphibole barometry, hygrometry and oxybarometry were utilised. The models presented here use phases that are present in all of the samples analysed and were calibrated for silicic, hydrous, volcanic systems. Each model is discussed and evaluated for applicability to this volcanic system. The multiple thermometers are compared as tools for determining whether the different mineral phases all shared a similar history immediately prior to eruption.

3.3.1 AMPHIBOLE THERMOBAROMETRY

3.3.1.1 Model

The amphibole thermobarometry of Ridolfi et al. (2010) provides a means of calculating the magma temperature, pressure, water content and oxygen fugacity from amphibole major element analysis. This thermobarometric system is based on the narrow physico-chemical range that amphibole in equilibrium with calc-alkaline melts crystallises. This provides a low variance system that enables the formulation of many pre-eruptive conditions of magmatic systems based on a single phase (amphibole). This model was calibrated using empirical data for calcic amphiboles of basaltic to rhyolitic magmas, specifically for subduction-related magmatism. Amphiboles must have a composition where aluminium number ($Al\# = [^6]Al/Al_T \leq 0.21$) and magnesium number ($Mg\# = Mg/Mg+Fe^{2+} > 0.5$). However, this model does not require the amphibole to be in equilibrium with coexisting melt or mineral phases as only the composition of the amphibole is used for the model. For this reason, it is especially useful for hybrid melts such as andesites.

For this study, all amphibole analyses that fitted the model requirements stated above were put through the amphibole thermobarometric model. These were divided into rims, cores and other zoning (any zones within the mantle of the crystal), with the rim and core analyses further investigated to determine whether there were multiple populations. In the case of rim analyses, there was one dominant, low pressure population that was considered to be in equilibrium with the melt. This was compared to temperatures modelled from the rims of other phenocryst phases. In samples SM-7P and SM-7R, two core populations (C1 and C2) were identified based on pressure and temperature.

3.3.1.2 Method

The amphibole thermometer is based on the silicon index (Si*) by the formula:

$$T = -151.487Si^* + 2041 \pm 22 \text{ } ^\circ\text{C} \quad \text{EQ 3.3}$$

$$\text{Where } Si^* = Si + \frac{[4]Al}{15} - 2[4]Ti - \frac{[6]Al}{2} - \frac{[6]Ti}{1.8} + \frac{Fe^{3+}}{9} + \frac{Fe^{2+}}{3.3} + \frac{Mg}{26} + \frac{B_{Ca}}{5} + \frac{B_{Na}}{1.3} - \frac{A_{Na}}{15} + \frac{A_{[]}}{2.3}$$

^[4]Al=tetrahedral Al; ^[4]Ti= tetrahedral Ti; ^[6]Al=octahedral Al; ^[6]Ti=octahedral Ti; ^BCa=Ca in the B site; ^BNa=Na in the B site; ^ANa=Na in the A site; ^A[]=any other cations in the A site not yet accounted for. All cations are calculated on the basis of 13 cations using the method of Leake et al. (1997).

The barometric formulation is based on total Al content (Al_T) by the equation:

$$P = 19.209e^{(1.438Al_T)} \pm 39 \text{ MPa} \quad \text{EQ 3.4}$$

Where Al_T = the total Al in amphibole calculated on the basis of 13 cations using the method of Leake et al. (1997).

The standard error of estimate (σ_{est}) is 54 MPa, but decreases to 39 MPa ($\pm 14\%$ average relative error) where pressures (P) are < 450 MPa. The magnitude of the errors associated with the pressure calculations is also related to how close to the amphibole stability curve the

amphibole analyses plot. The amphiboles modelled here all plot near the amphibole stability curve reducing pressure errors further to $< \pm 11\%$ average relative error.

Other amphibole barometers (eg. Hammarstrom & Zen, 1986; Hollister et al., 1987; Johnson & Rutherford, 1989; Schmidt, 1992) were calibrated for a very specific mineral assemblage, including the presence of quartz, making them unsuitable for use in this system.

The water content of the melt (H_2O_{melt}) is strongly correlated with octahedral Al ($^{[6]}Al$) and this relationship is improved upon by using an octahedral aluminium index ($^{[6]}Al^*$) which is related to H_2O_{melt} by the equation:

$$H_2O_{\text{melt}} = 5.215^{[6]}Al^* + 12.28 \pm 0.41 \text{ wt\%} \quad \text{EQ 3.5}$$

$$\text{Where } ^{[6]}Al^* = ^{[6]}Al + \frac{[4]Al}{13.9} - \frac{Si + [6]Ti}{5} - \frac{CFe^{2+}}{3} - \frac{Mg}{1.7} + \frac{B_{Ca+A[]}}{1.2} + \frac{ANa}{2.7} - 1.56K - \frac{Fe\#}{1.6}$$

$^{[6]}Al$ =octahedral Al; $^{[4]}Al$ =tetrahedral Al; $^{[6]}Ti$ =octahedral Ti; CFe^{2+} = Fe^{2+} in the C site; B_{Ca} =Ca in B site; $A[]$ = any cations in the A site not already accounted for; ANa =Na in the A site; $Fe\#$ = $Fe^{3+}/(Fe^{3+}+Mg+Fe^{2+}+Mn)$. All cations were calculated on the basis of 13 cations using the method of Leake et al. (1997).

As magnesiohastingsite was not included in the calibration data, and this is the dominant species at Mt Taranaki, the true errors are likely to be at the upper end of those stated above. This is comparable to the plagioclase-melt hygrometer of Lange et al. (2009) and is an improvement on those of Putirka (2005; 2008).

Oxygen fugacity is best correlated to Mg content in amphibole and the use of a Mg index (Mg^*) improves this relationship ($R^2=0.84$ to 0.89) and is described by the equation 2:

$$\Delta NNO = 1.644Mg^* - 4.01 \pm 0.22 \text{ log unit} \quad \text{EQ 3.6}$$

$$\text{Where } Mg^* = Mg + \frac{Si}{47} + \frac{[6]Al}{9} - 1.3^{[6]}Ti + \frac{Fe^{3+}}{3.7} + \frac{Fe^{2+}}{5.2} - \frac{BCa}{20} - \frac{ANa}{2.8} + \frac{A[]}{9.5}$$

Table 3.9 Amphibole analyses used for thermobarometry. Core analyses are divided into two populations (C1 and C2) where there are two distinct groups of amphibole cores.

Analysis	Zone ¹	Temp °C	Pressure MPa	H ₂ O _{melt} wt%	logfO ₂	Analysis	Zone ¹	Temp °C	Pressure MPa	H ₂ O _{melt} wt%	logfO ₂
<u>SM-6A</u>						<u>SM-6C</u>					
6aA10_3	C	961	286	3.73	-9.87	6cA5_5	C	1035	684	6.84	-9.67
6aA7_1	C	966	318	4.19	-9.92	6cA9_4	C	1012	539	6.71	-9.71
6aA1_4	C	1011	447	5.99	-9.05	6cA4_7	C	1011	514	5.61	-9.19
6aA11_4	C	1011	530	5.90	-8.97	6cA6_3	C	1008	505	5.68	-9.23
6aA3_3	C	1009	487	5.37	-8.90	6cA7_6	C	1021	571	6.14	-9.18
6aA7_4	C	948	295	3.66	-10.64	6cA8_2	C	1008	502	5.69	-9.11
6aA9_6	C	978	386	4.95	-10.13	6cA5_2	R*	1028	631	6.78	-9.55
6aA5_3	C	971	389	5.12	-10.15	6cA9_1	R*	1032	646	6.97	-9.54
6aA11_5	C	992	411	4.71	-9.68	6cA6_1	R	1002	469	5.45	-9.24
6aA3_5	C	1011	527	5.59	-9.24	6cA7_1	R	1010	501	5.60	-9.17
6aA1_1	R	928	262	4.12	-10.35	6cA8_1	R	1006	522	5.83	-9.23
6aA10_1	R	976	330	4.12	-9.78	6cA4_2	Z	1016	530	5.66	-9.08
6aA11_1	R	975	356	4.60	-9.81	6cA4_3	Z	1017	539	5.73	-9.00
6aA3_1	R	970	329	4.18	-9.72	6cA4_4	Z	988	394	4.93	-9.20
6aA4_2	R	953	335	4.66	-10.32	6cA4_5	Z	1010	510	5.62	-9.22
6aA5_1	R*	974	405	5.53	-10.28	6cA6_2	Z	1004	456	5.36	-9.11
6aA7_2	R*	1008	503	5.54	-9.57	6cA6_4	Z	1006	491	5.69	-9.21
6aA9_3	R*	1012	549	5.63	-9.40	6cA7_2	Z	1002	478	5.48	-9.18
6aA4_7	Z	985	501	6.06	-9.80	6cA7_3	Z	998	453	5.32	-9.09
6aA1_2	Z	983	432	5.65	-9.37	6cA7_4	Z	1012	530	5.81	-9.33
6aA10_2	Z	964	290	3.71	-10.04	6cA7_5	Z	960	303	4.27	-9.85
6aA10_4	Z	973	335	4.47	-9.75	6cA9_2	Z	1032	659	6.89	-9.51
6aA11_2	Z	979	353	4.40	-9.75	6cA9_3	Z	1027	637	6.91	-9.59
6aA11_3	Z	1007	478	5.49	-9.28						
6aA3_2	Z	1002	455	5.25	-9.51						
6aA9_4	Z	962	349	4.05	-10.62						
6aA9_5	Z	998	481	5.43	-9.96						
6aA7_3	Z	980	438	5.04	-10.29						
Mean	C	986	408	4.92	-9.65	Mean	C	1016	552	6.11	-9.35
Mean	R	960	323	4.34	-10.00	Mean	R	1006	498	5.63	-9.21
Mean	Z	983	411	4.96	-9.84	Mean	Z	1006	498	5.64	-9.28
Mean	all	982	402	4.90	-9.79	Mean	all	1011	524	5.87	-9.31

Analysis	Zone ¹	Temp °C	Pressure MPa	H ₂ O _{melt} wt%	logfO ₂	Analysis	Zone ¹	Temp °C	Pressure MPa	H ₂ O _{melt} wt%	logfO ₂
<u>SM-6K</u>						<u>SM-7P</u>					
6kA1_3	C	981	387	5.14	-9.90	7pA2_6	C1	1003	612	7.35	-10.08
6kA10_6	C	996	457	5.57	-9.32	7pA1_5	C1	924	228	3.97	-10.65
6kA12_2	C	994	426	5.37	-9.84	7pA3_5	C1	915	214	3.95	-10.89
6kA13_2	C	935	290	4.04	-11.07	7pA4_2	C1	921	212	3.80	-10.73
6kA14_6	C	1028	589	5.03	-8.75	7pA5_3	C1	914	219	4.20	-10.85
6kA17_2	C	1017	574	6.11	-9.55	7pA7_4	C1	917	218	3.78	-11.02
6kA4_1	C	970	371	5.29	-10.07	7pA8_3	C1	922	215	3.72	-10.70
6kA5_1	C	1001	457	5.17	-8.93	7pA11_3	C1	921	216	3.71	-10.78
6kA6_1	C	938	270	4.18	-10.36	7pA6_2	C2	985	436	6.15	-10.05
6kA7_1	C	985	407	5.30	-9.73	7pA1_6	C2	984	436	5.93	-9.93
6kA9_1	C	1010	567	6.49	-9.69	7pA3_2	C2	987	441	5.95	-10.09
6kA11_1	C	936	250	3.94	-10.35	7pA5_4	C2	986	442	5.81	-10.12
6kA11_2	C	1012	558	6.32	-9.52	7pA7_3	C2	991	469	6.08	-10.30
6kA14_4	R*	1020	580	5.94	-9.29	7pA8_2	C2	1008	542	6.27	-10.00
6kA2_1	R*	1000	492	6.00	-9.52	7pA11_2	C2	979	392	5.46	-10.09
6kA1_1	R	939	299	4.04	-11.01	7pA4_3	C2	969	405	5.96	-10.24
6kA13_1	R	970	329	4.22	-10.10	7pA1_1	R	929	221	3.68	-10.64
6kA17_1	R	967	308	4.04	-9.99	7pA3_1	R	913	207	3.96	-10.88
6kA5_4	R	936	255	4.06	-10.08	7pA4_1	R	927	227	3.99	-10.76
6kA7_2	R	945	262	4.02	-10.11	7pA5_1	R	923	226	3.94	-10.61
6kA11_3	Z	952	281	3.87	-10.38	7pA6_1	R	912	215	3.92	-10.99
6kA11_4	Z	987	416	5.30	-9.96	7pA2_3	R	910	210	4.11	-10.98
6kA11_6	Z	954	303	4.40	-10.28	7pA8_1	R	918	207	3.76	-10.77
6kA14_5	Z	1016	578	5.88	-9.34	7pA11_1	R	919	215	3.93	-10.83
6kA2_2	Z	965	327	4.32	-10.15	7pA1_2	Z	962	343	5.11	-10.48
6kA4_2	Z	998	452	5.57	-9.20	7pA1_3	Z	915	204	3.83	-10.72
6kA4_3	Z	947	274	4.25	-10.12	7pA2_2	Z	978	435	6.38	-10.24
6kA5_2	Z	1008	558	5.91	-8.97	7pA2_5	Z	990	545	7.13	-10.18
6kA5_3	Z	1008	488	5.52	-9.00	7pA7_2	Z	1009	522	6.22	-9.86
6kA6_2	Z	930	243	3.82	-10.58	7pA5_2	Z	928	241	4.37	-10.57
6kA1_2	Z	936	254	4.00	-10.85						
Mean	C	985	431	5.27	-9.78	Mean	C1	930	267	4	-11
Mean	R	951	291	4.07	-10.26	Mean	C2	986	445	6	-10
Mean	Z	973	379	4.80	-9.89	Mean	R	919	216	3.91	-10.81
Mean	all	977	397	4.95	-9.87	Mean	Z	964	382	5.51	-10.34
						Mean	all	949	324	4.88	-10.50

Table 3.9 continued

Analysis SM-7R	Zone ¹	Temp °C	Pressure MPa	H ₂ O _{init} wt%	logfO ₂ ¹ SM-7U	Analysis	Zone ¹	Temp °C	Pressure MPa	H ₂ O _{init} wt%	logfO ₂ ¹ SM-7U	Analysis	Zone ¹	Temp °C	Pressure MPa	H ₂ O _{init} wt%	logfO ₂
7rA13_7	C1	930	246	4.34	-10.62	7uA1_3	C	950	285	4.64	-10.63	7uA16_3	Z	930	242	4.29	-10.87
7rA12_2	C1	914	201	3.70	-10.81	7uA10_2	C	990	499	6.63	-9.87	7uA16_4	Z	964	350	5.00	-10.71
7rA9_2	C1	912	206	3.92	-10.83	7uA11_2	C	988	456	6.23	-9.92	7uA16_5	Z	942	271	4.11	-10.77
7rA14_10	C1	933	266	4.82	-10.56	7uA12_4	C	974	420	6.20	-9.93	7uA16_6	Z	972	318	4.32	-10.20
7rA10_3	C1	962	362	5.93	-10.35	7uA14_5	C	964	379	5.98	-9.97	7uA16_7	Z	1014	583	6.54	-9.71
7rA15_3	C1	929	227	3.84	-10.49	7uA2_4	C	1009	587	6.98	-9.91	7uA16_8	Z	942	253	3.95	-10.65
7rA14_9	C2	1025	706	7.54	-9.58	7uA4_5	C	908	197	3.72	-10.88	7uA16_9	Z	967	325	4.65	-10.54
7rA5_6	C2	1001	543	6.75	-10.33	7uA9_4	C	972	385	5.07	-9.99	7uA3_10	Z	973	359	5.02	-10.43
7rA9_3	C2	1008	575	6.69	-9.71	7uA16_10	C	957	304	4.59	-10.56	7uA3_11	Z	944	267	4.50	-10.52
7rA14_11	C2	1013	586	6.65	-9.83	7uA3_13	C	963	341	5.13	-10.35	7uA3_14	Z	986	397	5.13	-10.18
7rA10_4	C2	981	413	5.95	-10.23	7uA8_11	C	1002	467	5.48	-9.47	7uA3_2	Z	994	497	6.39	-10.30
7rA15_2	C2	1006	509	5.93	-9.79	7uA16_11	C	1019	592	5.96	-9.89	7uA3_3	Z	933	256	4.09	-10.92
7rA7_1	R*	983	406	5.48	-10.11	7uA3_12	C	984	394	5.18	-10.40	7uA3_4	Z	925	235	4.42	-10.92
7rA5_1	R*	1011	580	6.70	-10.23	7uA7_3	C	1004	550	6.54	-9.61	7uA3_5	Z	985	406	5.49	-10.33
7rA6_1	R*	973	375	5.61	-10.66	7uA8_10	C	1018	582	6.17	-9.67	7uA3_6	Z	945	282	4.63	-10.72
7rA13_2	R	922	220	3.85	-10.54	7uA1_1	R	916	245	5.15	-11.25	7uA3_7	Z	949	297	4.52	-10.70
7rA9_1	R	909	200	3.80	-10.78	7uA10_1	R	987	481	6.68	-10.09	7uA3_8	Z	935	261	4.04	-10.89
7rA14_1	R	918	214	4.06	-10.76	7uA12_1	R	927	241	4.06	-10.56	7uA3_9	Z	938	267	4.57	-10.79
7rA12_1	R	930	259	4.50	-10.59	7uA14_1	R	921	221	3.94	-10.55	7uA4_2	Z	970	364	5.47	-10.28
7rA2_3	Z	921	216	3.93	-11.16	7uA15_1	R	903	196	3.73	-10.78	7uA4_4	Z	929	240	4.15	-10.79
7rA13_3	Z	907	211	4.22	-10.85	7uA16_1	R	899	205	3.64	-11.40	7uA7_2	Z	915	213	3.86	-10.70
7rA13_4	Z	946	275	4.38	-10.42	7uA2_1	R	937	253	4.51	-10.67	7uA7_4	Z	917	222	3.89	-10.78
7rA13_5	Z	952	303	4.63	-10.39	7uA3_1	R	938	250	4.24	-10.70	7uA8_2	Z	993	470	6.01	-9.93
7rA13_6	Z	934	278	4.38	-10.83	7uA4_1	R	914	209	3.92	-10.89	7uA8_3	Z	922	208	3.73	-10.70
7rA8_2	Z	924	234	4.09	-10.75	7uA7_1	R	913	207	3.66	-10.60	7uA8_4	Z	923	213	3.84	-10.69
7rA9_4	Z	981	454	6.27	-10.08	7uA8_1	R	925	216	3.77	-10.65	7uA8_5	Z	922	214	3.80	-10.82
7rA14_2	Z	949	299	4.90	-10.54	7uA1_2	Z	978	419	5.99	-10.24	7uA8_6	Z	935	236	3.76	-10.67
7rA14_3	Z	915	214	3.94	-10.82	7uA12_2	Z	951	309	5.10	-10.28	7uA8_7	Z	925	198	3.55	-10.50
7rA14_4	Z	948	299	4.62	-10.60	7uA12_3	Z	998	529	6.67	-9.91	7uA8_8	Z	968	322	4.40	-10.15
7rA14_5	Z	932	242	4.23	-10.72	7uA14_6	Z	983	445	6.32	-9.77	7uA8_9	Z	941	250	3.97	-10.21
7rA14_6	Z	945	285	4.55	-10.47	7uA14_7	Z	960	346	5.68	-9.98	7uA9_2	Z	950	385	6.34	-10.67
7rA14_7	Z	998	491	6.06	-9.86	7uA14_8	Z	978	417	6.08	-9.94	7uA9_3	Z	933	239	3.99	-10.49
7rA14_8	Z	1005	529	6.41	-9.67	7uA15_2	Z	924	230	4.23	-10.55	7uA4_3	Z	918	226	4.46	-10.72
7rA14_12	Z	1002	495	5.88	-9.96	7uA16_12	Z	944	272	3.99	-10.65						
7rA10_2	Z	956	331	5.19	-10.44	7uA16_2	Z	981	421	5.79	-10.41						
Mean	C1	930	251	4.42	-10.61		C	980	429	5.63			C	980	429	5.63	-10.07
Mean	C2	1006	555	6.58	-9.91		R	926	248	4.30			R	926	248	4.30	-10.74
Mean	Z	951	322	4.86	-10.47		Z	952	316	4.78			Z	952	316	4.78	-10.48
Mean	all	956	350	5.08	-10.41		all	954	330	4.89			all	954	330	4.89	-10.43

*=not included in rim average as part of 'true' rim composition

¹ C=core analyses, C1= population 1 core analyses, C2=population 2 core analyses, R= rim analyses, Z=zoning that is neither cores nor rims, R* refers to rim analyses that were not included in the rim mean calculations as they do not represent the main rim population that is thought to be in equilibrium with the final melt composition

⁶Al=octahedral Al; ⁶Ti=octahedral Ti; ^BCa= Ca in the B site; ^ANa=Na in the A site; ^A[]=any cations in the A site not accounted for. All cations were calculated on the basis of 13 cations using the method of Leake et al. (1997).

The absence of ilmenite in the Taranaki samples precludes the use of ilmenite-magnetite oxybarometry, making the amphibole thermobarometer the only suitable quantification of oxygen fugacity conditions.

3.3.2 CLINOPYROXENE-MELT THERMOMETRY

3.3.2.1 Model

Clinopyroxene-melt thermometry was carried out using the jadeite (Jd; NaAlSi₂O₆)-diopside/hedenbergite (DiHd; Ca(Mg,Fe)Si₂O₆) exchange thermometer of Putirka (2008).

$$T(K) = 7.53 - 0.14 \ln \left(\frac{X_{Jd}^{cpx} X_{CaO}^{liq} X_{Fm}^{liq}}{X_{DiHd}^{cpx} X_{Na}^{liq} X_{Al}^{liq}} \right) + 0.07 (H_2O^{liq}) - 14.9 (X_{CaO}^{liq} X_{SiO_2}^{liq}) - 0.08 \ln (X_{TiO_2}^{liq}) - 3.62 (X_{NaO_{0.5}}^{liq} + X_{KO_{0.5}}^{liq}) - 1.1 (Mg\#^{liq}) - 0.18 \ln (X_{EnFs}^{cpx}) - 0.027P(kbar) \pm 42 \text{ } ^\circ\text{C} \quad \text{EQ 3.7}$$

$$P(kbar) = -48.7 + 271 \frac{T(K)}{10^4} + 32 \frac{T(K)}{10^4} \ln \left[\frac{X_{NaAlSi_2O_6}^{cpx}}{X_{NaO_{0.5}}^{liq} X_{AlO_{1.5}}^{liq} (X_{SiO_2}^{liq}) X_{NaO_{0.5}}^{liq} X_{AlO_{1.5}}^{liq} (X_{SiO_2}^{liq})^2} \right] - 8.2 \ln (X_{FeO}^{liq}) + 4.6 \ln (X_{MgO}^{liq}) - 0.96 \ln (X_{KO_{0.5}}^{liq}) - 2.2 \ln (X_{DiHd}^{cpx}) - 31 (Mg\#^{liq}) + 56 (X_{NaO_{0.5}}^{liq} + X_{KO_{0.5}}^{liq}) + 0.76 (H_2O^{liq}) \pm 3.6 \text{ kbar} \quad \text{EQ 3.8}$$

Where $X_{component}^{liq}$ = the liquid component calculated as cation fractions on an anhydrous basis, not renormalized to 100; $X_{component}^{cpx}$ = the clinopyroxene component calculated as cations per formula unit on an anhydrous basis not renormalized to 100.

$$X_{Jd}^{cpx} = X_{Al(VI)}^{cpx} \text{ or } X_{Na}^{cpx} \text{ whichever is less where } X_{Al(VI)}^{cpx} = X_{Al}^{cpx} - X_{Al(IV)}^{cpx} \text{ and } X_{Al(IV)}^{cpx} = 2 - X_{Si}^{cpx} \quad X_{Fm}^{liq} = X_{Fe}^{liq} + X_{Mg}^{liq}$$

$$X_{DiHd}^{cpx} = X_{Ca}^{cpx} - X_{CaTs}^{cpx} - X_{CrCaTs}^{cpx} \text{ where } X_{CaTs}^{cpx} = X_{Al(VI)}^{cpx} - X_{Jd}^{cpx} \text{ and } X_{CrCaTs}^{cpx} = X_{Cr}^{cpx} / 2$$

H_2O^{liq} = the water content of the melt in wt%

$Mg\#^{liq} = (Mg^{liq} / (Mg^{liq} + Fe^{liq}))$ calculated as a mole fraction basis

$$X_{EnFs}^{cpx} = [X_{Fe}^{cpx} + X_{Mg}^{cpx} - X_{DiHd}^{cpx}] / 2$$

This model is based on the Jd-DiHd exchange thermometers of Putirka et al. (1996; 2003), but with reduced uncertainties due to global calibrations of experimental data conducted at pressures of < 70 kbars. This resulted in an overall error reduction of 10-20 °C to ± 42 °C. This model has been calibrated for hydrous systems with SiO₂ up to 71.3 wt% (Putirka, 2008; Putirka et al., 2003).

3.3.2.2 Method

Equation 3.8 (eq 30, Putirka, 2008) was solved with Equation 3.7 as this thermometer requires a pressure input and was designed to be solved simultaneously to give the best results. Equation 3.8 was used as the pressure input because it best reproduces the hydrous data at P < 10 kbars, although Eq. 31 of Putirka (2008) has better overall statistics (Figure 3.2). The model error associated with the clinopyroxene-liquid barometers are on the order of ± 3 kbar and have 2 sd of up to 5 kbar when applied to these samples.

Equation 3.7 is only slightly pressure dependent so varying the pressure input from 0 to 10 kbar (extremes likely to be outside of this system) reduces the resulting temperature calculation by around 40 °C (Table 3.10), which is within the model error. Clinopyroxene-liquid barometry was used in conjunction with the thermometry, rather than inputting the pressures obtained from the amphibole barometry as it cannot be certain that the amphibole rims crystallised at the same pressures as the clinopyroxene rims. Therefore, although the clinopyroxene-liquid barometry has large errors associated with it, it is more appropriate to solve the clinopyroxene thermometry and barometry simultaneously as was intended by Putirka (2008). The H_2O_{melt}

input was obtained from the Ridolfi et al. (2010) hygrometer as this is the most reliable constraint on H_2O_{melt} .

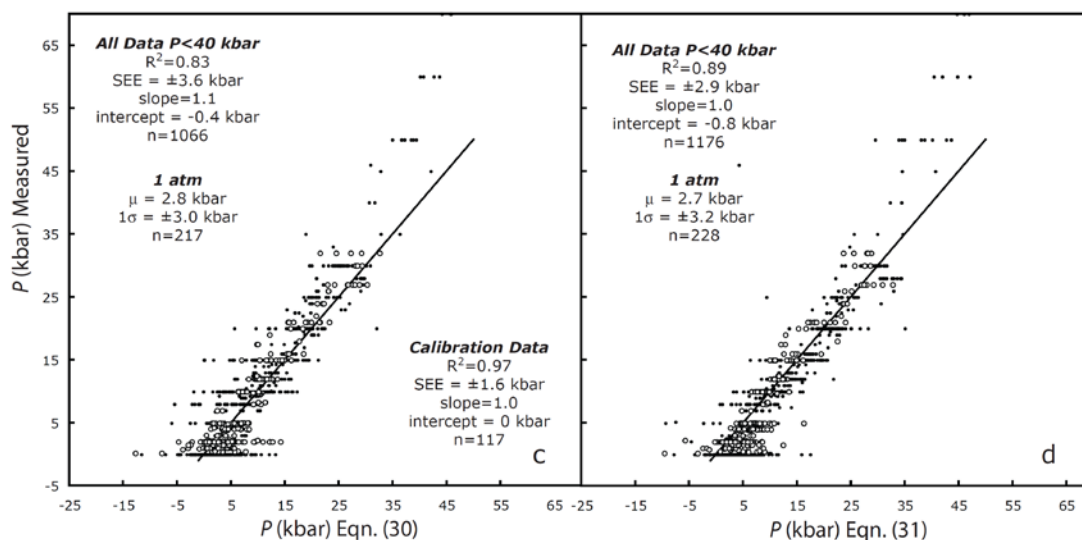


Figure 3.2 Comparison of two clinopyroxene-liquid barometers from Putirka (2008) shows that Eqn. 30 (equation 6) better reproduces the low pressure, hydrous data, although Eqn. 31 has better overall statistics. From Putirka (2008).

Table 3.10 Temperature ($^{\circ}\text{C}$) calculated from equation 5 using variable pressure and water content inputs. These variables are not well constrained, but within the variation expected in this system and the calculated temperature is within or very close to the model error ($\pm 42^{\circ}\text{C}$)

Pressure kbars	Water content			
	0%	1%	4%	2 SD
Eq 6 ¹	959	951	925	35.15
0	953	943	912	42.29
5	973	962	931	43.65
10	993	982	950	45.07
2 SD	36	35	31	

¹ Using equation 6 as the pressure input and solving pressure simultaneously with equation 5

EMPA analyses of glass adhered to clinopyroxene crystals and clinopyroxene-hosted melt inclusions $>10\ \mu\text{m}$ were paired with adjacent clinopyroxene analyses in order to ensure that glass and clinopyroxene compositions are in equilibrium if the crystal cargo was in equilibrium with the melt at the time of eruption. It also preserves any heterogeneities within each sample and allows for easy identification of pairs that do not represent chemical equilibrium. The glass analyses compared well with those of the matrix glass for each sample except SM-6C. These showed depletion in CaO, Al_2O_3 and MgO and enrichment in alkalis. For this reason, the average matrix glass was used for this sample.

3.3.2.3 Equilibrium

The use of clinopyroxene-melt thermometry requires the melt and clinopyroxene to be in equilibrium with one another. Putirka (2008) provides numerous methods to test this criteria as no single method is conclusive.

Fe-Mg exchange coefficients

If the clinopyroxene and liquid compositions are in equilibrium (at least in terms of Fe and Mg) then the $(\text{Fe}/\text{Mg})^{\text{cpx}}/(\text{Fe}/\text{Mg})^{\text{liq}} = K_D(\text{Fe-Mg})^{\text{cpx-liq}}$. The Fe-Mg exchange coefficient is 0.28 ± 0.08 with a range of 0.04-0.68 and a slight temperature dependence which can be accounted for by:

$$\ln K_D(\text{Fe} - \text{Mg})^{\text{cpx-liq}} = -0.107 - \frac{1719}{T(K)} \pm 0.08 \quad \text{EQ 3.9}$$

Although with a $R^2=0.12$ this poorly reproduces $K_D(\text{Fe-Mg})^{\text{cpx-liq}}$. Most of the K_D values calculated from these samples were much lower than 0.28 and the temperature dependent K_D value (0.193-0.233) (Table 3.11). Half of the samples could be considered to be in equilibrium if the temperature dependent $K_D \pm 0.08$ is used. However, Fe-Mg exchange between melt and clinopyroxene is dependent on many factors including pressure, oxygen fugacity and melt composition, rather than just temperature as is assumed in this model (Bedard, 2010). Therefore both constant and temperature dependent $K_D(\text{Fe-Mg})^{\text{cpx-liq}}$ used by Putirka (2008), are a rough approximation and failure to meet this condition does not rule out equilibrium between the liquid and crystal phases.

Clinopyroxene components

Equilibrium can also be determined on the basis of predicted clinopyroxene components (e.g. CaTs, EnFs, DiHd) based on the melt composition compared with the observed clinopyroxene components. This is a more robust test of clinopyroxene-melt equilibrium as it examines whether the individual clinopyroxene components are in equilibrium rather than assuming that these are in equilibrium if Fe-Mg are. Figure 3.3 indicates how well this data fits the criteria.

Melt inclusion/host data appears to be close to equilibrium, but the glass/rim pairs are less conclusive.

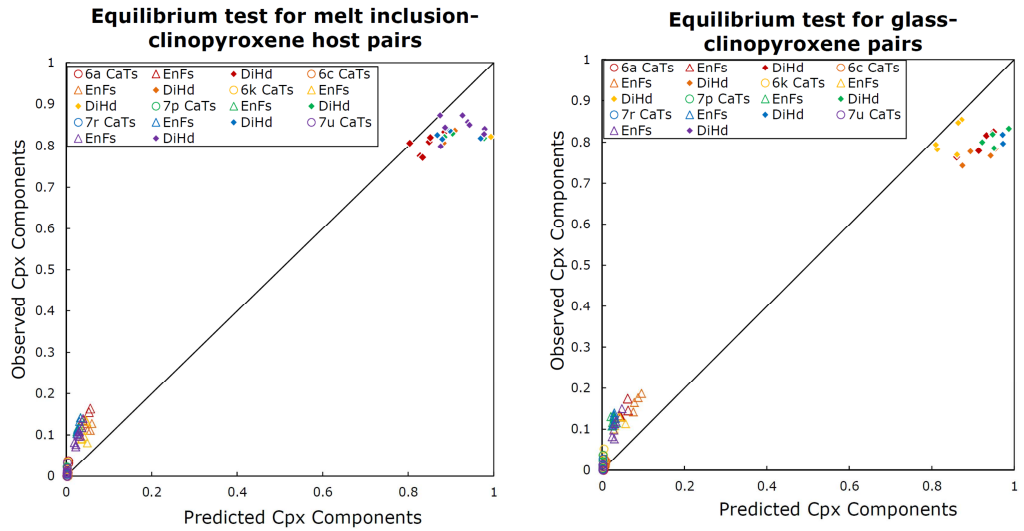


Figure 3.3 Predicted clinopyroxene components based on the melt composition vs the observed clinopyroxene components calculated from clinopyroxene analyses for glass-clinopyroxene pairs and melt inclusion-clinopyroxene host pairs. Modified after Putirka (2008).

Clinopyroxene saturation

Equation 3.10 is used as a test of the temperatures obtained from equation 3.7 as this gives the clinopyroxene saturation temperature of a melt at a given pressure. Therefore the result from this model should agree with that of equation 3.7 if the two phases are in equilibrium. The results were considered in agreement if they were within ± 45 °C of each other.

$$\frac{10^4}{T(K)} = 6.39 + 0.076(H_2O^{liq}) - 5.55(X_{CaO}^{liq}X_{SiO_2}^{liq}) - 0.386\ln(X_{MgO}^{liq}) - 0.046P(kbar) + 2.2 \times 10^{-4}[P(kbar)]^2 \quad \pm 45 \text{ } ^\circ\text{C} \quad \text{EQ 3.10}$$

Where H_2O^{liq} = the water content of the melt in wt% and $X_{component}^{liq}$ = the liquid component calculated as cation fractions on an anhydrous basis, but not renormalized to 100.

Any clinopyroxene-melt pairs that did not fit the clinopyroxene saturation equilibrium requirement were not considered to be in equilibrium and removed. Other equilibrium conditions are satisfied as indicated in Table 3.11.

Table 3.11 Glass/melt inclusion data and the associated clinopyroxene analyses with the calculated clinopyroxene temperature, pressure and equilibrium test results for each pair. If the clinopyroxene and liquid compositions are in equilibrium, the Jd-DiHd temperature and saturation temperature will be within $\pm 45^\circ\text{C}$ and the $K_D(\text{Fe-Mg})$ and predicted $K_D(\text{Fe-Mg})$ will be ± 0.08

Glass	Analysis pairs				Saturation				Analysis pairs				Saturation				Temp dependent KD(Fe-Mg)cpx-liq
	SM-6A	H ₂ O melt=4%	Cpx (kbar)	Jd-Di-Hd Temp (°C)	Temp KD(Fe-Mg) (°C)	KD(Fe-Mg)cpx-liq	SM-6A	Melt inclusions	H ₂ O melt=4%	Cpx (kbar)	Jd-Di-Hd Temp (°C)	Temp (°C)	KD(Fe-Mg)	Temp (°C)	KD(Fe-Mg)cpx-liq		
6a9G2	6acpx9_1	4.2	947	972	0.162	0.220	6a11MI1	6acpx11_6	5.5	926	951	0.136	0.224				
6a7G1	6acpx7_1	3.7	939	969	0.139	0.218	6a10MI1	6acpx10_3	3.8	890	923	0.083	0.217				
6a6G1	6acpx6_1	4.7	945	963	0.149	0.219	6a22MI1	6acpx22_6	3.7	898	926	0.080	0.213				
6a67G1	6acpx67_1	4.1	925	954	0.134	0.214	6a33MI1	6acpx33_5	2.3	928	952	0.140	0.254				
	Mean	4.2	939	965	0.146	0.218		Mean	3.8	910	938	0.109	0.227				
	2 SD	0.8	20	16	0.025	0.005		2 SD	2.5	39	31	0.065	0.037				
SM-6C	H₂O melt=5.5%																
6c_average	6ccpx16_1	3.8	978	991	0.172	0.227	SM-6C	6ccpx29_4	5.1	934	972	0.174	0.216				
6c_average	6ccpx16_6	7.0	1000	1013	0.214	0.233	6c31MI1	6ccpx31_3	5.1	929	964	0.154	0.215				
6c_average	6ccpx15_3	5.2	993	999	0.178	0.231	6c6MI1	6ccpx6_1	6.4	930	959	0.141	0.215				
6c_average	6ccpx28_1	3.6	977	988	0.184	0.227		Mean	5.5	931	965	0.156	0.216				
	Mean	4.9	987	998	0.187	0.230		2 SD	1.5	5	14	0.033	0.001				
	2 SD	3.2	23	23	0.038	0.006		H₂O melt=4%									
SM-6K	H₂O melt=4%																
6k45G	6kcp45_1	2.9	893	933	0.133	0.206	SM-6K	6kcp6_5	4.9	916	947	0.158	0.212				
6k12G	6kcp12_13	4.2	920	951	0.214	0.213	6k6MI	6kcp8_10	3.2	896	931	0.136	0.207				
6k15G	6kcp15_7	3.6	912	944	0.140	0.211	6k8MI	6kcp55_4	1.0	910	947	0.142	0.210				
6k58G	6kcp58_8	4.5	910	938	0.143	0.210	6k55MI	6kcp57_3	2.9	909	943	0.129	0.210				
6k75G	6kcp75_1	4.7	917	947	0.140	0.212	6k57MI										
	Mean	4.0	910	943	0.154	0.210		Mean	3.0	908	942	0.141	0.210				
	2 SD	1.5	21	14	0.067	0.006		2 SD	3.3	16	15	0.025	0.004				

Table 3.11 continued

Glass	Analysis pairs			Jd-Di-Hd		Saturation		Temp KD(Fe-Mg) (°C)	Temp dependent KD(Fe-Mg)/cpx-liq	Melt inclusions SM-7P	Cpx H ₂ O melt=4%	P (kbar)	Temp (°C)	Saturation Temp (°C)	KD(Fe-Mg) (°C)	Temp dependent KD(Fe-Mg)/cpx-liq
	SM-7P	H ₂ O melt=4%	Cpx	P (kbar)	Temp (°C)	Temp (°C)	Temp (°C)									
7p5G1	7p5G1	7p5G1	5.3	883	906	0.094	0.203	7p9MI1	7p9MI1	4.4	875	900	0.091	0.201		
7p10G1	7p10G1	7p10G1	5.8	884	905	0.133	0.203	7p34MI1	7p34MI1	-1.6	832	871	0.094	0.190		
7p15G1	7p15G1	7p15G1	3.0	863	890	0.085	0.198	7p35MI1	7p35MI1	2.7	853	878	0.096	0.195		
7p17G1	7p17G1	7p17G1	5.5	878	901	0.092	0.202	7p41MI1	7p41MI1	-0.5	845	877	0.087	0.193		
7p20G1	7p20G1	7p20G1	4.8	871	896	0.089	0.200									
7p35G1	7p35G1	7p35G1	4.7	868	897	0.089	0.199									
7p39G1	7p39G1	7p39G1	1.4	858	874	0.092	0.197									
7p26G1	7p26G1	7p26G1	4.1	866	893	0.080	0.199									
	Mean	Mean	4.3	872	895	0.094	0.200			1.2	851	882	0.092	0.195		
	2 SD	2 SD	3.0	19	20	0.032	0.005			5.5	36	26	0.008	0.010		
SM-7R								SM-7R								
7r2G1	7r2G1	7r2G1	4.7	871	894	0.096	0.200	7r4MI1	7r4MI1	4.0	870	900	0.084	0.200		
7r1G1	7r1G1	7r1G1	3.8	862	892	0.085	0.198	7r22MI1	7r22MI1	2.1	872	893	0.082	0.200		
7r24G1	7r24G1	7r24G1	4.4	871	894	0.082	0.200	7r48MI1	7r48MI1	4.0	879	906	0.093	0.202		
7r21G1	7r21G1	7r21G1	2.9	856	880	0.078	0.196	7r57MI1	7r57MI1	4.9	897	921	0.109	0.207		
7r35G1	7r35G1	7r35G1	3.5	857	885	0.084	0.196									
	Mean	Mean	3.9	863	889	0.085	0.198			3.8	880	905	0.092	0.202		
	2 SD	2 SD	1.4	14	12	0.013	0.004			2.3	25	24	0.024	0.007		
SM-7U								SM-7U								
7u4G1	7u4G1	7u4G1	2.3	866	908	0.105	0.199	7u22MI2	7u22MI2	2.5	872	901	0.104	0.200		
7u2G1	7u2G1	7u2G1	2.9	893	915	0.096	0.206	7u9MI1	7u9MI1	4.0	884	920	0.095	0.203		
7u22G1	7u22G1	7u22G1	4.0	897	914	0.091	0.207	7u36MI1	7u36MI1	3.0	881	911	0.111	0.203		
7u42G1	7u42G1	7u42G1	4.1	881	915	0.097	0.203	7u42MI1	7u42MI1	2.7	864	904	0.084	0.198		
7u47G1	7u47G1	7u47G1	3.8	881	912	0.098	0.203	7u56MI1	7u56MI1	2.3	868	903	0.112	0.199		
	Mean	Mean	3.4	884	913	0.097	0.203			2.9	874	908	0.101	0.201		
	2 SD	2 SD	1.6	24	6	0.010	0.006			1.3	16	16	0.023	0.004		

¹ Temperature and pressure calculated simultaneously using EQ 3.7 and EQ 3.8 respectively

² Calculated using EQ 3.10. This temperature should be within 45°C of the Jd-DiHd temperature

³ $K_D(\text{Fe-Mg}) = (\text{FeO/MgO})^{\text{cpx}} / (\text{FeO/MgO})^{\text{liquid}}$ calculated using cation fractions

⁴ The Fe-Mg exchange coefficient at the given temperature calculated using EQ 3.9 using the Jd-DiHd temperatures.

3.3.2.4 Other clinopyroxene thermometers

Clinopyroxene thermobarometry was reviewed and updated by Putirka (2008). The Jd-DiHd thermometer was used as this best fits the global calibration data for hydrous systems with the highest R^2 of 0.86 and the lowest $\sigma_{\text{est}} \pm 42$ °C. This model accurately reproduced hydrous calibration data from 800-1200 °C.

Clinopyroxene-melt thermometry requires the extra criteria of equilibrium between the melt and clinopyroxene phases be satisfied. This is not necessary for clinopyroxene-only thermometry, but these models are much less reliable with $R^2=0.22-0.36$ and $\sigma_{\text{est}} \pm 95$ and 87 for Nimis & Taylor (2000) and Putirka (2008) respectively.

3.3.3 PLAGIOCLASE-MELT THERMOMETRY

3.3.3.1 Model

The exchange of anorthite and albite between plagioclase and the coexisting melt is strongly dependent on both temperature and the water content of the melt. Multiple models have been devised to exploit this relationship by formulating thermometers and hygrometers (e.g. Sugawara, 2001; Ghiorso et al., 2002; Putirka, 2005; 2008; Lange et al., 2009)

The plagioclase-melt thermometer of Putirka (2008) was used to calculate magmatic temperatures using EMPA analyses of plagioclase rims and matrix glass. This model is based on plagioclase-melt equilibria, specifically the relationship between anorthite/albite content and temperature.

$$\frac{10^4}{T(K)} = 6.4706 + 0.3128 \ln \left(\frac{X_{An}^{pl}}{X_{CaO}^{liq} (X_{AlO_{1.5}}^{liq})^2 (X_{SiO_2}^{liq})^2} \right) - 8.103 (X_{SiO_2}^{liq}) + 4.872 (X_{K_{0.5}}^{liq}) + 1.5346 (X_{Ab}^{pl})^2 + 8.661 (X_{SiO_2}^{liq})^2 - 3.341 \times 10^{-2} (P(kbar)) + 0.18047 (H_2O^{liq}) \pm 36 \text{ °C}$$

EQ 3.11

Where $X_{component}^{liq}$ = the melt component calculated as cation fractions on an anhydrous basis, not renormalized to 100 and $X_{component}^{pl}$ = plagioclase components calculated as cation fractions on an anhydrous basis without renormalisation of weight percent values.

$$X_{An}^{pl} = X_{CaO}^{pl} / (X_{CaO}^{pl} + X_{NaO_{0.5}}^{pl} X_{KO_{0.5}}^{pl})$$

$$X_{Ab}^{pl} = X_{NaO_{0.5}}^{pl} / (X_{CaO}^{pl} + X_{NaO_{0.5}}^{pl} X_{KO_{0.5}}^{pl})$$

H_2O^{liq} = the water content of the melt in wt%

3.3.3.2 Method

The matrix glass for each sample was averaged as it was homogeneous. This was paired with plagioclase rim analyses that appeared to be in equilibrium with the surrounding glass based on crystal texture and anorthite content. Only compositions which were in the dominant rim population were included.

This model requires both a pressure and H_2O_{melt} input. The pressure and H_2O_{melt} from the amphibole thermobarometry were used as this is the best constraint on these parameters. Plagioclase-liquid thermometry is very H_2O_{melt} sensitive and varying this parameter by 4 wt% can change the resulting temperature by >100 °C.

3.3.3.3 Equilibrium

As this is a two phase model, it is essential that the two phases of interest are in equilibrium. Putirka (2008) provides two such tests, one is based on the anorthite-albite exchange constant (Equation 3.12) while the other calculates the temperature a melt will become plagioclase saturated at a given pressure (Equation 3.13)

$$K_D (An - Ab)^{pl-liq} = \frac{X_{Ab}^{pl} X_{AlO_{1.5}}^{liq} X_{CaO}^{liq}}{X_{An}^{pl} X_{NaO_{0.5}}^{liq} X_{SiO_2}^{liq}} = 0.10 \pm 0.05 \text{ at } T < 1050 \text{ } ^\circ\text{C} \quad \text{EQ 3.12}$$

$$\begin{aligned} \frac{10^4}{T(K)} = & 10.86 - 9.7654(X_{SiO_2}^{liq}) + 4.241(X_{CaO}^{liq}) - 55.56(X_{CaO}^{liq}X_{AlO_{1.5}}^{liq}) + \\ & 37.50(X_{K_{0.5}O}^{liq}X_{AlO_{1.5}}^{liq}) + 11.206(X_{SiO_2}^{liq})^3 - 3.151 \times \\ & 10^{-2}(P(kbar)) + 0.1709(H_2O^{liq}) \pm 37 \text{ } ^\circ\text{C} \end{aligned} \quad \text{EQ 3.13}$$

Where $X_{component}^{liq}$ = the liquid component calculated as cation fractions on an anhydrous basis, not renormalized to 100 and $X_{component}^{pl}$ = plagioclase components calculated as cation fractions on an anhydrous basis without renormalisation of weight percent values

$$X_{An}^{pl} = X_{CaO}^{pl} / (X_{CaO}^{pl} + X_{Na_{0.5}O}^{pl} + X_{K_{0.5}O}^{pl})$$

$$X_{Ab}^{pl} = X_{Na_{0.5}O}^{pl} / (X_{CaO}^{pl} + X_{Na_{0.5}O}^{pl} + X_{K_{0.5}O}^{pl})$$

H_2O^{liq} = the water content of the melt in wt%

The temperatures obtained from equations 3.11 and 3.13 are in agreement with one another to $\leq 15 \text{ } ^\circ\text{C}$ which is well within the model error of $\pm 37 \text{ } ^\circ\text{C}$. All samples except SM-6C were in equilibrium using the K_D An-Ab exchange.

3.3.3.4 Other plagioclase-melt thermometers

The Putirka (2008) model was used as this is calibrated for hydrous and anhydrous systems with a temperature range of greater than 800-1300 $^\circ\text{C}$, while earlier models such as Sugawara (2001) and Ghiorso et al. (2002) only proved accurate for temperatures $>1100 \text{ } ^\circ\text{C}$ (Putirka, 2005).

Lange et al. (2009) also present a thermometer and hygrometer based on the plagioclase-liquid exchange reaction between anorthite and albite. This model is calibrated as a hygrometer that requires temperature as an input. Where water content is used as an input, temperature can be calculated (Lange et al., 2009). This thermometer is comparable to that of Putirka (2005; 2008).

Table 3.12 Plagioclase analyses used for thermometry. The glass composition used was the average matrix glass values for each sample. The mean temperature and plagioclase saturation temperature are within $\pm 15^\circ\text{C}$ for each sample and $K_D=0.10 \pm 0.05$ for all samples except SM-6C.

SM-6A			SM-6C			SM-6K			SM-7P			SM-7R			SM-7U		
Analysis	Temp °C	K_D (An-Ab) ²	Analysis	Temp °C	K_D (An-Ab) ²	Analysis	Temp °C	K_D (An-Ab) ²	Analysis	Temp °C	K_D (An-Ab) ²	Analysis	Temp °C	K_D (An-Ab) ²	Analysis	Temp °C	K_D (An-Ab) ²
6aP1_2	937	0.083	6cP3_4	968	0.152	6kP1_1	928	0.062	7pP1_1	892	0.061	7rP19_1	872	0.073	7uP1_1	895	0.029
6aP4_1	942	0.072	6cP5_1	965	0.177	6kP2_1	915	0.116	7pP3_1	879	0.069	7rP1_1	873	0.055	7uP3_1	882	0.062
6aP5_1	939	0.084	6cP7_1	968	0.149	6kP3_1	925	0.078	7pP4_1	884	0.057	7rP5_1	872	0.057	7uP4_2	874	0.084
6aP9_1	942	0.077	6cP9_2	966	0.171	6kP4_1	923	0.080	7pP5_1	893	0.033	7rP6_4	871	0.060	7uP6_1	878	0.070
6aP10_1	942	0.075	6cP11_1	964	0.191	6kP5_1	926	0.070	7pP9_1	880	0.065	7rP8_1	871	0.057	7uP21_1	878	0.068
6aP11_1	944	0.068	6cP12_1	970	0.136	6kP6_1	924	0.079	7pP10_1	881	0.064	7rP21_1	872	0.056	7uP7_1	878	0.069
6aP12_1	937	0.093	6cP16_1	967	0.166	6kP7_1	926	0.068	7pP11_1	879	0.066	7rP22_1	871	0.060	7uP9_1	879	0.067
6aP15_1	945	0.064	6cP18_1	968	0.156	6kP8_1	928	0.065	7pP13_1	882	0.059	7rP9_1	871	0.059	7uP10_2	881	0.063
6aP17_1	933	0.098				6kP10_1	927	0.066	7pP14_5	886	0.051	7rP10_1	872	0.056	7uP11_1	880	0.065
6aP19_2	951	0.038				6kP16_6	926	0.069	7pP15_1	878	0.074	7rP11_1	873	0.054	7uP14_2	872	0.095
6aP20_1	941	0.078				6kP16_8	927	0.066	7pP15_8	889	0.042	7rP12_1	871	0.069	7uP15_1	876	0.077
6aP21_1	936	0.102				6kP17_1	926	0.069	7pP21_1	900	0.022	7rP14_1	870	0.061	7uP16_2	881	0.062
						6kP21_1	930	0.055	7pP15b	880	0.059	7rP24_1	871	0.059	7uP16_13	899	0.021
												7rP25_1	867	0.077	7uP19_1	879	0.066
												7rP15_1	874	0.051			
												7rP15_4	874	0.052			
												7rP16_7	876	0.047			
												7rP17_1	871	0.071			
												7rP17_3	871	0.059			
												7rP17_5	872	0.058			
Plag saturation (°C) ³	933			959			925			894			887			893	
Mean	941	0.078		966	0.162		925	0.073		885	0.055		872	0.060		881	0.064
2 SD	10	0.034	4		0.035	7		0.030		14	0.030	3		0.015		15	0.038

¹ Temperature calculated using Eq A3.11

² An-Ab exchange equilibrium calculated using Eq A3.12

³ Plagioclase saturation temperature calculated with Eq A3.13

3.3.4 COMPARISON OF RESULTS FROM DIFFERENT THERMOMETERS

Amphibole thermobarometry is the most reliable for the Taranaki eruptive system as all the model conditions are met and there is no requirement for equilibrium conditions so long as the host melt is calc-alkalic. The clinopyroxene-liquid thermometry, although not satisfying all equilibrium conditions stated by the model, appears to be in equilibrium. The melt inclusion/host and glass/rim clinopyroxene pairs give the same temperatures (± 30 °C) except for sample SM-6C, which further confirms the reproducibility of this method. This combined with the fact that these temperatures are in agreement with those of amphibole gives confidence that these temperatures are accurate. The plagioclase-liquid thermometer, while also giving consistent results, is less trustworthy due to the H_2O_{melt} dependence. As melt water content is not a well constrained parameter, the errors associated with this model are much larger than those stated. However, these results are also in agreement with the temperatures obtained from amphibole and clinopyroxene-liquid thermometry adding confidence to these temperatures. The rim temperatures of three mineral phases all returned the same temperatures, suggesting these rims were all formed at the same melt at the same magmatic conditions and therefore had a common final history (Table 3.13). Amphibole-plagioclase thermometry is not considered appropriate for this study. As model requirements were not met by all samples and this thermometer is only appropriate for temperatures < 900 °C. It is therefore not suitable for samples SM-6A, SM-6C or SM-6K and the significantly lower temperatures obtained from this model are indicative of this. This model also gives consistently lower temperatures for samples SM-7P, SM-7R and SM-7U which generally give temperatures of < 900 °C using the other thermometers assessed here. As both the phases used in this model were also used in other models evaluated here, the temperatures should correspond with one or both of these if the model is effective. Therefore, this model is not considered appropriate for this study. The results of the clinopyroxene-liquid thermometry are used in diffusion modelling, while the results of the amphibole thermobarometry are also reported in the results section of this thesis.

Table 3.13 Summary of thermometry results. For more details see Tables 3.9 3.11, 3.12

Inputs ¹	Sample		Amphibole	Cpx-melt	Cpx-melt- MI	Plag- melt
4% H ₂ O 3 kbars	<u>SM-6A</u>	Mean	960	939	910	941
		2 SD	41	20	39	10
5.5% H ₂ O 5 kbars	<u>SM-6C</u>	Mean	1006	987	931	966
		2 SD	8	23	5	4
4% H ₂ O 3 kbars	<u>SM-6K</u>	Mean	951	910	908	925
		2 SD	32	21	16	7
4% H ₂ O 2 kbars	<u>SM-7P</u>	Mean	919	872	851	885
		2 SD	14	19	36	14
4% H ₂ O 2 kbars	<u>SM-7R</u>	Mean	919	863	880	872
		2 SD	18	14	25	3
4% H ₂ O 2 kbars	<u>SM-7U</u>	Mean	919	884	873	881
		2 SD	26	24	16	15
	Model error	°C	±22	±42	±42	±36

¹ inputs obtained from amphibole thermobarometry of Ridolfi et al. (2010)

3.4 DIFFUSION MODELLING

3.4.1 INTRODUCTION TO DIFFUSION MODELLING THEORY

3.4.1.1 DIFFUSION IN MINERALS

Diffusion can be defined as “the relative motion of one or more particles of a system relative to other particles of the same system” (Onsager, 1945). Diffusion in solid silicates is a powerful tool for tracking timescales of subvolcanic processes, some of which occur in the lead up to an eruption (e.g. Zellmer et al., 2003; Morgan et al., 2004; Martin et al., 2008). The diffusion rates of commonly measured elements vary considerably for different mineral species, so depending on the mineral-element pair that is being studied, a range of processes can be investigated on timescales ranging from hours to millennia (Chakraborty, 2008).

When the magmatic system surrounding a crystal experiences a change in melt chemistry, temperature, pressure and/or oxygen fugacity, a new crystal zone in equilibrium with the new conditions may grow (Figure 3.4a). The boundary between the new zone and crystal interior is, in effect, a disequilibrium feature that immediately begins to re-equilibrate by diffusion (Figure 3.4). Due to the exponential temperature dependence of elemental diffusion rates, diffusion effectively ceases on eruption for most elements applied to volcanic systems. If eruption occurs before complete diffusive re-equilibration can be attained, a snapshot of the incomplete element exchange occurring over that boundary is preserved. Therefore, calculating the length of time during which diffusion occurred between mineral zones provides valuable constraints on the timescales of pre-eruptive magmatic conditions independent of sample age.

3.4.1.2 DIFFUSION MECHANISMS

Diffusion is ubiquitous, occurring randomly as the movement of atoms is driven by their thermal energy (Costa et al., 2008). Atoms migrate away from their starting position given a driving force such as a concentration gradient (or more strictly, chemical potential), resulting in an initially heterogeneous phase becoming homogeneous. Given its random nature, the process is defined statistically, averaging the movement of a large number of atoms using a Gaussian function (Chakraborty, 2008).

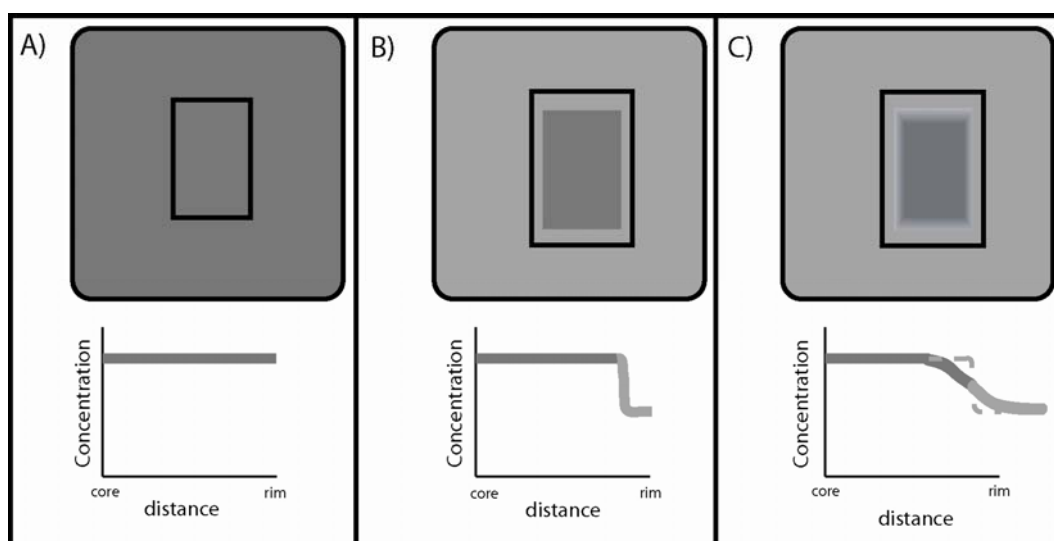


Figure 3.4 Schematic representation of the history of a crystal and how diffusion modelling of crystal zoning represents magmatic events. A) The crystal has grown in a melt at a specific set of conditions resulting in a homogeneous crystal. B) The conditions of the melt have changed resulting in the growth of a new zone with a different composition and a sharp compositional boundary. C) With time this initially sharp zone boundary is smoothed as a result of diffusion. By constraining the shape of the diffusion modified boundary, and with knowledge of the temperature and diffusion coefficient of the element of interest in the mineral, one can constrain the time between event B and eruption. Modified after Costa et al. (2008).

There are four main processes by which atoms migrate within a crystal lattice: (1) vacancy diffusion, whereby an atom jumps to a vacancy; (2) interstitial, when atoms are small enough to fit into interstitial sites within the crystal lattice; (3) exchange, during which atoms swap places; and (4) ring exchange, when more than two atoms exchange places in a circuit (Figure 3.5; Watson & Baxter, 2007; Costa et al., 2008). The most common of these is vacancy diffusion (Dimanov & Wiedenbeck, 2006; Chakraborty, 2008; Costa et al., 2008). Vacancies form when ions are forced out of their site, which requires energy. Energy is also required to allow the atoms to make the ‘jump’ to fill the vacancy. Therefore, temperature is a pivotal factor in determining the diffusion rate (Chakraborty, 2008).

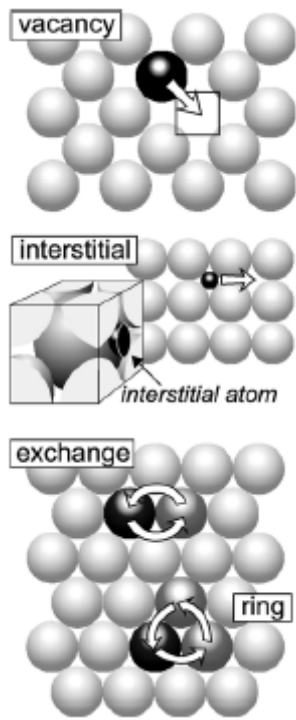


Figure 3.5 Schematic representation of the different types of diffusion mechanisms in minerals. Figure taken from Watson & Baxter (2007).

3.4.1.3 DIFFUSION EQUATIONS

The evolution of the concentration gradient due to diffusion is governed by Fick's First Law:

$$J_i = -D_i \frac{\partial C_i}{\partial x} \quad \text{EQ 3.15}$$

Where J_i = flux of diffusing component i

D_i = diffusion coefficient of component i

$\frac{\partial C_i}{\partial x}$ = concentration gradient

To determine timescales Fick's Second Law is applied, which introduces changes in concentration with time:

$$\frac{\partial C_{x,t}}{\partial t} = D_i \frac{\partial^2 C_{x,t}}{\partial x^2} \quad \text{EQ 3.16}$$

Where $C_{x,t}$ = the concentration at point x and time t
 t = time
 D_i = diffusion coefficient of component i
 x = position within the system

There are many analytical solutions to this equation and selection of an appropriate solution is dependent on the nature of the system being modelled including variables such as the dimensions, geometry, amount of diffusion that has occurred, boundary and initial conditions of the system (Crank, 1975). Appropriate models can be found in Crank (1975) and Carslaw & Jaeger (1986).

3.4.2 FE-MG INTERDIFFUSION IN CLINOPYROXENE

3.4.2.1 MODEL PARAMETERS

Interdiffusion of Fe and Mg in clinopyroxene crystals is modelled using the method of Morgan et al. (2004) to calculate the timescales between the growth of a mineral zone and eruption. The basis of this model and its application are briefly discussed here.

This is a simple 1-dimensional model that assumes a stepwise initial concentration gradient between mineral zones (Figure 3.6A). While the crystal is at magmatic temperatures, this gradient is progressively smoothed over time by diffusion in a manner that can be mathematically modelled in the form of a progressively modified error function (erf) or complementary error function (erfc) curve (Figure 3.6). Therefore a solution to Fick's Second Law from Crank (1975) is used.

$$\frac{(C-C_0)}{(C_1-C_0)} = 1 - \left[0.5 \operatorname{erfc} \left(\frac{h}{2\sqrt{Dt}} \right) \right] \quad \text{EQ 3.17}$$

Where C_1 and C_0 = the end member concentrations
 C = composition at point h and time t
 h = extent of diffusion from the half width

D = diffusion coefficient

t = time

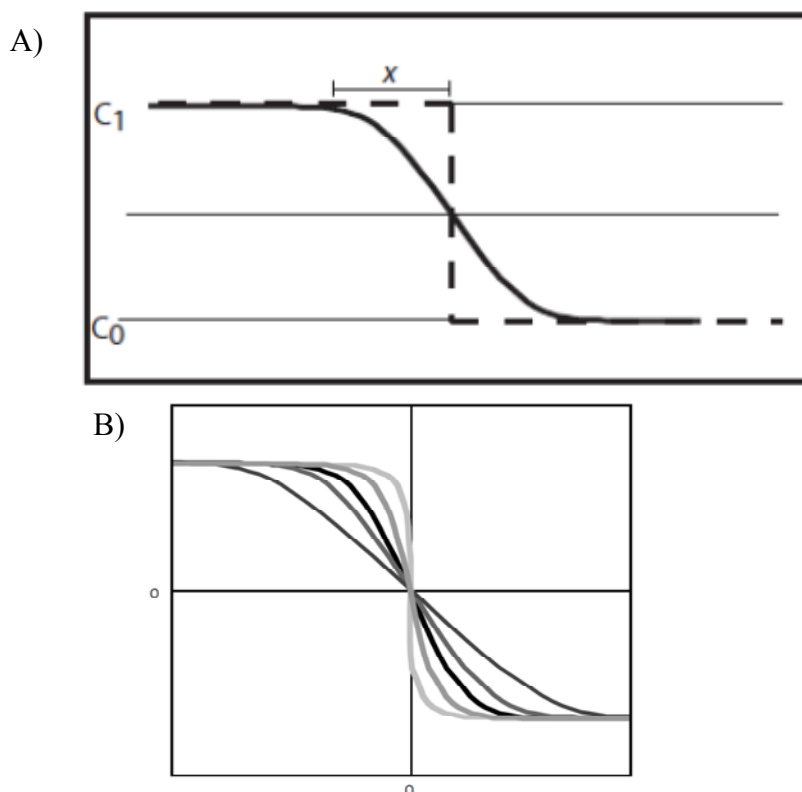


Figure 3.6 A) The dashed line represents an initial sharp chemical boundary in a mineral as is assumed in this model and the solid line illustrates how this profile looks some time later once partially smoothed to an erfc function. The parameters of EQA4.4 are identified. Figures modified after Morgan et al. (2004) and Costa et al. (2008). B) Shows the geometry of various erfc curves. Each of these could be the diffusion profile across a zone at various points in time, starting with the steepest profile and becoming progressively wider with time.

The erf function is uniquely defined because any point on the curve other than the origin has a single solution (Figure 3.6B). This enables the better constrained central 80% of the curve to be modelled and reduces the errors associated with defining the full width of the diffusion curve, as the tails of the profile are often lost to compositional noise (Morgan et al., 2004). Equation 3.17 is modified to account for this and for the limited spatial resolution resulting from the pixellated nature of the data. Therefore the diffusion equation used is:

$$C_{x,t} = \frac{n}{2(n+1)} = 1 - \left[0.5 \operatorname{erfc} \left(\frac{x}{2\sqrt{Dt}} \right) \right] \quad \text{EQ 3.18}$$

Where $C_{x,t}$ = concentration at point x and time t

C = compositional contrast on a scale of 0-0.5

x = half-width

D = diffusion coefficient

t = time since zone formed

n = number of grades of contrast over the diffusion profile

3.4.2.2 MODEL CONDITIONS

Initial conditions

A step-like initial condition was selected because the diffusion widths being modelled are generally narrow ($\leq 5\mu\text{m}$) and the renewal of crystal growth with a different composition is assumed to be abrupt and sharp. Any smoothing of this profile is attributed to diffusion which results in the calculation of a maximum age. A 1-dimensional model is justified as the lengths of the modelled diffusion profiles are very small in comparison to the size of the crystals (Costa et al., 2008).

An additional factor to consider in the diffusion process is how crystal growth affects calculated timescales. Magma evolution in response to fractionation during crystal growth can also produce smooth concentration profiles between crystal zones (Costa et al., 2008). In this case the assumption of an initially sharp, step-like profile is not valid, and could result in overestimating calculated timescales. For this reason, only zones that could reliably be inferred to have originally had sharp boundaries were modelled. Wherever possible, this was verified by observations of incongruent and congruent portions of individual boundaries. Incongruent boundaries, where there is a mismatch of the crystal lattice, diffuse at a much slower rate than congruent boundaries and therefore the curved sections of zones appear to remain sharp when straight sections have diffused (Morgan, 2003). This property was used to confirm the initial boundary sharpness by checking that the incongruent section of a modelled zone appeared crisp in backscatter electron (BSE) images. Only zones that met this criterion were modelled.

Boundary Conditions

Simple boundary conditions were used in the models assuming an isothermal, closed system. Thermometry results from both mineral rim and internal zones consistently returned the same temperature within the model error ($\pm 42^\circ \text{C}$) suggesting there was no overall heating or cooling trend affecting the zones of interest, justifying the use of an isothermal model. A closed system was assumed, as the growth rate appears to be relatively fast ($\sim 10^{-12} \text{ms}^{-1}$), which has the effect of isolating newly formed zones from the surrounding melt *ca.* 1000 s after formation (D. Morgan, pers. comm.). This time period is significantly shorter than the resolution of the model and will therefore have no impact on the calculated timescales (see discussion of model resolution below).

Diffusion Coefficient

The diffusion coefficient is calculated from an Arrhenius type equation (Equation 3.19). This is mainly related to the temperature-controlled concentration of vacancies. Other variables such as pressure, oxygen fugacity, composition and crystallographic orientation can also affect the diffusion coefficient depending on the mineral and element of interest (e.g. Costa & Dungan, 2005). The pre-exponential factor (D_0) and activation energy (Q) have been previously determined experimentally for each element-mineral pair. The temperature is determined separately.

Dimanov & Sautter (2000) experimentally investigated Fe-Mg interdiffusion in clinopyroxene and calculated a D_0 value of $9.55 \times 10^{-5} \text{m}^2\text{s}^{-1}$ and Q of 406 kJ. During these original experiments the oxygen fugacity spanned five orders of magnitude, from 10^{-18} to 10^{-13} . Earlier studies had shown that the activation energy varies depending on whether the oxygen fugacity is fixed or buffered (e.g. Chakraborty & Ganguly, 1992). Dimanov & Sautter (2000) postulated that their activation energy of 406 kJ/mol was an overestimate and Dimanov & Wiedenbeck (2006) confirmed this by calculating an activation energy $\sim 25\%$ lower of 297 ± 31 kJ/mol. The revised activation energy is in better agreement with other published studies of divalent cation diffusion in Fe-Mg silicates, which typically give values between 200-300

kJ/mol (e.g. Fe self-diffusion in clinopyroxene, Azough & Freer, 2000; Pb in clinopyroxene, Cherniak, 2001; Dimanov & Wiedenbeck, 2006).

The Fe-Mg interdiffusion coefficient for clinopyroxene used here is calculated using the Dimanov & Wiedenbeck (2006) equation:

$$D = D_0 \left(\frac{pO_2}{pO_2^{ref}} \right)^n \exp \left(-\frac{Q}{RT} \right) \quad \text{EQ 3.19}$$

Where D = the diffusion coefficient (cm^2/s)

D_0 = the pre-exponential factor (7.68×10^{-2})

pO_2 = oxygen partial pressure

pO_2^{ref} = a reference oxygen partial pressure (0.21 atm)

n = the oxygen fugacity exponent (0.22 ± 0.02)

Q = the activation energy (297 ± 31 kJ/mol)

R = the gas constant (8.314 J/mol/K)

T = temperature ($^{\circ}$ K)

Dimanov & Wiedenbeck (2006) investigated Fe-Mg interdiffusion in clinopyroxene along the [001] axis assuming compositional independence. A strong sensitivity to oxygen fugacity was found, which was quantified and incorporated as a separate factor into the above model.

3.4.3 METHOD

Greyscale values from BSE images are used as a proxy for Fe and Mg concentrations and allow the shape of the diffusion profile to be defined and modelled. These images were imported into the image manipulation program ImageJ[®] and rotated so that the boundary of interest was vertical (Figure 3.7). Greyscale values were calculated using an area of between 100 and 300 pixels along the length of the zone to calculate average values and reduce the amount of noise. Care was taken to minimise interference from imaging imperfections that may affect the greyscale such as polishing scratches, grease marks and light interactions (Figure 3.7).

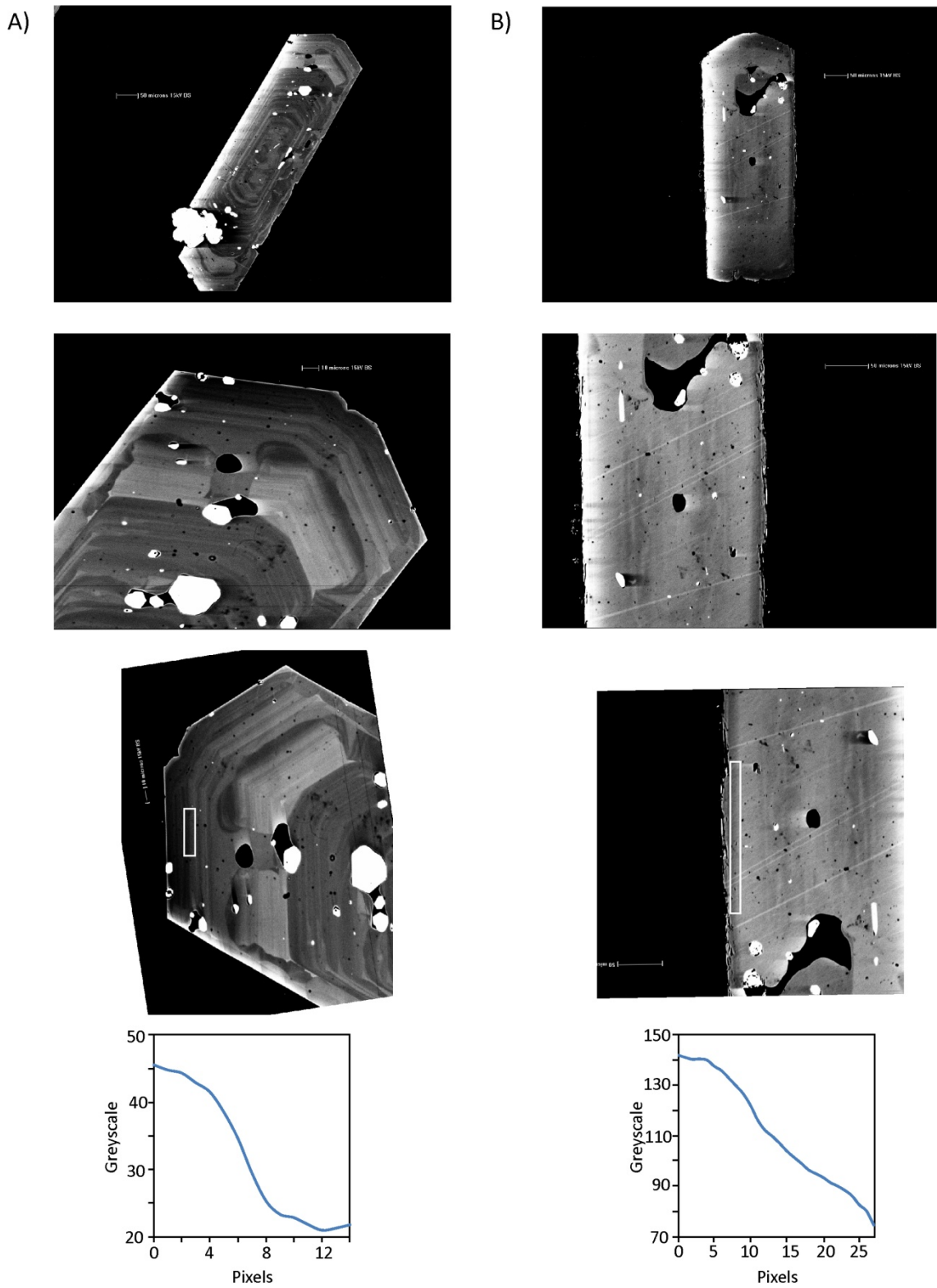


Figure 3.7 Examples of how diffusion profiles are obtained from BSE images. From top to bottom- an overview of the entire crystal is shown; an expanded image of the zones of interest; the image is rotated so the boundary of interest is vertical; the resulting profile across the modelled zone. A) an example of a good zone to model and the resulting smooth curve. B) an example of an inappropriate zone to model.

BSE images were obtained using a JEOL 733 Superprobe Electron Probe Micro-Analyser (EMPA) at Victoria University of Wellington (VUW). The greyscale intensity of these images was used as a proxy for concentration rather than compositional traverses as images provide better resolution with submicron as compared with micron resolution. The intensity of backscattering is related to the mean atomic number of the mineral beneath the rastered electron beam (Reed, 1975). Fe has the highest atomic number (56) of the major elements in clinopyroxene so it has the strongest influence on the BSE image greyscale (Figure 3.8). BSE imaging does not strongly differentiate between Mg, Al and Si as they have similar atomic numbers (24, 27 and 28 respectively) (Reed, 1975; Figure 3.8). Therefore the contrast observed in BSE images of clinopyroxene largely reflects variations in Fe making it an effective proxy for tracking Fe and Mg variation within clinopyroxene crystals (Morgan et al., 2004). BSE images provide a 2-dimensional map of the distribution of Fe-Mg zoning which more completely characterises the nature and distribution of the zoning than can be achieved by point analyses, enabling multiple zones in a crystal to be modelled (Ginibre et al., 2002b).

Energy dispersive spectrometry (EDS) mapping shows Al is the only other major element that shows zoning on the scale of Fe and Mg and therefore may affect the greyscale variations within BSE images. The affects of Al are however negligible as it has a similar atomic number to Mg and Si. In addition, its tetrahedral coordination within the crystal lattice results in a high activation energy that means it diffuses three orders of magnitude slower than Fe-Mg interdiffusion (Sautter et al., 1988; Dimanov & Sautter, 2000). This makes Al diffusion in pyroxenes negligible on geologic timescales at temperatures of < 1000 °C (Sautter et al., 1988). The overall affect of Al on the greyscale values is that it introduces some noise but has a minimal affect on the calculated timescale (D. Morgan, pers. comm.).

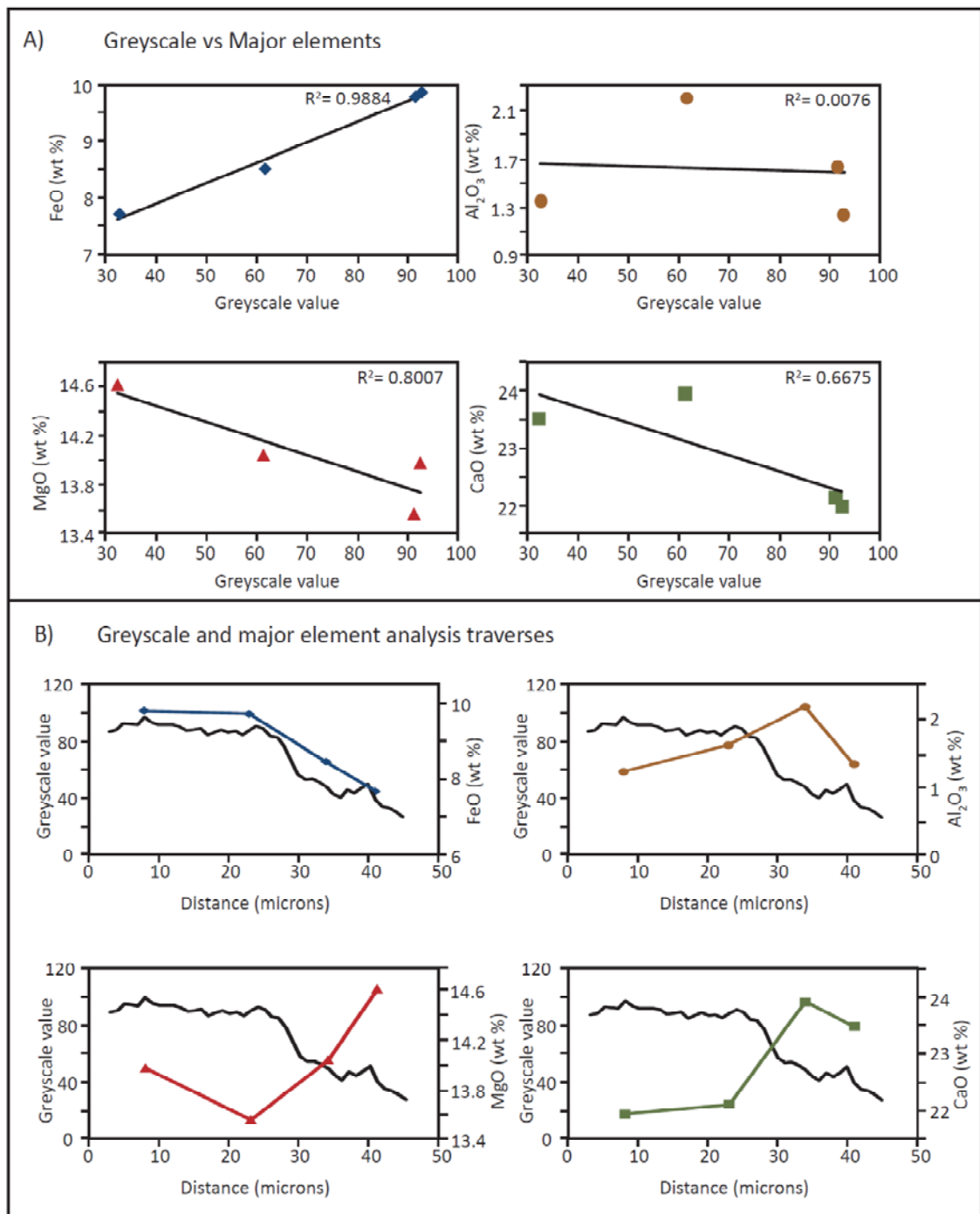


Figure 3.8 Graphs illustrating the relationship between greyscale and selected major elements. A) Greyscale plotted against selected major elements. Linear trend lines have been fitted to each graph and the regression value shown. Greyscale most closely correlates with FeO and Mg# and has a very poor correlation with Al₂O₃ and CaO. This indicates that the greyscale value of clinopyroxene is primarily controlled by the Fe content. B) A transect across a clinopyroxene zone comparing greyscale values (black line) and major element analyses (coloured lines). Also note the much better resolution provided by greyscale than EMPA analyses.

3.4.3.1 MINIMUM RESOLUTION OF THE MODEL

The spatial resolution of the data is dependent on pixel size and therefore the magnification of the image. The minimum resolution of the model with regards to timescale was calculated by modelling a perfectly sharp boundary, that is, a boundary that has undergone no diffusion and should therefore represent a diffusion timescale of zero. This was carried out on cracks and the edge of crystals (where the crystal meets epoxy) as these are discrete boundaries. This was done at a range of magnifications for each sample as each sample has a different diffusion coefficient due to their different temperatures. A numerical relationship was determined to calculate the minimum resolution for any given magnification and diffusion coefficient (Equation 3.20) and the results from these calculations are shown in figure 3.9.

$$y=ax^{-1.598} \quad \text{EQ 3.20}$$

Where y = the minimum resolution of the model in years

x = the magnification of the image

a = the pre-exponential factor which is determined by the diffusion coefficient

These times represent the error related to the resolution of the data and are assumed to be the minimum temporal resolution of the model. Any zones that return timescales at or below this threshold cannot be resolved using this model and are considered to represent boundaries not significantly modified by diffusion and therefore with diffusion timescales of zero age. Each calculated age was checked against its specific minimum resolution (dependent on image magnification and diffusion coefficient). No crystal zones modelled in this study returned ages at or near this threshold.

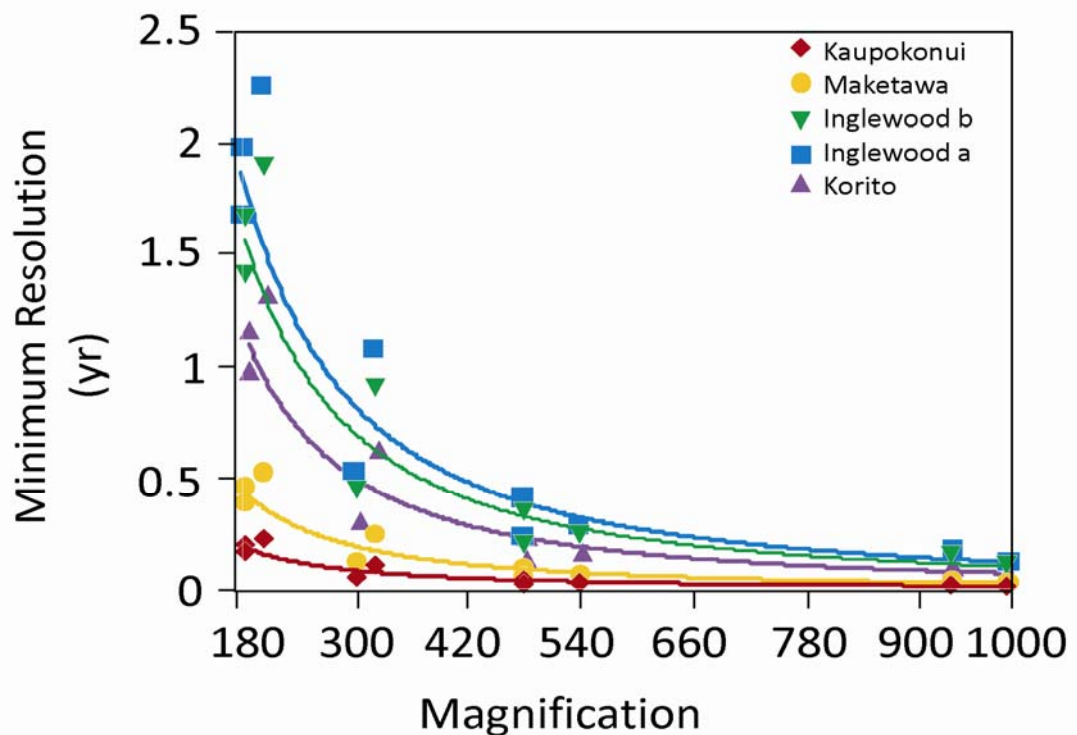


Figure 3.9 Graph illustrating the power function relationship between magnification of BSE image and minimum temporal resolution of the diffusion model as determined by EQ 3.20. This is calculated for each sample as the diffusion coefficient is different for each sample due to differences in temperature and oxygen fugacity. Image magnifications used in modelling range from 180x - 1000x, but most (~75%) modelled images were taken at a magnification of 400x – 800x.

3.4.4 SOURCES OF ERROR

There are a number of simplifications made in this model that will result in the propagation of errors and these effects must be considered. It is important to note that the same values of D_0 and Q were used for all calculations. Therefore the errors associated with D_0 and Q will affect the absolute ages, but not the relative ages. Temperature is the greatest source of error as the diffusion coefficient is exponentially dependent on temperature. It is therefore the only error quantified and factored into the age calculations. This is considered to be the total error as the other sources of error would fall within the range already defined by the temperature uncertainty. Other sources of error such as those associated with the simplifications necessary for the model have been reduced where possible and are assumed to be minimal.

3.4.4.1 DIFFUSION COEFFICIENT

The diffusion coefficient used from Dimanov & Wiedenbeck (2006) is a simplistic model as it does not take into account anisotropy or compositional dependence, as these variables are either currently not constrained or considered insignificant for clinopyroxene (Dimanov & Sautter, 2000; Dimanov & Wiedenbeck, 2006). However, these factors are both significant in the diffusivity within other mineral phases, specifically Fe-Mg interdiffusion in olivine (e.g. Costa & Dungan, 2005; Martin et al., 2008) and orthopyroxene (e.g. Ganguly & Tazzoli, 1994; Cherniak, 2001). It could therefore be expected to affect the Fe-Mg interdiffusion coefficient of clinopyroxene.

Anisotropy

The diffusion coefficient of Dimanov & Wiedenbeck (2006) was calculated for the plane parallel to the [001] axis (c-axis). However, the zoning in this direction was generally too narrow to model. To minimise any affects of anisotropy, clinopyroxene crystals were orientated during sample preparation and the [101] plane was primarily modelled. Therefore any error associated with this will affect only the absolute ages and not the relative ages. In addition, where possible, zones parallel to the [001] axis were modelled and these returned the same timescales within the error of the model.

Composition

Dimanov & Wiedenbeck (2006) assumed the rate of Fe-Mg interdiffusion in clinopyroxene was composition independent. This is justified by the previous work on interdiffusion rates in clinopyroxenes as the rates are very similar regardless of whether the clinopyroxene has a Fe-rich or Mg-rich composition (Dimanov & Sautter, 2000; Dimanov & Wiedenbeck, 2006). However, diffusivity is thought to be more sensitive to composition at higher oxygen fugacities (Dimanov & Wiedenbeck, 2006). The oxygen fugacity of the samples modelled here are above the QFM buffer in the range where composition may have a larger effect (Dimanov & Wiedenbeck, 2006). The diffusion coefficient was determined for Mg_{87} which is more

magnesium rich than the majority of clinopyroxene crystals modelled here. Any affect this has should be minimised as the Mg# ($\text{Mg}/\text{Mg}+\text{Fe}^{2+}$) for these samples is restricted to 75-90 with the bulk of compositions clustering around Mg#=80-85.

Temperature

The largest source of error in diffusion modelling is related to temperature. Temperature is the key energy input into the system, so it therefore determines the number of vacancies formed and whether atoms have enough energy to ‘jump’ into vacancies. The temperatures used here were calculated using the clinopyroxene-liquid thermometer of Putirka (2008) as discussed above in the thermobarometry section. The error associated with this thermometry is ± 42 °C (standard error of estimate). Two other thermometers were applied to these samples (amphibole - Ridolfi et al., 2010; plagioclase-melt - Putirka, 2008) which returned temperatures within error of those used here. This adds further confidence to the thermometry results and suggests the model error of ± 42 °C is a maximum uncertainty.

3.4.4.2 SECTIONING EFFECTS

Sampling a three dimensional crystal in two dimensions can result in some geometric complexities whereby the crystal is not sectioned perpendicular to the zones of interest (Costa & Morgan, in press). This has the effect of blurring the boundaries, making them appear more diffuse than they actually are and modelling of these boundaries will overestimate timescales (Figure 3.10; Ganguly et al., 2000). To reduce this effect, crystals were orientated on the [010] axis in epoxy blocks and polished approximately half way through the crystal. Sectioning in this way also enables the ‘real’ texture to be viewed and therefore the context of the diffusion ages may be better understood. When the crystal is sectioned obliquely, the same zone will appear more diffuse on one side of the crystal as compared to the other. Where this occurred, the narrowest zone was modelled as this is less affected by the sectioning and therefore more closely reflects the true diffusion length and therefore timescale (Ganguly et al., 2000). Rim zones are the least affected by sectioning, and this effect becomes more pronounced towards the cores, meaning the rim zones in general give more accurate timescales than the cores (D.

Morgan, pers. comm.). The majority of zones modelled in this study were crystal rims, or within the outer $\sim 50 \mu\text{m}$ of the crystals so this affect is minimised.

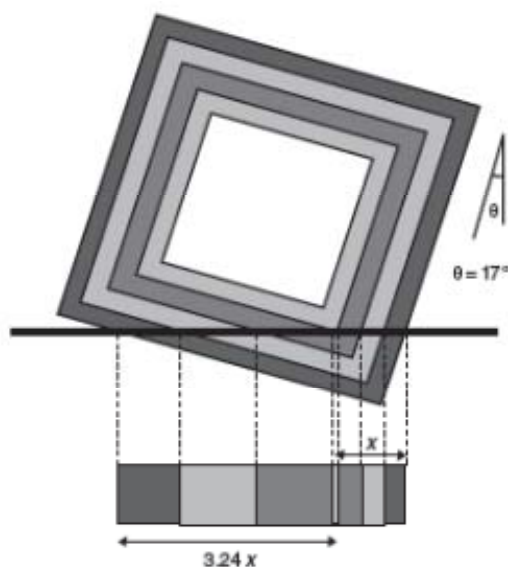


Figure 3.10 Schematic representation of the effect of oblique sectioning on the 2-dimensional view of the crystal. Note the smearing out affect of the crystal zones and therefore boundaries and hence the calculated timescales. From Costa & Morgan (2010).

3.4.4.3 IMAGE PARAMETERS

The effects of image parameters on calculated timescales were investigated. In particular whether there was any variation in the timescales calculated using variable resolution, magnification, contrast or brightness settings. It was found that there was no change in the timescale calculated using these variable parameters (Figure 3.11). The only affect these had was the minimum resolution of the images, which increased with increasing magnification as discussed previously.

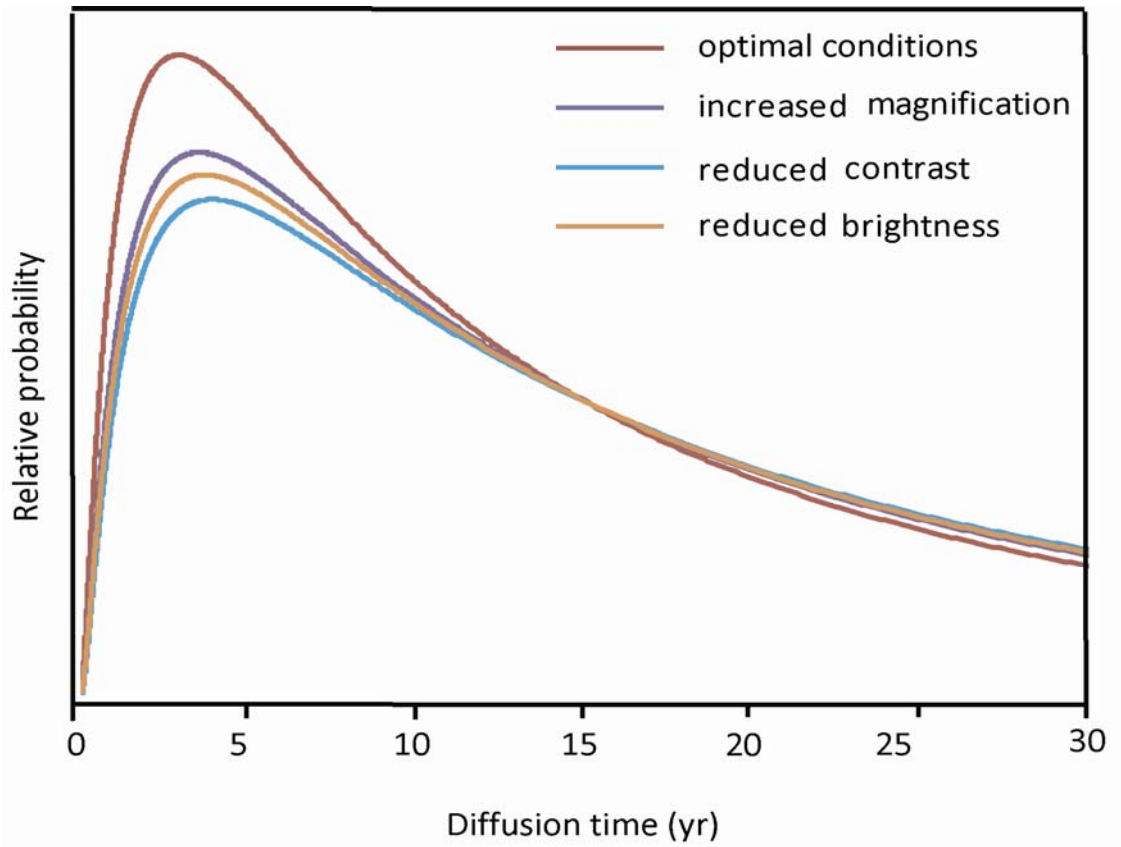


Figure 3.11 Calculated diffusion ages on the same zone in the same crystal using variable image parameters

CHAPTER 4: **RESULTS**

4.1 PETROLOGY

The six samples investigated in this study are pumice-lithic lapillis and classified as andesite-basaltic andesite based on whole rock compositions (Neall et al., 1986; Price et al., 1992; Stewart et al., 1996; Price et al., 1999, 2005). The pumice clasts are vesicular (~30-55 vol. % vesicles) and crystal rich (~20-30 %). Mineral phases range from microlites (~10 µm) to 2 mm in length and include plagioclase, clinopyroxene, amphibole and Fe-Ti oxides with rare olivine and orthopyroxene. Glomerocrysts are common and include clinopyroxene and Fe-Ti oxides with occasional plagioclase, amphibole, olivine and orthopyroxene. Xenoliths are present in SM-6C and contain plagioclase, orthopyroxene and amphibole. A summary of the petrology of each sample is given in Table 4.1.

Table 4.1 Summary of the petrographic variation observed within Taranaki eruptives investigated in this study. Mineral proportions were estimated visually under a petrographic microscope.

ID	Sample	Vesicle content	Glass content¹	Phenocryst content¹	Plag¹	Cpx¹	Amph¹	Oxides¹	Olivine¹	Opx¹
SM-6A	Kaupokonui	~40%	~50%	~50%	~25%	~10%	~15%	< 2%	-	-
SM-6C	SM-6C	~40%	~65%	~35%	~25%	~10%	<< 5%	< 5%	<< 1%	<1%
SM-6K	Maketawa	≥ 50%	~40%	~60%	~40%	~10%	~10%	< 10%	-	-
SM-7P	Inglewood b	~30%	~60%	~40%	~20%	~15%	~5%	< 5%	-	-
SM-7R	Inglewood a	~55%	~35%	~65%	45%	~10%	~10%	< 5%	-	-
SM-7U	Korito	~55%	~35%	~65%	~55%	<5%	~10%	< 1%	-	-

¹ Proportions of glass and minerals calculated on a vesicle free basis.

4.1.1 PLAGIOCLASE

Plagioclase is the most common mineral phase within Taranaki eruptives and is present in all samples. Crystals are generally euhedral to subhedral and range in size from ~20 µm to 2 mm. Plagioclase crystals are typically individual crystals, but occasionally form glomerocrysts with other plagioclase crystals as well as amphibole and Fe-Ti oxides. On the basis of mineral texture, three different types of plagioclase have been identified, although there is overlap

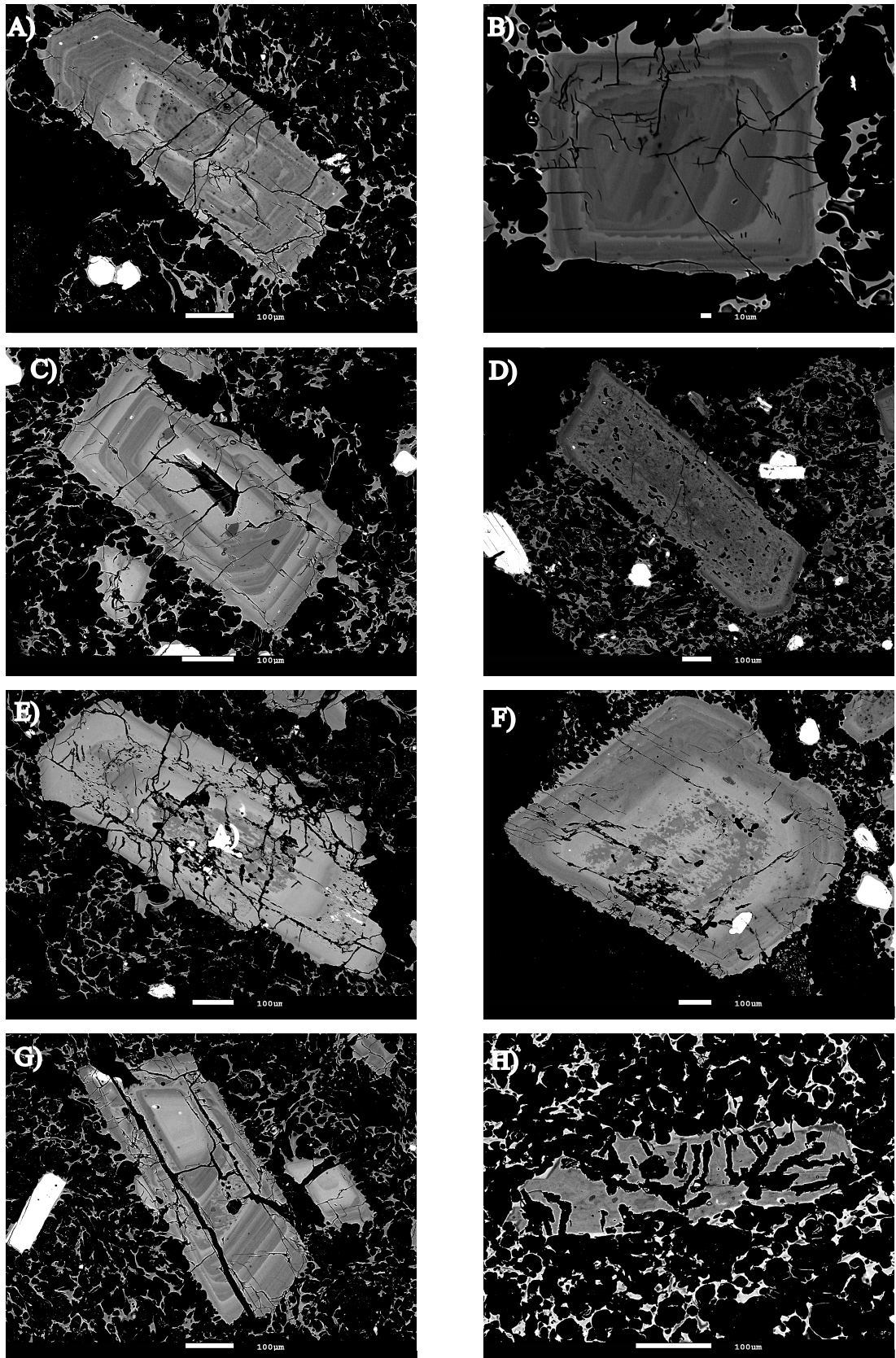


Figure 4.1 Backscattered electron images of representative plagioclase crystals. A) and B) Oscillatory zoned; C) Homogeneous high anorthite core with oscillatory rim; D) Sieved core with a thin rim; E) Patchy textured core and sieved zone; F) Patchy textured core with an oscillatory zoned rim; G) Patchy textured zone within oscillatory texture; H) Partially dissolved crystal.

between these. Plagioclase textures are: (1) oscillatory zoned; (2) patchy zoned and sieve textured; (3) dissolved textures (Figure 4.1).

Oscillatory zoned plagioclase crystals are the most common population and comprise 50% of plagioclase crystals in each sample except SM-6C (< 20%). The oscillatory zoning spans most of the compositional range of plagioclase (An_{36-84}) and usually extends from crystal rim to core (Figure 4.1a and b). About 50% of the older three samples have near homogeneous anorthite-rich cores (An_{67-82}) which, in some cases started to resorb (Figure 4.1c). Oscillations occur on a range of scales from < 5 to 60 microns. The finest scale oscillations do not appear to have any resorption associated with them, but larger scale zones occur with minor and major resorption zones with changes of up to 20 mol% in anorthite content. Despite the wide range in compositions, the rims are consistently low anorthite for any given sample (An_{36-60}).

Plagioclase exhibits sieved and/or patchy textures in 30-50% (~90% for SM-6C) of crystals in each sample. This generally affects the crystal core, which in some cases is surrounded by only a thin rim (Figure 4.1d), although specific zones in oscillatory crystals may be affected and both the crystal core as well as a distinct zone can be sieved or patchy (Figure 4.1e). Sieved and patchy textured crystals have low anorthite, oscillatory zoned rims which are compositionally the same as those of the oscillatory population rims. In some cases, the crystals appear identical to those of the oscillatory zoned population, but have a patchy texture in the core (Figure 4.1f). Sieved areas of crystals generally have a high anorthite content (An_{66-92}) and patchy areas display a bimodal composition with the high anorthite peak corresponding to sieved zones and the low anorthite composition corresponding to the oscillatory rims. It is therefore interpreted that the calcic composition is the original core/zone, which underwent partial resorption. Sieved and patchy textures differ in that areas with a patchy texture underwent recrystallisation.

Partially dissolved crystals that have undergone extensive resorption account for < 10% of the plagioclase crystals and are mostly found in sample SM-6C. These have undergone almost entire resorption and no or very little recrystallisation has occurred (Figure 4.1h). These crystals have very high anorthite contents (An_{86-92}).

4.1.2 CLINOPYROXENE

Clinopyroxene crystals range in size from microlites 10 μm to 1.5 mm in length and occur as isolated crystals with abundant Fe-Ti oxide and melt inclusions, but also commonly form glomerocrysts with Fe-Ti oxides and rare plagioclase and amphibole. Clinopyroxene crystals are primarily euhedral and compositionally have $\text{Mg}^{\#}_{70-92}$ with $\sim 80\%$ restricted to $\text{Mg}^{\#}_{76-86}$. Clinopyroxene crystals exhibit a wide range of textures, with most of this variability evident in the younger three samples. These samples contain crystals with patchy cores and oscillatory rims (all samples), patchy cores with Mg-rich rims (Maketawa, SM-6C, Kaupokonui) and multiply zoned crystals (Figure 4.2a; Maketawa and SM-6C). The two most abundant textural types are described in more detail below.

4.1.2.1 Patchy core and oscillatory rims

This is the dominant population within the samples investigated here and is the only clinopyroxene texture observed in Inglewood a and b and Korito, where the form of this texture in these three samples is near identical. The patchy cores contain abundant melt inclusions associated with the optically dark areas, indicating that the optically light areas represent the original core that underwent resorption and recrystallised as optically dark clinopyroxene (Figure 4.2c). Occasionally, the 'original' core exhibits oscillatory zoning (in the older 3 samples) (Figure 4.2d). A small population ($< 10\%$) within Maketawa has a distinct high-Mg resorption core ($\text{Mg}^{\#}_{87-94}$) (Figure 4.2e). Oscillatory zoning ranges in size from $\sim 20 \mu\text{m}$ to comprising the entire crystal (Figure 4.2b). Oscillations occur on multiple scales with fine zoning ($\leq 10 \mu\text{m}$) superimposed on coarser zoning (10-60 μm). These are commonly straight, asymmetric boundaries and various degrees of resorption is common. In some cases resorption is extensive and results in a zone or series of oscillatory zones more closely resembling a patchy texture. SM-6C contains a distinct population of oscillatory zoned crystals where oscillations are very fine ($< 10 \mu\text{m}$) and are more like fine lamellae (Figure 4.2f).

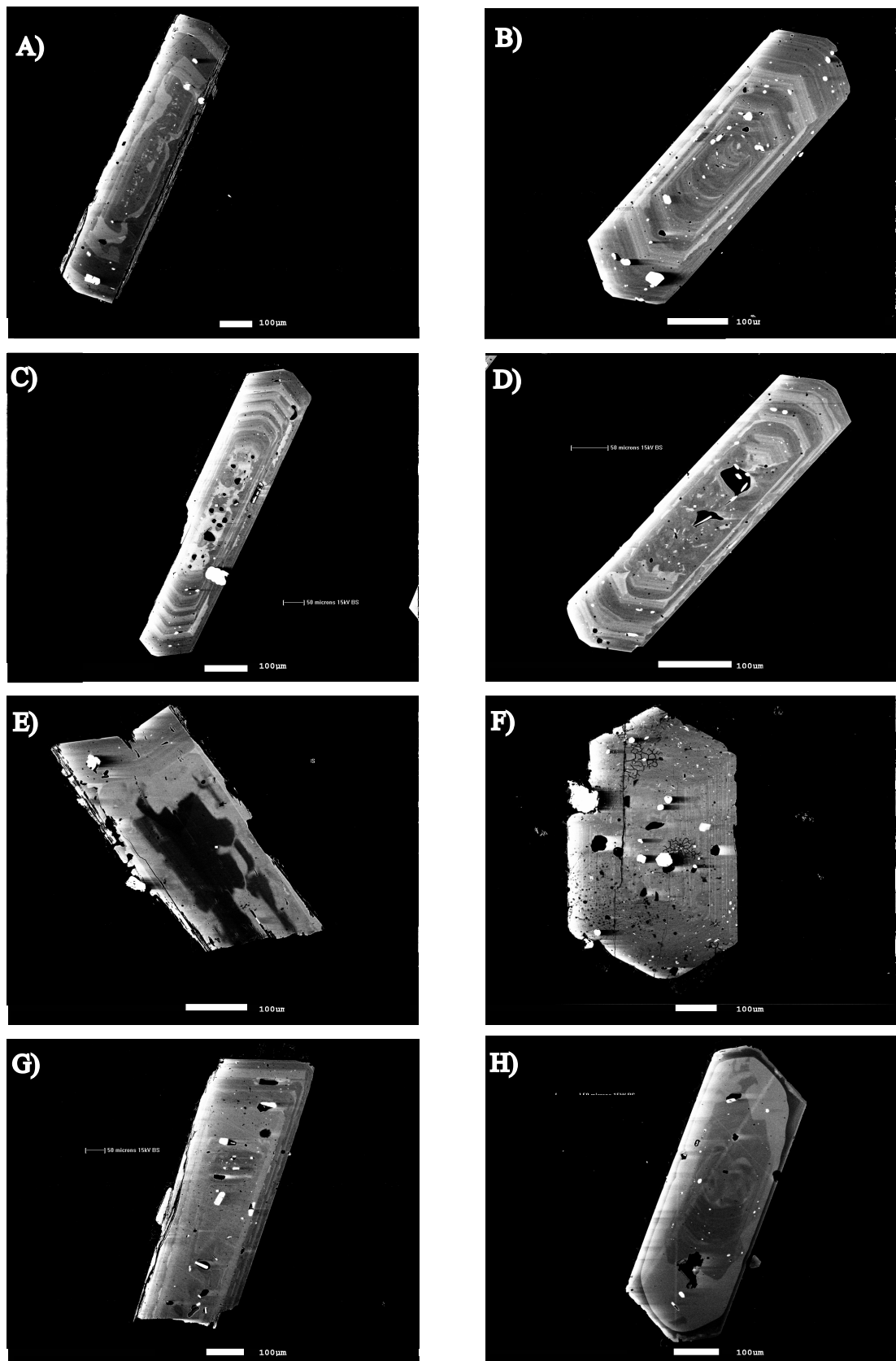


Figure 4.2 Backscattered electron images of representative clinopyroxene crystals. A) Multiple zoned; B) Oscillatory zoned; C) Patchy textured core with melt inclusions associated with the optically darker patches surrounded by an oscillatory rim; D) Resorbed oscillatory zoning; E) High-Mg resorbed core; F) Fine laminar zoning; G) Dark rim from Maketawa; H) Dark rim from Kaupokonui

4.1.2.2 Dark rim

A dark rim is present in the younger 3 samples as a final coarse oscillatory or multiple zone (Figure 4.2g), or the rim on a Fe-rich patchy textured core with abundant, large melt inclusions (Figure 4.2h). This dark rim is most pronounced in Kaupokonui where it is commonly associated with a large degree of resorption and can have a thin overgrowth of more Fe-rich clinopyroxene.

4.1.3 AMPHIBOLE

Amphibole is most abundant as euhedral to subhedral individual crystals 20 μm to 1 mm in size and can contain small Fe-Ti oxides and occasional melt inclusions. Occasionally amphibole is found in glomerocrysts with clinopyroxene \pm plagioclase \pm Fe-Ti oxides. Amphibole compositions are magnesio-hastingsite and range in composition from $\text{Mg}^{\#}_{60-92}$ with a shift to higher values in younger samples. A range of textures is observed across the sample suite including patchy zoning (~50%), simple zoning (~20%), multiple zoning (~15%), unzoned (~10%) and oscillatory zoning (~5%).

Patchy zoning occurs in all samples and is typically limited to the core which is then overgrown with an optically dark rim. Specifically there is a distinct population where a low Mg and high Al ($\text{Mg}^{\#}_{68-78}$; $\text{Al}_2\text{O}_3 = 12-15$ wt %) resorption core is recrystallised with a high Mg and low Al rim ($\text{Mg}^{\#}_{74-82}$; $\text{Al}_2\text{O}_3 = 9.5-11$ wt %) (Figure 4.3a). In some cases, this rim has oscillatory zoning (Figure 4.3b). This population is the sole amphibole type in Inglewood b and is dominant (~50%) in Inglewood a and Korito and typically restricted to the smaller size fraction (<150 μm , 20 μm in Maketawa). Simple zoning is most common in the younger three samples and typically comprises an optically light core with a dark rim (Figure 4.3c), although the reverse is also observed (Figure 4.3d). Multiple zoning occurs in the Korito, Inglewood a, Maketawa and Kaupokonui sample amphiboles (Figure 4.3e). Unzoned amphibole is present in all samples but Inglewood b and is observed only as microcrystals (<30 μm) (Figure 4.3f). Oscillatory zoning occurs in Korito, Inglewood a and SM-6C and is always present in only the largest amphibole size fraction (≥ 500 μm) or as part of a glomerocryst (Figure 4.3g and h).

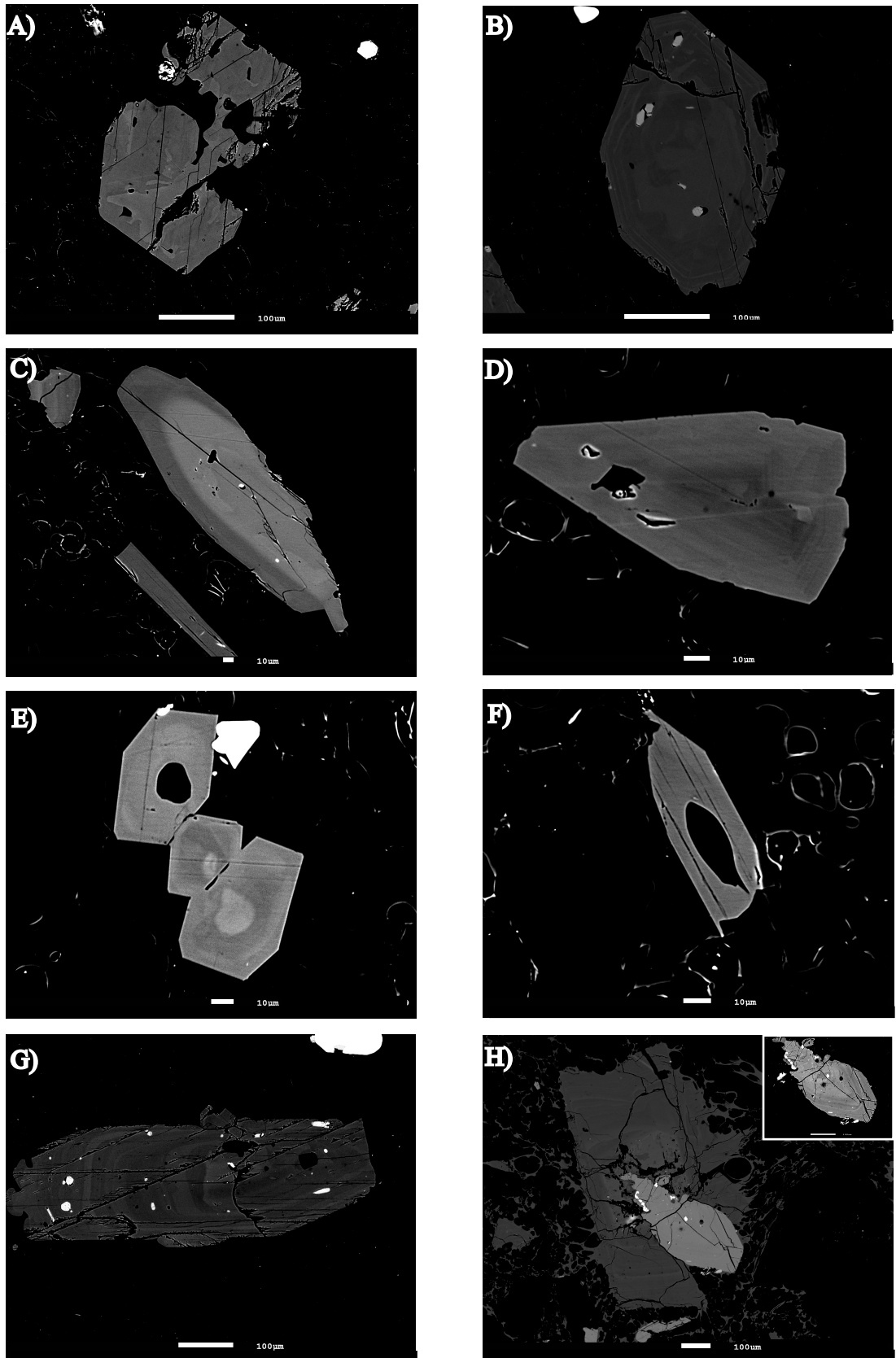


Figure 4.3 Backscattered electron images of representative amphibole crystals. A) Patchy textured core; B) Patchy core with oscillatory rim; C) Simple zoning with a light core and dark rim; D) Simple zoning with a dark core and light rim; E) Multiple zoning; F) Oscillatory zoning; G) Plagioclase and amphibole glomerocryst-inset highlights the oscillatory zoning of the amphibole

4.1.4 FE-TI OXIDES

The main Fe-Ti oxide phase is titanomagnetite, although rare ilmenite is also present. Titanomagnetite occurs as individual crystals, clusters of crystals and as inclusions in clinopyroxene and amphibole. These range in composition from $X_{Usp} \sim 0.1-0.3$. There are two populations of single crystal titanomagnetites based on morphology. (1) Large (50-300 μm) subhedral to anhedral crystals which appear to be resorbed and contain abundant apatite inclusions ($\sim 70\%$). In sample SM-6C, a small amount of these are very large ($\sim 200-300 \mu\text{m}$) and fragmented (Figure 4.4a). (2) Small euhedral to subhedral crystals 10-50 μm in size ($\sim 30\%$) (Figure 4.4b). Titanomagnetite also occurs as inclusions in, or forms glomerocrysts with, clinopyroxene and amphibole crystals ranging in size from <10 to 200 μm and are typically subhedral to anhedral in shape.

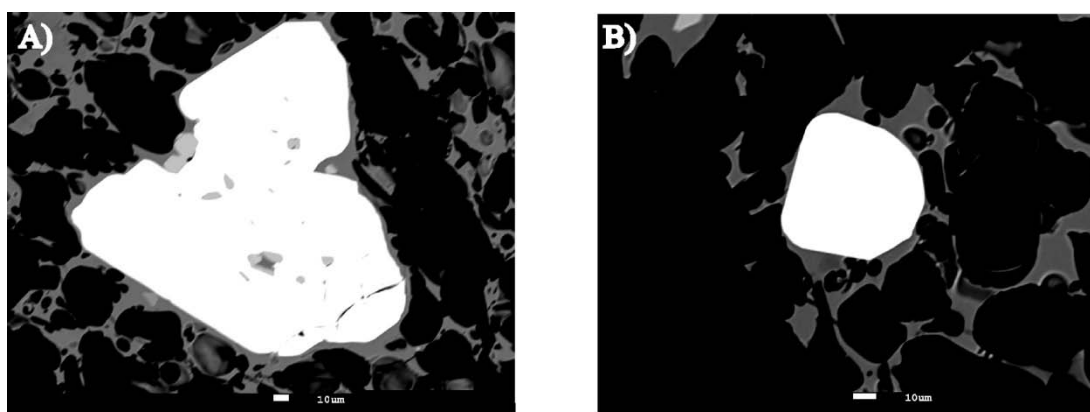


Figure 4.4 Backscattered electron images of titanomagnetite. A) Large, resorbed crystal; B) small euhedral crystal.

4.1.5 ORTHOPYROXENE

Orthopyroxene crystals are only present in sample SM-6C where they form euhedral to anhedral crystals 100-400 μm in size (Figure 4.5a). There is little compositional variation ($\text{Mg}\# = 70-81$) and weak zoning. Orthopyroxene crystals contain abundant melt and Fe-Ti oxide inclusions and rare crystals have an olivine core (Figure 4.5b).

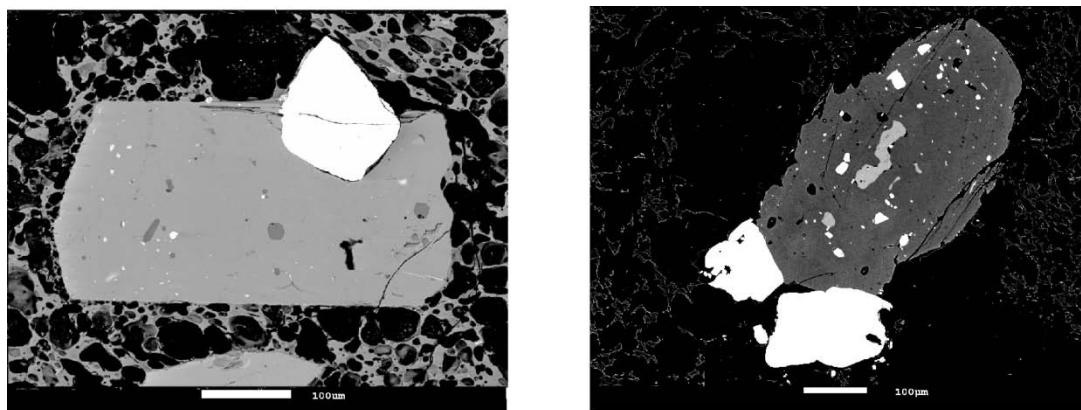


Figure 4.5 Backscattered electron images of orthopyroxene crystals. Left: weakly zoned euhedral crystal; Right: olivine cored orthopyroxene crystal.

4.2 MAJOR ELEMENT CHEMISTRY

4.2.1 GLASS MAJOR ELEMENT CHEMISTRY

Taranaki eruptives are classified as high K_2O andesites on the basis of whole rock data, however, glass data compositions have been shown to be dacitic (e.g. Price et al., 2005; Platz et al., 2007a). The glass major element data from this study are in agreement with this, but extend the range of glass compositions from andesite with slightly elevated K_2O content to high K_2O rhyolite (Figure 4.6). The overall trend of the glass major element chemistry is that of fractional crystallisation as FeO, MgO and CaO all decrease as SiO_2 increases (Figure 4.6). Five of the six samples form a continuous trend from dacitic to rhyolitic glass compositions that broadly corresponds to the chronologic order of these eruptions from youngest to oldest (Figure 4.6). Inglewood a and b and Korito are the most evolved samples and cluster at the rhyolite end of the spectrum. Maketawa and Kaupokonui are less evolved being dacitic in composition. Sample SM-6C falls on the same geochemical trend but is distinct because it is significantly less evolved than the other samples with lower SiO_2 and K_2O and higher Al_2O_3 , FeO, MgO, CaO and TiO_2 . There is limited scatter within each sample, indicating that the glass composition is relatively homogeneous.

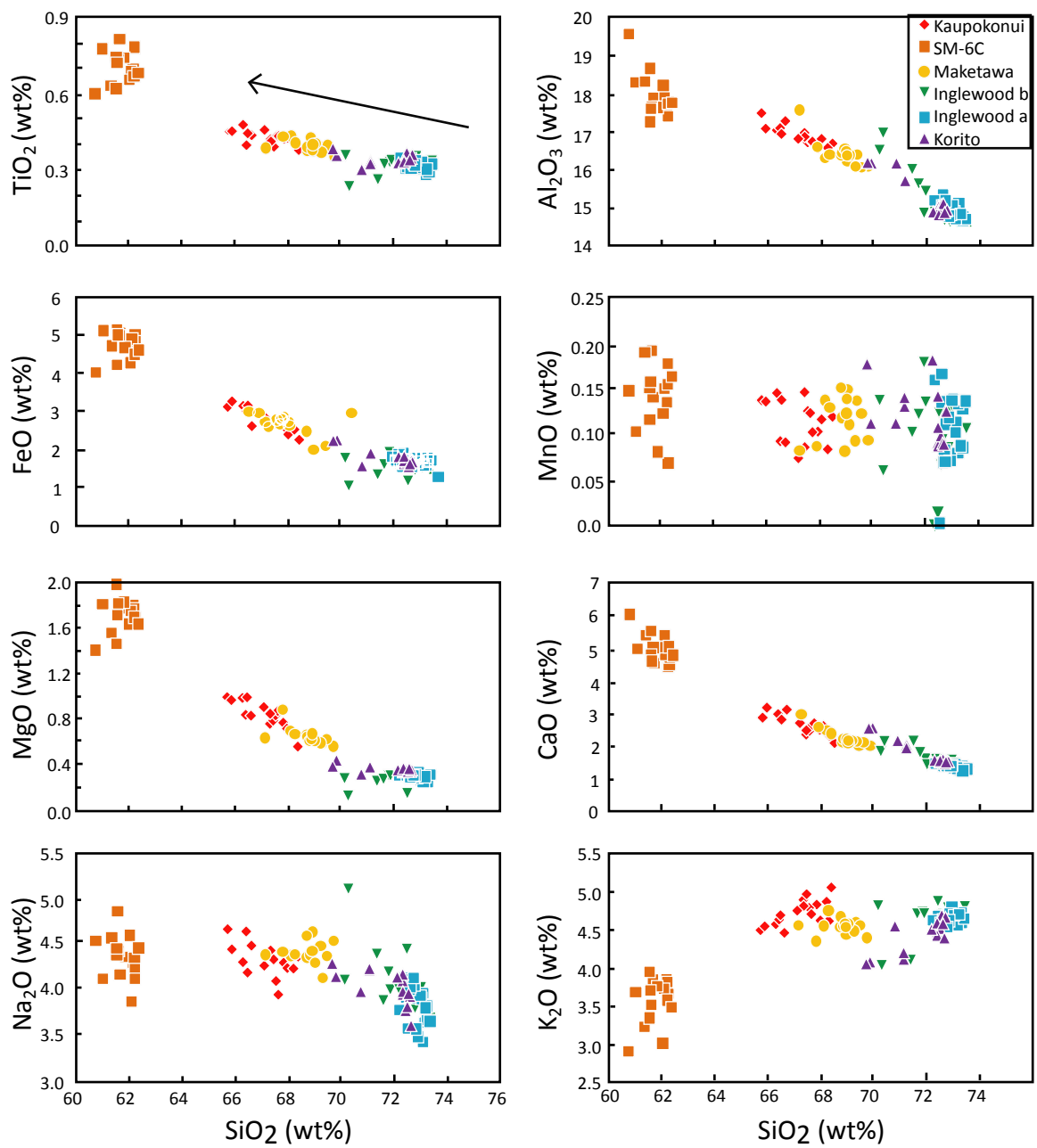


Figure 4.6 Major element analyses of glass determined by EMPA plotted versus SiO₂. A broad trend is evident from least to more evolved compositions with decreasing eruption age as indicated by the arrow. SM-6C is falls off this trend.

4.2.2 MELT INCLUSION MAJOR ELEMENT CHEMISTRY

The melt inclusion data shows the same general trend as the groundmass glass data, but with more scatter (Figure 4.7). The amphibole-hosted melt inclusions correspond most clearly to the glass compositions. Clinopyroxene-hosted melt inclusions are consistently 1-2 wt% lower in total alkalis (Figure 4.7c). The plagioclase melt inclusions from Inglewood a and b are less evolved than the glass compositions.

SM-6C however, has much more evolved melt inclusions compared with the glass data with the exception of the single amphibole-hosted melt inclusion analysed which overlaps with the glass field (Figure 4.7d).

4.2.3 MINERAL MAJOR ELEMENT CHEMISTRY

4.2.3.1 Plagioclase

Plagioclase compositions range from anorthite (An) 34-94 ($An=100 \times (Ca/(Ca+Na+K))$) (Figure 4.8). The peak in anorthite content for each sample is at the sodic end of this range with Inglewood a and b and Korito exhibiting almost identical patterns where the dominant composition is ca. An_{45} . Kaupokonui, SM-6C and Maketawa generally contain more calcic plagioclase crystals with a mode of around An_{55-60} , and SM-6C has some plagioclase crystals with the highest anorthite contents.

Most samples show a bimodal distribution with the high anorthite population (An_{70-80}) consisting primarily of core analyses and the low anorthite (An_{45-55}) population comprising both cores and rims. SM-6C and Maketawa consist of one main peak which has an anorthite content intermediate between the two populations of the other samples. The cores of these samples also have higher overall anorthite content than the rims.

Each sample contains oscillatory zoned and sieve textured crystals. Where recrystallisation has occurred within the sieved crystals a patchy texture is evident. As both the initial zone undergoing dissolution and the recrystallising composition were analysed and classified as

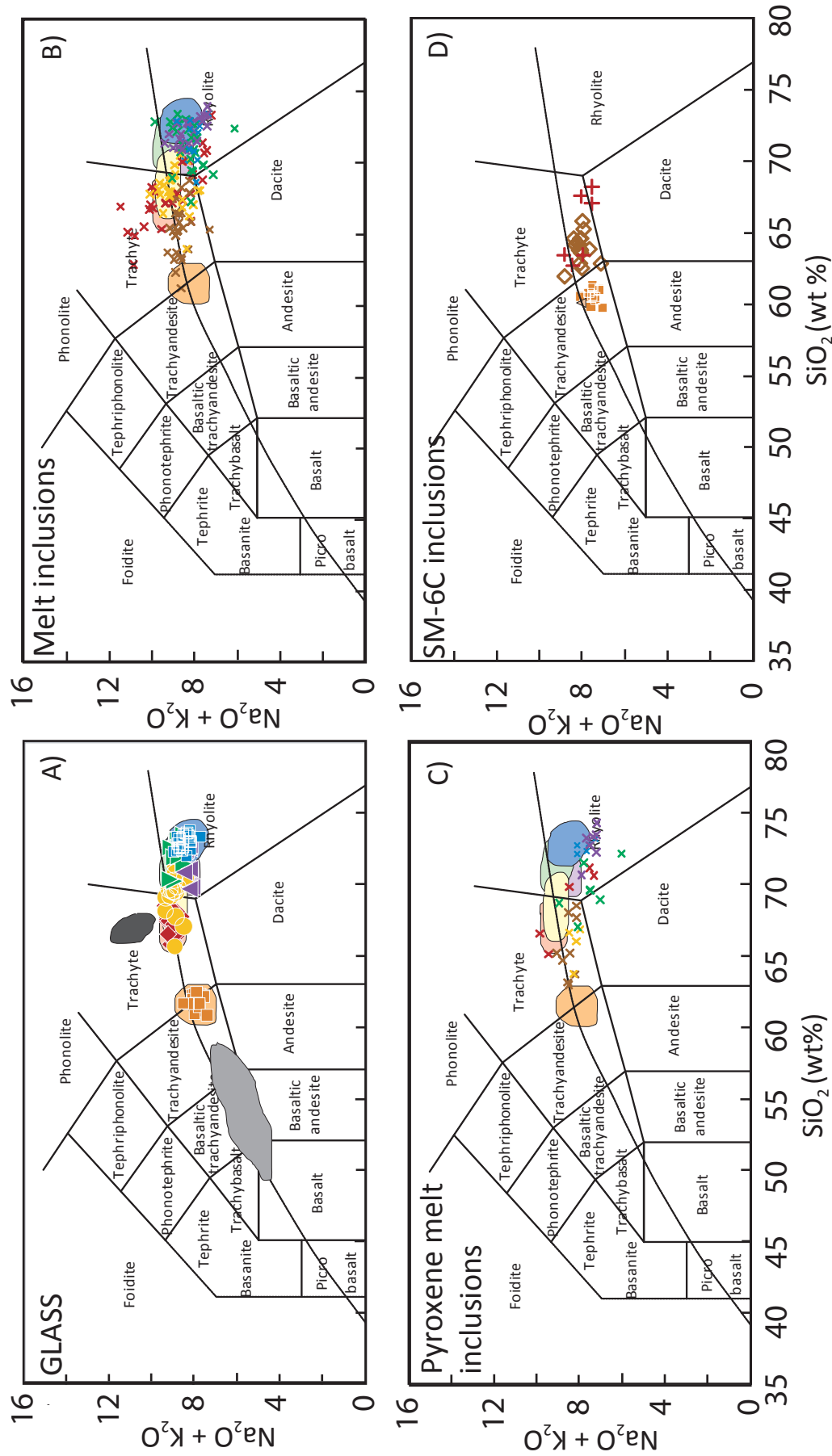


Figure 4.7 Total alkali-silica diagram of A) glass analyses; B) all melt inclusion analyses; C) clinopyroxene hosted melt inclusions; D) melt inclusions classified by host mineral for SM-6C. Red shades=Kaupokonui, orange/brown shades=SM-6C, yellow shades=Maketawa, green shades=Ingelwood b, blue shades=Ingelwood a, Purple shades=Korito. Fields indicate the glass analyses of each sample for comparison to melt inclusion data. For A) light grey field is published whole rock data from Price et al. (1999) and Turner et al. (2008); dark grey is glass data from Price et al. (2005); For D) filled squares represent glass, open diamonds are plagioclase hosted inclusions, crosses are clinopyroxene hosted

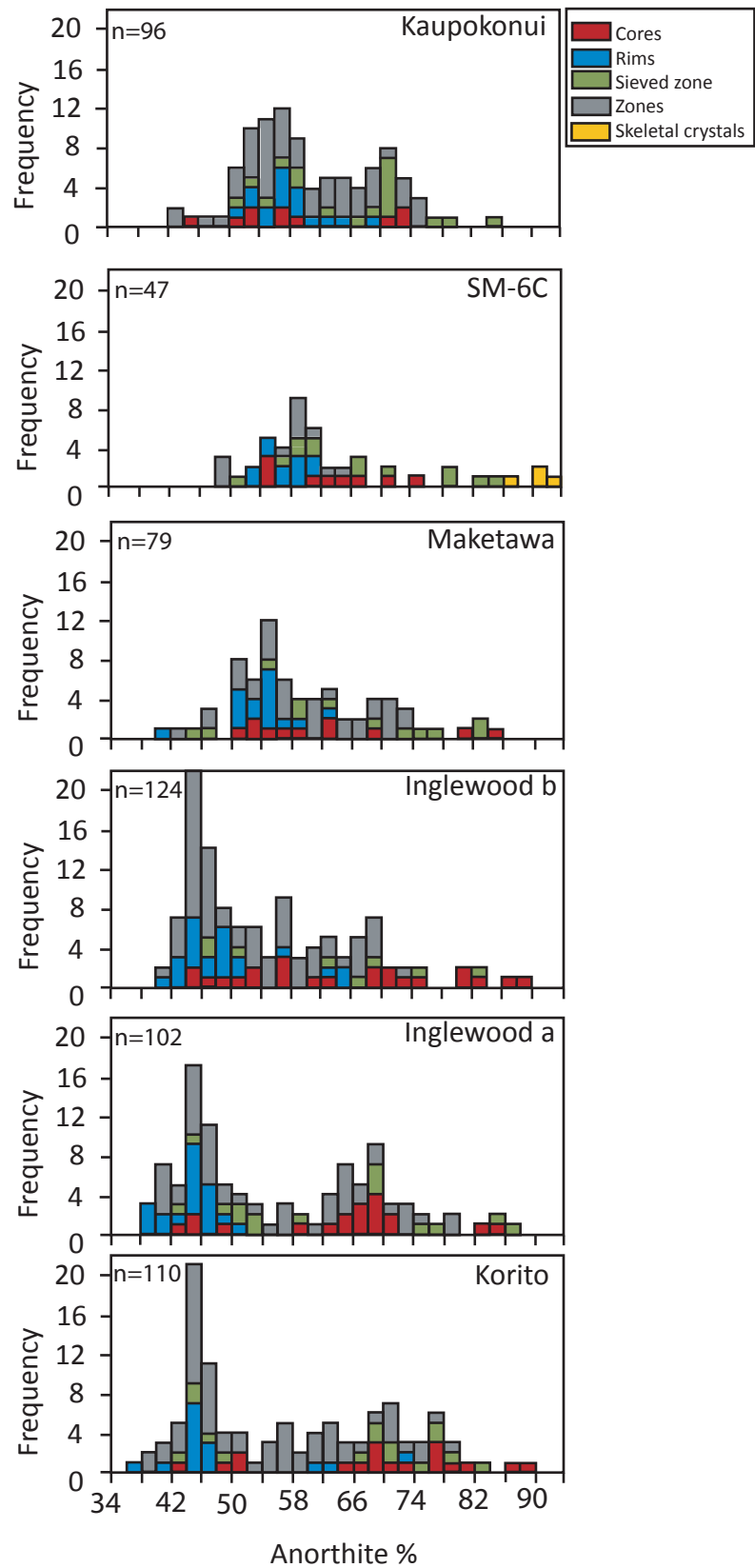


Figure 4.8 Anorthite content of plagioclase by crystal zone in each sample. Zoning refers to oscillatory zoning that is not a distinct core or rim zone. Sieved zoning occurs in both crystal cores and mantles. Core values span most of the range of each sample but rim compositions typically form a low anorthite peak.

sieved/patchy, a bimodal compositional pattern is observed for these zones. This gives the composition of the disequilibrium zone and the plagioclase composition that is in equilibrium with the new magmatic conditions. Sample SM-6C contains an additional crystal population referred to here as skeletal, where most of the crystal has been dissolved away. This population represents the most calcic plagioclase crystals (An_{86-92}).

4.2.3.2 Clinopyroxene

Clinopyroxene crystals from this study have diopside and augite compositions and show limited variation in major element chemistry. Mg# ($Mg\# = 100 \times (Mg/(Mg+Fe^{2+}))$) for all six samples fall within the range of Mg_{75-90} with a peak at 80-85 (Figure 4.9). Sample SM-6C exhibits slightly lower Mg# values on average and Kaupokonui has slightly elevated Mg# values. SiO_2 increases and TiO_2 and Al_2O_3 decrease with increasing Mg#. Other major elements show no clear trend.

Most clinopyroxene crystals have a patchy textured core with an oscillatory zoned rim. Kaupokonui also contains crystals with a distinct high-Mg rim or zone near the rim. In SM-6C and Korito a Fe-rich zone can be identified in some crystal populations. This zone is the mantle for SM-6C (between a Mg rich core and rim) and between the patchy core and oscillatory zoned rim for Korito. As a population, the clinopyroxene cores and rims are not distinguishable on the basis of major element data and aside from the distinctive zones already identified, no other pattern can be recognized on the basis of crystal zoning or texture.

4.2.3.3 Orthopyroxene

Orthopyroxene is a minor phase in the eruptives of Mt. Taranaki. It was detected only in SM-6C where it was present in cumulates and in reaction rims that mantled olivine cores. The orthopyroxene generally contain Fe-Ti oxides and melt inclusions. There is no clear distinction between cores and rims as these overlap with a $Mg\#_{75-80}$. Crystals associated with cumulates had a lower Mg# ($Mg\#_{66-70}$).

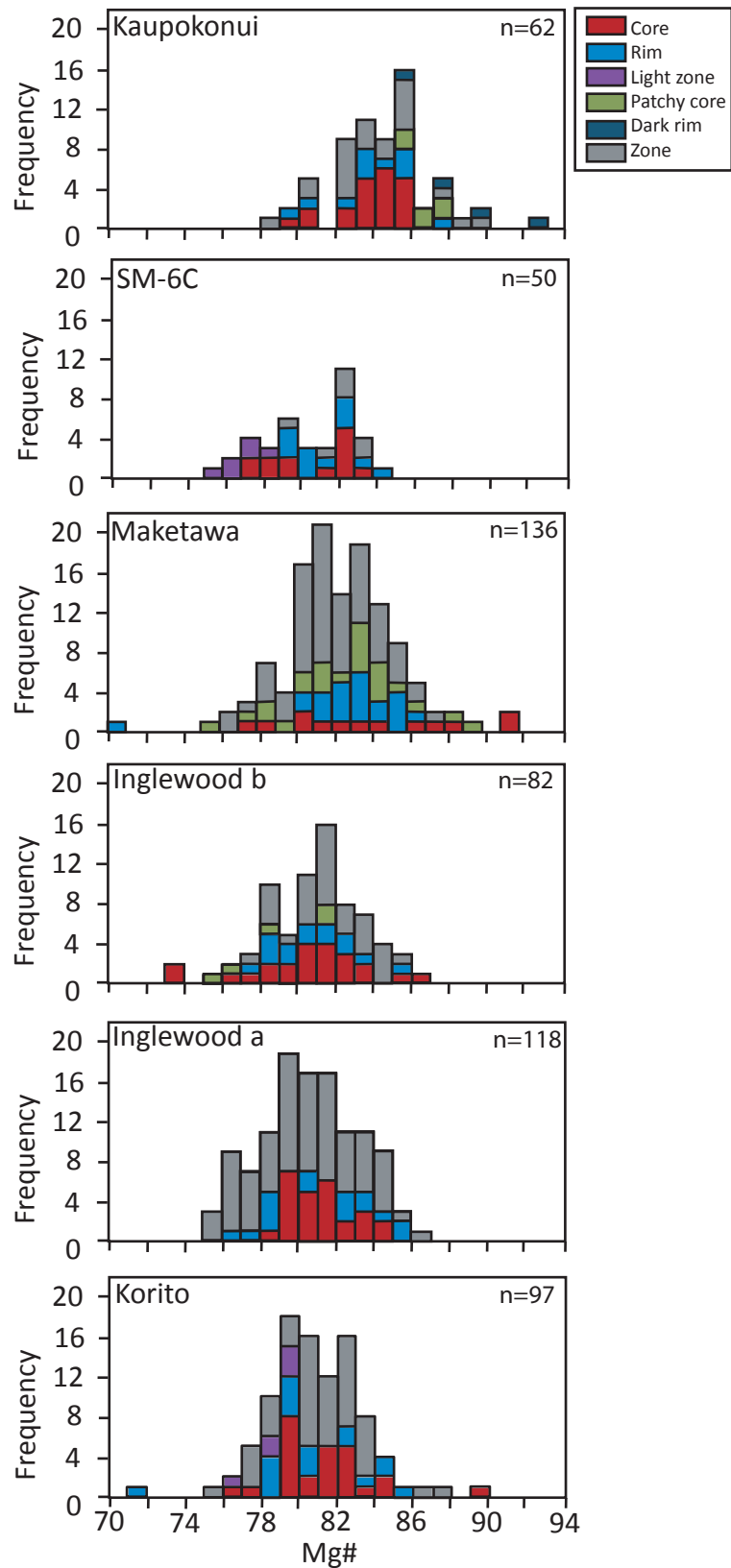


Figure 4.9 Histograms of clinopyroxene zones by Mg#. Analyses are divided into cores and rims. Light zones are a distinctive zone that appears to be correlated between crystals within a particular sample. Patchy textured cores that appear to have two compositions are plotted as 'patchy cores'. Dark rims refer to a Mg-rich rim population present only in Kaupokonui. Zones adjacent to the rim with similar characteristics are also in this group. Zoning that is not distinct is classified as 'zones'. There is no clear distinction between core and rim composition on the basis of Mg#.

4.2.3.4 Amphibole

Amphibole Mg# ($Mg\# = Mg/(Mg+Fe)$) varies from 0.6-0.9 with a dominant population of 0.7-0.8. This peak shifts to slightly higher Mg# values with time. Cores and rims overlap for each sample with core compositions spanning the entire Mg# range for each sample. There is a high Mg# population of rims in each sample ($Mg\# = 0.76-0.8$) and a population of low Mg rims in some samples (Maketawa and Inglewood a) which clusters around 0.66-0.7. In most cases the higher Mg rim population overlaps a peak in the core composition. This is especially well illustrated in Inglewood b where two core populations are distinguished on the basis of crystal texture as well as chemistry and the rim compositions overlap with the high Mg, 'dark core' population.

SM-6C does not follow most of the trends discussed above. This sample shows a bimodal distribution that falls on either side of the peak Mg# of all other samples (Figure 4.10a). The core compositions fall within a discrete peak and the rim compositions are bimodal with one population overlapping with the cores and the other coinciding with the low Mg# rim population observed in other samples.

The Al content (Al_2O_3 wt%) of amphibole crystals distinguishes cores and rims more effectively than Mg# for Inglewood a and b and Korito (Figure 4.10b). Core compositions again span the entire range but there is a dominant low Al rim population common to these three samples. The same pattern is observed in the Al data as has been identified in the Mg values for Kaupokonui, SM-6C and Maketawa.

4.2.3.5 Fe-Ti oxides

Titanomagnetite is the dominant Fe-Ti oxide phase found in these eruptives at Mt Taranaki. It is present in the groundmass as euhedral to subhedral crystals ranging in size from < 10 to 200 μm . Titanomagnetite is commonly found associated with, or as inclusions in, clinopyroxene, orthopyroxene, amphibole and rare plagioclase crystals. Fe-Ti oxides are particularly common

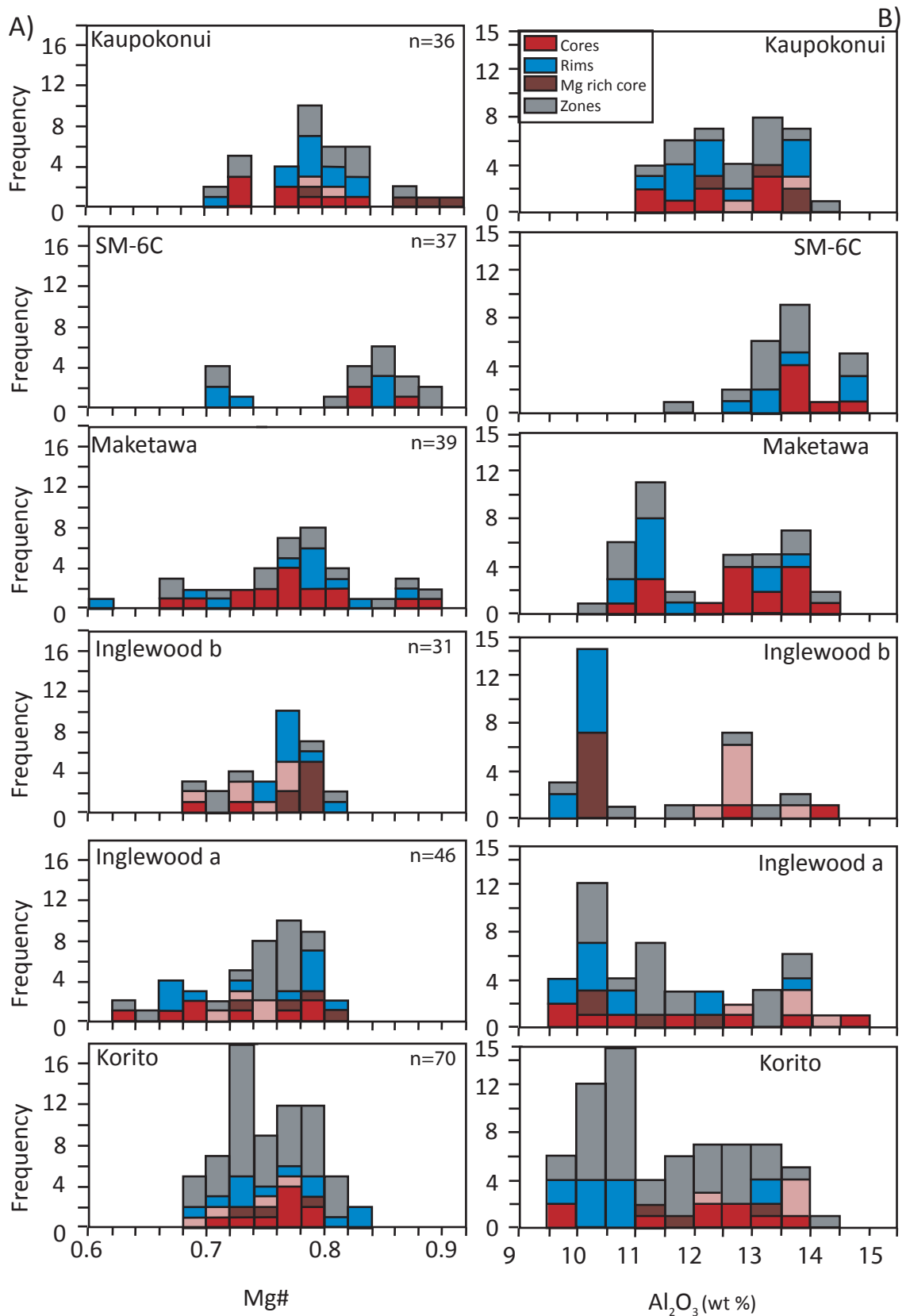


Figure 4.10 Histograms of amphibole composition by (A) Mg# and (B) Al₂O₃. Analyses have been divided into cores, rims and zoning that is not distinct. In some crystals there are different populations of cores on the basis of texture and these have been categorised separately as light or dark cores. Core values generally span the entire compositional range whereas rim concentrations are often clustered at low Al₂O₃, high Mg# values or bimodal in nature.

in clinopyroxene where smaller, anhedral to subhedral inclusions are present in the core and larger subhedral crystals form with the rim.

The samples can be divided into 4 groups on the basis of titanomagnetite major element chemistry (Figure 4.11): (1) A low ulvospinel population ($X'_{\text{usp}}_{0.15-0.19}$) with moderate Al_2O_3 and MnO , and high MgO and Fe_2O_3 that encompasses samples Kaupokonui and Maketawa. (2) Inglewood a and b and Korito are enriched in MnO with low concentrations of MgO and Al_2O_3 at an ulvospinel content of 0.16-0.21. (3) Amphibole hosted and broken groundmass crystals from SM-6C have a low ulvospinel content that overlaps with group 1. (4) Groundmass and clinopyroxene hosted oxides from sample SM-6C which have a high ulvospinel content ($X'_{\text{usp}}_{0.23-0.27}$). Groups 3 and 4 broadly overlap in other major elements and are relatively enriched in Al_2O_3 and MgO and depleted in MnO , FeO and Fe_2O_3 .

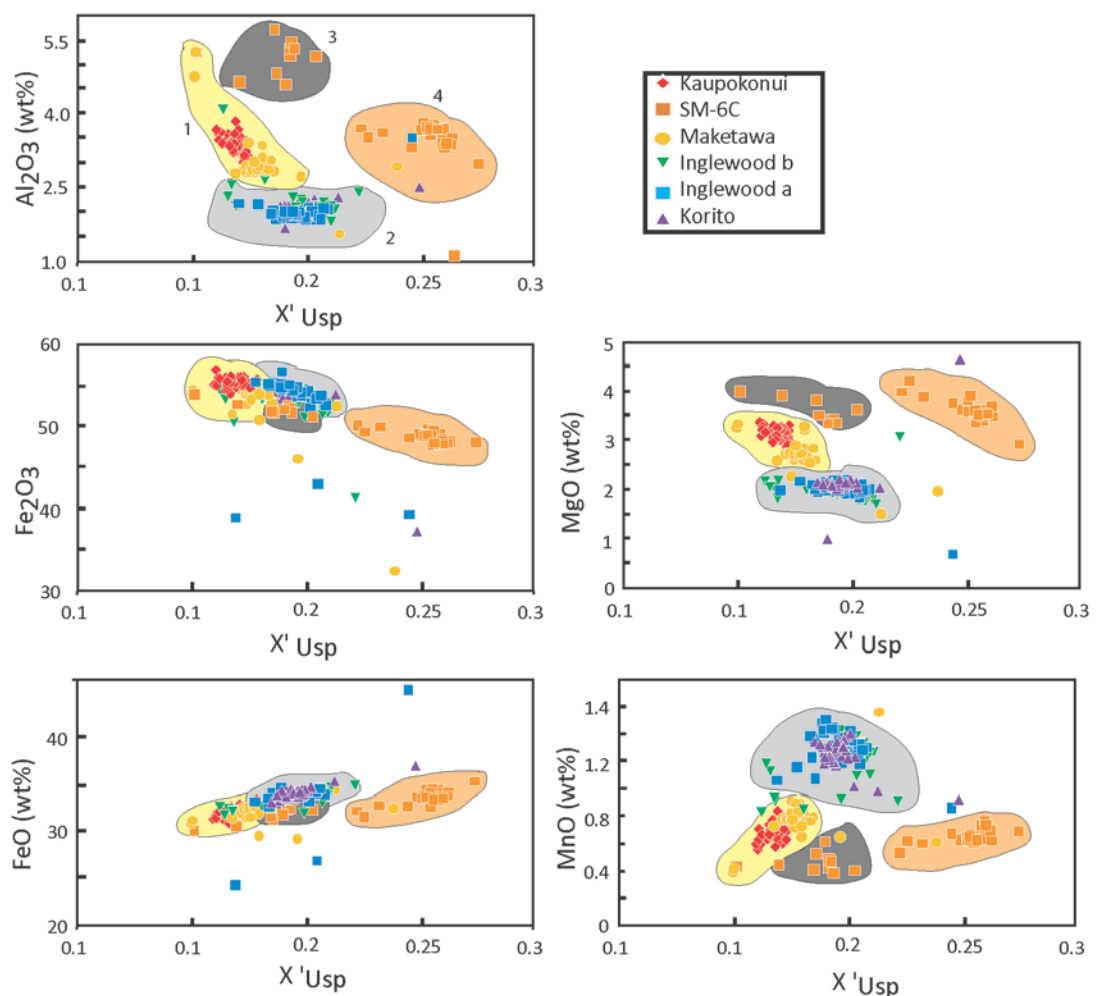


Figure 4.11 Bivariate diagrams of ulvospinel versus selected element oxides. Ulvospinel (X'_{Usp}) was calculated using the method of Stormer (1983). Four groups of titanomagnetite can be identified and this is particularly well illustrated in a plot of X'_{Usp} vs Al_2O_3

4.3 TRACE ELEMENT CHEMISTRY

4.3.1 GLASS TRACE ELEMENT CHEMISTRY

Most trace elements show a negative relationship with SiO₂ as illustrated in Figure 4.12. Compatible elements such as Co, Sc, V and Sr form a linear trend with SM-6C sometimes plotting above this line. Other trace elements show less variation and the negative correlation is less pronounced. Inglewood b is enriched in these elements and therefore plots off the trend for incompatible elements. Fluid mobile elements, in particular the LILEs are enriched in Kaupokonui and Inglewood b. SM-6C, Maketawa, Inglewood a and Korito all show similar trends for all trace elements. SM-6C is enriched in all elements with the most significant enrichments in compatible elements.

The rare earth element (REE) diagram shows enrichment in the light REEs (LREE) and depletion in the middle REEs (MREE) for each of the six samples (Figure 4.13a). Maketawa, Inglewood b and Korito have similar chondrite normalised REE concentrations. Inglewood a and SM-6C have relative depletion and enrichment in REEs respectively, with SM-6C exhibiting the larger offset. Each of the samples also exhibits a marked negative Eu anomaly (Eu/Eu*). Most samples have similar Eu/Eu* of around 0.8 but Kaupokonui and Maketawa have smaller Eu anomalies. Maketawa has a slight negative europium anomaly with Eu/Eu* of 0.94.

A multi-element diagram (Figure 4.13b) shows a typical subduction signature when normalised to N-MORB. There is an enrichment in the LILEs such as Cs, Rb and Ba and other fluid mobile elements like Pb. There is also a depletion in high field strength elements (HFSE) especially Nb and Ta as well as Sr and Ti which are strongly compatible in commonly crystallising phases of these eruptives. The variation between the samples is similar to that illustrated by the REE diagram where SM-6C is relatively enriched in these elements and Inglewood a is slightly depleted compared with the other samples. This offset is similar for each element except Li which is homogeneous across all samples. Inglewood b has a slight enrichment in Zr and Hf.

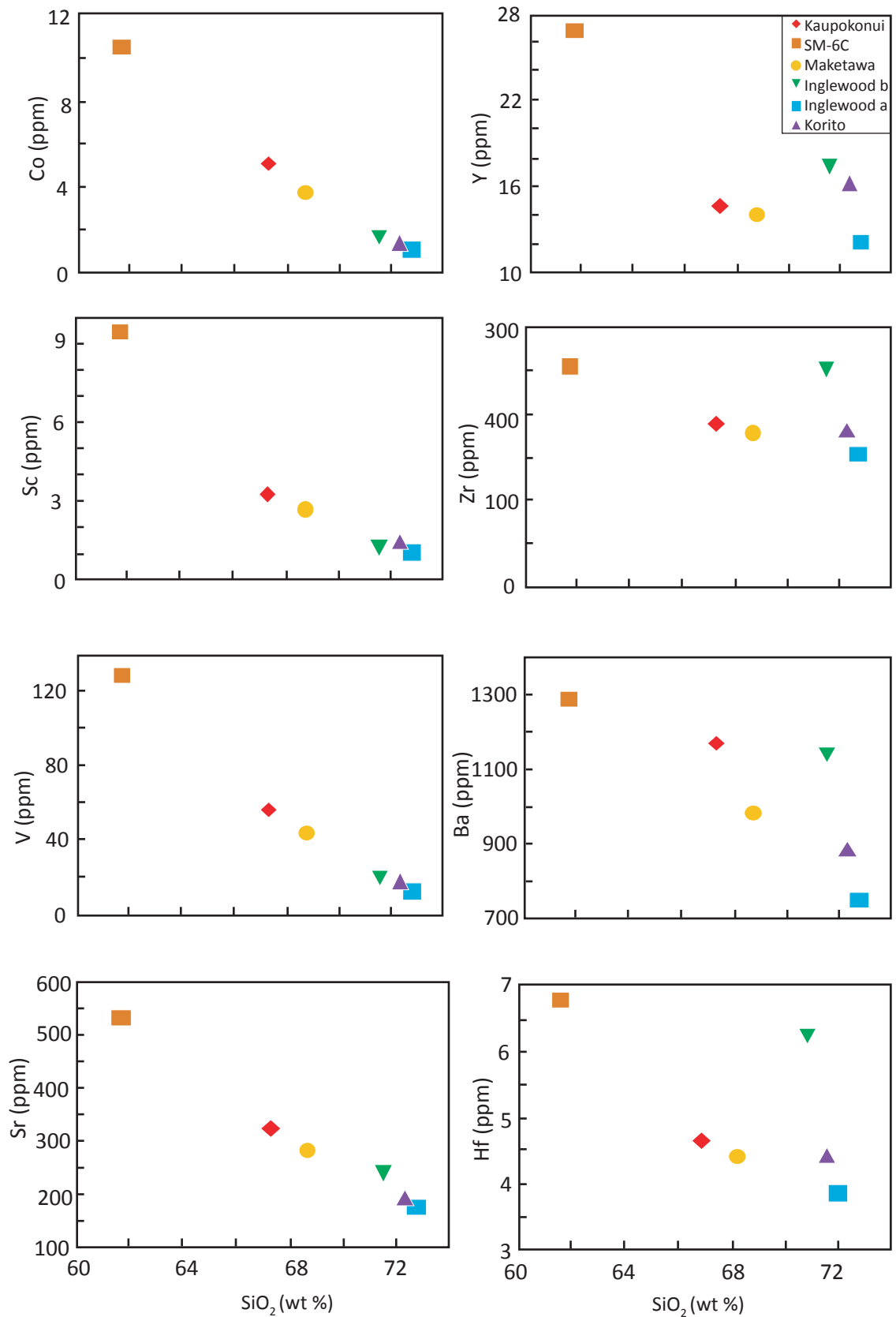


Figure 4.12 Representative trace elements plotted versus SiO₂ of the glass compositions of Taranaki eruptives. Compatible elements such as Co, Sc, V and Sr show a negative linear trend with SiO₂. Less variability is observed with other trace element concentrations (Y, Nb, Ba and Hf). 2 SD errors are smaller than graph symbols

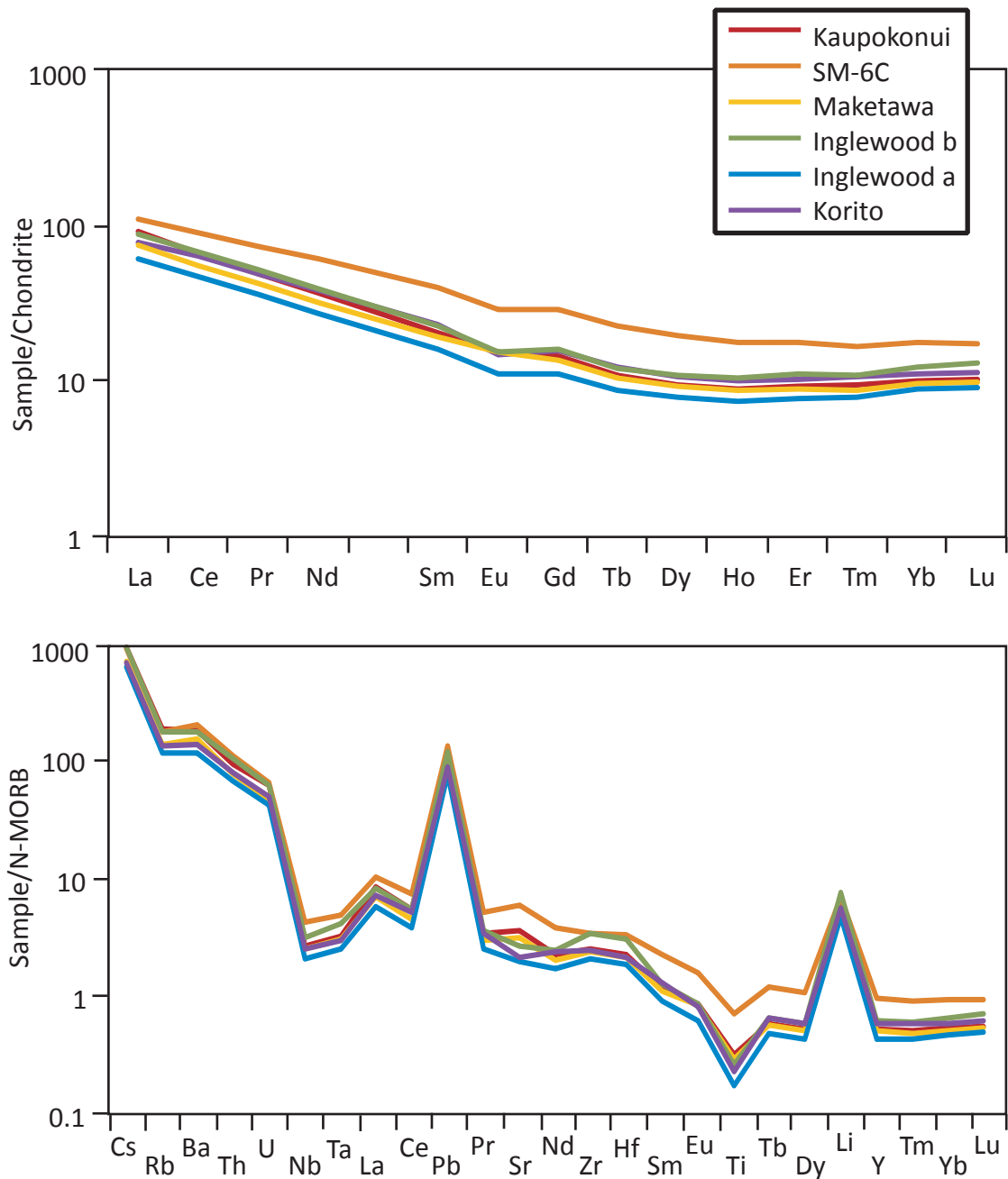


Figure 4.13 Diagrams of glass compositions illustrating the pattern and variation of Taranaki eruptives. All samples show the same broad trends. SM-6C is relatively enriched and Inglewood a is relatively depleted in trace elements. Normalising values for N-MORB were taken from Sun & McDonough (1989). (A) chondrite-normalised rare earth element diagram. All samples show enrichment in light REEs, a negative Eu anomaly characteristic of plagioclase fractionation and a trough in the MREEs attributed to amphibole fractionation. (B) Multi-element diagram normalised to N-MORB. All samples show an enrichment in LILE, Pb and Li and depletion in HFSE and compatible elements.

4.3.2 MINERAL TRACE ELEMENT CHEMISTRY

Trace element concentrations generally correlate with the major element data as positive correlations are observed for compatible elements and negative relationships for incompatible elements (Figures 4.14, 4.16 and 4.18). However, a large degree of variability is also evident within this trace element data set.

The overall patterns of the mineral specific multi-element plots are controlled by the partition coefficients of the mineral phase of interest and the composition of the equilibrium melt as discussed above (Figures 4.15, 4.17 and 4.19). There is a slight distinction between core and rim analyses with one population containing a greater number of relatively enriched compositions than the other. These two populations overlap substantially so the core/rim distinction identified in the major element data is generally less evident, in part because of the logarithmic scale of these plots. The variation within a sample is greater than the variation between samples.

4.3.2.1 Plagioclase

The trace elements measured in plagioclase show negative correlations with anorthite content with the exception of Sr. (Figure 4.14). There is a large degree of variability as concentrations range by a factor of 2-10 at a given anorthite content and by up to an order of magnitude for the entire sample suite. The deviations from this trend include an anomalous enrichment of Li in the rims of Kaupokonui and Maketawa plagioclase and a change in the trend of Sr and Ba correlations at $An > 70$ for Inglewood a and b and Korito plagioclase. Sr changes from a positive to a negative relationship with An content and the Ba contents of these analyses decreases at a slower rate as anorthite content increases.

The same multi-element pattern is observed in all plagioclase analyses and the range of values for each sample overlaps (Figure 4.15). The variation within each sample is up to an order of magnitude and this largely reflects the variation in the core compositions whereas the rim compositions are consistent between and within samples. Crystal rims are relatively more

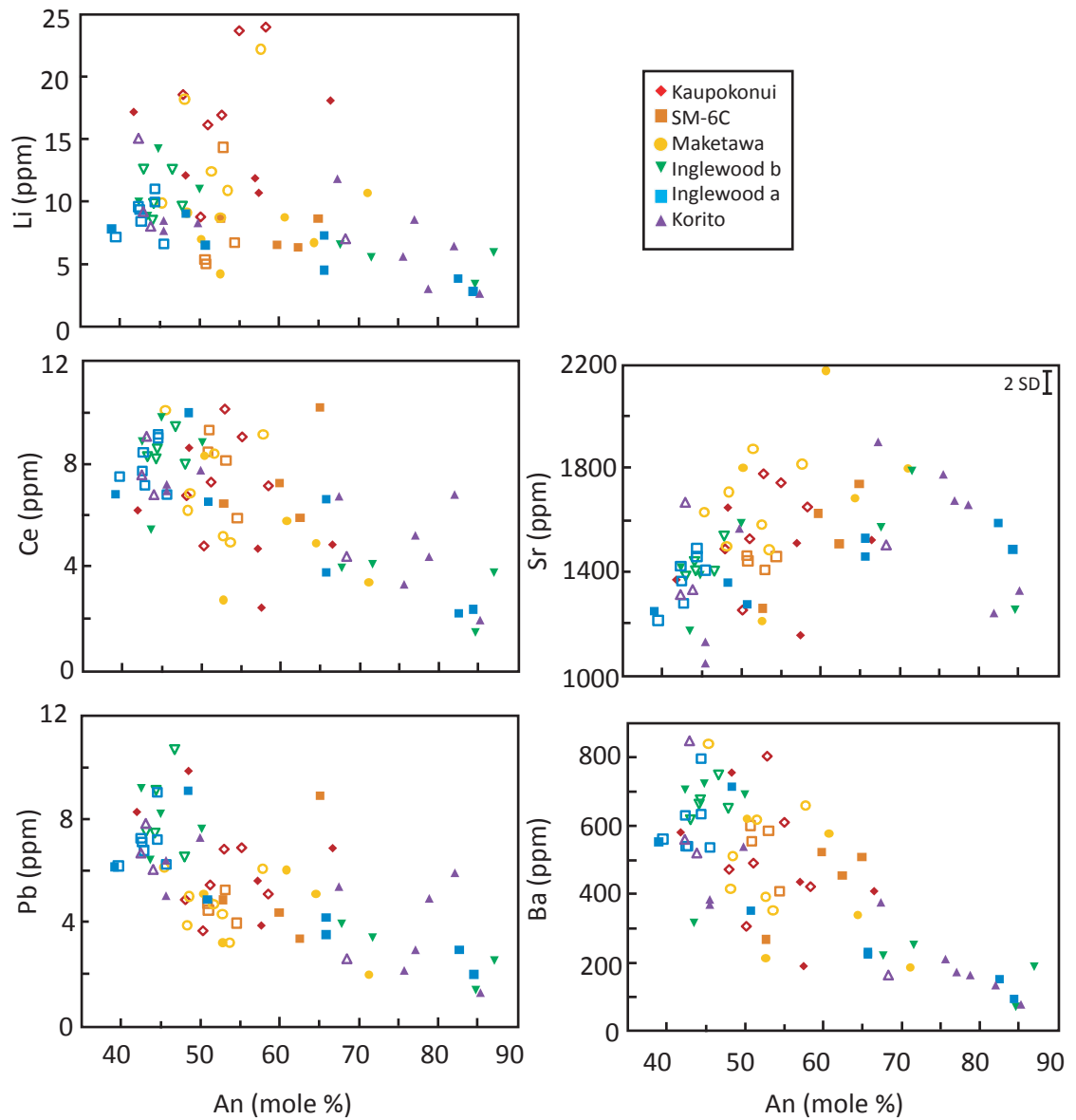


Figure 4.14 Selected trace elements plotted versus anorthite content of plagioclase crystals. Open symbols represent rim compositions and filled symbols indicate core analyses. Each of the trace elements except Sr show a negative correlation with anorthite content. Sr has a positive correlation with anorthite content except at the high anorthite end member where Sr values decrease. Kaupokonui and Maketawa show relative enrichments in Li and Sr. Errors as stated or smaller than symbol.

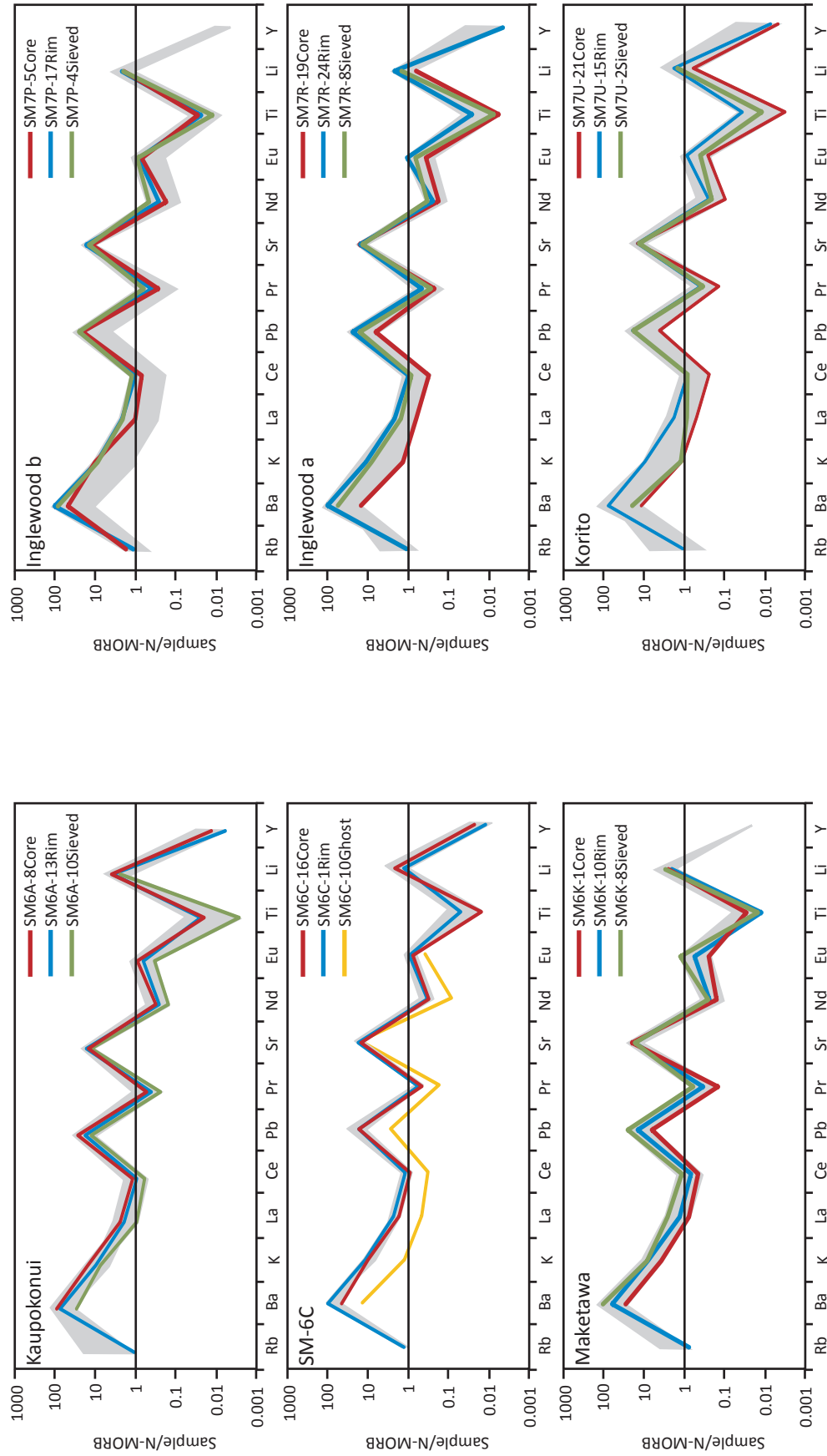


Figure 4.15 Multi-element diagrams of plagioclase trace element analyses classified by sample and mineral zone. The overall pattern is identical for each sample and the range of compositions overlaps between samples. Core analyses generally span the range of sample variability and rim analyses are consistent between and within samples. Grey fields indicate the range of compositions of that particular sample (excluding outliers). Red and blue lines are representative core and rim analyses respectively and green and yellow are representative sieved and ghost crystals.

evolved than cores in Inglewood a and b, Korito and SM-6C but the core analyses are enriched in Kaupokonui and Maketawa. The sieved zone compositions generally overlap the rims but extend to lower values. The ghost crystals present in SM-6C are around 7 times lower in trace element concentration than the dominant population. Sr values are the most consistent with a total variation of less than 2 ppm.

4.3.2.2 Clinopyroxene

There is a large range in the trace element chemistry of clinopyroxene crystals from Taranaki eruptives on the order of a factor of two to five (Figure 4.16). There is a slight positive correlation between Mg# and elements compatible in clinopyroxene such as Sc, V and Ni and elements that are compatible in other major mineral phases such as Sr. Negative correlations are evident in the incompatible elements at Mg# > 85 which primarily relates to the rims of Kaupokonui. Kaupokonui, SM-6C and Maketawa are enriched in compatible trace elements and depleted in incompatible elements compared with Inglewood a and b and Korito. There is no widespread differentiation between core and rim analyses although the rims of the two most primitive samples appear to contain higher abundance of compatible trace elements.

The overall trend observed in the multi-element diagrams (Figure 4.17) show little variability between samples and the dominant population of each sample is coincident in most cases. The exception is Maketawa, which is relatively depleted. In detail there are also fluctuations in the REEs and Li on the order of less than a factor of three.

Within the main population in each sample a distinction between the core and rim analyses can be identified. The trace element concentrations of cores are generally higher for SM-6C, Maketawa, Inglewood a and b but the rims are relatively enriched in Kaupokonui and Korito. This distinction is weak and the two groups overlap each other.

The high Mg#, dark rim population present in Kaupokonui displays a different trace element pattern. These are depleted in most elements with some present in concentrations of up to a factor of seven lower than the main population. Crystal 4 in Korito exhibits a different

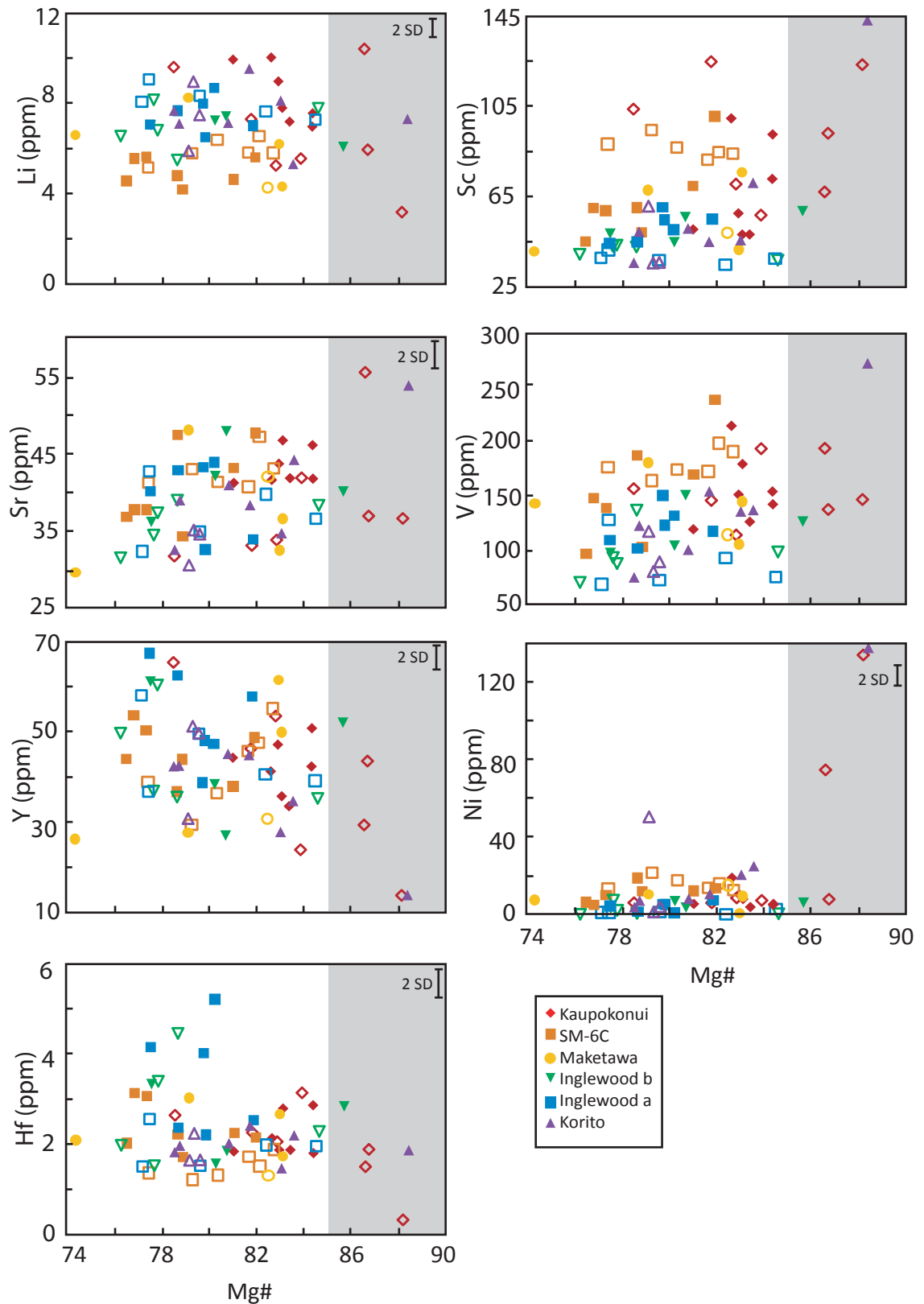


Figure 4.16 Selected trace elements plotted versus Mg# of clinopyroxene crystals. Open symbols represent rim compositions and filled symbols indicate core analyses. Kaupokonui, SM-6C and Maketawa show relative enrichments in compatible elements (Sc, V, Ni) compared to Inglewood a and b and Korito. Shaded area highlights Mg# > 85. Error bars as stated or smaller than symbol.

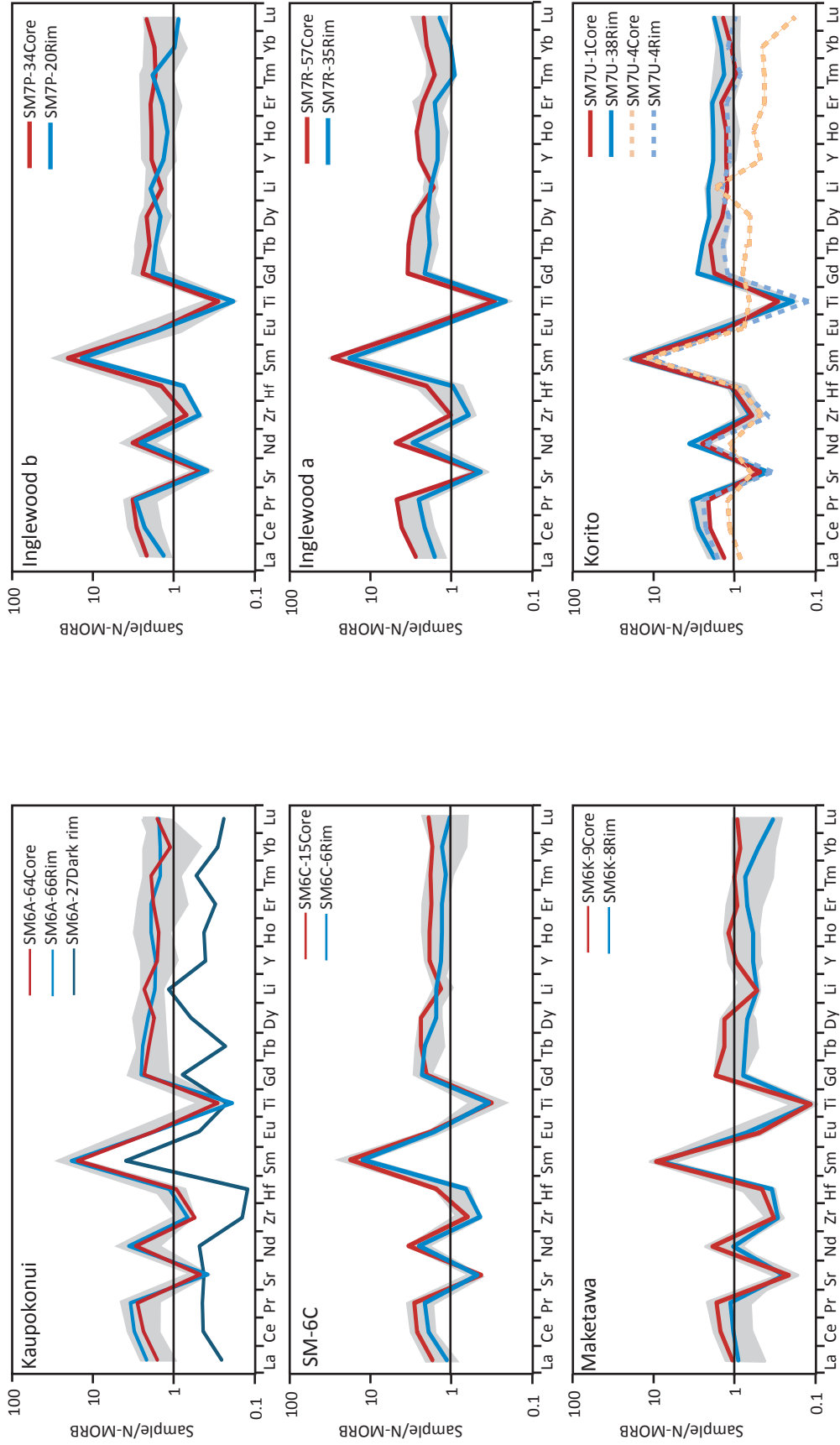


Figure 4.17 Multi-element diagrams of clinopyroxene trace element analyses plotted by sample. A representative core and rim analysis is plotted for each sample and the grey shaded field shows the variation of the main population for that sample. Any other distinct population is also represented, such as the Mg-rich dark rims in Kaupokonui and crystal SM7U-4 in Korito. The core and rim compositions overlap but one population is generally more enriched than the other. All analyses display the same general trends with a few exceptions such as Li and Lu.

chemistry, especially in its core. This is depleted in trace elements with a peak in Li and a lack of a negative anomaly at Ti. This unusual chemistry can also be identified as an outlier in Figure 4.16.

4.3.2.3 Amphibole

There is a large amount of variability in amphibole trace element concentrations with most elements varying by a factor of four (Figure 4.18). Most of this variability is at low Mg# values (Mg# <80). There is a weak correlation between Mg# and trace element concentrations. Compatible elements such as Sc, V and Ni have a slight positive correlation with Mg#. All other trace elements except Sr have a slight negative trend. The trace element data more clearly distinguish between samples, with Kaupokonui and SM-6C showing the least evolved chemistry (higher compatible and lower incompatible element concentrations), followed by Maketawa and Inglewood a and b displaying the most evolved chemistry in a trend which mimics that of the glass chemistry. Korito breaks this pattern, because although it is one of the evolved samples, it has Sr and incompatible trace element concentrations that overlap those of the less evolved samples.

The overall range of trace element compositions for each sample is broadly the same. There are two populations within each sample: Population 1 which is relatively depleted in trace elements and Population 2 which has a relatively enriched chemistry with negative anomalies at Th, U, Pb, Sr, Hf, Zr and Li (Figure 4.19). One population typically dominates a sample with ~10-20% of analyses comprising the minor group. This minor group is typically a population of amphibole core analyses except for Korito where this is rim analyses. Population 1 dominates in Kaupokonui, SM-6C and Korito samples, while Population 2 is the major group for the other 3 samples.

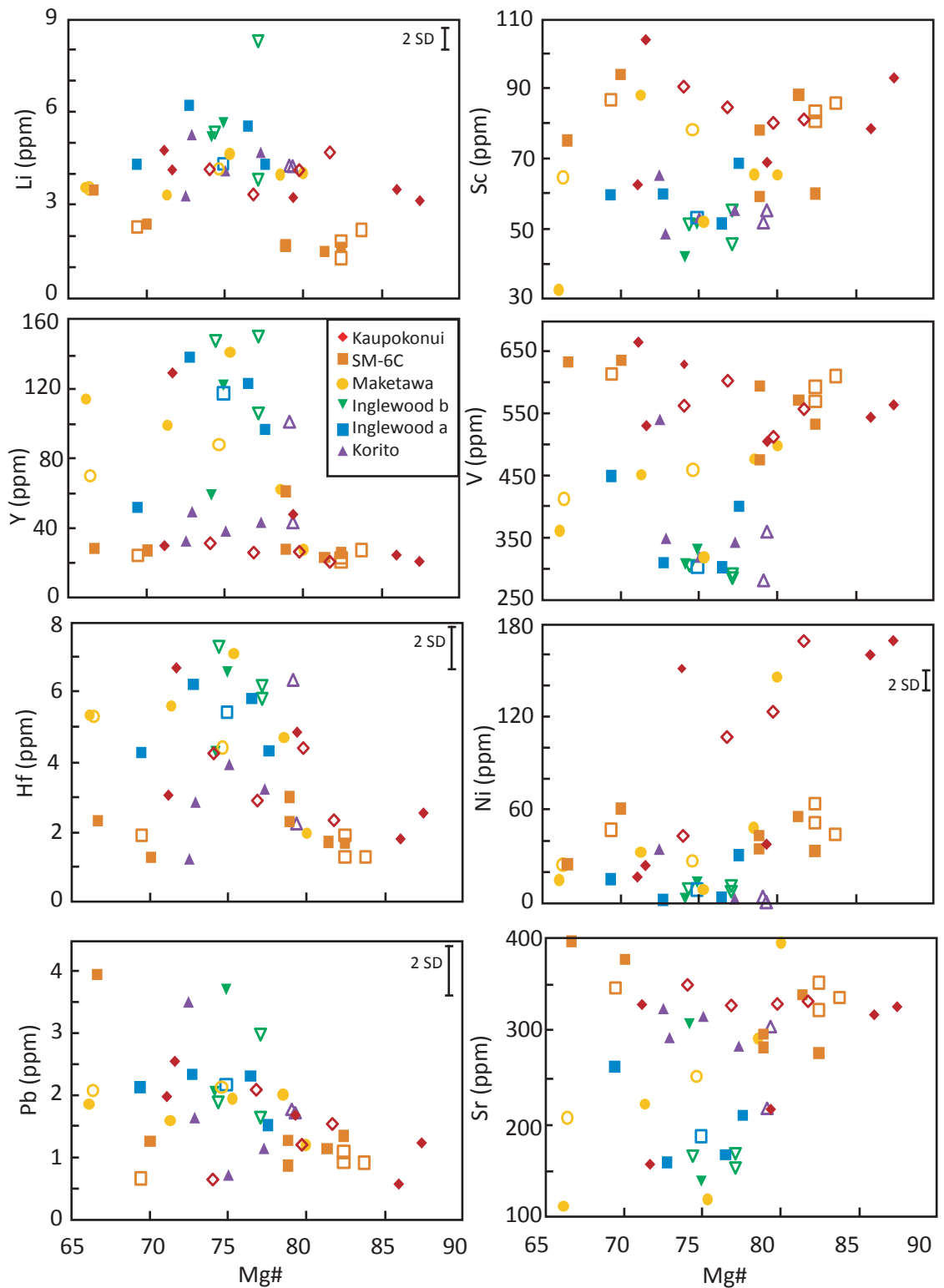


Figure 4.18 Selected trace elements versus Mg# for amphibole crystals. Open symbols represent rim compositions and filled symbols indicate core analyses. Kaupokonui, SM-6C and Maketawa have more primitive compositions with higher concentrations of compatible elements (Sc, V, Ni and Sr) and lower concentrations of incompatible elements (Li, Y, Hf and Pb). There is a large variation in trace elements concentration of a factor of 4 to 10 at a given Mg# where Mg# < 80. Error bars as stated or smaller than the symbol size.

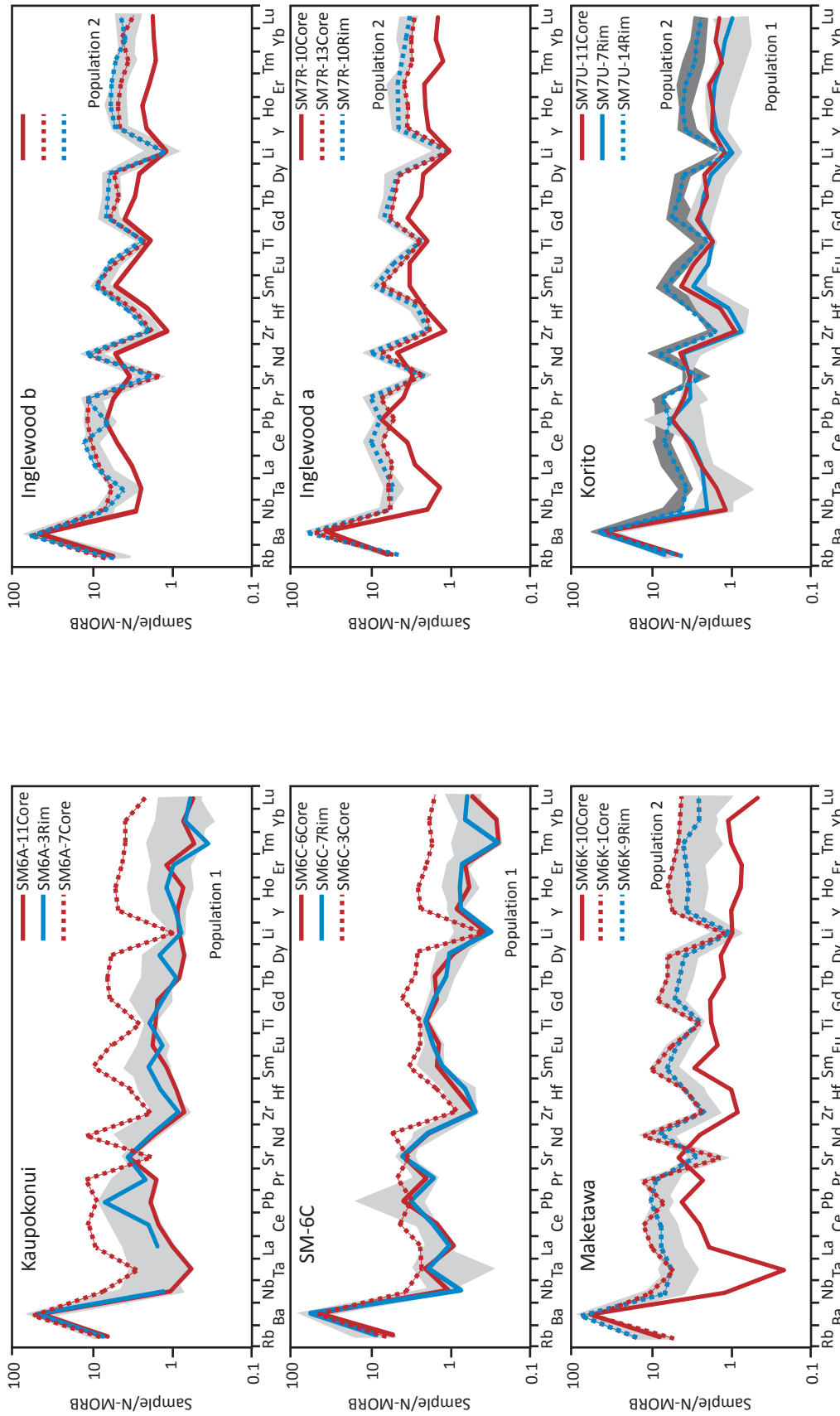


Figure 4.19 Multi-element diagrams of amphibole trace element analyses. Two populations can be identified in each sample with the solid lines representing Population 1 and the dashed lines representing Population 2. Grey shading indicates the range of each population where there are more than 2 analyses otherwise a representative analysis is displayed. Red and blue lines indicate representative core and rim analyses respectively. Population 1 encompasses mostly core analyses and Population 2 rim compositions except SM-6C and Kaupokonui where these associations reverse.

4.4 THERMOBAROMETRY

4.4.1 THERMOMETRY

All four thermometers applied to the sample suite returned the same temperature for each sample within the ± 42 °C model error (Figure 4.20). All six samples are also within model error of one another, however Inglewood a and b and Korito consistently return lower temperatures of ~860-920 °C compared with Kaupokonui, SM-6C and Maketawa, which have temperatures ~910-1000 °C. Sample SM-6C is the hottest sample. These temperatures are broadly consistent with the SiO₂ content of the samples with those highest in SiO₂ recording the coolest temperatures and vice versa.

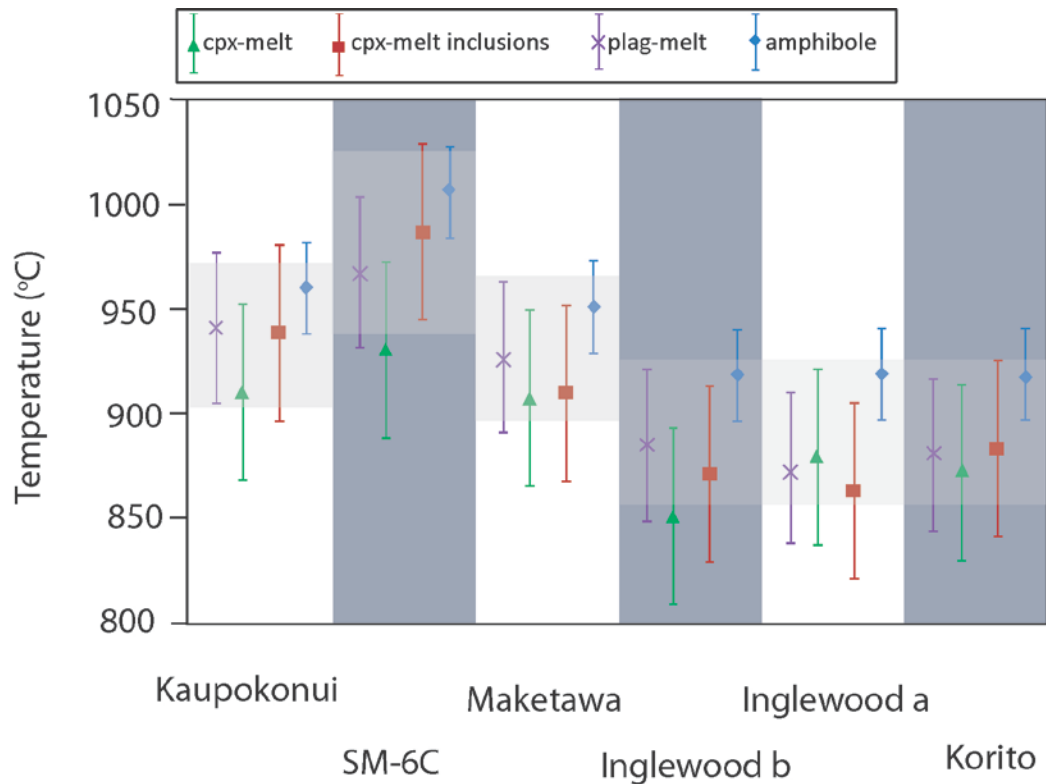


Figure 4.20 Summary of thermobarometry models. Symbols represent sample averages and error bars indicate the model error.

4.4.2 AMPHIBOLE THERMOBAROMETRY

Each sample spans a similar range of temperature, pressure, melt water content (H_2O_{melt}) and oxygen fugacity (Figures 4.21, 4.22, 4.23). Amphibole core values generally extend the range of observed values (temperature ~ 1050 to 900 °C; pressure ~ 200 to 600 MPa; $H_2O_{\text{melt}} \sim 4$ to 7 wt%; $\log fO_2 \sim -11$ to -9) but rims are typically clustered at low end member values, with a minor rim population overlapping the high core values. This is especially well illustrated by Inglewood b where there are two distinct amphibole populations. One is hotter, deeper as well as more hydrous and oxidised, and is comprised entirely of cores and zoning. The low temperature population is tightly constrained and contains amphibole rim values and the remaining cores and zones. This core-rim distinction is not present in Kaupokonui and SM-6C as cores and rims overlap the range observed in these samples. These samples also do not extend to values as low as most others and SM-6C exhibits the highest values for each variable. The older three samples have the lowest temperature, pressure, water content and oxygen fugacity.

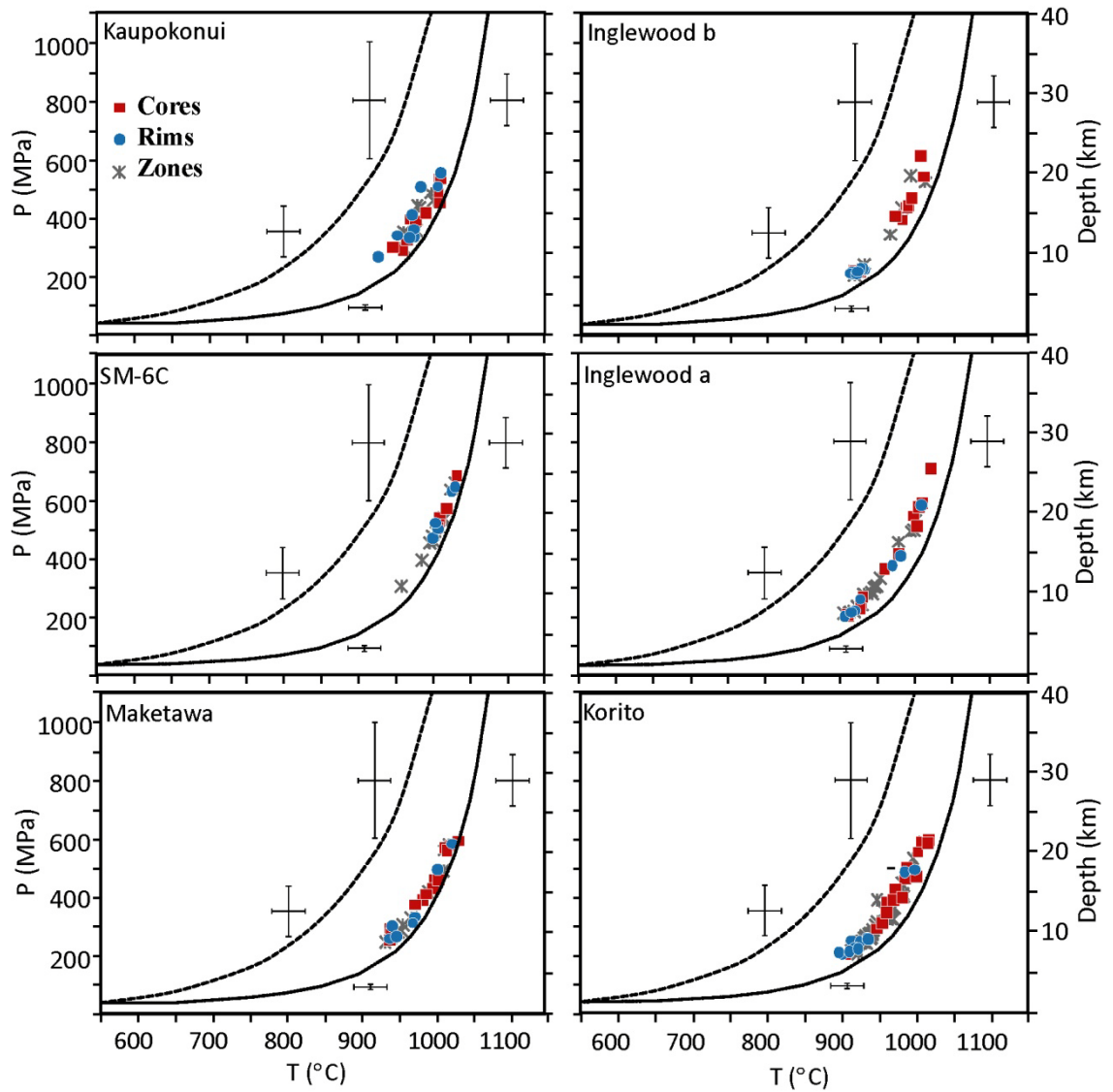


Figure 4.21 Amphibole thermobarometry results. Black curves outline the range of amphiboles this model is appropriate for, the base of which is determined by the amphibole stability curve. Temperature errors are constant $\pm 22^{\circ}\text{C}$, pressure errors range from 11% near the amphibole stability curve to 25% at the upper limit of appropriate amphibole values. The errors for these values are closer to 11% as they plot near the amphibole stability curve. Depth is calculated based on average specific weights of 2.7g/cm^3

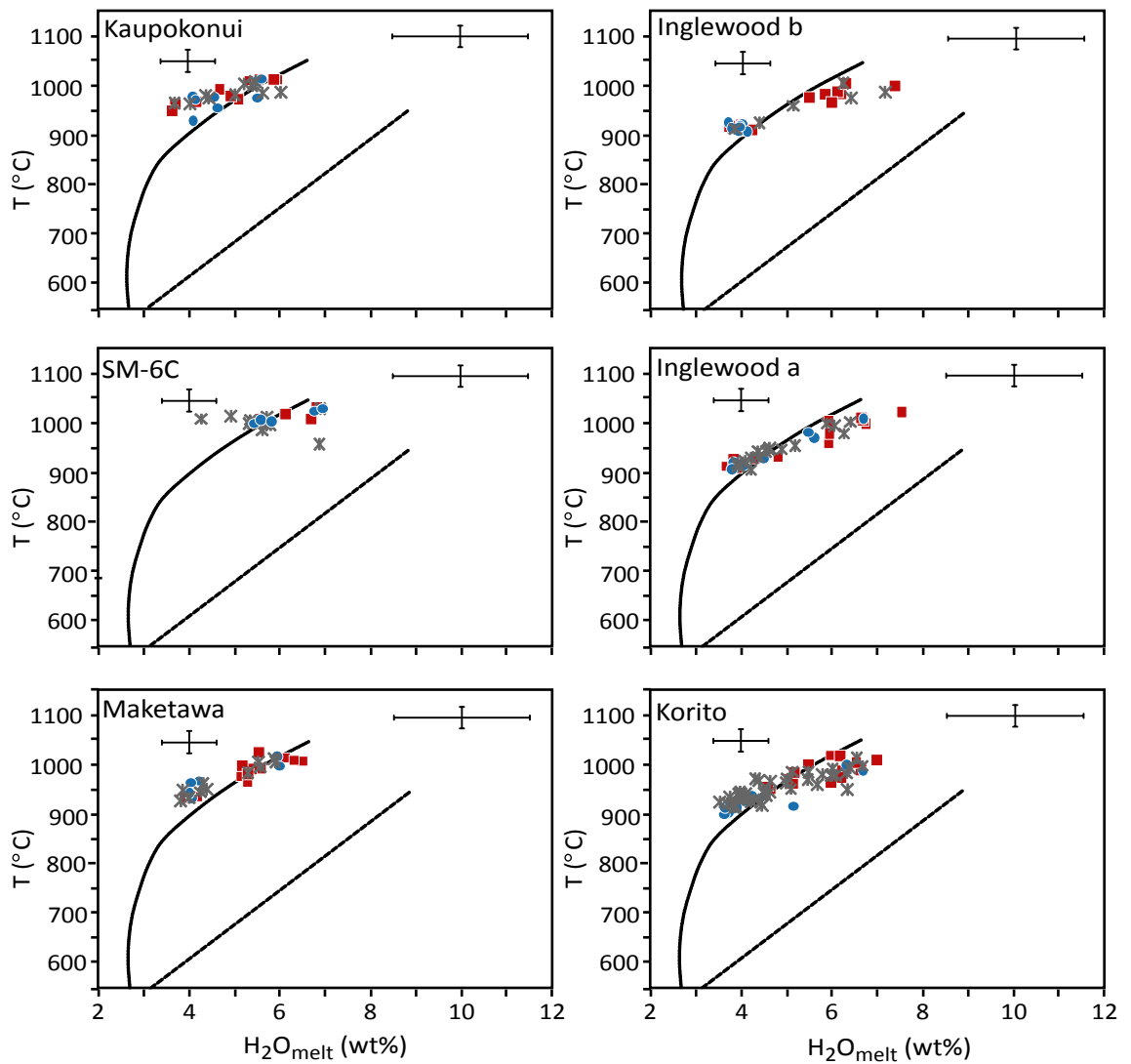


Figure 4.22 H₂O_{melt} vs temperature from amphibole thermometry and hygrometry models. Errors for temperature are constant at $\pm 22^\circ\text{C}$ and H₂O_{melt} errors are 15%. Black curves outline the range of amphiboles which are suitable for this model. The extended stability of some of these amphiboles is also evident in the Ridolfi et al. (2010) magnesiohastingsite data set and attributed to large amounts of CO₂ in the system at relatively high temperatures and low H₂O_{melt} stabilising magnesiohastingsite compositions. Symbols as for Figure 4.21.

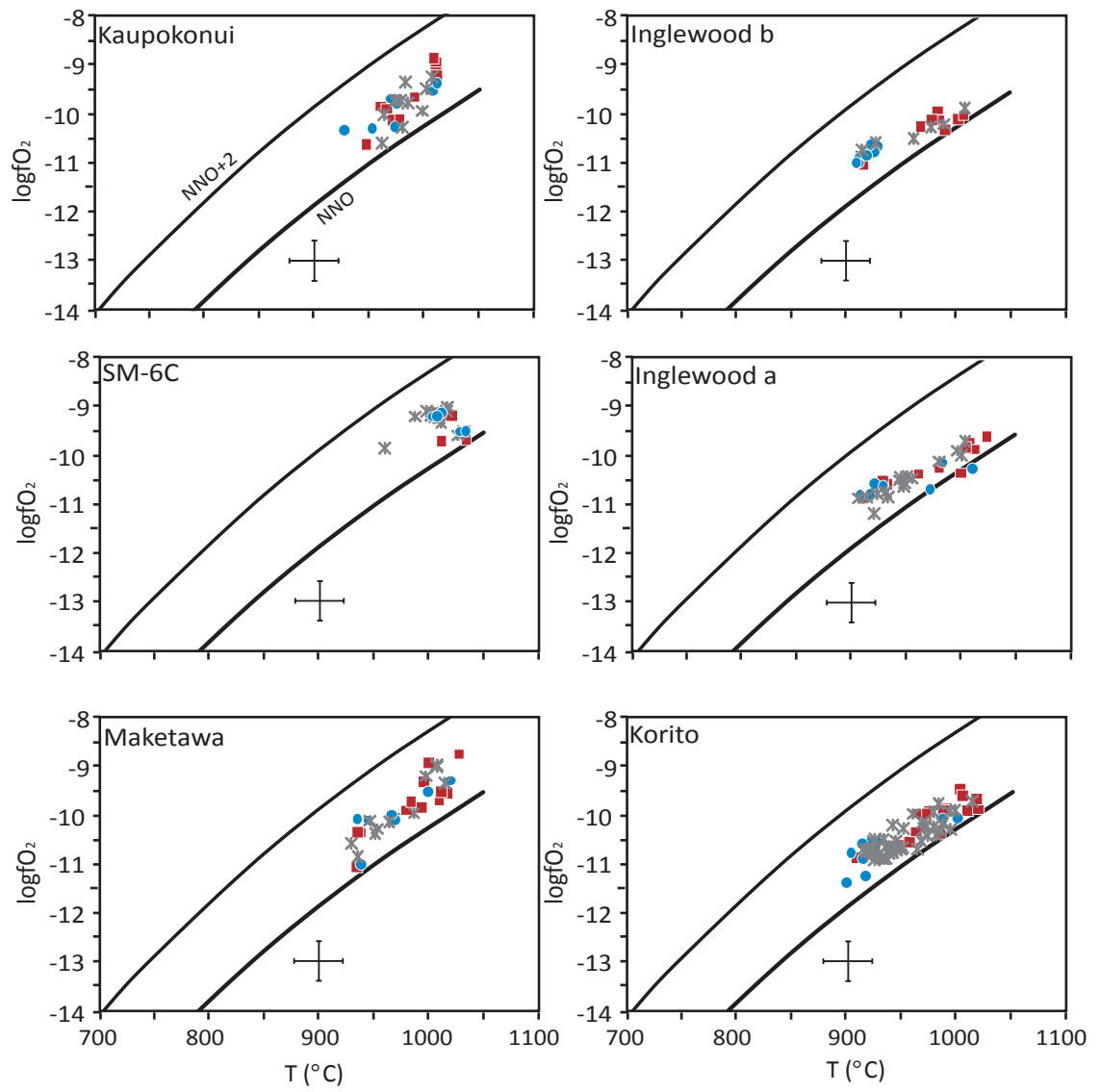


Figure 4.23 Temperature-oxygen fugacity results from amphibole thermometry and oxybarometry. Black curves represent Nickel-nickel oxide buffer (NNO) and NNO +2. Errors are constant at ± 22 C for themometry and 0.4 log unit for oxygen fugacity. Symbols as for Figure 4.21.

CHAPTER 5:
DISCUSSION

5.1 GLASS CHEMISTRY

Most of the previous geochemical studies of Mt Taranaki eruptives analysed whole rock samples (Price et al., 1992, 1999; Turner et al., 2008). Whole rock data is the weighted average of the heterogeneous crystal cargo and host melt (Davidson et al., 2007a). Glass represents the residual melt phase of the magma, which may or may not be related to the crystal cargo. Therefore these represent two different aspects of the magma system which provide different information about andesite petrogenesis. Whole rock information provides an overview of the system and detects broad scale processes and inputs into the system, whereas glass gives a snapshot of melt evolution and can be used in conjunction with mineral chemistry to unravel the complexities of the sub-volcanic magmatic system.

5.1.1 COMPARISON WITH PUBLISHED GLASS STUDIES

Much of the published glass analyses are from distal sites and have been investigated from a tephrostratigraphic perspective. Tephra layers originating at Taranaki have been identified distally in sediment cores from lakes (e.g. Lowe, 1988; Shane, 2005). These tephra records are better constrained chronologically than lava flow sequences. For example, the lava flow sequences are grouped into units encompassing 700 yr to 5000 yr and those eruptions that pre-date major sector collapse events are broadly grouped into Young Egmont Ring Plain and Old Egmont Ring Plain, which encompass thousands of years and tens of thousands of years, respectively (Stewart et al., 1996; Price et al., 1999). The tephrostratigraphic record provides a higher resolution, temporally constrained record that extends back as far as 70,000 yr (Shane, 2005). However, correlating between these units is challenging due to the typically heterogeneous nature of andesitic glass (Shane, 2005; Platz et al., 2007b).

The major element results from this study are consistent with published glass data from distal sites (Lowe, 1988; Shane, 2005) and proximal sites (Platz et al., 2007b; Figure 5.1). The groundmass glass compositions of Price et al. (2005) fall off this trend, most likely due to microlite crystallisation during and after lava emplacement. Published data from distal tephras from the past 70,000 yr show the same degree of major element variability as the ~3000 yr

record represented by the six samples investigated in this thesis. Unit Eg-2 from Lowe (1988) represents Inglewood a (Alloway et al., 1995). These values overlap when the SiO₂ errors of Eg-2 are considered (± 0.99 wt%).

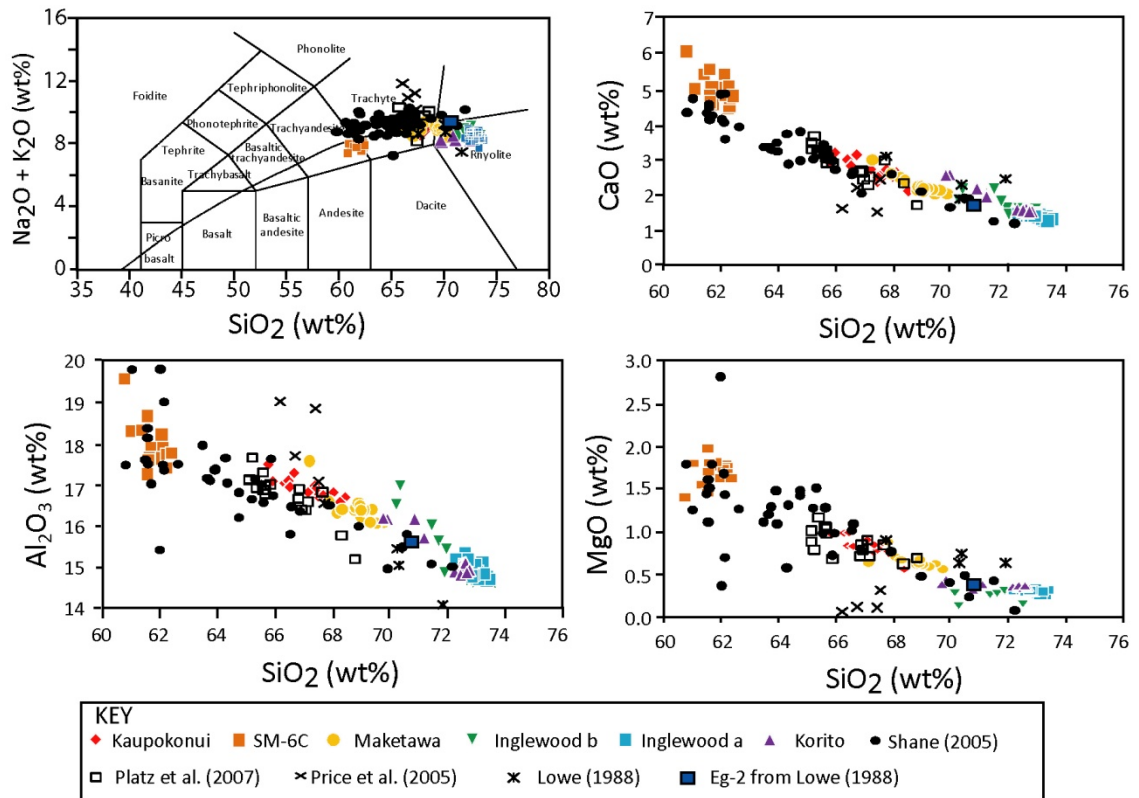


Figure 5.1 Comparison of glass data from this study and selected published data using selected major elements. Analyses are recalculated to 100% on a volatile free basis. Published data are mean analyses for a specific unit where 1 sd range from: SiO₂ = 0.45-3.83 wt%; CaO = 0.1-1.49; MgO = 0.06-0.76; Na₂O = 0.12-1.38; K₂O = 0.18-1.38 (except Platz et al., 2007a which are representative EMP analyses).

5.1.2 COMPARISON WITH WHOLE ROCK GEOCHEMISTRY

Taranaki major element glass data (this study; Price et al., 2005; Platz et al., 2007a) are more evolved than the associated whole rock data: the SiO₂ content of the glass ~60-75 wt% compared with ~53-57 wt% for the associated whole rock. Glass is also relatively depleted in most other major elements (except K₂O and Na₂O) when compared with whole rock analyses (Figure 5.2; Price et al., 1992, 1999; Stewart et al., 1996; Turner et al., 2008). The discrepancy between the two data types is due to the incorporation of mineral phases in the whole rock analyses, rather than different chemistries of the eruptives. This is illustrated by the major element data which show that whole rock and glass values are related by crystal accumulation

of plagioclase, clinopyroxene and amphibole. This has been quantified using least squares mixing modelling, which confirms that the whole rock chemistry of contemporaneous lava flows can be reproduced using a realistic mixture of phenocryst mineral assemblages and glass (Table 5.1). The modal mineral abundances used in this modelling broadly agree (i.e. $r^2 < 1$) with those estimated for lava flow sequences from Stewart et al. (1996), Price et al. (1999) and Turner et al. (2008) (Table 5.1). The plagioclase modal proportion model input is up to 10% higher than the published estimates probably due to the high abundance of plagioclase microlites in the whole rocks which were not included in these published estimates. The major element data from this study are in agreement with that of previous studies once the least squares mixing modelling has accounted for the comparison of glass and whole rock data.

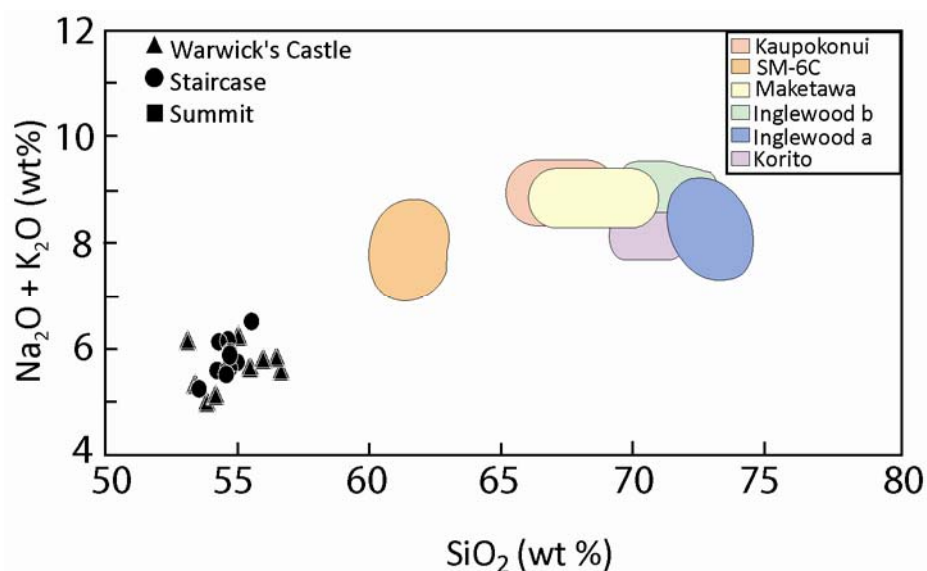


Figure 5.2 Total alkalis-silica plot of Taranaki eruptives. Whole rock data as compared with glass data from this study (coloured fields). Filled symbols represent published whole rock data and open symbols represent temporally associated published glass data. Published data taken from Stewart et al. (1996), Price et al. (1999; 2005), Platz et al. (2007a) and Turner et al. (2008).

Representative glass samples from this study were paired up with the average whole rock values for the contemporaneous lava flow sequences and used for least squares mixing modelling. However, the eruptions investigated in this study are unlikely to be directly represented in the lava flow sequences, but were paired up with the lava flow sequence which temporally coincides with the age of the associated tephra unit. The whole rock major element values for the Warwick's Castle and Staircase group lavas overlap and exhibit limited compositional variability (Figure

Korito		Warwick's Castle Group lava sequence							Model Whole rock	Difference between measured whole rock - model
		Whole rock			2 SD ¹					
Oxide (wt %)	Plagioclase	Clinopyroxene	Amphibole	Fe-Ti Oxides	Orthopyroxene	Glass				
Proportions	35%	5%	21%	4%	0%	35%				
SiO ₂	54.41	52.88	41.73	0.06	-	70.94	55.70	3.00	55.28	0.42
TiO ₂	0.03	0.33	2.70	7.13	-	0.34	0.85	0.25	1.00	-0.14
Al ₂ O ₃	29.40	1.93	11.16	2.08	-	14.81	18.09	0.76	18.00	0.09
FeO	0.51	7.88	12.85	88.42	-	1.63	7.22	1.52	7.38	-0.16
MnO	0.01	0.69	0.44	1.26	-	0.11	0.16	0.02	0.22	-0.06
MgO	0.03	14.79	13.11	2.06	-	0.34	3.30	1.79	3.70	-0.40
CaO	11.36	22.03	11.72	0.01	-	1.58	8.13	1.27	8.09	0.04
Na ₂ O	4.55	0.35	2.11	-	-	3.85	3.60	0.59	3.40	0.20
K ₂ O	0.51	-	0.92	-	-	4.46	2.21	0.70	1.93	0.28
									Σr ²	0.51

SM-6C		Staircase Group lava sequence							Model Whole rock	Difference between measured whole rock - model
		Whole rock			2 SD ¹					
Oxide (wt %)	Plagioclase	Clinopyroxene	Amphibole	Fe-Ti Oxides	Orthopyroxene	Glass				
Proportions	20%	9%	1%	4%	1%	65%				
SiO ₂	51.99	52.59	40.77	0.09	53.60	60.08	54.64	0.55	55.13	-0.49
TiO ₂	0.05	0.46	2.49	8.14	0.34	0.67	0.91	0.06	0.84	0.07
Al ₂ O ₃	29.60	2.53	13.29	4.05	1.18	17.56	17.60	0.32	17.87	-0.27
FeO	0.68	8.06	11.31	82.65	16.16	4.51	8.00	0.51	7.86	0.14
MnO	-	0.42	0.15	0.59	-	0.14	0.16	0.01	0.16	0.01
MgO	0.06	15.47	13.74	3.61	26.01	1.63	3.64	0.38	3.79	-0.14
CaO	12.42	20.86	12.26	0.11	1.45	4.98	8.30	0.33	7.79	0.51
Na ₂ O	3.86	0.39	2.14	-	0.03	4.32	3.57	0.57	3.64	-0.07
K ₂ O	0.54	-	1.00	-	-	3.38	2.27	0.10	2.32	-0.05
									Σr ²	0.63

Oxide (wt %)	Kaupokonui										Staircase Group lava sequence			Difference between measured whole rock - model		
	Plagioclase		Clinopyroxene		Amphibole		Fe-Ti Oxides		Orthopyroxene		Glass		Whole rock		2 SD ¹	Model Whole rock
	30%	9%	14%	5%	0%	42%	Whole rock	2 SD ¹	Model Whole rock							
Proportions	30%	9%	14%	5%	0%	42%	Whole rock	2 SD ¹	Model Whole rock							
SiO ₂	53.51	52.76	40.91	0.07	-	66.53	54.64	0.55	54.48	0.16						
TiO ₂	0.03	0.34	2.45	6.13	-	0.43	0.91	0.06	0.87	0.04						
Al ₂ O ₃	29.61	2.28	11.96	3.33	-	16.65	17.60	0.32	17.92	-0.32						
FeO	0.54	7.56	12.02	87.49	-	2.71	8.00	0.51	8.04	-0.04						
MnO	-	0.50	0.24	0.68	-	0.10	0.16	0.01	0.16	0.01						
MgO	0.05	15.76	13.28	3.08	-	0.83	3.64	0.38	3.79	-0.15						
CaO	11.91	21.30	11.82	0.06	-	2.69	8.30	0.33	8.28	0.02						
Na ₂ O	4.23	0.44	2.02	-	-	4.21	3.57	0.57	3.36	0.21						
K ₂ O	0.52	-	1.10	-	-	4.65	2.27	0.10	2.27	0.00						
							Σr²		0.20							

Table 5.1 Least squares mixing modelling results for selected samples. Using average glass and mineral compositions for each sample, the proportions of each phase were adjusted to give a whole rock composition that best fit the average whole rock data for the lava sequence which temporally overlaps the tephra unit.

¹ Two standard deviation of published whole rock data for lava flow sequence of interest using data from Stewart et al. (1996), Price et al. (1999) and Turner et al. (2008)

5.2; Stewart et al., 1996; Price et al., 1999; Turner et al., 2008). The close fit of each sample to this limited whole rock range may point to some of the samples having approximately the same major element whole rock compositions with the observed variations in major element glass chemistry due to late stage crystallisation. Price et al. (2005) came to a similar conclusion when comparing modal groundmass abundance with whole rock compositions for flow groups of Ruapehu eruptives, postulating that 20-30% of the crystal populations could have formed during closed system crystallisation.

Xenoliths are common in Taranaki eruptives and are dominated by plagioclase-hornblende-clinopyroxene-glass assemblages that have similar crystal textures and compositions to the phenocrysts in Taranaki andesites (Stewart et al., 1996; Price et al., 2005; Gruender et al., 2010). Therefore many of the phenocrysts in andesites such as the Ruapehu and Taranaki eruptives may be xenocrysts derived from the disaggregation of microxenoliths (Price et al., 2005). The close match produced by the least squares mixing model supports this as whole rock analyses would have included any xenoliths, which were not included as inputs into the model. Therefore it is possible that xenocrysts were analysed as a population of the mineral phases and therefore incorporated into the average mineral compositions input into the model, or alternatively, not analysed but having a similar composition to the phenocrysts and therefore not altering whole rock geochemistry.

5.1.3 THE RELATIONSHIP BETWEEN GLASS AND MINERAL PHASES

The relationship between the glass and mineral phases can be addressed by considering two end-member scenarios: 1) where they are directly related by closed system processes such as crystallisation and; 2) where the crystals have no genetic relationship to the melt in which they are found but were mixed immediately prior to eruption. Closed system processes would result in phenocryst assemblages in equilibrium with the glass and crystallisation that would drive the composition of the magma to more evolved compositions. Where the melt and crystals have evolved separately, they are unlikely to be in equilibrium and features such as sieve textured crystals, may be apparent.

A combination of these processes appears to be occurring at Taranaki as there is both a phenocryst population of plagioclase, clinopyroxene and amphibole that are in equilibrium with the host melt (see Section 3.3 for equations used to calculate equilibrium and associated discussion) as well as other mineral populations of these phases with more complex zoning and crystallisation histories. The cores of these complex crystals display a range of major and trace element compositions suggesting these crystals are from multiple magma sources (maybe including xenoliths) and were incorporated into the host magma at a later stage. The rim compositions of these complex crystals have little variability and generally coincide with that of the phenocryst population so also likely grew from the host melt. This rim is absent in a small population of crystals which display less evolved major and trace element chemistry and are therefore probably a final addition to this magma

These findings are consistent with recently proposed concepts of intermediate magmas as a mixture of silicic melt and assorted minerals derived from various sources (e.g. Eichelberger, 1978; Davidson et al., 2005; Price et al., 2005; Reubi & Blundy, 2009). Silicic melts appear to be formed in the lower crust by processes such as crystallisation of hydrous basalts, melting of mafic source rocks (Hildreth and Moorbath, 1988; Annen et al., 2006) and/or interaction of a mantle-derived melt with the lower crust (Price et al., 2005). Melt differentiation at depth is favoured as melt inclusions are consistently silicic regardless of the location within the host crystal (Price et al., 2005; Annen et al., 2006; Reubi & Blundy, 2009). Although melt inclusion compositions are more variable than the groundmass glass, the average SiO₂ content overlaps that of the glass for each sample and Gruender et al. (2010) found the glass composition of xenoliths also coincides with that of the Taranaki glass. The dominance of type II xenoliths comprising mostly cumulates and granulites suggest a large degree of involvement with the lower crust (Stewart et al., 1996; Gruender et al., 2010).

These silicic lower crustal melts incorporate minerals from various sources as they traverse the crust resulting in a complex crystal cargo containing xenocrysts, antecrysts and phenocrysts with a range of textures and chemistries. Xenoliths are incorporated largely in the lower crust and silicic melts migrate through the crust as crystal and lithic rich magmas to recharge the

shallow magmatic system (Stewart et al., 1996; Price et al., 2005; Turner et al., 2008). As these magmas migrate to the surface, the crystal cargo is further modified by incorporation of antecrysts due to interaction with the shallow magmatic system and crystallisation of phenocrysts and growth of equilibrium rims on xenocrysts and antecrysts. The complex interplay of magma storage, recharge and subsequent mixing in the shallow magmatic system results in a mixture of crystal cargo that has originated from different parts of this system and therefore may have little or no relationship to the host magma. The following section will explore the nature of the mineral cargo using a detailed examination of mineral chemistry to decipher the history of the various mineral populations.

5.2 MINERAL CHEMISTRY

Unravelling the history of mineral populations requires detailed examination of both chemical and textural evidence. In particular, the use of in situ techniques to construct a crystal stratigraphy enables the investigation of magmatic evolution through time. Mineral phases can form at different stages of magmatic evolution prior to eruption and are sensitive to different processes. Therefore each phase provides distinct insights into the sub-volcanic magmatic system, and populations within these phases can identify complex open system processes. The chemistry and textures of plagioclase, clinopyroxene and amphibole crystals in this section will be discussed individually in the context of magmatic processes operating beneath Mt Taranaki.

5.2.1 PLAGIOCLASE

Plagioclase is a particularly useful mineral for investigating magmatic processes. The major element chemistry recorded during crystallisation is preserved due to the slow rate of NaSi-CaAl interdiffusion, hence preserving the mineral zoning (Morse, 1984; Grove et al., 1984). Plagioclase crystallises over a range of magmatic conditions and is sensitive to changes in magmatic parameters and composition. However, distinguishing uniquely between these factors is not always straightforward. Melt composition and temperature are the most important variables in influencing plagioclase anorthite content, with a small change in either of these parameters producing a large effect (Zellmer et al., 2003; Humphreys et al., 2006). Pressure and

$p\text{H}_2\text{O}$ also affect plagioclase crystallisation and chemistry, with decreasing pressure of a water undersaturated system inducing resorption. Decompression of a water saturated system is also able to produce crystallisation of more sodic plagioclase (Vance, 1965; Nelson & Montana, 1992). Given these basic relationships, the range of plagioclase textures and populations observed in the Taranaki eruptives provide evidence for different crystallisation histories.

Plagioclase crystals in the Taranaki eruptives typically display one or all of the following textures: sieved or patchy textures (~30-50%) and oscillatory zoning (> 50%). Oscillatory zoning is the dominant texture, particularly in crystal rims. Sieved and patchy textures are usually features of plagioclase phenocryst cores but can also occur outside the core in isolated zones that interrupt oscillatory zoning.

5.2.1.1 Patchy/sieved textured crystals

As patchy textures simply represent crystallisation of the melt within the sieved regions (Streck, 2008), there is no clear distinction between patchy and sieved textures and they will be discussed together. Sieve texturing is limited to the high anorthite zones ($\text{An} > 60$) of crystals and the nature of the patchy zoning indicates sodic plagioclase crystallised within calcic plagioclase. This is further supported by the association of melt inclusions with the sodic plagioclase (e.g. Humphreys et al., 2006). In previous work, this texture has been interpreted to result from either rapid growth or resorption (Streck, 2008). In this case, the rounded nature of the sieving favours a resorption origin as rapid, skeletal growth would likely form a boxy cellular texture with square melt inclusions (Figure 5.3; Streck, 2008).

Formation of calcic cores with sodic rims requires that the cores crystallised from either a magma which was hotter, more mafic or at considerably higher $p\text{H}_2\text{O}$, and these textures are generally attributed to crystal cumulates which were then resorbed during water undersaturated decompression (Zellmer et al., 2003; Humphreys et al., 2006; Berlo et al., 2007; Turner et al., 2008). The patchy and sieved textures which are found in cores and mantles appear similar (Figure 5.3) and are interpreted to be formed by the same process. The effects of decompression

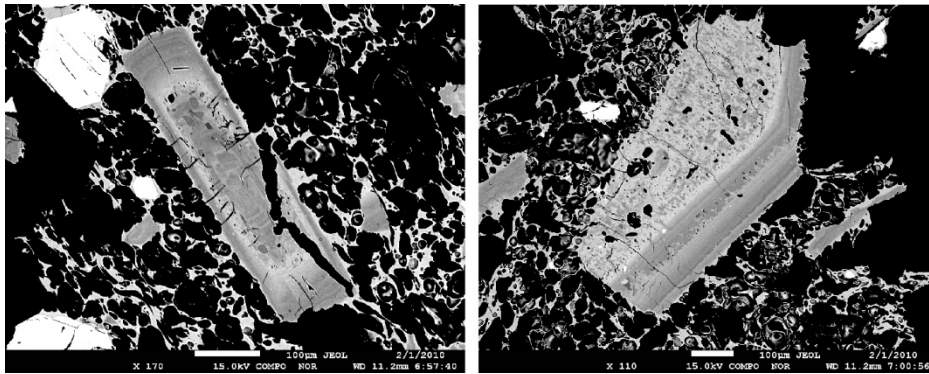


Figure 5.3 Examples of plagioclase crystals with sieved/patchy core and mantle from Kaupokonui (crystals= left: 6a_P9, right: 6a_P10). Note the similarity of the patchy/sieved texture in the core and mantle and the rounded nature of the melt inclusions. These patchy/sieved zones appear to be partially crystallised highlighting the continuum between the patchy and sieved textures.

could account for indiscriminate sieving of an entire core, but not the isolated bands of sieving which interrupt oscillatory zoning (Figure 5.3). The sieved zoning is therefore more likely to be the result of changing melt composition and temperature, possibly due to the intrusion of a hotter and/or more mafic magma into the magmatic system/magma chamber.

Browne et al. (2006) observed a similar feature in the eruptive products of Mt Unzen, where a population of oscillatory zoned crystals contained a resorbed zone. This was attributed to being locally engulfed by a basaltic injection, which resorbed the oscillatory zoning and crystallised higher anorthite plagioclase. Afterwards, the basalt may have dispersed into the silicic body and oscillatory zoning resumed. These authors correlated the increase in anorthite content with increased Sr/Ba ratios, an indicator of more mafic magma. The heterogeneous and melt inclusion-rich nature of the patchy/sieved zones in this study generally precluded LA-ICP-MS analysis of the high anorthite patches of the zones. Therefore it was difficult to distinguish between mixing of mafic magma and reheating of the system by a hotter magma on the basis of geochemical data. Interaction with a less evolved magma is favoured because the dissolution penetrated the crystal, rather than exhibiting a simple smoothing of crystal edges which may have been attributed to magma heating (Tsuchiyama, 1985; Singer et al., 1995).

Dissolved crystals

Dissolved crystals are mostly confined to sample SM-6C and are characterised by very high anorthite ($An > 86$), and REE concentrations that are almost an order of magnitude lower than other plagioclase crystals from this sample. These are therefore interpreted to be plagioclase crystals from a more primitive melt that were incorporated into the host melt or, alternatively, may represent the remnants of disaggregated xenoliths.

5.2.1.2 Oscillatory zoned crystals

Oscillatory zoning has been attributed to a number of processes including kinetic effects (e.g. Pearce & Kolisnik, 1990; Ginibre et al., 2002b), convection (Pearce & Kolisnik, 1990; Singer et al., 1995), decompression-heating cycles (Blundy et al., 2006) and magma recharge (e.g. Sparks & Marshall, 1986; Singer et al., 1995; Davidson & Tepley, 1997; Ginibre et al., 2002a). There are multiple scales of oscillatory zoning observed in the Taranaki samples, and these were likely produced by different mechanisms. Different scales of zoning are superimposed on one another. The finest scale zoning occurs on a scale of $< 5 \mu\text{m}$, exhibits very minor changes in anorthite content and do not appear to have any resorption associated with them. These are similar to the Low Amplitude Oscillatory (LAO-type) zoning of Ginibre et al. (2002b), which are thought to form at near equilibrium conditions by kinetic effects (e.g. Bottinga et al., 1966; Sibley et al., 1976; Haase et al., 1980; Allegre et al., 1981; Anderson, 1984). These conditions occur where a super-saturated liquid forms a local boundary layer as element diffusion is too slow to replenish the melt at the interface (Bottinga et al., 1966). The interface is periodically destroyed by a pulse of new melt with slightly different composition and possibly also different temperature, resulting in a minor, but sudden change in anorthite composition (Ginibre et al., 2002b).

The more common, broader scale oscillatory zoning ranges in scale from 5 to 60 μm with changes in anorthite content of ~ 10 to 20 mol%. These are saw-tooth shaped with sharp increases in anorthite content following resorption surfaces which then trend to lower anorthite values until truncation by another resorption surface. These resorption-associated oscillations

resemble a range of documented textures including the saw-tooth pattern with resorption zoning (STR-type) of Ginibre et al. (2002b) and the Type II of Pearce & Kolisnik (1990). The smaller oscillations can be repeated tens to hundreds of times, while the larger features may occur only twice. Turner et al. (2008) attributed all oscillatory zoning in plagioclase and clinopyroxene to kinetic effects operating in a shallow magma chamber. While this process may be responsible for the finest scale zoning, most oscillatory zoning in the Taranaki eruptives from the present study is likely due to other mechanisms, as kinetic effects are unlikely to produce the observed resorption and the compositional variation observed is difficult to produce with kinetic effects (Ginibre et al., 2002a; Humphreys et al., 2006).

Oscillatory zoning has been attributed by Blundy et al. (2006) to the complex interplay between decompression, crystallisation and heating. In this model, decompression of a hydrous magma crystallises plagioclase with decreasing anorthite content. However, this crystallisation releases latent heat which slightly resorbs the sodic plagioclase and crystallises more calcic plagioclase. This would produce many oscillations and may be a mechanism for producing the finer scale of the resorption related oscillations. Similarly, rhythmic oscillatory zoning associated with resorption has also been related to growth during convection within the magma chamber as a response to a weak thermal gradient (Singer et al., 1995). In this model, dissolution occurs as the crystals descend, interact with hotter magma, and crystallisation renews on ascent into cooler magma. A combination of these factors likely account for the small scale, rhythmic oscillatory zoning observed in some crystals. In contrast, the larger scale oscillatory zones are interpreted to result from repeated mafic recharge. The heat from these intrusions resorbs the outside of the equilibrium plagioclase before crystallising the higher anorthite, higher temperature plagioclase. As the heat dissipates, progressively lower anorthite plagioclase crystallises (Singer et al., 1995). All of these processes are a function of intensive and extensive parameters operating on a shallow magma chamber. Equilibrium calculations based on major element concentrations indicate that the rims of plagioclase crystals are in equilibrium with the host glass. Therefore, in general, the oscillatory zoning is considered to have formed in the host silicic magma.

5.2.1.3 Calculated plagioclase equilibrium melt compositions

The trace element chemistry of plagioclase crystals reflects that of the melt from which it crystallised, and is controlled by partition coefficients. The trace element concentrations of the equilibrium melts were calculated using the partition coefficients of Blundy & Wood (1991) and Bindeman et al. (1998), using temperatures obtained from plagioclase-melt thermometry (Putirka, 2008) (Table 5.2). Calculation of the melt composition as opposed to directly interpreting the plagioclase trace element concentrations is important because temperature and anorthite content affect the partitioning of most trace elements (Blundy & Wood, 1991; Bindeman et al., 1998). As variation in anorthite content can be caused by a number of factors, reconstructing the trace element composition of the plagioclase melt provides useful constraints on changes in the melt composition. This information can be used to distinguish between changing melt composition and changes in physical parameters.

Plagioclase			925° C
Element	a	b	An ₄₅
Li	-6900	-12100	0.22
Mg	-26100	-25700	0.02
Rb	-40000	-15100	0.04
Sr	-26700	26800	4.37
Ba	-38200	10200	0.49
La	-10800	-12400	0.18
Ce	-17500	-12400	0.13
Pr	-22500	-9300	0.14
Nd	-19900	-9400	0.16
Sm	-25700	-7700	0.14
Eu	-16100	-14200	0.12
Pb	-60500	25300	0.81

Table 5.2 Plagioclase-melt partition coefficients used in this study. These partition coefficients are strongly dependent on anorthite content and temperature so have been calculated for each analysis using the equation: $RT \ln D_{\text{element}} = b - a * X_{\text{An}}$ where R is the gas constant (8.314JK^{-1}) and T is temperature in Kelvin. A representative set of partition coefficients are given using An₄₅ and T=925°C (=1198° K). a and b values are from Bindeman et al. (1998), except Sr and Ba which are from Blundy & Wood (1991).

Diffusion effects

Trace element compositions of plagioclase can be modified by diffusion. Strontium in particular diffuses within plagioclase on timescales of decades to centuries which are relevant to

magmatic processes operating at andesitic volcanoes (e.g. Zellmer et al., 1999; 2003; Saunders et al., 2010). Following the example of Smith et al. (2009) it will be shown that Sr and Ba diffusion has not significantly altered the trace element concentrations of plagioclase from this study and therefore the trends observed do indeed reflect melt compositions.

The effect of diffusion on trace elements cannot be assessed directly because these measurements are point analyses on a scale of 25-35 μm . Therefore the behaviour of Mg, a minor element in plagioclase, which has been analysed by EMPA transects, is used to qualitatively determine the effects of diffusion on these samples. The rate of diffusion for these elements in plagioclase with an anorthite content of ~30-58 at 850°C fall within the following ranges: Mg – 3.4×10^{-6} to 5.8×10^{-5} mm^2/s (Costa et al., 2003); Sr – 2.1×10^{-8} to 5.4×10^{-7} mm^2/s (Giletti & Casserly, 1994); and Ba – 1.5×10^{-11} to 1.4×10^{-9} mm^2/s (Cherniak, 2002). As Mg diffuses ~100 times more quickly than Sr and 10 000 times quickly than Ba, if the Mg profile has not been heavily modified by diffusion, Sr and Ba will not have been affected on the scale of interest here.

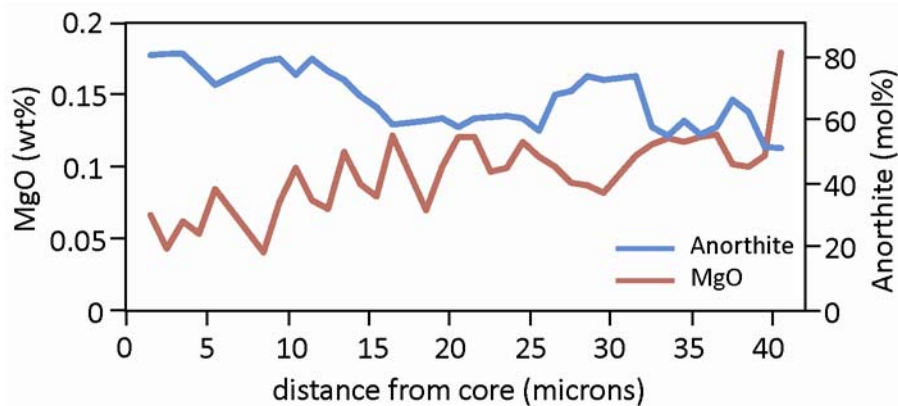


Figure 5.4 An example of a plagioclase transect (crystal SM-6C Pg) showing the anti-correlation between MgO and anorthite content indicating that the Sr and Ba trace element composition of plagioclase crystals have not been modified by diffusion.

There is a weak compositional sensitivity of Mg partitioning into plagioclase – it is slightly more compatible at lower anorthite content (Bindeman et al., 1998). Based on this relationship, Mg would initially vary inversely with anorthite content, and diffusion would act to smooth the Mg profile to a near flat equilibrium profile. As illustrated by Figure 5.4, An and Mg vary

inversely in plagioclase. Therefore, Mg is not considered to have diffused significantly and diffusion of Sr and Ba has not modified plagioclase trace element compositions.

The overall trend of each sample shows decreasing Sr and Ba trending towards the measured matrix glass value for that sample (Figure 5.5). The close agreement of many of the rim-calculated melt values with the measured matrix glass concentrations verifies the use of these partition coefficients and further supports the hypothesis that the oscillatory rims are host-derived. Inglewood a and b and Korito samples contain two distinct groups: the melts in equilibrium with the anorthite-rich cores and sieved cores and zones ('core melt') and those calculated from the oscillatory zoning, rims and infilling plagioclase ('rim melt') (Figure 5.5). The 'core melt' was a less evolved composition, relatively enriched in Sr and depleted in La compared with the 'rim melt'. The calcic and sieved cores may be a restite of partial melting of the lower crust with resorption related to decompression in a water undersaturated system (Zellmer et al., 2003; Humphreys et al., 2006; Berlo et al., 2007). Alternatively, these may be remnants of an earlier phase of crystallisation or introduced by mixing with a mafic magma (Zellmer et al., 2003). Calcic cores that do not exhibit resorption may be an artefact of crystal orientation during sectioning, so that the core was not exposed in the observed two-dimensional plane. Alternatively, these crystals may have experienced continuous or episodic crystallisation (Berlo et al., 2007). The sieving may also be feasibly attributed to disequilibrium conditions during which calcic plagioclase entered the silicic melt before its rim crystallised. Given the available data it is not immediately clear whether these cores crystallised from the same melt, but the plagioclase assemblages imply that there were mafic additions to a shallow, silicic magma chamber, occurring as a single, or episodic, injection of more mafic magma.

The 'rim melt' forms a distinct group in Ba-Sr space, suggesting these are linked by a common process (Figure 5.5). The decrease in Sr may be a crystallisation trend as Sr is compatible in plagioclase. However, the crystallising assemblage does not account for the decreasing Ba due to its incompatible behaviour in the fractionating assemblage of plagioclase, clinopyroxene and amphibole. Published partition coefficients for Ba in these

	Starting composition	k_D		
		plag	cpx	amph
Sr	663.0	4	0.101	0.49
Nd	21.4	0.15	0.38	1.24
Ce	37.8	0.12	0.25	0.63
fractionating assemblage				
	Kaupokonui	0.4	0.1	0.15
	SM-6C	0.5	0.1	0.05
	Maketawa	0.4	0.05	0.05
	Inglewood b	0.35	0.1	0.1
	Inglewood a	0.4	0.1	0.1
	Korito	0.4	0.05	0.1

Table 5.3 The starting composition, partition coefficients (k_D) and the fractionating assemblage used to model fractional crystallisation in this study.

mineral phases are all < 1 (e.g. Rollinson, 1993 and references therein; Ewart & Griffin, 1994; Blundy & Wood, 1991; Severs et al., 2009). This is consistent with the trace element data from this study because the Ba concentrations of the host melt are higher than the equilibrium rims of the dominant mineral assemblage. For example, in Inglewood b, the glass Ba concentration is 1140 ppm compared with ~600-700 ppm in plagioclase rims and ~300-400 ppm in amphibole rims (values are below the detection limit in clinopyroxene). Therefore crystallisation of this assemblage will concentrate Ba in the melt producing the opposite trend to that observed in Figure 5.5. Quantitative modelling of fractional crystallisation also shows that the plagioclase compositions cannot be reproduced by fractional crystallisation.

Humphreys et al. (2006) identified a similar trend of decreasing Sr and Ba which was interpreted as melt evolution during fractional crystallisation. However, these authors invoked the presence of phlogopite in the crystallising cumulate body, in which Ba is compatible. This is an unlikely solution for the Taranaki eruptives due to the absence of phlogopite, and because the anomalous trend appears to be recorded in the shallow magma chamber, host melt or some parent thereof. The decreasing Sr-Ba trend must therefore reflect open system processes, with the linear nature of this trend further indicating possible mixing with a melt high in Sr and Ba.

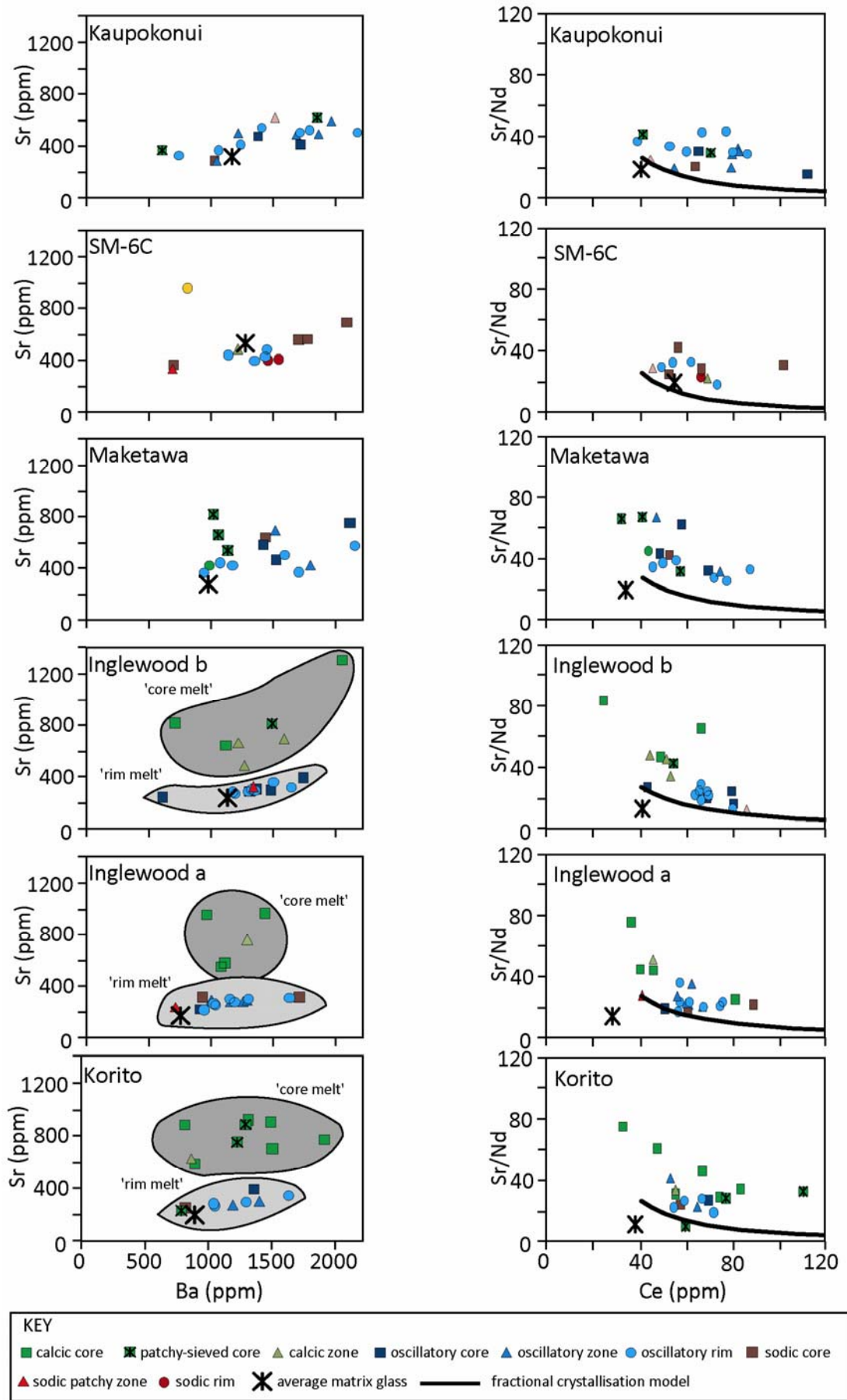


Figure 5.5 Trace element concentrations of plagioclase equilibrium melt. Fractional crystallisation was modelled using the parameters in Table 5.3.

The melt compositions from which the plagioclase cores crystallised in sample SM-6C fall on a linear trend with those of the rims and matrix glass, and generally trend toward lower values. The single point representing dissolved crystals is separate from this trend as it is significantly enriched in Sr and depleted in Ba. Therefore it appears to have crystallised from a distinct, less evolved, higher Sr and more mafic melt.

The trace element data for Kaupokonui and Maketawa indicate a more complex relationship between plagioclase crystals. The overall trend of decreasing Sr and Ba of the oscillatory zoning is evident, but exhibits more scatter and the oscillatory zoning appears to fall into distinct groups. The greater degree of variability of the oscillatory zoning may indicate that these crystallised from two different magma bodies that were mixed prior to eruption or crystallised within a single magma chamber that was compositionally variable. Determining the history of the plagioclase crystals is further complicated by the lack of trace element data for anorthite-rich, sieved/patchy zoning for these crystals, limiting interpretation of the host melt of disequilibrium cores.

5.2.2 CLINOPYROXENE

The major element chemistry of clinopyroxene responds to changes in magmatic conditions primarily by variations in Mg# ($= \text{Mg}/(\text{Mg} + \text{Fe}^{2+})$). This value is illustrated in backscattered electron imaging with higher Mg# portions appearing darker. Clinopyroxene textures in conjunction with major and trace element data therefore provide important information related to the processes which have formed these crystals. Fe-Mg interdiffusion is significant over the timescales of magmatic processes ($1.17 \times 10^{-22} \text{ m}^2/\text{s}$ at 900° C), and are not necessarily an accurate representation of the original zoning. As a result, clinopyroxene crystals give a clearer picture of later stage processes such as those occurring in the shallow crust and in the lead up to eruption.

5.2.2.1 Clinopyroxene textures

Simple and multiple zoning forms from one or more changes in magmatic conditions such as melt composition, temperature and oxygen fugacity. Patchy textured cores are indicative of disequilibrium conditions and can form by both partial dissolution of the pre-existing core followed by recrystallisation of equilibrium clinopyroxene (Simonetti et al., 1996), and by diffusion from melt inclusions formed during partial dissolution of the core (Tomiya & Takahashi, 2005; Streck et al., 2007). Most crystal cores are melt inclusion-rich and major element analyses of these melt inclusions show that these compositions overlap with that of the host glass for any particular sample. Therefore it is interpreted that melt inclusions were open until a later stage of crystallisation in the host melt (or similar melt), and so cores may re-equilibrate to rim compositions.

Oscillatory zoning is found in all the samples investigated here and shows cyclical changes in Mg# (Mg#₇₅₋₈₅) with varying amounts of resorption associated with the changes in composition. As with plagioclase, oscillatory zoning in clinopyroxene crystals has been attributed to a range of processes including kinetic effects (e.g. Turner et al., 2008), cyclical changes within a shallow magma chamber such as convection (e.g. Morgan et al., 2004) and multiple replenishment events (Nakagawa et al., 1999). Clinopyroxene oscillatory zoning occurs on a number of scales and may not be clearly attributable to any single process. As this textural feature is similar to that of plagioclase, it is assumed to be produced by similar processes within a shallow magma chamber.

5.2.2.2 Clinopyroxene chemistry

Mg# is typically used as an index of crystallising conditions, with increasing Mg# attributed to crystallisation from a more mafic and/or hotter melt (e.g. Nakagawa et al., 1999; Turner et al., 2008). However, there is little correlation between Mg# and other major and trace elements in the samples investigated here (Figure 5.7). The exception to this is clinopyroxene with Mg# > 85, showing a positive relationship between Mg#, Al₂O₃ and compatible trace elements (e.g. Ni,

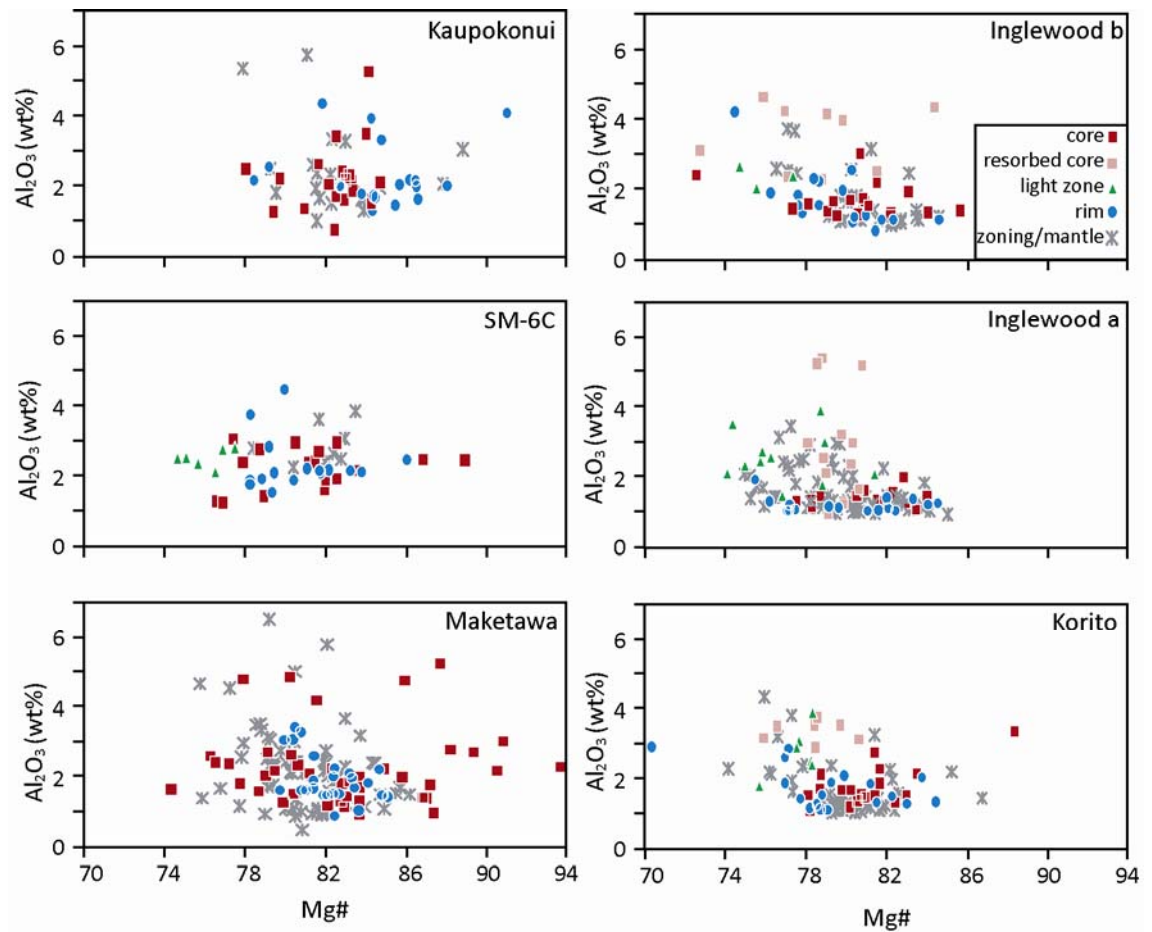


Figure 5.6 Mg# vs Al₂O₃ content of clinopyroxene cores, rims and zoning in each of the samples investigated in this study

Cr, V, Sc) and a negative relationship with incompatible trace elements (e.g. Hf, Ce). Therefore this clinopyroxene population may be recording melt evolution. Streck (2008) stated that Mg# does not necessarily record melt evolution in pyroxene which crystallised from felsic melts, so the observed termination of the Mg#-trace element correlations may reflect the transition from crystallisation of mafic-intermediate melts to more silicic melts. Where Mg# < 85 cores, rims and mantles/zoning can be differentiated on the basis of Al₂O₃ for all samples (with the exception of SM-6C), and Mg# for the younger three samples (Figure 5.6). Variation in clinopyroxene Mg#, which is independent of trace element concentrations, is generally attributed to changes in physical parameters such as temperature and oxygen fugacity (Nakagawa et al., 2002).

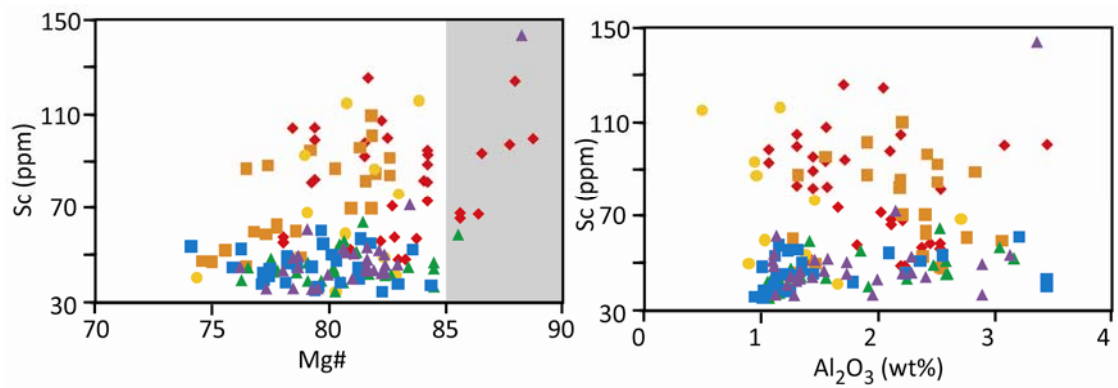


Figure 5.7 Mg# and Al₂O₃ plotted against a representative trace element (Sc) to illustrate the lack of correlation between major element indices and trace element chemistry. The grey shaded area highlights Mg >85 where a positive correlation is observed in a relatively small number of crystals. Symbols relate to samples as in Figure 4.6.

Variations in Al concentrations within clinopyroxene have also been related to changes in melt composition, pressure and temperature (e.g. Umino & Horio, 1998; Streck et al., 2005; Turner et al., 2008; Putirka, 2008). Melt composition is an unlikely cause of the observed variation in clinopyroxene composition as Al₂O₃ does not correlate with major or trace element compositions (Figure 5.7). Streck et al. (2005) and Turner et al. (2008) attribute high Al/low Mg# clinopyroxene to crystallisation from a melt which has undergone extensive crystallisation of mafic phases such as olivine and pyroxene, but limited plagioclase crystallisation. However, this too would be reflected in trace element chemistry as this melt is implied to be less evolved due to limited plagioclase crystallisation resulting in a high Sr melt. Also the disequilibrium textures associated with the high-Al zones indicate a sudden change in conditions, implying either different melt or a change in physical parameters.

Al contents in clinopyroxene have been used as a barometer (e.g. Nimis, 1995; 1999; Putirka et al., 1996; Putirka, 2005; 2008). The errors associated with these quantitative models are large (\pm 2-5 kbars), therefore these models are not applied to these samples. However, the general relationship of increasing Al incorporation into clinopyroxene at greater pressures can potentially be used as a qualitative indicator of pressure (e.g. Simonetti et al., 1996).

Umino & Horio (1998) also observed variations in Al₂O₃ rather than Mg# between clinopyroxene populations. The authors attributed this to mixing between a low temperature rhyolitic melt with a higher temperature dacite, where low Al clinopyroxene crystallised from

the more silicic melt. They also did not observe dissolution of the low-Al core due to near-homogeneous Mg# amongst the different clinopyroxene populations.

Melt Chemistry

To gain further insights into the magmatic conditions as recorded by clinopyroxene, the trace element composition of the equilibrium melt was calculated using partition coefficients from Bacon & Druitt (1988), Rollinson (1993) and Severs et al. (2009) (Table 5.4). This shows that while the trace element concentrations are variable, the clinopyroxene appear to be related primarily by fractional crystallisation processes in most samples (Figure 5.8). Therefore crystals have formed from a genetically related suite of melts.

Clinopyroxene					
Element	K _D	Element	K _D	Element	K _D
Sc	3.306	Sr	0.101	Gd	0.907
Ti	0.412	Y	0.949	Tb	1.1 ^b
V	1.532	Zr	0.097	Dy	0.926
Cr	30 ^a	La	0.082	Ho	1.009
Mn	2.877	Ce	0.25 ^b	Er	1.33 ^b
Ni	6 ^b	Nd	0.38	Yb	0.973
Cu	0.66 ^b	Sm	0.61	Lu	0.665 ^b
Zn	2 ^a	Eu	0.626	Hf	0.171

Table 5.4 Clinopyroxene-melt (andesite to dacite) partition coefficients used in this study. Values are from Severs et al. (2009) unless otherwise stated. ^a Bacon & Druitt (1988)=andesite values; ^b Rollinson (1993) and references therein=dacite values.

5.2.2.3 Inglewood a, Inglewood b and Korito Processes

The three older samples are dominated by two clinopyroxene populations. One contains patchy textured cores and oscillatory rims and the other is comprised entirely of oscillatory zoning. Patchy textured cores have resorbed, high-Al clinopyroxene that is replaced by low-Al clinopyroxene. Oscillatory rims are primarily comprised of low Al clinopyroxene which is periodically interrupted by low Al/low Mg# bands (indicated by a light zone in BSE images). High Al cores may originate from a greater depth and be resorbed by decompression. However, this cannot also explain the light zones which are more likely to result from changes in temperature or oxygen fugacity of the magma, possibly as a result of repeated recharge of the shallow magma chamber.

5.2.2.4 Kaupokonui, SM-6C and Maketawa Processes

Clinopyroxene in the three younger samples are distinguished primarily on the basis of Mg#. As the variation in Mg# is not associated with changes in trace elements, this is likely due to changes in temperature and/or oxygen fugacity (Nakagawa et al., 2002; Turner et al., 2008). Additionally, there is a high-Al₂O₃ population, which is assumed to have the same origin as those in the older three samples. The variation of Mg rather than Al in these samples may be because they are recording different processes or the same processes in a different way. These younger samples also contain two populations of clinopyroxene crystals, each providing evidence for open system processes such as magma mixing.

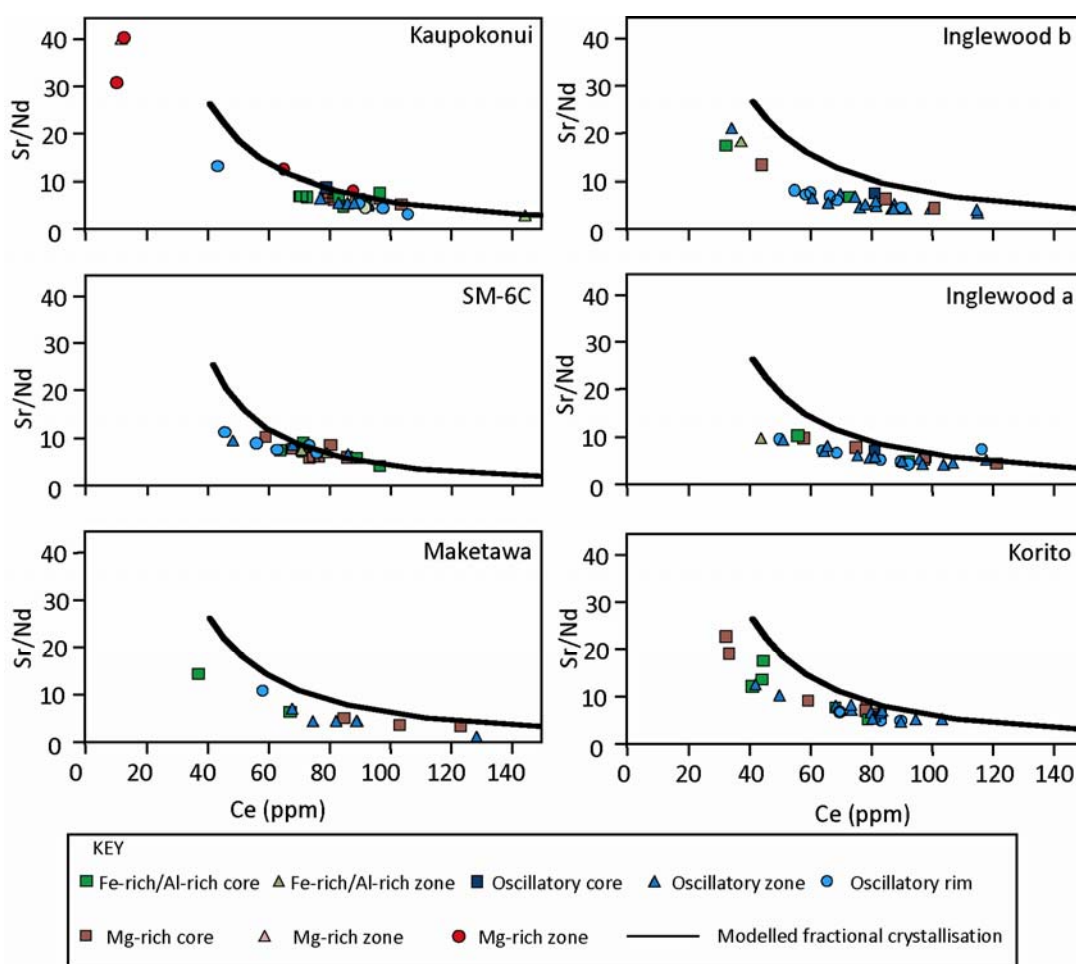


Figure 5.8 Ce vs Sr/Nd of the clinopyroxene equilibrium melt. Fractional crystallisation was modelled using the parameters defined in Table 5.3

Some crystals in Kaupokonui and Maketawa contain highly resorbed, high Mg# cores which appear to be from a more mafic magma. These cores were likely later incorporated into a

more silicic melt by magma mixing or incorporation of cumulates. Most crystals in these samples have a variable but high-Mg rim, implying there was an increase in the temperature and/or oxygen fugacity of the magma chamber shortly before eruption. However, the influence on individual crystals differed. Some crystals within the Kaupokonui sample have extremely zoned rims, where $Mg\# > 85$ and compatible elements such as Cr and Ni are enriched, and incompatible elements are depleted. These are interpreted as crystallising from a less evolved melt. The high $Mg\#$ rims and the variability observed within these rims can be explained by a model based on that of Nakagawa et al. (2002), where an invading high temperature melt can displace the host melt and engulf some crystals, resulting in extremely zoned rims. This melt then mixes with the more silicic host melt. The subsequent rim compositions reflect that of the corresponding ratio of the melt components, producing progressively less extreme zonation. As a small proportion of crystals (~ 15%) record the higher compatible element signature, the intruding magma is volumetrically small compared with the host silicic melt and so it is efficiently mixed and the host melt remains silicic. It is after this magma mixing, or during ascent and cooling, that the thin Fe-rich overgrowths form. The low Cr (~385 ppm) and Ni (~130 ppm) content of the extremely zoned rims indicates that the intruding magma had already undergone extensive differentiation and so was probably at least intermediate in composition.

The multiple zoning observed in Maketawa may reflect a similar process whereby a more chemically similar, but hotter, melt was injected into the host. This would produce Mg-rich rims without a strong trace element signature. In sample SM-6C, homogeneous and laminar crystals have a similar $Mg\#$ to the rims of the simple and multiple zoned crystals of this sample. Those crystals with more Fe-rich cores were therefore incorporated into a hotter, possibly more mafic melt which hosted the laminar and homogeneous crystals via mixing or incorporation of cumulate material.

5.2.3 AMPHIBOLE

Amphiboles are compositionally complex and record changes in melt composition, pressure, temperature, melt water content (H_2O_{melt}) and oxygen fugacity (fO_2).

Thermobarometric models (e.g. Ridolfi et al., 2010) have enabled quantification of physical-chemical conditions in equilibrium, with individual zones resulting in a less ambiguous interpretation of amphibole chemistry. This can enable pathways of magma ascent to be reconstructed.

5.2.3.1 Physical Conditions of Amphibole Crystallisation

The pressure-temperature- H_2O_{melt} - fO_2 values are consistent with some amphibole crystallisation occurring at depth in a hotter, water-rich magma before ascending through the crust and cooling with time. The highest pressure population of amphiboles indicate crystallisation depths of ~20-25 km. Given that the crust in the Taranaki region is 25-35 km thick (Stern & Davey, 1987; 1990), these high pressure amphibole crystals represent mid- to lower crustal conditions. There is also a dominant low pressure, temperature, H_2O_{melt} and fO_2 population in most samples, which indicates a shallow magma chamber at ~8-10 km depth. This is in agreement with 3-dimensional tomographic imaging indicating a high- V_p low V_p/V_s structure that extends to at least 10 km depth (Sherburn et al., 2006). The authors interpreted this as the 'roots' of Mt Taranaki. Amphibole trace element concentrations indicate crystallisation from two different melts, where the less evolved melt corresponds to the higher pressure amphibole (Figure 5.9). However, other high pressure amphiboles have trace element concentrations similar to those that crystallised at cooler, shallower conditions. This may indicate two crystallising conditions from distinct melts that mix in the mid-crust, or alternatively, that an evolved melt ascended and both crystallised amphibole and entrained cumulates. It is difficult to distinguish between these two options on the basis of trace element data due to the limited analyses of amphibole that crystallised at higher pressures. The exception to this is Kaupokonui sample where there is a clear trend between the high pressure, less evolved trace element amphiboles (Population 1) and the more evolved, low pressure amphiboles (Population 2). In some samples, most notably Inglewood b, textural evidence supports a cumulate origin. Thornber et al. (2008) proposed that those amphibole crystals with patchy-resorbed cores and subhedral overgrowths reflect xenocryst assimilation at depth. The temperatures calculated from the low pressure population are in agreement with those calculated from other mineral phases, and this likely represents

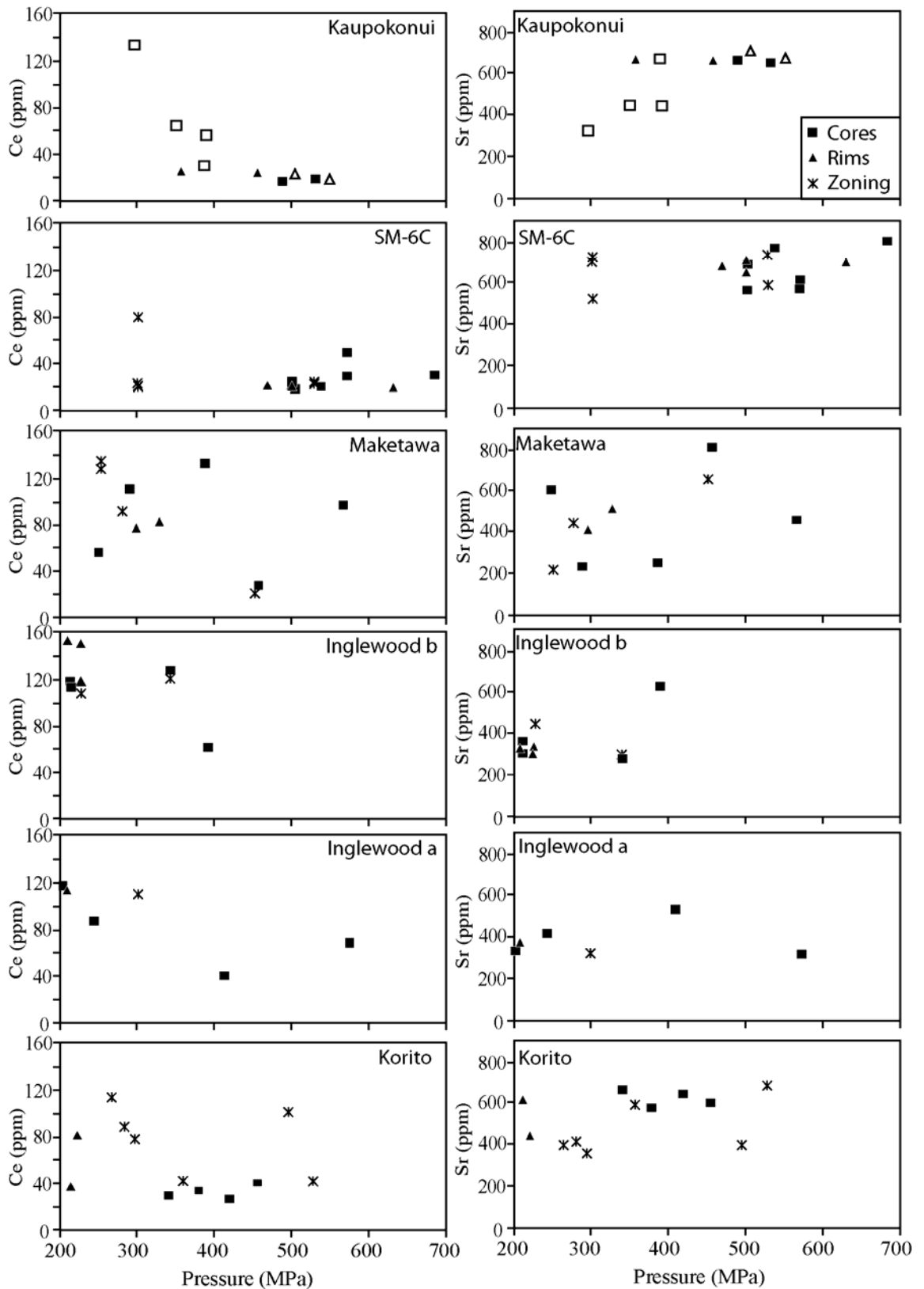


Figure 5.9 Graphs of amphibole crystallisation pressure versus Ce and Sr concentrations of the melt in equilibrium with the amphibole. Amphibole analyses are classified as cores, rims and other zoning for each sample except Kaupokonui, where there are two populations of amphibole (filled and open symbols). Equilibrium melts were calculated using partition coefficients from the GERM database as given in Table 5.5.

crystallisation in a shallow magma chamber from which the eruption originated. Major and trace element data are consistent with most amphibole rims crystallising in this shallow magma chamber and some crystals growing entirely from this melt (phenocrysts). Therefore the majority of amphibole crystals either grew from, or stalled at, this shallow magma chamber. The exception to this is a small population of crystals which only record lower crustal conditions.

Most crystals exhibit sharp changes between zones, indicating that the amphibole experienced large scale changes in parameters consistent with periods of rapid ascent between each zone. Most amphibole crystals from this study display simple or multiple zoning, so melts likely stalled once or twice in the mid- to upper crust. The near continuous range of magmatic conditions apparent in some samples is most likely a function of multiple magma batches which stalled at various levels within the crust before finally intruding into the shallow magma chamber (Figure 5.10).

Amphibole begins to breakdown and be replaced by anhydrous minerals such as pyroxene, plagioclase and Fe-Ti oxides during magma ascent, forming reaction rims which are a common feature of amphibole in many arc magmas (Rutherford & Devine, 1988; Rutherford & Hill, 1993). Amphibole is unstable at low pressures due to the decreasing H_2O_{melt} and at Mt Taranaki this upper limit of amphibole stability is at ~5.2 km depth (Platz et al., 2007a). The amphibole crystals from this study do not have reaction rims, which provides important constraints on the minimum magma ascent rate. Amphibole begins to break down after ~6 days outside of the stability field (Rutherford & Hill, 1993; Rutherford & Devine, 2003; Browne & Gardner, 2006). Therefore, the ascent rate for magmas stored in the shallow magma chamber is >1.3 km/day. Those samples which do not show evidence for accumulation in a shallow magma chamber may have ascent rates twice this. The shallow magma chamber values are in agreement with the ascent rates of fresh amphibole from other arc volcanoes such as Mt St Helens (>1.6 km/day; Rutherford & Hill, 1993; >1.2 km/day; Thornber et al., 2008) and Soufriere Hills (>1.6 km/day; Rutherford & Devine, 2003).

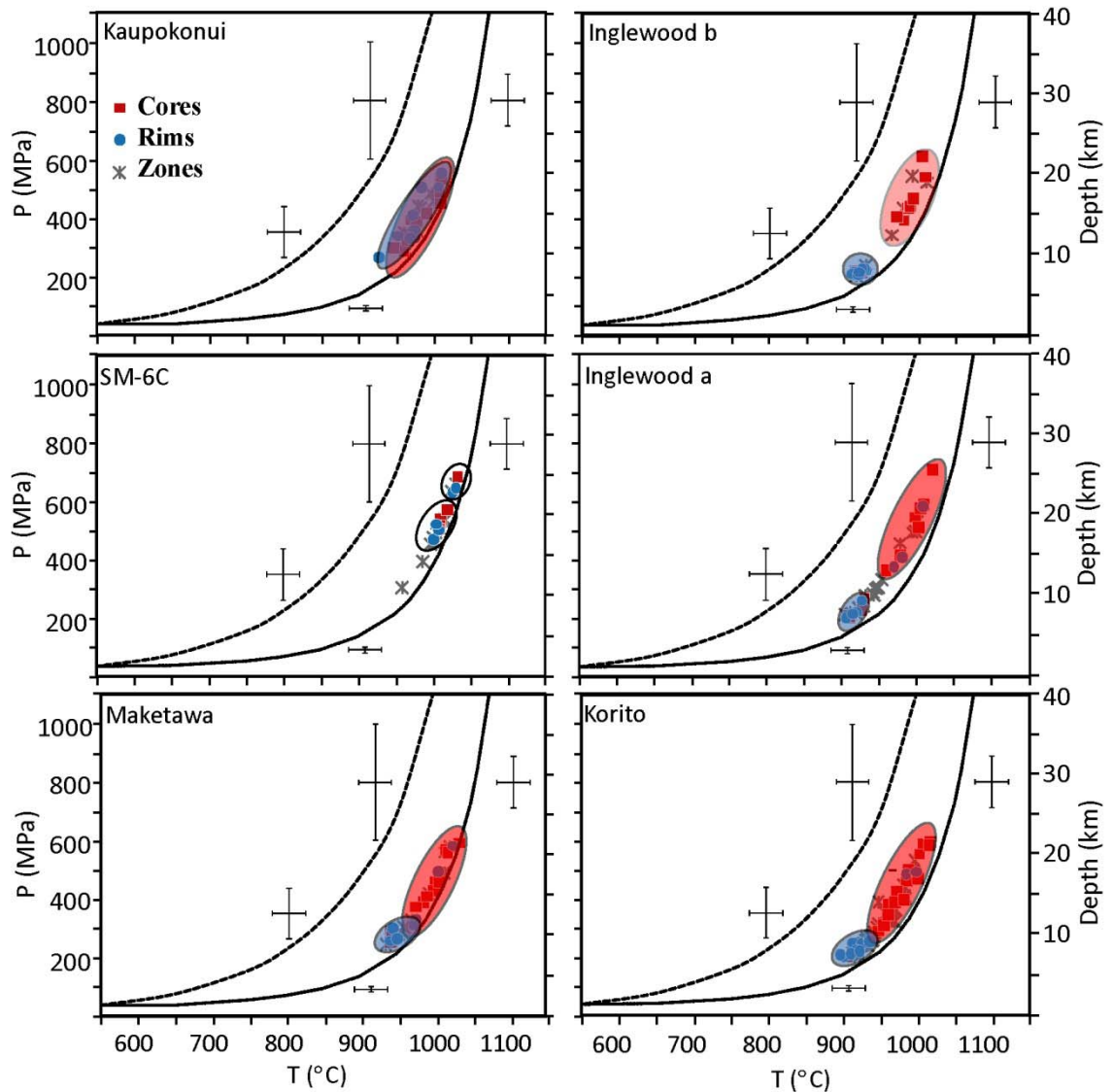


Figure 5.10 Amphibole thermobarometry results. The key populations are identified where red and blue fields represent populations that are dominated by cores and rims respectively. SM-6C contains two populations which appear to be independent of cores/rims.

A distinct amphibole population within the Kaupokonui sample records higher pressure, temperature, H_2O_{melt} and fO_2 within the crystal rims when compared with the cores. These rims record the highest values for this sample, overlapping with cores of other crystal populations. The required increase in pressure during crystallisation of these crystals is 100-200 MPa (~3-7 km). As this is limited to, and consistent within, a specific amphibole population it is probably not analytical error, however, it is difficult to reconcile with geological processes. Rutherford & Devine (2008) explained cyclically zoned amphibole with a Fe- and Al-rich central zone by convection within the storage chamber. As crystallisation does not occur in the sinking magma, there is a sharp chemical transition between the cores and rims. However, the cores from the

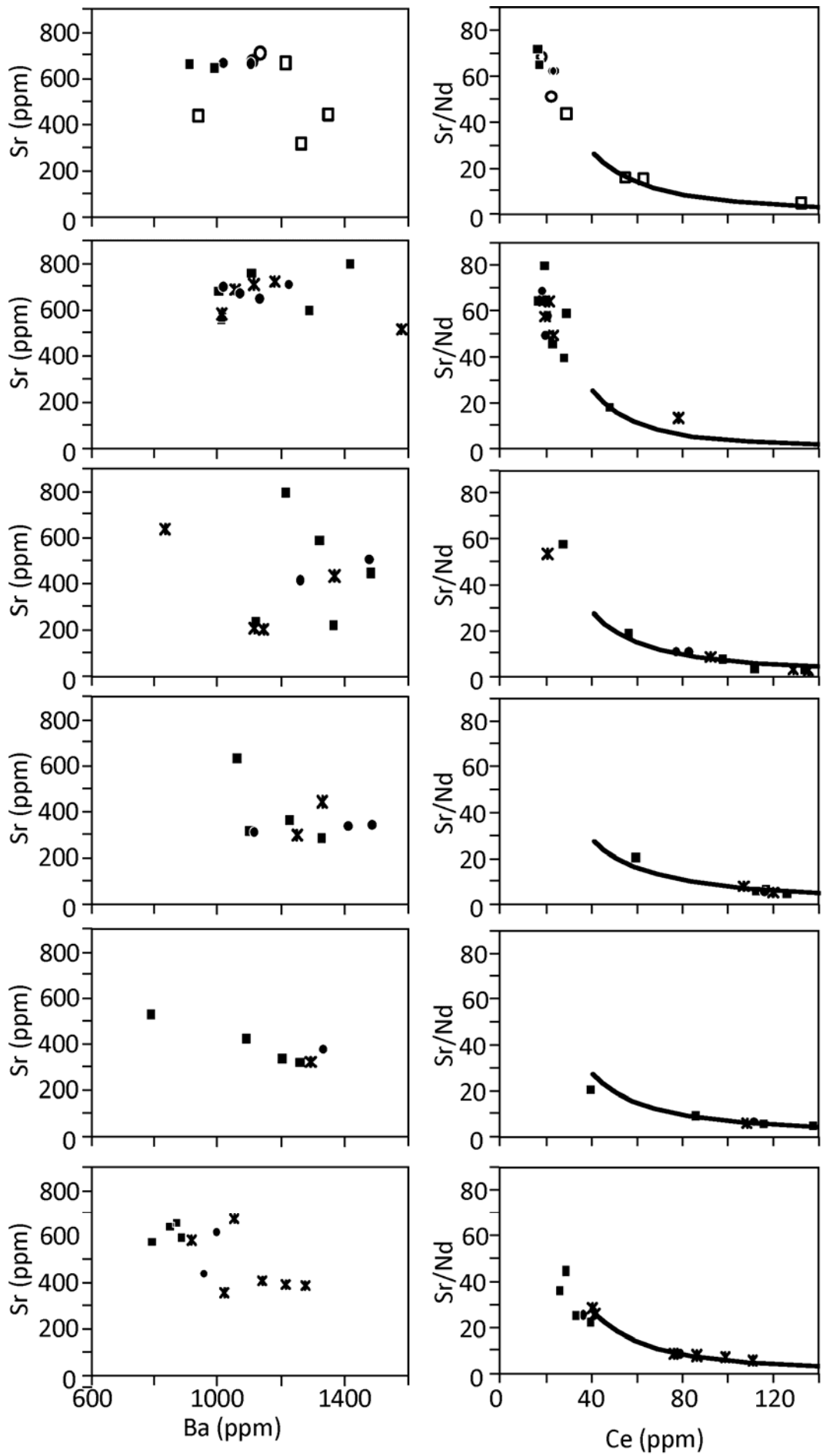


Figure 5.11 Selected trace elements concentrations of amphibole equilibrium melt. Fractional crystallisation was modelled using the parameters in Table 5.3

reversely zoned amphibole population from Taranaki contain enriched trace element chemistries (2 to 9 times higher REE concentrations). This requires the cores and rims to have grown from different melts at different conditions. Mixing with a hotter, more mafic magma can account for the increased temperature and more primitive trace element concentrations of the rims, but not the recorded increase in pressure. The same is true if the cores were xenocrysts incorporated into the host magma. There may be a combination of processes operating where intrusion of a hotter, more mafic magma causes convection or the convecting magma incorporates xenocrysts.

There are two populations of amphibole present in sample SM-6C which differ primarily in pressure, H_2O_{melt} and fO_2 and only slightly in temperature (Figure 5.10). These samples overlap the high pressure, less evolved end members of the other samples, but do not display the trend to lower values present in all other samples. Amphibole is a minor phase in this sample (< 5%). This may be related to the lack of amphibole crystallisation at shallower levels (where the dominant amphibole populations of other samples crystallised) due to rapid ascent from the 15 km depth recorded by rim compositions or, alternatively, due to magma stalling at conditions outside of the amphibole stability field.

Browne & Gardner (2006) found that amphibole dissolution does not necessarily result in the formation of reaction rims, but can round crystal edges and reduce the modal abundance of amphibole. This typically occurs at ~75-90 MPa, which is the pressure range where amphibole dissolution is greatest (Browne & Gardner, 2006). The subhedral to euhedral nature of amphibole crystals from this sample in conjunction with the low modal abundance suggests that magma stalled at ~2-3 km depth during ascent. Thornber et al. (2008) came to a similar conclusion for a small population of resorbed amphibole crystals from the 2004-6 Mt St Helens dacite.

5.2.3.2 Melt Differentiation

Trace element compositions of the melt in equilibrium with various amphibole zones were calculated using the amphibole-dacite partition coefficients from the GERM database (Table 5.5). The Sr content of the back calculated melts were used to estimate the SiO₂ content of amphibole equilibrium melts using the relationship between SiO₂ and Sr in the measured matrix glass. The amphibole cores that record crystallisation depths of ~25 km crystallised from melts with ~530-800 ppm Sr for Population 1 and 250-650 ppm for Population 2, which are inferred to have SiO₂ contents of ~52-62 wt% and 57-70 wt% SiO₂ (basaltic andesite to rhyolite). Early melt differentiation is also supported by the low compatible trace element concentrations recorded by other mineral phases, most notably Cr levels below detection, and low V and Sc in clinopyroxene. This is in agreement with models where melt differentiation occurred in the lower crust (Price et al., 2005; Annen et al., 2006). The Price et al. (2005) model states that dacitic to rhyolitic compositions are generated in the lower crust, whereas Annen et al. (2006) propose that a range of compositions from basaltic andesite to rhyolite can be generated depending on both how evolved the deep crustal hot zone is and the depth within the hot zone.

Amphibole							
Element	K _D	Element	K _D	Element	K _D	Element	K _D
Li	0.18	Cu	1.2	Ba	0.28	Tb	3.08
Sc	35	Zn	10.7	La	0.26	Er	2.34
Ti	3.66	Rb	0.18	Ce	0.63	Yb	1.31
V	4.92	Sr	0.49	Nd	1.24	Lu	1.75
Cr	21	Y	2.46	Sm	2.38	Pb	0.53
Mn	15.7	Zr	0.34	Eu	5.9		
Ni	9.3	Nb	2.5	Gd	2		

Table 5.5 Amphibole-melt (andesite-dacite) partition coefficients used in this study. All values are from the GERM database (<http://earthref.org/GERM/>)

5.2.3.3 Amphibole Model

The amphibole data from most samples are consistent with a model where amphibole crystallises in the lower crust at depths of ~20 km from a differentiated hydrous, oxidised melt. The amphibole and the associated melt migrates through the crust possibly through a series of

sills and dykes similar to that described by Price et al. (1997) and Gamble et al. (1999). As the melt moves through the crust, cumulates may be incorporated and amphibole continues to crystallise. This melt stalls at a depth of ~8 km for the older three samples and ~10 km for Maketawa and Kaupokonui samples, where a large proportion of amphibole crystallises. Many of the deeper-sourced amphibole crystals grow a rim in this shallow magma chamber. However, a small population do not, suggesting these spent a very limited time at these conditions before eruption. Magma ascent from the storage zone to the surface was rapid, as indicated by a lack of break down textures in amphibole crystals.

Sample SM-6C records a different history where amphibole crystallises at ~25 km depth before migrating to a depth of ~15-20 km in association with an increase in melt fO_2 . Melt ascent from this depth was rapid, stalling briefly at ~2-3 km depth before eruption.

5.2.4 FE-TI OXIDES

The chemistry of Fe-Ti oxides reflect temperature, oxygen fugacity and melt composition of the magmatic system immediately prior to eruption because they equilibrate rapidly (on the order of a few years at 900° C; Freer & Hauptman, 1978; Frost & Lindsley, 1991; Devine et al., 2003; Tomiya & Takahashi, 2005). This is reflected in the restricted chemistry of oxides within each sample. The chemical variations between samples can be used to further investigate the differences in the pre-eruptive magmatic conditions among samples.

Four compositionally distinct groups of Fe-Ti oxides have been identified and are differentiated primarily by Ti content (X'_{Usp}), Al_2O_3 , MnO and MgO (Figure 5.12). The Ti content of magnetite records changes in temperature or oxygen fugacity and has been widely used to infer magma mixing and reheating events (e.g. Nakamura, 1995; Devine et al., 2003; Chertkoff & Gardner, 2004; Turner et al., 2008). The Al_2O_3 content of magnetite reflects that of the melt and therefore reflects melt evolution (Chertkoff & Gardner, 2004; Tomiya & Takahashi, 2005) and the Mg/Mn ratio is indicative of magmatic temperature (Bacon & Hirschmann, 1988). There is a strong relationship between Al_2O_3 and Mg/Mn indicating that these parameters are reflecting melt evolution where high Al_2O_3 and Mg/Mn oxides crystallised

from a hotter melt that has experienced less plagioclase crystallisation. This is consistent with the glass analyses and thermometry results for these samples as Inglewood a and b and Korito are the most evolved, lowest temperature samples and Kaupokonui, SM-6C and Maketawa are the most evolved, lowest temperature samples and Kaupokonui, SM-6C and Maketawa are the less evolved and hottest magmas. The X'_{Usp} content does not correspond with the relative magmatic temperatures calculated or the Mg/Mn ratio and is therefore most likely recording changes in fO_2 .

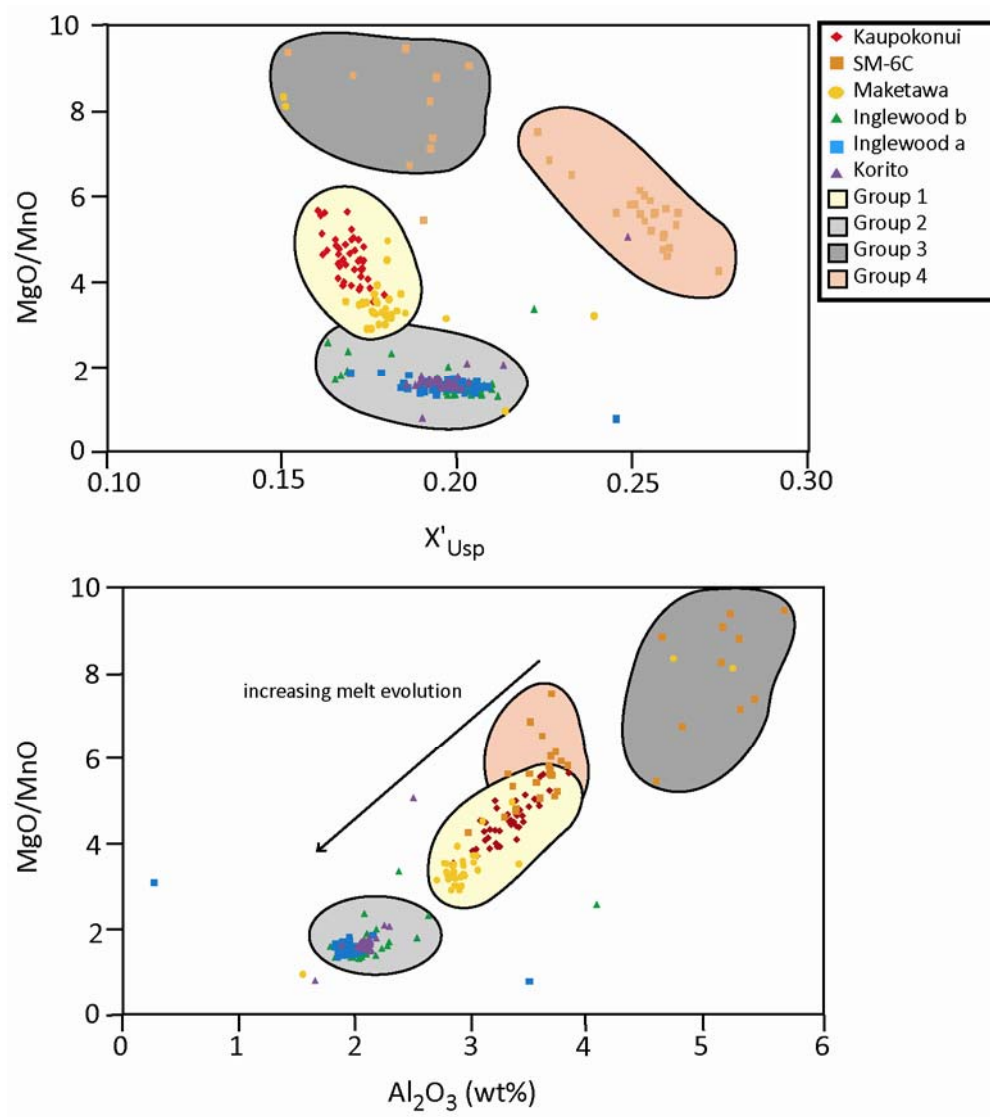


Figure 5.12 Selected major element chemistry of Fe-Ti oxides.

5.2.4.1 SM-6C

SM-6C has two populations of Fe-Ti oxides, recording two different magmatic conditions and that have crystallised from two different melts. Other studies (e.g. Nakamura, 1995; Venezky & Rutherford, 1999; Devine et al., 2003; Turner et al., 2008) have used the presence of two oxide populations to infer that magma mixing must have occurred shortly before eruption. However, most of the oxides which record the least evolved magmatic compositions are amphibole hosted and thus have been isolated from the new melt conditions. The few groundmass oxides which also fall into this population are broken up so these may have formed part of a cumulate which was later disaggregated. Therefore the presence of these two populations cannot constrain the timescales of any mixing event, but does demonstrate that incorporation of xenoliths or antecrystic material occurred.

Amphibole oxybarometry results show two populations of amphibole crystals within SM-6C on the basis of fO_2 . Qualitatively, groundmass oxides would relate to the higher pressure amphibole population (the groundmass population and the high pressure population have the lower fO_2 of the two groups). This may mean that lower pressure amphibole population from SM-6C are cumulates or xenoliths which were incorporated into the host magma during ascent.

5.2.5 RELATIONSHIP BETWEEN MINERAL PHASES

There are a number of common textures within the dominant mineral assemblage that are most likely formed by the same set of processes (e.g. Humphreys et al., 2006). Most notably plagioclase and clinopyroxene exhibit similar textural and chemical features that indicate a similar history. However, various mineral phases can respond differently to magmatic processes. The interpretations of mineral textures in this study are strongly influenced by the nature of BSE imaging as this was the basis of mineral characterisation. Zoning highlighted by BSE imaging for plagioclase and clinopyroxene minerals are those chemical variations which are particularly sensitive to magmatic conditions (anorthite content and Mg#). Zoning in amphibole also primarily reflects variations in Mg# which in turn is most strongly controlled by oxygen fugacity (Ridolfi et al., 2010).

5.2.5.1 Crystal cores

Trace element data show that those plagioclase cores which are high in anorthite and/or patchy did not form in conjunction with high pressure amphibole (Figure 5.13). This is consistent with suppression of plagioclase crystallisation at high H_2O_{melt} (Gaetani et al., 1993) such as those recorded by the high pressure amphibole cores. The high Al clinopyroxene cores may have formed with either the high anorthite and sieved plagioclase cores or the high pressure amphibole cores. The clinopyroxene major element data and textures are consistent with both crystallisation at high pressure with amphibole, or a less evolved and/or hotter melt with the plagioclase cores. Distinguishing between these is difficult due to the limited trace element analyses of the high Al cores and the ambiguous interpretation of clinopyroxene major element data. As plagioclase and clinopyroxene share many other common textural and chemical features, it is considered more likely that these have a similar origin.

5.2.5.2 Zoning and rims

Magma mixing where a hotter and/or less evolved melt is injected into the shallow magma body will be recorded differently by individual crystals depending on the proximity to the site of the intrusion (Murphy et al., 2000). Those with the strongest disequilibrium features such as sieved zones in plagioclase and distinctive, strongly resorbed zones in clinopyroxene crystals, were formed when these crystals were engulfed by a hotter magma (Nakagawa et al., 2002; Browne et al., 2006). Other crystals primarily recorded heating of the system and are most likely represented by the multiple zoning within clinopyroxene and the larger scale oscillatory zoning in plagioclase (~50 μm , 15-20 mol% change in anorthite). These textures are evidence for disequilibrium conditions, but do not record large changes in melt chemistry. Other crystals appear to be unaffected, and the overall result is a wide range of textures within each sample.

Plagioclase and clinopyroxene crystals as well as some amphibole rims are comprised of oscillatory zoning. These textures are probably formed by a combination of processes including kinetic effects, convection and recharge which results in slightly different morphologies and scales of oscillatory zoning.

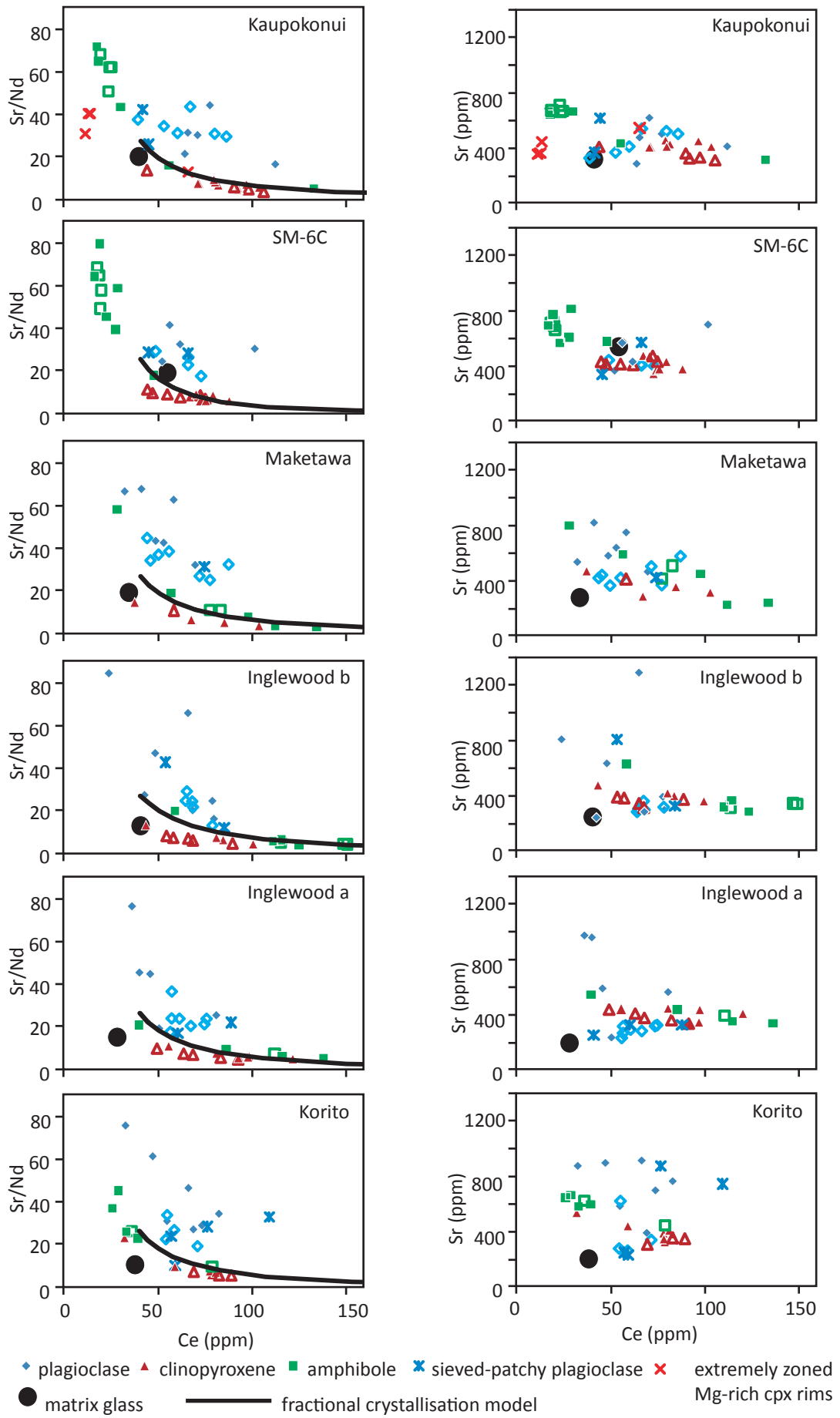


Figure 5.13 Trace element concentrations of melt in equilibrium with the plagioclase, clinopyroxene and amphibole. Ce vs Sr/Nd is used as an index of fractional crystallisation and the composition of the equilibrium melts is compared with the modelled evolution of the melt as driven by fractionation of plagioclase, clinopyroxene and amphibole using the parameters from Table 5.3. Ce vs Sr is also shown as Nd is present in low concentrations in plagioclase (1-4 ppm) so the consistent offset apparent in the Ce vs Sr/Nd of the plagioclase data is most likely related to the low accuracy of the Nd data which is then amplified by the affect of modelling melt composition values using partition coefficients.

Amphibole crystallisation primarily reflects the evolution of the host melt as it ascends the crust because the trace element compositions of both the high and low amphibole population follows a fractional crystallisation trend (Figure 5.13). Plagioclase and clinopyroxene oscillatory zoning coincide with this fractional crystallisation trend marked by the low pressure amphibole. This trend is particularly dominant in the older three samples. The younger three samples display more variability within the trace element chemistry (e.g. Sr values for this 'equilibrium assemblage' vary by up to 400 ppm at a fixed Ce concentration). This may relate to a stronger mixing signature in these younger samples shortly before eruption that is apparent in the mineral textures.


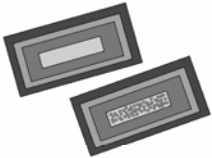


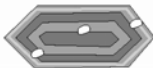





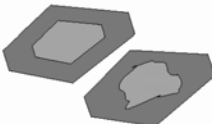



	Mineral Texture	Observation	Interpretation
<i>Plagioclase</i>		Oscillatory zoning	Crystallisation in a shallow magma chamber
		Calcic and sieved cores	Crystallisation from a hotter more mafic magma
		Sieved zone	Engulfed by hotter and/or mafic magma which is then mixed into the host
		Dissolved crystals	Xenoliths or crystals from a much more mafic magma
<i>Clinopyroxene</i>		Oscillatory zoning	Crystallisation in a shallow magma chamber
		Multiple zoning	Records perturbations to a shallow magma chamber e.g. heating
		Resorbed zone	Heated, possibly by interaction with a hotter magma
		Patchy core	Crystallisation at depth or in a hotter and/or mafic magma
		Extreme Mg-rich rim	Engulfed by an andesitic magma which is then mixed into the dacitic host
<i>Amphibole</i>		Unzoned	Equilibrium crystallised in a shallow magma chamber from the host melt
		Simple zoning	Cores crystallise at depth, rims crystallised in shallow storage chamber
		Oscillatory rim	Cores crystallise at depth, rims crystallised in shallow storage chamber, probably for a longer period of time than simple zoning
		Patchy-resorbed core	Cumulate origin?
		Multiple zoning	Records multiple periods of magma stalling during ascent of the crust

Figure 5.14 Summary of the mineral textures observed in the Holocene Taranaki eruptions and the associated interpretation.

5.3 TEMPORAL VARIABILITY

The long term temporal variability at Mt Taranaki shows that these eruptives are becoming more potassic with time (Price et al., 1999). Over shorter time periods (100's to 1000's of years), the degree of variability is much greater, a trend that has been noted at other andesitic volcanoes such as Mt Ruapehu (Gamble et al., 1999), Tongariro (Hobden et al., 1999) and Tataru San Pedro (Dungan et al., 2001). Long term geochemical variability is controlled by broad scale processes such as variations in the mantle source, slab flux and subducted sediment as well as crustal processes related to the evolution of the magmatic system including crustal assimilation and fractional crystallisation (Graham & Hackett, 1987; Stewart et al., 1996). In contrast, short term variability is related to the complexity of andesitic plumbing systems and is controlled by magma system processes such as magma recharge, mixing and mingling as well as which parts of the system are tapped (Gamble et al., 1999; Stewart 2010).

The six samples investigated here span a time frame from ~4000 years to ~2000 years ago. This is not a complete record of the volcanic history during this period, but represents the larger sub-plinian eruptions. The geochemistry results indicate that Taranaki eruptives over this time period became less silicic with time. It has been emphasised in the discussion thus far that the samples investigated fall into three populations on the basis of petrology and chemistry: 1) The older three samples, Inglewood a and b and Korito; 2) Maketawa and Kaupokonui; and 3) SM-6C. The short-term variations in petrology and chemistry of these eruptions may in part be related to complexities in the sub-volcanic system.

The older three samples have the most evolved glass ($\text{SiO}_2=70-74$ wt%), and are the lowest temperature (850-900° C) and largest eruptive units in the suite. These samples are almost indistinguishable on the basis of petrology and chemistry (except Group 1 amphibole in Korito) (Figure 5.15). Amphibole thermobarometry data indicate that each of these magmas ascended through the crust in a similar way, stalling and crystallising from ~ 20 km depth to the shallow storage system at ~6 km depth.

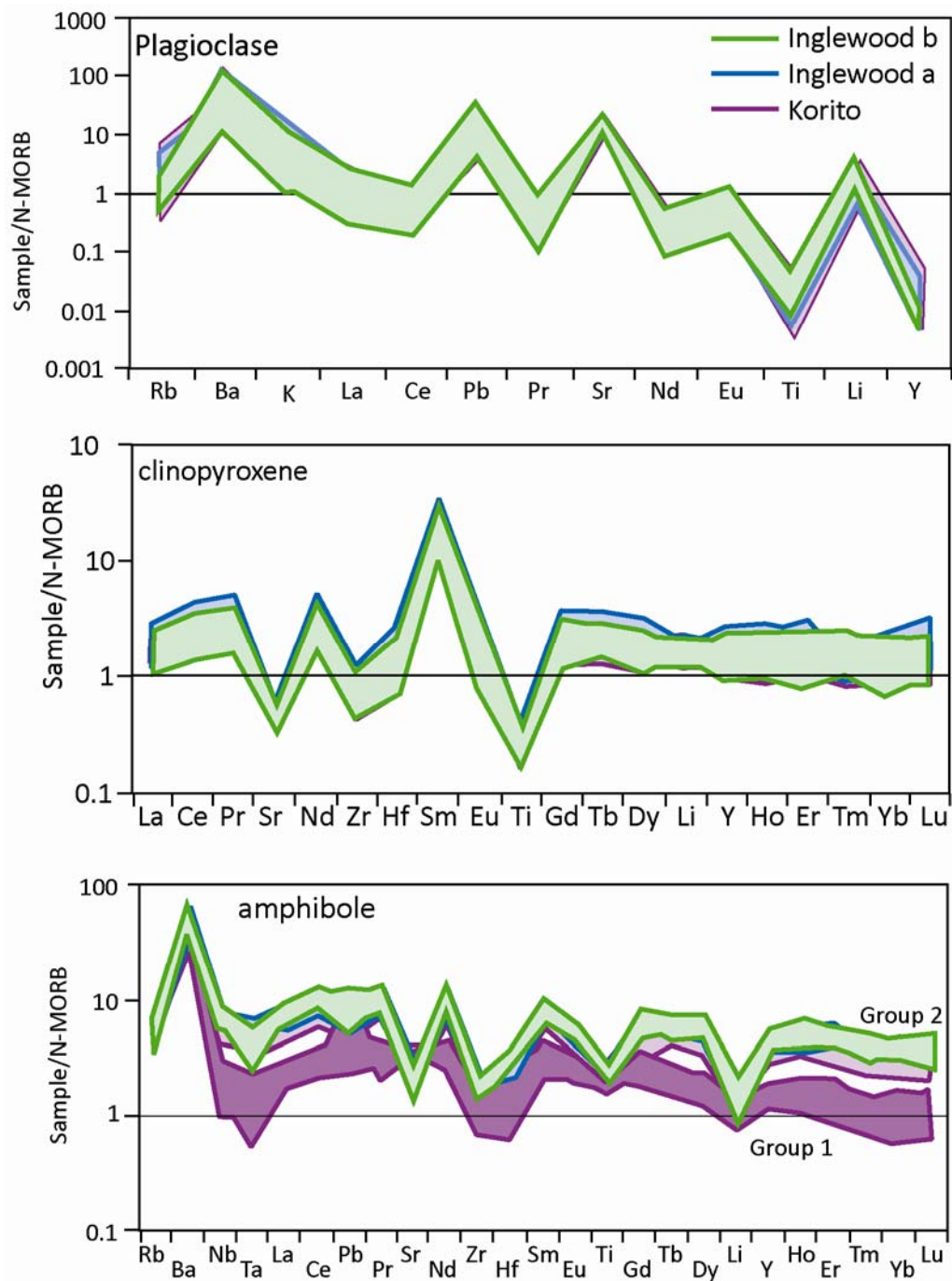


Figure 5.15 Multi-element diagrams of mineral trace element analyses for samples Inglewood a and b and Korito. The trace element chemistry for each mineral phase is very similar between these samples with the exception of Group 1 amphibole in Korito.

In contrast, the Maketawa and Kaupokonui are hotter (900-950° C), less evolved samples with dacitic glass compositions ($\text{SiO}_2=66-69$ wt%). Trace element chemistry of both glass and mineral phases indicates that these formed from similar magmas. Thermobarometry modelling also implicates a similar history of ascent through the crust, with crystallisation occurring continuously from ~20 km to ~8 km.

SM-6C is consistently identified as a distinctly different sample within this suite. SM-6C is the least evolved sample as indicated by major element glass chemistry ($\text{SiO}_2=60-62$ wt% $\text{K}_2\text{O}=3-4$ wt%). It is also petrographically distinct due to the presence of orthopyroxene and olivine, which are notably absent from the other samples. The plagioclase, clinopyroxene, amphibole and titanomagnetite from this sample exhibit a range of textures that are not observed in the other samples from this study.

The origin of geochemical distinctions between different groups of eruptions has been examined at many andesitic volcanic systems (e.g. Tataru-San Pedro Complex, Dungan et al., 2001; Ngauruhoe, Price et al., 2010). These variations have been related to factors including variability of the parental magma composition, changes in the magma supply rate and reorganisation of the sub-volcanic magmatic system (Dungan et al., 2001). Geochemically similar groups of lava flows at Taranaki can erupt for periods of 1000 to 2000 years (Downey et al., 1994). This relates to broader-scale replenishment of the magmatic system, while localised interactions within the storage region give rise to shorter period events (Stewart, 2010). The older three Taranaki samples span a time range of ~500 years (4150-3580 years B.P.) and Maketawa and Kaupokonui are ~1000 yrs apart from each other. Gross differences between the older samples and the Maketawa/Kaupokonui are therefore likely related to large scale replenishment.

These two groups of eruptions relate to different pulses of magma from the lower crust. Therefore they will have started with slightly different magmatic compositions that were further modified during ascent and storage in the crust. Additionally, there appears to be shift in the nature of the magmatic plumbing system between these two groups of eruptions based on amphibole thermobarometry data. The older three samples appear to have stalled in a shallow magma chamber at ~6-8 km depth, whereas Kaupokonui and Maketawa stalled at ~8-10 km depth. This reorganisation of the sub-volcanic reservoir system may have resulted in changes in the degree and style of mixing and the contamination components (Dungan et al., 2001). The deeper, less evolved and volumetrically smaller nature of the Kaupokonui and Maketawa eruptions may have caused the stronger apparent mixing signal in these samples. Additionally,

the nature of the mixing component is likely to have also changed as a result of this larger scale replenishment to a less evolved composition (e.g. Gardner et al., 1995). In comparison, the three older samples have a stronger fractional crystallisation signature, possibly as a result of a longer residence time in a shallower storage system.

SM-6C is interpreted to be an eruption from the satellite vent of Fanthams Peak. The reported petrology of eruptions from Fanthams Peak more closely fits that observed in this sample than the summit vent eruptions. Fanthams Peak eruptions are less evolved, with basaltic to basaltic andesite whole rock compositions (e.g. Neall et al., 1986; Stewart et al., 1996). They are significantly lower in K_2O and contain orthopyroxene and rare olivine, which is consistent with the mineralogy of SM-6C. The limited published major element mineral data for Fanthams Peak eruptives (Stewart et al., 1996; Turner et al., 2008) show a general agreement with that of SM-6C. Plagioclase anorthite content is significantly higher in those units sourced from Fanthams peak (An_{80-90} compared with An_{45-75}) and SM-6C plagioclase compositions extend to higher anorthite values than the other samples from this study, overlapping the reported values from Fanthams Peak. Amphibole Al_2O_3 content is 12.5-15 wt% in Fanthams Peak eruptives, which is higher than the 10-11 wt% published for the corresponding summit vent eruptions from these same studies. The high Al content has been attributed to amphibole crystallisation from a greater depth. Both the higher Al_2O_3 and deeper crystallisation pressures are features of SM-6C. Clinopyroxene data is less conclusive, as the published core values correspond to most of the samples in this study (including SM-6C) but the rim values do not. Glass trace element chemistry shows that the five samples assumed to be from the summit vent form a straight line trend in SiO_2 -compatible trace element space. This is interpreted as a mixing trend and indicates that these samples may be related. SM-6C plots off this trend, showing that it has not interacted with the magmatic systems of the other samples.

5.4 TIMESCALES OF MAGMATIC PROCESSES

Modelling of Fe-Mg interdiffusion in clinopyroxene was applied to quantify the timescales of magma storage and mixing. The model of Morgan et al. (2004) was applied using the diffusion coefficient of Dimanov & Wiedenbeck (2006) (Chapter 3). Clinopyroxene from all samples were modelled except those from SM-6C, which did not contain zoning characteristics appropriate for this model. The outermost zone from a number texturally diverse crystals was modelled in each sample. Where possible, zones closer to the core were also modelled to better constrain residence times.

5.4.1 CLINOPYROXENE RESIDENCE TIMES

The minimum residence times (ages) of clinopyroxene crystals in the host magma are of the order of months to years as recorded by the outermost rims of these crystals (Figure 5.16). The total range of ages for these outermost crystal rims range from *ca.* 0.3-3 yr for Korito, Maketawa and Kaupokonui and *ca.* 1-10 yr for Inglewood a and b, with the distribution skewed towards younger ages (Figure 5.15). A range of zones within the oscillatory zoning bands of individual crystals were also modelled for Kaupokonui, Inglewood a and b and Korito samples. These give residence times of 2-5 yr for Inglewood a and b and Korito, 0.5 to 2 yr for Maketawa and months (indistinguishable from the outermost rims) for Kaupokonui (Figure 5.17).

5.4.1.1 Magma storage

Oscillatory zoning has been attributed to crystallisation conditions within the main storage magma chamber (e.g. Browne et al., 2006; Humphreys et al., 2006). The boundary between clinopyroxene cores and oscillatory zoning is generally resorbed and not appropriate for diffusion modelling. Therefore, the 'inner oscillatory zone' population provides the best estimate for crystal residence times within this storage chamber. These ages indicate that clinopyroxene crystals were stored in a shallow level magma chamber at least 5 yr prior to eruption for Inglewood a and b and Korito, and 1 yr prior to the eruption of the Kaupokonui and Maketawa samples. The variability in the range of ages calculated for a population of zones

increases towards the core of the crystal. This relates to the nature of oscillatory zoning because the zones cannot be correlated between crystals (Ginibre et al., 2002b). The older three samples are the most silicic, containing rhyolitic glass compositions ($\text{SiO}_2 = 70\text{-}74 \text{ wt}\%$). These also record the longest residence times in the storage chamber. Therefore these samples may have undergone more fractional crystallisation and subsequently more evolution of the melt phase.

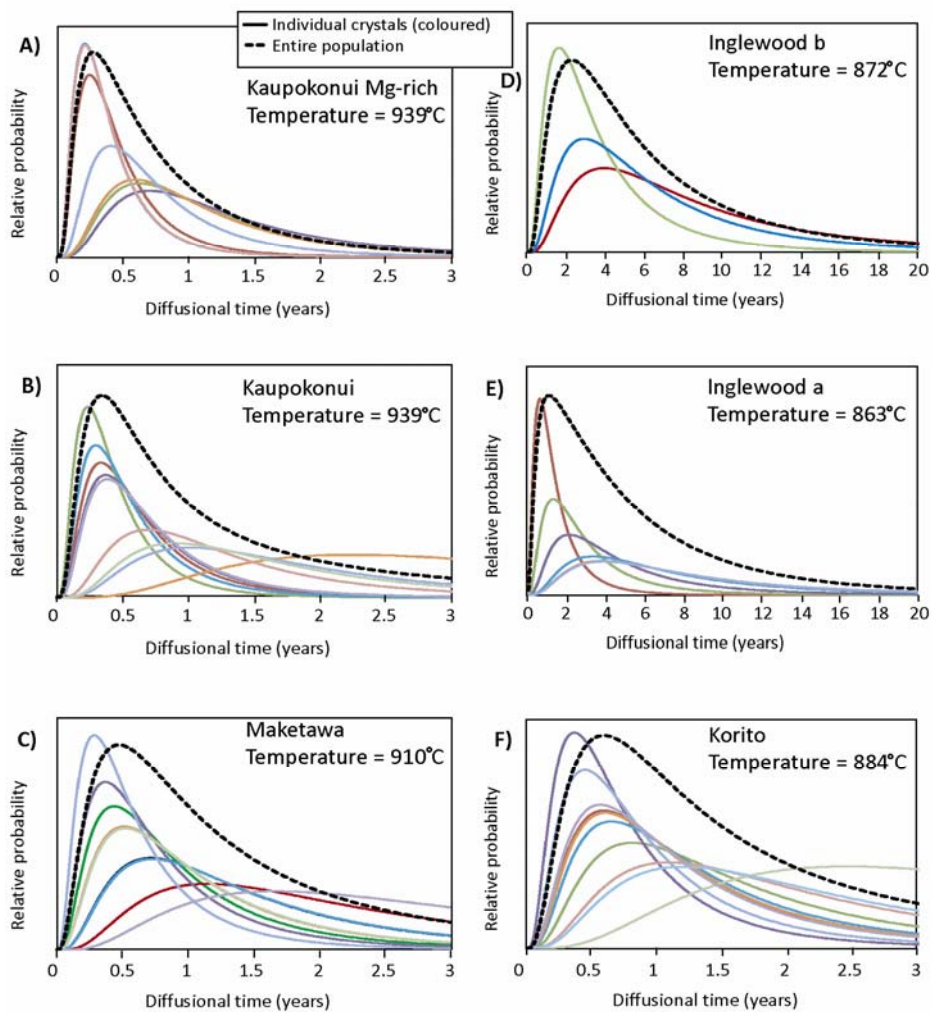


Figure 5.16 Probability density functions showing the results of diffusion modelling for the rims of each sample. The high-Mg rims from Kaupokonui are presented separately from the oscillatory rims from this sample. Temperatures shown are those used in the modelling.

5.4.1.2 Mixing

Diffusion modelling of the Mg-rich rims from Kaupokonui, which are proposed to record the intrusion of a hotter, intermediate (andesitic-dacitic) magma, also returned residence times of months. This short time between magma mixing and eruption suggests it may have been the eruption triggering event. In comparison it is more difficult to decipher whether mixing

events triggered the other eruptions investigated in this study because the mixing is between magmas of similar composition. Some of the broader scale oscillatory and multiple zoning may record perturbations to the magma chamber induced by magma mixing. Addition of clinopyroxene to the shallow magma chamber may have occurred as a consequence of a mixing event. In this case, the residence times of the oscillatory zoning provides a minimum timescale for magma mixing.

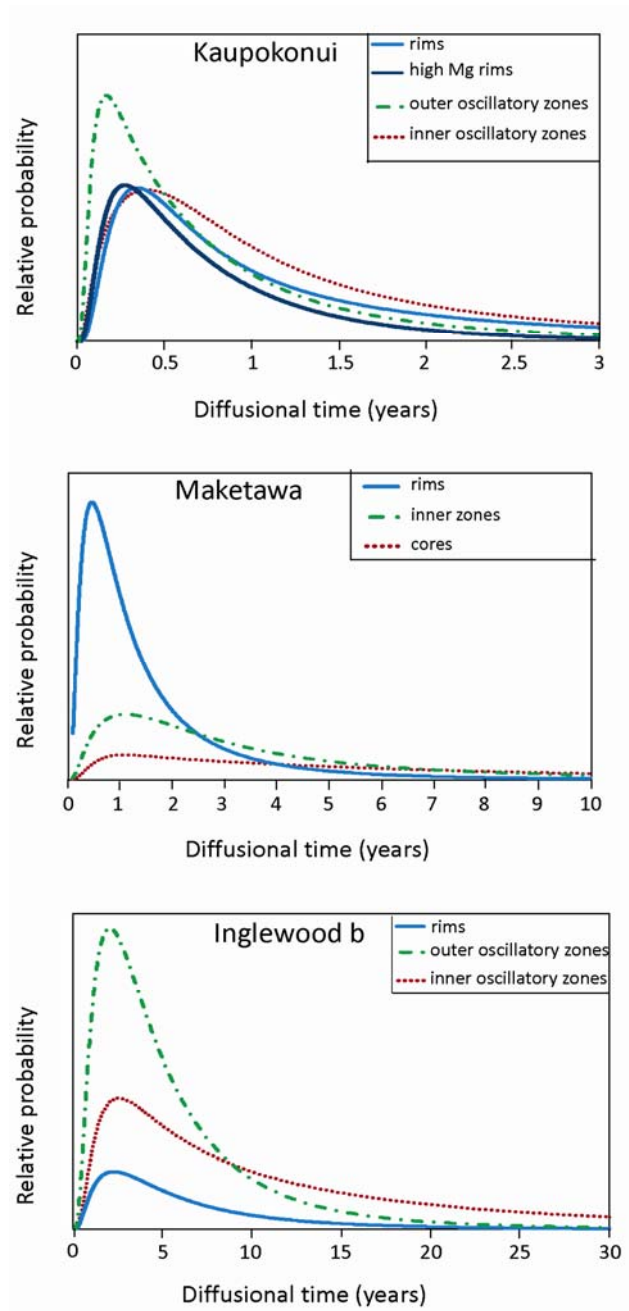


Figure 5.17 Probability density functions of representative samples showing the results of diffusion modelling zones that are not the outermost rim (shown in Figure 5.16).

5.4.2 COMPARISON WITH OTHER STUDIES

The timescales obtained from these Taranaki samples are similar to those found in other studies of andesitic volcanoes. Timescales of the order of months to years fall within the intermediate range for magma mixing in general, and are relatively short for crystal residence times in shallow magma chambers. The same diffusion model was applied by Morgan et al. (2004), who used Fe-Mg interdiffusion in clinopyroxene to constrain the open system processes occurring during the 1944 eruption at Vesuvius. The authors calculated a range of residence times of Fe-rich rims from 4.5 months to 9 yr, with the shorter ages predominant. This was interpreted to be related to recharge of the magma chamber, and concluded that the bulk of the magma was intruded < 6 months prior to the eruption. A population with no measurable diffusion was also identified, signifying the final input into the system and triggering of the eruption. The diffusion coefficient used by Morgan et al. (2004) was 1.7979×10^{-20} at a temperature of 1077° C from Dimanov & Sautter (2000). For comparison, the residence times of Morgan et al. (2004) were recalculated applying a diffusion coefficient determined using the method of Dimanov & Wiedenbeck (2006) (6.35×10^{-21}). This increased the timescales by a factor of 2.72, resulting in residence times of 1 to 25 yr. The recalculated values are on a scale of years to decades compared with the months to years presented in this thesis for Taranaki.

Other published studies that investigated crystal residence times typically return ages that are longer than those calculated in this study (Table 5.6). In general, the studies that use crystal residence times to infer timescales of crystallisation and crustal residence times (e.g. Zellmer et al., 1999; Morgan & Blake, 2006) are measuring a longer lived process than the shallow magma chamber residence times constrained in this study.

The timescales of magma mixing have been investigated using diffusion modelling at a number of volcanoes returning timescales ranging from days to centuries (Table 5.6). Much of the focus on magma mixing has been on systems where basaltic magma intrudes into a silicic reservoir (e.g. Martin et al., 2008; Kent et al., 2010; Costa & Chakraborty, 2004). Martin et al.

(2008) used Fe-Mg interdiffusion in olivine to constrain a basaltic magma injection on a timescale of *ca.* 1 month at Santorini, making this intrusion the probable triggering event.

Table 5.6 Summary of previous studies applying diffusion modelling to volcanic systems. Modified from Costa & Chakraborty (2004).

Case Study	Method	Time (prior to eruption)	Process	Reference
Curtis Ridge episode, Mt Taranaki (New Zealand)	Fe-Ti oxide zoning	Hours to weeks	Andesite-andesite mixing	Turner et al. (2008)
Montserrat (Lesser Antilles)	Fe-Ti oxide zoning	Days to weeks	Andesite remobilisation by mafic intrusions	Devine et al. (2003)
Usu (Japan)	Fe-Ti oxide zoning	Days to weeks	Basalt-rhyolite-andesite; dacite-rhyolite; dacite-dacite mixing	Tomiya & Takahashi (2005)
Ceboruco (Mexico)	Fe-Ti oxide zoning	Days to 6 months	Rhyodacite-dacite-mafic mixing	Chertkoff & Gardner (2004)
Unzen (Japan)	Fe-Ti oxide zoning	Weeks to months	Dacite-dacite mixing	Venezky & Rutherford (1999)
Unzen (Japan)	Fe-Ti oxide zoning	Weeks to months	Dacite-dacite mixing	Nakamura (1995)
Trident (Alaska)	Fe-Ti oxide zoning and Fe-Mg olivine zoning	Days to 2 years	Dacite-andesite mixing	Coombs et al. (2000)
1944 eruption - Vesuvius (Italy)	Fe-Mg zoning in clinopyroxene	Months to years	Magma recharge	Morgan et al. (2004)
Santorini (Greece)	Fe-Mg olivine zoning	1 month	Basaltic –andesite mixing	Martin et al. (2008)
Tatara-San Pedro (Chile)	Fe-Mg, Mn, Ni zoning in olivine	Months to 10 years	Magmatic assimilation of hydrous mafic to ultramafic cumulates by ascending basalts	Costa & Dungan (2005)
San Pedro (Chile)	Fe-Mg olivine zoning	Year to decades	Basaltic andesite-dacite mixing at depth	Costa & Chakraborty (2004)
Mt St. Helens (Washington)	Li in plagioclase	< 1 year	Vapour transfer and accumulation at the top of the magma reservoir	Kent et al. (2007)
Mt Hood (Oregon)	Mg zoning in plagioclase	Days	Mafic-silicic mixing	Kent et al. (2010)
San Pedro (Chile)	Mg zoning in plagioclase	Decades to 100 years	Metasomatism of xenoliths	Costa et al. (2003)
Santorini (Greece); Montserrat (Lesser Antilles)	Sr zoning in plagioclase	100 - 450 years	Crystal residence time	Zellmer et al. (1999)
Montserrat (Lesser Antilles)	Sr and Ba zoning in plagioclase	10 -1200 years	Andesite remobilisation by mafic intrusions	Zellmer et al. (2003)
A.D. 79 eruption- Vesuvius (Italy)	Ba zoning in sanidine	Decades	Episodic recharge	Morgan et al. (2006)
Bishop Tuff (California)	Sr and Ba zoning in sanidine	114 000 years	Crystal residence time	Morgan & Blake (2006)
<i>Mt Taranaki (New Zealand)</i>	<i>Fe-Mg zoning in clinopyroxene</i>	<i>Months to years</i>	<i>Intermediate-silicic mixing; residence in a shallow storage chamber</i>	<i>This work</i>

However, Costa & Chakraborty (2004) calculated timescales of years to decades at San Pedro, Chile, meaning the basaltic input did not necessarily trigger the eruption. Rather, it was induced by collapse of the eastern flank of the volcano. These authors also proposed that the mixing occurred at depths of ~6 km (Costa et al., 2004), so there would be a longer time span between mixing and eruption than if this mixing occurred in the conduit.

5.4.2.1 Previous work using Fe-Ti diffusion in oxides

Ti diffusion in Fe-Ti oxides is the most frequently applied diffusion technique for investigating andesite petrogenesis, including processes such as magma recharge, mixing and reheating on a short timescale (e.g. Nakamura, 1995; Devine et al., 2003; Tomiya & Takahashi, 2005; Turner et al., 2008). This method was outside the scope of the present study as the Fe-Ti oxides did not show compositional variability appropriate for diffusion modelling. The samples did not contain Fe-Ti oxides with zoning and all but SM-6C contained only one population. Although SM-6C did contain two oxide populations, one of these was considered to be isolated from the melt and therefore not record magmatic perturbations. As such, this section discusses previous work employing this technique in andesitic complexes and identifies the conclusions relevant to an understanding of the Taranaki magma system.

Ti diffuses so rapidly in Fe-Ti oxides that the Ti distribution homogenises within a few years (at 900° C) (Freer & Hauptman, 1978). Therefore Ti disequilibrium within these minerals indicates a perturbation to the magmatic system on a timescale shorter than a few years. The presence of Fe-Ti oxides preserving the unaffected ‘original’ composition, when independent evidence indicates a late stage perturbation, may suggest shorter timescales still (Devine et al., 2003). However, these minerals reset so quickly that they only record the final reheating event before eruption, thereby provide different information about pre-eruptive processes than silicate minerals (Turner & Costa, 2007). This can lead to the calculation of conflicting timescales. For example, Zellmer et al. (2003) and Devine et al. (2003) both investigated the shallow magmatic processes at Soufriere Hills, Montserrat. Zellmer et al. (1999) obtained residence times from Ba and Sr zoning in plagioclase crystals of 10-1200 yr which they interpreted as multiple pulses of

magma into the shallow crust over this period of time. Devine et al. (2003) used Ti zoning within Fe-Ti oxides to infer that reheating and subsequent remobilisation of the andesite body by a hotter, mafic magma occurred days to weeks before eruption and continued throughout this eruption. At Soufriere Hills, the plagioclase crystals recorded the intrusion of the various andesitic pulses into the upper crust and the formation of the magma body which was eventually erupted. The Fe-Ti oxides recorded the remobilisation of this andesite and therefore constrained the triggering events of these eruptions and quantified the timescales between eruption triggering and the subsequent eruption.

Turner et al. (2008) used Ti diffusion in titanomagnetite to identify a recharge triggering event hours to weeks prior to the eruption of the Curtis Ridge episode from Mt Taranaki on the basis of two distinct Fe-Ti oxide populations present in the groundmass of the eruptives. There was no Ti compositional gradient in these oxides and therefore no Ti diffusion. This led the authors to conclude that one population was part of a triggering injection which cryptically mixed with the resident magma hours to weeks prior to eruption. The clinopyroxene crystals from the Turner et al. (2008) study are similar to those of the oscillatory rim population found in Korito and Inglewood a and b presented here. Turner et al. (2008) attribute the change from patchy cores to oscillatory rims of the clinopyroxene crystals in the Curtis Ridge sample to the same triggering event – results which are inconsistent with the work of this thesis. However, separate eruptions are investigated and therefore different processes and/or slightly different timescales may be expected to occur. Also, Fe-Ti oxides generally record separate events to silicate minerals, and the interpretation of Turner et al. that the recharge event introduced both the high Ti magnetite population and a population of clinopyroxene crystals, which then crystallised an oscillatory zoned rim, may not be valid. Clinopyroxene crystals (along with plagioclase and amphibole) may have been introduced into the magma chamber months to years prior to eruption before a final injection of magma triggering the eruption as is observed at Montserrat and Vesuvius (Devine et al., 2003; Zellmer et al., 2003; Morgan et al., 2004). Most of the samples investigated here appear to have been cryptically mixed by the injection of a compositionally similar magma as discussed by Turner et al. (2008). This is most evident in the

Kaupokonui sample where the extreme high-Mg rims are clear evidence for interaction with a hotter, more mafic magma.

The long relative timescales for magma mixing calculated in this study when compared with the results of other diffusion modelling used to constrain the timescales of mixing between intermediate to silicic end members may be related to the use of magnetite rather than silicate minerals. Diffusion modelling in silicate minerals has primarily been applied to mixing between more extreme end members (basalt and silicic melt). This may be because mixing between intermediate and silicic end-members as has been proposed at Taranaki is not clearly recorded in silicate minerals.

Magma mixing and recharge has been strongly linked to eruption triggering by a number of studies (e.g. Sparks et al., 1977; Eichelberger & Izbekov, 2000; Murphy et al., 2000; Martin et al., 2008; Kent et al., 2010). However, magma mixing does not necessarily trigger eruptions (Costa & Chakraborty, 2004). This is supported by the results of this thesis, which establish that clinopyroxene disequilibrium features related to mixing events are present in older parts of the crystals formed prior to the mixing event constrained by diffusion modelling.

The range in timescales inferred by diffusion modelling for magma mixing processes has been linked to the end member compositions involved in the mixing (Turner & Costa, 2007) and the mode of andesite formation (Costa & Chakraborty, 2004). The summary of previous work presented in Table 5.6 does not support the idea that timescales of magma mixing are controlled by the end member compositions. Mixing between basalt-dacite and dacite-dacite have both been estimated to occur on short timescales (days to weeks) at various volcanoes. However, the mode of andesite formation is likely to be a more important control on the timescales of magmatic processes. Diffusion modelling timescales is most strongly related to the nature of the formative process, and this is in turn dependent on the mineral-element pair being modelled. Other factors such as the magma composition(s) may play a minor role.

5.4.3 RELATIONSHIPS BETWEEN THE OLDER THREE ERUPTIONS

Diffusion modelling can be used to test two hypotheses about the geochemically and petrographically similar, older three samples: (1) they represent three separate magma batches formed by the same petrogenetic processes, producing similar eruptives over a period of time; or (2) they are from the same magma batch, which is periodically remobilised and erupted. The diffusion ages for these three samples get progressively older as the eruptions get younger, by *ca.* six months to a year. However, these timescales are too small to infer that the eruptions are from a single magma batch, as Inglewood a and b erupted *ca.* 50 yr apart (Alloway et al., 1995 and references therein). The Korito is around 100-400 yr older than the Inglewood Tephra (Alloway et al., 1995 and references therein) and is therefore even more difficult to reconcile with the diffusion ages assuming a single magma batch (Alloway et al., 1995 and references therein). These timescales can be reconciled if the diffusion process is slowed down to a near negligible rate by cooling of the magma to temperatures around 700° C (D. Morgan, pers comm.). This requires a cooling of the magma body by *ca.* 150° C, followed by subsequent reheating within 6 months to a year. Cooling on this timescale is unlikely in context of other magmatic systems. For example, Ngauruhoe erupted in 1975, and eight years later Giggenbach (1982) recorded a gas temperature of 650° C. Magmatic systems do not typically cool on the timescale of months required for these eruptions to represent progressive eruptions from a single host magma. This is in agreement with Hildreth & Moorbath (1988), who favour the repeated input of new magma preferentially following established conduits, rather than the continuous evolution of a single magma batch.

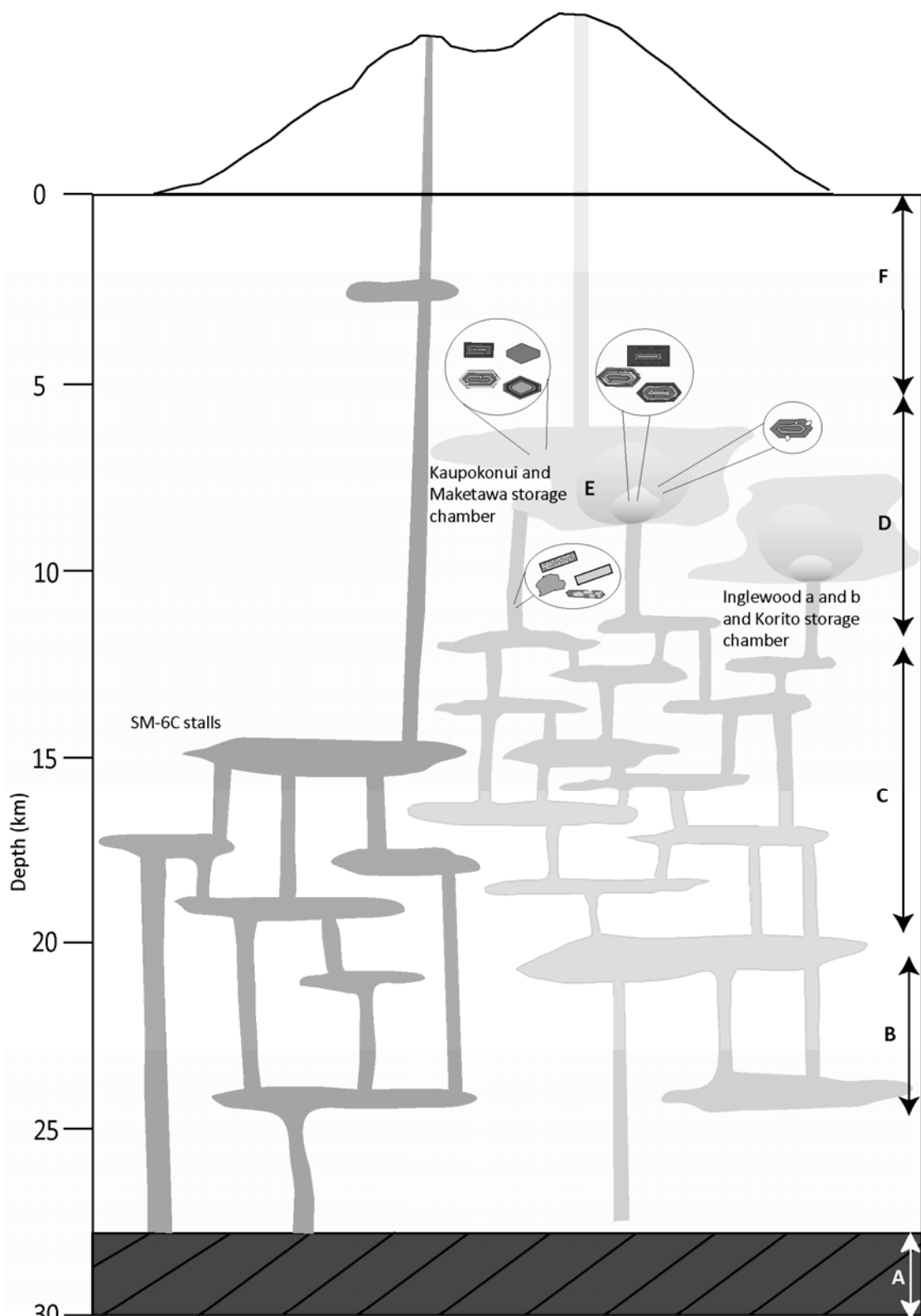
In summary, these three samples represent three separate magma batches which record a similar ascent through the crust and were formed by very similar petrogenetic processes. Amphibole barometry indicates that the Inglewood a and Korito continuously record crystallisation between the 20 km initial depth and 6 km storage depth. However, Inglewood b does not record crystallisation between ~12 and 8 km depth, suggesting that it used the magmatic plumbing system established by the previous eruptions and therefore ascended more rapidly.

5.5 ANDESITE PETROGENESIS AT MT TARANAKI

The petrogenesis of the Taranaki andesites investigated in this study is described within the context of previous work using a four-stage model in which: (i) Melt is differentiated at depth (> *ca.* 25 km) to an intermediate - silicic composition; (ii) The melt migrates through the crust via a complex plumbing system, possibly consisting of interconnected sills and dykes; (iii) Magma stalls in the upper crust, where decompression crystallisation and magma mixing between compositionally similar end members occurs during ascent and storage; and (iv) Fractional crystallisation takes place in the shallow magma chamber, imprinting a dominant signature on these magmas (Figure 5.18). Geochemical and textural evidence for each of these stages will be discussed in detail in the following sections.

i. Differentiation of melt at depth

Melt differentiation occurring at depth of greater than *ca.* 20 km as indicated by the evolved nature of the glass and mineral trace element chemistry, including the earliest crystallising phases. There is little evidence for basaltic melt in the upper crust due to the evolved nature of mixing end-members and the notable absence of erupted basaltic melt. The Annen et al. (2006) model is favoured for melt differentiation, in which evolved melts are produced in a deep crustal hot zone. Partial crystallisation of hydrous basalt and partial melting of the surrounding crust is induced by heat and volatiles provided by the intruding hydrous basalt. This provides a mechanism for producing crystal-poor, differentiated melts with a range of compositions from andesite to rhyolite. The mineral chemistry data do not suggest that large quantities of crystals originated from the lower crust (25-35 km; Stern & Davey, 1987, 1990), as was proposed by Price et al. (2005). Rather, the earliest crystallising amphiboles record pressures that equate to depths of around 20-25 km. Trace element chemistry of these amphibole crystals indicates that those crystals crystallised directly from the evolving host melt, and do not represent xenocrystic material.



A: Differentiation at depth in a deep crust hot zone

B: Amphibole crystallisation begins around 20-25 km.

C: Magmas migrate through the crust via a complex plumbing system. Crystallisation continues and some mixing occurs.

D: Magma which erupt from the main vent stall at a shallow storage chamber.

E: Cryptic mixing-intruding magma is hotter and more mafic. This magma engulfs some crystals forming zones of disequilibrium, other crystals crystallise zones which are in equilibrium with a the hotter melt. Other crystals further from the source of the intrusion are not affected.

F: Magma ascends from the shallow storage chamber to the surface at a rate of > 1.3 km/day

Figure 5.18 Schematic diagram of the petrogenetic processes operating at Mt Taranaki during the Holocene.

ii. Magma ascent through the crust

Magma ascent from a deep origin is inferred from amphibole barometry. The pressure records indicate near-continuous crystallisation between the onset of deep-seated crystallisation, and storage in a shallow magma chamber (*ca.* 6-10 km). Magmatic ascent is therefore relatively slow and suggests a complex plumbing system such as a series of sills and dykes that would have impeded ascent (Price et al., 1997; Gamble et al., 1999). As the system developed, evidence for increased interaction with the crust is provided by the long term geochemical trends at Taranaki, including increasing K₂O and ⁸⁷Sr/⁸⁶Sr ratios (Price et al., 1999). This is in contrast to the style of ascent proposed by Annen et al. (2006), invoking rapid ascent of melt through the crust via a series of dykes due to the low viscosity and density of the crystal poor, water-rich melts. The slower ascent occurring at Taranaki may be related to a range of extensive parameters such as the nature of the crust at this site and the mass flux rate.

iii. Stagnation of magma in the upper crust

Magma stall in the shallow crust as a result of decompression crystallisation (Blundy & Cashman, 2001). For example, Blundy & Cashman (2001) calculated an isothermal crystallisation rate of 0.23% per MPa for a water-saturated andesitic magma at 900° C. The combined effect of increased crystal content and decreased melt water content causes stagnation at this point for a period of months to years as calculated from clinopyroxene residence times. The abundant crystal growth occurring at this depth is reflected in the dominance of oscillatory zoning in plagioclase and clinopyroxene, as well as a strong fractional crystallisation signature evident in the least squares mixing modelling. There is a significant correlation between the silica content of the melt, the depth of the storage magma chamber and the residence time within this chamber, and a number of feedbacks are possible. For example, a shallow emplacement depth would favour higher rates of crystallisation (Blundy & Cashman, 2001), which would in turn evolve the melt to a more silicic composition.

In contrast to the other samples investigated in this study, SM-6C magma likely ascended from a slightly shallower depth of *ca.* 15 km, stalling briefly in the upper crust (*ca.* 2-3 km) for

a few days. It did not therefore experience the same degree of decompression crystallisation as the others, as reflected by a lower silica and crystal content.

iv. Magma mixing

Magma mixing is a key process occurring at Mt Taranaki and is a primary source of variability within these eruptives. The magma mixing at Taranaki is not occurring in the traditional manner where a basaltic magma injects a shallow silicic body, often triggering an eruption. Rather, the mixing is between compositionally similar end-members, which enables efficient mixing. This process leaves behind little evidence, except within mineral phases where disequilibrium features and variable trace element chemistry indicate open system processes. The mixing is likely occurring in both the plumbing system and the shallow storage chamber as magmas traverse the crust using existing pathways (Hildreth & Moorbath, 1988; Gamble et al., 1999, 2003).

‘Cryptic’ magma mixing reflects repeated, efficient mixing of small batches of magma with similar compositions (Humphreys et al., 2006). Such efficient mixing is attributed to similar physical properties and the small volume of the intruding magma (Sparks & Marshall, 1986). This has a variable effect on the magma chamber-hosted minerals depending on the spatial distribution of the intrusion and crystal assemblage. Therefore, individual crystals will record the event differently. Humphreys et al. (2006) noted little overlap in the mineral textures of Shiveluch Volcano, which was attributed to spatial and temporal isolation of the mineral populations. Crystals near the intrusion may be incorporated into the intruding melt, inducing extreme disequilibrium features such as sieving and resorption of zones. Crystals that are nearby, but not close enough to be engulfed, may just record hotter conditions, while other crystals will not record this intrusion at all. This makes the correlation of such disequilibrium features challenging, and has been used to account for disequilibrium textures in plagioclase at Unzen, Japan (Browne et al., 2006), and clinopyroxene at Ruapehu, New Zealand (Nakagawa et al., 2002).

This work dominantly discusses the intrusion of hotter melts, but occurrence of magma mixing and recharge may also occur by intrusion of a more silicic melt into a relatively mafic host. Identifying the latter style is challenging, as calcic cores are more resistant to dissolution when immersed in a more felsic melt (Nakamura & Shimakita, 1998; Larsen, 2005); the textural record is therefore less conclusive. Also, the dominant textures apparent from magma mixing will be induced by the cooler, more felsic-hosted minerals interacting with a hotter, more mafic melt. This does not necessarily indicate which magma was the host.

Magma mixing appears to be occurring in all the samples investigated here. However, it appears more dominant in the younger three samples as evident in the mineral textures, major element and trace element chemistry. Mineral textures illustrate more variability and more disequilibrium textures. Major element chemistry shows that there is less of a distinction between cores and rims, a feature also apparent in the amphibole thermobarometry results. Trace element chemistry shows that minerals from the younger three samples have chemistries typical of a less evolved melt and show more variability in compatible trace elements (e.g. V in clinopyroxene).

The shorter term variability noted in the Taranaki eruptives are thought to be related to pulses of magma from the lower crust that then migrate through the crust. The samples investigated in this study appear to cover the transition from one magma pulse to another. The older three samples are more evolved, stalled for longer in the shallow storage chamber and appear to be following established magmatic pathways through the crust. Kaupokonui and Maketawa may represent the initial stages of the next pulse of melt. The chemistry is different, and magma has not had time to accumulate large quantities of magma and therefore the mixing signature is stronger because the host magma batches are smaller. The more basaltic nature of the later samples may be inherent to the new magma pulse, or may be related to the fact that this is the early stages of a magma pulse which has therefore not evolved and differentiated via intra-crustal processes.

Overall, variations in these processes, including magma ascent path, degree of fractional crystallisation, and the nature and extent of magma mixing, contribute to short term (100's to 1000's yr) variability at the Mt Taranaki system. Signatures from these processes are therefore superimposed on the longer term magmatic evolution, and resulting geochemical characteristics.

CHAPTER 6:
CONCLUSIONS

6.1 CONCLUSIONS

This thesis has presented detailed crystal specific and glass geochemical data for six subplinian eruptions from Mt Taranaki. Intensive magmatic parameters and crystal residence times were quantified. This investigation has resulted in the following conclusions:

- 1) These ‘andesites’ are the product of a complex set of processes including magma mixing and fractional crystallisation. This results in a large degree of geochemical variability on a timescale of 100’s to 1000’s yr that is superimposed on the longer term evolution of the magmatic system.
- 2) In situ crystal specific studies of plagioclase, clinopyroxene and amphibole record magmatic evolution and provide evidence for processes such as cryptic magma mixing and reheating of the magma chamber. Combining petrographic techniques with major and trace element analyses enables petrogenetic processes to be better constrained.
- 3) Magma mixing is cryptic, occurring between evolved and compositionally similar end-members. This mixing is most prominent when it occurs in the shallow storage chamber (6-10 km depth). However, it is most likely also occurring throughout the magmatic plumbing system. The volumetrically small nature of the intruding magma results in a heterogeneous effect on the host magma, imprinting a range of textural and chemical features on the resident crystal population. This means correlating zoning between individual minerals is often not possible.
- 4) Melt differentiates at depth (*ca.* 30 km) to an andesitic – silicic composition and ascends the crust gradually via a complex plumbing system.
- 5) Most crystallisation occurs in the shallow crust within a storage magma chamber as shown by mineral textures and thermobarometry modelling. This is due to decompression driven crystallisation and results in a dominant fractional crystallisation signature. The fractional crystallisation signature is further evident by the relationship between glass data from this study and published whole rock data as quantified by the least squares mixing modelling.

- 6) Residence times obtained from diffusion modelling show that magma mixing does not always trigger eruptions. Clinopyroxene residence times obtained from Fe-Mg interdiffusion modelling indicates that magmas are resident in a shallow storage chamber for months to years prior to eruption. Magma mixing is implicated as a triggering event for the Kaupokonui Tephra, however other samples do not show such conclusive evidence for magma mixing as a triggering event.

6.2 SUGGESTIONS FOR FUTURE WORK

The data acquired and ideas proposed in this thesis lend themselves to further study to be properly tested. Some recommendations for further study are summarised below:

- 1) Much of the ambiguity relating to the cause of disequilibrium textures and the origins of non-host derived cores is related to the lack of trace element data for these zones due to the spot size required for LA-ICP-MS analysis. The use of Secondary Ion Mass Spectrometry (SIMS) which obtains trace element analyses on a scale of 1µm would enable the trace element composition of these features to be obtained and therefore better constrain the origin.
- 2) It is suggested that the sample SM-6C represents an unknown eruption from the satellite vent of Fantham's Peak. In order to test this, glass analyses from an eruption known to have been sourced from Fantham's Peak (such as the Manganui Tephra) could be compared with the glass from SM-6C. The same could be done for the Curtis Ridge Episode, which is the other eruption this unit may relate to.
- 3) Sample SM-6C could be further constrained by detailed investigation of the nature of the deposits. Mapping and the construction of isopachs would also aid in determining whether this sample is sourced from Fantham's Peak and whether this sample represents the Curtis Ridge Episode investigated by Turner et al. (2008).
- 4) Residence times of clinopyroxene crystals were modelled using Fe-Mg interdiffusion. Modelling of additional mineral phases such as Mg and Sr diffusion in plagioclase and Fe-Ti diffusion in titanomagnetite may constrain different magmatic processes that

occur on a different timescales from the months to years that are accessible by clinopyroxene diffusion modelling.

- 5) Open system processes could be further investigated by using Sr-Nd-Hf-Pb isotopic data for specific mineral phases. Whole rock isotopic analyses have been published by Price et al. (1992, 1999) which provides constraints on the overall degree of crustal contamination. In situ isotopic analyses of individual mineral phases would enable the isotopic evolution of the magma system to be resolved and the various open system inputs to the system such as magma mixing and crustal contamination to be further constrained.

REFERENCES

- Adams, R. D. & Ware, D. E. (1977). Subcrustal earthquakes beneath New Zealand: locations determined with a laterally inhomogeneous velocity model. *New Zealand Journal of Geology and Geophysics* **20**, 59-83.
- Allan, A. S. R. (2008). An elemental and isotopic investigation of Quaternary silicic Taupo Volcanic Zone tephra from ODP Site 1123: Chronostratigraphic and petrogenetic applications. M.Sc. Dissertation, Victoria University of Wellington, 210 pp.
- Allan, A. S. R., Baker, J. A., Carter, L. & Wysoczanski, R. J. (2008). Reconstructing the Quaternary evolution of the world's most active silicic volcanic system: insights from an similar to 1.65 Ma deep ocean tephra record sourced from Taupo Volcanic Zone, New Zealand. *Quaternary Science Reviews* **27**, 2341-2360.
- Allegre, C. J., Provost, A. & Jaupart, C. (1981). Oscillatory zoning - a pathological case of crystal-growth. *Nature* **294**, 223-228.
- Allis, R. G., Armstrong, P. A. & Funnell, R. H. (1995). Implications for a high heat-flow anomaly around New Plymouth, North Island, New Zealand. *New Zealand Journal of Geology and Geophysics* **38**, 121-130.
- Alloway, B. (1989). Late Quaternary cover-bed stratigraphy and tephra-chronology of north-eastern and central Taranaki region, New Zealand. Ph.D Dissertation, Massey University.
- Alloway, B., Neall, V. E. & Vucetich, C. G. (1995). Late Quaternary (post 28,000 year BP) tephrostratigraphy of northeast and central Taranaki, New Zealand. *Journal of the Royal Society of New Zealand* **25**, 385-458.
- Anderson, A. T. (1976). Magma mixing [mdash] petrological process and volcanological tool. *Journal of Volcanology and Geothermal Research* **1**, 3-33.
- Anderson, D. L. (1982). Isotopic evolution of the mantle - The role of magma mixing. *Earth and Planetary Science Letters* **57**, 1-12.
- Anderson, A. T. (1984). Probable relations between plagioclase zoning and magma dynamics, Fuego Volcano, Guatemala. *American Mineralogist* **69**, 660-676.
- Anderson, H. & Webb, T. (1994). New Zealand Seismicity: Patterns revealed by the upgraded National Seismic Network. *New Zealand Journal of Geology and Geophysics* **37**, 477-493.
- Annen, C. & Sparks, R. S. J. (2002). Effects of repetitive emplacement of basaltic intrusions on thermal evolution and melt generation in the crust. *Earth and Planetary Science Letters* **203**, 937-955.

- Annen, C., Blundy, J. D. & Sparks, R. S. J. (2006). The genesis of intermediate and silicic magmas in deep crustal hot zones. *Journal of Petrology* **47**, 505-539.
- Azough, F. & Freer, R. (2000). Iron diffusion in single-crystal diopside. *Physics and Chemistry of Minerals* **27**, 732-740.
- Bachmann, O. & Bergantz, G. W. (2004). On the origin of crystal-poor rhyolites: Extracted from batholithic crystal mushes. *Journal of Petrology* **45**, 1565-1582.
- Bachmann, O., Dungan, M. A. & Lipman, P. W. (2002). The Fish Canyon magma body, San Juan volcanic field, Colorado: Rejuvenation and eruption of an upper-crustal batholith. *Journal of Petrology* **43**, 1469-1503.
- Bacon, C. R. & Druitt, T. H. (1988). Compositional evolution of the zoned calcalkaline magma chamber of Mount Mazama, Crater Lake, Oregon. *Contributions to Mineralogy and Petrology* **98**, 224-256.
- Bedard, J. H. (2010). Parameterization of the Fe=Mg exchange coefficient (k_d) between clinopyroxene and silicate melts. *Chemical Geology* **274**, 169-176.
- Berlo, K., Blundy, J., Turner, S. & Hawkesworth, C. (2007). Textural and chemical variation in plagioclase phenocrysts from the 1980 eruptions of Mount St. Helens, USA. *Contributions to Mineralogy and Petrology* **154**, 291-308.
- Bibby, H. M., Caldwell, T. G., Davey, F. J. & Webb, T. H. (1995). Geophysical evidence on the structure of the Taupo Volcanic Zone and its hydrothermal circulation. *Journal of Volcanology and Geothermal Research* **68**, 29-58.
- Bindeman, I. N., Davis, A. M. & Drake, M. J. (1998). Ion microprobe study of plagioclase-basalt partition experiments at natural concentration levels of trace elements. *Geochimica et Cosmochimica Acta* **62**, 1175-1193.
- Blundy, J. D. & Wood, B. (1991). Crystal-chemical controls on the partitioning of Sr and Ba between plagioclase feldspar, silicate melts, and hydrothermal solutions. *Geochimica et Cosmochimica Acta* **55**, 193-209.
- Blundy, J. & Cashman, K. (2001). Ascent-driven crystallisation of dacite magmas at Mount St Helens, 1980-1986. *Contributions to Mineralogy and Petrology* **140**, 631-650.
- Blundy, J., Cashman, K. & Humphreys, M. C. S. (2006). Magma heating by decompression-driven crystallisation beneath andesite volcanoes. *Nature* **443**, 76-80.
- Boddington, T., Parkin, C. J. & Gubbins, D. (2004). Isolated deep earthquakes beneath the North Island of New Zealand. *Geophysical Journal International* **158**, 972-982.

- Bohrson, W. A. & Spera, F. J. (2001). Energy-constrained open-system magmatic processes II: Application of energy-constrained assimilation-fractional crystallization (EC-AFC) model to magmatic systems. *Journal of Petrology* **42**, 1019-1041.
- Bottinga, Y., Kudo, A. & Weill, D. (1966). Some observations on oscillatory zoning and crystallization of magmatic plagioclase. *American Mineralogist* **51**, 792-806.
- Browne, B. L. & Gardner, J. E. (2006). The influence of magma ascent path on the texture, mineralogy, and formation of hornblende reaction rims. *Earth and Planetary Science Letters* **246**, 161-176.
- Browne, B. L., Eichelberger, J. C., Patino, L. C., Vogel, T. A., Uto, K. & Hoshizumi, H. (2006). Magma mingling as indicated by texture and Sr/Ba ratios of plagioclase phenocrysts from Unzen volcano, SW Japan. *Journal of Volcanology and Geothermal Research* **154**, 103-116.
- Carslaw, H. S. & Jaeger, J. C. (1986). *Conduction of Heat in Solids*. New York: Oxford University Press.
- Chakraborty, S. (2008). Diffusion in solid silicates: A tool to track timescales of processes comes of age. *Annual Review of Earth and Planetary Sciences* **36**, 153-190.
- Chakraborty, S. & Ganguly, J. (1992). Cation diffusion in aluminosilicate garnets - experimental-determination in spessartine-almandine diffusion couples, evaluation of effective binary diffusion-coefficients, and applications. *Contributions to Mineralogy and Petrology* **111**, 74-86.
- Challis, G. A., Johnston, M. R., Lauder, W. R. & Suggate, R. P. (1994). *Geology of the Lake Rotoroa area, Nelson*. Institute of Geological and Nuclear Sciences geological map 8. 1 sheet + 32 . Lower Hutt, New Zealand: Institute of Geological and Nuclear Sciences Limited.
- Cherniak, D. J. (2001). Pb diffusion in Cr diopside, augite, and enstatite, and consideration of the dependence of cation diffusion in pyroxene on oxygen fugacity. *Chemical Geology* **177**, 381-397.
- Cherniak, D. J. (2002). Ba diffusion in feldspar. *Geochimica et Cosmochimica Acta* **66**, 1641-1650.
- Chertkoff, D. G. & Gardner, J. E. (2004). Nature and timing of magma interactions before, during, and after the caldera-forming eruption of Volcan Ceboruco, Mexico. *Contributions to Mineralogy and Petrology* **146**, 715-735.
- Coombs, M. L., Eichelberger, J. C. & Rutherford, M. J. (2000). Magma storage and mixing conditions for the 1953-1974 eruptions of Southwest Trident volcano, Katmai National Park, Alaska. *Contributions to Mineralogy and Petrology* **140**, 99-118.

- Cooper, K. M. & Reid, M. R. (2003). Re-examination of crystal ages in recent Mount St. Helens lavas: implications for magma reservoir processes. *Earth and Planetary Science Letters* **213**, 149-167.
- Cooper, K. M., Reid, M. R., Murrell, M. T. & Clague, D. A. (2001). Crystal and magma residence at Kilauea Volcano, Hawaii: Th-230-Ra-226 dating of the 1955 east rift eruption. *Earth and Planetary Science Letters* **184**, 703-718.
- Costa, F. & Chakraborty, S. (2004). Decadal time gaps between mafic intrusion and silicic eruption obtained from chemical zoning patterns in olivine. *Earth and Planetary Science Letters* **227**, 517-530.
- Costa, F. & Dungan, M. (2005). Short time scales of magmatic assimilation from diffusion modeling of multiple elements in olivine. *Geology* **33**, 837-840.
- Costa, F., Chakraborty, S. & Dohmen, R. (2003). Diffusion coupling between trace and major elements and a model for calculation of magma residence times using plagioclase. *Geochimica et Cosmochimica Acta* **67**, 2189-2200.
- Costa, F., Scaillet, B. & Pichavant, M. (2004). Petrologic and experimental constraints on the pre-eruption conditions of Holocene dacite from Volcan San Pedro (36°S, Chilean Andes) and the importance of sulfur in silicic subduction-related magmas. *Journal of Petrology* **45**, 855-881.
- Costa, F., Dohmen, R. & Chakraborty, S. (2008). *Time Scales of Magmatic Processes from Modeling the Zoning Patterns of Crystals*. In: Putirka, K. D. & Tepley, F. J. (eds.) *Minerals, Inclusions and Volcanic Processes*, 545-594.
- Costa, F. & Morgan, D. J. (2010). *Time constraints from chemical equilibrium in magmatic crystals*. In: Dosseto, A., Turner, S. & Van Orman, J. A. (eds.) *Timescales of Magmatic Processes: From core to atmosphere*: Blackwell Publishing Limited.
- Crank, J. (1975). *The mathematics of diffusion*. London: Oxford Press.
- Davidson, J. P. & Tepley, F. J. (1997). Recharge in volcanic systems: Evidence from isotope profiles of phenocrysts. *Science* **275**, 826-829.
- Davidson, J. P., Hora, J. M., Garrison, J. M. & Dungan, M. A. (2005). Crustal forensics in arc magmas. *Journal of Volcanology and Geothermal Research* **140**, 157-170.
- Davidson, J. P., Morgan, D. J. & Charlier, B. L. A. (2007a). Isotopic microsampling of magmatic rocks. *Elements* **3**, 253-259.

- Davidson, J. P., Morgan, D. J., Charlier, B. L. A., Harlou, R. & Hora, J. M. (2007b). Microsampling and isotopic analysis of igneous rocks: Implications for the study of magmatic systems. *Annual Review of Earth and Planetary Sciences* **35**, 273-311.
- Defant, M. J. & Drummond, M. S. (1990). Derivation of some modern arc magmas by melting of young subducted lithosphere. *Nature* **347**, 662-665.
- Demets, C., Gordon, R. G., Argus, D. F. & Stein, S. (1994). Effect of recent revisions to the geomagnetic reversal time-scale on estimates of current plate motions. *Geophysical Research Letters* **21**, 2191-2194.
- DePaolo, D. J. (1981). Trace element and isotopic effects of combined wallrock assimilation and fractional crystallization. *Earth and Planetary Science Letters* **53**, 189-202.
- Devine, J. D., Rutherford, M. J., Norton, G. E. & Young, S. R. (2003). Magma storage region processes inferred from geochemistry of Fe-Ti oxides in andesitic magma, Soufriere Hills Volcano, Montserrat, W.I.. *Journal of Petrology* **44**, 1375-1400.
- Dimanov, A. & Sautter, V. (2000). "Average" interdiffusion of (Fe,Mn)-Mg in natural diopside. *European Journal of Mineralogy* **12**, 749-760.
- Dimanov, A. & Wiedenbeck, M. (2006). (Fe,Mn)-Mg interdiffusion in natural diopside: effect of pO₂. *European Journal of Mineralogy* **18**, 705-718.
- Downey, W. S., Kellett, R. J., Smith, I. E. M., Price, R. C. & Stewart, R. B. (1994). New palaeomagnetic evidence for the recent eruptive activity of Mt. Taranaki, New Zealand. *Journal of Volcanology and Geothermal Research* **60**, 15-27.
- Dungan, M. A. & Davidson, J. (2004). Partial assimilative recycling of the mafic plutonic roots of arc volcanoes: an example from the Chilean Andes. *Geology* **32**, 773-776.
- Dungan, M. A., Wulff, A. & Thompson, R. (2001). Eruptive stratigraphy of the Tatara-San Pedro complex, 36 degrees S, southern volcanic zone, Chilean Andes: Reconstruction method and implications for magma evolution at long-lived arc volcanic centers. *Journal of Petrology* **42**, 555-626.
- Eichelberger, J. C. (1975). Origin of andesite and dacite - evidence of mixing at Glass Mountain in California and at other circum-Pacific volcanos. *Geological Society of America Bulletin* **86**, 1381-1391.
- Eichelberger, J. C. (1978). Andesitic volcanism and crustal evolution. *Nature* **275**, 21-27.

- Eichelberger, J. C. & Izbekov, P. E. (2000). Eruption of andesite triggered by dyke injection: contrasting cases at Karymsky Volcano, Kamchatka and Mt Katmai, Alaska. *Philosophical Transactions of the Royal Society of London. Series A: Mathematical, Physical and Engineering Sciences* **358**, 1465-1485.
- Eichelberger, J. C., Izbekov, P. E. & Browne, B. L. (2006). Bulk chemical trends at arc volcanoes are not liquid lines of descent. *Lithos* **87**, 135-154.
- Elliott, T., Plank, T., Zindler, A., White, W. & Bourdon, B. (1997). Element transport from slab to volcanic front at the Mariana arc. *Journal of Geophysical Research* **102**, 14,991-15,019.
- Ewart, A. & Griffin, W. L. (1994). Application of proton-microprobe data to trace-element partitioning in volcanic rocks. *Chemical Geology* **117**, 251-284.
- Ferrara, G., Petrini, R., Serri, G. & Tonarini, S. (1989). Petrology and isotope-geochemistry of San Vincenzo rhyolites (Tuscany, Italy). *Bulletin of Volcanology* **51**, 379-388.
- Fowler, S. J. & Spera, F. J. (2010). A metamodel for crustal magmatism: Phase equilibria of giant ignimbrites. *Journal of Petrology* **51**, 1783-1830.
- Foxworthy, B. L. & Hill, M. (1982). *Volcanic Eruptions of 1980 at Mount St. Helens: The First 100 Days*. Washington: United States Government Printing Office.
- Freer, R. & Hauptman, Z. (1978). An experimental study of magnetite-titanomagnetite interdiffusion. *Physics of the Earth and Planetary Interiors* **16**, 223-231.
- Frost, B. R. & Lindsley, D. H. (1991). Occurrence of iron-titanium oxides in igneous rocks. *Reviews in Mineralogy and Petrology* **25**, 433-468.
- Gaetani, G. A., Grove, T. L. & Bryan, W. B. (1993). The influence of water on the petrogenesis of subduction-related igneous rocks. *Nature* **365**, 332-334.
- Gamble, J. A., Wood, C. P., Price, R. C., Smith, I. E. M., Stewart, R. B. & Waight, T. (1999). A fifty year perspective of magmatic evolution on Ruapehu Volcano, New Zealand: verification of open system behaviour in an arc volcano. *Earth and Planetary Science Letters* **170**, 301-314.
- Gamble, J. A., Price, R. C., Smith, I. E. M., McIntosh, W. C. & Dunbar, N. W. (2003). Ar-40/Ar-39 geochronology of magmatic activity, magma flux and hazards at Ruapehu volcano, Taupo Volcanic Zone, New Zealand. *Journal of Volcanology and Geothermal Research* **120**, 271-287.

- Ganguly, J. & Tazzoli, V. (1994). Fe²⁺-Mg interdiffusion in ortho-pyroxene - retrieval from the data on intracrystalline exchange-reaction. *American Mineralogist* **79**, 930-937.
- Ganguly, J., Dasgupta, S., Cheng, W. J. & Neogi, S. (2000). Exhumation history of a section of the Sikkim Himalayas, India: records in the metamorphic mineral equilibria and compositional zoning of garnet. *Earth and Planetary Science Letters* **183**, 471-486.
- Gardner, J. E., Carey, S., Rutherford, M. J. & Sigurdsson, H. (1995). Petrologic diversity in Mount St. Helens dacites during the last 4,000 years: implications for magma mixing. *Contributions to Mineralogy and Petrology* **119**, 224-238.
- Ghiorso, M. S., Hirschmann, M. M., Reiners, P. W. & Kress, V. C. I. (2002). The pMELTS: a revision of MELTS for improved calculation of phase relations and major element partitioning related to partial melting of the mantle to 3 GPa. *Geochemistry, Geophysics, Geosystems* **3**, 1-36.
- Giba, M., Nicol, A. & Walsh, J. J. (2010). Evolution of faulting and volcanism in a back-arc basin and its implications for subduction processes. *Tectonics* **29**, TC4020.
- Giggenbach, W. (1982). The chemical and isotopic composition of gas discharges from New Zealand andesitic volcanoes. *Bulletin of Volcanology* **45**, 253-255.
- Giletti, B. J. & Casserly, J. E. D. (1994). Strontium diffusion kinetics in plagioclase feldspars. *Geochimica et Cosmochimica Acta* **58**, 3785-3793.
- Gill, J. B. (1981). *Orogenic Andesites and Plate Tectonics*. New York: Springer-Verlag.
- Ginibre, C., Worner, G. & Kronz, A. (2002a). Minor- and trace-element zoning in plagioclase: implications for magma chamber processes at Parinacota volcano, northern Chile. *Contributions to Mineralogy and Petrology* **143**, 300-315.
- Ginibre, C., Kronz, A. & Worner, G. (2002b). High-resolution quantitative imaging of plagioclase composition using accumulated backscattered electron images: new constraints on oscillatory zoning. *Contributions to Mineralogy and Petrology* **142**, 436-448.
- Ginibre, C., Worner, G. & Kronz, A. (2007). Crystal zoning as an archive for magmatic evolution. *Elements* **3**, 261-266.
- Goldlich, M. S., Ingamells, C. O., Suhr, N. H. & Anderson, D. T. (1967). Analyses of silicate rock and mineral standards. *Canadian Journal of Earth Sciences* **4**, 747-755.

- Gow, A. J. (1968). Petrographic and petrochemical studies of Mt Egmont andesites. *New Zealand Journal of Geology and Geophysics* **11**, 166-190.
- Graham, I. J. & Hackett, W. R. (1987). Petrology of calc-alkaline lavas from Ruapehu volcano and related vents, Taupo Volcanic Zone, New Zealand. *Journal of Petrology* **28**, 531-567.
- Green, T. H. (1981). Experimental evidence for the role of accessory phases in magma genesis. *Journal of Volcanology and Geothermal Research* **10**, 405-422.
- Grove, T. L. & Kinzler, R. J. (1986). Petrogenesis of Andesites. *Annual Review of Earth and Planetary Sciences* **14**, 417-454.
- Grove, T. L., Baker, M. B. & Kinzler, R. J. (1984). Coupled CaAl-NaSi diffusion in plagioclase feldspar - experiments and applications to cooling rate speedometry. *Geochimica et Cosmochimica Acta* **48**, 2113-2121.
- Grove, T. L., Donnelly-Nolan, J. M. & Housh, T. (1997). Magmatic processes that generated the rhyolite of Glass Mountain, Medicine Lake volcano, N. California. *Contributions to Mineralogy and Petrology* **127**, 205-223.
- Grove, T. L., Elkins-Tanton, L. T., Parman, S. W., Chatterjee, N., Muntener, O. & Gaetani, G. A. (2003). Fractional crystallisation and mantle-melting controls on calc-alkaline differentiation trends. *Contributions to Mineralogy and Petrology* **145**, 515-533.
- Gruender, K., Stewart, R. B. & Foley, S. (2010). Xenoliths from the sub-volcanic lithosphere of Mt Taranaki, New Zealand. *Journal of Volcanology and Geothermal Research* **190**, 192-202.
- Jochum, K. P., Stoll, B., Herwig, K., Willbold, M., Hofmann, A. W., Amini, M., Aarburg, S., Abouchami, W., Hellebrand, E., Mocek, B., Raczek, I., Stracke, A., Alard, O., Bouman, C., Becker, S., Dücking, M., Bratz, H., Klemm, R., de Bruin, D., Canil, D., Cornell, D., de Hoog, C. J., Dalpe, C., Danyushevsky, L., Eisenhauer, A., Gao, Y. J., Snow, J. E., Goschopf, N., Günther, D., Latkoczy, C., Guillong, M., Hauri, E. H., Hofer, H. E., Lahaye, Y., Horz, K., Jacob, D. E., Kasemann, S. A., Kent, A. J. R., Ludwig, T., Zack, T., Mason, P. R. D., Meixner, A., Rosner, M., Misawa, K. J., Nash, B. P., Pfänder, J., Premo, W. R., Sun, W. D., Tiepolo, M., Vannucci, R., Vennemann, T., Wayne, D. & Woodhead, J. D. (2006). MPI-DING reference glasses for in situ microanalysis: New reference values for element concentrations and isotope ratios. *Geochemistry Geophysics Geosystems* **7**.Q02008, doi:10.1029/2005GC001060.
- Haase, C. S., Chadam, J., Fein, D. & Ortoleva, P. (1980). Oscillatory zoning in plagioclase feldspar. *Science* **209**, 272-274.

- Hammarstrom, J. M. & Zen, E. A. (1986). Aluminium in hornblende - An empirical igneous geobarometer. *American Mineralogist* **71**, 1297-1313.
- Harrison, A. J. & White, R. S. (2004). Crustal structure of the Taupo Volcanic Zone, New Zealand: Stretching and igneous intrusion. *Geophysical Research Letters* **31**, L13615.
- Hawkesworth, C. J. & Kemp, A. I. S. (2006). Evolution of the continental crust. *Nature* **443**, 811-817.
- Hawkesworth, C. J., Turner, S. P., McDermott, F., Peate, D. W. & van Calstern, P. (1997). U-Th isotopes in arc magmas: Implications for element transfer from the subducted crust. *Science* **276**, 551-555.
- Hawkesworth, C., George, R., Turner, S. & Zellmer, G. (2004). Time scales of magmatic processes. *Earth and Planetary Science Letters* **218**, 1-16.
- Heiken, G. & Eichelberger, J. C. (1980). Eruptions at Chaos Crags, Lassen Volcanic National Park, California. *Journal of Volcanology and Geothermal Research* **7**, 443-481.
- Hermann, J., Spandler, C., Hack, A. & Korsakov, A. V. (2006). Aqueous fluids and hydrous melts in high-pressure and ultra-high pressure rocks: Implications for element transfer in subduction zones. *Lithos* **92**, 399-417.
- Herzer, R. H. (1995). Seismic stratigraphy of a buried volcanic arc, Northland, New Zealand and implications for Neogene subduction. *Marine and Petroleum Geology* **12**, 511-531.
- Hildreth, W. (2004). Volcanological perspectives on Long Valley, Mammoth Mountain, and Mono Craters: several contiguous but discrete systems. *Journal of Volcanology and Geothermal Research* **136**, 169-198.
- Hildreth, W. & Moorbath, S. (1988). Crustal contributions to arc magmatism in the Andes of Central Chile. *Contributions to Mineralogy and Petrology* **98**, 455-489.
- Hobden, B. J., Houghton, B. F., Davidson, J. P. & Weaver, S. D. (1999). Small and short-lived magma batches at composite volcanoes: time windows at Tongariro volcano, New Zealand. *Journal of the Geological Society* **156**, 865-868.
- Hogg, A. G., Lowe, D. J. & Hendeby, C. H. (1987). University of Waikato radiocarbon dates I. *Radiocarbon* **29**, 263-301.
- Hollister, L. S., Grissom, G. C., Peters, E. K., Stowell, H. H. & Sisson, V. B. (1987). Confirmation of the empirical correlation of Al in hornblende with pressure of solidification of calc-alkaline plutons. *American Mineralogist* **72**, 231-239.

- Houghton, B. F., Wilson, C. J. N., McWilliams, M. O., Lanphere, M. A., Weaver, S. D., Briggs, R. M. & Pringle, M. S. (1995). Chronology and dynamics of a large silicic magmatic system: Central Taupo Volcanic Zone, New Zealand. *Geology* **23**, 13-16.
- Humphreys, M. C. S., Blundy, J. D. & Sparks, R. S. J. (2006). Magma evolution and open-system processes at Shiveluch Volcano: insights from phenocryst zoning. *Journal of Petrology* **47**, 2303-2334.
- Ingamells, C. O. (1980). Analyzed minerals for electron microprobe standards. *Geostandards Newsletter* **2**, 115.
- Ingamells, C. O. (1983). Microprobe Column. *Geostandards Newsletter* **7**, 243-244.
- Jarosweich, E., Nelen, J. A. & Norber, J. A. (1980). Reference samples for electron microprobe analysis. *Geostandards Newsletter* **4**, 43-47.
- Jerram, D. A. & Martin, V. M. (2008). Understanding crystal populations and their significance through the magma plumbing system. *Geological Society, London, Special Publications* **304**, 133-148.
- Johnson, M. C. & Plank, T. (1999). Dehydration and melting experiments constrain the fate of subducted sediments. *Geochemistry, Geophysics, Geosystems* **1**, 1-26.
- Johnson, M. C. & Rutherford, M. J. (1989). Experimental calibration of the aluminium-in-hornblende geobarometer with application to Long-Valley Caldera (California) volcanic-rocks. *Geology* **17**, 837-841.
- Kamp, P. J. J., Vonk, A. J., Bland, K. J., Hansen, R. J., Hendy, A. J. W., McIntyre, A. P., Ngatai, M., Cartwright, S. J., Hayton, S. & Nelson, C. S. (2004). Neogene stratigraphic architecture and tectonic evolution of Wanganui, King Country, and eastern Taranaki Basins, New Zealand. *New Zealand Journal of Geology and Geophysics* **47**, 625-644.
- Kay, R. W. (1978). Aleutian magnesian andesites - melts from subducted Pacific Ocean crust. *Journal of Volcanology and Geothermal Research* **4**, 117-132.
- Kay, R. W. (1980). Volcanic arc magmas - Implications of a melting-mixing model for element recycling in the crust-upper mantle system. *Geology* **88**, 497-522.
- Kent, A. J. R., Blundy, J., Cashman, K. V., Cooper, K. M., Donnelly, C., Pallister, J. S., Reagan, M., Rowe, M. C. & Thornber, C. R. (2007). Vapor transfer prior to the October 2004 eruption of Mount St. Helens, Washington. *Geology* **35**, 231-234.
- Kent, A. J. R., Darr, C., Koleszar, A. M., Salisbury, M. J. & Cooper, K. M. (2010). Preferential eruption of andesitic magmas through recharge filtering. *Nature Geoscience* **3**, 631-636.

- Kessel, R., Schmidt, M. W., Ulmer, P. & Pettke, T. (2005). Trace element signature of subduction-zone fluids, melts and supercritical liquids at 120-180 km depth. *Nature* **437**, 724-727.
- Kimura, J.-I., Kent, A. J. R., Rowe, M. C., Katakuse, M., Nakano, F., Hacker, B. R., van Keken, P. E., Kawabata, H. & Stern, R. J. (2010). Origin of cross-chain geochemical variation in Quaternary lavas from the northern Izu arc: Using a quantitative mass balance approach to identify mantle sources and mantle wedge processes. *Geochemistry, Geophysics Geosystems* **11**, Q10011.
- King, P. R. & Thrasher, G. P. (1996). Cretaceous-Cenozoic Geology and Petroleum Systems of the Taranaki Basin, New Zealand. *Institute of Geological and Nuclear Sciences Monograph* **13**, 243 pp.
- Klugel, A., Hansteen, T. H. & Galipp, K. (2005). Magma storage and underplating beneath Cumbre Vieja volcano, La Palma (Canary Islands). *Earth and Planetary Science Letters* **236**, 211-226.
- Kogiso, T., Omori, S. & Maruyama, S. (2009). Magma genesis beneath Northeast Japan arc: A new perspective on subduction zone magmatism. *Gondwana Research* **16**, 446-457.
- Kushiro, I. (1983). On the lateral variation in chemical composition and volume of Quaternary volcanic rocks across Japan arc. *Journal of Volcanology and Geothermal Research* **18**, 435-447.
- Lange, R. A., Frey, H. M. & Hector, J. (2009). A thermodynamic model for the plagioclase-liquid hygrometer/thermometer. *American Mineralogist* **94**, 494-506.
- Larocque, J. & Canil, D. (2010). The role of amphibole in the evolution of arc magmas and crust: the case from the Jurassic Bonanza arc section, Vancouver Island, Canada. *Contributions to Mineralogy and Petrology* **159**, 475-492.
- Larsen, J. F. (2005). Experimental study of plagioclase rim growth around anorthite seed crystals in rhyodacitic melt. *American Mineralogist* **90**, 417-427.
- Leake, B. E., Woolley, A. R., Arps, C. E. S., Birch, W. D., Gilbert, M. C., Grice, J. D., Hawthorne, F. C., Kato, A., Kisch, H. J., Krivovichev, V. G., Linthout, K., Laird, J., Mandarino, J., Maresch, W. V., Nickel, E. H., Rock, N. M. S., Schumacher, J. C., Smith, D. C., Stephenson, N. C. N., Ungaretti, L., Whittaker, E. J. W. & Youzhi, G. (1997). Nomenclature of amphiboles: Report of the Subcommittee on Amphiboles of the International Mineralogical Association Commission on New Minerals and Mineral Names. *Mineralogical Magazine* **61**, 295-321.
- Lepage, L. D. (2003). ILMAT: an Excel worksheet for ilmenite-magnetite geothermometry and geobarometry. *Computers & Geosciences* **29**, 673-678.

- Locke, C. A. & Cassidy, J. (1997). Egmont Volcano, New Zealand: three-dimensional structure and its implications for evolution. *Journal of Volcanology and Geothermal Research* **76**, 149-161.
- Locke, C. A., Cassidy, J. & MacDonald, A. (1993). Three-dimensional structure of relict stratovolcanoes in Taranaki, New Zealand: evidence from gravity data. *Journal of Volcanology and Geothermal Research* **59**, 121-130.
- Locke, C. A., Cassidy, J. & MacDonald, A. (1994). Constraints on the evolution of the Taranaki volcanoes, New Zealand, based on aeromagnetic data. *Bulletin of Volcanology* **56**, 552-560.
- Lowe, D. J. (1988). Stratigraphy, age, composition, and correlation of late Quaternary tephra interbedded with organic sediments in Waikato lakes, North Island, New Zealand. *New Zealand Journal of Geology and Geophysics* **31**, 125-165.
- Martin, H. (1999). Adakitic magmas: Modern analogues of Archaean granitoids. *Lithos* **46**, 411-429.
- Martin, H., Smithies, R. H., Rapp, R., Moyen, J. F. & Champion, D. (2005). An overview of adakite, tonalite-trondhjemite-granodiorite (TTG), and sanukitoid: relationships and some implications for crustal evolution. *Lithos* **79**, 1-24.
- Martin, V. M., Morgan, D. J., Jerram, D. A., Caddick, M. J., Prior, D. J. & Davidson, J. P. (2008). Bang! Month-scale eruption triggering at Santorini Volcano. *Science* **321**, 1178.
- McCulloch, M. T. & Gamble, J. A. (1991). Geochemical and geodynamical constraints on subduction zone magmatism. *Earth and Planetary Science Letters* **102**, 358-374.
- McGlone, M. S., Neall, V. E. & Clarkson, B. D. (1988). The effect of recent volcanic events and climatic changes on the vegetation of Mt Egmont (Mt Taranaki), New Zealand. *New Zealand Journal of Botany* **26**, 123-144.
- Mibe, K., Fujii, T. & Yasuda, A. (1999). Control of the location of the volcanic front in island arcs by aqueous fluid connectivity in the mantle wedge. *Nature* **401**, 259-262.
- Morgan, D. J. (2003). Timescales of crystal residence and magmatic differentiation: Vesuvius. Ph.D. Dissertation, University of Durham
- Morgan, D. J. & Blake, S. (2006). Magmatic residence times of zoned phenocrysts: introduction and application of the binary element diffusion modelling (BEDM) technique. *Contributions to Mineralogy and Petrology* **151**, 58-70.

- Morgan, D. J., Blake, S., Rogers, N. W., DeVivo, B., Rolandi, G., Macdonald, R. & Hawkesworth, C. J. (2004). Time scales of crystal residence and magma chamber volume from modelling of diffusion profiles in phenocrysts: Vesuvius 1944. *Earth and Planetary Science Letters* **222**, 933-946.
- Morgan, D. J., Blake, S., Rogers, N. W., De Vivo, B., Rolandi, G. & Davidson, J. P. (2006). Magma chamber recharge at Vesuvius in the century prior to the eruption of A.D. 79. *Geology* **34**, 845-848.
- Morse, S. A. (1984). Cation diffusion in plagioclase feldspar. *Science* **225**, 504-505.
- Mortimer, N., Tulloch, A. J. & Ireland, T. R. (1997). Basement geology of Taranaki and Wanganui Basins, New Zealand. *New Zealand Journal of Geology and Geophysics* **40**, 223-236.
- Mortimer, N., Gans, P. B., Palin, J. M., Meffre, S., Herzer, R. H. & Skinner, D. N. B. (2010). Location and migration of Miocene-Quaternary volcanic arcs in the SW Pacific region. *Journal of Volcanology and Geothermal Research* **190**, 1-10.
- Muir, R. J., Bradshaw, J. D., Weaver, S. D. & Laird, M. G. (2000). The influence of basement structure on the evolution of the Taranaki Basin, New Zealand. *Journal of the Geological Society* **157**, 1179-1185.
- Murphy, J. B. (2007). Arc Magmatism II: Geochemical and Isotopic Characteristics. *Geoscience Canada* **34**, 7-35.
- Murphy, M. D., Sparks, R. S. J., Barclay, J., Carroll, M. R. & Brewer, T. S. (2000). Remobilisation of andesite magma by intrusion of mafic magma at Soufriere Hills Volcano, Montserrat, West Indies. *Journal of Petrology* **41**, 21-42.
- Nakagawa, M., Wada, K., Thordarson, T., Wood, C. P. & Gamble, J. A. (1999). Petrologic investigations of the 1995 and 1996 eruptions of Ruapehu volcano, New Zealand: formation of discrete and small magma pockets and their intermittent discharge. *Bulletin of Volcanology* **61**, 15-31.
- Nakagawa, M., Wada, K. & Wood, C. P. (2002). Mixed magmas, mush chambers and eruption triggers: Evidence from zoned clinopyroxene phenocrysts in andesitic scoria from the 1995 eruptions of Ruapehu volcano, New Zealand. *Journal of Petrology* **43**, 2279-2303.
- Nakamura, M. (1995). Continuous mixing of crystal mush and replenished magma in the ongoing Unzen eruption. *Geology* **23**, 807-810.
- Nakamura, M. & Shimakita, S. (1998). Dissolution origin and syn-entrapment compositional change of melt inclusion in plagioclase. *Earth and Planetary Science Letters* **161**, 119-133.

- Neall, V. E. (1979). *Sheets P19, P20 & P21 New Plymouth, Egmont and Mania*. Geological Map of New Zealand 1:50 000. Wellington: New Zealand Geological Survey Department of Scientific and Industrial Research, 3 maps and notes, 36p.
- Neall, V. E. & Alloway, B. A. (1986). Quaternary volcanoclastics and volcanic hazards of Taranaki. *New Zealand Geological Survey Report* **12**, 101-137.
- Neall, V. E., Stewart, R. B. & Smith, I. E. M. (1986). History and Petrology of the Taranaki Volcanoes. *The Royal Society of New Zealand Bulletin* **23**, 251-263.
- Nelson, S. T. & Montana, A. (1992). Sieve-textured plagioclase in volcanic rocks produced by rapid decompression. *American Mineralogist* **77**, 1242-1249.
- Nimis, P. (1995). A clinopyroxene geobarometer for basaltic systems based on crystal-structure modeling. *Contributions to Mineralogy and Petrology* **121**, 115-125.
- Nimis, P. (1999). Clinopyroxene geobarometry of magmatic rocks. Part 2. Structural geobarometers for basic to acid, tholeiitic and mildly alkaline magmatic systems. *Contributions to Mineralogy and Petrology* **135**, 62-74.
- Nimis, P. & Taylor, W. R. (2000). Single clinopyroxene thermobarometry for garnet peridotites. Part I. Calibration and testing of a Cr-in-Cpx barometer and an enstatite-in-Cpx thermometer. *Contributions to Mineralogy and Petrology* **139**, 541-554.
- Onsager, L. (1945). Theories and problems of liquid diffusion. *Annals of the New York Academy of Sciences* **46**, 241-265.
- Pallister, J. S., Hoblitt, R. P. & Reyes, A. G. (1992). A Basalt Trigger for the 1991 Eruptions of Pinatubo Volcano? *Nature* **356**, 426-428.
- Peacock, S. M., Rushmer, T. & Thompson, A. B. (1994). Partial melting of subducting oceanic crust. *Earth and Planetary Science Letters* **121**, 227-244.
- Pearce, J. A. & Cann, J. R. (1973). Tectonic setting of basic volcanic rocks determined using trace element analyses. *Earth and Planetary Science Letters* **19**, 290-300.
- Pearce, T. H. & Kolisnik, A. M. (1990). Observations of plagioclase zoning using interference imaging. *Earth Science Reviews* **29**, 9-26.
- Petford, N. & Atherton, M. (1996). Na-rich partial melts from newly underplated basaltic crust: the Cordillera Blanca Batholith, Peru. *Journal of Petrology* **37**, 1491-1521.

- Petford, N. & Gallagher, K. (2001). Partial melting of mafic (amphibolitic) lower crust by periodic influx of basaltic magma. *Earth and Planetary Science Letters* **193**, 483-499.
- Pichavant, M., Martel, C., Bourdier, J.-L. & Scaillet, B. (2002). Physical conditions, structure, and dynamics of a zoned magma chamber: Mount Pelée (Martinique, Lesser Antilles Arc). *Journal of Geophysical Research* **107**, (B5)2093.
- Plank, T. (2005). Constraints from thorium/lanthanum on sediment recycling at subduction zones and the evolution of the continents. *Journal of Petrology* **46**, 921-944.
- Plank, T. & Langmuir, C. H. (1988). An evaluation of the global variations in the major element chemistry of arc basalts. *Earth and Planetary Science Letters* **90**, 349-370.
- Platz, T. (2007). Understanding aspects of andesitic dome-forming eruptions through the last 1000 yrs of volcanism at Mt Taranaki, New Zealand. Ph.D. Dissertation, Massey University, 264 pp.
- Platz, T., Cronin, S. J., Cashman, K., Stewart, R. B. & Smith, I. E. M. (2007a). Transition from effusive to explosive phases in andesite eruptions- A case-study from the AD1655 eruption of Mt. Taranaki, New Zealand. *Journal of Volcanology and Geothermal Research* **161**, 15-34.
- Platz, T., Cronin, S. J., Smith, I. E. M., Turner, M. P. & Stewart, R. P. (2007b). Improving the reliability of microprobe-based analyses of andesitic glasses for tephra correlation. *Holocene* **17**, 573-583.
- Price, R. C., McCulloch, M. T., Smith, I. E. M. & Stewart, R. B. (1992). Pb-Nd-Sr isotopic compositions and trace element characteristics of young volcanic rocks from Egmont Volcano and comparisons with basalts and andesites from the Taupo Volcanic Zone, New Zealand. *Geochimica et Cosmochimica Acta* **56**, 941-953.
- Price, R. C., Waight, T. E., Chapman, J. R., Beyer, E. E., Smith, I. E. M. & Stewart, R. B. (1997). The geochemical evolution of arc magmas in a continental setting: evidence from detailed chemo-stratigraphy at Ruapehu, New Zealand. *Geological Society of Australia Abstracts* **45**, 79-81.
- Price, R. C., Stewart, R. B., Woodhead, J. D. & Smith, I. E. M. (1999). Petrogenesis of high-K arc magmas: evidence from Egmont Volcano, North Island, New Zealand. *Journal of Petrology* **40**, 167-197.
- Price, R. C., Gamble, J. A., Smith, I. E. M., Stewart, R. B., Eggins, S. & Wright, I. C. (2005). An integrated model for the temporal evolution of andesites and rhyolites and crustal development in New Zealand's North Island. *Journal of Volcanology and Geothermal Research* **140**, 1-24.

- Price, R. C., Turner, S., Cook, C., Hobden, B., Smith, I. E. M., Gamble, J. A., Handley, H., Maas, R. & Möbis, A. (2010). Crustal and mantle influences and U-Th-Ra disequilibrium in andesitic lavas of Ngauruhoe volcano, New Zealand. *Chemical Geology* **277**, 355-373.
- Prouteau, G. & Scaillet, B. (2003). Experimental constraints on the origin of the 1991 Pinatubo dacite. *Journal of Petrology* **44**, 2203-2241.
- Putirka, K. A. (2005). Igneous thermometers and barometers based on plagioclase plus liquid equilibria: Tests of some existing models and new calibrations. *American Mineralogist* **90**, 336-346.
- Putirka, K. D. (2008). *Thermometers and Barometers for Volcanic Systems*. In: Putirka, K. D. & Tepley, F. J. (eds.) *Minerals, Inclusions and Volcanic Processes*, 61-120.
- Putirka, K., Johnson, M., Kinzler, R., Longhi, J. & Walker, D. (1996). Thermobarometry of mafic igneous rocks based on clinopyroxene-liquid equilibria, 0-30 kbar. *Contributions to Mineralogy and Petrology* **123**, 92-108.
- Putirka, K. D., Mikaelian, H., Ryerson, F. & Shaw, H. (2003). New clinopyroxene-liquid thermobarometers for mafic, evolved, and volatile-bearing lava compositions, with applications to lavas from Tibet and the Snake River Plain, Idaho. *American Mineralogist* **88**, 1542-1554.
- Rattenbury, M. S., Cooper, R. A. & Johnston, M. R. (1998). Geology of the Nelson area. Institute of Geological and Nuclear Sciences 1:250 000 geological map 9.1 sheet + 67 p. Lower Hutt, New Zealand: Institute of Geological and Nuclear Sciences Limited.
- Reed. (1975). *Electron Microprobe Analysis*. Cambridge: Cambridge University Press.
- Reubi, O. & Blundy, J. (2009). A dearth of intermediate melts at subduction zone volcanoes and the petrogenesis of arc andesites. *Nature* **461**, 1269-1273.
- Reyners, M. (1983). Lateral Segmentation of the Subducted Plate at the Hikurangi Margin, New Zealand: Seismological Evidence. *Tectonophysics* **96**, 203-223.
- Reyners, M., Eberhart-Phillips, D., Stuart, G. & Nishimura, Y. (2006). Imaging subduction from the trench to 300 km depth beneath the central North Island, New Zealand, with Vp and Vp/Vs. *Geophysical Journal International* **165**, 565-583.
- Ridolfi, F., Renzulli, A. & Puerini, M. (2010). Stability and chemical equilibrium of amphibole in calc-alkaline magmas: an overview, new thermobarometric formulations and application to subduction-related volcanoes. *Contributions to Mineralogy and Petrology* **160**, 45-66.

- Rollinson, H. (1993). *Using Geochemical Data: Evaluation, Presentation, Interpretation*. London: Longman Group Limited.
- Rudnick, R. L. (1995). Making continental crust. *Nature* **378**, 571-578.
- Rudnick, R. L. & Gao, S. (2003). *Composition of the Continental Crust*. In: Heinrich, D. H. & Karl, K. T. (eds.) *Treatise on Geochemistry*. Oxford: Pergamon, 1-64.
- Rutherford, M. J. & Devine, J. D. (1988). The May 18, 1980, eruption of Mount St Helens. 3. Stability and chemistry of amphibole in the magma chamber. *Journal of Geophysical Research-Solid Earth and Planets* **93**, 11949-11959.
- Rutherford, M. J. & Hill, P. M. (1993). Magma ascent rates from amphibole breakdown - An experimental study applied to the 1980-1986 Mount St-Helens eruptions. *Journal of Geophysical Research* **98**, 19667-19685.
- Rutherford, M. J. & Devine, J. D. (2003). Magmatic conditions and magma ascent as indicated by hornblende phase equilibria and reactions in the 1995-2002 Soufriere Hills magma. *Journal of Petrology* **44**, 1433-1454.
- Rutherford, M. J. & Devine, J. D. (eds.) (2008). *Magmatic conditions and processes in the storage zone of the 2004-2006 Mount St. Helens eruption: The record in amphibole and plagioclast phenocrysts*. In: Sherrod, D. R., Scott, W. E. and Stauffer, P. H. (eds.) *A volcano rekindled: the first year of renewed eruption at Mount St. Helens, 2004-2006*. US Geological Survey Professional Paper 1750, ch 31.
- Sakuyama, M. (1979). Evidence of magma mixing: Petrological study of Shirouma-Oike calc-alkaline andesite volcano, Japan. *Journal of Volcanology and Geothermal Research* **5**, 179-208.
- Saunders, K. E., Morgan, D. J., Baker, J. A. & Wysoczanski, R. J. (2010). The magmatic evolution of the Whakamaru supereruption, New Zealand, constrained by a microanalytical study of plagioclase and quartz. *Journal of Petrology* **51**, 2465-2488.
- Sautter, V., Jaoul, O. & Abel, F. (1988). Aluminium diffusion in diopside using the Al-27(P, gamma) Si-28 nuclear-reaction - preliminary results. *Earth and Planetary Science Letters* **89**, 109-114.
- Schmidt, M. W. (1992). Amphibole composition in tonalite as a function of pressure - An experimental calibration of the Al-in-hornblende barometer. *Contributions to Mineralogy and Petrology* **110**, 304-310.
- Schmidt, M. W. & Poli, S. (1998). Experimentally based water budgets for dehydrating slabs and consequences for arc magma generation. *Earth and Planetary Science Letters* **163**, 361-379.

- Severs, M. J., Beard, J. S., Fedele, L., Hanchar, J. M., Mutchler, S. R. & Bodnar, R. J. (2009). Partitioning behaviour of trace elements between dacitic melt and plagioclase, orthopyroxene, and clinopyroxene based on laser ablation ICPMS analysis of silicate melt inclusions. *Geochimica et Cosmochimica Acta* **73**, 2123-2141.
- Shane, P. (2005). Towards a comprehensive distal andesitic tephrostratigraphic framework for New Zealand based on eruptions from Egmont volcano. *Journal of Quaternary Science* **20**, 45-57.
- Sherburn, S. & White, R. S. (2005). Crustal seismicity in Taranaki, New Zealand using accurate hypocentres from a dense network. *Geophysical Journal International* **162**, 494-506.
- Sherburn, S., White, R. S. & Chadwick, M. (2006). Three-dimensional tomographic imaging of the Taranaki volcanoes, New Zealand. *Geophysical Journal International* **166**, 957-969.
- Sibley, D. F., Vogel, T. A., Walker, B. M. & Byerly, G. (1976). Origin of oscillatory zoning in plagioclase - diffusion and growth controlled model. *American Journal of Science* **276**, 275-284.
- Simonetti, A., Shore, M. & Bell, K. (1996). Diopside phenocrysts from a nephelinite lavas, Napak Volcano, Eastern Uganda: Evidence for magma mixing. *The Canadian Mineralogist* **34**, 411-421.
- Singer, B. S., Dungan, M. A. & Layne, G. D. (1995). Textures and Sr, Ba, Mg, K and Ti compositional profiles in volcanic plagioclase - Clues to the dynamics of calc-alkaline magma chambers. *American Mineralogist* **80**, 776-798.
- Sisson, T. W. & Grove, T. L. (1993). Experimental investigations of the role of H₂O in calc-alkaline differentiation and subduction zone magmatism. *Contributions to Mineralogy and Petrology* **113**, 143-166.
- Smith, V. C., Blundy, J. D. & Arce, J. L. (2009). A temporal record of magma accumulation and evolution beneath Nevado de Toluca, Mexico, preserved in plagioclase phenocrysts. *Journal of Petrology* **50**, 405-426.
- Sparks, R. S. J. & Marshall, L. A. (1986). Thermal and mechanical constraints on mixing between mafic and silicic magmas. *Journal of Volcanology and Geothermal Research* **29**, 99-124.
- Sparks, R. S. J., Sigurdsson, H. & Wilson, L. (1977). Magma mixing: a mechanism for triggering acid explosive eruptions. *Nature* **267**, 315-318.
- Stagpoole, V. & Funnell, R. (2001). Arc magmatism and hydrocarbon generation in the northern Taranaki Basin, New Zealand. *Petroleum Geoscience* **7**, 255-267.
- Stagpoole, V. & Nicol, A. (2008). Regional structure and kinematic history of a large subduction back thrust: Taranaki Fault, New Zealand. *Journal of Geophysical Research* **113**, B01403.

- Stern, R. J. (2002). Subduction zones. *Reviews of Geophysics* **40**, 3-1.
- Stern, T. A. (1985). A back-arc basin formed within the continental lithosphere - The Central Volcanic Region of New Zealand. *Tectonophysics* **112**, 385-409.
- Stern, T. A. & Davey, F. J. (1987). A seismic investigation of the crustal and upper mantle structure within the Central Volcanic Region of New Zealand. *New Zealand Journal of Geology and Geophysics* **30**, 217-231.
- Stern, T. A. & Davey, F. J. (1990). Deep seismic expression of a foreland basin - Taranaki Basin, New Zealand. *Geology* **18**, 979-982.
- Stern, T., Smith, E. G. C., Davey, F. J. & Muirhead, K. J. (1987). Crustal and upper mantle structure of the Northwestern North Island, New Zealand, from seismic refraction data. *Geophysical Journal of the Royal Astronomical Society* **91**, 913-936.
- Stewart, R. B. (2010). Andesites as magmatic liquids or liquid-crystal mixtures; Insights from Egmont and Ruapehu Volcanoes, New Zealand. *Central European Journal of Geosciences* **2**, 329-338.
- Stewart, R. B., Price, R. C. & Smith, I. E. M. (1996). Petrogenesis of high-K arc magmas: Evidence from Egmont Volcano, North Island, New Zealand. *Journal of Volcanology and Geothermal Research* **74**, 275-295.
- Stormer, J. C. J. (1983). The effects of recalculation on estimates of temperature and oxygen fugacity from analyses of multi-component iron-titanium oxides. *American Mineralogist* **68**, 589-594.
- Stratford, W. R. & Stern, T. A. (2004). Strong seismic reflections and melts in the mantle of a continental back-arc basin. *Geophysical Research Letters* **31**, L06622.
- Streck, M. J. (2008). Mineral textures and zoning as evidence for open system processes. *Reviews in Mineralogy and Geochemistry* **69**, 595-622.
- Streck, M. J., Dungan, M. A., Malavassi, E., Reagan, M. & Bussy, F. (2002). The role of basalt replenishment in the generation of basaltic andesites of the ongoing activity at Arenal volcano, Costa Rica: evidence from clinopyroxene and spinel. *Bulletin of Volcanology* **64**, 316-327.
- Streck, M. J., Dungan, M. A., Bussy, F. & Malavassi, E. (2005). Mineral inventory of continuously erupting basaltic andesites at Arenal volcano, Costa Rica: implications for interpreting monotonous, crystal-rich, mafic arc stratigraphies. *Journal of Volcanology and Geothermal Research* **140**, 133-155.
- Streck, M. J., Leeman, W. P. & Chesley, J. (2007). High-magnesian andesite from Mount Shasta: A product of magma mixing and contamination, not a primitive mantle melt. *Geology* **35**, 351-354.

- Sugawara, T. (2001). Ferric iron partitioning between plagioclase and silicate liquid: thermodynamics and petrological applications. *Contributions to Mineralogy and Petrology* **141**, 659-686.
- Sun, S.-s. & McDonough, W. F. (1989). Chemical and isotopic systematics of oceanic basalts: implications for mantle composition and processes. *Geological Society, London, Special Publications* **42**, 313-345.
- Tatsumi, Y. & Eggins, S. (1995). *Subduction Zone Magmatism*. Oxford: Blackwell Scientific.
- Tatsumi, Y. & Takahashi, T. (2006). Operation of subduction factory and production of andesite. *Journal of Mineralogical and Petrological Sciences* **101**, 145-153.
- Taylor, S. R. & McLennan, S. M. (1995). The geochemical evolution of the continental crust. *Reviews in Geophysics* **33**, 241-265.
- Thornber, C. R., Pallister, J. S., Lowers, H. A., Rowe, M. C., Mandeville, C. W. & Meeker, G. P. (eds.) (2008). *Chemistry, mineralogy, and petrology of amphibole in Mount St. Helens 2004-2006 dacite* In: Sherrod, D.R., Scott, W.E., and Stauffer, P.H., (eds.) *A volcano rekindled; the renewed eruption of Mount St. Helens, 2004–2006*. U.S. Geological Survey Professional Paper 1750, ch 32.
- Tomiya, A. & Takahashi, E. (2005). Evolution of the magma chamber beneath Usu volcano since 1663: A natural laboratory for observing changing phenocryst compositions and textures. *Journal of Petrology* **46**, 2395-2426.
- Tsuchiyama, A. (1985). Dissolution kinetics of plagioclase in the melt of the system diopside-albite-anorthite, and origin of dusty plagioclase in andesites. *Contributions to Mineralogy and Petrology* **89**, 1-16.
- Turner, M. B. (2008). Eruption Cycles and Magmatic Processes at a Reawakening Volcano, Mt Taranaki, New Zealand. Ph.D. Dissertation, Massey University, 409 pp.
- Turner, S. & Costa, F. (2007). Measuring timescales of magmatic evolution. *Elements* **3**, 267-272.
- Turner, S., George, R., Jerram, D. A., Carpenter, N. & Hawkesworth, C. (2003). Case studies of plagioclase growth and residence times in island arc lavas from Tonga and the Lesser Antilles, and a model to reconcile discordant age information. *Earth and Planetary Science Letters* **214**, 279-294.
- Turner, M. B., Cronin, S. J., Smith, I. E. M., Stewart, R. B. & Neall, V. E. (2008). Eruption episodes and magma recharge events in andesitic systems: Mt Taranaki, New Zealand. *Journal of Volcanology and Geothermal Research* **177**, 1063-1076.
- Turner, M. B., Bebbington, M., Cronin, S. J. & Stewart, R. B. (2009). Merging eruption datasets: building an integrated Holocene eruptive record for Mt Taranaki, New Zealand. *Bulletin of Volcanology* **71**, 903-918.

- Umino, S. & Horio, A. (1998). Multistage Magma Mixing Revealed in Phenocryst Zoning of the Yunokuchi Pumice Akagi Volcano, Japan. *Journal of Petrology* **39**, 101-124.
- Vance, J. A. (1965). Zoning in igneous plagioclase: patchy zoning. *Geology* **73**, 636-651.
- Venezky, M. J. & Rutherford, M. J. (1999). Petrology and Fe-Ti oxide reequilibration of the 1991 Mount Unzen mixed magma. *Journal of Volcanology and Geothermal Research* **89**, 213-230.
- Wallace, L. M., Beavan, J., McCaffrey, R. & Darby, D. (2004). Subduction zone coupling and tectonic block rotations in the North Island, New Zealand. *Journal of Geophysical Research* **109**, B12406.
- Watson, E. B. & Baxter, E. F. (2007). Diffusion in solid-Earth systems. *Earth and Planetary Science Letters* **253**, 307-327.
- Wilson, C. J. N., Houghton, B. F., McWilliams, M. O., Lanphere, M. A., Weaver, S. D. & Briggs, R. M. (1995). Volcanic and structural evolution of Taupo Volcanic Zone, New Zealand - A review. *Journal of Volcanology and Geothermal Research* **68**, 1-28.
- Witham, C. S. (2005). Volcanic disasters and incidents: A new database. *Journal of Volcanology and Geothermal Research* **148**, 191-233.
- Woodhead, J., Eggins, S. & Gamble, J. (1993). High field strength and transition element systematics in island arc and back-arc basin basalts: Evidence for multi-phase melt extraction and a depleted mantle wedge. *Earth and Planetary Science Letters* **114**, 491-504.
- Zellmer, G. F., Blake, S., Vance, D., Hawkesworth, C. & Turner, S. (1999). Plagioclase residence times at two island arc volcanoes (Kameni Islands, Santorini, and Soufriere, St. Vincent) determined by Sr diffusion systematics. *Contributions to Mineralogy and Petrology* **136**, 345-357.
- Zellmer, G. F., Sparks, R. S. J., Hawkesworth, C. J. & Wiedenbeck, M. (2003). Magma emplacement and remobilization timescales beneath Montserrat: Insights from Sr and Ba zonation in plagioclase phenocrysts. *Journal of Petrology* **44**, 1413-1431.
- Zernack, A. V., Procter, J. N. & Cronin, S. J. (2009). Sedimentary signatures of cyclic growth and destruction of stratovolcanoes: A case study from Mt. Taranaki, New Zealand. *Sedimentary Geology* **220**, 288-305.

APPENDICES:

Appendix 1: Sample list

Appendix 2: Major element data

Appendix 3: Trace element data

**Appendix 4: Diffusion modelling images
and profiles**

APPENDIX 1:

Table A1.1 SAMPLE LIST

Table A1.1 List of tephra samples used in this thesis.

Sample ID	Inferred Unit / ID	Age (yr BP)	Description
SM-6A	Kaupokonui	< 1950±90	Pumice lapilli; dark brown; friable; clast supported; maximum clast diameter = 50mm, mean clast diameter = 3mm.
SM-6C	SM-6C	< 1950±90	Pumice lapilli; 80% pumice, 20% lithics; dark brown, matrix supported, maximum clast = 40mm, mean clast = 5mm, reverse graded.
SM-6K	Maketawa	< 2890±100	Pumice lapilli; 80% pumice, 20% lithics; reddish brown, maximum clast = 20mm, mean clast = 5mm.
SM-7P	Inglewood b	>3610±60	Pumice lapilli; 90% pumice, 10% lithics, reddish brown, maximum clast = 30mm, mean clast = 2mm.
SM-7R	Inglewood a	< 3870±110	Pumice lapilli; 90% pumice, 10% lithics;reddish brown; friable; maximum clast = 50mm, mean clast = 4mm; reverse graded.
SM-7U	Korito	4150-3580	Pumice lapilli; yellowish brown; friable; moderately sorted; maximum clast = 50mm, mean clast = 4mm; slight reverse grading.

Age estimates from Alloway et al. (1995) and references therein, and are based on radiocarbon ages of peat and wood between tephra units. Maximum or minimum ages are indicated, based on dated material found stratigraphically below or above the tephra unit. A range of values is given where ages are available directly above and below the unit.

APPENDIX 2:

MAJOR ELEMENT DATA

Table A2.1 Glass major element data

Table A2.2 Melt inclusion major element data

Table A2.3 Plagioclase major element data

Table A2.4 Clinopyroxene major element data

Table A2.5 Orthopyroxene major element data

Table A2.6 Amphibole major element data

Table A2.7 Oxides major element data

Table A2.1 Major element glass compositions analysed by EMPA.

Sample	Kaupokonui	Kaupokonui	Kaupokonui	Kaupokonui	Kaupokonui	Kaupokonui	Kaupokonui	Kaupokonui	Kaupokonui	Kaupokonui	Kaupokonui
ID	G1	G2	G3	G4	G5	G6	G7	G8	G9	G9	G9
SiO ₂	66.14	66.93	67.15	65.63	68.00	64.77	65.72	66.30	66.71	66.71	66.71
TiO ₂	0.44	0.42	0.43	0.42	0.43	0.45	0.44	0.41	0.46	0.46	0.46
Al ₂ O ₃	17.15	16.33	16.66	16.24	16.81	16.79	16.75	16.60	16.71	16.71	16.71
FeO	2.59	2.56	2.68	2.70	2.40	3.19	3.10	2.60	2.82	2.82	2.82
MnO	0.09	0.10	0.12	0.10	0.12	0.13	0.14	0.08	0.07	0.07	0.07
MgO	0.82	0.75	0.82	0.84	0.71	0.95	0.97	0.83	0.89	0.89	0.89
CaO	3.09	2.47	2.62	2.62	2.61	3.12	2.88	2.45	2.69	2.69	2.69
Na ₂ O	4.45	4.24	4.07	3.83	4.24	4.37	4.14	4.36	4.24	4.24	4.24
K ₂ O	4.42	4.77	4.76	4.57	4.62	4.47	4.64	4.74	4.72	4.72	4.72
Total	99.20	98.57	99.31	96.95	99.95	98.24	98.79	98.36	99.32	99.32	99.32
K ₂ O+Na ₂ O	8.87	9.00	8.83	8.39	8.86	8.83	8.78	9.10	8.96	8.96	8.96

Any number before 'G' in the ID designates the clinopyroxene crystal to which analysed glass was adhered. Otherwise, analysis is of matrix glass. All Fe is reported as FeO.

Table A2.1 Major element glass compositions analysed by EMPA.

Sample	Kaupokonui	Kaupokonui	Kaupokonui	Kaupokonui	Kaupokonui	Kaupokonui	Kaupokonui	Kaupokonui	Kaupokonui	Kaupokonui	SMI-6C	SMI-6C	SMI-6C	SMI-6C
ID	G10	6G1	7G1	9G2	34G1	35G	67G1	G1	G4	G5	G6			
SiO ₂	67.92	66.51	64.54	65.88	68.90	68.33	66.95	57.85	59.80	59.95	60.32			
TiO ₂	0.42	0.40	0.45	0.48	0.38	0.40	0.42	0.64	0.72	0.72	0.64			
Al ₂ O ₃	16.50	17.11	17.17	16.93	16.81	16.93	16.87	16.74	17.06	17.16	17.71			
FeO	2.51	3.00	3.05	3.11	2.27	2.70	2.59	4.56	4.51	4.86	4.15			
MnO	0.08	0.09	0.13	0.14	0.12	0.13	0.15	0.14	0.08	0.19	0.12			
MgO	0.68	0.83	0.97	0.97	0.56	0.79	0.75	1.62	1.76	1.76	1.58			
CaO	2.31	2.82	2.82	2.96	2.12	2.50	2.35	4.47	4.85	4.87	5.23			
Na ₂ O	4.21	4.64	4.58	4.27	4.39	4.39	4.40	3.60	4.21	4.30	4.46			
K ₂ O	4.85	4.64	4.41	4.54	5.09	5.03	4.87	3.48	3.64	3.42	2.93			
Total	99.48	100.05	98.13	99.29	100.65	101.20	99.34	93.10	96.64	97.23	97.15			
K ₂ O+Na ₂ O	9.06	9.28	8.99	8.82	9.49	9.42	9.27	7.08	7.85	7.72	7.40			

Any number before 'G' in the ID designates the clinopyroxene crystal to which analysed glass was adhered. Otherwise, analysis is of matrix glass. All Fe is reported as FeO.

Table A2.1 Major element glass compositions analysed by EMPA.

Sample	SMI-6C	SMI-6C	SMI-6C	SMI-6C	SMI-6C	SMI-6C	SMI-6C	SMI-6C	SMI-6C	SMI-6C	SMI-6C	SMI-6C	SMI-6C	Maketawa	Maketawa	Maketawa
ID	G7	G8	G8	G10	G11	G12	G13	15G1	16G1	16G2	28G1	G3	G4	G5		
SiO ₂	61.17	59.71	60.83	60.52	60.42	59.52	60.77	60.23	61.34	60.33	61.67	68.26	68.87	68.93		
TiO ₂	0.66	0.73	0.63	0.61	0.60	0.65	0.72	0.64	0.67	0.70	0.63	0.44	0.40	0.37		
Al ₂ O ₃	17.45	16.75	18.16	18.34	19.44	16.94	17.38	16.41	15.93	16.32	15.77	16.72	15.94	16.02		
FeO	4.42	5.00	4.67	4.15	3.99	4.39	4.93	4.16	3.78	3.74	3.65	2.77	2.15	2.41		
MnO	0.15	0.15	0.19	0.11	0.15	0.16	0.16	0.16	0.14	0.15	0.10	0.09	0.12	0.09		
MgO	1.66	1.92	1.54	1.43	1.39	1.55	1.68	1.37	1.06	1.13	1.04	0.89	0.62	0.58		
CaO	4.95	4.63	5.33	5.42	5.98	4.56	4.53	3.59	3.00	3.29	2.68	2.60	2.10	2.13		
Na ₂ O	4.27	4.25	4.52	4.38	4.51	4.25	4.79	4.34	4.30	4.45	4.29	4.44	4.33	4.45		
K ₂ O	3.52	3.83	3.21	3.29	2.90	3.33	3.66	4.30	4.50	4.54	4.52	4.38	4.52	4.47		
Total	98.25	96.95	99.07	98.26	99.38	95.35	98.61	95.19	94.72	94.66	94.35	100.58	99.04	99.46		
K ₂ O+Na ₂ O	7.79	8.08	7.73	7.67	7.40	7.58	8.45	8.64	8.80	8.99	8.81	8.82	8.85	8.92		

Any number before 'G' in the ID designates the clinopyroxene crystal to which analysed glass was adhered. Otherwise, analysis is of matrix glass. All Fe is reported as FeO.

Table A2.1 Major element glass compositions analysed by EMPA.

Sample	Maketawa	Maketawa	Maketawa	Maketawa	Maketawa	Maketawa	Maketawa	Maketawa	Maketawa	Maketawa	Maketawa	Maketawa	Maketawa	Maketawa	Maketawa
ID	G6	G7	G8	G12	G13	G14	G16	12G	15G	45G	58G				
SiO ₂	67.88	66.13	67.52	65.17	66.35	65.83	68.01	65.68	65.21	67.03	69.09				
TiO ₂	0.37	0.38	0.42	0.38	0.39	0.37	0.40	0.42	0.39	0.38	0.35				
Al ₂ O ₃	16.18	15.83	16.25	17.05	15.76	15.76	16.16	15.73	15.66	15.86	15.94				
FeO	2.36	2.24	2.20	2.11	2.21	2.19	2.23	2.72	2.38	2.26	2.13				
MnO	0.15	0.11	0.08	0.08	0.11	0.12	0.14	0.13	0.12	0.13	0.09				
MgO	0.65	0.62	0.59	0.61	0.59	0.60	0.66	0.67	0.64	0.57	0.55				
CaO	2.09	2.14	2.17	2.89	2.10	2.00	2.15	2.40	2.29	1.95	1.99				
Na ₂ O	4.53	4.19	4.30	4.25	4.13	4.22	4.36	4.22	4.18	3.99	4.49				
K ₂ O	4.49	4.50	4.46	4.42	4.41	4.37	4.48	4.39	4.54	4.45	4.36				
Total	98.70	96.14	97.99	96.97	96.04	95.45	98.60	96.36	95.41	96.62	99.01				
K ₂ O+Na ₂ O	9.02	8.68	8.76	8.67	8.53	8.60	8.84	8.61	8.72	8.44	8.85				

Any number before 'G' in the ID designates the clinopyroxene crystal to which analysed glass was adhered. Otherwise, analysis is of matrix glass. All Fe is reported as FeO.

Table A2.1 Major element glass compositions analysed by EMPA.

Sample	Maketawa	Inglewood b	Inglewood b	Inglewood b	Inglewood b	Inglewood b	Inglewood b	Inglewood b	Inglewood b	Inglewood b
ID	75G	G1	G2	G4	G5	G6	G7	G8	G9	G10
SiO ₂	68.63	68.65	70.19	68.05	69.49	65.64	62.57	67.24	68.30	68.73
TiO ₂	0.38	0.31	0.31	0.30	0.33	0.30	0.32	0.23	0.28	0.32
Al ₂ O ₃	16.15	13.72	14.56	14.01	14.58	13.62	14.72	16.21	14.37	14.22
FeO	2.36	1.34	1.53	1.46	1.54	1.38	1.57	0.97	1.08	1.83
MnO	0.15	0.10	0.06	0.12	0.01	0.11	0.12	0.06	0.09	0.17
MgO	0.63	0.26	0.30	0.29	0.32	0.27	0.24	0.12	0.14	0.29
CaO	2.14	1.13	1.42	1.37	1.46	1.28	1.64	2.04	1.31	1.54
Na ₂ O	4.61	3.44	3.91	3.30	3.80	3.59	3.65	4.87	4.18	4.00
K ₂ O	4.42	4.49	4.51	4.39	4.45	4.42	4.30	3.86	4.37	4.53
Total	99.47	93.45	96.79	93.30	95.99	90.60	89.13	95.59	94.12	95.63
K ₂ O+Na ₂ O	9.02	7.94	8.42	7.69	8.26	8.01	7.95	8.72	8.55	8.53

Any number before 'G' in the ID designates the clinopyroxene crystal to which analysed glass was adhered. Otherwise, analysis is of matrix glass. All Fe is reported as FeO.

Table A2.1 Major element glass compositions analysed by EMPA.

Sample	Inglewood b	Inglewood b	Inglewood b	Inglewood b	Inglewood b	Inglewood b	Inglewood b	Inglewood b	Inglewood b	Inglewood b	Inglewood b	Inglewood b
ID	G11	G12	G13	5G1	10G1	15G1	17G1	20G1	26G1	35G1		
SiO ₂	67.14	63.53	63.34	70.48	70.57	70.29	70.18	71.87	71.55	71.94		
TiO ₂	0.30	0.30	0.29	0.34	0.30	0.34	0.30	0.32	0.32	0.30		
Al ₂ O ₃	14.65	13.64	13.29	14.25	14.18	14.33	14.35	14.78	14.82	14.39		
FeO	1.49	1.51	1.55	1.62	1.50	1.51	1.38	1.52	1.64	1.47		
MnO	0.11	0.12	0.00	0.12	0.13	0.12	0.10	0.08	0.12	0.13		
MgO	0.25	0.26	0.27	0.29	0.27	0.28	0.26	0.26	0.26	0.27		
CaO	1.69	1.27	1.40	1.44	1.52	1.32	1.31	1.36	1.43	1.31		
Na ₂ O	3.63	3.53	3.50	3.93	3.85	3.66	3.85	3.97	3.99	3.95		
K ₂ O	4.41	4.16	4.00	4.57	4.55	4.60	4.62	4.57	4.57	4.65		
Total	93.68	88.31	87.64	97.03	96.87	96.45	96.36	98.73	98.70	98.41		
K ₂ O+Na ₂ O	8.04	7.69	7.50	8.49	8.40	8.26	8.47	8.54	8.56	8.60		

Any number before 'G' in the ID designates the clinopyroxene crystal to which analysed glass was adhered. Otherwise, analysis is of matrix glass. All Fe is reported as FeO.

Table A2.1 Major element glass compositions analysed by EMPA.

Sample	Inglewood b	Inglewood a	Inglewood a	Inglewood a	Inglewood a	Inglewood a	Inglewood a	Inglewood a	Inglewood a	Inglewood a
ID	39G1	G1	G2	G3	G4	G5	G6	G7	G8	G9
SiO ₂	69.80	70.91	70.27	68.45	66.67	68.02	69.92	70.09	70.38	70.29
TiO ₂	0.26	0.32	0.33	0.29	0.29	0.29	0.31	0.32	0.30	0.30
Al ₂ O ₃	15.65	14.74	14.63	14.00	14.12	14.06	14.02	14.14	14.29	14.67
FeO	1.28	1.44	1.47	1.47	1.46	1.50	1.37	1.44	1.36	1.46
MnO	0.10	0.11	0.13	0.13	0.06	0.13	0.13	0.10	0.08	0.00
MgO	0.25	0.31	0.32	0.31	0.29	0.27	0.30	0.29	0.28	0.29
CaO	2.10	1.42	1.44	1.35	1.36	1.27	1.25	1.28	1.21	1.43
Na ₂ O	4.28	3.81	3.80	3.27	3.28	3.33	3.48	3.77	3.65	4.00
K ₂ O	4.01	4.48	4.47	4.50	4.31	4.40	4.43	4.50	4.52	4.54
Total	97.72	97.54	96.88	93.79	91.84	93.27	95.20	95.94	96.07	96.99
K₂O+Na₂O	8.29	8.30	8.27	7.77	7.59	7.73	7.91	8.28	8.17	8.54

Any number before 'G' in the ID designates the clinopyroxene crystal to which analysed glass was adhered. Otherwise, analysis is of matrix glass. All Fe is reported as FeO.

Table A2.1 Major element glass compositions analysed by EMPA.

Sample	Inglewood a	Inglewood a	Inglewood a	Inglewood a	Inglewood a	Inglewood a	Inglewood a	Inglewood a	Inglewood a	Inglewood a	Inglewood a	Inglewood a
ID	G10	G11	G12	G13	G15	G16	G1	2G1	3G1	21G1		
SiO ₂	68.59	71.27	71.33	70.53	70.30	71.29	67.44	71.42	72.07	70.63		
TiO ₂	0.34	0.31	0.34	0.33	0.30	0.32	0.27	0.30	0.31	0.29		
Al ₂ O ₃	14.45	14.82	14.71	14.37	14.71	14.50	13.64	14.49	14.62	14.25		
FeO	1.70	1.44	1.57	1.43	1.40	1.51	1.44	1.45	1.37	1.45		
MnO	0.15	0.16	0.08	0.07	0.07	0.12	0.13	0.11	0.08	0.12		
MgO	0.29	0.30	0.28	0.30	0.28	0.30	0.25	0.26	0.25	0.24		
CaO	1.41	1.38	1.40	1.38	1.35	1.38	1.27	1.35	1.26	1.25		
Na ₂ O	3.58	4.04	3.93	3.91	3.89	4.04	3.35	3.81	3.91	3.53		
K ₂ O	4.39	4.52	4.56	4.48	4.43	4.44	4.31	4.52	4.66	4.55		
Total	94.91	98.25	98.18	96.80	96.73	97.90	92.10	97.71	98.53	96.31		
K ₂ O+Na ₂ O	7.98	8.55	8.48	8.39	8.32	8.49	7.66	8.33	8.56	8.08		

Any number before 'G' in the ID designates the clinopyroxene crystal to which analysed glass was adhered. Otherwise, analysis is of matrix glass. All Fe is reported as FeO.

Table A2.1 Major element glass compositions analysed by EMPA.

Sample	Inglewood a	Inglewood a	Korito	Korito	Korito	Korito	Korito	Korito	Korito	Korito	Korito	Korito
ID	24G1	35G1	G1	G2	G3	G4	G5	G6	G7	G8	G9	G9
SiO ₂	71.57	70.21	71.02	71.48	71.72	72.50	70.14	70.56	69.01	71.68	71.67	71.67
TiO ₂	0.32	0.31	0.34	0.37	0.34	0.35	0.32	0.32	0.35	0.33	0.34	0.34
Al ₂ O ₃	14.33	14.55	14.77	14.90	14.81	14.91	14.49	14.71	14.20	14.69	14.71	14.71
FeO	1.50	1.56	1.68	1.63	1.67	1.68	1.74	1.48	1.57	1.78	1.58	1.58
MnO	0.08	0.13	0.09	0.10	0.14	0.12	0.18	0.09	0.12	0.11	0.09	0.09
MgO	0.26	0.23	0.35	0.34	0.34	0.34	0.34	0.33	0.33	0.36	0.36	0.36
CaO	1.32	1.30	1.54	1.58	1.51	1.54	1.53	1.44	1.46	1.55	1.50	1.50
Na ₂ O	3.73	3.29	3.87	3.72	4.13	3.91	4.02	3.71	3.42	3.94	3.90	3.90
K ₂ O	4.49	4.38	4.42	4.46	4.39	4.39	4.38	4.57	4.43	4.55	4.52	4.52
Total	97.60	95.95	98.07	98.56	99.04	99.73	97.14	97.21	94.88	98.98	98.67	98.67
K ₂ O+Na ₂ O	8.22	7.67	8.29	8.17	8.52	8.30	8.40	8.27	7.85	8.48	8.43	8.43

Any number before 'G' in the ID designates the clinopyroxene crystal to which analysed glass was adhered. Otherwise, analysis is of matrix glass. All Fe is reported as FeO.

Table A2.1 Major element glass compositions analysed by EMPA.

Sample	Korito	Korito	Korito	Korito	Korito	Korito	Korito	Korito	Korito
ID	G11	2G1	4G1	15G1	22G1	30G1	42G1	47G1	
SiO₂	69.61	69.01	70.59	70.88	68.31	71.18	70.89	70.71	
TiO₂	0.30	0.36	0.40	0.34	0.38	0.29	0.34	0.33	
Al₂O₃	15.91	15.99	15.03	14.76	15.88	15.66	15.71	15.64	
FeO	1.52	2.20	1.96	1.57	2.17	1.82	1.86	1.87	
MnO	0.11	0.11	0.11	0.09	0.17	0.09	0.13	0.14	
MgO	0.31	0.43	0.35	0.33	0.37	0.40	0.37	0.37	
CaO	2.13	2.52	2.02	1.53	2.49	1.94	2.03	1.94	
Na₂O	3.91	4.09	1.32	4.01	4.20	1.82	4.20	4.20	
K₂O	4.48	4.03	3.95	4.39	3.97	4.33	4.10	4.18	
Total	98.28	98.74	95.73	97.89	97.94	97.53	99.63	99.37	
K₂O+Na₂O	8.39	8.12	5.27	8.39	8.17	6.15	8.30	8.38	

Any number before 'G' in the ID designates the clinopyroxene crystal to which analysed glass was adhered. Otherwise, analysis is of matrix glass. All Fe is reported as FeO.

Table A2.2 Major element melt inclusion compositions analysed by EMPA

Sample ID	Kaupokonui P9MI4		Kaupokonui P10MI1		Kaupokonui P10MI2		Kaupokonui P10MI3		Kaupokonui P20MI1		Kaupokonui P20MI2		Kaupokonui P21MI1		Kaupokonui P21MI2		Kaupokonui 8MI1	
	plag	cpx	plag	cpx	plag	cpx	plag	cpx	plag	cpx	plag	cpx	plag	cpx	plag	cpx	plag	cpx
SiO ₂	63.88		64.19		64.43		61.93		66.27		65.36		66.76		67.24		65.55	
TiO ₂	0.37		0.42		0.41		0.33		0.29		0.35		0.37		0.38		0.45	
Al ₂ O ₃	15.89		16.19		15.95		15.60		15.08		15.95		16.04		16.14		17.33	
FeO ^t	2.67		2.85		2.87		2.42		1.47		1.74		2.40		2.38		2.75	
MnO	0.11		0.12		0.12		0.13		0.10		0.08		0.14		0.11		0.13	
MgO	0.89		0.96		0.95		0.71		0.34		0.47		0.71		0.65		0.86	
CaO	2.18		2.37		2.24		2.07		1.55		1.85		2.05		2.08		2.65	
Na ₂ O	3.28		4.38		4.66		2.94		2.51		3.12		4.09		4.16		4.48	
K ₂ O	4.86		5.45		5.38		4.69		4.64		4.82		5.22		5.26		4.65	
Total	94.12		96.92		97.02		90.83		92.26		93.73		97.80		98.39		98.86	
K ₂ O+Na ₂ O	8.14		9.83		10.05		7.63		7.16		7.94		9.32		9.41		9.13	

Number before 'G' in ID relates to the host crystal. All Fe reported as FeO. Mineral host where plag=plagioclase, cpx=clinopyroxene, opx=orthopyroxene, amph=amphibole.

Table A2.2 Major element melt inclusion compositions analysed by EMPA

Sample ID	Kaupokonui		Kaupokonui		Kaupokonui		Kaupokonui		Kaupokonui		Kaupokonui	
	10MI1	11MI1	16MI1	22MI1	33MI1	A6MI1	A3MI1	A4MI1	A5MI1	amph	amph	amph
Host	cpx	cpx	cpx	cpx	cpx	cpx	amph	amph	amph	amph	amph	amph
SiO ₂	66.24	65.14	65.61	64.95	65.11	67.16	66.49	66.41	65.78	66.41	66.41	65.78
TiO ₂	0.39	0.42	0.32	0.40	0.39	0.44	0.45	0.37	0.41	0.37	0.37	0.41
Al ₂ O ₃	15.64	14.75	15.18	16.84	16.36	16.83	15.93	16.78	16.56	16.78	16.78	16.56
FeO ^t	2.30	2.58	2.42	2.56	2.43	2.43	2.51	2.42	2.88	2.42	2.42	2.88
MnO	0.12	0.10	0.13	0.11	0.07	0.08	0.11	0.05	0.10	0.05	0.05	0.10
MgO	0.44	0.56	0.59	0.48	0.84	0.42	0.48	0.39	0.62	0.39	0.39	0.62
CaO	1.56	2.24	2.11	2.03	2.60	2.16	2.18	2.32	2.38	2.32	2.32	2.38
Na ₂ O	2.80	3.06	3.48	4.56	3.57	4.60	3.31	5.61	4.93	5.61	5.61	4.93
K ₂ O	4.69	4.22	4.64	4.62	4.52	5.04	4.46	5.03	4.67	5.03	5.03	4.67
Total	94.18	93.07	94.49	96.55	95.89	99.15	95.93	99.39	98.34	99.39	99.39	98.34
K ₂ O+Na ₂ O	7.48	7.27	8.12	9.19	8.09	9.64	7.77	10.64	9.60	10.64	10.64	9.60

Number before 'G' in ID relates to the host crystal. All Fe reported as FeO. Mineral host where plag=plagioclase, cpx=clinopyroxene, opx=orthopyroxene, amph=amphibole.

Table A2.2 Major element melt inclusion compositions analysed by EMPA

Sample ID	Kaupokonui		Kaupokonui		SM-6C		SM-6C		SM-6C		SM-6C		SM-6C	
	A8MI1 amph	A9MI1 amph	A10MI1 amph	P5MI1 plag	P5MI2 plag	P5MI3 plag	P5MI4 plag	P5MI5 plag	P5MI6 plag	P5MI7 plag	P7MI1 plag	P7MI2 plag		
SiO ₂	63.39	62.40	64.79	58.97	58.71	58.33	58.12	58.27	57.25	61.58	61.19	61.36		
TiO ₂	0.36	0.49	0.38	0.70	0.62	0.72	0.71	0.75	0.70	0.67	0.63	0.72		
Al ₂ O ₃	17.43	15.22	16.18	13.67	13.15	13.58	13.73	14.29	14.70	16.04	16.19	16.26		
FeO [†]	3.28	2.52	2.61	3.66	3.57	3.92	4.18	4.08	3.84	3.61	3.76	3.76		
MnO	0.07	0.14	0.08	0.13	0.11	0.21	0.13	0.13	0.16	0.16	0.12	0.12		
MgO	0.87	0.71	0.59	0.85	0.85	0.95	0.95	0.91	0.94	1.11	1.23	1.16		
CaO	3.27	2.73	2.20	3.18	3.04	3.28	3.18	3.84	5.08	2.75	2.81	2.84		
Na ₂ O	5.53	3.25	3.64	2.53	2.48	2.55	2.67	2.62	2.67	3.73	3.75	3.78		
K ₂ O	4.65	4.24	4.40	4.90	4.91	4.99	5.18	4.63	4.04	4.41	4.31	4.37		
Total	98.85	91.71	94.87	88.59	87.43	88.54	88.83	89.51	89.39	94.06	93.99	94.37		
K ₂ O+Na ₂ O	10.18	7.49	8.04	7.43	7.39	7.54	7.84	7.25	6.71	8.14	8.06	8.14		

Number before 'G' in ID relates to the host crystal. All Fe reported as FeO. Mineral host where plag=plagioclase, cpx=clinopyroxene, opx=orthopyroxene, amph=amphibole.

Table A2.2 Major element melt inclusion compositions analysed by EMPA

Sample	SM-6C		SM-6C		SM-6C		SM-6C		SM-6C		SM-6C		SM-6C		SM-6C		SM-6C																								
ID	P7MI3	P8MI1	P8MI2	P9MI1	P11MI1	P16MI1	P18MI1	6MI1	17MI1	26MI1	29MI1	31MI1	12MI1	Host	plag	cpx	plag	cpx	plag	cpx	plag	cpx	plag	cpx	plag	cpx	plag	cpx	plag	cpx	plag	cpx	plag	cpx	plag	cpx	plag	cpx			
SiO₂	61.38	60.30	61.42	61.83	60.13	62.58	59.30	62.76	62.93	61.17	62.79	64.55	59.80																												
TiO₂	0.73	0.76	0.69	0.67	0.87	0.63	0.78	0.48	0.48	0.65	0.64	0.51	0.65																												
Al₂O₃	16.36	16.32	16.26	16.00	16.03	15.78	16.12	14.22	14.62	15.83	16.47	14.95	15.48																												
FeO[†]	3.80	4.42	3.65	3.47	4.10	3.52	4.19	3.31	2.73	3.58	3.88	3.39	4.13																												
MnO	0.17	0.18	0.16	0.10	0.15	0.12	0.14	0.17	0.11	0.18	0.16	0.17	0.12																												
MgO	1.27	1.53	1.32	1.17	1.40	1.13	1.47	0.75	0.79	0.94	1.10	0.93	1.08																												
CaO	2.89	3.13	2.90	2.61	3.15	2.80	3.17	2.40	2.44	2.67	2.83	2.81	2.75																												
Na₂O	3.83	3.78	3.84	3.63	3.82	4.17	4.43	3.38	3.70	3.99	4.10	3.79	3.79																												
K₂O	4.24	4.24	4.22	4.42	4.24	4.29	4.37	4.51	3.82	4.56	4.07	4.02	4.38																												
Total	94.67	94.65	94.46	93.90	93.87	95.00	93.97	92.00	91.62	93.57	96.03	95.12	92.17																												
K₂O+Na₂O	8.07	8.02	8.06	8.05	8.05	8.45	8.80	7.90	7.52	8.55	8.17	7.81	8.17																												

Number before 'G' in ID relates to the host crystal. All Fe reported as FeO. Mineral host where plag=plagioclase, cpx=clinopyroxene, opx=orthopyroxene, amph=amphibole.

Table A2.2 Major element melt inclusion compositions analysed by EMPA

Sample ID	Host	SM-6C 7MI1 amph	Maketawa		Maketawa		Maketawa		Maketawa		Maketawa		Maketawa		Maketawa	
			P6MI1 plag	P6MI2 plag	P10MI1 plag	P10MI2 plag	P10MI3 plag	P10MI4 plag	P10MI5 plag	P10MI6 plag	P16MI1 plag	P16MI2 plag				
SiO ₂		59.36	66.14	66.48	65.52	66.53	62.41	65.69	66.19	66.58	65.06	63.13				
TiO ₂		0.57	0.39	0.39	0.33	0.36	0.34	0.33	0.38	0.35	0.31	0.31				
Al ₂ O ₃		17.29	16.02	16.04	16.47	16.44	15.72	16.39	16.59	17.05	15.61	16.28				
FeO ^t		5.32	2.41	2.56	2.35	2.35	2.49	2.21	2.29	2.08	1.99	1.99				
MnO		0.18	0.14	0.13	0.13	0.15	0.13	0.14	0.18	0.16	0.06	0.08				
MgO		1.58	0.69	0.73	0.67	0.69	0.74	0.66	0.67	0.59	0.57	0.52				
CaO		4.48	2.07	2.31	2.28	2.29	2.28	2.32	2.40	2.95	2.00	3.39				
Na ₂ O		4.84	4.58	4.41	4.14	4.27	3.21	4.29	4.33	4.15	3.56	4.03				
K ₂ O		3.44	4.73	4.64	4.50	4.51	4.14	4.31	4.41	4.26	4.33	3.67				
Total		97.05	97.18	97.70	96.38	97.61	91.45	96.34	97.43	98.18	93.48	93.42				
K₂O+Na₂O		8.28	9.31	9.05	8.63	8.79	7.35	8.60	8.74	8.41	7.89	7.70				

Number before 'G' in ID relates to the host crystal. All Fe reported as FeO. Mineral host where plag=plagioclase, cpx=clinopyroxene, opx=orthopyroxene, amph=amphibole.

Table A2.2 Major element melt inclusion compositions analysed by EMPA

Sample	Maketawa	Maketawa	Maketawa	Maketawa	Maketawa	Maketawa	Maketawa	Maketawa	Maketawa	Maketawa	Maketawa	Maketawa	Maketawa
ID	P21MI1	P21MI2	P21MI3	P21MI4	PJMI1	PJMI2	PJMI3	1MI	6MI	8MI	45MI		
Host	plag	plag	plag	plag	plag	plag	plag	cpx	cpx	cpx	cpx		
SiO ₂	64.54	66.86	66.33	65.77	67.71	67.37	67.34	64.40	62.57	64.46	65.28		
TiO ₂	0.28	0.39	0.35	0.39	0.39	0.39	0.38	0.39	0.50	0.38	0.29		
Al ₂ O ₃	15.17	16.07	16.32	15.90	16.17	16.22	16.22	15.51	14.88	13.86	15.05		
FeO ^t	2.03	2.36	2.23	2.25	2.40	2.37	2.34	2.25	2.61	2.18	2.29		
MnO	0.13	0.08	0.12	0.10	0.12	0.15	0.14	0.12	0.12	0.16	0.13		
MgO	0.47	0.62	0.61	0.66	0.68	0.72	0.68	0.59	0.50	0.48	0.42		
CaO	1.76	2.09	2.18	2.17	2.07	2.04	2.13	2.08	2.53	2.19	1.86		
Na ₂ O	3.57	4.54	4.47	4.47	4.19	4.31	4.28	2.81	2.12	2.82	2.29		
K ₂ O	4.41	4.50	4.57	4.31	4.45	4.44	4.51	4.18	4.41	4.22	3.72		
Total	92.36	97.51	97.19	96.02	98.18	98.01	98.03	92.32	90.25	90.74	91.34		
K ₂ O+Na ₂ O	7.98	9.04	9.04	8.79	8.64	8.75	8.79	6.99	6.53	7.04	6.01		

Number before 'G' in ID relates to the host crystal. All Fe reported as FeO. Mineral host where plag=plagioclase, cpx=clinopyroxene, opx=orthopyroxene, amph=amphibole.

Table A2.2 Major element melt inclusion compositions analysed by EMPA

Sample ID	Maketawa		Maketawa		Maketawa		Maketawa		Maketawa		Maketawa		Inglewood b		Inglewood b						
	51MI	55MI	57MI	A12MI1	A9MI1	A13MI1	A13MI42	P4MI1	P4MI2	P4MI3	51MI	55MI	57MI	A12MI1	A9MI1	A13MI1	A13MI42	P4MI1	P4MI2	P4MI3	
Host	cpx	cpx	cpx	amph	amph	amph	amph	amph	amph	amph	amph	amph	amph	plag	plag	plag	amph	amph	plag	plag	plag
SiO ₂	63.15	64.11	65.90	65.88	65.72	65.74	65.69	64.94	60.21	63.70	63.15	64.11	65.90	65.88	65.72	65.74	65.69	64.94	60.21	63.70	63.15
TiO ₂	0.44	0.36	0.37	0.34	0.37	0.37	0.43	0.41	0.24	0.46	0.44	0.36	0.37	0.34	0.37	0.37	0.43	0.41	0.24	0.46	0.44
Al ₂ O ₃	15.01	16.16	15.60	15.70	16.57	16.08	15.47	14.13	18.68	14.25	15.01	16.16	15.60	15.70	16.57	16.08	15.47	14.13	18.68	14.25	15.01
FeO ^t	2.37	2.60	2.38	2.14	2.92	3.19	2.64	1.96	1.58	1.90	2.37	2.60	2.38	2.14	2.92	3.19	2.64	1.96	1.58	1.90	2.37
MnO	0.08	0.11	0.13	0.09	0.07	0.07	0.05	0.18	0.14	0.15	0.08	0.11	0.13	0.09	0.07	0.07	0.05	0.18	0.14	0.15	0.08
MgO	0.51	0.85	0.67	0.48	1.05	0.95	0.66	0.44	0.33	0.49	0.51	0.85	0.67	0.48	1.05	0.95	0.66	0.44	0.33	0.49	0.51
CaO	2.11	2.54	2.10	2.09	2.40	2.37	2.17	1.79	6.03	1.83	2.11	2.54	2.10	2.09	2.40	2.37	2.17	1.79	6.03	1.83	2.11
Na ₂ O	2.61	3.59	3.72	4.15	4.74	3.72	4.27	3.26	4.33	2.70	2.61	3.59	3.72	4.15	4.74	3.72	4.27	3.26	4.33	2.70	2.61
K ₂ O	4.22	3.89	4.41	4.16	4.19	4.01	4.11	4.37	2.53	4.42	4.22	3.89	4.41	4.16	4.19	4.01	4.11	4.37	2.53	4.42	4.22
Total	90.52	94.20	95.28	95.02	98.03	96.51	95.47	91.47	94.07	89.91	90.52	94.20	95.28	95.02	98.03	96.51	95.47	91.47	94.07	89.91	90.52
K ₂ O+Na ₂ O	6.84	7.48	8.13	8.30	8.93	7.73	8.38	7.62	6.86	7.12	6.84	7.48	8.13	8.30	8.93	7.73	8.38	7.62	6.86	7.12	6.84

Number before 'G' in ID relates to the host crystal. All Fe reported as FeO. Mineral host where plag=plagioclase, cpx=clinopyroxene, opx=orthopyroxene, amph=amphibole.

Table A2.2 Major element melt inclusion compositions analysed by EMPA

Sample	Inglewood b	Inglewood b	Inglewood b	Inglewood b	Inglewood b	Inglewood b	Inglewood b	Inglewood b	Inglewood b	Inglewood b
ID	P4MI4	P4MI5	P5MI1	P7MI1	P7MI2	P14MI1	P20MI1	P20MI2	P20MI1	P21MI1
Host	plag	plag	plag	plag	plag	plag	plag	plag	plag	plag
SiO₂	64.31	62.21	66.58	63.53	64.50	64.52	62.92	64.37	62.92	66.48
TiO₂	0.46	0.42	0.41	0.32	0.32	0.32	0.53	0.34	0.53	0.29
Al₂O₃	13.76	14.17	14.01	14.16	13.52	13.66	14.04	14.05	14.04	13.76
FeO[†]	2.13	2.02	2.28	1.93	1.62	1.47	2.50	1.69	2.50	1.47
MnO	0.01	0.16	0.18	0.09	0.13	0.20	0.18	0.15	0.18	0.10
MgO	0.40	0.42	0.56	0.40	0.29	0.33	0.59	0.40	0.59	0.29
CaO	1.60	3.03	2.86	1.77	1.52	1.52	1.67	1.57	1.67	1.50
Na₂O	3.27	3.22	3.65	3.12	2.85	2.93	2.97	2.91	2.97	3.11
K₂O	4.39	3.98	3.75	4.57	4.17	4.36	4.27	4.29	4.27	4.30
Total	90.34	89.63	94.28	89.88	88.93	89.30	89.67	89.77	89.67	91.31
K₂O+Na₂O	7.66	7.20	7.40	7.69	7.03	7.29	7.24	7.21	7.24	7.41

Number before 'G' in ID relates to the host crystal. All Fe reported as FeO. Mineral host where plag=plagioclase, cpx=clinopyroxene, opx=orthopyroxene, amph=amphibole.

Table A2.2 Major element melt inclusion compositions analysed by EMPA

Sample	Inglewood b	Inglewood b	Inglewood b	Inglewood b	Inglewood b	Inglewood b	Inglewood b	Inglewood b	Inglewood b	Inglewood b	Inglewood b
ID	9MI1	19MI1	34MI1	35MI1	41MI1	A1MI1	A2MI1	A3MI1	A3MI2		
Host	cpx	cpx	cpx	cpx	cpx	amph	amph	amph	amph		
SiO ₂	66.37	67.10	67.68	69.21	67.76	67.61	66.39	67.88	67.67		
TiO ₂	0.29	0.31	0.30	0.31	0.30	0.34	0.32	0.37	0.32		
Al ₂ O ₃	14.13	14.06	14.71	14.29	14.20	14.16	14.05	14.11	13.96		
FeO ^t	1.61	1.50	1.59	1.66	1.65	1.81	1.80	1.70	1.70		
MnO	0.14	0.07	0.08	0.14	0.13	0.00	0.10	0.09	0.17		
MgO	0.27	0.26	0.30	0.23	0.30	0.34	0.22	0.27	0.31		
CaO	1.51	1.48	1.48	1.34	1.44	1.58	1.41	1.40	1.46		
Na ₂ O	3.08	2.28	2.93	3.51	2.82	3.97	3.42	3.96	4.09		
K ₂ O	4.42	4.40	4.28	4.25	4.24	4.29	4.26	4.26	4.28		
Total	91.81	91.47	93.36	94.94	92.84	94.09	91.97	94.03	93.97		
K₂O+Na₂O	7.50	6.68	7.21	7.76	7.07	8.25	7.67	8.22	8.37		

Number before 'G' in ID relates to the host crystal. All Fe reported as FeO. Mineral host where plag=plagioclase, cpx=clinopyroxene, opx=orthopyroxene, amph=amphibole.

Table A2.2 Major element melt inclusion compositions analysed by EMPA

Sample	Inglewood b	Inglewood b	Inglewood b	Inglewood b	Inglewood b	Inglewood a	Inglewood a	Inglewood a	Inglewood a
ID	A6MI1	A7MI1	A8MI1	A9MI1	A11MI1	P5MI1	P9MI1	P12MI1	P12MI2
Host	amph	amph	amph	amph	amph	plag	plag	plag	plag
SiO ₂	67.52	66.01	67.72	66.45	66.31	62.95	66.01	64.64	64.49
TiO ₂	0.30	0.47	0.34	0.34	0.33	0.41	0.43	0.31	0.27
Al ₂ O ₃	14.06	14.68	13.78	13.80	13.73	15.84	14.04	15.39	17.86
FeO [†]	1.46	3.28	1.57	1.50	1.50	2.07	1.97	1.58	1.29
MnO	0.08	0.13	0.13	0.15	0.00	0.11	0.20	0.14	0.12
MgO	0.18	0.30	0.25	0.32	0.25	0.39	0.47	0.33	0.29
CaO	0.97	1.63	1.26	1.39	1.39	2.86	1.39	2.65	4.10
Na ₂ O	3.60	3.91	3.90	3.57	3.99	3.11	2.64	3.24	2.24
K ₂ O	5.24	3.90	4.26	4.23	4.24	4.06	4.44	3.88	2.41
Total	93.41	94.32	93.22	91.76	91.74	91.80	91.58	92.16	93.05
K₂O+Na₂O	8.84	7.81	8.16	7.80	8.23	7.17	7.09	7.12	4.64

Number before 'G' in ID relates to the host crystal. All Fe reported as FeO. Mineral host where plag=plagioclase, cpx=clinopyroxene, opx=orthopyroxene, amph=amphibole.

Table A2.2 Major element melt inclusion compositions analysed by EMPA

Sample	Inglewood a	Inglewood a	Inglewood a	Inglewood a	Inglewood a	Inglewood a	Inglewood a	Inglewood a	Inglewood a	Inglewood a	Inglewood a
ID	P12MI3	P16MI1	P19MI2	P21MI1	P21MI2	P22MI1	4MI1	9MI1	19MI1		
Host	plag	plag	plag	plag	plag	plag	cpx	cpx	cpx		
SiO ₂	66.87	65.84	64.30	68.33	70.01	64.62	67.71	67.73	67.35		
TiO ₂	0.33	0.46	0.27	0.28	0.30	0.37	0.32	0.33	0.34		
Al ₂ O ₃	14.81	14.64	14.77	16.00	14.05	14.04	14.15	13.96	14.14		
FeO [†]	1.66	2.03	1.76	1.37	1.54	2.21	1.56	1.55	1.68		
MnO	0.11	0.12	0.11	0.14	0.14	0.15	0.10	0.11	0.08		
MgO	0.34	0.45	0.49	0.26	0.28	0.42	0.28	0.29	0.32		
CaO	2.25	1.77	2.04	3.00	1.38	1.58	1.42	1.47	1.55		
Na ₂ O	3.78	3.22	3.03	4.40	3.83	2.58	2.77	2.69	2.70		
K ₂ O	4.17	4.35	4.15	3.74	4.53	4.46	4.14	4.43	4.31		
Total	94.33	92.89	90.91	97.51	96.06	90.44	92.46	92.57	92.47		
K₂O+Na₂O	7.96	7.57	7.18	8.14	8.36	7.05	6.92	7.12	7.01		

Number before 'G' in ID relates to the host crystal. All Fe reported as FeO. Mineral host where plag=plagioclase, cpx=clinopyroxene, opx=orthopyroxene, amph=amphibole.

Table A2.2 Major element melt inclusion compositions analysed by EMPA

Sample	Inglewood a	Inglewood a	Inglewood a	Inglewood a	Inglewood a	Inglewood a	Inglewood a	Inglewood a	Korito	Korito	Korito
ID	22MI1	48MI1	57MI1	74MI1	A2MI1	A7MI1	A13MI1	P9MI1	P9MI2	P9MI3	
Host	cpx	cpx	cpx	cpx	amph	amph	amph	plag	plag	plag	
SiO ₂	67.35	66.28	65.89	67.31	68.56	68.03	68.83	66.91	67.67	70.26	
TiO ₂	0.31	0.29	0.38	0.20	0.25	0.34	0.36	0.33	0.34	0.37	
Al ₂ O ₃	14.45	13.70	14.70	13.51	15.34	13.96	14.34	14.14	14.08	14.57	
FeO ^t	1.69	1.52	1.65	1.57	1.73	1.48	1.83	1.49	1.60	1.69	
MnO	0.11	0.10	0.13	0.09	0.06	0.10	0.10	0.06	0.13	0.11	
MgO	0.30	0.30	0.37	0.26	0.33	0.25	0.30	0.32	0.33	0.34	
CaO	1.82	1.53	1.87	1.49	1.76	1.28	1.33	1.36	1.43	1.47	
Na ₂ O	2.73	2.73	3.00	2.63	3.86	3.71	3.33	2.80	3.04	3.95	
K ₂ O	4.12	3.95	4.23	4.09	4.15	4.35	4.04	4.69	4.53	4.93	
Total	92.88	90.40	92.21	91.14	96.03	93.50	94.48	92.11	93.15	97.69	
K ₂ O+Na ₂ O	6.85	6.68	7.23	6.72	8.00	8.06	7.38	7.49	7.57	8.88	

Number before 'G' in ID relates to the host crystal. All Fe reported as FeO. Mineral host where plag=plagioclase, cpx=clinopyroxene, opx=orthopyroxene, amph=amphibole.

Table A2.2 Major element melt inclusion compositions analysed by EMPA

Sample ID	Korito P9MI4		Korito P11MI1		Korito P14MI1		Korito P14MI2		Korito P16MI1		Korito P16MI2		Korito P16MI3		Korito P16MI4		Korito P21MI1		Korito P23MI1		Korito P23MI2		
	plag	plag	plag	plag	plag	plag	plag	plag	plag	plag	plag	plag	plag	plag	plag	plag	plag	plag	plag	plag	plag	plag	
SiO ₂	67.13	64.10	65.71	62.80	66.19	69.13	66.01	66.04	67.63	68.23	66.11												
TiO ₂	0.32	0.44	0.32	0.19	0.41	0.36	0.36	0.35	0.30	0.23	0.23												
Al ₂ O ₃	13.74	13.98	14.04	17.62	14.43	14.76	13.96	14.16	13.81	14.53	14.33												
FeO ^t	1.62	2.00	1.79	1.46	2.08	1.79	1.84	1.88	1.78	2.16	2.28												
MnO	0.07	0.13	0.11	0.05	0.14	0.13	0.10	0.14	0.10	0.11	0.11												
MgO	0.32	0.47	0.36	0.29	0.40	0.35	0.37	0.38	0.39	0.66	0.63												
CaO	1.49	1.49	1.61	4.37	1.52	1.44	1.33	1.39	1.44	1.69	1.71												
Na ₂ O	3.12	2.74	2.96	4.43	3.43	4.23	3.20	3.23	3.27	3.78	3.26												
K ₂ O	4.49	4.60	4.26	2.88	4.59	4.78	4.63	4.67	4.34	4.76	4.66												
Total	92.31	89.95	91.15	94.10	93.20	96.96	91.80	92.24	93.06	96.15	93.30												
K₂O+Na₂O	7.62	7.35	7.22	7.32	8.02	9.00	7.83	7.90	7.61	8.54	7.92												

Number before 'G' in ID relates to the host crystal. All Fe reported as FeO. Mineral host where plag=plagioclase, cpx=clinopyroxene, opx=orthopyroxene, amph=amphibole.

Table A2.2 Major element melt inclusion compositions analysed by EMPA

Sample ID	Korito P23MI3		Korito 3MI1		Korito 4MI1		Korito 9MI1		Korito 22MI1		Korito 22MI2		Korito 36MI1		Korito 42MI1	
	Host	plag	cpx	cpx	cpx	cpx	cpx	cpx	cpx	cpx	cpx	cpx	cpx	cpx	cpx	cpx
SiO ₂	64.59		68.39	65.86	66.50	67.03	66.46	67.59	66.46	67.03	66.46	66.59	67.59	66.46	67.59	67.59
TiO ₂	0.19		0.30	0.32	0.30	0.31	0.38	0.34	0.38	0.31	0.38	0.34	0.34	0.38	0.34	0.32
Al ₂ O ₃	16.63		14.76	15.03	14.64	14.21	14.63	14.83	14.63	14.21	14.63	14.83	14.83	14.63	14.83	14.41
FeO ^t	1.94		2.25	2.00	1.96	1.86	1.97	1.78	1.97	1.86	1.97	1.78	1.78	1.97	1.78	1.90
MnO	0.10		0.11	0.09	0.12	0.05	0.11	0.13	0.11	0.05	0.11	0.13	0.13	0.11	0.13	0.11
MgO	0.55		0.21	0.32	0.39	0.36	0.33	0.38	0.33	0.36	0.33	0.38	0.38	0.33	0.38	0.33
CaO	3.61		2.07	1.88	1.68	1.73	1.77	1.61	1.77	1.73	1.77	1.61	1.61	1.77	1.61	1.53
Na ₂ O	1.86		3.66	2.33	2.81	2.91	3.02	2.82	3.02	2.91	3.02	2.82	2.82	3.02	2.82	2.80
K ₂ O	3.74		3.73	4.73	4.15	4.06	4.41	4.14	4.41	4.06	4.41	4.14	4.14	4.41	4.14	4.01
Total	93.21		95.49	92.55	92.55	92.52	93.08	93.62	93.08	92.52	93.08	93.62	93.62	93.08	93.62	93.00
K₂O+Na₂O	5.59		7.39	7.07	6.96	6.97	7.43	6.96	7.43	6.97	7.43	6.96	6.96	7.43	6.96	6.81

Number before 'G' in ID relates to the host crystal. All Fe reported as FeO. Mineral host where plag=plagioclase, cpx=clinopyroxene, opx=orthopyroxene, amph=amphibole.

Table A2.2 Major element melt inclusion compositions analysed by EMPA

Sample ID	Korito	Korito	Korito	Korito	Korito	Korito	Korito	Korito	Korito
Host	53MI1	56MI1	59MI1	A3MI1	A6MI1	A8MI1	A15MI1	A16MI1	
	cpx	cpx	cpx	amph	amph	amph	amph	amph	
SiO ₂	67.38	67.02	67.64	66.50	71.72	67.70	66.97	68.41	
TiO ₂	0.35	0.31	0.33	0.28	0.34	0.31	0.38	0.35	
Al ₂ O ₃	14.44	15.49	14.47	14.80	14.81	15.50	14.52	14.44	
FeO [†]	1.47	2.00	1.78	1.68	1.67	1.77	1.92	1.79	
MnO	0.04	0.09	0.14	0.09	0.14	0.10	0.17	0.10	
MgO	0.33	0.35	0.32	0.30	0.34	0.35	0.30	0.26	
CaO	1.44	1.85	1.57	1.69	1.51	1.54	1.54	1.38	
Na ₂ O	2.69	3.16	2.82	3.69	4.13	3.50	3.65	3.27	
K ₂ O	4.75	4.15	4.12	4.29	4.39	4.42	4.27	4.33	
Total	92.89	94.42	93.18	93.33	99.04	95.19	93.72	94.33	
K₂O+Na₂O	7.44	7.31	6.94	7.98	8.52	7.92	7.91	7.60	

Number before 'G' in ID relates to the host crystal. All Fe reported as FeO. Mineral host where plag=plagioclase, cpx=clinopyroxene, opx=orthopyroxene, amph=amphibole.

Table A2.3 Major element plagioclase compositions analysed by EMPA.

Sample ID	Kaupokonui		Kaupokonui		Kaupokonui		Kaupokonui		Kaupokonui		Kaupokonui		Kaupokonui			
	P1_2	P1_3	P1_4	P1_5	P1_7	P1_8	P1_9	P1_10	P1_11	rim	sieved	sieved	zone	core	zone	zone
SiO ₂	54.95	49.52	49.15	55.15	55.53	52.25	54.97	50.86	52.30							
TiO ₂	0.04	0.00	0.06	0.03	0.04	0.03	0.03	0.02	0.01							
Al ₂ O ₃	28.55	32.70	32.66	28.79	28.28	29.99	28.72	31.78	30.28							
FeO	0.56	0.48	0.62	0.43	0.43	0.43	0.40	0.49	0.38							
Fe ₂ O ₃	0.62	0.54	0.69	0.47	0.48	0.47	0.45	0.54	0.42							
MgO	0.07	0.04	0.08	0.03	0.01	0.04	0.03	0.04	0.04							
CaO	10.67	15.43	15.41	10.64	10.31	12.13	10.82	14.17	12.92							
Na ₂ O	4.70	2.67	2.51	4.84	4.98	3.95	4.79	3.22	3.87							
K ₂ O	0.32	0.12	0.21	0.36	0.31	0.19	0.27	0.15	0.21							
Total	99.93	101.01	100.77	100.31	99.94	99.07	100.07	100.78	100.06							
An	54.55	75.63	76.30	53.69	52.34	62.16	54.60	70.22	64.03							
Ab	43.51	23.65	22.48	44.16	45.79	36.65	43.77	28.87	34.74							
Or	1.95	0.72	1.23	2.16	1.87	1.19	1.63	0.91	1.23							
Cations																
Si	2.480	2.245	2.236	2.479	2.502	2.389	2.477	2.301	2.374							
Al	1.519	1.747	1.751	1.525	1.502	1.616	1.525	1.695	1.620							
Ti	0.001	0.000	0.002	0.001	0.001	0.001	0.001	0.001	0.000							
Fe ³⁺	0.021	0.018	0.024	0.016	0.016	0.016	0.015	0.018	0.014							
Mg	0.004	0.001	0.003	0.001	0.000	0.001	0.001	0.001	0.001							
Ca	0.516	0.749	0.751	0.513	0.498	0.594	0.522	0.687	0.628							
Na	0.412	0.234	0.221	0.422	0.435	0.351	0.419	0.282	0.341							
K	0.018	0.007	0.012	0.021	0.018	0.011	0.016	0.009	0.012							
Total	4.972	5.001	5.000	4.977	4.972	4.981	4.976	4.995	4.991							

Analysis ID relates to crystal number_spot number. All Fe assumed to be Fe2O3. Cations calculated on a 8 oxygen basis.

Table A2.3 Major element plagioclase compositions analysed by EMPA.

Sample ID	Kaupokonui		Kaupokonui		Kaupokonui		Kaupokonui		Kaupokonui		Kaupokonui	
	P2_1 rim	P2_2 zone	P2_3 zone	P2_4 zone	P2_5 sieved	P4_1 rim	P4_2 zone	P4_3 sieved	P4_4 sieved	P4_3 sieved	P4_4 sieved	
SiO ₂	55.40	51.44	53.62	50.09	57.28	53.71	53.92	50.60	54.52	50.60	54.52	
TiO ₂	0.03	0.03	0.00	0.05	0.04	0.03	0.04	0.02	0.04	0.02	0.04	
Al ₂ O ₃	29.02	31.56	30.19	32.68	27.51	29.18	29.16	31.47	29.14	31.47	29.14	
FeO	0.54	0.46	0.50	0.62	0.38	0.59	0.56	0.56	0.58	0.56	0.58	
Fe ₂ O ₃	0.60	0.51	0.56	0.69	0.42	0.65	0.62	0.62	0.64	0.62	0.64	
MgO	0.08	0.05	0.06	0.08	0.08	0.07	0.04	0.03	0.04	0.03	0.04	
CaO	11.28	13.48	11.78	15.37	9.12	11.78	11.54	14.41	11.46	14.41	11.46	
Na ₂ O	4.39	3.65	4.27	2.89	5.11	4.51	4.61	3.25	4.76	3.25	4.76	
K ₂ O	0.31	0.21	0.26	0.14	0.42	0.58	0.54	0.29	0.60	0.29	0.60	
Total	101.11	100.94	100.72	102.00	99.99	100.52	100.48	100.69	101.19	100.69	101.19	
An	57.55	66.27	59.47	73.98	48.36	57.10	56.20	69.85	55.13	69.85	55.13	
Ab	40.53	32.49	38.99	25.21	48.99	39.58	40.68	28.50	41.45	28.50	41.45	
Or	1.91	1.24	1.54	0.82	2.65	3.32	3.12	1.66	3.42	1.66	3.42	
Cations												
Si	2.473	2.320	2.409	2.251	2.565	2.428	2.434	2.298	2.445	2.298	2.445	
Al	1.526	1.678	1.599	1.731	1.452	1.554	1.552	1.685	1.540	1.685	1.540	
Ti	0.001	0.001	0.000	0.002	0.002	0.001	0.001	0.001	0.001	0.001	0.001	
Fe ³⁺	0.020	0.017	0.019	0.023	0.014	0.022	0.021	0.021	0.022	0.021	0.022	
Mg	0.005	0.003	0.002	0.003	0.003	0.005	0.003	0.001	0.001	0.001	0.001	
Ca	0.539	0.651	0.567	0.740	0.438	0.570	0.558	0.701	0.550	0.701	0.550	
Na	0.380	0.319	0.372	0.252	0.443	0.395	0.404	0.286	0.414	0.286	0.414	
K	0.018	0.012	0.015	0.008	0.024	0.033	0.031	0.017	0.034	0.017	0.034	
Total	4.962	5.002	4.983	5.009	4.939	5.009	5.004	5.009	5.007	5.009	5.007	

Analysis ID relates to crystal number_spot number. All Fe assumed to be Fe2O3. Cations calculated on a 8 oxygen basis.

Table A2.3 Major element plagioclase compositions analysed by EMPA.

Sample ID	Kaupokonui		Kaupokonui		Kaupokonui		Kaupokonui		Kaupokonui		Kaupokonui	
	P4_6 sieved	P5_1 rim	P5_3 zone	P5_4 zone	P5_5 zone	P5_6 zone	P5_7 core	P8_1 rim	P8_5 zone			
SiO ₂	53.68	54.82	50.91	51.27	55.62	53.90	57.59	51.09	55.07			
TiO ₂	0.03	0.06	0.04	0.02	0.04	0.03	0.00	0.03	0.02			
Al ₂ O ₃	29.49	28.76	31.51	31.06	28.13	29.50	26.67	30.37	28.41			
FeO	0.55	0.56	0.59	0.65	0.39	0.48	0.44	0.69	0.41			
Fe ₂ O ₃	0.61	0.62	0.66	0.72	0.43	0.53	0.49	0.77	0.46			
MgO	0.03	0.04	0.04	0.07	0.04	0.04	0.05	0.06	0.03			
CaO	11.60	10.71	14.19	13.77	10.54	11.64	8.80	13.07	10.52			
Na ₂ O	4.47	4.78	3.30	3.51	4.99	4.43	5.94	3.33	4.85			
K ₂ O	0.51	0.64	0.32	0.34	0.66	0.55	0.97	0.37	0.73			
Total	100.43	100.44	100.98	100.77	100.45	100.63	100.52	99.09	100.09			
An	57.15	53.24	69.05	67.10	51.76	57.28	42.50	66.90	52.16			
Ab	39.85	42.96	29.10	30.94	44.38	39.48	51.95	30.86	43.51			
Or	2.99	3.79	1.86	1.96	3.86	3.23	5.55	2.24	4.33			
Cations												
Si	2.424	2.469	2.304	2.324	2.501	2.428	2.580	2.348	2.486			
Al	1.570	1.526	1.681	1.659	1.490	1.566	1.408	1.645	1.511			
Ti	0.001	0.002	0.001	0.001	0.001	0.001	0.000	0.001	0.001			
Fe ³⁺	0.021	0.021	0.022	0.025	0.015	0.018	0.016	0.027	0.016			
Mg	0.001	0.001	0.001	0.002	0.001	0.001	0.002	0.002	0.001			
Ca	0.561	0.517	0.688	0.669	0.508	0.562	0.422	0.644	0.509			
Na	0.391	0.417	0.290	0.308	0.435	0.387	0.516	0.297	0.424			
K	0.029	0.037	0.018	0.020	0.038	0.032	0.055	0.022	0.042			
Total	4.999	4.991	5.007	5.007	4.988	4.996	5.000	4.985	4.990			

Analysis ID relates to crystal number_spot number. All Fe assumed to be Fe2O3. Cations calculated on a 8 oxygen basis.

Table A2.3 Major element plagioclase compositions analysed by EMPA.

Sample ID	Kaupokonui	P8_7	Kaupokonui	P8_8	Kaupokonui	P8_9	Kaupokonui	P8_10	Kaupokonui	P8_11	Kaupokonui	P9_1	Kaupokonui	P9_2	Kaupokonui	P9_3	Kaupokonui	P9_4	
zone	zone	zone	core	rim	sieved	rim	zone	rim	sieved	rim	zone	rim	zone	zone	zone	zone	zone	zone	
SiO ₂	57.65	52.07	54.68	52.83	51.54	54.40	54.72	55.33	50.98										
TiO ₂	0.03	0.02	0.02	0.04	0.00	0.04	0.02	0.02	0.02										
Al ₂ O ₃	26.40	30.61	27.97	30.15	31.33	29.25	28.48	27.95	30.98										
FeO	0.38	0.42	0.37	0.60	0.74	0.56	0.57	0.54	0.46										
Fe ₂ O ₃	0.43	0.47	0.41	0.66	0.83	0.63	0.63	0.60	0.51										
MgO	0.01	0.01	0.01	0.06	0.08	0.05	0.06	0.04	0.05										
CaO	8.36	13.13	10.04	12.87	14.39	11.51	10.73	9.85	13.51										
Na ₂ O	5.67	3.54	4.79	3.86	3.36	4.73	4.84	4.97	3.35										
K ₂ O	1.14	0.43	0.71	0.52	0.44	0.70	0.77	0.78	0.35										
Total	99.69	100.27	98.64	100.99	101.95	101.31	100.24	99.54	99.75										
An	41.85	65.49	51.35	62.88	68.56	55.08	52.60	49.83	67.55										
Ab	51.33	31.98	44.31	34.10	28.94	40.92	42.89	45.46	30.36										
Or	6.82	2.53	4.34	3.03	2.50	4.01	4.51	4.71	2.10										
Cations																			
Si	2.598	2.361	2.499	2.381	2.314	2.438	2.473	2.508	2.328										
Al	1.402	1.636	1.507	1.602	1.658	1.545	1.516	1.493	1.668										
Ti	0.001	0.001	0.001	0.001	0.000	0.001	0.001	0.001	0.001										
Fe ³⁺	0.014	0.016	0.014	0.022	0.028	0.021	0.022	0.020	0.018										
Mg	0.000	0.000	0.000	0.002	0.003	0.002	0.002	0.001	0.002										
Ca	0.404	0.638	0.492	0.622	0.692	0.553	0.519	0.478	0.661										
Na	0.495	0.311	0.424	0.337	0.292	0.411	0.424	0.437	0.297										
K	0.066	0.025	0.042	0.030	0.025	0.040	0.045	0.045	0.020										
Total	4.980	4.988	4.979	4.998	5.013	5.011	5.001	4.984	4.994										

Analysis ID relates to crystal number_spot number. All Fe assumed to be Fe2O3. Cations calculated on a 8 oxygen basis.

Table A2.3 Major element plagioclase compositions analysed by EMPA.

Sample ID	kaupokonui sieved	P9_5	kaupokonui sieved	P9_6	kaupokonui sieved	P9_7	kaupokonui sieved	P9_9	kaupokonui zone	P9_10	kaupokonui core	P9_11	kaupokonui rim	P10_1	kaupokonui zone	P10_2	kaupokonui sieved	P10_3	
SiO ₂	51.47	52.48	55.53	53.86	52.37	53.49	53.95	54.70	50.86										
TiO ₂	0.03	0.00	0.03	0.00	0.01	0.03	0.02	0.01	0.02										
Al ₂ O ₃	30.95	29.93	27.93	28.53	29.91	29.10	28.79	28.34	31.28										
FeO	0.55	0.56	0.60	0.54	0.56	0.52	0.53	0.51	0.43										
Fe ₂ O ₃	0.61	0.62	0.67	0.60	0.62	0.58	0.58	0.56	0.48										
MgO	0.04	0.05	0.05	0.04	0.06	0.04	0.03	0.05	0.02										
CaO	13.46	12.34	10.06	10.79	12.17	11.49	11.03	10.59	13.95										
Na ₂ O	3.57	3.98	5.04	4.42	3.98	4.41	4.40	4.77	3.19										
K ₂ O	0.42	0.51	0.75	0.65	0.45	0.56	0.66	0.68	0.34										
Total	100.55	99.90	100.05	98.89	99.58	99.70	99.48	99.71	100.13										
An	65.92	61.27	50.14	55.16	61.09	57.07	55.75	52.87	69.33										
Ab	31.66	35.74	45.41	40.88	36.20	39.61	40.27	43.09	28.68										
Or	2.42	2.99	4.45	3.96	2.70	3.32	3.98	4.04	2.00										
Cations																			
Si	2.335	2.388	2.507	2.463	2.389	2.433	2.455	2.480	2.316										
Al	1.654	1.605	1.486	1.538	1.608	1.560	1.544	1.514	1.678										
Ti	0.001	0.000	0.001	0.000	0.000	0.001	0.001	0.001	0.001										
Fe ³⁺	0.021	0.021	0.023	0.021	0.021	0.020	0.020	0.019	0.016										
Mg	0.001	0.002	0.002	0.002	0.002	0.001	0.002	0.003	0.001										
Ca	0.654	0.601	0.487	0.529	0.595	0.560	0.538	0.514	0.681										
Na	0.314	0.351	0.441	0.392	0.352	0.389	0.388	0.419	0.282										
K	0.024	0.029	0.043	0.038	0.026	0.033	0.038	0.039	0.020										
Total	5.005	4.998	4.989	4.981	4.994	4.996	4.986	4.989	4.994										

Analysis ID relates to crystal number_spot number. All Fe assumed to be Fe2O3. Cations calculated on a 8 oxygen basis.

Table A2.3 Major element plagioclase compositions analysed by EMPA.

Sample ID	zone	P10_4	zone	P10_5	zone	P10_6	sieved	P10_8	sieved	P10_10	rim	P11_1	zone	P11_2	zone	P11_3	zone	P11_4	
SiO ₂	54.47	52.71	50.05	46.90	53.70	53.83	52.47	50.00	53.58	53.83	52.47	50.00	53.58	52.47	50.00	53.58	52.47	50.00	53.58
TiO ₂	0.04	0.02	0.03	0.00	0.00	0.00	0.04	0.00	0.04	0.00	0.00	0.00	0.04	0.04	0.03	0.04	0.03	0.04	0.04
Al ₂ O ₃	28.31	30.63	31.89	33.93	29.24	29.19	30.02	31.53	28.87	29.19	30.02	31.53	28.87	30.02	31.53	28.87	30.02	31.53	28.87
FeO	0.50	0.53	0.52	0.63	0.50	0.53	0.65	0.70	0.64	0.50	0.53	0.70	0.64	0.65	0.70	0.64	0.70	0.64	0.64
Fe ₂ O ₃	0.55	0.59	0.58	0.70	0.55	0.59	0.72	0.78	0.71	0.55	0.59	0.78	0.71	0.72	0.78	0.71	0.78	0.71	0.71
MgO	0.05	0.04	0.04	0.04	0.05	0.06	0.03	0.07	0.05	0.05	0.06	0.07	0.05	0.03	0.07	0.05	0.07	0.05	0.05
CaO	10.44	12.99	14.45	16.76	11.50	11.80	12.84	14.71	11.49	11.50	11.80	14.71	11.49	12.84	14.71	11.49	12.84	14.71	11.49
Na ₂ O	4.79	3.95	3.06	1.77	4.33	4.27	3.84	2.91	4.23	4.33	4.27	2.91	4.23	3.84	2.91	4.23	3.84	2.91	4.23
K ₂ O	0.64	0.46	0.29	0.15	0.55	0.57	0.44	0.30	0.53	0.55	0.57	0.30	0.53	0.44	0.30	0.53	0.44	0.30	0.53
Total	99.30	101.39	100.38	100.24	99.92	100.31	100.40	100.33	99.50	99.92	100.31	100.33	99.50	100.40	100.33	99.50	100.33	99.50	99.50
An	52.55	62.81	71.07	83.25	57.53	58.40	63.23	72.36	58.11	57.53	58.40	72.36	58.11	63.23	72.36	58.11	72.36	58.11	58.11
Ab	43.58	34.56	27.25	15.89	39.19	38.22	34.18	25.91	38.71	39.19	38.22	25.91	38.71	34.18	25.91	38.71	34.18	25.91	38.71
Or	3.86	2.63	1.68	0.87	3.28	3.39	2.58	1.73	3.18	3.28	3.39	1.73	3.18	2.58	1.73	3.18	2.58	1.73	3.18
Cations																			
Si	2.479	2.367	2.280	2.155	2.435	2.434	2.379	2.283	2.441	2.435	2.434	2.283	2.441	2.379	2.283	2.441	2.379	2.283	2.441
Al	1.519	1.621	1.712	1.837	1.562	1.555	1.604	1.696	1.550	1.562	1.555	1.696	1.550	1.604	1.696	1.550	1.696	1.550	1.550
Ti	0.001	0.001	0.001	0.000	0.000	0.000	0.001	0.001	0.001	0.000	0.000	0.001	0.001	0.001	0.001	0.001	0.001	0.001	0.001
Fe ³⁺	0.019	0.020	0.020	0.024	0.019	0.020	0.025	0.027	0.024	0.019	0.020	0.027	0.024	0.025	0.027	0.024	0.027	0.024	0.024
Mg	0.002	0.001	0.001	0.001	0.002	0.002	0.001	0.002	0.002	0.002	0.002	0.002	0.002	0.001	0.002	0.002	0.002	0.002	0.002
Ca	0.509	0.625	0.705	0.825	0.559	0.572	0.624	0.720	0.561	0.559	0.572	0.720	0.561	0.624	0.720	0.561	0.720	0.561	0.561
Na	0.422	0.344	0.270	0.157	0.381	0.374	0.337	0.258	0.374	0.381	0.374	0.258	0.374	0.337	0.258	0.374	0.337	0.258	0.374
K	0.037	0.026	0.017	0.009	0.032	0.033	0.026	0.017	0.031	0.032	0.033	0.017	0.031	0.026	0.017	0.031	0.026	0.017	0.031
Total	4.988	5.005	5.006	5.008	4.989	4.990	4.997	5.003	4.983	4.989	4.990	5.003	4.983	4.997	5.003	4.983	4.997	5.003	4.983

Analysis ID relates to crystal number_spot number. All Fe assumed to be Fe2O3. Cations calculated on a 8 oxygen basis.

Table A2.3 Major element plagioclase compositions analysed by EMPA.

Sample ID	zone	zone	zone	rim	zone	zone	core	core	rim	core
	P11_5	P11_6	P11_7	P12_1	P12_2	P12_3	P12_5	P12_6	P12_7	
	zone	zone	zone	rim	zone	core	core	rim	core	core
SiO ₂	51.64	50.57	52.32	56.13	55.80	51.05	51.72	54.56	50.57	50.57
TiO ₂	0.03	0.03	0.03	0.01	0.02	0.01	0.07	0.05	0.03	0.03
Al ₂ O ₃	30.68	31.71	29.43	28.69	29.14	32.43	32.15	30.06	30.67	30.67
FeO	0.57	0.64	0.64	0.59	0.59	0.64	0.53	0.64	0.82	0.82
Fe ₂ O ₃	0.64	0.71	0.71	0.65	0.65	0.71	0.59	0.71	0.91	0.91
MgO	0.04	0.03	0.05	0.04	0.05	0.05	0.04	0.03	0.04	0.04
CaO	13.58	14.82	12.17	10.31	10.58	14.18	14.27	11.74	13.56	13.56
Na ₂ O	3.53	3.07	3.81	5.12	4.95	3.14	3.23	4.48	2.93	2.93
K ₂ O	0.38	0.34	0.63	0.71	0.65	0.28	0.34	0.59	0.29	0.29
Total	100.52	101.28	99.16	101.65	101.84	101.85	102.41	102.22	99.00	99.00
An	66.52	71.33	61.39	50.51	52.07	70.22	69.51	57.14	70.60	70.60
Ab	31.26	26.73	34.80	45.37	44.09	28.10	28.51	39.46	27.64	27.64
Or	2.22	1.94	3.81	4.13	3.83	1.67	1.98	3.41	1.77	1.77
Cations										
Si	2.343	2.287	2.399	2.495	2.476	2.288	2.305	2.422	2.329	2.329
Al	1.640	1.690	1.590	1.503	1.524	1.713	1.689	1.573	1.665	1.665
Ti	0.001	0.001	0.001	0.000	0.001	0.000	0.002	0.002	0.001	0.001
Fe ³⁺	0.022	0.024	0.025	0.022	0.022	0.024	0.020	0.024	0.031	0.031
Mg	0.001	0.001	0.002	0.001	0.002	0.002	0.001	0.001	0.001	0.001
Ca	0.660	0.718	0.598	0.491	0.503	0.681	0.681	0.558	0.669	0.669
Na	0.310	0.269	0.339	0.441	0.426	0.272	0.279	0.385	0.262	0.262
K	0.022	0.020	0.037	0.040	0.037	0.016	0.019	0.033	0.017	0.017
Total	5.000	5.010	4.991	4.993	4.991	4.997	4.997	4.998	4.976	4.976

Analysis ID relates to crystal number_spot number. All Fe assumed to be Fe2O3. Cations calculated on a 8 oxygen basis.

Table A2.3 Major element plagioclase compositions analysed by EMPA.

Sample ID	kaupokonui	kaupokonui	kaupokonui	kaupokonui	kaupokonui	kaupokonui	kaupokonui	kaupokonui	kaupokonui	kaupokonui	kaupokonui
zone	P13_1	P13_2	P13_3	P13_4	P13_5	P13_6	P13_8	P15_1	P15_2	rim	zone
SiO ₂	56.32	55.70	55.18	53.78	56.10	56.39	55.96	53.20	52.51	53.20	52.51
TiO ₂	0.07	0.03	0.03	0.06	0.05	0.03	0.07	0.03	0.03	0.03	0.03
Al ₂ O ₃	28.74	28.59	29.10	29.97	28.60	28.03	28.71	29.61	30.59	29.61	30.59
FeO	0.58	0.60	0.57	0.57	0.49	0.40	0.47	0.65	0.58	0.65	0.58
Fe ₂ O ₃	0.65	0.66	0.64	0.64	0.54	0.45	0.52	0.72	0.64	0.72	0.64
MgO	0.05	0.04	0.04	0.05	0.02	0.05	0.03	0.07	0.06	0.07	0.06
CaO	10.92	10.38	10.99	12.14	10.45	9.90	10.49	12.07	13.27	12.07	13.27
Na ₂ O	5.07	5.02	4.80	4.26	5.02	5.34	4.92	4.09	3.96	4.09	3.96
K ₂ O	0.75	0.72	0.60	0.50	0.71	0.77	0.69	0.52	0.49	0.52	0.49
Total	102.56	101.14	101.37	101.38	101.50	100.96	101.39	100.30	101.56	100.30	101.56
An	52.04	51.12	53.93	59.41	51.25	48.36	51.90	60.10	63.13	60.10	63.13
Ab	43.69	44.69	42.59	37.69	44.60	47.19	44.04	36.85	34.09	36.85	34.09
Or	4.27	4.19	3.48	2.90	4.15	4.46	4.06	3.06	2.78	3.06	2.78
Cations											
Si	2.487	2.489	2.463	2.409	2.496	2.519	2.492	2.409	2.359	2.409	2.359
Al	1.495	1.506	1.531	1.582	1.500	1.476	1.507	1.580	1.619	1.580	1.619
Ti	0.002	0.001	0.001	0.002	0.002	0.001	0.002	0.001	0.001	0.001	0.001
Fe ³⁺	0.021	0.022	0.021	0.021	0.018	0.015	0.017	0.025	0.022	0.025	0.022
Mg	0.002	0.001	0.001	0.002	0.001	0.002	0.001	0.002	0.002	0.002	0.002
Ca	0.517	0.497	0.525	0.582	0.498	0.474	0.501	0.586	0.639	0.586	0.639
Na	0.434	0.435	0.415	0.370	0.433	0.463	0.425	0.359	0.345	0.359	0.345
K	0.042	0.041	0.034	0.028	0.040	0.044	0.039	0.030	0.028	0.030	0.028
Total	5.000	4.993	4.993	4.996	4.988	4.993	4.984	4.992	5.015	4.992	5.015

Analysis ID relates to crystal number_spot number. All Fe assumed to be Fe2O3. Cations calculated on a 8 oxygen basis.

Table A2.3 Major element plagioclase compositions analysed by EMPA.

Sample ID	Kaupokonui	P15_3	Kaupokonui	P15_4	Kaupokonui	P15_5	Kaupokonui	P15_6	Kaupokonui	P15_7	Kaupokonui	P15_8	Kaupokonui	P17_1	Kaupokonui	P17_2	Kaupokonui	P17_3	
zone	zone	zone	zone	zone	zone	zone	zone	zone	zone	zone	rim	zone	zone	rim	zone	zone	zone	zone	
SiO ₂	54.69	54.03	55.39	55.42	54.65	54.23	55.86	51.69	55.27										
TiO ₂	0.03	0.02	0.04	0.02	0.02	0.02	0.06	0.06	0.04										
Al ₂ O ₃	28.41	28.87	28.25	27.69	29.35	28.52	27.88	30.93	27.60										
FeO	0.54	0.51	0.56	0.44	0.41	0.48	0.53	0.45	0.59										
Fe ₂ O ₃	0.60	0.57	0.62	0.49	0.46	0.54	0.59	0.50	0.65										
MgO	0.06	0.05	0.03	0.05	0.05	0.04	0.07	0.09	0.06										
CaO	10.87	11.07	10.33	9.82	11.66	10.89	9.82	13.09	9.71										
Na ₂ O	4.68	4.48	4.85	5.01	4.71	4.63	5.13	3.62	4.98										
K ₂ O	0.66	0.59	0.70	0.75	0.67	0.62	0.39	0.19	0.36										
Total	99.99	99.67	100.20	99.26	101.58	99.48	99.79	100.16	98.67										
An	54.03	55.73	51.81	49.67	55.59	54.43	50.22	65.90	50.68										
Ab	42.08	40.76	44.04	45.83	40.61	41.90	47.43	32.96	47.08										
Or	3.89	3.51	4.15	4.50	3.81	3.67	2.35	1.14	2.23										
Cations																			
Si	2.475	2.453	2.496	2.517	2.441	2.466	2.519	2.346	2.521										
Al	1.515	1.545	1.501	1.482	1.545	1.528	1.482	1.654	1.483										
Ti	0.001	0.001	0.001	0.001	0.001	0.001	0.002	0.002	0.001										
Fe ³⁺	0.021	0.019	0.021	0.017	0.015	0.018	0.020	0.017	0.022										
Mg	0.002	0.002	0.001	0.002	0.002	0.001	0.002	0.003	0.002										
Ca	0.527	0.539	0.499	0.478	0.558	0.531	0.475	0.636	0.474										
Na	0.410	0.394	0.424	0.441	0.408	0.408	0.448	0.318	0.441										
K	0.038	0.034	0.040	0.043	0.038	0.036	0.022	0.011	0.021										
Total	4.989	4.986	4.983	4.981	5.007	4.990	4.971	4.987	4.965										

Analysis ID relates to crystal number_spot number. All Fe assumed to be Fe2O3. Cations calculated on a 8 oxygen basis.

Table A2.3 Major element plagioclase compositions analysed by EMPA.

Sample ID	zone	P17_4	P17_5	P19_2	P20_1	P20_2	P20_3	P20_4	P20_5	P20_6
zone	zone	sieved	zone	rim	zone	zone	zone	zone	zone	core
SiO ₂	55.33	51.11	50.32	55.06	54.91	57.46	58.73	54.64	56.32	
TiO ₂	0.03	0.03	0.01	0.03	0.00	0.03	0.03	0.02	0.03	
Al ₂ O ₃	28.28	31.43	32.10	28.94	29.35	27.09	26.50	29.58	28.28	
FeO	0.41	0.50	0.61	0.48	0.58	0.47	0.43	0.43	0.45	
Fe ₂ O ₃	0.45	0.56	0.68	0.54	0.64	0.52	0.47	0.48	0.50	
MgO	0.05	0.05	0.09	0.05	0.03	0.03	0.04	0.03	0.03	
CaO	10.21	13.77	14.84	11.08	11.26	9.04	8.11	11.55	10.02	
Na ₂ O	4.89	3.37	2.96	4.58	4.70	5.61	5.93	4.48	5.19	
K ₂ O	0.36	0.17	0.15	0.64	0.62	0.96	1.13	0.58	0.78	
Total	99.59	100.49	101.15	100.89	101.52	100.76	100.94	101.37	101.15	
An	52.40	68.63	72.82	55.07	54.92	44.44	40.18	56.75	49.23	
Ab	45.39	30.37	26.32	41.17	41.48	49.91	53.16	39.84	46.20	
Or	2.21	1.00	0.86	3.77	3.60	5.65	6.66	3.41	4.57	
Cations										
Si	2.501	2.317	2.275	2.468	2.450	2.567	2.611	2.441	2.512	
Al	1.507	1.679	1.711	1.528	1.543	1.427	1.389	1.557	1.487	
Ti	0.001	0.001	0.000	0.001	0.000	0.001	0.001	0.001	0.001	
Fe ³⁺	0.015	0.019	0.023	0.018	0.022	0.018	0.016	0.016	0.017	
Mg	0.002	0.002	0.003	0.003	0.002	0.001	0.001	0.001	0.001	
Ca	0.494	0.669	0.719	0.532	0.538	0.433	0.386	0.553	0.479	
Na	0.428	0.296	0.260	0.398	0.407	0.486	0.511	0.388	0.449	
K	0.021	0.010	0.008	0.036	0.035	0.055	0.064	0.033	0.044	
Total	4.968	4.993	5.000	4.984	4.997	4.988	4.980	4.990	4.990	

Analysis ID relates to crystal number_spot number. All Fe assumed to be Fe2O3. Cations calculated on a 8 oxygen basis.

Table A2.3 Major element plagioclase compositions analysed by EMPA.

Sample ID	Kaupokonui		Kaupokonui		Kaupokonui		Kaupokonui		Kaupokonui		SM-6C		SM-6C		SM-6C		SM-6C	
	P21_1 rim	P21_2 zone	P21_3 zone	P21_4 sieved	P21_5 sieved	P21_9 sieved	P1_2 rim	P1_6 core	P3_1 rim	P3_2 skeletal	P3_4 rim	P3_7 core						
SiO ₂	56.68	53.20	56.69	51.33	50.46	51.70	53.89	50.58	52.41	44.69	52.71	52.70						
TiO ₂	0.04	0.01	0.03	0.02	0.01	0.02	0.06	0.03	0.05	0.02	0.03	0.05						
Al ₂ O ₃	28.21	30.53	27.77	31.83	31.64	31.49	27.40	29.86	28.48	34.93	28.72	28.70						
FeO	0.48	0.60	0.56	0.61	0.68	0.53	0.64	0.66	0.93	0.69	0.70	0.67						
Fe ₂ O ₃	0.54	0.66	0.62	0.68	0.76	0.59	0.71	0.73	1.04	0.76	0.78	0.74						
MgO	0.04	0.05	0.05	0.02	0.04	0.02	0.06	0.06	0.10	0.04	0.08	0.07						
CaO	9.81	12.52	9.66	14.23	13.66	13.76	9.98	13.06	11.96	18.45	11.59	11.66						
Na ₂ O	5.32	4.03	5.37	3.19	3.09	3.49	4.82	3.60	4.19	1.02	4.44	4.27						
K ₂ O	0.83	0.49	0.85	0.31	0.33	0.37	0.81	0.45	0.58	0.08	0.62	0.59						
Total	101.46	101.49	101.04	101.60	99.99	101.44	97.74	98.36	98.81	99.99	98.97	98.78						
An	48.02	61.38	47.37	69.88	69.57	67.09	50.76	64.94	59.10	90.50	56.91	58.05						
Ab	47.15	35.77	47.69	28.31	28.45	30.75	44.32	32.37	37.50	9.05	39.45	38.44						
Or	4.83	2.85	4.94	1.82	1.98	2.16	4.92	2.69	3.39	0.45	3.65	3.51						
Cations																		
Si	2.520	2.383	2.531	2.307	2.302	2.325	2.778	2.347	2.418	2.072	2.422	2.425						
Al	1.478	1.612	1.462	1.686	1.701	1.669	0.936	1.633	1.548	1.908	1.556	1.556						
Ti	0.001	0.000	0.001	0.001	0.000	0.001	0.037	0.001	0.002	0.001	0.001	0.002						
Fe ³⁺	0.018	0.022	0.021	0.023	0.026	0.020	0.231	0.025	0.036	0.027	0.027	0.026						
Mg	0.003	0.003	0.002	0.001	0.001	0.001	0.164	0.002	0.007	0.003	0.003	0.003						
Ca	0.467	0.601	0.462	0.685	0.668	0.663	0.283	0.649	0.591	0.916	0.570	0.574						
Na	0.459	0.350	0.465	0.278	0.273	0.304	0.356	0.324	0.375	0.092	0.395	0.380						
K	0.047	0.028	0.048	0.018	0.019	0.021	0.220	0.027	0.034	0.005	0.037	0.035						
Total	4.993	4.999	4.992	4.997	4.991	5.002	5.01	5.01	5.01	5.02	5.01	5.00						

Analysis ID relates to crystal number_spot number. All Fe assumed to be Fe2O3. Cations calculated on a 8 oxygen basis.

Table A2.3 Major element plagioclase compositions analysed by EMPA.

Sample	SM-6C	SM-6C	SM-6C	SM-6C	SM-6C	SM-6C	SM-6C	SM-6C	SM-6C	SM-6C	SM-6C	SM-6C	SM-6C	SM-6C	SM-6C	SM-6C	SM-6C	SM-6C	SM-6C	
ID	P3_8	P5_1	P5_3	P5_5	P7_1	P7_2	P7_3	P7_4	P7_5	P7_7	P7_8	P9_2	P9_3	P9_4	P9_5	zone	core	rim	zone	zone
zone	sieved	rim	sieved	sieved	rim	sieved	zone	sieved	sieved	zone	core	rim	zone	core	zone	zone	core	rim	zone	zone
SiO ₂	48.21	54.76	53.53	48.48	53.39	51.31	55.87	50.42	54.01	53.17	49.52	54.30	53.10	54.26	55.93					
TiO ₂	0.04	0.06	0.05	0.04	0.02	0.02	0.01	0.04	0.04	0.06	0.00	0.05	0.04	0.06	0.03					
Al ₂ O ₃	32.40	28.44	29.08	32.54	29.21	30.56	27.32	30.67	28.18	28.99	31.83	28.38	29.07	28.19	27.20					
FeO	0.77	0.59	0.77	0.64	0.61	0.69	0.55	0.66	0.70	0.67	0.70	0.74	0.64	0.52	0.60					
Fe ₂ O ₃	0.86	0.65	0.86	0.71	0.67	0.76	0.61	0.73	0.78	0.75	0.77	0.82	0.71	0.58	0.66					
MgO	0.06	0.05	0.08	0.03	0.07	0.05	0.05	0.06	0.09	0.06	0.04	0.05	0.08	0.04	0.07					
CaO	15.84	10.64	11.96	15.53	11.59	13.36	9.45	13.54	10.70	11.53	14.66	10.68	11.43	10.60	9.55					
Na ₂ O	2.37	4.75	4.06	2.35	4.36	3.58	5.28	3.19	4.59	4.30	2.84	4.60	4.22	4.58	5.17					
K ₂ O	0.31	0.70	0.58	0.22	0.61	0.44	0.89	0.41	0.67	0.62	0.29	0.71	0.58	0.69	0.91					
Total	100.09	100.05	100.20	99.88	99.93	100.07	99.48	99.05	99.05	99.47	99.95	99.59	99.23	99.02	99.52					
An	77.29	53.04	59.80	77.50	57.37	65.59	47.12	68.36	54.05	57.49	72.76	53.79	57.87	53.79	47.76					
Ab	20.92	42.80	36.77	21.19	39.05	31.83	47.61	29.19	41.95	38.82	25.50	41.97	38.64	42.05	46.82					
Or	1.79	4.16	3.44	1.31	3.59	2.57	5.27	2.45	4.01	3.70	1.74	4.24	3.49	4.16	5.41					
Cations																				
Si	2.217	2.476	2.427	2.227	2.426	2.341	2.534	2.323	2.470	2.427	2.269	2.470	2.427	2.478	2.536					
Al	1.756	1.516	1.554	1.762	1.564	1.643	1.460	1.665	1.519	1.560	1.719	1.521	1.566	1.517	1.454					
Ti	0.001	0.002	0.002	0.001	0.001	0.001	0.000	0.001	0.001	0.002	0.000	0.002	0.001	0.002	0.001					
Fe ³⁺	0.030	0.022	0.029	0.024	0.023	0.026	0.021	0.025	0.027	0.026	0.027	0.028	0.024	0.020	0.023					
Mg	0.002	0.003	0.003	0.001	0.002	0.002	0.002	0.002	0.003	0.002	0.001	0.002	0.003	0.001	0.002					
Ca	0.780	0.516	0.581	0.764	0.564	0.653	0.459	0.668	0.524	0.564	0.719	0.520	0.560	0.519	0.464					
Na	0.211	0.416	0.357	0.209	0.384	0.317	0.464	0.285	0.407	0.381	0.252	0.406	0.374	0.405	0.455					
K	0.018	0.040	0.033	0.013	0.035	0.026	0.051	0.024	0.039	0.036	0.017	0.041	0.034	0.040	0.053					
Total	5.02	4.99	4.99	5.00	5.00	5.01	4.99	5.00	4.99	5.00	5.00	4.99	4.99	4.98	4.99					

Analysis ID relates to crystal number_spot number. All Fe assumed to be Fe2O3. Cations calculated on a 8 oxygen basis.

Table A2.3 Major element plagioclase compositions analysed by EMPA.

Sample ID	SM-6C P10_1		SM-6C P11_1		SM-6C P11_2		SM-6C P11_3		SM-6C P11_4		SM-6C P12_1		SM-6C P12_2		SM-6C P12_3		SM-6C P15_2		SM-6C P15_5		SM-6C P16_1		SM-6C P16_2		SM-6C P16_4				
	skeletal	rim	zone	sieved	sieved	zone	sieved	sieved	sieved	rim	rim	zone	core	rim	core	rim	core	rim	core	rim	sieved	sieved	rim	sieved	sieved	sieved			
SiO ₂	44.90	54.22	54.79	47.40	52.58	53.46	54.23	50.97	51.92	53.06	51.04	53.06	51.92	53.06	51.04	53.06	51.92	53.06	51.04	53.06	51.04	53.06	51.04	53.06	51.04	53.06	51.04	53.06	51.04
TiO ₂	0.00	0.04	0.04	0.01	0.06	0.10	0.12	0.06	0.06	0.08	0.08	0.12	0.06	0.08	0.08	0.12	0.06	0.08	0.08	0.08	0.05	0.08	0.05	0.08	0.05	0.08	0.05	0.08	
Al ₂ O ₃	34.43	27.62	29.55	33.11	29.10	28.42	27.92	29.13	29.10	29.13	28.42	27.92	29.13	29.13	28.42	27.92	29.13	29.35	27.93	30.34	27.33	30.34	27.33	30.34	27.33	30.34	27.33	30.34	27.33
FeO	0.64	0.55	0.69	0.68	0.60	0.71	0.72	0.89	0.67	0.74	0.71	0.72	0.89	0.67	0.71	0.72	0.89	0.67	0.80	0.75	0.53	0.75	0.53	0.75	0.53	0.75	0.53	0.75	
Fe ₂ O ₃	0.71	0.61	0.77	0.75	0.67	0.79	0.80	0.99	0.67	0.82	0.79	0.80	0.99	0.75	0.83	0.80	0.99	0.75	0.88	0.83	0.59	0.83	0.59	0.83	0.59	0.83	0.59	0.83	
MgO	0.04	0.05	0.07	0.05	0.05	0.06	0.06	0.10	0.05	0.09	0.06	0.06	0.10	0.07	0.05	0.06	0.10	0.07	0.06	0.05	0.04	0.05	0.04	0.05	0.04	0.05	0.04	0.05	
CaO	18.06	10.10	11.79	16.48	11.83	10.88	10.32	12.31	11.83	12.35	10.88	10.32	12.31	12.29	13.37	12.31	12.29	13.37	13.37	9.86	13.37	9.86	13.37	9.86	13.37	9.86	13.37	9.86	
Na ₂ O	1.18	4.86	4.12	2.06	4.12	4.41	4.79	3.58	4.12	4.22	4.41	4.79	3.58	3.77	4.54	3.58	3.77	4.54	3.59	5.06	4.54	5.06	4.54	5.06	4.54	5.06	4.54	5.06	
K ₂ O	0.08	0.80	0.57	0.18	0.59	0.65	0.70	0.43	0.59	0.54	0.65	0.70	0.43	0.49	0.46	0.43	0.49	0.46	0.46	0.81	0.46	0.81	0.46	0.81	0.46	0.81	0.46	0.81	
Total	99.40	98.30	101.70	100.04	98.99	98.75	98.93	97.58	98.69	99.89	98.75	98.93	97.58	98.69	99.72	98.69	98.69	99.72	99.72	98.72	99.72	98.72	99.72	98.72	99.72	98.72	99.72	98.72	
An	89.01	50.89	59.17	80.73	59.20	55.43	52.05	63.76	62.43	54.46	65.52	63.76	62.43	54.46	65.52	62.43	54.46	65.52	65.52	49.35	49.35	49.35	49.35	49.35	49.35	49.35	49.35	49.35	
Ab	10.50	44.33	37.45	18.23	37.28	40.66	43.73	33.59	34.61	41.30	31.81	45.85	34.61	41.30	31.81	45.85	34.61	41.30	31.81	45.85	45.85	45.85	45.85	45.85	45.85	45.85	45.85	45.85	
Or	0.50	4.78	3.38	1.04	3.52	3.91	4.21	2.65	2.96	4.24	2.66	4.81	2.96	4.24	2.66	4.81	2.96	4.24	2.66	4.81	4.81	4.81	4.81	4.81	4.81	4.81	4.81	4.81	
Cations																													
Si	2.091	2.494	2.441	2.182	2.413	2.453	2.481	2.379	2.393	2.456	2.339	2.456	2.393	2.456	2.339	2.456	2.393	2.456	2.339	2.515	2.456	2.515	2.456	2.339	2.515	2.456	2.339	2.515	
Al	1.890	1.497	1.552	1.797	1.574	1.537	1.506	1.603	1.594	1.524	1.638	1.594	1.524	1.638	1.474	1.594	1.524	1.638	1.474	1.474	1.474	1.474	1.474	1.474	1.474	1.474	1.474	1.474	
Ti	0.000	0.001	0.001	0.000	0.002	0.004	0.004	0.002	0.002	0.003	0.004	0.004	0.002	0.002	0.002	0.002	0.002	0.002	0.002	0.002	0.002	0.002	0.002	0.002	0.002	0.002	0.002	0.002	
Fe ³⁺	0.025	0.021	0.026	0.026	0.023	0.027	0.027	0.035	0.026	0.028	0.027	0.027	0.035	0.026	0.029	0.026	0.026	0.029	0.029	0.020	0.029	0.020	0.029	0.020	0.029	0.020	0.029	0.020	
Mg	0.001	0.004	0.005	0.002	0.002	0.002	0.002	0.007	0.002	0.003	0.002	0.002	0.007	0.002	0.003	0.002	0.002	0.002	0.003	0.001	0.001	0.001	0.001	0.003	0.001	0.001	0.001	0.001	
Ca	0.901	0.498	0.563	0.813	0.582	0.535	0.506	0.616	0.607	0.537	0.656	0.607	0.537	0.656	0.484	0.607	0.537	0.656	0.484	0.484	0.484	0.484	0.484	0.484	0.484	0.484	0.484	0.484	
Na	0.106	0.434	0.356	0.184	0.366	0.392	0.425	0.324	0.336	0.407	0.319	0.407	0.319	0.407	0.319	0.407	0.319	0.407	0.319	0.449	0.449	0.449	0.449	0.449	0.449	0.449	0.449	0.449	
K	0.005	0.047	0.032	0.010	0.035	0.038	0.041	0.026	0.029	0.042	0.027	0.041	0.026	0.029	0.042	0.029	0.042	0.027	0.042	0.047	0.047	0.047	0.047	0.047	0.047	0.047	0.047	0.047	
Total	5.02	5.00	4.98	5.01	5.00	4.99	4.99	4.99	4.99	5.01	4.99	4.99	4.99	4.99	5.01	4.99	4.99	5.01	4.99	4.99	4.99	4.99	4.99	5.01	4.99	4.99	4.99		

Analysis ID relates to crystal number_spot number. All Fe assumed to be Fe2O3. Cations calculated on a 8 oxygen basis.

Table A2.3 Major element plagioclase compositions analysed by EMPA.

Sample ID	SM-6C P16_6 zone	SM-6C P16_7 zone	SM-6C P16_8 core	SM-6C P18_1 rim	SM-6C P18_2 sieved	SM-6C P18_3 zone	SM-6C P18_4 sieved	SM-6C P19_2 core	SM-6C P23_1 core	SM-6C P24_1 zone	SM-6C Pp1_1 rim	SM-6C Pp1_2 skeletal	SM-6C Pp1_3 core
SiO ₂	53.16	51.93	54.10	53.04	52.69	52.70	46.91	52.01	50.51	55.88	54.22	45.82	53.99
TiO ₂	0.03	0.01	0.02	0.06	0.07	0.06	0.00	0.10	0.08	0.28	0.07	0.03	0.09
Al ₂ O ₃	28.66	29.71	28.01	28.87	28.47	28.28	33.25	29.50	31.32	25.87	28.37	34.66	28.76
FeO	0.52	0.54	0.60	0.81	0.67	0.77	0.78	0.67	1.05	1.28	0.58	0.75	0.72
Fe ₂ O ₃	0.58	0.60	0.67	0.89	0.75	0.86	0.87	0.75	1.16	1.42	0.64	0.83	0.80
MgO	0.05	0.05	0.07	0.06	0.06	0.06	0.04	0.07	0.08	0.28	0.05	0.02	0.05
CaO	11.35	12.23	10.58	11.32	11.31	11.41	16.88	12.05	14.74	9.48	11.00	17.93	11.48
Na ₂ O	4.37	3.91	4.78	4.45	4.32	4.34	1.93	4.04	3.49	4.91	4.56	1.13	4.38
K ₂ O	0.57	0.48	0.70	0.66	0.63	0.63	0.16	0.54	0.43	1.19	0.67	0.07	0.61
Total	98.77	98.92	98.92	99.35	98.30	98.33	100.03	99.06	101.82	99.31	99.58	100.49	100.16
An	56.92	61.52	52.74	56.17	56.89	57.01	82.08	60.21	68.38	47.95	54.86	89.39	57.02
Ab	39.69	35.61	43.12	39.95	39.34	39.26	16.99	36.57	29.26	44.90	41.14	10.21	39.36
Or	3.40	2.87	4.14	3.88	3.77	3.73	0.94	3.22	2.36	7.14	4.00	0.40	3.61
Cations													
Si	2.440	2.386	2.476	2.427	2.434	2.436	2.165	2.389	2.284	2.553	2.466	2.107	2.446
Al	1.550	1.609	1.511	1.557	1.550	1.541	1.808	1.597	1.669	1.393	1.521	1.878	1.535
Ti	0.001	0.000	0.001	0.002	0.003	0.002	0.000	0.003	0.003	0.010	0.002	0.001	0.003
Fe ³⁺	0.020	0.021	0.023	0.031	0.026	0.030	0.030	0.026	0.040	0.049	0.022	0.029	0.027
Mg	0.002	0.002	0.002	0.002	0.002	0.002	0.001	0.002	0.003	0.009	0.002	0.001	0.002
Ca	0.558	0.602	0.519	0.555	0.560	0.565	0.834	0.593	0.714	0.464	0.536	0.883	0.557
Na	0.389	0.349	0.424	0.395	0.387	0.389	0.173	0.360	0.306	0.435	0.402	0.101	0.385
K	0.033	0.028	0.041	0.038	0.037	0.037	0.010	0.032	0.025	0.069	0.039	0.004	0.035
Total	4.99	5.00	5.00	5.01	5.00	5.00	5.02	5.00	5.04	4.98	4.99	5.00	4.99

Analysis ID relates to crystal number_spot number. All Fe assumed to be Fe2O3. Cations calculated on a 8 oxygen basis.

Table A2.3 Major element plagioclase compositions analysed by EMPA.

Sample ID	SM-6C		SM-6C		SM-6C		SM-6C		SM-6C		SM-6C		SM-6C		SM-6C		SM-6C		SM-6C			
	Pg2	Pg3	Pg4	Pg5	Pg6	Pg9	Pg10	Pg11	Pg12	Pg13	Pg14	Pg15	Pg16	Pg17	core	traverse	traverse	traverse	traverse	traverse	traverse	
SiO ₂	47.90	47.74	48.07	49.14	50.64	48.75	47.97	49.39	48.24	49.32	50.10	52.10	52.74	53.72								
TiO ₂	0.04	0.05	0.05	0.00	0.05	0.14	0.02	0.14	0.01	0.03	0.03	0.07	0.03	0.07								
Al ₂ O ₃	32.55	32.94	32.88	31.62	30.95	32.22	32.26	31.44	32.33	31.69	31.26	30.32	29.82	28.94								
FeO	0.58	0.48	0.62	0.55	0.79	0.57	0.62	0.64	0.66	0.54	0.64	0.61	0.50	0.55								
Fe ₂ O ₃	0.64	0.53	0.69	0.61	0.88	0.63	0.69	0.71	0.74	0.60	0.71	0.68	0.55	0.61								
MgO	0.07	0.04	0.06	0.05	0.08	0.04	0.08	0.10	0.08	0.07	0.11	0.09	0.08	0.12								
CaO	16.85	16.87	17.18	15.77	14.80	16.31	16.64	15.47	16.43	15.77	15.14	14.04	13.50	12.36								
Na ₂ O	2.21	2.17	2.24	2.65	3.19	2.39	2.35	2.77	2.34	2.71	3.08	3.62	4.07	4.67								
K ₂ O	0.13	0.07	0.10	0.15	0.25	0.18	0.11	0.32	0.12	0.21	0.18	0.23	0.25	0.35								
Total	100.39	100.42	101.26	99.99	100.83	100.67	100.11	100.34	100.29	100.42	100.61	101.15	101.06	100.85								
An	80.24	80.78	80.49	76.03	70.91	78.19	79.19	74.11	78.92	75.35	72.33	67.29	63.78	58.24								
Ab	19.04	18.83	18.97	23.09	27.68	20.76	20.21	24.05	20.37	23.44	26.64	31.38	34.81	39.79								
Or	0.72	0.40	0.54	0.88	1.41	1.05	0.60	1.84	0.71	1.22	1.04	1.33	1.40	1.97								
Cations																						
Si	2.199	2.189	2.190	2.256	2.303	2.227	2.208	2.262	2.214	2.256	2.284	2.352	2.379	2.423								
Al	1.761	1.780	1.766	1.711	1.658	1.735	1.750	1.696	1.749	1.708	1.679	1.613	1.585	1.539								
Ti	0.001	0.002	0.002	0.000	0.002	0.005	0.001	0.005	0.001	0.001	0.001	0.002	0.001	0.002								
Fe ³⁺	0.022	0.018	0.024	0.021	0.030	0.022	0.024	0.024	0.025	0.021	0.024	0.023	0.019	0.021								
Mg	0.005	0.003	0.004	0.004	0.006	0.003	0.005	0.007	0.005	0.005	0.008	0.006	0.005	0.008								
Ca	0.829	0.829	0.838	0.776	0.721	0.798	0.821	0.759	0.808	0.773	0.739	0.679	0.652	0.598								
Na	0.197	0.193	0.198	0.236	0.281	0.212	0.209	0.246	0.209	0.240	0.272	0.317	0.356	0.408								
K	0.007	0.004	0.006	0.009	0.014	0.011	0.006	0.019	0.007	0.012	0.011	0.013	0.014	0.020								
Total	5.02	5.02	5.03	5.01	5.01	5.01	5.02	5.02	5.02	5.02	5.02	5.00	5.01	5.02								

Analysis ID relates to crystal number_spot number. All Fe assumed to be Fe2O3. Cations calculated on a 8 oxygen basis.

Table A2.3 Major element plagioclase compositions analysed by EMPA.

Sample ID	SM-6C		SM-6C		SM-6C		SM-6C		SM-6C		SM-6C		SM-6C		SM-6C		SM-6C			
	Pg19	Pg20	Pg21	Pg22	Pg23	Pg24	Pg25	Pg26	Pg27	Pg28	Pg29	Pg30	Pg32	zone	transect	transect	transect	transect	transect	
SiO ₂	53.38	53.62	53.95	52.70	52.75	53.02	52.74	53.39	50.91	50.48	49.74	50.09	50.14							
TiO ₂	0.06	0.05	0.06	0.04	0.09	0.08	0.10	0.08	0.01	0.07	0.01	0.12	0.05							
Al ₂ O ₃	29.14	29.00	28.81	29.42	29.14	29.32	29.33	28.83	30.60	30.98	31.68	31.13	31.86							
FeO	0.69	0.53	0.66	0.56	0.56	0.60	0.62	0.54	0.55	0.68	0.58	0.82	0.58							
Fe ₂ O ₃	0.77	0.59	0.74	0.62	0.63	0.67	0.69	0.60	0.61	0.75	0.64	0.91	0.65							
MgO	0.07	0.10	0.07	0.10	0.07	0.06	0.08	0.09	0.06	0.07	0.09	0.05	0.09							
CaO	12.64	12.44	12.11	12.65	12.60	12.82	12.59	11.65	14.14	14.48	15.31	15.23	14.88							
Na ₂ O	4.49	4.32	4.73	4.33	4.35	4.28	4.34	4.75	3.60	3.44	2.92	3.11	2.83							
K ₂ O	0.36	0.34	0.34	0.37	0.28	0.34	0.35	0.37	0.22	0.21	0.21	0.17	0.16							
Total	100.91	100.47	100.80	100.23	99.91	100.59	100.24	99.77	100.16	100.49	100.60	100.81	100.65							
An	59.67	60.19	57.50	60.45	60.58	61.13	60.33	56.29	67.59	69.08	73.43	72.32	73.70							
Ab	38.33	37.82	40.60	37.43	37.81	36.97	37.65	41.56	31.14	29.70	25.37	26.74	25.37							
Or	2.01	1.99	1.90	2.12	1.61	1.91	2.02	2.15	1.27	1.21	1.20	0.94	0.93							
Cations																				
Si	2.410	2.425	2.434	2.395	2.403	2.401	2.397	2.430	2.324	2.301	2.268	2.282	2.278							
Al	1.551	1.545	1.531	1.575	1.564	1.564	1.571	1.546	1.646	1.665	1.702	1.672	1.706							
Ti	0.002	0.002	0.002	0.001	0.003	0.003	0.003	0.003	0.000	0.003	0.000	0.004	0.002							
Fe ³⁺	0.026	0.020	0.025	0.021	0.021	0.023	0.024	0.021	0.021	0.026	0.022	0.031	0.022							
Mg	0.005	0.007	0.005	0.007	0.005	0.004	0.005	0.006	0.004	0.004	0.006	0.003	0.006							
Ca	0.611	0.603	0.585	0.616	0.615	0.622	0.613	0.568	0.692	0.707	0.748	0.744	0.724							
Na	0.393	0.379	0.413	0.381	0.384	0.376	0.383	0.419	0.319	0.304	0.258	0.275	0.249							
K	0.021	0.020	0.019	0.022	0.016	0.019	0.021	0.022	0.013	0.012	0.012	0.010	0.009							
Total	5.02	5.00	5.02	5.02	5.01	5.01	5.02	5.01	5.02	5.02	5.02	5.02	5.00							

Analysis ID relates to crystal number_spot number. All Fe assumed to be Fe2O3. Cations calculated on a 8 oxygen basis.

Table A2.3 Major element plagioclase compositions analysed by EMPA.

Sample ID	SM-6C		SM-6C		SM-6C		SM-6C		SM-6C		SM-6C		Maketawa		Maketawa		Maketawa		
	Pg33	Pg34	Pg35	Pg36	Pg37	Pg38	Pg39	Pg40	Pg41	P1_1	P1_2	P1_3	P2_1	P1_1	P1_2	P1_3	P2_1	P2_1	
zone	transect	transect	transect	transect	transect	transect	transect	transect	rim	zone	sieved	rim	rim	rim	zone	sieved	rim	rim	
SiO ₂	53.09	54.38	53.48	55.09	53.82	51.50	52.55	55.63	55.38	54.41	50.55	48.47	58.63	54.41	50.55	48.47	58.63	58.63	
TiO ₂	0.09	0.08	0.05	0.06	0.06	0.08	0.11	0.05	0.00	0.03	0.04	0.07	0.05	0.03	0.04	0.07	0.05	0.05	
Al ₂ O ₃	28.26	28.47	28.94	28.50	28.94	30.55	29.53	27.74	27.42	27.87	0.71	0.71	0.50	27.87	0.71	0.71	0.50	0.50	
FeO	0.96	0.68	0.60	0.61	0.59	0.70	0.59	0.72	0.62	0.54	31.24	32.45	26.03	0.54	31.24	32.45	26.03	26.03	
Fe ₂ O ₃	1.06	0.75	0.67	0.68	0.66	0.78	0.66	0.79	0.69	0.60	0.79	0.79	0.56	0.60	0.79	0.79	0.56	0.56	
MgO	0.07	0.05	0.10	0.08	0.09	0.07	0.07	0.06	0.08	0.04	0.05	0.10	0.05	0.04	0.05	0.10	0.05	0.05	
CaO	11.76	11.52	12.42	11.73	12.29	13.78	12.84	10.45	10.62	10.46	14.35	15.91	7.69	10.46	14.35	15.91	7.69	7.69	
Na ₂ O	4.60	5.00	4.43	4.96	4.77	3.71	4.12	5.23	5.27	4.45	3.04	1.93	6.09	4.45	3.04	1.93	6.09	6.09	
K ₂ O	0.35	0.43	0.37	0.40	0.36	0.30	0.32	0.44	0.53	0.55	0.27	0.32	1.02	0.55	0.27	0.32	1.02	1.02	
Total	99.28	100.68	100.46	101.51	100.99	100.78	100.19	100.41	99.99	98.41	69.79	68.31	74.58	98.41	69.79	68.31	74.58	74.58	
An	57.38	54.67	59.52	55.36	57.55	66.05	62.10	51.13	51.10	54.57	71.12	80.38	38.57	54.57	71.12	80.38	38.57	38.57	
Ab	40.60	42.92	38.36	42.38	40.42	32.21	36.07	46.28	45.89	41.99	27.30	17.66	55.32	41.99	27.30	17.66	55.32	55.32	
Or	2.03	2.40	2.12	2.26	2.03	1.74	1.83	2.59	3.02	3.45	1.58	1.95	6.12	3.45	1.58	1.95	6.12	6.12	
Cations																			
Si	2.434	2.454	2.422	2.463	2.425	2.336	2.388	2.506	2.507	2.494	2.304	2.225	2.626	2.494	2.304	2.225	2.626	2.626	
Al	1.527	1.514	1.544	1.502	1.537	1.633	1.582	1.473	1.463	1.506	1.678	1.756	1.374	1.506	1.678	1.756	1.374	1.374	
Ti	0.003	0.003	0.002	0.002	0.002	0.003	0.004	0.002	0.000	0.001	0.001	0.002	0.002	0.001	0.001	0.002	0.002	0.002	
Fe ³⁺	0.037	0.026	0.023	0.023	0.022	0.027	0.023	0.027	0.023	0.021	0.027	0.027	0.019	0.021	0.027	0.027	0.019	0.019	
Mg	0.005	0.003	0.007	0.005	0.006	0.005	0.004	0.004	0.005	0.003	0.003	0.003	0.002	0.003	0.003	0.003	0.002	0.002	
Ca	0.578	0.557	0.603	0.562	0.593	0.670	0.625	0.504	0.515	0.513	0.701	0.783	0.369	0.513	0.701	0.783	0.369	0.369	
Na	0.409	0.437	0.388	0.430	0.417	0.327	0.363	0.456	0.463	0.395	0.269	0.172	0.529	0.395	0.269	0.172	0.529	0.529	
K	0.020	0.024	0.022	0.023	0.021	0.018	0.018	0.026	0.030	0.032	0.016	0.019	0.058	0.032	0.016	0.019	0.058	0.058	
Total	5.01	5.02	5.01	5.01	5.02	5.02	5.01	5.00	5.01	4.97	5.00	4.99	4.98	4.97	5.00	4.99	4.98	4.98	

Analysis ID relates to crystal number_spot number. All Fe assumed to be Fe2O3. Cations calculated on a 8 oxygen basis.

Table A2.3 Major element plagioclase compositions analysed by EMPA.

Sample ID	Maketawa		Maketawa		Maketawa		Maketawa		Maketawa		Maketawa		Maketawa		Maketawa			
	P2_2 zone	P2_3 zone	P2_4 zone	P2_5 core	P3_1 rim	P3_2 zone	P3_3 zone	P3_4 zone	P3_5 core	P4_1 rim	P4_2 zone	P3_2 zone	P3_3 zone	P3_4 zone	P3_5 core	P4_1 rim	P4_2 zone	
SiO ₂	57.02	51.26	53.62	53.26	56.61	54.01	55.26	57.58	55.23	55.73	53.50							
TiO ₂	0.03	0.04	0.02	0.06	0.05	0.06	0.02	0.03	0.05	0.04	0.02							
Al ₂ O ₃	0.55	0.68	0.51	0.57	0.53	0.50	0.56	0.52	0.50	0.55	0.62							
FeO	27.10	31.47	29.21	29.88	27.35	28.66	27.64	26.08	27.63	27.58	29.41							
Fe ₂ O ₃	0.61	0.76	0.57	0.63	0.59	0.56	0.62	0.58	0.55	0.61	0.68							
MgO	0.04	0.04	0.04	0.03	0.03	0.04	0.03	0.04	0.04	0.05	0.05							
CaO	9.06	14.07	11.55	12.31	9.63	11.11	9.88	7.99	9.94	9.67	11.85							
Na ₂ O	5.51	3.22	4.29	4.10	5.11	4.50	5.12	5.84	4.98	5.26	4.09							
K ₂ O	0.79	0.30	0.45	0.45	0.83	0.52	0.70	0.95	0.67	0.68	0.47							
Total	73.62	70.37	71.05	71.43	73.37	71.30	72.19	73.52	71.96	72.60	71.28							
An	45.37	69.48	58.20	60.73	48.46	55.91	49.45	40.58	50.29	48.35	59.83							
Ab	49.93	28.75	39.12	36.61	46.54	40.95	46.38	53.71	45.65	47.57	37.34							
Or	4.69	1.77	2.68	2.65	5.00	3.14	4.17	5.72	4.06	4.08	2.83							
Cations																		
Si	2.562	2.314	2.434	2.402	2.545	2.457	2.513	2.608	2.514	2.523	2.423							
Al	1.435	1.674	1.563	1.588	1.449	1.537	1.481	1.392	1.482	1.472	1.570							
Ti	0.001	0.002	0.001	0.002	0.002	0.002	0.001	0.001	0.002	0.001	0.001							
Fe ³⁺	0.021	0.026	0.019	0.022	0.020	0.019	0.021	0.020	0.019	0.021	0.023							
Mg	0.001	0.001	0.001	0.001	0.001	0.001	0.001	0.001	0.001	0.004	0.004							
Ca	0.436	0.681	0.562	0.595	0.464	0.541	0.481	0.388	0.484	0.469	0.575							
Na	0.480	0.282	0.378	0.359	0.445	0.397	0.451	0.513	0.440	0.461	0.359							
K	0.045	0.017	0.026	0.026	0.048	0.030	0.041	0.055	0.039	0.040	0.027							
Total	4.98	5.00	4.98	4.99	4.97	4.98	4.99	4.98	4.98	4.99	4.98							

Analysis ID relates to crystal number_spot number. All Fe assumed to be Fe₂O₃. Cations calculated on a 8 oxygen basis.

Table A2.3 Major element plagioclase compositions analysed by EMPA.

Sample ID	Maketawa P4_3 zone	Maketawa P4_4 zone	Maketawa P4_5 sieved	Maketawa P4_6 sieved	Maketawa P5_1 rim	Maketawa P5_2 zone	Maketawa P5_3 zone	Maketawa P5_4 core	Maketawa P5_5 zone	Maketawa P5_6 zone	Maketawa P5_7 zone
SiO ₂	53.56	54.65	49.32	54.05	54.85	50.71	54.03	54.44	51.04	54.20	51.82
TiO ₂	0.01	0.03	0.02	0.04	0.04	0.03	0.03	0.03	0.01	0.03	0.03
Al ₂ O ₃	0.62	0.56	0.68	0.48	0.52	0.56	0.52	0.42	0.60	0.51	0.64
FeO	29.28	28.42	32.27	28.75	27.82	30.32	28.23	27.73	30.31	27.59	30.14
Fe ₂ O ₃	0.68	0.62	0.75	0.53	0.58	0.62	0.58	0.47	0.67	0.57	0.71
MgO	0.05	0.07	0.03	0.02	0.06	0.04	0.04	0.03	0.04	0.03	0.04
CaO	11.85	10.79	15.24	11.31	10.25	13.29	10.68	10.21	13.27	10.18	13.04
Na ₂ O	4.16	4.71	2.54	4.44	4.91	3.43	4.63	4.87	3.60	4.90	3.82
K ₂ O	0.44	0.53	0.20	0.54	0.63	0.33	0.57	0.59	0.36	0.64	0.39
Total	71.37	71.95	68.78	71.40	71.83	69.00	71.09	71.07	69.59	71.06	70.50
An	59.56	54.09	75.91	56.62	51.54	66.80	54.10	51.76	65.64	51.39	63.86
Ab	37.82	42.76	22.91	40.19	44.68	31.22	42.44	44.66	32.23	44.74	33.85
Or	2.62	3.15	1.18	3.19	3.78	1.98	3.46	3.57	2.13	3.86	2.30
Cations											
Si	2.428	2.476	2.251	2.454	2.499	2.340	2.473	2.497	2.344	2.495	2.362
Al	1.564	1.517	1.736	1.539	1.494	1.649	1.523	1.499	1.641	1.497	1.619
Ti	0.001	0.001	0.001	0.001	0.001	0.001	0.001	0.001	0.000	0.001	0.001
Fe ³⁺	0.023	0.021	0.026	0.018	0.020	0.021	0.020	0.016	0.023	0.020	0.024
Mg	0.002	0.002	0.001	0.001	0.002	0.001	0.001	0.001	0.001	0.001	0.001
Ca	0.575	0.523	0.745	0.550	0.500	0.657	0.524	0.502	0.653	0.502	0.637
Na	0.365	0.414	0.225	0.391	0.434	0.307	0.411	0.433	0.321	0.437	0.338
K	0.025	0.031	0.012	0.031	0.037	0.019	0.033	0.035	0.021	0.038	0.023
Total	4.98	4.98	5.00	4.99	4.99	5.00	4.99	4.98	5.00	4.99	5.01

Analysis ID relates to crystal number_spot number. All Fe assumed to be Fe2O3. Cations calculated on a 8 oxygen basis.

Table A2.3 Major element plagioclase compositions analysed by EMPA.

Sample ID	Maketawa rim	P6_1	Maketawa zone	P6_2	Maketawa sieved	P6_4	Maketawa sieved	P6_6	Maketawa sieved	P6_9	Maketawa zone	P6_10	Maketawa core	P7_1	Maketawa rim	P7_2	Maketawa zone	P7_3	Maketawa zone	P7_4	Maketawa zone	P7_5	Maketawa zone		
SiO ₂	56.06	50.53	51.49	49.29	51.61	53.06	54.13	51.75	54.15	53.69	51.75	54.15	50.56	53.69	51.75	54.15	50.56	53.69	51.75	54.15	50.56	53.69	51.75	54.15	
TiO ₂	0.06	0.02	0.05	0.05	0.00	0.04	0.02	0.04	0.02	0.04	0.04	0.02	0.04	0.02	0.04	0.04	0.06	0.02	0.04	0.04	0.06	0.02	0.04	0.02	
Al ₂ O ₃	0.54	0.57	0.54	0.64	0.57	0.48	0.57	0.66	0.57	0.48	0.66	0.57	0.77	0.60	0.57	0.66	0.77	0.60	0.66	0.66	0.77	0.60	0.66	0.60	
FeO	27.25	30.82	30.29	31.10	29.69	28.79	27.91	29.42	28.36	28.79	29.42	27.91	30.39	28.37	27.91	29.42	30.39	28.36	28.36	29.42	30.39	28.37	27.91	28.37	
Fe ₂ O ₃	0.60	0.63	0.60	0.72	0.64	0.54	0.63	0.74	0.67	0.54	0.74	0.63	0.85	0.67	0.63	0.74	0.85	0.67	0.67	0.74	0.85	0.67	0.63	0.67	
MgO	0.05	0.05	0.04	0.04	0.04	0.04	0.06	0.06	0.04	0.04	0.06	0.06	0.05	0.04	0.06	0.06	0.05	0.04	0.04	0.06	0.05	0.04	0.06	0.04	
CaO	9.68	13.70	12.91	14.02	12.80	11.59	10.53	12.16	10.90	11.59	12.16	10.53	13.46	10.90	10.53	12.16	13.46	10.90	10.90	12.16	13.46	10.90	10.53	10.90	
Na ₂ O	5.24	3.27	3.69	2.77	3.74	4.36	4.87	3.87	4.79	4.36	3.87	4.87	3.40	4.61	4.87	3.87	3.40	4.79	4.79	3.87	3.40	4.61	4.87	4.61	
K ₂ O	0.77	0.31	0.37	0.26	0.41	0.49	0.61	0.41	0.56	0.41	0.41	0.61	0.34	0.58	0.61	0.41	0.34	0.56	0.56	0.41	0.34	0.58	0.61	0.58	
Total	73.01	69.09	69.70	67.79	69.80	70.61	71.43	69.68	71.74	70.61	69.68	71.43	69.49	71.11	71.43	69.68	69.49	71.74	71.74	69.68	69.49	71.11	71.43	71.11	
An	48.20	68.54	64.44	72.47	63.83	57.74	52.50	61.87	53.88	57.74	61.87	52.50	67.21	54.66	52.50	61.87	67.21	53.88	53.88	61.87	67.21	54.66	52.50	54.66	
Ab	47.22	29.61	33.35	25.92	33.75	39.34	43.89	35.67	42.85	39.34	35.67	43.89	30.76	41.86	43.89	35.67	30.76	42.85	42.85	35.67	30.76	41.86	43.89	41.86	
Or	4.58	1.85	2.22	1.61	2.42	2.92	3.62	2.47	3.28	2.92	2.47	3.62	2.03	3.48	3.62	2.47	2.03	3.28	3.28	2.47	2.03	3.48	3.62	3.48	
Cations																									
Si	2.536	2.321	2.357	2.291	2.375	2.433	2.480	2.390	2.465	2.433	2.390	2.480	2.330	2.459	2.480	2.390	2.330	2.465	2.465	2.390	2.330	2.459	2.480	2.459	
Al	1.453	1.668	1.634	1.704	1.610	1.555	1.507	1.601	1.522	1.555	1.601	1.507	1.651	1.531	1.507	1.601	1.651	1.522	1.522	1.601	1.651	1.531	1.507	1.531	
Ti	0.002	0.001	0.002	0.002	0.000	0.001	0.001	0.001	0.001	0.000	0.001	0.001	0.001	0.001	0.001	0.001	0.001	0.001	0.001	0.001	0.001	0.001	0.001	0.001	0.001
Fe ³⁺	0.021	0.022	0.021	0.025	0.022	0.019	0.022	0.026	0.023	0.022	0.026	0.022	0.030	0.023	0.022	0.026	0.030	0.023	0.023	0.026	0.030	0.023	0.022	0.023	0.023
Mg	0.002	0.002	0.002	0.001	0.001	0.001	0.002	0.002	0.001	0.001	0.001	0.002	0.001	0.001	0.002	0.002	0.001	0.001	0.001	0.001	0.002	0.001	0.001	0.001	0.001
Ca	0.469	0.674	0.633	0.698	0.631	0.570	0.517	0.602	0.532	0.631	0.602	0.517	0.664	0.535	0.517	0.602	0.664	0.532	0.532	0.602	0.664	0.535	0.517	0.535	
Na	0.460	0.291	0.328	0.250	0.334	0.388	0.432	0.347	0.423	0.334	0.388	0.432	0.304	0.410	0.432	0.347	0.304	0.423	0.423	0.347	0.304	0.410	0.432	0.410	
K	0.045	0.018	0.022	0.016	0.024	0.029	0.036	0.024	0.032	0.024	0.029	0.036	0.020	0.034	0.036	0.024	0.020	0.032	0.032	0.024	0.020	0.034	0.036	0.034	
Total	4.99	5.00	5.00	4.99	5.00	5.00	5.00	4.99	5.00	5.00	4.99	5.00	5.00	4.99	5.00	4.99	5.00	5.00	5.00	4.99	5.00	4.99	5.00	4.99	

Analysis ID relates to crystal number_spot number. All Fe assumed to be Fe₂O₃. Cations calculated on a 8 oxygen basis.

Table A2.3 Major element plagioclase compositions analysed by EMPA.

Sample ID	Maketawa	Maketawa	Maketawa	Maketawa	Maketawa	Maketawa	Maketawa	Maketawa	Maketawa	Maketawa	Maketawa	Maketawa	Maketawa
zone	P7_6	P8_1	P8_2	P8_3	P8_4	P8_5	P8_6	P8_7	P9_2	P9_3	P10_1	core	rim
SiO ₂	50.25	54.68	53.09	57.42	54.53	50.93	48.11	56.10	49.45	45.87	54.49		
TiO ₂	0.05	0.06	0.01	0.03	0.02	0.04	0.02	0.00	0.03	0.03	0.02		
Al ₂ O ₃	0.65	0.59	0.57	0.39	0.41	0.49	0.52	0.34	0.62	0.67	0.59		
FeO	30.73	28.27	29.61	26.29	28.04	30.68	33.06	27.27	30.87	33.29	28.04		
Fe ₂ O ₃	0.72	0.65	0.63	0.43	0.46	0.54	0.58	0.38	0.69	0.74	0.66		
MgO	0.03	0.04	0.06	0.03	0.01	0.02	0.03	0.01	0.03	0.03	0.05		
CaO	13.48	10.71	12.48	8.39	10.46	13.32	15.99	9.24	14.24	16.89	10.49		
Na ₂ O	3.32	4.72	4.22	5.69	4.85	3.48	2.28	5.32	3.24	1.80	4.73		
K ₂ O	0.31	0.62	0.53	0.89	0.62	0.33	0.15	0.70	0.30	0.14	0.60		
Total	68.80	72.07	71.59	73.26	71.35	69.16	67.66	72.08	68.60	66.18	71.63		
An	67.88	53.59	60.12	42.49	52.35	66.57	78.84	46.92	69.60	83.16	53.06		
Ab	30.25	42.73	36.83	52.16	43.96	31.47	20.30	48.86	28.63	15.99	43.32		
Or	1.87	3.68	3.06	5.35	3.70	1.96	0.86	4.22	1.77	0.85	3.62		
Cations													
Si	2.319	2.480	2.401	2.598	2.488	2.335	2.204	2.547	2.291	2.144	2.486		
Al	1.672	1.511	1.578	1.402	1.508	1.658	1.785	1.459	1.685	1.834	1.508		
Ti	0.002	0.002	0.000	0.001	0.001	0.001	0.001	0.000	0.001	0.001	0.001		
Fe ³⁺	0.025	0.022	0.021	0.015	0.016	0.019	0.020	0.013	0.024	0.026	0.023		
Mg	0.001	0.001	0.002	0.001	0.000	0.001	0.001	0.001	0.001	0.001	0.002		
Ca	0.667	0.520	0.605	0.407	0.511	0.654	0.785	0.449	0.707	0.846	0.513		
Na	0.297	0.415	0.370	0.499	0.429	0.309	0.202	0.468	0.291	0.163	0.419		
K	0.018	0.036	0.031	0.051	0.036	0.019	0.009	0.040	0.018	0.009	0.035		
Total	5.00	4.99	5.01	4.97	4.99	5.00	5.01	4.98	5.02	5.02	4.98		

Analysis ID relates to crystal number_spot number. All Fe assumed to be Fe2O3. Cations calculated on a 8 oxygen basis.

Table A2.3 Major element plagioclase compositions analysed by EMPA.

Sample ID	Maketawa P10_3		Maketawa P10_4		Maketawa P10_5		Maketawa P10_6		Maketawa P16_1		Maketawa P16_2		Maketawa P16_3		Maketawa P16_4		Maketawa P16_5		Maketawa P16_6		Maketawa P16_7	
	zone	core	zone	core	sieved	core	sieved	core	rim	zone	core	zone	core	zone	core	zone	core	rim	core	rim	core	core
SiO ₂	54.80		50.21		54.67		47.55		58.38		51.82		56.08		53.46		56.15		55.56		54.89	
TiO ₂	0.02		0.00		0.00		0.05		0.12		0.05		0.00		0.02		0.05		0.00		0.07	
Al ₂ O ₃	0.47		0.72		0.47		0.65		0.74		0.67		0.46		0.47		0.43		0.52		0.60	
FeO	28.19		31.13		28.22		32.97		27.25		30.01		27.58		29.03		27.41		28.16		28.24	
Fe ₂ O ₃	0.52		0.80		0.52		0.72		0.82		0.74		0.51		0.52		0.48		0.58		0.66	
MgO	0.04		0.04		0.03		0.04		0.06		0.04		0.05		0.04		0.03		0.04		0.04	
CaO	10.56		14.18		10.55		16.10		9.83		12.81		9.76		11.80		9.71		10.43		10.59	
Na ₂ O	4.85		3.11		4.84		2.04		4.99		3.65		5.25		4.29		5.18		4.89		4.82	
K ₂ O	0.60		0.30		0.60		0.16		1.15		0.36		0.66		0.48		0.73		0.64		0.61	
Total	71.85		69.36		71.68		67.30		76.10		70.13		72.79		71.07		72.76		72.67		72.28	
An	52.66		70.30		52.68		80.57		48.57		64.53		48.67		58.60		48.69		52.05		52.85	
Ab	43.77		27.94		43.76		18.48		44.65		33.33		47.38		38.54		46.97		44.14		43.52	
Or	3.56		1.76		3.55		0.95		6.77		2.14		3.95		2.86		4.34		3.82		3.63	
Cations																						
Si	2.487		2.302		2.484		2.194		2.567		2.371		2.530		2.432		2.536		2.501		2.484	
Al	1.508		1.682		1.511		1.793		1.412		1.618		1.466		1.557		1.459		1.494		1.506	
Ti	0.001		0.000		0.000		0.002		0.004		0.002		0.000		0.001		0.002		0.000		0.002	
Fe ³⁺	0.018		0.028		0.018		0.025		0.027		0.025		0.017		0.018		0.016		0.020		0.023	
Mg	0.001		0.001		0.001		0.001		0.004		0.002		0.002		0.001		0.001		0.001		0.001	
Ca	0.513		0.696		0.514		0.796		0.463		0.628		0.472		0.575		0.470		0.503		0.513	
Na	0.427		0.277		0.427		0.183		0.426		0.324		0.459		0.378		0.453		0.427		0.423	
K	0.035		0.017		0.035		0.009		0.065		0.021		0.038		0.028		0.042		0.037		0.035	
Total	4.99		5.00		4.99		5.00		4.97		4.99		4.98		4.99		4.98		4.98		4.99	

Analysis ID relates to crystal number_spot number. All Fe assumed to be Fe2O3. Cations calculated on a 8 oxygen basis.

Table A2.3 Major element plagioclase compositions analysed by EMPA.

Sample ID	Maketawa rim	P16_8	Maketawa core	P16_9	Maketawa rim	P17_1	Maketawa sieved	P17_3	Maketawa zone	P17_5	Maketawa core	P17_6	Maketawa rim	P21_1	Maketawa zone	P21_2	Maketawa zone	P21_3	Maketawa sieved	P21_6	Maketawa sieved	P21_7
SiO ₂	54.92	47.97	55.04	50.22	56.61	53.03	52.35	54.88	54.84	49.27	56.18											
TiO ₂	0.03	0.00	0.04	0.00	0.04	0.04	0.04	0.01	0.03	0.01	0.03											
Al ₂ O ₃	0.57	0.49	0.59	0.55	0.55	0.59	0.55	0.46	0.54	0.47	0.44											
FeO	28.45	33.05	27.79	31.35	27.04	29.41	28.58	27.67	27.42	31.79	26.72											
Fe ₂ O ₃	0.63	0.55	0.65	0.61	0.61	0.66	0.61	0.51	0.59	0.52	0.49											
MgO	0.04	0.02	0.04	0.06	0.05	0.04	0.08	0.04	0.05	0.04	0.04											
CaO	10.75	15.99	10.28	14.40	9.09	12.01	11.63	10.25	9.73	15.04	9.08											
Na ₂ O	4.87	2.18	4.86	2.92	5.40	4.13	4.36	4.96	5.09	2.89	5.51											
K ₂ O	0.63	0.18	0.68	0.28	0.83	0.42	0.49	0.63	0.69	0.23	0.80											
Total	72.43	67.38	72.18	69.03	73.18	70.91	70.11	71.73	71.55	68.46	72.56											
An	52.94	79.39	51.71	71.97	45.78	60.06	57.86	51.32	49.25	73.21	45.39											
Ab	43.37	19.56	44.24	26.38	49.25	37.41	39.26	44.91	46.60	25.47	49.87											
Or	3.68	1.04	4.06	1.65	4.97	2.53	2.87	3.77	4.15	1.32	4.74											
Cations																						
Si	2.477	2.203	2.502	2.298	2.557	2.413	2.423	2.504	2.514	2.262	2.559											
Al	1.512	1.789	1.489	1.691	1.439	1.577	1.559	1.488	1.482	1.720	1.434											
Ti	0.001	0.000	0.001	0.000	0.001	0.001	0.001	0.000	0.001	0.000	0.001											
Fe ³⁺	0.021	0.019	0.022	0.021	0.021	0.022	0.021	0.018	0.021	0.018	0.017											
Mg	0.001	0.001	0.001	0.002	0.002	0.001	0.003	0.002	0.002	0.001	0.001											
Ca	0.520	0.787	0.501	0.706	0.440	0.585	0.577	0.501	0.478	0.740	0.443											
Na	0.426	0.194	0.428	0.259	0.473	0.365	0.391	0.438	0.452	0.257	0.487											
K	0.036	0.010	0.039	0.016	0.048	0.025	0.029	0.037	0.040	0.013	0.046											
Total	4.99	5.00	4.98	4.99	4.98	4.99	5.00	4.99	4.99	5.01	4.99											

Analysis ID relates to crystal number_spot number. All Fe assumed to be Fe2O3. Cations calculated on a 8 oxygen basis.

Table A2.3 Major element plagioclase compositions analysed by EMPA.

Sample ID	Maketawa		Maketawa		Maketawa		Maketawa		Maketawa		Maketawa		Ingleswood b		Ingleswood b	
	P30_1 sieved	P31_1 zone	PD_24core core	PD_24rim rim	PJ_6 rim	PJ_7 zone	PJ_8 sieved	P1_1 rim	P1_2 zone	P1_3 zone	PJ_6 rim	PJ_7 zone	PJ_8 sieved	P1_1 rim	P1_2 zone	P1_3 zone
SiO ₂	50.42	54.59	55.72	53.46	55.22	50.55	55.90	59.88	57.67	55.96						
TiO ₂	0.06	0.05	0.04	0.11	0.08	0.04	0.04	0.06	0.06	0.06						
Al ₂ O ₃	0.86	0.66	0.54	0.61	0.51	0.55	0.46	25.96	26.04	27.97						
FeO	29.43	28.37	28.06	28.84	27.85	29.80	28.13	0.64	0.43	0.36						
Fe ₂ O ₃	0.96	0.73	0.60	0.68	0.57	0.61	0.51	0.71	0.48	0.39						
MgO	0.08	0.06	0.06	0.06	0.08	0.05	0.06	0.04	0.02	0.02						
CaO	12.76	10.58	11.56	12.52	10.91	14.38	12.12	8.42	8.00	10.11						
Na ₂ O	3.56	4.70	4.91	4.24	5.23	3.42	4.87	5.25	5.95	5.15						
K ₂ O	0.44	0.60	0.35	0.23	0.39	0.18	0.33	1.89	0.85	0.59						
Total	69.15	71.97	73.80	71.90	72.99	69.79	74.30	102.21	99.06	100.26						
An	64.68	53.45	55.39	61.19	52.34	69.18	56.82	41.77	40.46	50.22						
Ab	32.65	42.94	42.59	37.47	45.45	29.79	41.35	47.10	54.45	46.30						
Or	2.68	3.62	2.02	1.34	2.21	1.02	1.83	11.13	5.09	3.48						
Cations																
Si	2.356	2.477	2.490	2.426	2.491	2.334	2.485	2.637	2.611	2.515						
Al	1.621	1.517	1.478	1.542	1.481	1.622	1.473	1.348	1.389	1.481						
Ti	0.002	0.002	0.002	0.004	0.003	0.002	0.001	0.002	0.002	0.002						
Fe ³⁺	0.034	0.025	0.020	0.023	0.019	0.021	0.017	0.023	0.016	0.013						
Mg	0.003	0.002	0.004	0.004	0.005	0.004	0.004	0.001	0.001	0.001						
Ca	0.639	0.514	0.553	0.608	0.527	0.711	0.577	0.397	0.388	0.487						
Na	0.323	0.413	0.426	0.373	0.458	0.306	0.420	0.448	0.522	0.449						
K	0.026	0.035	0.020	0.013	0.022	0.011	0.019	0.106	0.049	0.034						
Total	5.00	4.98	4.99	4.99	5.01	5.01	5.00	4.96	4.98	4.98						

Analysis ID relates to crystal number_spot number. All Fe assumed to be Fe2O3. Cations calculated on a 8 oxygen basis.

Table A2.3 Major element plagioclase compositions analysed by EMPA.

Sample ID	Inglewood b		Inglewood b		Inglewood b		Inglewood b		Inglewood b		Inglewood b		Inglewood b	
	P1_4 zone	P1_7 core	P3_1 rim	P3_2 zone	P3_4 zone	P3_5 zone	P3_6 zone	P3_7 zone	P3_8 zone	P3_9 core				
SiO ₂	57.42	50.93	57.55	54.40	54.57	56.82	55.01	56.43	57.45	54.85				
TiO ₂	0.04	0.00	0.05	0.01	0.00	0.02	0.05	0.05	0.00	0.05				
Al ₂ O ₃	26.59	31.01	26.48	29.00	28.44	27.23	28.58	27.14	26.62	27.93				
FeO	0.44	0.64	0.63	0.50	0.46	0.48	0.50	0.43	0.43	0.50				
Fe ₂ O ₃	0.49	0.71	0.70	0.55	0.51	0.53	0.55	0.48	0.47	0.55				
MgO	0.03	0.03	0.02	0.03	0.04	0.02	0.03	0.03	0.03	0.03				
CaO	8.47	13.69	8.33	11.07	10.66	8.89	10.62	8.97	8.41	10.01				
Na ₂ O	5.81	3.43	5.89	4.67	4.76	5.47	4.84	5.45	5.69	4.83				
K ₂ O	0.79	0.28	0.82	0.52	0.51	0.70	0.48	0.70	0.80	0.55				
Total	99.64	100.06	99.83	100.24	99.50	99.68	100.17	99.25	99.48	98.79				
An	42.53	67.69	41.74	54.97	53.61	45.34	53.22	45.60	42.78	51.60				
Ab	52.74	30.68	53.39	41.95	43.34	50.44	43.91	50.14	52.39	45.04				
Or	4.72	1.63	4.87	3.08	3.05	4.22	2.87	4.26	4.83	3.36				
Cations														
Si	2.588	2.323	2.591	2.455	2.477	2.561	2.480	2.556	2.591	2.502				
Al	1.412	1.667	1.405	1.542	1.522	1.446	1.519	1.448	1.415	1.502				
Ti	0.001	0.000	0.002	0.000	0.000	0.001	0.002	0.002	0.000	0.002				
Fe ³⁺	0.016	0.024	0.024	0.019	0.017	0.018	0.019	0.016	0.016	0.019				
Mg	0.001	0.001	0.001	0.002	0.001	0.001	0.001	0.001	0.001	0.001				
Ca	0.409	0.669	0.402	0.535	0.519	0.429	0.513	0.435	0.406	0.489				
Na	0.507	0.303	0.514	0.408	0.419	0.478	0.423	0.478	0.498	0.427				
K	0.045	0.016	0.047	0.030	0.030	0.040	0.028	0.041	0.046	0.032				
Total	4.98	5.00	4.99	4.99	4.99	4.97	4.98	4.98	4.97	4.97				

Analysis ID relates to crystal number_spot number. All Fe assumed to be Fe₂O₃. Cations calculated on a 8 oxygen basis.

Table A2.3 Major element plagioclase compositions analysed by EMPA.

Sample ID	Inglewood b P3_10 zone	Inglewood b P4_1 rim	Inglewood b P4_2 zone	Inglewood b P4_3 zone	Inglewood b P4_4 zone	Inglewood b P4_5 sieved	Inglewood b P4_7 sieved	Inglewood b P4_9 zone	Inglewood b P4_12 core	Inglewood b P5_1 rim
SiO ₂	50.87	55.88	52.85	56.76	54.32	47.37	55.66	50.24	46.76	52.53
TiO ₂	0.03	0.02	0.02	0.03	0.01	0.01	0.02	0.01	0.00	0.03
Al ₂ O ₃	31.02	27.73	30.43	27.50	29.06	33.56	27.79	31.56	34.11	29.33
FeO	0.68	0.40	0.53	0.43	0.45	0.59	0.45	0.66	0.56	0.69
Fe ₂ O ₃	0.75	0.44	0.59	0.47	0.50	0.65	0.50	0.73	0.63	0.76
MgO	0.02	0.01	0.03	0.02	0.02	0.03	0.04	0.03	0.00	0.07
CaO	13.45	9.26	12.21	8.93	10.79	15.78	9.93	14.12	17.20	11.95
Na ₂ O	3.34	5.38	4.17	5.62	4.74	2.00	5.20	3.11	1.67	4.10
K ₂ O	0.28	0.72	0.37	0.77	0.52	0.15	0.66	0.27	0.09	0.36
Total	99.77	99.44	100.65	100.11	99.94	99.56	99.79	100.07	100.46	99.15
An	67.84	46.65	60.45	44.58	54.00	80.57	49.35	70.36	84.60	60.34
Ab	30.46	49.05	37.37	50.84	42.92	18.51	46.72	28.01	14.85	37.48
Or	1.69	4.31	2.19	4.58	3.08	0.92	3.93	1.63	0.56	2.18
Cations										
Si	2.325	2.529	2.384	2.550	2.456	2.184	2.516	2.294	2.145	2.406
Al	1.671	1.479	1.617	1.456	1.549	1.823	1.480	1.699	1.844	1.583
Ti	0.001	0.001	0.001	0.001	0.000	0.000	0.001	0.000	0.000	0.001
Fe³⁺	0.026	0.015	0.020	0.016	0.017	0.023	0.017	0.025	0.022	0.026
Mg	0.001	0.001	0.002	0.001	0.001	0.001	0.001	0.001	0.000	0.002
Ca	0.659	0.449	0.590	0.430	0.523	0.779	0.481	0.691	0.845	0.587
Na	0.296	0.472	0.365	0.490	0.415	0.179	0.455	0.275	0.148	0.364
K	0.016	0.041	0.021	0.044	0.030	0.009	0.038	0.016	0.006	0.021
Total	4.99	4.99	5.00	4.99	4.99	5.00	4.99	5.00	5.01	4.99

Analysis ID relates to crystal number_spot number. All Fe assumed to be Fe2O3. Cations calculated on a 8 oxygen basis.

Table A2.3 Major element plagioclase compositions analysed by EMPA.

Sample ID	Inglewood b		Inglewood b		Inglewood b		Inglewood b		Inglewood b		Inglewood b		Inglewood b	
	P5_2 zone	P5_4 sieved	P5_10 zone	P5_12 core	P8_3 zone	P9_1 rim	P9_2 zone	P9_4 core	P10_2 zone	P10_3 zone	P5_2 zone	P5_4 sieved	P5_10 zone	P5_12 core
SiO ₂	51.44	51.97	52.90	56.41	50.86	57.58	53.29	57.56	51.25	56.73				
TiO ₂	0.04	0.04	0.08	0.04	0.03	0.01	0.00	0.04	0.01	0.02				
Al ₂ O ₃	30.49	30.61	29.29	26.70	30.79	27.37	30.55	26.98	30.11	26.71				
FeO	0.62	0.71	0.57	0.42	0.61	0.10	0.53	0.45	0.45	0.47				
Fe ₂ O ₃	0.69	0.79	0.64	0.47	0.68	0.11	0.59	0.50	0.50	0.52				
MgO	0.05	0.07	0.02	0.00	0.05	0.03	0.02	0.04	0.01	0.02				
CaO	13.10	13.69	11.74	8.56	13.22	8.69	12.06	8.59	12.33	8.67				
Na ₂ O	3.59	3.64	4.25	5.63	3.69	5.82	4.32	5.92	3.51	5.44				
K ₂ O	0.27	0.42	0.40	0.76	0.33	0.79	0.38	0.79	0.30	0.74				
Total	99.68	101.24	99.31	98.57	99.64	100.40	101.21	100.42	98.02	98.85				
An	65.72	65.87	58.98	43.57	65.12	43.08	59.28	42.44	64.78	44.67				
Ab	32.64	31.72	38.64	51.83	32.91	52.26	38.47	52.93	33.37	50.77				
Or	1.64	2.42	2.38	4.60	1.96	4.67	2.25	4.63	1.85	4.56				
Cations														
Si	2.350	2.345	2.416	2.571	2.329	2.571	2.389	2.576	2.370	2.576				
Al	1.641	1.628	1.576	1.434	1.661	1.440	1.615	1.423	1.641	1.429				
Ti	0.001	0.001	0.003	0.001	0.001	0.000	0.000	0.001	0.000	0.001				
Fe ³⁺	0.024	0.027	0.022	0.016	0.023	0.004	0.020	0.017	0.017	0.018				
Mg	0.002	0.002	0.001	0.000	0.002	0.001	0.001	0.001	0.001	0.001				
Ca	0.641	0.662	0.575	0.418	0.649	0.416	0.579	0.412	0.611	0.422				
Na	0.318	0.319	0.377	0.497	0.328	0.504	0.376	0.514	0.315	0.479				
K	0.016	0.024	0.023	0.044	0.020	0.045	0.022	0.045	0.017	0.043				
Total	4.99	5.01	4.99	4.98	5.01	4.98	5.00	4.99	4.97	4.97				

Analysis ID relates to crystal number_spot number. All Fe assumed to be Fe2O3. Cations calculated on a 8 oxygen basis.

Table A2.3 Major element plagioclase compositions analysed by EMPA.

Sample ID	Inglewood b		Inglewood b		Inglewood b		Inglewood b		Inglewood b		Inglewood b		Inglewood b			
	P10_4	P10_5	P10_6	P10_7	P10_9	P10_1	P10_11	P10_12	P11_1	P11_3	zone	rim	core	rim	zone	
SiO ₂	51.36	56.74	53.04	57.89	51.36	57.26	57.60	52.92	57.83	54.86						
TiO ₂	0.02	0.00	0.03	0.04	0.03	0.04	0.00	0.02	0.02	0.00						
Al ₂ O ₃	30.92	26.85	29.61	26.31	31.22	26.76	26.75	30.17	27.03	29.95						
FeO	0.47	0.36	0.51	0.36	0.48	0.43	0.42	0.63	0.41	0.52						
Fe ₂ O ₃	0.52	0.40	0.57	0.40	0.53	0.47	0.47	0.70	0.45	0.57						
MgO	0.03	0.03	0.03	0.03	0.01	0.02	0.01	0.04	0.02	0.01						
CaO	13.40	8.88	11.76	7.80	13.49	8.67	8.18	12.36	8.69	12.25						
Na ₂ O	3.45	5.44	4.00	5.81	3.37	5.70	5.67	3.98	5.86	4.71						
K ₂ O	0.32	0.73	0.40	0.79	0.30	0.81	0.83	0.35	0.71	0.47						
Total	100.03	99.07	99.44	99.08	100.31	99.72	99.51	100.54	100.61	102.82						
An	66.91	45.32	60.36	40.49	67.64	43.48	42.11	61.88	43.17	57.42						
Ab	31.19	50.22	37.18	54.61	30.55	51.71	52.78	36.04	52.65	39.98						
Or	1.90	4.46	2.46	4.90	1.81	4.81	5.11	2.08	4.18	2.60						
Cations																
Si	2.338	2.571	2.415	2.614	2.331	2.579	2.594	2.390	2.581	2.424						
Al	1.659	1.434	1.589	1.400	1.670	1.421	1.420	1.606	1.421	1.559						
Ti	0.001	0.000	0.001	0.001	0.001	0.001	0.000	0.001	0.001	0.000						
Fe ³⁺	0.018	0.014	0.019	0.014	0.018	0.016	0.016	0.024	0.015	0.019						
Mg	0.001	0.001	0.001	0.001	0.000	0.001	0.000	0.001	0.001	0.000						
Ca	0.653	0.431	0.574	0.377	0.656	0.418	0.395	0.598	0.415	0.580						
Na	0.304	0.478	0.353	0.509	0.296	0.497	0.495	0.348	0.507	0.404						
K	0.019	0.042	0.023	0.046	0.018	0.046	0.048	0.020	0.040	0.026						
Total	4.99	4.97	4.98	4.96	4.99	4.98	4.97	4.99	4.98	5.01						

Analysis ID relates to crystal number_spot number. All Fe assumed to be Fe2O3. Cations calculated on a 8 oxygen basis.

Table A2.3 Major element plagioclase compositions analysed by EMPA.

Sample ID	Inglewood b P11_4 zone	Inglewood b P11_5 zone	Inglewood b P11_6 zone	Inglewood b P11_7 core	Inglewood b P13_1 rim	Inglewood b P13_2 sieved	Inglewood b P13_3 sieved	Inglewood b P13_4 zone	Inglewood b P13_5 core	Inglewood b P13_10 zone
SiO ₂	57.63	57.94	57.71	54.59	57.44	53.39	57.45	51.59	46.61	58.71
TiO ₂	0.06	0.01	0.03	0.01	0.02	0.01	0.03	0.00	0.00	0.01
Al ₂ O ₃	27.23	27.24	26.90	29.25	27.70	30.03	27.12	31.27	34.86	26.91
FeO	0.49	0.44	0.46	0.51	0.42	0.58	0.40	0.58	0.63	0.43
Fe ₂ O ₃	0.54	0.48	0.51	0.56	0.47	0.64	0.44	0.64	0.70	0.47
MgO	0.03	0.03	0.05	0.02	0.02	0.02	0.03	0.03	0.01	0.02
CaO	8.97	9.08	8.66	11.41	8.84	12.05	8.96	13.41	17.71	8.59
Na ₂ O	5.90	5.99	5.97	4.79	5.34	4.04	5.47	3.44	1.42	5.82
K ₂ O	0.73	0.78	0.77	0.51	0.66	0.36	0.69	0.28	0.08	0.83
Total	101.08	101.56	100.60	101.15	100.49	100.53	100.20	100.65	101.38	101.35
An	43.74	43.53	42.46	55.14	45.81	60.89	45.50	67.19	86.94	42.71
Ab	52.03	52.02	53.02	41.92	50.09	36.94	50.30	31.16	12.60	52.39
Or	4.24	4.45	4.52	2.94	4.09	2.17	4.20	1.65	0.46	4.90
Cations										
Si	2.565	2.568	2.579	2.446	2.562	2.407	2.573	2.334	2.121	2.598
Al	1.429	1.423	1.417	1.544	1.456	1.596	1.431	1.667	1.870	1.403
Ti	0.002	0.000	0.001	0.000	0.001	0.000	0.001	0.000	0.000	0.000
Fe ³⁺	0.018	0.016	0.017	0.019	0.016	0.022	0.015	0.022	0.024	0.016
Mg	0.001	0.001	0.002	0.001	0.001	0.001	0.001	0.001	0.000	0.001
Ca	0.428	0.431	0.415	0.548	0.422	0.582	0.430	0.650	0.863	0.407
Na	0.509	0.515	0.518	0.416	0.462	0.353	0.475	0.301	0.125	0.499
K	0.041	0.044	0.044	0.029	0.038	0.021	0.040	0.016	0.005	0.047
Total	4.99	5.00	4.99	5.00	4.96	4.98	4.97	4.99	5.01	4.97

Analysis ID relates to crystal number_spot number. All Fe assumed to be Fe2O3. Cations calculated on a 8 oxygen basis.

Table A2.3 Major element plagioclase compositions analysed by EMPA.

Sample ID	Inglewood b		Inglewood b		Inglewood b		Inglewood b		Inglewood b		Inglewood b		Inglewood b	
	P13_11	P13_12	P14_2	P14_3	P14_4	P14_5	P14_6	P14_7	P14_8	P14_10	zone	core	zone	zone
SiO ₂	54.59	56.62	57.43	54.60	57.12	55.78	57.10	54.48	50.00		54.48	50.00	54.48	56.08
TiO ₂	0.03	0.05	0.04	0.00	0.01	0.00	0.04	0.02	0.04		0.02	0.04	0.02	0.00
Al ₂ O ₃	29.12	27.96	26.88	28.39	26.82	27.72	26.79	29.23	31.61		29.23	31.61	29.23	27.67
FeO	0.66	0.47	0.35	0.54	0.35	0.52	0.43	0.49	0.61		0.49	0.61	0.49	0.43
Fe ₂ O ₃	0.73	0.53	0.39	0.60	0.38	0.57	0.48	0.54	0.67		0.54	0.67	0.54	0.48
MgO	0.02	0.01	0.02	0.04	0.03	0.01	0.03	0.04	0.03		0.04	0.03	0.04	0.03
CaO	10.72	9.36	8.85	10.76	8.81	9.83	8.66	11.50	14.41		11.50	14.41	11.50	9.88
Na ₂ O	4.49	5.16	5.63	4.54	5.47	5.12	5.54	4.56	2.90		4.56	2.90	4.56	5.03
K ₂ O	0.48	0.64	0.78	0.50	0.78	0.64	0.77	0.50	0.21		0.50	0.21	0.50	0.63
Total	100.17	100.33	100.03	99.44	99.42	99.68	99.42	100.87	99.88		100.87	99.88	100.87	99.82
An	55.23	48.09	44.33	54.99	44.88	49.55	44.18	56.49	72.36		56.49	72.36	56.49	50.06
Ab	41.83	48.00	51.04	41.98	50.39	46.64	51.13	40.56	26.38		40.56	26.38	40.56	46.15
Or	2.95	3.91	4.63	3.04	4.72	3.81	4.69	2.95	1.26		2.95	1.26	2.95	3.80
Cations														
Si	2.462	2.536	2.578	2.479	2.578	2.522	2.578	2.446	2.287		2.446	2.287	2.446	2.530
Al	1.547	1.476	1.422	1.519	1.427	1.477	1.426	1.547	1.704		1.547	1.704	1.547	1.471
Ti	0.001	0.002	0.001	0.000	0.001	0.000	0.001	0.001	0.001		0.001	0.001	0.001	0.000
Fe ³⁺	0.025	0.018	0.013	0.020	0.013	0.020	0.016	0.018	0.023		0.018	0.023	0.018	0.016
Mg	0.001	0.000	0.002	0.003	0.001	0.000	0.001	0.001	0.001		0.001	0.001	0.001	0.001
Ca	0.518	0.449	0.426	0.524	0.426	0.476	0.419	0.553	0.706		0.553	0.706	0.553	0.478
Na	0.392	0.448	0.490	0.400	0.478	0.448	0.485	0.397	0.257		0.397	0.257	0.397	0.440
K	0.028	0.036	0.044	0.029	0.045	0.037	0.045	0.029	0.012		0.029	0.012	0.029	0.036
Total	4.97	4.97	4.98	4.97	4.97	4.98	4.97	4.99	4.99		4.99	4.99	4.99	4.97

Analysis ID relates to crystal number_spot number. All Fe assumed to be Fe2O3. Cations calculated on a 8 oxygen basis.

Table A2.3 Major element plagioclase compositions analysed by EMPA.

Sample ID	Inglewood b		Inglewood b		Inglewood b		Inglewood b		Inglewood b		Inglewood b		Inglewood b			
	P14_11	P15_1	P15_2	P15_5	P15_6	P15_7	P15_8	P15_9	P16_1	P16_2	zone	rim	core	rim	zone	
SiO ₂	56.97	57.57	56.79	52.26	47.90	56.68	54.57	53.97	56.49	52.00						52.00
TiO ₂	0.03	0.04	0.01	0.00	0.00	0.02	0.03	0.04	0.01	0.02						0.02
Al ₂ O ₃	27.25	26.03	26.70	30.15	33.05	26.97	28.35	28.32	27.79	31.04						31.04
FeO	0.43	0.44	0.44	0.51	0.74	0.45	0.69	0.78	0.49	0.60						0.60
Fe ₂ O ₃	0.48	0.49	0.48	0.56	0.83	0.50	0.77	0.86	0.54	0.66						0.66
MgO	0.02	0.03	0.03	0.03	0.04	0.02	0.05	0.06	0.03	0.07						0.07
CaO	9.07	7.95	8.75	12.70	16.22	8.85	10.91	10.87	9.48	13.49						13.49
Na ₂ O	5.38	6.03	5.68	3.92	2.09	5.70	4.69	4.65	5.45	3.61						3.61
K ₂ O	0.71	0.87	0.77	0.31	0.13	0.79	0.48	0.50	0.58	0.26						0.26
Total	99.92	99.00	99.22	99.94	100.27	99.54	99.86	99.26	100.37	101.16						101.16
An	46.15	39.98	43.87	63.00	80.42	43.99	54.63	54.68	47.29	66.35						66.35
Ab	49.55	54.83	51.52	35.15	18.79	51.30	42.52	42.30	49.25	32.12						32.12
Or	4.31	5.18	4.62	1.85	0.79	4.70	2.85	3.01	3.47	1.53						1.53
Cations																
Si	2.561	2.609	2.573	2.377	2.197	2.562	2.473	2.463	2.534	2.342						2.342
Al	1.444	1.390	1.425	1.616	1.787	1.437	1.514	1.523	1.469	1.647						1.647
Ti	0.001	0.001	0.000	0.000	0.000	0.001	0.001	0.001	0.000	0.001						0.001
Fe ³⁺	0.016	0.017	0.017	0.019	0.029	0.017	0.026	0.030	0.018	0.023						0.023
Mg	0.001	0.002	0.002	0.001	0.001	0.001	0.002	0.002	0.001	0.003						0.003
Ca	0.437	0.386	0.425	0.619	0.797	0.429	0.530	0.531	0.455	0.651						0.651
Na	0.469	0.529	0.499	0.345	0.186	0.500	0.412	0.411	0.474	0.315						0.315
K	0.041	0.050	0.045	0.018	0.008	0.046	0.028	0.029	0.033	0.015						0.015
Total	4.97	4.98	4.98	5.00	5.01	4.99	4.99	4.99	4.98	5.00						5.00

Analysis ID relates to crystal number_spot number. All Fe assumed to be Fe2O3. Cations calculated on a 8 oxygen basis.

Table A2.3 Major element plagioclase compositions analysed by EMPA.

Sample ID	Inglewood b P16_4 zone	Inglewood b P16_5 core	Inglewood b P16_6 zone	Inglewood b P17_2 rim	Inglewood b P17_4 zone	Inglewood b P17_5 zone	Inglewood b P17_7 zone	Inglewood b P17_10 sieved	Inglewood b P17_11 core	Inglewood b P20_2 zone
SiO ₂	56.18	54.58	58.18	56.22	53.40	57.08	54.82	56.52	50.07	58.76
TiO ₂	0.02	0.03	0.02	0.03	0.00	0.02	0.02	0.03	0.00	0.03
Al ₂ O ₃	28.22	29.50	26.82	27.46	29.64	26.57	28.51	27.06	31.71	27.30
FeO	0.37	0.52	0.45	0.41	0.54	0.47	0.37	0.37	0.47	0.41
Fe ₂ O ₃	0.42	0.58	0.50	0.46	0.60	0.52	0.42	0.41	0.52	0.45
MgO	0.02	0.02	0.00	0.02	0.01	0.03	0.02	0.03	0.01	0.01
CaO	9.98	11.53	8.29	9.63	12.09	8.61	10.73	9.13	14.44	8.49
Na ₂ O	5.42	4.76	6.12	5.35	4.27	5.56	4.71	5.47	2.88	5.76
K ₂ O	0.55	0.46	0.80	0.67	0.42	0.77	0.49	0.73	0.23	0.77
Total	100.79	101.46	100.74	99.85	100.44	99.16	99.72	99.38	99.85	101.57
An	48.82	55.73	40.82	47.88	59.47	43.94	54.07	45.88	72.47	42.84
Ab	47.95	41.63	54.50	48.13	38.05	51.40	42.96	49.76	26.14	38.33
Or	3.23	2.63	4.68	3.99	2.48	4.66	2.96	4.36	1.39	5.11
Cations										
Si	2.512	2.438	2.593	2.536	2.413	2.584	2.481	2.557	2.289	2.592
Al	1.487	1.553	1.409	1.460	1.579	1.418	1.520	1.443	1.708	1.419
Ti	0.001	0.001	0.001	0.001	0.000	0.001	0.001	0.001	0.000	0.001
Fe³⁺	0.014	0.020	0.017	0.016	0.020	0.018	0.014	0.014	0.018	0.015
Mg	0.001	0.001	0.000	0.002	0.000	0.001	0.001	0.001	0.000	0.000
Ca	0.478	0.552	0.396	0.466	0.585	0.417	0.520	0.443	0.707	0.401
Na	0.469	0.412	0.529	0.468	0.374	0.488	0.413	0.480	0.255	0.492
K	0.032	0.026	0.045	0.039	0.024	0.044	0.028	0.042	0.014	0.043
Total	4.99	5.00	4.99	4.99	5.00	4.97	4.98	4.98	4.99	4.96

Analysis ID relates to crystal number_spot number. All Fe assumed to be Fe2O3. Cations calculated on a 8 oxygen basis.

Table A2.3 Major element plagioclase compositions analysed by EMPA.

Sample ID	Inglewood b P20_3 core	Inglewood b P20_4 core	Inglewood b P21_1 rim	Inglewood b P21_2 zone	Inglewood b P21_3 sieved	Inglewood b P21_4 sieved	Inglewood b P21_5 sieved	Inglewood b p1a zone	Inglewood b p1b core	Inglewood b p2a core
SiO ₂	51.69	46.36	51.13	58.33	50.99	58.72	48.46	57.13	57.81	58.61
TiO ₂	0.00	0.01	0.05	0.02	0.02	0.00	0.01	0.00	0.02	0.07
Al ₂ O ₃	31.88	35.79	30.19	27.25	31.80	26.88	34.12	27.22	28.06	27.00
FeO	0.61	0.59	0.45	0.44	0.50	0.36	0.60	0.47	0.43	0.37
Fe ₂ O ₃	0.67	0.65	0.50	0.48	0.56	0.41	0.66	0.52	0.48	0.41
MgO	0.04	0.00	0.04	0.03	0.02	0.01	0.03	0.04	0.10	0.06
CaO	14.02	18.29	13.68	8.55	14.41	8.15	16.54	10.08	10.31	9.31
Na ₂ O	3.09	1.04	3.14	5.72	3.00	5.96	2.02	5.82	5.79	6.19
K ₂ O	0.22	0.05	0.31	0.79	0.25	0.82	0.13	0.43	0.42	0.47
Total	101.61	102.20	99.03	101.17	101.05	100.94	101.98	101.26	103.00	102.12
An	70.55	90.40	69.33	43.09	71.58	40.92	81.25	47.71	48.41	44.17
Ab	17.85	5.36	18.32	37.98	16.97	39.94	10.81	49.86	49.22	53.17
Or	1.24	0.26	1.82	5.25	1.42	5.49	0.72	2.43	2.37	2.66
Cations										
Si	2.317	2.094	2.351	2.586	2.302	2.605	2.183	2.545	2.531	2.580
Al	1.684	1.905	1.635	1.423	1.692	1.406	1.812	1.429	1.448	1.401
Ti	0.000	0.000	0.002	0.001	0.001	0.000	0.000	0.000	0.001	0.002
Fe ³⁺	0.023	0.022	0.017	0.016	0.019	0.014	0.022	0.018	0.016	0.014
Mg	0.001	0.000	0.001	0.001	0.001	0.000	0.001	0.001	0.003	0.002
Ca	0.673	0.885	0.674	0.406	0.697	0.387	0.798	0.481	0.484	0.439
Na	0.269	0.091	0.280	0.491	0.262	0.513	0.177	0.503	0.492	0.528
K	0.012	0.003	0.018	0.045	0.014	0.046	0.008	0.025	0.024	0.026
Total	4.98	5.00	4.98	4.97	4.99	4.97	5.00	5.00	5.00	4.99

Analysis ID relates to crystal number_spot number. All Fe assumed to be Fe2O3. Cations calculated on a 8 oxygen basis.

Table A2.3 Major element plagioclase compositions analysed by EMPA.

Sample ID	Inglewood b		Inglewood b		Inglewood b		Inglewood b		Inglewood b		Inglewood b		Inglewood b	
	p2b zone	p2core zone	p2d zone	p7a core	p7b zone	p7core zone	p7d zone	p7e zone	p7f zone	p7g zone				
SiO ₂	52.32	57.24	57.92	57.84	58.92	58.14	58.64	57.96	58.76	54.37				
TiO ₂	0.08	0.07	0.04	0.05	0.05	0.02	0.05	0.02	0.04	0.03				
Al ₂ O ₃	30.89	27.27	27.30	27.38	26.92	27.30	26.98	27.21	27.11	29.17				
FeO	0.53	0.42	0.55	0.53	0.44	0.42	0.48	0.33	0.38	0.53				
Fe ₂ O ₃	0.59	0.47	0.62	0.58	0.49	0.46	0.53	0.37	0.43	0.58				
MgO	0.01	0.04	0.05	0.05	0.05	0.07	0.01	0.01	0.05	0.05				
CaO	13.50	9.23	8.88	9.87	8.80	9.08	8.69	8.88	8.83	11.54				
Na ₂ O	4.01	6.17	6.18	5.93	6.16	6.21	6.18	6.36	6.45	4.81				
K ₂ O	0.22	0.42	0.56	0.42	0.56	0.45	0.53	0.51	0.49	0.26				
Total	101.62	100.91	101.54	102.13	101.97	101.74	101.61	101.32	102.15	100.82				
An	64.23	44.15	42.82	46.77	42.68	43.53	42.38	42.27	41.90	56.14				
Ab	34.55	53.46	53.98	50.85	54.06	53.90	54.56	54.86	55.33	42.37				
Or	1.22	2.39	3.20	2.38	3.26	2.57	3.06	2.87	2.77	1.49				
Cations														
Si	2.347	2.553	2.566	2.553	2.594	2.569	2.591	2.571	2.584	2.442				
Al	1.633	1.433	1.425	1.424	1.397	1.421	1.404	1.422	1.405	1.545				
Ti	0.003	0.002	0.001	0.002	0.002	0.001	0.002	0.001	0.001	0.001				
Fe ³⁺	0.020	0.016	0.021	0.019	0.016	0.015	0.018	0.012	0.014	0.020				
Mg	0.000	0.001	0.002	0.002	0.002	0.002	0.000	0.000	0.002	0.002				
Ca	0.649	0.441	0.421	0.467	0.415	0.430	0.411	0.422	0.416	0.556				
Na	0.349	0.534	0.531	0.508	0.526	0.532	0.529	0.547	0.550	0.419				
K	0.012	0.024	0.032	0.024	0.032	0.025	0.030	0.029	0.027	0.015				
Total	5.01	5.01	5.00	5.00	4.98	5.00	4.98	5.00	5.00	5.00				

Analysis ID relates to crystal number_spot number. All Fe assumed to be Fe2O3. Cations calculated on a 8 oxygen basis.

Table A2.3 Major element plagioclase compositions analysed by EMPA.

Sample ID	Inglewood b		Inglewood b		Inglewood b		Inglewood b		Inglewood b		Inglewood b		Inglewood b	
	p7h zone	p7i zone	p7p rim	p9a core	p9core rim	p11a core	p11b zone	p11core zone	p11d rim	p11b zone	p11core zone	p11d rim	p12b core	
SiO ₂	55.33	56.16	52.19	50.33	59.44	54.05	55.15	60.12	59.04	55.15	60.12	59.04	48.31	
TiO ₂	0.07	0.05	0.07	0.05	0.00	0.05	0.04	0.01	0.14	0.04	0.01	0.14	0.10	
Al ₂ O ₃	28.74	28.45	30.39	31.23	26.91	29.62	29.13	26.26	26.91	29.13	26.26	26.91	32.55	
FeO	0.47	0.46	0.60	0.61	0.46	0.45	0.47	0.39	0.39	0.47	0.39	0.39	0.55	
Fe ₂ O ₃	0.52	0.51	0.66	0.67	0.51	0.50	0.52	0.44	0.44	0.52	0.44	0.44	0.61	
MgO	0.09	0.01	0.07	0.01	0.00	0.05	0.06	0.04	0.06	0.06	0.04	0.06	0.07	
CaO	10.98	10.47	13.22	14.07	8.38	12.15	11.74	8.24	8.91	11.74	8.24	8.91	16.06	
Na ₂ O	5.41	5.46	4.00	3.36	6.50	4.59	4.97	6.55	6.25	4.97	6.55	6.25	2.41	
K ₂ O	0.32	0.38	0.21	0.18	0.44	0.28	0.34	0.50	0.51	0.34	0.50	0.51	0.10	
Total	101.45	101.49	100.80	99.90	102.17	101.28	101.97	102.16	102.25	101.97	102.16	102.25	100.21	
An	51.92	50.33	63.85	69.14	40.56	58.47	55.54	39.85	42.78	55.54	39.85	42.78	78.20	
Ab	46.27	47.47	34.93	29.83	56.92	39.95	42.56	57.27	54.28	42.56	57.27	54.28	21.19	
Or	1.81	2.20	1.21	1.03	2.52	1.58	1.90	2.88	2.94	1.90	2.88	2.94	0.60	
Cations														
Si	2.469	2.498	2.359	2.302	2.607	2.421	2.452	2.635	2.592	2.452	2.635	2.592	2.215	
Al	1.511	1.491	1.619	1.683	1.391	1.563	1.526	1.356	1.393	1.526	1.356	1.393	1.759	
Ti	0.002	0.002	0.002	0.002	0.000	0.002	0.001	0.000	0.004	0.001	0.000	0.004	0.003	
Fe ³⁺	0.017	0.017	0.023	0.023	0.017	0.017	0.018	0.014	0.014	0.018	0.014	0.014	0.021	
Mg	0.003	0.000	0.002	0.000	0.000	0.002	0.002	0.001	0.002	0.002	0.001	0.002	0.002	
Ca	0.525	0.499	0.640	0.690	0.394	0.583	0.559	0.387	0.419	0.559	0.387	0.419	0.789	
Na	0.468	0.471	0.350	0.298	0.552	0.398	0.428	0.556	0.532	0.428	0.556	0.532	0.214	
K	0.018	0.022	0.012	0.010	0.024	0.016	0.019	0.028	0.029	0.019	0.028	0.029	0.006	
Total	5.01	5.00	5.01	5.01	4.99	5.00	5.01	4.98	4.99	5.01	4.98	4.99	5.01	

Analysis ID relates to crystal number_spot number. All Fe assumed to be Fe2O3. Cations calculated on a 8 oxygen basis.

Table A2.3 Major element plagioclase compositions analysed by EMPA.

Sample ID	Inglewood b		Inglewood b		Inglewood b		Inglewood b		Inglewood b		Inglewood b		Inglewood b							
	p12core	rim	p12d	rim	p12e	rim	p15a	core	p15b	rim	p16a	core	p16b	zone	p16core	rim	p17a	core	p17b	rim
SiO ₂	53.14		48.73		56.97		51.37		57.11		50.45		59.08		58.85		55.01		55.63	
TiO ₂	0.07		0.01		0.01		0.07		0.06		0.06		0.05		0.00		0.06		0.08	
Al ₂ O ₃	30.66		32.90		27.09		31.83		27.66		31.21		26.49		27.22		27.69		27.42	
FeO	0.68		0.63		0.49		0.48		0.48		0.54		0.42		0.37		0.48		0.39	
Fe ₂ O ₃	0.75		0.69		0.54		0.53		0.54		0.60		0.47		0.41		0.53		0.43	
MgO	0.04		0.05		0.04		0.06		0.05		0.03		0.07		0.05		0.05		0.08	
CaO	13.28		16.75		9.94		14.78		9.70		14.42		8.83		9.46		10.68		10.07	
Na ₂ O	4.09		2.44		5.76		3.16		5.89		3.30		6.34		6.32		5.37		5.46	
K ₂ O	0.23		0.10		0.43		0.15		0.47		0.17		0.51		0.46		0.39		0.43	
Total	102.26		101.68		100.79		101.95		101.48		100.24		101.83		102.77		99.77		99.59	
An	63.40		78.66		47.61		71.50		46.36		69.99		42.24		44.10		51.23		49.21	
Ab	35.32		20.75		49.92		27.64		50.97		29.01		54.88		53.34		46.57		48.29	
Or	1.28		0.58		2.46		0.85		2.68		1.00		2.88		2.55		2.20		2.50	
Cations																				
Si	2.368		2.207		2.549		2.301		2.537		2.301		2.605		2.576		2.494		2.519	
Al	1.610		1.756		1.428		1.680		1.448		1.677		1.377		1.404		1.480		1.464	
Ti	0.002		0.000		0.000		0.002		0.002		0.002		0.002		0.000		0.002		0.003	
Fe ³⁺	0.025		0.024		0.018		0.018		0.018		0.021		0.016		0.013		0.018		0.015	
Mg	0.001		0.002		0.001		0.002		0.002		0.001		0.002		0.002		0.002		0.003	
Ca	0.634		0.813		0.476		0.709		0.462		0.704		0.417		0.444		0.519		0.488	
Na	0.353		0.214		0.499		0.274		0.507		0.292		0.542		0.537		0.472		0.479	
K	0.013		0.006		0.025		0.008		0.027		0.010		0.028		0.026		0.022		0.025	
Total	5.01		5.02		5.00		5.00		5.00		5.01		4.99		5.00		5.01		5.00	

Analysis ID relates to crystal number_spot number. All Fe assumed to be Fe2O3. Cations calculated on a 8 oxygen basis.

Table A2.3 Major element plagioclase compositions analysed by EMPA.

Sample ID	Inglewood b		Inglewood a		Inglewood a		Inglewood a		Inglewood a		Inglewood a		Inglewood a	
	p18 sieved	P1_1 rim	P1_3 zone	P1_4 zone	P1_5 zone	P1_6 zone	P1_7 zone	P1_8 zone	P1_9 core	P5_1 rim				
SiO ₂	51.64	61.29	58.09	57.11	53.71	56.77	50.56	54.27	47.26	56.59				
TiO ₂	0.06	0.11	0.03	0.03	0.00	0.04	0.00	0.05	0.00	0.01				
Al ₂ O ₃	31.05	25.09	26.24	27.03	29.00	26.84	31.27	28.69	33.43	27.31				
FeO	0.56	0.49	0.35	0.39	0.45	0.38	0.52	0.45	0.55	0.42				
Fe ₂ O ₃	0.62	0.54	0.39	0.44	0.50	0.43	0.58	0.50	0.61	0.47				
MgO	0.07	0.08	0.02	0.03	0.04	0.03	0.03	0.04	0.02	0.03				
CaO	13.99	7.11	7.99	8.75	11.32	8.88	13.79	10.98	16.61	9.12				
Na ₂ O	3.79	5.89	6.15	5.88	4.64	5.98	3.25	4.76	1.88	5.65				
K ₂ O	0.16	1.40	0.91	0.77	0.43	0.77	0.25	0.47	0.11	0.76				
Total	101.38	101.51	99.82	100.03	99.65	99.74	99.73	99.76	99.92	99.96				
An	66.47	36.58	39.57	43.11	55.94	43.07	69.04	54.46	82.49	45.01				
Ab	32.62	54.86	55.08	52.38	41.51	52.46	29.46	42.75	16.88	50.49				
Or	0.91	8.55	5.36	4.51	2.55	4.47	1.50	2.79	0.63	4.49				
Cations														
Si	2.326	2.697	2.610	2.567	2.441	2.563	2.312	2.461	2.176	2.549				
Al	1.648	1.301	1.390	1.432	1.553	1.428	1.685	1.533	1.813	1.449				
Ti	0.002	0.004	0.001	0.001	0.000	0.001	0.000	0.002	0.000	0.000				
Fe ³⁺	0.021	0.018	0.013	0.015	0.017	0.014	0.020	0.017	0.021	0.016				
Mg	0.002	0.005	0.001	0.001	0.001	0.001	0.001	0.001	0.001	0.002				
Ca	0.675	0.335	0.385	0.421	0.551	0.429	0.675	0.533	0.819	0.440				
Na	0.331	0.502	0.536	0.512	0.409	0.523	0.288	0.419	0.168	0.494				
K	0.009	0.078	0.052	0.044	0.025	0.045	0.015	0.027	0.006	0.044				
Total	5.02	4.94	4.99	4.99	5.00	5.00	5.00	4.99	5.00	4.99				

Analysis ID relates to crystal number_spot number. All Fe assumed to be Fe2O3. Cations calculated on a 8 oxygen basis.

Table A2.3 Major element plagioclase compositions analysed by EMPA.

Sample ID	Inglewood a P5_2 zone	Inglewood a P5_3 zone	Inglewood a P5_4 sieved	Inglewood a P5_5 sieved	Inglewood a P5_6 sieved	Inglewood a P6_2 zone	Inglewood a P6_3 zone	Inglewood a P6_4 rim	Inglewood a P6_5 core	Inglewood a P8_1 rim
SiO ₂	49.75	51.10	47.54	55.62	53.59	57.02	53.85	56.97	55.89	57.56
TiO ₂	0.02	0.03	0.01	0.04	0.01	0.03	0.04	0.04	0.01	0.00
Al ₂ O ₃	31.62	31.09	34.06	27.71	28.79	26.74	29.60	26.81	27.80	26.54
FeO	0.61	0.53	0.64	0.48	0.54	0.43	0.57	0.50	0.51	0.45
Fe ₂ O ₃	0.68	0.58	0.71	0.53	0.59	0.48	0.63	0.55	0.57	0.50
MgO	0.02	0.02	0.02	0.03	0.02	0.03	0.03	0.02	0.02	0.02
CaO	14.15	13.28	16.50	9.60	10.61	8.82	11.83	8.88	9.73	8.70
Na ₂ O	2.90	3.43	1.84	5.18	4.17	5.72	4.49	5.70	5.43	5.89
K ₂ O	0.22	0.26	0.14	0.64	0.55	0.75	0.41	0.78	0.62	0.83
Total	99.36	99.80	100.81	99.36	98.34	99.58	100.88	99.74	100.09	100.05
An	71.96	67.08	82.54	48.66	56.40	43.95	57.84	44.13	47.92	42.77
Ab	26.71	31.36	16.65	47.48	40.14	51.62	39.75	51.24	48.42	52.35
Or	1.32	1.56	0.81	3.87	3.46	4.43	2.40	4.63	3.66	4.88
Cations										
Si	2.286	2.331	2.168	2.522	2.459	2.573	2.422	2.569	2.519	2.587
Al	1.712	1.671	1.831	1.481	1.557	1.422	1.569	1.425	1.477	1.406
Ti	0.001	0.001	0.000	0.001	0.000	0.001	0.001	0.001	0.000	0.000
Fe ³⁺	0.023	0.020	0.024	0.018	0.021	0.016	0.021	0.019	0.019	0.017
Mg	0.001	0.001	0.001	0.001	0.001	0.002	0.001	0.001	0.001	0.001
Ca	0.697	0.649	0.806	0.466	0.522	0.426	0.570	0.429	0.470	0.419
Na	0.259	0.303	0.163	0.455	0.371	0.501	0.392	0.498	0.475	0.513
K	0.013	0.015	0.008	0.037	0.032	0.043	0.024	0.045	0.036	0.048
Total	4.99	4.99	5.00	4.98	4.96	4.98	5.00	4.99	5.00	4.99

Analysis ID relates to crystal number_spot number. All Fe assumed to be Fe2O3. Cations calculated on a 8 oxygen basis.

Table A2.3 Major element plagioclase compositions analysed by EMPA.

Sample ID	Inglewood a zone	Inglewood a P8_3 zone	Inglewood a P8_4 sieved	Inglewood a P8_5 sieved	Inglewood a P8_6 rim	Inglewood a P8_7 core	Inglewood a P9_1 rim	Inglewood a P9_2 zone	Inglewood a P9_3 zone	Inglewood a P9_4 zone
SiO ₂	52.52	57.09	55.70	49.87	58.63	58.21	57.57	53.69	57.30	50.89
TiO ₂	0.03	0.01	0.01	0.00	0.05	0.04	0.02	0.00	0.03	0.00
Al ₂ O ₃	29.98	26.81	28.29	31.81	26.25	26.36	26.47	28.48	27.05	30.67
FeO	0.48	0.40	0.49	0.60	0.48	0.49	0.50	0.51	0.40	0.49
Fe ₂ O ₃	0.54	0.44	0.54	0.67	0.53	0.55	0.55	0.56	0.45	0.55
MgO	0.01	0.00	0.04	0.02	0.03	0.02	0.02	0.03	0.02	0.02
CaO	12.33	8.96	10.44	14.61	8.02	8.42	8.71	10.85	9.16	13.24
Na ₂ O	4.09	5.80	5.19	2.99	6.21	6.13	5.92	4.83	5.92	3.36
K ₂ O	0.36	0.74	0.61	0.21	0.91	0.81	0.84	0.49	0.76	0.29
Total	99.86	99.86	100.82	100.17	100.64	100.54	100.09	98.94	100.68	99.03
An	61.17	44.07	50.79	72.06	39.41	41.12	42.68	53.75	44.05	67.32
Ab	36.73	51.58	45.67	26.70	55.24	54.18	52.44	43.33	51.58	30.92
Or	2.10	4.35	3.54	1.24	5.35	4.70	4.88	2.92	4.37	1.76
Cations										
Si	2.388	2.571	2.496	2.277	2.615	2.601	2.587	2.456	2.563	2.339
Al	1.607	1.423	1.494	1.712	1.380	1.388	1.402	1.536	1.426	1.661
Ti	0.001	0.000	0.000	0.000	0.002	0.001	0.001	0.000	0.001	0.000
Fe ³⁺	0.018	0.015	0.018	0.023	0.018	0.018	0.019	0.019	0.015	0.019
Mg	0.000	0.000	0.001	0.001	0.001	0.001	0.002	0.002	0.001	0.001
Ca	0.601	0.432	0.501	0.715	0.383	0.403	0.420	0.532	0.439	0.652
Na	0.361	0.506	0.451	0.265	0.537	0.531	0.515	0.428	0.514	0.299
K	0.021	0.043	0.035	0.012	0.052	0.046	0.048	0.029	0.044	0.017
Total	5.00	4.99	5.00	5.00	4.99	4.99	4.99	5.00	5.00	4.99

Analysis ID relates to crystal number_spot number. All Fe assumed to be Fe2O3. Cations calculated on a 8 oxygen basis.

Table A2.3 Major element plagioclase compositions analysed by EMPA.

Sample ID	Inglewood a P9_5 zone	Inglewood a P9_6 zone	Inglewood a P9_7 zone	Inglewood a P9_8 core	Inglewood a P9_9 zone	Inglewood a P9_10 core	Inglewood a P10_1 rim	Inglewood a P10_2 zone	Inglewood a P10_3 zone	Inglewood a P10_4 zone
SiO ₂	57.40	53.25	58.30	57.08	56.84	50.58	56.32	57.09	55.94	54.48
TiO ₂	0.03	0.04	0.01	0.03	0.02	0.02	0.07	0.06	0.00	0.02
Al ₂ O ₃	26.40	29.51	25.81	26.49	26.75	31.37	26.20	26.12	27.29	28.62
FeO	0.44	0.37	0.37	0.43	0.36	0.48	0.44	0.49	0.43	0.47
Fe ₂ O ₃	0.49	0.41	0.41	0.48	0.40	0.54	0.49	0.55	0.48	0.52
MgO	0.03	0.03	0.00	0.03	0.02	0.03	0.02	0.03	0.04	0.01
CaO	8.25	11.99	7.78	8.46	8.82	14.13	8.64	8.36	9.60	11.18
Na ₂ O	5.91	4.33	6.24	5.84	5.69	3.19	5.80	5.82	5.25	4.81
K ₂ O	0.86	0.44	0.94	0.81	0.76	0.26	0.78	0.82	0.68	0.55
Total	99.37	100.01	99.49	99.21	99.30	100.10	98.30	98.85	99.28	100.20
An	41.33	58.93	38.54	42.30	44.06	69.92	43.06	42.07	48.22	54.43
Ab	53.57	38.50	55.93	52.86	51.42	28.55	52.32	53.02	47.71	42.39
Or	5.10	2.57	5.52	4.84	4.53	1.53	4.61	4.91	4.07	3.18
Cations										
Si	2.594	2.415	2.627	2.585	2.572	2.306	2.577	2.594	2.538	2.462
Al	1.406	1.577	1.371	1.413	1.427	1.685	1.413	1.399	1.459	1.525
Ti	0.001	0.001	0.000	0.001	0.001	0.001	0.002	0.002	0.000	0.001
Fe ³⁺	0.017	0.014	0.014	0.016	0.014	0.018	0.017	0.019	0.016	0.018
Mg	0.001	0.001	0.000	0.001	0.001	0.001	0.001	0.002	0.001	0.000
Ca	0.399	0.582	0.375	0.410	0.428	0.690	0.423	0.407	0.466	0.542
Na	0.518	0.380	0.545	0.513	0.499	0.282	0.514	0.513	0.461	0.422
K	0.049	0.025	0.054	0.047	0.044	0.015	0.045	0.048	0.039	0.032
Total	4.98	5.00	4.99	4.99	4.98	5.00	4.99	4.98	4.98	5.00

Analysis ID relates to crystal number_spot number. All Fe assumed to be Fe2O3. Cations calculated on a 8 oxygen basis.

Table A2.3 Major element plagioclase compositions analysed by EMPA.

Sample ID	Inglewood a		Inglewood a		Inglewood a		Inglewood a		Inglewood a		Inglewood a		Inglewood a	
	P10_5	P10_6	P10_7	P10_8	P10_9	P11_1	P11_2	P11_3	P11_4	P11_1	P11_2	P11_3	P11_4	P12_1
zone	zone	zone	core	zone	zone	rim	zone	zone	core	rim	zone	zone	core	rim
SiO ₂	51.34	57.57	56.68	51.28	52.99	56.87	52.29	49.36	47.66	55.96				
TiO ₂	0.02	0.00	0.05	0.01	0.01	0.00	0.00	0.04	0.03	0.02				
Al ₂ O ₃	30.56	27.01	27.25	30.63	29.91	26.61	30.04	32.83	33.18	26.80				
FeO	0.69	0.49	0.45	0.71	0.54	0.47	0.63	0.53	0.55	0.45				
Fe ₂ O ₃	0.76	0.55	0.50	0.79	0.59	0.52	0.69	0.59	0.61	0.50				
MgO	0.04	0.03	0.02	0.01	0.02	0.04	0.03	0.02	0.03	0.03				
CaO	13.23	8.71	9.49	13.55	12.19	8.93	12.73	15.61	16.13	8.99				
Na ₂ O	3.58	5.86	5.53	3.55	4.14	5.66	3.80	2.36	1.89	5.47				
K ₂ O	0.33	0.77	0.69	0.30	0.39	0.79	0.34	0.16	0.13	0.71				
Total	99.84	100.50	100.21	100.13	100.23	99.42	99.92	100.95	99.66	98.47				
An	65.84	43.05	46.73	66.63	60.53	44.39	63.63	77.81	81.87	45.58				
Ab	32.23	52.42	49.22	31.58	37.20	50.92	34.34	21.27	17.34	50.14				
Or	1.93	4.53	4.05	1.78	2.28	4.70	2.03	0.92	0.79	4.28				
Cations														
Si	2.344	2.575	2.547	2.338	2.400	2.573	2.379	2.239	2.195	2.556				
Al	1.644	1.424	1.444	1.646	1.596	1.419	1.610	1.755	1.801	1.443				
Ti	0.001	0.000	0.002	0.000	0.000	0.000	0.000	0.001	0.001	0.001				
Fe ³⁺	0.026	0.018	0.017	0.027	0.020	0.018	0.024	0.020	0.021	0.017				
Mg	0.001	0.001	0.001	0.000	0.001	0.003	0.002	0.001	0.001	0.002				
Ca	0.647	0.417	0.457	0.662	0.591	0.433	0.620	0.759	0.796	0.440				
Na	0.317	0.508	0.482	0.314	0.363	0.497	0.335	0.207	0.169	0.484				
K	0.019	0.044	0.040	0.018	0.022	0.046	0.020	0.009	0.008	0.041				
Total	5.00	4.99	4.99	5.00	4.99	4.99	4.99	4.99	4.99	4.98				

Analysis ID relates to crystal number_spot number. All Fe assumed to be Fe2O3. Cations calculated on a 8 oxygen basis.

Table A2.3 Major element plagioclase compositions analysed by EMPA.

Sample ID	Inglewood a P12_2 zone	Inglewood a P12_3 zone	Inglewood a P12_4 zone	Inglewood a P12_5 sieved	Inglewood a P12_6 sieved	Inglewood a P12_7 sieved	Inglewood a P12_8 sieved	Inglewood a P14_1 rim	Inglewood a P14_2 core	Inglewood a P15_1 rim
SiO ₂	51.86	57.88	54.65	50.90	50.74	55.87	50.90	59.25	52.06	58.03
TiO ₂	0.02	0.00	0.03	0.04	0.02	0.04	0.01	0.05	0.02	0.02
Al ₂ O ₃	30.34	26.47	27.93	30.84	30.84	27.50	30.56	25.73	29.94	25.11
FeO	0.44	0.40	0.46	0.43	0.48	0.36	0.42	0.49	0.73	0.50
Fe ₂ O ₃	0.49	0.44	0.51	0.48	0.53	0.40	0.47	0.54	0.82	0.55
MgO	0.02	0.03	0.03	0.04	0.02	0.02	0.03	0.00	0.04	0.01
CaO	12.87	8.56	10.15	13.52	13.52	9.64	13.28	7.70	12.65	7.33
Na ₂ O	3.83	6.05	4.88	3.47	3.46	5.27	3.54	5.97	3.83	6.35
K ₂ O	0.34	0.83	0.53	0.30	0.28	0.64	0.28	1.15	0.37	1.08
Total	99.76	100.26	98.71	99.58	99.42	99.37	99.06	100.39	99.72	98.49
An	63.68	41.77	51.75	67.12	67.20	48.34	66.32	38.75	63.21	36.46
Ab	34.32	53.40	45.05	31.13	31.13	47.85	32.03	54.38	34.58	57.13
Or	2.00	4.83	3.20	1.75	1.67	3.81	1.65	6.88	2.20	6.41
Cations										
Si	2.364	2.594	2.497	2.329	2.326	2.531	2.339	2.644	2.376	2.643
Al	1.630	1.398	1.504	1.663	1.667	1.468	1.655	1.353	1.611	1.348
Ti	0.001	0.000	0.001	0.001	0.001	0.001	0.000	0.002	0.001	0.001
Fe ³⁺	0.017	0.015	0.017	0.017	0.018	0.014	0.016	0.018	0.028	0.019
Mg	0.002	0.001	0.001	0.001	0.001	0.001	0.001	0.000	0.001	0.001
Ca	0.628	0.411	0.497	0.663	0.664	0.468	0.654	0.368	0.619	0.358
Na	0.339	0.526	0.432	0.307	0.308	0.463	0.316	0.517	0.339	0.561
K	0.020	0.048	0.031	0.017	0.017	0.037	0.016	0.065	0.022	0.063
Total	5.00	4.99	4.98	5.00	5.00	4.98	5.00	4.97	5.00	4.99

Analysis ID relates to crystal number_spot number. All Fe assumed to be Fe₂O₃. Cations calculated on a 8 oxygen basis.

Table A2.3 Major element plagioclase compositions analysed by EMPA.

Sample ID	Inglewood a		Inglewood a		Inglewood a		Inglewood a		Inglewood a		Inglewood a		Inglewood a	
	P15_2	P15_4	P15_5	P16_2	P16_3	P16_4	P16_5	P16_6	P16_7	P16_8	core	zone	rim	zone
SiO ₂	51.13	56.20	56.77	56.29	57.54	51.70	57.61	50.96	55.37	51.51				
TiO ₂	0.03	0.01	0.00	0.01	0.02	0.04	0.06	0.03	0.02	0.03				0.03
Al ₂ O ₃	30.59	26.98	26.56	26.88	26.21	30.20	25.64	30.95	27.06	30.22				
FeO	0.73	0.39	0.45	0.50	0.46	0.45	0.35	0.55	0.46	0.82				
Fe ₂ O ₃	0.81	0.43	0.50	0.55	0.51	0.50	0.39	0.61	0.51	0.91				
MgO	0.05	0.04	0.03	0.03	0.01	0.02	0.02	0.02	0.02	0.05				
CaO	13.57	9.31	8.73	8.84	8.20	12.96	7.55	13.67	9.31	13.09				
Na ₂ O	3.41	5.39	5.81	5.54	5.88	3.90	6.14	3.41	5.46	3.73				
K ₂ O	0.23	0.71	0.80	0.72	0.83	0.35	0.84	0.28	0.68	0.30				
Total	99.83	99.06	99.21	98.86	99.22	99.67	98.26	99.94	98.42	99.84				
An	67.77	46.78	43.22	44.85	41.34	63.43	38.40	67.73	46.56	64.82				
Ab	30.87	48.99	52.08	50.83	53.68	34.56	56.49	30.61	49.40	33.41				
Or	1.36	4.22	4.70	4.33	4.98	2.02	5.11	1.65	4.04	1.77				
Cations														
Si	2.336	2.553	2.574	2.560	2.603	2.362	2.625	2.325	2.535	2.354				
Al	1.647	1.444	1.420	1.441	1.397	1.626	1.377	1.665	1.460	1.628				
Ti	0.001	0.000	0.000	0.000	0.001	0.001	0.002	0.001	0.001	0.001				
Fe ³⁺	0.028	0.015	0.017	0.019	0.018	0.017	0.013	0.021	0.018	0.031				
Mg	0.002	0.001	0.001	0.001	0.000	0.001	0.001	0.001	0.001	0.002				
Ca	0.664	0.453	0.424	0.431	0.397	0.634	0.369	0.668	0.456	0.641				
Na	0.303	0.475	0.511	0.488	0.516	0.346	0.542	0.302	0.484	0.330				
K	0.013	0.041	0.046	0.042	0.048	0.020	0.049	0.016	0.040	0.018				
Total	4.99	4.98	4.99	4.98	4.98	5.01	4.98	5.00	5.00	5.00				

Analysis ID relates to crystal number_spot number. All Fe assumed to be Fe2O3. Cations calculated on a 8 oxygen basis.

Table A2.3 Major element plagioclase compositions analysed by EMPA.

Sample ID	Inglewood a		Inglewood a		Inglewood a		Inglewood a		Inglewood a		Inglewood a		Inglewood a	
	P16_9	P17_1	P17_2	P17_3	P17_4	P17_5	P17_6	P19_1	P19_2	P19_3	core	rim	core	zone
SiO ₂	51.57	54.93	52.57	60.51	51.06	57.24	52.55	57.37	57.46	57.34				
TiO ₂	0.02	0.05	0.01	0.07	0.02	0.02	0.02	0.03	0.00	0.02				
Al ₂ O ₃	30.40	27.10	29.86	25.31	30.79	26.67	29.94	26.51	26.87	27.01				
FeO	0.83	0.50	0.72	0.49	0.58	0.44	0.63	0.51	0.45	0.38				
Fe ₂ O ₃	0.92	0.55	0.80	0.55	0.64	0.49	0.70	0.57	0.50	0.43				
MgO	0.05	0.02	0.04	0.04	0.04	0.03	0.04	0.04	0.05	0.02				
CaO	13.05	9.18	12.44	7.51	13.76	8.73	12.44	8.00	8.68	8.73				
Na ₂ O	3.73	4.89	3.88	6.01	3.33	5.78	4.05	6.00	5.96	5.92				
K ₂ O	0.34	0.59	0.38	1.30	0.24	0.78	0.40	0.77	0.78	0.74				
Total	100.06	97.30	99.98	101.30	99.89	99.74	100.14	99.28	100.30	100.20				
An	64.62	48.99	62.48	37.65	68.54	43.39	61.46	40.45	42.55	42.98				
Ab	33.39	47.25	35.25	54.59	30.04	51.98	36.21	54.92	52.88	52.70				
Or	1.99	3.76	2.27	7.76	1.43	4.63	2.33	4.63	4.57	4.33				
Cations														
Si	2.351	2.537	2.390	2.674	2.331	2.579	2.387	2.593	2.576	2.572				
Al	1.634	1.475	1.600	1.318	1.657	1.417	1.602	1.412	1.420	1.428				
Ti	0.001	0.002	0.000	0.002	0.001	0.001	0.001	0.001	0.000	0.001				
Fe ³⁺	0.032	0.019	0.027	0.018	0.022	0.017	0.024	0.019	0.017	0.014				
Mg	0.002	0.001	0.001	0.001	0.002	0.001	0.001	0.001	0.002	0.001				
Ca	0.637	0.454	0.606	0.355	0.673	0.422	0.605	0.387	0.417	0.419				
Na	0.329	0.438	0.342	0.515	0.295	0.505	0.357	0.526	0.518	0.514				
K	0.020	0.035	0.022	0.073	0.014	0.045	0.023	0.044	0.045	0.042				
Total	5.00	4.96	4.99	4.96	4.99	4.99	5.00	4.98	4.99	4.99				

Analysis ID relates to crystal number_spot number. All Fe assumed to be Fe2O3. Cations calculated on a 8 oxygen basis.

Table A2.3 Major element plagioclase compositions analysed by EMPA.

Sample ID	Inglewood a P19_4 zone	Inglewood a P19_5 zone	Inglewood a P19_6 zone	Inglewood a P19_7 sieved	Inglewood a P21_1 rim	Inglewood a P21_2 zone	Inglewood a P21_3 sieved	Inglewood a P21_4 sieved	Inglewood a P21_5 zone	Inglewood a P21_6 core
SiO ₂	57.17	58.27	49.37	46.54	56.35	49.69	56.73	55.75	58.00	50.90
TiO ₂	0.01	0.02	0.02	0.01	0.03	0.01	0.03	0.01	0.02	0.03
Al ₂ O ₃	27.19	25.98	31.70	34.12	26.48	31.28	26.71	27.98	25.92	30.63
FeO	0.49	0.47	0.56	0.55	0.43	0.61	0.38	0.46	0.50	0.52
Fe ₂ O ₃	0.54	0.52	0.63	0.61	0.48	0.68	0.42	0.51	0.56	0.58
MgO	0.04	0.02	0.03	0.02	0.04	0.03	0.01	0.00	0.03	0.03
CaO	8.96	7.77	14.73	17.43	8.62	14.17	8.60	10.33	7.85	13.18
Na ₂ O	5.67	6.14	2.83	1.72	5.60	3.05	5.76	5.17	6.19	3.56
K ₂ O	0.73	0.94	0.22	0.10	0.71	0.23	0.77	0.67	0.89	0.29
Total	100.30	99.67	99.54	100.55	98.30	99.15	99.04	100.43	99.45	99.21
An	44.59	38.85	73.22	84.34	43.98	71.01	43.11	50.46	39.05	65.99
Ab	51.07	55.54	25.50	15.08	51.69	27.63	52.27	45.65	55.68	32.27
Or	4.34	5.60	1.28	0.58	4.33	1.36	4.62	3.89	5.27	1.74
Cations										
Si	2.563	2.622	2.270	2.136	2.575	2.290	2.574	2.507	2.617	2.337
Al	1.437	1.377	1.718	1.845	1.426	1.699	1.428	1.483	1.378	1.657
Ti	0.000	0.001	0.001	0.000	0.001	0.000	0.001	0.000	0.001	0.001
Fe ³⁺	0.018	0.018	0.022	0.021	0.017	0.024	0.014	0.017	0.019	0.020
Mg	0.001	0.001	0.001	0.001	0.003	0.002	0.000	0.000	0.001	0.001
Ca	0.430	0.375	0.726	0.857	0.422	0.700	0.418	0.498	0.380	0.648
Na	0.493	0.536	0.253	0.153	0.496	0.272	0.507	0.450	0.541	0.317
K	0.042	0.054	0.013	0.006	0.042	0.013	0.045	0.038	0.051	0.017
Total	4.98	4.98	5.00	5.02	4.98	5.00	4.99	4.99	4.99	5.00

Analysis ID relates to crystal number_spot number. All Fe assumed to be Fe2O3. Cations calculated on a 8 oxygen basis.

Table A2.3 Major element plagioclase compositions analysed by EMPA.

Sample ID	Inglewood a		Inglewood a		Inglewood a		Inglewood a		Inglewood a		Inglewood a		Inglewood a		
	P22_1 rim	P22_2 zone	P22_3 zone	P22_4 zone	P22_5 core	P24_1 rim	P24_2 sieved	P24_3 sieved	P25_1 rim	P25_2 zone	P22_1 rim	P22_2 zone	P22_3 zone	P22_4 zone	
SiO ₂	56.38	53.14	56.49	50.42	51.54	58.05	49.40	56.56	57.11	52.15					
TiO ₂	0.05	0.03	0.02	0.03	0.04	0.03	0.00	0.07	0.03	0.00					
Al ₂ O ₃	26.61	29.75	27.03	31.42	30.42	27.05	32.75	27.39	26.71	30.05					
FeO	0.40	0.45	0.38	0.51	0.53	0.47	0.55	0.43	0.44	0.51					
Fe ₂ O ₃	0.44	0.50	0.42	0.56	0.59	0.52	0.61	0.48	0.49	0.57					
MgO	0.02	0.03	0.03	0.02	0.03	0.04	0.03	0.02	0.02	0.03					
CaO	8.95	12.27	9.12	14.10	13.12	8.73	15.35	9.32	8.69	12.57					
Na ₂ O	5.67	4.20	5.77	3.07	3.58	6.01	2.59	5.56	5.81	3.92					
K ₂ O	0.77	0.41	0.82	0.25	0.31	0.81	0.18	0.72	0.77	0.32					
Total	98.90	100.33	99.70	99.87	99.63	101.24	100.92	100.12	99.64	99.61					
An	44.47	60.23	44.42	70.65	65.72	42.43	75.79	46.07	43.19	62.70					
Ab	51.00	37.35	50.85	27.88	32.46	52.86	23.13	49.70	52.24	35.42					
Or	4.53	2.42	4.73	1.47	1.82	4.71	1.08	4.23	4.57	1.88					
Cations															
Si	2.565	2.404	2.553	2.303	2.354	2.578	2.242	2.544	2.577	2.379					
Al	1.427	1.586	1.439	1.691	1.637	1.416	1.752	1.452	1.420	1.615					
Ti	0.002	0.001	0.001	0.001	0.001	0.001	0.000	0.002	0.001	0.000					
Fe ³⁺	0.015	0.017	0.014	0.019	0.020	0.017	0.021	0.016	0.017	0.019					
Mg	0.001	0.001	0.001	0.001	0.001	0.003	0.002	0.001	0.001	0.001					
Ca	0.436	0.595	0.441	0.690	0.642	0.416	0.746	0.449	0.420	0.614					
Na	0.501	0.369	0.505	0.272	0.317	0.518	0.228	0.484	0.508	0.347					
K	0.044	0.024	0.047	0.014	0.018	0.046	0.011	0.041	0.044	0.018					
Total	4.99	5.00	5.00	4.99	4.99	4.99	5.00	4.99	4.99	4.99					

Analysis ID relates to crystal number_spot number. All Fe assumed to be Fe2O3. Cations calculated on a 8 oxygen basis.

Table A2.3 Major element plagioclase compositions analysed by EMPA.

Sample ID	Inglewood a		Inglewood a		Korito		Korito		Korito		Korito		Korito	
	P25_3 zone	P25_4 zone	P25_5 zone	P1_1 core	P1_2 rim	P2_1 rim	P2_2 sieved	P2_3 sieved	P2_4 sieved	P3_1 rim	P3_2 zone	P3_3 sieved	P3_4 sieved	Korito
SiO ₂	52.44	48.57	51.73	52.38	58.02	52.89	48.88	47.75	57.44	56.75	53.22	50.42	50.72	
TiO ₂	0.03	0.00	0.01	0.02	0.00	0.04	0.01	0.02	0.02	0.05	0.00	0.04	0.00	
Al ₂ O ₃	30.30	32.52	31.03	30.63	26.99	31.19	33.61	34.91	27.79	27.18	29.99	31.99	31.69	
FeO	0.51	0.47	0.55	0.55	0.64	0.71	0.69	0.71	0.55	0.56	0.61	0.63	0.61	
Fe ₂ O ₃	0.56	0.52	0.61	0.61	0.71	0.78	0.77	0.79	0.61	0.62	0.68	0.70	0.68	
MgO	0.04	0.03	0.05	0.05	0.04	0.03	0.02	0.00	0.02	0.04	0.04	0.03	0.04	
CaO	12.63	15.20	13.36	12.86	8.92	12.77	15.49	16.70	8.95	8.99	12.04	14.23	14.13	
Na ₂ O	3.89	2.41	3.52	3.72	5.93	4.14	2.44	1.97	5.89	5.49	4.24	3.19	3.19	
K ₂ O	0.31	0.14	0.23	0.29	0.72	0.38	0.17	0.09	0.80	0.76	0.37	0.30	0.28	
Total	100.19	99.38	100.53	100.56	101.34	102.22	101.39	102.23	101.52	99.88	100.58	100.91	100.73	
An	63.03	77.07	66.79	64.48	43.50	61.65	77.00	81.97	43.54	45.32	59.74	69.86	69.83	
Ab	35.14	22.09	31.87	33.79	52.30	36.16	21.96	17.48	51.84	50.09	38.06	28.36	28.50	
Or	1.83	0.84	1.34	1.73	4.21	2.19	1.03	0.55	4.62	4.59	2.20	1.78	1.67	
Cations														
Si	2.377	2.236	2.342	2.367	2.577	2.357	2.211	2.150	2.548	2.556	2.402	2.284	2.300	
Al	1.619	1.765	1.655	1.631	1.413	1.638	1.792	1.852	1.453	1.443	1.595	1.708	1.693	
Ti	0.001	0.000	0.000	0.001	0.000	0.001	0.000	0.001	0.001	0.002	0.000	0.001	0.000	
Fe ³⁺	0.019	0.018	0.021	0.021	0.024	0.026	0.026	0.027	0.021	0.021	0.023	0.024	0.023	
Mg	0.001	0.001	0.002	0.003	0.003	0.002	0.001	0.000	0.001	0.001	0.001	0.001	0.001	
Ca	0.613	0.750	0.648	0.622	0.425	0.610	0.751	0.806	0.426	0.434	0.582	0.691	0.687	
Na	0.342	0.215	0.309	0.326	0.510	0.358	0.214	0.172	0.507	0.479	0.371	0.280	0.280	
K	0.018	0.008	0.013	0.017	0.041	0.022	0.010	0.005	0.045	0.044	0.021	0.018	0.016	
Total	4.99	4.99	4.99	4.99	4.99	5.01	5.01	5.01	5.00	4.98	5.00	5.01	5.00	

Analysis ID relates to crystal number_spot number. All Fe assumed to be Fe2O3. Cations calculated on a 8 oxygen basis.

Table A2.3 Major element plagioclase compositions analysed by EMPA.

Sample ID	Korito P3_6 sieved	Korito P3_7 zone	Korito P3_8 zone	Korito P3_9 core	Korito P3_10 core	Korito P3_11 sieved	Korito P3_12 sieved	Korito P4_2 zone	Korito P4_3 zone	Korito P4_4 core	Korito P5_4 core	Korito P6_1 rim	Korito P6_2 zone	Korito P6_3 sieved
SiO ₂	51.26	57.69	53.40	49.24	51.14	50.39	47.31	58.47	51.50	49.70	51.95	57.72	51.62	52.67
TiO ₂	0.04	0.03	0.04	0.03	0.05	0.03	0.00	0.09	0.03	0.02	0.01	0.05	0.04	0.02
Al ₂ O ₃	31.06	26.87	30.47	32.73	31.78	32.40	34.68	25.06	30.94	31.65	31.38	26.70	31.85	31.17
FeO	0.53	0.40	0.43	0.63	0.54	0.52	0.54	0.46	0.65	0.54	0.65	0.54	0.60	0.43
Fe ₂ O ₃	0.58	0.45	0.48	0.70	0.60	0.57	0.60	0.51	0.72	0.60	0.72	0.60	0.67	0.47
MgO	0.02	0.03	0.05	0.03	0.05	0.04	0.02	0.06	0.05	0.04	0.04	0.06	0.05	0.03
CaO	13.51	8.42	12.44	15.36	14.07	14.67	17.35	7.27	13.92	14.84	13.81	8.34	13.97	13.17
Na ₂ O	3.46	5.81	4.25	2.63	3.19	2.85	1.58	6.03	3.39	2.50	3.41	5.82	3.44	3.42
K ₂ O	0.30	0.82	0.37	0.17	0.23	0.21	0.09	0.81	0.24	0.17	0.31	0.75	0.22	0.58
Total	100.23	100.11	101.49	100.89	101.11	101.16	101.63	98.31	100.77	99.52	101.64	100.05	101.85	101.53
An	67.11	42.31	60.45	75.58	69.95	73.09	85.37	37.99	68.48	75.84	67.88	42.18	68.32	65.72
Ab	31.12	52.80	37.42	23.42	28.68	25.66	14.09	57.00	30.14	23.15	30.30	53.29	30.42	30.86
Or	1.77	4.89	2.13	1.00	1.37	1.25	0.54	5.01	1.38	1.01	1.82	4.53	1.26	3.42
Cations														
Si	2.330	2.586	2.389	2.237	2.307	2.275	2.143	2.660	2.336	2.284	2.331	2.593	2.315	2.361
Al	1.664	1.419	1.606	1.753	1.689	1.724	1.852	1.344	1.654	1.714	1.659	1.414	1.683	1.646
Ti	0.001	0.001	0.001	0.001	0.002	0.001	0.000	0.003	0.001	0.001	0.000	0.002	0.001	0.001
Fe ³⁺	0.020	0.015	0.016	0.024	0.020	0.020	0.020	0.008	0.011	0.009	0.024	0.009	0.010	0.007
Mg	0.001	0.001	0.002	0.001	0.002	0.001	0.001	0.004	0.002	0.001	0.001	0.004	0.003	0.001
Ca	0.658	0.404	0.596	0.748	0.680	0.709	0.842	0.355	0.677	0.731	0.664	0.401	0.671	0.632
Na	0.305	0.505	0.369	0.232	0.279	0.249	0.139	0.532	0.298	0.223	0.296	0.507	0.299	0.297
K	0.017	0.047	0.021	0.010	0.013	0.012	0.005	0.047	0.014	0.010	0.018	0.043	0.012	0.033
Total	5.00	4.98	5.00	5.01	4.99	4.99	5.00	4.95	4.99	4.97	4.99	4.97	5.00	4.98

Analysis ID relates to crystal number_spot number. All Fe assumed to be Fe2O3. Cations calculated on a 8 oxygen basis.

Table A2.3 Major element plagioclase compositions analysed by EMPA.

Sample ID	Korito P6_5 sieved	Korito P6_6 zone	Korito P6_7 sieved	Korito P7_1 rim	Korito P7_2 zone	Korito P7_4 core	Korito P8_2 zone	Korito P8_3 zone	Korito P8_4 zone	Korito P8_5 zone	Korito P8_6 zone	Korito P8_7 zone	Korito P8_8 core	Korito P9_1 rim	Korito P9_2 zone
SiO ₂	58.38	51.07	56.96	57.10	54.57	51.45	55.48	58.63	57.95	52.59	57.38	54.51	58.21	57.85	54.17
TiO ₂	0.05	0.02	0.03	0.01	0.02	0.01	0.02	0.02	0.03	0.06	0.03	0.04	0.04	0.01	0.03
Al ₂ O ₃	26.98	32.05	27.56	27.39	29.02	31.73	29.21	26.80	27.06	30.90	27.84	29.77	26.69	27.11	29.43
FeO	0.39	0.58	0.50	0.48	0.52	0.55	0.44	0.37	0.44	0.51	0.41	0.41	0.39	0.42	0.64
Fe ₂ O ₃	0.44	0.65	0.55	0.54	0.57	0.62	0.49	0.41	0.49	0.56	0.46	0.46	0.43	0.47	0.71
MgO	0.02	0.02	0.01	0.03	0.02	0.01	0.03	0.03	0.02	0.03	0.03	0.04	0.02	0.03	0.02
CaO	8.43	14.26	9.03	8.45	10.49	13.59	10.64	8.15	8.75	12.95	9.48	11.87	8.47	8.68	11.19
Na ₂ O	6.15	3.27	5.52	5.82	4.68	3.45	5.03	6.25	5.98	3.90	5.62	4.56	6.05	5.80	4.49
K ₂ O	0.87	0.23	0.67	0.79	0.48	0.28	0.50	0.87	0.80	0.33	0.70	0.47	0.81	0.79	0.47
Total	101.32	101.57	100.33	100.13	99.84	101.14	101.41	101.15	101.06	101.33	101.54	101.73	100.71	100.76	100.50
An	40.96	69.73	45.55	42.40	53.73	67.35	52.34	39.75	42.65	63.49	46.30	57.39	41.57	43.12	56.28
Ab	54.02	28.95	50.43	52.88	43.37	30.98	44.74	55.20	52.71	34.56	49.63	39.91	53.71	52.18	40.92
Or	5.02	1.32	4.02	4.72	2.90	1.67	2.92	5.04	4.64	1.94	4.07	2.70	4.72	4.70	2.80
Cations															
Si	2.591	2.299	2.555	2.566	2.470	2.321	2.474	2.603	2.581	2.364	2.546	2.431	2.597	2.579	2.440
Al	1.411	1.701	1.457	1.450	1.548	1.687	1.535	1.402	1.420	1.636	1.456	1.565	1.403	1.424	1.562
Ti	0.002	0.001	0.001	0.000	0.001	0.000	0.001	0.001	0.001	0.002	0.001	0.001	0.001	0.000	0.001
Fe ³⁺	0.007	0.010	0.008	0.008	0.009	0.009	0.007	0.006	0.007	0.009	0.007	0.007	0.006	0.016	0.024
Mg	0.001	0.001	0.000	0.001	0.001	0.000	0.001	0.001	0.001	0.001	0.001	0.001	0.001	0.002	0.001
Ca	0.401	0.688	0.434	0.407	0.509	0.657	0.508	0.388	0.417	0.624	0.451	0.567	0.405	0.415	0.540
Na	0.529	0.286	0.480	0.507	0.410	0.302	0.435	0.538	0.516	0.339	0.483	0.395	0.523	0.502	0.392
K	0.049	0.013	0.038	0.045	0.027	0.016	0.028	0.049	0.045	0.019	0.040	0.027	0.046	0.045	0.027
Total	4.99	5.00	4.97	4.98	4.97	4.99	4.99	4.99	4.99	4.99	4.98	4.99	4.98	4.98	4.99

Analysis ID relates to crystal number_spot number. All Fe assumed to be Fe2O3. Cations calculated on a 8 oxygen basis.

Table A2.3 Major element plagioclase compositions analysed by EMPA.

Sample ID	Korito P9_3		Korito P9_4		Korito P9_5		Korito P9_7		Korito P9_9		Korito P9_10		Korito P10_2		Korito P10_3		Korito P10_4		Korito P10_5		Korito P10_6		Korito P10_7		Korito P10_8		
	zone	zone	zone	sieved	zone	core	zone	zone	core	zone	zone	rim	zone	zone	zone	zone	zone	zone	zone	zone	zone	zone	zone	zone	zone	zone	zone
SiO ₂	57.36	53.94	56.55	52.21	56.31	53.29	57.48	58.16	54.97	58.03	57.35	58.97	58.16	54.97	58.03	57.35	58.97	58.16	54.97	58.03	57.35	58.97	58.16	54.97	58.03	57.35	58.97
TiO ₂	0.03	0.03	0.04	0.03	0.03	0.02	0.02	0.01	0.00	0.03	0.02	0.02	0.01	0.00	0.03	0.02	0.05	0.01	0.00	0.03	0.02	0.05	0.01	0.00	0.03	0.02	0.05
Al ₂ O ₃	27.27	29.94	27.75	31.26	27.84	29.94	27.20	26.52	29.07	26.97	27.09	26.15	26.52	29.07	26.97	27.09	26.15	26.52	29.07	26.97	27.09	26.15	26.52	29.07	26.97	27.09	26.15
FeO	0.46	0.51	0.49	0.64	0.41	0.51	0.49	0.54	0.41	0.45	0.57	0.47	0.42	0.52	0.39	0.45	0.42	0.42	0.52	0.39	0.45	0.42	0.42	0.52	0.39	0.45	0.42
Fe ₂ O ₃	0.51	0.56	0.54	0.71	0.45	0.57	0.54	0.46	0.41	0.45	0.57	0.47	0.46	0.57	0.43	0.50	0.47	0.46	0.57	0.43	0.50	0.47	0.46	0.57	0.43	0.50	0.47
MgO	0.03	0.02	0.03	0.03	0.02	0.04	0.02	0.03	0.02	0.02	0.04	0.02	0.03	0.02	0.03	0.03	0.02	0.03	0.02	0.03	0.03	0.02	0.02	0.03	0.03	0.03	0.02
CaO	8.81	11.69	9.27	13.19	9.88	12.04	9.08	8.57	11.15	8.65	8.99	8.09	8.57	11.15	8.65	8.99	8.09	8.57	11.15	8.65	8.99	8.09	8.57	11.15	8.65	8.99	8.09
Na ₂ O	5.81	4.35	5.43	3.55	5.23	4.20	5.70	5.90	4.78	5.93	5.73	6.23	5.90	4.78	5.93	5.73	6.23	5.90	4.78	5.93	5.73	6.23	5.90	4.78	5.93	5.73	6.23
K ₂ O	0.79	0.44	0.66	0.34	0.68	0.44	0.76	0.80	0.48	0.72	0.71	0.87	0.80	0.48	0.72	0.71	0.87	0.80	0.48	0.72	0.71	0.87	0.80	0.48	0.72	0.71	0.87
Total	100.60	100.97	100.27	101.33	100.44	100.55	100.81	100.45	101.06	100.78	100.41	100.85	100.45	101.06	100.78	100.41	100.85	100.45	101.06	100.78	100.41	100.85	100.45	101.06	100.78	100.41	100.85
An	43.50	58.22	46.60	65.88	49.01	59.69	44.73	42.43	54.72	42.74	44.50	39.68	42.43	54.72	42.74	44.50	39.68	42.43	54.72	42.74	44.50	39.68	42.43	54.72	42.74	44.50	39.68
Ab	51.86	39.18	49.43	32.07	46.95	37.68	50.84	52.87	42.45	53.05	51.34	55.23	52.87	42.45	53.05	51.34	55.23	52.87	42.45	53.05	51.34	55.23	52.87	42.45	53.05	51.34	55.23
Or	4.63	2.60	3.97	2.05	4.04	2.63	4.43	4.70	2.83	4.21	4.16	5.10	4.70	2.83	4.21	4.16	5.10	4.70	2.83	4.21	4.16	5.10	4.70	2.83	4.21	4.16	5.10
Cations																											
Si	2.564	2.420	2.537	2.345	2.526	2.405	2.565	2.599	2.461	2.585	2.568	2.622	2.599	2.461	2.585	2.568	2.622	2.599	2.461	2.585	2.568	2.622	2.599	2.461	2.585	2.568	2.622
Al	1.437	1.583	1.468	1.655	1.472	1.592	1.430	1.397	1.534	1.416	1.429	1.370	1.397	1.534	1.416	1.429	1.370	1.397	1.534	1.416	1.429	1.370	1.397	1.534	1.416	1.429	1.370
Ti	0.001	0.001	0.001	0.001	0.001	0.001	0.001	0.000	0.000	0.001	0.001	0.002	0.000	0.000	0.001	0.001	0.002	0.000	0.000	0.001	0.001	0.002	0.000	0.000	0.001	0.001	0.002
Fe ³⁺	0.017	0.019	0.018	0.024	0.015	0.019	0.018	0.016	0.019	0.015	0.017	0.016	0.016	0.019	0.015	0.017	0.016	0.016	0.019	0.015	0.017	0.016	0.016	0.019	0.015	0.017	0.016
Mg	0.001	0.001	0.001	0.001	0.001	0.001	0.001	0.001	0.001	0.001	0.001	0.001	0.001	0.001	0.001	0.001	0.001	0.001	0.001	0.001	0.001	0.001	0.001	0.001	0.001	0.001	0.001
Ca	0.422	0.562	0.445	0.635	0.475	0.582	0.434	0.410	0.535	0.413	0.431	0.386	0.410	0.535	0.413	0.431	0.386	0.410	0.535	0.413	0.431	0.386	0.410	0.535	0.413	0.431	0.386
Na	0.503	0.378	0.473	0.309	0.455	0.367	0.493	0.511	0.415	0.512	0.497	0.537	0.511	0.415	0.512	0.497	0.537	0.511	0.415	0.512	0.497	0.537	0.511	0.415	0.512	0.497	0.537
K	0.045	0.025	0.038	0.020	0.039	0.026	0.043	0.045	0.028	0.041	0.040	0.050	0.045	0.028	0.041	0.040	0.050	0.045	0.028	0.041	0.040	0.050	0.045	0.028	0.041	0.040	0.050
Total	4.99	4.99	4.98	4.99	4.98	4.99	4.99	4.98	4.99	4.98	4.98	4.98	4.98	4.99	4.98	4.98	4.98	4.98	4.99	4.98	4.98	4.98	4.98	4.98	4.99	4.98	4.98

Analysis ID relates to crystal number_spot number. All Fe assumed to be Fe2O3. Cations calculated on a 8 oxygen basis.

Table A2.3 Major element plagioclase compositions analysed by EMPA.

Sample ID	Korito P10_9		Korito P10_10		Korito P10_11		Korito P11_1		Korito P11_3		Korito P11_4		Korito P11_5		Korito P11_6		Korito P11_7		Korito P11_8		Korito P11_9		Korito P14_2		Korito P14_4		
	zone	zone	zone	zone	core	rim	zone	zone	zone	zone	zone	zone	zone	zone	zone	zone	zone	zone	zone	zone	zone	core	rim	rim	zone	zone	
SiO ₂	56.74	51.31	51.05	57.16	53.16	54.38	50.85	55.81	57.17	49.04	46.68	60.25	58.33														
TiO ₂	0.05	0.00	0.03	0.05	0.05	0.05	0.04	0.00	0.04	0.00	0.00	0.05	0.01														
Al ₂ O ₃	27.74	31.35	31.76	27.04	30.10	29.48	31.66	28.70	27.34	33.09	35.02	25.92	26.92														
FeO	0.48	0.54	0.50	0.53	0.57	0.47	0.57	0.44	0.39	0.63	0.63	0.38	0.40														
Fe ₂ O ₃	0.53	0.60	0.56	0.59	0.63	0.52	0.63	0.48	0.43	0.70	0.70	0.43	0.44														
MgO	0.03	0.02	0.01	0.03	0.01	0.04	0.04	0.03	0.03	0.06	0.02	0.02	0.02														
CaO	9.85	14.05	14.22	8.74	12.38	11.26	14.12	10.35	9.08	15.69	17.76	7.08	8.44														
Na ₂ O	5.44	3.36	3.21	5.65	4.03	4.58	3.11	5.05	5.56	2.41	1.39	6.70	6.15														
K ₂ O	0.62	0.24	0.22	0.77	0.42	0.47	0.25	0.58	0.75	0.15	0.07	1.01	0.77														
Total	100.99	100.94	101.06	100.02	100.77	100.77	100.71	101.01	100.40	101.15	101.63	101.46	101.09														
An	48.22	68.83	70.07	43.94	61.37	56.00	70.47	51.30	45.33	77.55	87.20	34.70	41.17														
Ab	48.17	29.76	28.63	51.44	36.14	41.24	28.06	45.28	50.22	21.54	12.37	59.41	54.35														
Or	3.61	1.41	1.30	4.62	2.49	2.76	1.47	3.42	4.45	0.91	0.43	5.88	4.48														
Cations																											
Si	2.532	2.319	2.305	2.569	2.396	2.441	2.304	2.493	2.559	2.224	2.119	2.656	2.591														
Al	1.459	1.670	1.690	1.432	1.599	1.560	1.690	1.511	1.442	1.768	1.873	1.347	1.409														
Ti	0.002	0.000	0.001	0.002	0.002	0.002	0.001	0.000	0.001	0.000	0.000	0.002	0.000														
Fe ³⁺	0.018	0.020	0.019	0.020	0.022	0.017	0.022	0.016	0.015	0.024	0.024	0.014	0.015														
Mg	0.001	0.001	0.000	0.002	0.000	0.001	0.001	0.001	0.001	0.002	0.001	0.001	0.001														
Ca	0.471	0.680	0.688	0.421	0.598	0.542	0.686	0.495	0.435	0.762	0.864	0.334	0.401														
Na	0.470	0.294	0.281	0.492	0.352	0.399	0.273	0.437	0.482	0.212	0.123	0.572	0.530														
K	0.035	0.014	0.013	0.044	0.024	0.027	0.014	0.033	0.043	0.009	0.004	0.057	0.044														
Total	4.99	5.00	5.00	4.98	4.99	4.99	4.99	4.99	4.98	5.00	5.01	4.98	4.99														

Analysis ID relates to crystal number_spot number. All Fe assumed to be Fe2O3. Cations calculated on a 8 oxygen basis.

Table A2.3 Major element plagioclase compositions analysed by EMPA.

Sample ID	Korito P14_5 zone	Korito P14_6 zone	Korito P14_7 zone	Korito P14_8 zone	Korito P14_9 zone	Korito P14_10 core	Korito P15_1 rim	Korito P15_2 zone	Korito P15_3 zone	Korito P15_4 zone	Korito P15_5 zone	Korito P15_6 zone	Korito P15_7 zone
SiO ₂	54.49	58.28	58.64	57.58	51.66	55.94	58.76	57.65	57.78	57.30	57.50	54.78	57.36
TiO ₂	0.02	0.03	0.03	0.03	0.06	0.01	0.01	0.05	0.02	0.03	0.04	0.02	0.04
Al ₂ O ₃	29.39	26.57	27.43	26.99	31.67	28.25	26.50	27.31	27.31	27.43	27.47	29.28	27.65
FeO	0.50	0.44	0.32	0.40	0.45	0.46	0.50	0.37	0.40	0.46	0.37	0.44	0.44
Fe ₂ O ₃	0.56	0.48	0.35	0.44	0.50	0.51	0.55	0.41	0.44	0.51	0.41	0.48	0.49
MgO	0.02	0.03	0.04	0.02	0.05	0.04	0.02	0.03	0.02	0.03	0.02	0.03	0.02
CaO	11.21	8.17	9.34	8.58	13.87	10.27	7.98	8.89	9.02	8.83	8.95	11.18	9.47
Na ₂ O	4.62	5.98	6.28	5.84	3.48	5.32	6.08	5.78	5.81	5.65	5.88	4.85	5.90
K ₂ O	0.42	0.77	0.85	0.73	0.26	0.59	0.85	0.75	0.72	0.70	0.74	0.48	0.70
Total	100.73	100.31	102.98	100.22	101.54	100.93	100.76	100.87	101.14	100.48	101.00	101.10	101.62
An	55.85	41.00	43.00	42.86	67.73	49.85	39.91	43.93	44.26	44.38	43.71	54.49	45.15
Ab	41.64	54.37	52.33	52.79	30.74	46.76	55.04	51.66	51.54	51.41	51.99	42.73	50.86
Or	2.51	4.63	4.67	4.34	1.53	3.40	5.05	4.41	4.20	4.21	4.30	2.78	3.99
Cations													
Si	2.447	2.604	2.566	2.579	2.319	2.503	2.614	2.567	2.568	2.562	2.560	2.452	2.544
Al	1.555	1.399	1.415	1.425	1.675	1.489	1.390	1.433	1.431	1.445	1.441	1.545	1.445
Ti	0.001	0.001	0.001	0.001	0.002	0.000	0.000	0.002	0.001	0.001	0.001	0.001	0.001
Fe ³⁺	0.019	0.016	0.012	0.015	0.017	0.017	0.018	0.014	0.015	0.017	0.014	0.016	0.016
Mg	0.001	0.001	0.001	0.001	0.002	0.001	0.002	0.002	0.001	0.001	0.001	0.001	0.001
Ca	0.539	0.391	0.438	0.412	0.667	0.492	0.380	0.424	0.430	0.423	0.427	0.536	0.450
Na	0.402	0.518	0.533	0.507	0.303	0.462	0.525	0.499	0.500	0.490	0.508	0.421	0.507
K	0.024	0.044	0.048	0.042	0.015	0.034	0.048	0.043	0.041	0.040	0.042	0.027	0.040
Total	4.99	4.98	5.01	4.98	5.00	5.00	4.98	4.98	4.99	4.98	4.99	5.00	5.00

Analysis ID relates to crystal number_spot number. All Fe assumed to be Fe2O3. Cations calculated on a 8 oxygen basis.

Table A2.3 Major element plagioclase compositions analysed by EMPA.

Sample ID	Korito P15_8	Korito P15_9	Korito P16_2	Korito P16_3	Korito P16_6	Korito P16_7	Korito P16_8	Korito P16_9	Korito P16_10	Korito P16_11	Korito P16_13	Korito P16_15	Korito P16_17
zone	zone	core	zone	zone	zone	zone	zone	zone	zone	core	rim	zone	core
SiO ₂	49.56	48.58	57.10	54.31	57.17	53.24	57.54	56.85	52.97	56.31	50.52	57.21	51.57
TiO ₂	0.02	0.04	0.04	0.04	0.03	0.02	0.05	0.02	0.04	0.00	0.03	0.05	0.01
Al ₂ O ₃	32.83	33.35	27.67	29.37	26.47	30.19	26.93	27.46	30.14	27.75	32.61	27.93	31.28
FeO	0.52	0.54	0.44	0.44	0.41	0.51	0.49	0.56	0.50	0.33	0.66	0.43	0.60
Fe ₂ O ₃	0.58	0.60	0.48	0.48	0.46	0.57	0.55	0.63	0.56	0.37	0.73	0.48	0.66
MgO	0.01	0.03	0.02	0.03	0.00	0.02	0.03	0.03	0.03	0.03	0.05	0.02	0.04
CaO	15.27	16.07	9.14	11.30	8.06	12.42	8.61	9.28	12.48	9.63	13.33	9.52	13.80
Na ₂ O	2.71	2.30	5.64	4.65	5.90	4.23	5.90	5.60	4.04	5.49	2.84	5.52	3.60
K ₂ O	0.20	0.15	0.70	0.47	0.74	0.42	0.77	0.64	0.35	0.60	0.27	0.66	0.25
Total	101.17	101.12	100.80	100.64	98.84	101.11	100.39	100.51	100.61	100.17	100.38	101.38	101.21
An	74.83	78.74	45.26	55.76	41.08	60.37	42.61	45.99	61.75	47.50	70.94	46.91	66.94
Ab	24.03	20.40	50.58	41.49	54.43	37.21	52.85	50.22	36.19	48.99	27.34	49.23	31.60
Or	1.14	0.86	4.15	2.76	4.49	2.42	4.54	3.78	2.06	3.51	1.72	3.86	1.46
Cations													
Si	2.243	2.206	2.547	2.442	2.593	2.393	2.576	2.547	2.391	2.530	2.289	2.540	2.325
Al	1.751	1.784	1.455	1.556	1.415	1.599	1.421	1.450	1.603	1.470	1.741	1.461	1.662
Ti	0.001	0.001	0.001	0.001	0.001	0.001	0.002	0.001	0.001	0.000	0.001	0.002	0.000
Fe ³⁺	0.020	0.020	0.016	0.016	0.016	0.019	0.019	0.021	0.019	0.012	0.025	0.016	0.023
Mg	0.000	0.001	0.001	0.001	0.000	0.001	0.001	0.001	0.001	0.001	0.002	0.001	0.001
Ca	0.741	0.782	0.437	0.544	0.392	0.598	0.413	0.445	0.603	0.464	0.647	0.453	0.666
Na	0.238	0.203	0.488	0.405	0.519	0.369	0.512	0.486	0.354	0.478	0.249	0.475	0.315
K	0.011	0.009	0.040	0.027	0.043	0.024	0.044	0.037	0.020	0.034	0.016	0.037	0.015
Total	5.00	5.01	4.99	4.99	4.98	5.00	4.99	4.99	4.99	4.99	4.97	4.98	5.01

Analysis ID relates to crystal number_spot number. All Fe assumed to be Fe2O3. Cations calculated on a 8 oxygen basis.

Table A2.3 Major element plagioclase compositions analysed by EMPA.

Sample ID	Korito P19_1 rim	Korito P19_2 zone	Korito P19_3 sieved	Korito P19_4 sieved	Korito P19_5 sieved	Korito P19_6 core	Korito P21_1 rim	Korito P21_2 zone	Korito P21_3 zone	Korito P21_4 zone	Korito P21_5 core	Korito P22_2 rim	Korito P22_3 zone
SiO ₂	57.18	55.95	49.57	49.14	57.51	49.39	58.00	58.10	50.15	50.41	47.52	54.42	58.16
TiO ₂	0.02	0.03	0.04	0.02	0.01	0.03	0.02	0.01	0.01	0.06	0.00	0.00	0.02
Al ₂ O ₃	27.33	28.22	32.95	32.44	27.44	32.61	26.70	27.32	32.12	32.18	34.44	30.06	26.95
FeO	0.51	0.49	0.61	0.68	0.45	0.56	0.38	0.46	0.67	0.58	0.64	0.62	0.39
Fe ₂ O ₃	0.56	0.54	0.68	0.75	0.50	0.63	0.42	0.51	0.75	0.64	0.71	0.69	0.44
MgO	0.02	0.03	0.03	0.04	0.03	0.02	0.01	0.04	0.05	0.05	0.04	0.04	0.04
CaO	8.67	9.70	15.22	14.46	8.71	14.66	8.76	8.88	14.89	15.00	17.34	12.01	8.57
Na ₂ O	5.70	5.31	2.72	2.55	5.71	2.68	5.93	5.93	2.88	2.91	1.61	4.47	5.93
K ₂ O	0.71	0.64	0.19	0.19	0.73	0.21	0.75	0.70	0.19	0.18	0.09	0.37	0.74
Total	100.19	100.42	101.40	99.61	100.64	100.23	100.60	101.48	101.04	101.42	101.75	102.06	100.84
An	43.72	48.33	74.76	74.91	43.76	74.20	43.00	43.43	73.24	73.25	85.20	58.43	42.49
Ab	52.00	47.88	24.13	23.92	51.89	24.56	52.62	52.48	25.65	25.70	14.28	39.41	53.17
Or	4.28	3.79	1.11	1.18	4.35	1.24	4.38	4.08	1.11	1.05	0.52	2.16	4.34
Cations													
Si	2.564	2.511	2.240	2.254	2.566	2.252	2.589	2.573	2.272	2.274	2.152	2.419	2.588
Al	1.444	1.493	1.755	1.754	1.443	1.753	1.405	1.426	1.715	1.711	1.837	1.574	1.413
Ti	0.001	0.001	0.001	0.001	0.000	0.001	0.001	0.000	0.000	0.002	0.000	0.000	0.001
Fe ³⁺	0.019	0.018	0.023	0.026	0.017	0.021	0.014	0.017	0.026	0.022	0.024	0.023	0.015
Mg	0.001	0.001	0.001	0.001	0.001	0.001	0.000	0.001	0.002	0.002	0.001	0.001	0.001
Ca	0.416	0.466	0.737	0.711	0.416	0.716	0.419	0.421	0.723	0.725	0.841	0.572	0.409
Na	0.495	0.462	0.238	0.227	0.494	0.237	0.513	0.509	0.253	0.254	0.141	0.386	0.511
K	0.041	0.037	0.011	0.011	0.041	0.012	0.043	0.040	0.011	0.010	0.005	0.021	0.042
Total	4.98	4.99	5.01	4.99	4.98	4.99	4.98	4.99	5.00	5.00	5.00	5.00	4.98

Analysis ID relates to crystal number_spot number. All Fe assumed to be Fe₂O₃. Cations calculated on a 8 oxygen basis.

Table A2.3 Major element plagioclase compositions analysed by EMPA.

Sample ID	Korito zone	P22_4	Korito sieved	P22_5	Korito sieved	P23_3	Korito sieved	P23_6	Korito core	P24_2	Korito zone	P24_3	Korito core
SiO ₂	59.13	50.19	51.54	49.58	53.14	53.18							
TiO ₂	0.06	0.03	0.04	0.00	0.06	0.01							
Al ₂ O ₃	25.84	31.86	30.96	33.10	30.59	30.67							
FeO	0.36	0.55	0.52	0.54	0.58	0.55							
Fe ₂ O ₃	0.40	0.61	0.58	0.60	0.64	0.61							
MgO	0.02	0.03	0.02	0.02	0.04	0.05							
CaO	7.58	14.91	13.32	15.76	12.62	12.68							
Na ₂ O	6.43	2.89	3.31	2.50	4.02	4.07							
K ₂ O	0.93	0.19	0.25	0.15	0.35	0.32							
Total	100.38	100.71	100.00	101.72	101.47	101.56							
An	37.31	73.21	67.96	77.00	62.12	62.11							
Ab	57.25	25.67	30.54	22.12	35.80	36.04							
Or	5.44	1.12	1.50	0.88	2.07	1.85							
Cations													
Si	2.638	2.280	2.343	2.234	2.380	2.379							
Al	1.359	1.705	1.659	1.758	1.615	1.617							
Ti	0.002	0.001	0.001	0.000	0.002	0.000							
Fe ³⁺	0.013	0.021	0.020	0.020	0.022	0.020							
Mg	0.001	0.001	0.001	0.001	0.001	0.002							
Ca	0.362	0.726	0.649	0.761	0.606	0.608							
Na	0.556	0.254	0.292	0.219	0.349	0.353							
K	0.053	0.011	0.014	0.009	0.020	0.018							
Total	4.98	5.00	4.98	5.00	4.99	5.00							

Analysis ID relates to crystal number_spot number. All Fe assumed to be Fe₂O₃. Cations calculated on a 8 oxygen basis.

Table A2.4 Major element clinopyroxene compositions analysed by EMPA.

Sample ID	Zone	Kaupokonui rim	Kaupokonui zone	Kaupokonui rim	Kaupokonui zone	Kaupokonui rim	Kaupokonui zone	Kaupokonui rim	Kaupokonui zone	Kaupokonui rim	Kaupokonui zone	Kaupokonui rim	Kaupokonui zone	Kaupokonui rim	Kaupokonui zone
		cpx4_2	cpx4_3	cpx4_4	cpx4_7	cpx4_11	cpx6_1	cpx6_3	cpx6_4	cpx7_3	cpx7_4	cpx7_3	cpx7_4	cpx7_3	cpx7_4
SiO ₂		53.41	54.45	53.90	53.67	52.25	50.47	52.86	52.77	53.61	52.77	52.86	52.77	53.61	52.77
TiO ₂		0.27	0.22	0.29	0.26	0.65	0.58	0.30	0.33	0.18	0.33	0.30	0.33	0.18	0.33
Al ₂ O ₃		2.20	1.06	1.86	2.11	3.47	3.37	2.00	1.92	0.81	1.92	2.00	1.92	0.81	1.92
Cr ₂ O ₃															
Fe ₂ O ₃		1.91	0.93	1.58	1.40	2.36	3.74	2.51	2.12	1.66	2.12	2.51	2.12	1.66	2.12
FeO		7.33	6.61	7.16	4.21	5.86	4.94	5.04	5.46	5.91	5.46	5.04	5.46	5.91	5.46
MnO		0.72	0.78	0.74	0.21	0.42	0.52	0.43	0.50	0.84	0.50	0.43	0.50	0.84	0.50
MgO		14.97	16.47	15.65	17.15	15.54	15.34	15.70	15.35	15.61	15.35	15.70	15.35	15.61	15.35
CaO		20.78	20.90	20.74	21.93	20.93	20.57	21.89	21.94	21.67	21.94	21.89	21.94	21.67	21.94
Na ₂ O		0.60	0.39	0.51	0.29	0.50	0.39	0.43	0.43	0.42	0.43	0.43	0.43	0.42	0.43
Total		102.20	101.81	102.44	101.22	101.98	99.91	101.17	100.82	100.70	100.82	101.17	100.82	100.70	100.82
Mg#		78.53	81.66	79.64	87.94	82.63	84.82	84.81	83.44	82.54	83.44	84.81	83.44	82.54	83.44
En		44.03	46.80	45.30	48.64	45.91	46.68	45.85	44.94	45.27	44.94	45.85	44.94	45.27	44.94
Fs		12.04	10.51	11.58	6.67	9.65	8.35	8.21	8.92	9.58	8.92	8.21	8.92	9.58	8.92
Wo		43.93	42.69	43.12	44.70	44.44	44.97	45.94	46.14	45.16	46.14	45.94	46.14	45.16	46.14
Si (Cations)		1.949	1.976	1.956	1.945	1.904	1.888	1.941	1.945	1.977	1.945	1.941	1.945	1.977	1.945
Ti		0.007	0.006	0.008	0.007	0.018	0.016	0.008	0.009	0.005	0.009	0.008	0.009	0.005	0.009
Al		0.095	0.045	0.079	0.090	0.149	0.149	0.086	0.083	0.035	0.083	0.086	0.083	0.035	0.083
Cr															
Fe ³⁺		0.052	0.025	0.043	0.038	0.064	0.104	0.069	0.058	0.046	0.058	0.069	0.058	0.046	0.058
Fe ²⁺		0.223	0.200	0.217	0.127	0.177	0.153	0.154	0.167	0.182	0.167	0.154	0.167	0.182	0.167
Mn		0.022	0.024	0.023	0.007	0.013	0.016	0.013	0.016	0.026	0.016	0.013	0.016	0.026	0.016
Mg		0.814	0.891	0.847	0.927	0.844	0.856	0.859	0.844	0.858	0.844	0.859	0.844	0.858	0.844
Ca		0.812	0.813	0.806	0.852	0.817	0.824	0.861	0.866	0.856	0.866	0.861	0.866	0.856	0.866
Na		0.043	0.027	0.036	0.020	0.035	0.028	0.031	0.031	0.030	0.031	0.031	0.031	0.030	0.031
Total		4.02	4.01	4.01	4.01	4.02	4.04	4.02	4.02	4.02	4.02	4.02	4.02	4.02	4.02

Abbreviations same as Table A2.3. Cations calculated on a 6 oxygen basis.

Table A2.4 Major element clinopyroxene compositions analysed by EMPA.

Sample ID	Kaupokonui dark zone	Kaupokonui rim	Kaupokonui core	Kaupokonui rim	Kaupokonui rim	Kaupokonui rim	Kaupokonui dark zone	Kaupokonui core	Kaupokonui rim	Kaupokonui rim	Kaupokonui dark zone
Zone	cpx7_5	cpx7_6	cpx8_3	cpx8_9	cpx9_1	cpx9_2	cpx9_5	cpx10_1	cpx10_2	cpx10_2	dark zone
SiO ₂	53.10	50.72	52.71	53.45	51.57	52.25	52.76	52.72	53.66	53.66	53.66
TiO ₂	0.25	0.62	0.42	0.23	0.56	0.36	0.45	0.29	0.27	0.27	0.27
Al ₂ O ₃	1.43	4.40	2.23	2.05	3.98	2.28	2.35	2.00	1.54	1.54	1.54
Cr ₂ O ₃											
Fe ₂ O ₃	1.88	2.99	2.51	1.19	3.20	2.79	2.38	1.72	2.08	2.08	2.08
FeO	5.17	5.72	5.60	4.30	5.08	4.60	5.46	5.89	5.02	5.02	5.02
MnO	0.52	0.32	0.64	0.14	0.31	0.43	0.50	0.36	0.51	0.51	0.51
MgO	15.71	14.42	15.33	17.93	15.24	15.98	15.16	15.97	16.51	16.51	16.51
CaO	22.06	21.58	21.56	21.20	21.76	21.38	21.90	21.34	21.63	21.63	21.63
Na ₂ O	0.39	0.41	0.49	0.12	0.39	0.42	0.53	0.28	0.38	0.38	0.38
Total	100.52	101.17	101.50	100.60	102.09	100.48	101.50	100.58	101.60	101.60	101.60
Mg#	84.47	81.91	83.09	88.18	84.34	86.16	83.27	82.90	85.49	85.49	85.49
En	45.60	43.55	45.17	50.40	45.22	47.13	44.66	46.16	47.37	47.37	47.37
Fs	8.39	9.62	9.19	6.76	8.39	7.57	8.97	9.52	8.04	8.04	8.04
Wo	46.02	46.84	45.64	42.84	46.39	45.31	46.36	44.32	44.60	44.60	44.60
Si (Cations)	1.958	1.874	1.934	1.943	1.883	1.930	1.934	1.942	1.954	1.954	1.954
Ti	0.007	0.017	0.012	0.006	0.015	0.010	0.012	0.008	0.007	0.007	0.007
Al	0.062	0.192	0.097	0.088	0.171	0.099	0.102	0.087	0.066	0.066	0.066
Cr											
Fe ³⁺	0.052	0.082	0.069	0.032	0.087	0.077	0.065	0.048	0.057	0.057	0.057
Fe ²⁺	0.159	0.175	0.171	0.130	0.154	0.141	0.166	0.181	0.152	0.152	0.152
Mn	0.016	0.010	0.020	0.004	0.010	0.014	0.016	0.011	0.016	0.016	0.016
Mg	0.864	0.794	0.839	0.972	0.830	0.880	0.829	0.877	0.896	0.896	0.896
Ca	0.872	0.854	0.847	0.826	0.851	0.846	0.860	0.842	0.844	0.844	0.844
Na	0.028	0.029	0.035	0.009	0.028	0.030	0.038	0.020	0.027	0.027	0.027
Total	4.02	4.03	4.02	4.01	4.03	4.03	4.02	4.02	4.02	4.02	4.02

Abbreviations same as Table A2.3. Cations calculated on a 6 oxygen basis.

Table A2.4 Major element clinopyroxene compositions analysed by EMPA.

Sample ID	Zone	Kaupokonui cpx10_3	Kaupokonui cpx10_5	Kaupokonui rim cpx11_1	Kaupokonui core cpx11_3	Kaupokonui core cpx11_7	Kaupokonui zone cpx11_8	Kaupokonui core cpx16_1	Kaupokonui rim cpx16_6	Kaupokonui core cpx16_7
SiO ₂	53.47	52.41	52.96	51.73	53.51	52.28	53.83	52.52	52.25	52.25
TiO ₂	0.28	0.39	0.24	0.25	0.37	0.34	0.27	0.31	0.31	0.31
Al ₂ O ₃	1.68	2.15	1.73	2.11	1.91	2.66	1.66	2.60	2.67	2.67
Cr ₂ O ₃										
Fe ₂ O ₃	1.66	2.74	2.30	3.66	2.22	2.13	1.85	2.04	3.00	3.00
FeO	5.54	4.92	5.12	5.65	5.95	6.08	5.82	6.78	5.87	5.87
MnO	0.50	0.55	0.53	0.69	0.44	0.29	0.63	0.54	0.53	0.53
MgO	16.08	15.31	15.67	14.51	16.84	14.93	15.89	14.47	14.63	14.63
CaO	21.50	21.93	21.84	21.24	20.18	22.20	21.80	21.39	21.43	21.43
Na ₂ O	0.42	0.48	0.43	0.59	0.45	0.31	0.42	0.56	0.62	0.62
Total	101.14	100.87	100.83	100.42	101.86	101.23	102.16	101.20	101.33	101.33
Mg#	83.86	84.81	84.57	82.20	83.54	81.48	83.02	79.26	81.73	81.73
En	46.44	45.28	45.79	44.09	48.59	43.55	45.66	43.03	43.94	43.94
Fs	8.94	8.11	8.35	9.55	9.57	9.90	9.34	11.26	9.82	9.82
Wo	44.62	46.61	45.86	46.36	41.83	46.55	45.01	45.71	46.24	46.24
Si (Cations)	1.956	1.934	1.950	1.934	1.945	1.924	1.955	1.936	1.928	1.928
Ti	0.008	0.011	0.007	0.007	0.010	0.010	0.007	0.009	0.009	0.009
Al	0.072	0.093	0.075	0.093	0.082	0.115	0.071	0.113	0.116	0.116
Cr										
Fe ³⁺	0.046	0.075	0.063	0.102	0.060	0.059	0.050	0.056	0.083	0.083
Fe ²⁺	0.169	0.151	0.157	0.175	0.180	0.186	0.176	0.208	0.180	0.180
Mn	0.015	0.017	0.017	0.022	0.013	0.009	0.019	0.017	0.017	0.017
Mg	0.877	0.842	0.860	0.809	0.913	0.819	0.860	0.795	0.805	0.805
Ca	0.843	0.867	0.862	0.850	0.786	0.875	0.848	0.845	0.847	0.847
Na	0.030	0.034	0.031	0.043	0.032	0.022	0.029	0.040	0.044	0.044
Total	4.02	4.03	4.02	4.03	4.02	4.02	4.02	4.02	4.03	4.03

Abbreviations same as Table A2.3. Cations calculated on a 6 oxygen basis.

Table A2.4 Major element clinopyroxene compositions analysed by EMPA.

Sample ID	Kaupokonui rim	Kaupokonui dark zone	Kaupokonui cpx22_2 zone	Kaupokonui cpx22_3 zone	Kaupokonui cpx22_6 core	Kaupokonui cpx27_1 rim	Kaupokonui cpx27_2 zone	Kaupokonui cpx27_5 zone	Kaupokonui cpx27_6 zone	Kaupokonui cpx27_7 zone
SiO ₂	53.23	52.58	53.07	53.76	53.38	49.52	52.87	52.24	53.02	
TiO ₂	0.40	0.38	0.29	0.25	0.28	0.58	0.32	0.31	0.26	
Al ₂ O ₃	2.03	2.12	1.98	1.55	1.82	5.39	3.10	2.55	1.56	
Cr ₂ O ₃										
Fe ₂ O ₃	2.18	2.64	2.60	1.71	1.89	3.63	1.70	2.13	2.17	
FeO	5.95	4.77	6.03	5.32	5.56	6.48	3.86	6.74	5.30	
MnO	0.69	0.53	0.67	0.59	0.50	0.31	0.17	0.61	0.58	
MgO	16.03	16.02	14.93	16.07	16.17	12.71	17.35	14.45	15.78	
CaO	20.72	21.47	21.31	21.89	21.69	22.43	21.52	21.16	21.74	
Na ₂ O	0.49	0.41	0.68	0.41	0.31	0.35	0.21	0.56	0.39	
Total	101.72	100.92	101.57	101.56	101.60	101.41	101.10	100.73	100.80	
Mg#	82.84	85.77	81.61	84.39	83.90	77.91	88.95	79.34	84.21	
En	46.82	46.97	44.43	46.22	46.38	39.19	49.62	43.23	45.93	
Fs	9.70	7.79	10.01	8.55	8.90	11.11	6.16	11.26	8.61	
Wo	43.48	45.23	45.56	45.23	44.71	49.70	44.22	45.51	45.46	
Si (Cations)	1.943	1.934	1.949	1.959	1.947	1.844	1.917	1.936	1.953	
Ti	0.011	0.011	0.008	0.007	0.008	0.016	0.009	0.009	0.007	
Al	0.087	0.092	0.086	0.067	0.078	0.237	0.132	0.111	0.068	
Cr										
Fe ³⁺	0.060	0.073	0.071	0.047	0.052	0.101	0.046	0.059	0.060	
Fe ²⁺	0.181	0.146	0.184	0.162	0.169	0.200	0.117	0.208	0.163	
Mn	0.021	0.017	0.021	0.018	0.015	0.010	0.005	0.019	0.018	
Mg	0.872	0.878	0.818	0.873	0.879	0.706	0.938	0.798	0.867	
Ca	0.810	0.846	0.838	0.855	0.847	0.895	0.836	0.840	0.858	
Na	0.035	0.029	0.048	0.029	0.022	0.026	0.015	0.040	0.028	
Total	4.02	4.02	4.02	4.02	4.02	4.03	4.02	4.02	4.02	

Abbreviations same as Table A2.3. Cations calculated on a 6 oxygen basis.

Table A2.4 Major element clinopyroxene compositions analysed by EMPA.

Sample ID	Zone	Kaupokonui cpx27_9 core	Kaupokonui cpx27_11 core	Kaupokonui cpx33_1 rim	Kaupokonui cpx33_7 core	Kaupokonui cpx33_9 core	Kaupokonui cpx34_1 rim	Kaupokonui cpx35_2 rim	Kaupokonui cpx35_5 core	Kaupokonui cpx64_1 rim
	SiO ₂	53.61	53.14	52.30	52.99	53.84	53.08	52.32	51.65	53.19
	TiO ₂	0.31	0.29	0.30	0.34	0.25	0.38	0.39	0.58	0.30
	Al ₂ O ₃	1.66	2.27	2.22	2.54	1.39	2.04	4.14	3.53	1.77
	Cr ₂ O ₃									
	Fe ₂ O ₃	1.62	1.54	2.91	1.71	1.25	2.93	2.91	3.80	1.79
	FeO	5.32	6.73	4.42	7.51	6.50	4.39	2.86	4.96	5.27
	MnO	0.59	0.66	0.61	0.75	0.67	0.53	0.12	0.43	0.54
	MgO	16.06	14.87	15.86	14.98	15.53	15.78	16.31	14.54	16.04
	CaO	21.93	21.49	21.71	20.56	21.99	22.60	23.32	22.55	21.77
	Na ₂ O	0.38	0.52	0.37	0.52	0.34	0.40	0.22	0.46	0.35
	Total	101.48	101.48	100.70	101.89	101.77	102.14	102.58	102.51	101.02
	Mg#	84.37	79.82	86.55	78.13	81.04	86.59	91.10	84.05	84.49
	En	46.17	43.63	46.74	44.12	44.41	45.78	47.04	43.39	46.32
	Fs	8.55	11.03	7.26	12.35	10.39	7.09	4.60	8.23	8.50
	Wo	45.29	45.33	45.99	43.53	45.20	47.13	48.36	48.37	45.18
	Si (Cations)	1.955	1.947	1.930	1.939	1.964	1.933	1.883	1.890	1.949
	Ti	0.008	0.008	0.008	0.009	0.007	0.010	0.011	0.016	0.008
	Al	0.071	0.098	0.096	0.110	0.060	0.088	0.176	0.152	0.076
	Cr									
	Fe ³⁺	0.044	0.042	0.080	0.047	0.034	0.080	0.078	0.104	0.049
	Fe ²⁺	0.162	0.205	0.136	0.229	0.198	0.133	0.086	0.150	0.161
	Mn	0.018	0.020	0.019	0.023	0.021	0.016	0.004	0.013	0.017
	Mg	0.873	0.812	0.872	0.817	0.844	0.857	0.875	0.793	0.876
	Ca	0.856	0.844	0.858	0.806	0.860	0.882	0.899	0.884	0.855
	Na	0.027	0.037	0.027	0.037	0.024	0.028	0.015	0.033	0.025
	Total	4.01	4.01	4.03	4.02	4.01	4.03	4.03	4.03	4.02

Abbreviations same as Table A2.3. Cations calculated on a 6 oxygen basis.

Table A2.4 Major element clinopyroxene compositions analysed by EMPA.

Sample ID	Kaupokonui dark zone	Kaupokonui cpx64_2	Kaupokonui cpx64_3	Kaupokonui cpx64_4	Kaupokonui cpx64_6	Kaupokonui cpx64_7	Kaupokonui cpx64_9	Kaupokonui cpx66_4	Kaupokonui cpx66_10	Kaupokonui cpx66_12
Zone	zone	zone	zone	zone	zone	zone	core	zone	core	core
SiO ₂	52.78	51.61	52.08	53.44	52.41	52.14	52.14	53.10	54.01	53.13
TiO ₂	0.31	0.41	0.34	0.26	0.32	0.40	0.40	0.26	0.22	0.38
Al ₂ O ₃	1.81	3.32	2.41	1.44	2.38	2.45	2.45	1.71	1.30	2.20
Cr ₂ O ₃										
Fe ₂ O ₃	2.66	3.24	3.10	2.01	3.23	3.46	3.46	1.99	1.49	2.15
FeO	5.43	5.47	5.91	5.29	5.82	5.60	5.60	5.91	6.77	5.54
MnO	0.79	0.28	0.57	0.59	0.68	0.65	0.65	0.67	0.70	0.64
MgO	16.58	14.91	14.64	15.93	15.08	15.10	15.10	14.82	14.67	15.55
CaO	20.15	22.14	21.40	22.05	21.05	21.08	21.08	22.16	22.36	21.91
Na ₂ O	0.40	0.31	0.57	0.35	0.57	0.56	0.56	0.51	0.55	0.42
Total	100.91	101.69	101.02	101.37	101.54	101.44	101.44	101.13	102.08	101.92
Mg#	84.57	83.04	81.64	84.37	82.30	82.90	82.90	81.79	79.49	83.41
En	48.64	44.02	43.96	45.88	45.07	45.26	45.26	43.52	42.50	45.22
Fs	8.88	8.99	9.88	8.50	9.69	9.34	9.34	9.69	10.96	9.00
Wo	42.49	46.99	46.16	45.62	45.23	45.40	45.40	46.79	46.54	45.79
Si (Cations)	1.942	1.898	1.930	1.956	1.930	1.924	1.924	1.956	1.972	1.937
Ti	0.009	0.011	0.009	0.007	0.009	0.011	0.011	0.007	0.006	0.010
Al	0.079	0.144	0.105	0.062	0.103	0.107	0.107	0.074	0.056	0.095
Cr										
Fe ³⁺	0.073	0.089	0.086	0.055	0.089	0.095	0.095	0.055	0.041	0.059
Fe ²⁺	0.166	0.167	0.182	0.161	0.178	0.171	0.171	0.181	0.206	0.168
Mn	0.025	0.009	0.018	0.018	0.021	0.020	0.020	0.021	0.022	0.020
Mg	0.909	0.817	0.809	0.869	0.828	0.831	0.831	0.813	0.799	0.845
Ca	0.794	0.872	0.849	0.864	0.831	0.833	0.833	0.874	0.874	0.856
Na	0.029	0.022	0.041	0.025	0.041	0.040	0.040	0.037	0.039	0.030
Total	4.02	4.03	4.03	4.02	4.03	4.03	4.03	4.02	4.01	4.02

Abbreviations same as Table A2.3. Cations calculated on a 6 oxygen basis.

Table A2.4 Major element clinopyroxene compositions analysed by EMPA.

Sample ID	Kaupokonui rim	Kaupokonui dark zone	Kaupokonui cpx67_2	Kaupokonui cpx67_3	Kaupokonui cpx67_4	Kaupokonui cpx67_5	Kaupokonui cpx67_6	Kaupokonui core	SM-6C cpx1_1 rim	SM-6C cpx1_2 zone
Zone										
SiO ₂	52.95	53.05	53.34	53.47	49.68	51.94	53.13	52.85	51.34	51.34
TiO ₂	0.34	0.32	0.26	0.25	0.70	0.39	0.34	0.44	0.59	0.59
Al ₂ O ₃	2.04	1.72	1.56	1.35	5.77	3.37	1.75	2.12	2.67	2.67
Cr ₂ O ₃										
Fe ₂ O ₃	1.63	2.72	1.75	1.61	3.49	2.87	2.31	1.39	2.44	2.44
FeO	5.84	4.53	5.83	5.45	5.61	5.66	5.69	6.41	6.06	6.06
MnO	0.51	0.58	0.61	0.60	0.27	0.30	0.67	0.41	0.42	0.42
MgO	15.69	16.45	15.23	16.01	13.41	14.75	15.05	16.00	15.74	15.74
CaO	21.53	21.39	22.11	21.89	22.20	22.07	22.13	20.85	20.35	20.35
Na ₂ O	0.37	0.42	0.46	0.33	0.40	0.43	0.50	0.34	0.29	0.29
Total	100.90	101.18	101.15	100.97	101.54	101.77	101.55	100.80	99.92	99.92
Mg#	82.79	86.70	82.38	84.01	81.12	82.38	82.58	81.70	82.32	82.32
En	45.59	47.91	44.31	46.03	41.28	43.68	44.09	46.29	46.64	46.64
Fs	9.48	7.35	9.47	8.76	9.61	9.34	9.30	10.37	10.02	10.02
Wo	44.93	44.74	46.22	45.21	49.11	46.97	46.60	43.34	43.34	43.34
Si (Cations)	1.945	1.944	1.959	1.961	1.837	1.905	1.950	1.941	1.912	1.912
Ti	0.009	0.009	0.007	0.007	0.019	0.011	0.009	0.012	0.016	0.016
Al	0.088	0.074	0.067	0.058	0.252	0.146	0.076	0.092	0.117	0.117
Cr										
Fe ³⁺	0.045	0.075	0.048	0.044	0.096	0.079	0.063	0.038	0.068	0.068
Fe ²⁺	0.179	0.138	0.178	0.167	0.172	0.172	0.174	0.196	0.188	0.188
Mn	0.016	0.018	0.019	0.019	0.008	0.009	0.021	0.013	0.013	0.013
Mg	0.859	0.899	0.834	0.876	0.739	0.807	0.823	0.876	0.874	0.874
Ca	0.847	0.839	0.870	0.860	0.880	0.867	0.870	0.820	0.812	0.812
Na	0.027	0.030	0.033	0.024	0.029	0.030	0.036	0.024	0.021	0.021
Total	4.02	4.03	4.02	4.01	4.03	4.03	4.02	4.01	4.02	4.02

Abbreviations same as Table A2.3. Cations calculated on a 6 oxygen basis.

Table A2.4 Major element clinopyroxene compositions analysed by EMPA.

Sample ID	SM-6C cpx1_3 core	SM-6C cpx2_1 rim	SM-6C cpx2_2 zone	SM-6C cpx2_3 zone	SM-6C cpx2_4 core	SM-6C cpx6_1 core	SM-6C cpx6_5 rim	SM-6C cpx9_1 rim	SM-6C cpx9_4 core	SM-6C cpx9_5 light zone
Zone										
SiO ₂	52.16	52.58	52.23	52.48	52.68	52.45	53.77	52.49	52.70	51.84
TiO ₂	0.52	0.43	0.49	0.39	0.32	0.34	0.37	0.39	0.25	0.33
Al ₂ O ₃	2.72	2.15	2.44	2.28	1.95	2.42	1.91	1.80	1.46	2.56
Cr ₂ O ₃										
Fe ₂ O ₃	1.90	2.42	1.80	1.95	1.71	1.80	0.75	-0.09	0.90	1.16
FeO	6.34	5.61	6.25	6.64	5.79	7.29	7.09	7.81	7.00	8.09
MnO	0.39	0.41	0.38	0.40	0.45	0.59	0.40	0.42	0.69	0.66
MgO	15.71	16.12	15.85	15.17	15.30	14.29	16.26	15.72	14.64	13.59
CaO	20.62	20.95	20.73	21.00	21.99	21.20	20.83	19.88	21.68	21.11
Na ₂ O	0.37	0.37	0.32	0.47	0.35	0.55	0.32	0.30	0.37	0.49
Total	100.74	101.04	100.48	100.77	100.54	100.91	101.70	98.71	99.70	99.82
Mg#	81.62	83.75	81.95	80.35	82.53	77.83	80.37	78.21	78.90	75.02
En	46.11	47.00	46.29	44.66	44.55	42.54	46.19	45.71	42.88	40.83
Fs	10.39	9.12	10.20	10.92	9.43	12.11	11.28	12.74	11.47	13.60
Wo	43.50	43.88	43.51	44.42	46.02	45.35	42.52	41.55	45.65	45.58
Si (Cations)	1.922	1.932	1.928	1.938	1.945	1.941	1.953	1.961	1.966	1.941
Ti	0.015	0.012	0.014	0.011	0.009	0.009	0.010	0.011	0.007	0.009
Al	0.118	0.093	0.106	0.099	0.085	0.105	0.082	0.079	0.064	0.113
Cr										
Fe ³⁺	0.053	0.067	0.050	0.054	0.047	0.050	0.020	-0.003	0.025	0.033
Fe ²⁺	0.194	0.171	0.192	0.204	0.178	0.225	0.215	0.244	0.218	0.253
Mn	0.012	0.013	0.012	0.012	0.014	0.018	0.012	0.013	0.022	0.021
Mg	0.863	0.883	0.872	0.835	0.842	0.788	0.881	0.875	0.814	0.759
Ca	0.814	0.825	0.820	0.831	0.870	0.841	0.811	0.796	0.866	0.847
Na	0.026	0.026	0.023	0.033	0.025	0.039	0.022	0.022	0.026	0.036
Total	4.02	4.02	4.02	4.02	4.02	4.02	4.01	4.00	4.01	4.01

Abbreviations same as Table A2.3. Cations calculated on a 6 oxygen basis.

Table A2.4 Major element clinopyroxene compositions analysed by EMPA.

Sample ID	SM-6C cpx15_1 rim	SM-6C cpx15_4 core	SM-6C cpx15_6 light zone	SM-6C cpx16_1 rim	SM-6C cpx16_4 light zone	SM-6C cpx16_7 core	SM-6C cpx18_1 rim	SM-6C cpx18_4 zone	SM-6C cpx20_1 rim	SM-6C cpx20_4 light zone
Zone										
SiO ₂	53.77	53.31	54.06	52.78	53.01	55.50	51.98	49.16	52.96	52.06
TiO ₂	0.35	0.58	0.34	0.40	0.30	0.27	0.63	0.93	0.39	0.32
Al ₂ O ₃	1.92	3.07	2.54	2.20	2.39	1.31	4.45	6.17	1.55	2.14
Cr ₂ O ₃										
Fe ₂ O ₃	0.26	0.04	0.53	1.56	0.99	-1.31	1.22	3.75	0.52	1.40
FeO	8.12	7.94	8.73	6.26	8.18	8.75	6.59	5.57	7.53	7.62
MnO	0.43	0.51	0.62	0.36	0.67	0.64	0.22	0.20	0.53	0.67
MgO	16.35	15.23	14.36	16.07	14.20	16.06	14.66	13.79	16.16	13.84
CaO	19.72	20.65	21.22	20.82	20.88	20.82	21.89	21.27	19.97	21.30
Na ₂ O	0.36	0.48	0.61	0.34	0.60	0.41	0.38	0.45	0.27	0.50
Total	101.27	101.81	103.00	100.79	101.22	102.44	102.01	101.30	99.89	99.85
Mg#	78.21	77.38	74.59	82.13	75.61	76.53	79.91	81.66	79.30	76.47
En	46.61	44.11	41.62	46.53	42.03	44.68	43.02	42.87	46.54	41.43
Fs	12.98	12.90	14.18	10.13	13.56	13.70	10.82	9.63	12.15	12.75
Wo	40.40	42.99	44.20	43.34	44.41	41.62	46.16	47.50	41.32	45.82
Si (Cations)	1.960	1.935	1.953	1.939	1.952	1.991	1.890	1.821	1.960	1.949
Ti	0.010	0.016	0.009	0.011	0.008	0.007	0.017	0.026	0.011	0.009
Al	0.082	0.131	0.108	0.095	0.104	0.056	0.191	0.269	0.068	0.094
Cr										
Fe ³⁺	0.007	0.001	0.014	0.043	0.027	-0.036	0.033	0.104	0.015	0.039
Fe ²⁺	0.247	0.241	0.264	0.192	0.251	0.263	0.200	0.171	0.233	0.238
Mn	0.013	0.016	0.019	0.011	0.021	0.019	0.007	0.006	0.017	0.021
Mg	0.888	0.824	0.773	0.880	0.779	0.859	0.795	0.761	0.892	0.773
Ca	0.770	0.803	0.821	0.820	0.824	0.800	0.853	0.844	0.792	0.854
Na	0.025	0.034	0.043	0.024	0.043	0.028	0.027	0.032	0.019	0.036
Total	4.00	4.00	4.00	4.01	4.01	3.99	4.01	4.03	4.00	4.01

Abbreviations same as Table A2.3. Cations calculated on a 6 oxygen basis.

Table A2.4 Major element clinopyroxene compositions analysed by EMPA.

Sample ID	SM-6C cpx20_5 core	SM-6C cpx25_2 rim	SM-6C cpx25_4 zone	SM-6C cpx25_5 core	SM-6C cpx28_1 rim	SM-6C cpx28_3 light zone	SM-6C cpx28_6 core	SM-6C cpx29_1 rim	SM-6C cpx29_2 light zone	SM-6C cpx29_3 zone
SiO ₂	53.30	52.37	51.61	51.75	52.61	51.55	51.77	52.51	52.02	52.51
TiO ₂	0.28	0.44	0.37	0.29	0.41	0.44	0.46	0.46	0.44	0.47
Al ₂ O ₃	1.27	2.12	2.80	1.63	1.94	2.80	2.96	2.24	2.84	2.21
Cr ₂ O ₃										
Fe ₂ O ₃	0.21	0.65	2.10	1.71	0.52	1.53	1.84	1.42	1.80	1.65
FeO	7.83	7.14	6.91	5.81	7.57	7.69	6.34	6.61	7.60	6.30
MnO	0.69	0.44	0.46	0.48	0.46	0.49	0.35	0.41	0.47	0.38
MgO	14.57	15.41	13.95	14.71	15.76	14.26	14.56	15.81	14.57	15.96
CaO	21.70	20.62	21.36	21.84	20.08	20.09	21.73	20.63	20.35	20.80
Na ₂ O	0.36	0.34	0.54	0.36	0.31	0.59	0.40	0.35	0.54	0.31
Total	100.20	99.54	100.09	98.59	99.65	99.43	100.42	100.42	100.63	100.60
Mg#	76.86	79.40	78.34	81.92	78.79	76.83	80.44	81.05	77.44	81.92
En	42.17	45.03	42.07	43.71	45.77	43.21	43.18	46.05	43.58	46.35
Fs	12.70	11.68	11.63	9.65	12.32	13.03	10.50	10.77	12.69	10.23
Wo	45.13	43.29	46.30	46.64	41.91	43.76	46.32	43.18	43.73	43.42
Si (Cations)	1.976	1.947	1.928	1.952	1.952	1.933	1.920	1.938	1.928	1.935
Ti	0.008	0.012	0.010	0.008	0.011	0.012	0.013	0.013	0.012	0.013
Al	0.056	0.093	0.123	0.072	0.085	0.124	0.130	0.097	0.124	0.096
Cr										
Fe ³⁺	0.006	0.018	0.059	0.048	0.015	0.043	0.051	0.039	0.050	0.046
Fe ²⁺	0.242	0.222	0.215	0.183	0.235	0.240	0.196	0.203	0.235	0.193
Mn	0.022	0.014	0.014	0.015	0.015	0.015	0.011	0.013	0.015	0.012
Mg	0.805	0.854	0.777	0.827	0.872	0.797	0.805	0.870	0.805	0.877
Ca	0.862	0.821	0.855	0.883	0.798	0.807	0.863	0.816	0.808	0.821
Na	0.026	0.024	0.039	0.026	0.022	0.043	0.029	0.025	0.039	0.022
Total	4.00	4.01	4.02	4.02	4.00	4.01	4.02	4.01	4.02	4.02

Abbreviations same as Table A2.3. Cations calculated on a 6 oxygen basis.

Table A2.4 Major element clinopyroxene compositions analysed by EMPA.

Sample ID	SM-6C cpx29_4 core	SM-6C cpx31_1 rim	SM-6C cpx31_2 core	SM-6C cpx31_4 core	SM-6C cpx33_2 zone	SM-6C cpx33_3 core	SM-6C Pa core	SM-6C Pb rim	SM-6C Pc1 core	SM-6C Pc12 zone
SiO ₂	51.96	52.54	52.17	52.40	52.17	52.87	51.85	51.98	50.91	51.72
TiO ₂	0.37	0.44	0.49	0.49	0.53	0.34	0.53	0.75	0.58	0.73
Al ₂ O ₃	2.77	2.19	2.43	2.41	2.52	1.91	2.18	3.76	2.96	3.09
Cr ₂ O ₃							0.02	0.11	0.08	0.06
Fe ₂ O ₃	2.05	1.64	1.86	1.62	2.09	1.77	2.32	1.71	2.40	2.34
FeO	6.82	6.33	6.26	6.58	5.84	6.15	5.57	7.50	5.87	5.73
MnO	0.51	0.41	0.41	0.41	0.35	0.40	0.32	0.32	0.06	0.23
MgO	14.03	15.76	15.33	15.73	15.60	15.60	15.94	15.11	15.52	15.60
CaO	21.72	20.95	21.24	20.66	21.34	21.50	20.57	20.38	20.46	21.12
Na ₂ O	0.51	0.34	0.35	0.35	0.33	0.36	0.29	0.42	0.35	0.36
Total	100.73	100.60	100.54	100.66	100.77	100.89	99.59	102.05	99.17	101.00
Mg#	78.66	81.67	81.43	81.05	82.72	81.96	83.60	78.21	82.51	82.91
En	41.95	45.88	44.97	45.93	45.63	45.24	47.09	44.48	46.31	45.90
Fs	11.38	10.30	10.25	10.74	9.53	9.96	9.24	12.39	9.82	9.46
Wo	46.67	43.82	44.77	43.34	44.84	44.81	43.68	43.13	43.87	44.64
Si (Cations)	1.928	1.937	1.929	1.931	1.923	1.946	1.931	1.896	1.907	1.903
Ti	0.010	0.012	0.014	0.014	0.015	0.009	0.015	0.021	0.016	0.020
Al	0.121	0.095	0.106	0.105	0.109	0.083	0.096	0.162	0.131	0.134
Cr							0.001	0.003	0.002	0.002
Fe ³⁺	0.057	0.045	0.052	0.045	0.058	0.049	0.065	0.047	0.068	0.065
Fe ²⁺	0.211	0.195	0.193	0.202	0.179	0.188	0.174	0.229	0.184	0.176
Mn	0.016	0.013	0.013	0.013	0.011	0.013	0.010	0.010	0.002	0.007
Mg	0.776	0.867	0.845	0.865	0.858	0.856	0.885	0.822	0.867	0.856
Ca	0.863	0.827	0.841	0.816	0.843	0.847	0.821	0.797	0.821	0.832
Na	0.036	0.024	0.025	0.025	0.024	0.026	0.021	0.030	0.025	0.026
Total	4.02	4.02	4.02	4.01	4.02	4.02	4.02	4.02	4.02	4.02

Abbreviations same as Table A2.3. Cations calculated on a 6 oxygen basis.

Table A2.4 Major element clinopyroxene compositions analysed by EMPA.

Sample ID	SM-6C Pc20 zone	SM-6C Pc31 zone	SM-6C Pc46 rim	SM-6C PN_3 core	SM-6C PO_2 rim	SM-6C PQ_2 core	SM-6C PX_4 rim	Maketawa cpx1_1 rim	Maketawa cpx1_2 core	Maketawa cpx1_3 core
SiO ₂	49.97	50.62	52.10	50.73	50.20	50.20	52.32	52.10	51.89	52.38
TiO ₂	0.85	0.81	0.67	0.41	0.48	0.48	0.44	0.28	0.29	0.31
Al ₂ O ₃	3.85	3.62	2.85	2.49	2.50	2.47	2.18	1.49	2.19	1.89
Cr ₂ O ₃	0.09	0.06	0.22	0.05	0.06	0.06	0.04			
Fe ₂ O ₃	3.34	2.33	0.99	4.58	3.52	4.07	2.50	1.73	2.70	2.07
FeO	5.37	6.13	7.27	4.22	4.55	3.60	5.91	6.03	6.43	5.50
MnO	0.29	0.30	0.35	0.52	0.51	0.50	0.50	0.56	0.59	0.52
MgO	15.14	15.26	15.48	15.48	15.64	16.05	16.37	15.30	13.89	15.22
CaO	20.24	20.14	20.19	20.19	20.19	20.46	20.06	21.41	21.79	22.01
Na ₂ O	0.42	0.40	0.39	0.54	0.36	0.34	0.36	0.27	0.57	0.34
Total	99.57	99.67	100.51	99.21	98.01	98.22	100.68	99.18	100.34	100.23
Mg#	83.41	81.62	79.15	86.74	85.97	88.83	83.16	81.96	79.49	83.22
En	46.30	46.01	45.44	47.85	47.83	48.98	48.01	44.94	41.93	44.63
Fs	9.21	10.36	11.97	7.32	7.81	6.16	9.72	9.89	10.82	9.00
Wo	44.49	43.63	42.59	44.84	44.36	44.86	42.27	45.17	47.25	46.37
Si (Cations)	1.873	1.889	1.921	1.912	1.909	1.904	1.929	1.953	1.939	1.943
Ti	0.024	0.023	0.019	0.012	0.014	0.014	0.012	0.008	0.008	0.009
Al	0.170	0.159	0.124	0.111	0.112	0.111	0.095	0.066	0.097	0.083
Cr	0.003	0.002	0.006	0.002	0.002	0.002	0.001			
Fe ³⁺	0.094	0.065	0.028	0.130	0.101	0.116	0.069	0.049	0.075	0.057
Fe ²⁺	0.168	0.191	0.224	0.133	0.145	0.114	0.182	0.188	0.200	0.170
Mn	0.009	0.009	0.011	0.016	0.016	0.016	0.016	0.018	0.019	0.016
Mg	0.846	0.849	0.851	0.870	0.887	0.908	0.900	0.855	0.774	0.842
Ca	0.813	0.805	0.798	0.815	0.822	0.831	0.793	0.860	0.872	0.875
Na	0.031	0.029	0.028	0.039	0.027	0.025	0.026	0.020	0.042	0.025
Total	4.03	4.02	4.01	4.04	4.03	4.04	4.02	4.02	4.03	4.02

Abbreviations same as Table A2.3. Cations calculated on a 6 oxygen basis.

Table A2.4 Major element clinopyroxene compositions analysed by EMPA.

Sample ID	Maketawa cpx1_4 core	Maketawa cpx2_1 rim	Maketawa cpx2_2 zone	Maketawa cpx2_3 zone	Maketawa cpx2_4 zone	Maketawa cpx2_5 core	Maketawa cpx2_6 core	Maketawa cpx2_7 core	Maketawa cpx6_1 rim
SiO ₂	51.75	52.13	50.43	52.22	51.33	51.40	51.03	51.72	52.66
TiO ₂	0.31	0.29	0.53	0.30	0.36	0.30	0.28	0.34	0.28
Al ₂ O ₃	1.56	1.91	3.08	1.62	2.38	2.22	1.99	2.42	1.54
Cr ₂ O ₃									
Fe ₂ O ₃	2.66	2.18	2.87	2.00	3.28	2.14	3.14	2.40	1.54
FeO	5.44	6.03	6.37	5.79	6.37	5.56	4.42	7.29	5.83
MnO	0.99	0.49	0.37	0.48	0.60	0.60	0.61	0.57	0.60
MgO	14.29	14.73	13.56	14.93	13.62	14.53	14.86	13.25	15.57
CaO	21.92	22.17	22.06	22.22	21.74	21.91	21.86	21.86	21.61
Na ₂ O	0.48	0.32	0.36	0.30	0.58	0.35	0.39	0.59	0.30
Total	99.40	100.24	99.62	99.86	100.26	99.03	98.58	100.43	99.92
Mg#	82.48	81.41	79.26	82.20	79.34	82.41	85.80	76.51	82.70
En	43.19	43.29	41.14	43.74	41.53	43.54	44.99	40.11	45.32
Fs	9.18	9.89	10.76	9.47	10.82	9.29	7.44	12.32	9.48
Wo	47.63	46.82	48.10	46.79	47.65	47.17	47.57	47.57	45.20
Si (Cations)	1.949	1.941	1.902	1.948	1.927	1.935	1.932	1.936	1.955
Ti	0.009	0.008	0.015	0.008	0.010	0.009	0.008	0.010	0.008
Al	0.069	0.084	0.137	0.071	0.105	0.099	0.089	0.107	0.067
Cr									
Fe ³⁺	0.075	0.061	0.081	0.056	0.092	0.060	0.089	0.067	0.043
Fe ²⁺	0.170	0.187	0.200	0.180	0.198	0.174	0.139	0.227	0.180
Mn	0.031	0.016	0.012	0.015	0.019	0.019	0.020	0.018	0.019
Mg	0.802	0.817	0.762	0.830	0.762	0.816	0.839	0.739	0.862
Ca	0.884	0.884	0.892	0.888	0.875	0.884	0.887	0.876	0.859
Na	0.035	0.023	0.026	0.022	0.042	0.026	0.028	0.043	0.021
Total	4.03	4.02	4.03	4.02	4.03	4.02	4.03	4.02	4.01

Abbreviations same as Table A2.3. Cations calculated on a 6 oxygen basis.

Table A2.4 Major element clinopyroxene compositions analysed by EMPA.

Sample ID	Maketawa cpx6_2 zone	Maketawa cpx6_4 zone	Maketawa cpx6_5 zone	Maketawa cpx6_6 zone	Maketawa cpx6_9 core	Maketawa cpx8_1 rim	Maketawa cpx8_4 zone	Maketawa cpx8_5 zone	Maketawa cpx8_6 zone
SiO ₂	50.59	51.15	48.84	52.64	49.77	53.21	52.49	52.37	52.03
TiO ₂	0.34	0.35	0.73	0.20	0.69	0.24	0.21	0.22	0.35
Al ₂ O ₃	2.45	2.47	4.65	0.90	4.74	0.89	1.03	1.04	1.72
Cr ₂ O ₃									
Fe ₂ O ₃	2.44	2.23	3.31	0.92	2.27	1.39	1.51	1.48	1.50
FeO	6.03	5.67	6.84	6.23	4.11	6.10	6.27	6.14	6.88
MnO	0.28	0.31	0.46	0.91	0.27	0.62	0.90	0.94	0.97
MgO	13.82	14.34	11.88	14.44	14.06	16.05	14.75	15.29	14.62
CaO	22.31	22.39	22.30	22.40	22.66	20.81	21.89	21.10	21.00
Na ₂ O	0.29	0.27	0.45	0.33	0.36	0.40	0.32	0.31	0.37
Total	98.53	99.19	99.47	98.96	98.94	99.72	99.37	98.89	99.46
Mg#	80.43	81.93	75.73	80.54	85.97	82.49	80.81	81.66	79.17
En	41.61	42.69	37.45	42.43	43.08	46.65	43.40	45.11	43.57
Fs	10.12	9.42	12.01	10.25	7.03	9.90	10.30	10.13	11.46
Wo	48.27	47.89	50.54	47.32	49.89	43.45	46.30	44.76	44.97
Si (Cations)	1.923	1.924	1.860	1.978	1.867	1.975	1.969	1.968	1.951
Ti	0.010	0.010	0.021	0.006	0.020	0.007	0.006	0.006	0.010
Al	0.110	0.109	0.209	0.040	0.210	0.039	0.045	0.046	0.076
Cr									
Fe ³⁺	0.069	0.063	0.094	0.026	0.064	0.039	0.042	0.042	0.042
Fe ²⁺	0.190	0.178	0.216	0.195	0.128	0.189	0.196	0.192	0.215
Mn	0.009	0.010	0.015	0.029	0.009	0.020	0.028	0.030	0.031
Mg	0.783	0.805	0.674	0.809	0.787	0.888	0.825	0.857	0.818
Ca	0.908	0.903	0.910	0.902	0.911	0.828	0.880	0.850	0.844
Na	0.021	0.020	0.033	0.024	0.026	0.029	0.023	0.023	0.027
Total	4.02	4.02	4.03	4.01	4.02	4.01	4.01	4.01	4.01

Abbreviations same as Table A2.3. Cations calculated on a 6 oxygen basis.

Table A2.4 Major element clinopyroxene compositions analysed by EMPA.

Sample ID	Maketawa cpx8_7 zone	Maketawa cpx8_8 zone	Maketawa cpx8_9 zone	Maketawa cpx8_10 core	Maketawa cpx9_1 rim	Maketawa cpx9_2 zone	Maketawa cpx9_3 zone	Maketawa cpx9_4 zone	Maketawa cpx9_5 zone
SiO ₂	51.95	51.40	52.20	50.70	51.92	50.55	52.13	51.73	52.32
TiO ₂	0.25	0.30	0.24	0.40	0.31	0.38	0.24	0.32	0.21
Al ₂ O ₃	1.24	1.69	1.13	2.72	1.98	2.75	1.11	1.79	0.96
Cr ₂ O ₃									
Fe ₂ O ₃	2.23	1.62	1.74	2.25	2.25	2.70	2.25	1.30	1.63
FeO	5.47	7.50	6.01	6.44	5.45	5.54	4.88	6.64	5.70
MnO	0.82	0.66	0.85	0.37	0.47	0.26	0.62	0.55	0.70
MgO	14.95	13.87	14.97	13.61	15.22	14.09	15.36	14.34	14.56
CaO	21.79	21.73	21.59	22.21	21.55	22.46	21.82	21.76	22.30
Na ₂ O	0.33	0.23	0.31	0.32	0.37	0.25	0.38	0.33	0.40
Total	99.04	98.99	99.05	99.02	99.53	98.98	98.78	98.76	98.77
Mg#	83.04	76.80	81.67	79.12	83.35	82.02	84.94	79.42	82.05
En	44.41	41.18	44.23	41.05	45.10	42.28	45.50	42.56	43.11
Fs	9.07	12.44	9.93	10.83	9.01	9.27	8.06	11.03	9.43
Wo	46.52	46.38	45.84	48.12	45.89	48.45	46.44	46.42	47.46
Si (Cations)	1.956	1.947	1.963	1.919	1.940	1.911	1.961	1.951	1.972
Ti	0.007	0.009	0.007	0.011	0.009	0.011	0.007	0.009	0.006
Al	0.055	0.075	0.050	0.121	0.087	0.123	0.049	0.080	0.043
Cr									
Fe ³⁺	0.063	0.046	0.049	0.064	0.063	0.076	0.063	0.037	0.046
Fe ²⁺	0.171	0.237	0.188	0.203	0.169	0.174	0.153	0.209	0.179
Mn	0.026	0.021	0.027	0.012	0.015	0.008	0.020	0.018	0.022
Mg	0.839	0.783	0.839	0.768	0.848	0.794	0.861	0.806	0.818
Ca	0.879	0.882	0.870	0.900	0.863	0.910	0.879	0.879	0.901
Na	0.024	0.017	0.023	0.024	0.027	0.018	0.028	0.024	0.029
Total	4.02	4.02	4.02	4.02	4.02	4.03	4.02	4.01	4.02

Abbreviations same as Table A2.3. Cations calculated on a 6 oxygen basis.

Table A2.4 Major element clinopyroxene compositions analysed by EMPA.

Sample ID	Maketawa cpx9_6 zone	Maketawa cpx9_8 zone	Maketawa cpx9_11 core	Maketawa cpx10_2 rim	Maketawa cpx10_3 zone	Maketawa cpx10_4 zone	Maketawa cpx10_5 zone	Maketawa cpx10_6 zone	Maketawa cpx10_7 core
SiO ₂	52.28	52.27	51.75	51.84	51.43	52.26	50.65	52.57	52.11
TiO ₂	0.18	0.22	0.30	0.30	0.35	0.32	0.32	0.28	0.20
Al ₂ O ₃	0.94	1.07	1.46	1.83	2.39	1.86	2.36	1.38	1.65
Cr ₂ O ₃									
Fe ₂ O ₃	1.52	1.18	2.13	2.43	2.53	2.71	3.42	1.25	2.01
FeO	6.55	6.50	5.37	5.10	5.69	5.78	5.88	6.54	7.99
MnO	0.64	0.82	0.67	0.57	0.41	0.56	0.62	0.61	0.81
MgO	13.79	14.91	14.72	15.10	14.45	15.09	13.46	15.16	12.93
CaO	22.65	21.41	22.03	21.78	22.39	21.82	21.97	21.66	22.00
Na ₂ O	0.41	0.30	0.36	0.39	0.28	0.35	0.49	0.26	0.53
Total	98.96	98.69	98.79	99.35	99.93	100.76	99.17	99.70	100.24
Mg#	79.03	80.39	83.09	84.13	81.99	82.41	80.46	80.58	74.35
En	40.89	43.93	43.87	44.94	42.86	44.40	41.40	44.10	38.94
Fs	10.85	10.72	8.93	8.47	9.41	9.48	10.05	10.63	13.44
Wo	48.26	45.35	47.20	46.59	47.72	46.13	48.55	45.27	47.62
Si (Cations)	1.975	1.970	1.952	1.942	1.924	1.938	1.924	1.960	1.958
Ti	0.005	0.006	0.009	0.009	0.010	0.009	0.009	0.008	0.006
Al	0.042	0.048	0.065	0.081	0.106	0.081	0.105	0.061	0.073
Cr									
Fe ³⁺	0.043	0.033	0.060	0.068	0.071	0.075	0.097	0.035	0.057
Fe ²⁺	0.206	0.204	0.168	0.159	0.177	0.178	0.185	0.203	0.250
Mn	0.020	0.026	0.021	0.018	0.013	0.017	0.020	0.019	0.026
Mg	0.777	0.837	0.828	0.843	0.806	0.834	0.762	0.843	0.725
Ca	0.917	0.864	0.890	0.874	0.897	0.867	0.894	0.865	0.886
Na	0.030	0.022	0.027	0.028	0.021	0.025	0.036	0.019	0.039
Total	4.01	4.01	4.02	4.02	4.02	4.03	4.03	4.01	4.02

Abbreviations same as Table A2.3. Cations calculated on a 6 oxygen basis.

Table A2.4 Major element clinopyroxene compositions analysed by EMPA.

Sample ID	Maketawa core	Maketawa rim	Maketawa cpx12_2	Maketawa cpx12_3	Maketawa cpx12_4	Maketawa cpx12_5	Maketawa cpx12_6	Maketawa cpx12_7	Maketawa cpx12_8	Maketawa core
Zone				zone	zone	zone	zone	zone	zone	core
SiO ₂	51.45	49.48	47.02	48.95	50.65	51.63	52.12	51.66	50.88	50.88
TiO ₂	0.38	0.51	1.03	0.66	0.48	0.23	0.18	0.22	0.23	0.23
Al ₂ O ₃	2.12	3.43	6.53	4.53	2.98	0.97	1.18	0.94	1.59	1.59
Cr₂O₃										
Fe ₂ O ₃	3.02	3.81	4.98	3.69	3.40	2.67	1.82	2.35	3.31	3.31
FeO	5.78	5.82	5.67	6.83	6.75	5.69	7.19	5.89	6.68	6.68
MnO	0.71	0.30	0.27	0.26	0.61	0.93	1.03	1.02	1.05	1.05
MgO	13.90	13.29	11.89	12.86	13.22	14.27	14.02	14.33	13.71	13.71
CaO	22.24	22.21	22.10	21.69	21.12	21.67	21.19	21.61	20.49	20.49
Na ₂ O	0.47	0.31	0.39	0.31	0.66	0.47	0.46	0.40	0.58	0.58
Total	100.06	99.16	99.88	99.76	99.86	98.51	99.20	98.42	98.52	98.52
Mg#	81.19	80.42	79.09	77.20	77.89	81.83	77.73	81.34	78.68	78.68
En	41.99	40.92	38.45	39.89	41.12	43.23	42.15	43.24	42.64	42.64
Fs	9.73	9.96	10.17	11.78	11.68	9.60	12.08	9.92	11.55	11.55
Wo	48.29	49.12	51.38	48.34	47.20	47.17	45.77	46.85	45.80	45.80
Si (Cations)	1.931	1.884	1.791	1.856	1.912	1.964	1.968	1.965	1.947	1.947
Ti	0.011	0.014	0.030	0.019	0.014	0.006	0.005	0.006	0.007	0.007
Al	0.094	0.154	0.293	0.203	0.132	0.044	0.052	0.042	0.072	0.072
Cr										
Fe ³⁺	0.085	0.108	0.141	0.104	0.096	0.076	0.051	0.067	0.095	0.095
Fe ²⁺	0.180	0.184	0.178	0.215	0.211	0.180	0.226	0.186	0.212	0.212
Mn	0.023	0.010	0.009	0.008	0.019	0.030	0.033	0.033	0.034	0.034
Mg	0.777	0.754	0.675	0.727	0.744	0.809	0.790	0.813	0.782	0.782
Ca	0.894	0.906	0.902	0.881	0.854	0.883	0.857	0.881	0.840	0.840
Na	0.034	0.023	0.029	0.022	0.049	0.034	0.034	0.030	0.043	0.043
Total	4.03	4.04	4.05	4.04	4.03	4.03	4.02	4.02	4.03	4.03

Abbreviations same as Table A2.3. Cations calculated on a 6 oxygen basis.

Table A2.4 Major element clinopyroxene compositions analysed by EMPA.

Sample ID	Maketawa core	Maketawa rim	Maketawa cpx15_1	Maketawa zone	Maketawa cpx15_2	Maketawa zone	Maketawa cpx15_3	Maketawa zone	Maketawa cpx15_5	Maketawa core	Maketawa cpx15_6	Maketawa zone	Maketawa cpx17_1	Maketawa rim	Maketawa cpx17_10	Maketawa core	Maketawa cpx17_3	Maketawa zone	
SiO ₂	51.08	52.26	50.58	51.75	51.56	47.86	53.10	51.69	52.53	51.56	47.86	53.10	51.69	52.53	51.69	52.53	51.69	52.53	51.69
TiO ₂	0.28	0.26	0.33	0.28	0.28	0.65	0.27	0.24	0.10	0.28	0.65	0.27	0.24	0.10	0.24	0.10	0.24	0.10	0.24
Al ₂ O ₃	1.32	1.45	2.40	1.54	1.43	5.76	1.49	1.15	0.49	1.43	5.76	1.49	1.15	0.49	1.15	0.49	1.15	0.49	1.15
Cr ₂ O ₃																			
Fe ₂ O ₃	3.13	2.36	3.90	2.99	3.24	4.82	1.32	2.58	1.79	3.24	4.82	1.32	2.58	1.79	2.58	1.79	2.58	1.79	2.58
FeO	5.37	4.88	4.64	4.67	4.09	4.94	6.17	5.26	5.99	4.09	4.94	6.17	5.26	5.99	5.26	5.99	5.26	5.99	5.26
MnO	0.91	0.60	0.48	0.58	0.58	0.26	0.59	1.03	1.08	0.58	0.26	0.59	1.03	1.08	1.03	1.08	1.03	1.08	1.03
MgO	14.33	15.59	13.97	15.32	15.02	12.45	15.87	14.26	14.13	15.02	12.45	15.87	14.26	14.13	14.26	14.13	14.26	14.13	14.26
CaO	21.62	21.82	22.55	21.88	22.30	22.51	21.02	22.15	22.70	22.30	22.51	21.02	22.15	22.70	22.15	22.70	22.15	22.70	22.15
Na ₂ O	0.40	0.33	0.42	0.35	0.42	0.36	0.38	0.43	0.34	0.42	0.36	0.38	0.43	0.34	0.43	0.34	0.43	0.34	0.43
Total	98.45	99.56	99.28	99.35	98.92	99.62	100.21	98.78	99.15	98.92	99.62	100.21	98.78	99.15	98.78	99.15	98.78	99.15	98.78
Mg#	82.74	85.12	84.41	85.49	86.85	81.98	82.14	82.95	80.86	86.85	81.98	82.14	82.95	80.86	82.95	80.86	82.95	80.86	82.95
En	43.61	45.86	42.65	45.53	45.08	39.70	46.09	43.07	41.82	45.08	39.70	46.09	43.07	41.82	43.07	41.82	43.07	41.82	43.07
Fs	9.10	8.02	7.88	7.73	6.83	8.73	10.02	8.86	9.90	6.83	8.73	10.02	8.86	9.90	8.86	9.90	8.86	9.90	8.86
Wo	47.29	46.12	49.47	46.74	48.09	51.57	43.88	48.08	48.28	48.09	51.57	43.88	48.08	48.28	48.08	48.28	48.08	48.28	48.08
Si (Cations)	1.947	1.951	1.915	1.943	1.945	1.820	1.962	1.959	1.982	1.945	1.820	1.962	1.959	1.982	1.959	1.982	1.959	1.982	1.959
Ti	0.008	0.007	0.009	0.008	0.008	0.019	0.008	0.007	0.003	0.008	0.019	0.008	0.007	0.003	0.007	0.003	0.007	0.003	0.007
Al	0.059	0.064	0.107	0.068	0.063	0.258	0.065	0.051	0.022	0.063	0.258	0.065	0.051	0.022	0.051	0.022	0.051	0.022	0.051
Cr																			
Fe ³⁺	0.089	0.066	0.110	0.084	0.091	0.136	0.037	0.073	0.051	0.091	0.136	0.037	0.073	0.051	0.073	0.051	0.073	0.051	0.073
Fe ²⁺	0.170	0.152	0.146	0.146	0.128	0.155	0.190	0.166	0.188	0.128	0.155	0.190	0.166	0.188	0.166	0.188	0.166	0.188	0.166
Mn	0.029	0.019	0.015	0.018	0.018	0.008	0.018	0.033	0.035	0.018	0.008	0.018	0.033	0.035	0.033	0.035	0.033	0.035	0.033
Mg	0.814	0.867	0.789	0.857	0.845	0.706	0.874	0.805	0.795	0.845	0.706	0.874	0.805	0.795	0.805	0.795	0.805	0.795	0.805
Ca	0.883	0.872	0.915	0.880	0.901	0.917	0.832	0.899	0.917	0.901	0.917	0.832	0.899	0.917	0.899	0.917	0.899	0.917	0.899
Na	0.030	0.024	0.031	0.025	0.031	0.027	0.028	0.031	0.025	0.031	0.027	0.028	0.031	0.025	0.031	0.025	0.031	0.025	0.031
Total	4.03	4.02	4.04	4.03	4.03	4.05	4.01	4.02	4.02	4.03	4.05	4.01	4.02	4.02	4.02	4.02	4.02	4.02	4.02

Abbreviations same as Table A2.3. Cations calculated on a 6 oxygen basis.

Table A2.4 Major element clinopyroxene compositions analysed by EMPA.

Sample ID	Maketawa cpx17_4 zone	Maketawa cpx17_5 zone	Maketawa cpx17_7 zone	Maketawa cpx17_9 core	Maketawa cpx32_1 rim	Maketawa cpx32_2 zone	Maketawa cpx32_3 zone	Maketawa cpx32_5 zone	Maketawa cpx32_8 core
SiO ₂	51.76	50.85	49.66	51.59	51.56	51.68	50.97	51.95	49.75
TiO ₂	0.22	0.39	0.51	0.25	0.28	0.27	0.34	0.30	0.54
Al ₂ O ₃	1.16	2.76	3.51	1.83	1.49	1.52	2.32	1.50	4.18
Cr ₂ O ₃									
Fe ₂ O ₃	2.41	2.76	3.94	2.58	2.35	2.86	2.90	2.51	3.77
FeO	5.01	6.22	6.36	6.80	4.88	4.39	5.28	4.84	5.34
MnO	0.64	0.38	0.37	0.89	0.49	0.50	0.34	0.54	0.39
MgO	14.62	13.67	12.90	13.26	15.21	15.29	14.35	14.94	13.10
CaO	22.40	22.47	22.23	21.72	21.89	22.14	22.43	22.32	22.49
Na ₂ O	0.37	0.31	0.37	0.61	0.31	0.34	0.30	0.39	0.47
Total	98.60	99.82	99.86	99.52	98.45	98.98	99.22	99.29	100.02
Mg#	83.96	79.78	78.51	77.76	84.83	86.20	82.97	84.70	81.52
En	43.63	41.08	39.81	40.59	45.18	45.44	42.95	44.36	40.64
Fs	8.33	10.41	10.90	11.61	8.08	7.28	8.81	8.01	9.21
Wo	48.03	48.51	49.29	47.80	46.73	47.28	48.24	47.63	50.15
Si (Cations)	1.959	1.913	1.883	1.950	1.948	1.944	1.922	1.949	1.873
Ti	0.006	0.011	0.015	0.007	0.008	0.008	0.010	0.008	0.015
Al	0.052	0.122	0.157	0.081	0.066	0.067	0.103	0.066	0.185
Cr									
Fe ³⁺	0.068	0.078	0.111	0.073	0.066	0.080	0.082	0.070	0.106
Fe ²⁺	0.158	0.194	0.200	0.214	0.153	0.137	0.166	0.151	0.167
Mn	0.021	0.012	0.012	0.029	0.016	0.016	0.011	0.017	0.012
Mg	0.825	0.767	0.730	0.747	0.857	0.858	0.807	0.836	0.735
Ca	0.908	0.906	0.903	0.880	0.886	0.892	0.906	0.897	0.907
Na	0.027	0.023	0.027	0.044	0.022	0.025	0.022	0.028	0.034
Total	4.02	4.03	4.04	4.02	4.02	4.03	4.03	4.02	4.04

Abbreviations same as Table A2.3. Cations calculated on a 6 oxygen basis.

Table A2.4 Major element clinopyroxene compositions analysed by EMPA.

Sample ID	Maketawa rim	Maketawa core	Maketawa cpx45_3 core	Maketawa cpx45_8 core	Maketawa rim cpx47_1	Maketawa zone cpx47_2	Maketawa zone cpx47_3	Maketawa zone cpx47_4	Maketawa zone cpx47_5	Maketawa core cpx47_8
Zone										
SiO ₂	52.01	51.94	52.47	52.04	52.04	51.53	51.61	51.35	51.77	51.58
TiO ₂	0.35	0.35	0.30	0.27	0.27	0.36	0.34	0.30	0.25	0.31
Al ₂ O ₃	2.26	2.39	1.53	1.53	1.53	2.09	2.01	2.04	1.44	1.72
Cr ₂ O ₃										
Fe ₂ O ₃	2.39	2.37	1.78	2.07	2.07	2.01	2.02	2.44	2.32	2.67
FeO	5.63	7.10	6.17	5.74	5.74	6.14	5.61	5.66	5.35	5.14
MnO	0.40	0.63	0.80	0.53	0.53	0.41	0.50	0.43	0.62	0.61
MgO	14.74	13.43	14.18	14.97	14.97	14.50	14.95	14.53	14.68	14.69
CaO	22.43	21.78	22.43	22.01	22.01	22.07	21.59	22.15	21.86	22.13
Na ₂ O	0.32	0.62	0.44	0.29	0.29	0.28	0.35	0.29	0.44	0.37
Total	100.52	100.60	100.10	99.45	99.45	99.39	98.97	99.18	98.73	99.22
Mg#	82.45	77.22	80.45	82.38	82.38	80.89	82.69	82.15	83.10	83.69
En	43.36	40.64	42.02	44.04	44.04	42.92	44.50	43.24	43.98	43.91
Fs	9.23	11.99	10.21	9.42	9.42	10.14	9.31	9.40	8.95	8.56
Wo	47.41	47.37	47.76	46.54	46.54	46.94	46.18	47.36	47.07	47.53
Si (Cations)	1.930	1.938	1.957	1.950	1.950	1.935	1.940	1.934	1.955	1.941
Ti	0.010	0.010	0.008	0.008	0.008	0.010	0.009	0.008	0.007	0.009
Al	0.099	0.105	0.067	0.067	0.067	0.093	0.089	0.090	0.064	0.076
Cr										
Fe ³⁺	0.066	0.066	0.050	0.058	0.058	0.056	0.057	0.069	0.066	0.075
Fe ²⁺	0.174	0.220	0.192	0.179	0.179	0.192	0.175	0.177	0.168	0.161
Mn	0.012	0.020	0.025	0.017	0.017	0.013	0.016	0.014	0.020	0.019
Mg	0.816	0.747	0.789	0.836	0.836	0.812	0.838	0.816	0.826	0.824
Ca	0.892	0.871	0.896	0.884	0.884	0.888	0.869	0.894	0.884	0.892
Na	0.023	0.045	0.032	0.021	0.021	0.021	0.025	0.021	0.032	0.027
Total	4.02	4.02	4.02	4.02	4.02	4.02	4.02	4.02	4.02	4.03

Abbreviations same as Table A2.3. Cations calculated on a 6 oxygen basis.

Table A2.4 Major element clinopyroxene compositions analysed by EMPA.

Sample ID	Maketawa cpx47_9 core	Maketawa cpx49_1 rim	Maketawa cpx49_4 zone	Maketawa cpx49_6 core	Maketawa cpx49_8 core	Maketawa cpx51_2 zone	Maketawa cpx51_3 zone	Maketawa cpx51_4 zone	Maketawa cpx51_5 core
SiO ₂	52.38	56.76	52.65	48.49	52.16	51.21	51.33	51.45	52.08
TiO ₂	0.20	0.53	0.20	0.73	0.24	0.36	0.39	0.33	0.28
Al ₂ O ₃	2.19	8.95	0.92	4.85	1.20	2.18	2.43	2.33	1.33
Cr ₂ O ₃									
Fe ₂ O ₃	2.06	-17.01	1.70	4.61	2.32	2.45	2.32	2.50	2.69
FeO	3.10	20.99	5.80	5.47	5.62	5.69	5.08	6.43	5.08
MnO	0.23	0.37	0.88	0.45	0.83	0.33	0.19	0.51	0.67
MgO	16.63	10.86	14.62	12.23	14.39	14.38	15.28	13.66	14.51
CaO	22.55	14.65	22.31	22.35	22.18	22.34	22.19	21.99	22.62
Na ₂ O	0.21	1.86	0.40	0.51	0.45	0.28	0.18	0.52	0.43
Total	99.55	97.97	99.48	99.70	99.38	99.23	99.39	99.71	99.68
Mg#	90.57	47.03	81.85	80.12	82.13	81.93	84.35	79.22	83.68
En	48.12	32.31	43.13	39.04	43.01	42.80	44.87	41.34	43.18
Fs	5.01	36.38	9.57	9.69	9.36	9.44	8.33	10.84	8.42
Wo	46.88	31.31	47.30	51.27	47.63	47.77	46.80	47.82	48.40
Si (Cations)	1.935	2.014	1.972	1.845	1.961	1.929	1.920	1.934	1.953
Ti	0.006	0.014	0.006	0.021	0.007	0.010	0.011	0.009	0.008
Al	0.095	0.374	0.041	0.218	0.053	0.097	0.107	0.103	0.059
Cr									
Fe ³⁺	0.057	-0.472	0.048	0.131	0.065	0.069	0.065	0.070	0.075
Fe ²⁺	0.095	0.647	0.181	0.172	0.176	0.178	0.158	0.201	0.158
Mn	0.007	0.011	0.028	0.015	0.026	0.011	0.006	0.016	0.021
Mg	0.916	0.575	0.816	0.694	0.807	0.808	0.852	0.766	0.811
Ca	0.892	0.557	0.895	0.911	0.894	0.901	0.889	0.886	0.909
Na	0.015	0.128	0.029	0.038	0.033	0.021	0.013	0.038	0.031
Total	4.02	3.85	4.02	4.04	4.02	4.02	4.02	4.02	4.03

Abbreviations same as Table A2.3. Cations calculated on a 6 oxygen basis.

Table A2.4 Major element clinopyroxene compositions analysed by EMPA.

Sample ID	Maketawa cpx51_6 core	Maketawa cpx53_1 rim	Maketawa cpx53_2 zone	Maketawa cpx53_3 zone	Maketawa cpx53_6 core	Maketawa cpx53_8 zone	Maketawa cpx55_1 rim	Maketawa cpx55_2 zone	Maketawa cpx55_3 zone
SiO ₂	50.36	52.35	50.86	51.46	51.66	48.67	53.14	53.29	53.35
TiO ₂	0.40	0.27	0.41	0.37	0.28	0.72	0.28	0.32	0.27
Al ₂ O ₃	2.25	1.64	3.03	2.57	3.02	5.00	1.63	1.67	1.71
Cr ₂ O ₃									
Fe ₂ O ₃	3.84	0.46	2.35	2.60	1.49	3.70	1.27	1.71	2.58
FeO	4.47	6.83	6.05	6.87	2.88	5.68	6.47	5.88	4.85
MnO	0.54	0.58	0.35	0.62	0.09	0.28	0.60	0.60	0.56
MgO	13.96	15.08	13.90	13.45	16.09	12.98	15.50	16.21	16.24
CaO	22.45	21.22	22.31	21.69	22.83	21.91	21.62	21.34	21.75
Na ₂ O	0.43	0.29	0.32	0.58	0.25	0.38	0.30	0.28	0.40
Total	98.69	98.74	99.58	100.20	98.58	99.31	100.80	101.32	101.72
Mg#	84.88	79.75	80.46	77.83	90.90	80.43	81.08	83.14	85.73
En	42.85	44.15	41.73	40.92	47.17	40.70	44.73	46.54	46.98
Fs	7.63	11.21	10.14	11.66	4.72	9.90	10.44	9.44	7.82
Wo	49.52	44.65	48.13	47.42	48.11	49.40	44.83	44.02	45.21
Si (Cations)	1.917	1.962	1.911	1.929	1.921	1.846	1.956	1.949	1.946
Ti	0.011	0.008	0.012	0.010	0.008	0.021	0.008	0.009	0.008
Al	0.101	0.072	0.134	0.114	0.132	0.223	0.071	0.072	0.073
Cr									
Fe ³⁺	0.109	0.013	0.066	0.073	0.042	0.105	0.035	0.047	0.070
Fe ²⁺	0.141	0.214	0.189	0.214	0.089	0.179	0.199	0.179	0.147
Mn	0.018	0.018	0.011	0.020	0.003	0.009	0.019	0.019	0.017
Mg	0.792	0.843	0.778	0.752	0.892	0.734	0.851	0.884	0.883
Ca	0.916	0.852	0.898	0.871	0.910	0.891	0.853	0.836	0.850
Na	0.032	0.021	0.023	0.042	0.018	0.028	0.022	0.020	0.028
Total	4.04	4.00	4.02	4.02	4.01	4.04	4.01	4.02	4.02

Abbreviations same as Table A2.3. Cations calculated on a 6 oxygen basis.

Table A2.4 Major element clinopyroxene compositions analysed by EMPA.

Sample ID	Maketawa cpx55_4 core	Maketawa cpx55_7 zone	Maketawa cpx55_8 rim	Maketawa cpx57_1 core	Maketawa cpx57_2 core	Maketawa cpx58_1 rim	Maketawa cpx58_2 zone	Maketawa cpx58_3 zone	Maketawa cpx58_4 zone
SiO ₂	53.08	50.90	52.42	52.31	48.78	53.78	52.14	52.93	51.93
TiO ₂	0.27	0.54	0.32	0.39	0.84	0.28	0.37	0.35	0.42
Al ₂ O ₃	1.79	3.68	2.22	2.79	5.22	1.63	3.15	2.45	3.34
Cr ₂ O ₃									
Fe ₂ O ₃	3.09	3.42	2.53	3.81	4.67	0.72	1.33	1.22	1.58
FeO	4.26	5.35	5.06	3.88	3.65	6.74	6.87	6.68	6.94
MnO	0.51	0.41	0.45	0.36	0.32	0.60	0.29	0.40	0.29
MgO	16.19	14.50	15.60	16.11	14.36	15.95	14.60	15.50	14.44
CaO	22.00	21.83	21.97	21.92	21.56	21.31	21.85	21.35	21.88
Na ₂ O	0.42	0.40	0.33	0.42	0.43	0.33	0.33	0.34	0.33
Total	101.61	101.02	100.91	101.99	99.83	101.34	100.93	101.22	101.13
Mg#	87.22	82.97	84.69	88.19	87.63	80.85	79.18	80.58	78.83
En	47.11	43.72	45.61	47.36	45.04	45.52	42.76	44.83	42.42
Fs	6.90	8.98	8.24	6.34	6.36	10.78	11.25	10.80	11.39
Wo	45.99	47.31	46.14	46.30	48.60	43.70	45.99	44.37	46.19
Si (Cations)	1.941	1.887	1.931	1.909	1.832	1.962	1.921	1.938	1.913
Ti	0.007	0.015	0.009	0.011	0.024	0.008	0.010	0.010	0.012
Al	0.077	0.161	0.097	0.120	0.231	0.070	0.137	0.106	0.145
Cr									
Fe ³⁺	0.084	0.095	0.070	0.104	0.130	0.020	0.037	0.034	0.044
Fe ²⁺	0.129	0.164	0.155	0.117	0.114	0.205	0.211	0.204	0.213
Mn	0.016	0.013	0.014	0.011	0.010	0.018	0.009	0.012	0.009
Mg	0.883	0.801	0.857	0.877	0.804	0.867	0.802	0.846	0.793
Ca	0.862	0.867	0.867	0.857	0.867	0.833	0.862	0.838	0.863
Na	0.030	0.029	0.024	0.029	0.031	0.023	0.024	0.024	0.023
Total	4.03	4.03	4.02	4.03	4.04	4.01	4.01	4.01	4.01

Abbreviations same as Table A2.3. Cations calculated on a 6 oxygen basis.

Table A2.4 Major element clinopyroxene compositions analysed by EMPA.

Sample ID	Maketawa cpx58_5 zone	Maketawa cpx58_6 core	Maketawa cpx58_7 zone	Maketawa cpx61_2 rim	Maketawa cpx61_3 zone	Maketawa cpx61_6 core	Maketawa cpx61_7 core	Maketawa cpx65_1 rim	Maketawa cpx65_2 zone
SiO ₂	53.60	53.81	53.46	52.88	52.61	51.77	53.54	52.37	51.13
TiO ₂	0.32	0.24	0.29	0.28	0.33	0.46	0.22	0.25	0.42
Al ₂ O ₃	2.15	1.28	1.80	1.49	2.30	2.65	0.94	1.69	3.54
Cr ₂ O ₃									
Fe ₂ O ₃	0.68	0.87	0.65	2.68	2.55	3.31	2.11	0.81	1.46
FeO	6.78	6.83	6.48	5.04	6.52	6.11	5.35	6.34	6.81
MnO	0.55	0.69	0.61	0.52	0.62	0.63	1.04	0.56	0.24
MgO	15.46	15.23	15.82	15.72	14.06	13.86	15.33	15.57	14.12
CaO	21.41	21.63	21.13	22.18	21.90	22.45	22.29	20.81	21.81
Na ₂ O	0.45	0.47	0.39	0.33	0.64	0.47	0.43	0.33	0.30
Total	101.39	101.06	100.64	101.12	101.55	101.70	101.24	98.72	99.83
Mg#	80.28	79.93	81.34	84.85	79.47	80.28	83.71	81.44	78.76
En	44.62	44.03	45.67	45.60	42.06	41.49	44.65	45.70	42.02
Fs	10.96	11.05	10.48	8.14	10.87	10.19	8.69	10.41	11.33
Wo	44.42	44.92	43.85	46.25	47.07	48.32	46.66	43.88	46.65
Si (Cations)	1.955	1.974	1.961	1.947	1.940	1.916	1.969	1.960	1.908
Ti	0.009	0.007	0.008	0.008	0.009	0.013	0.006	0.007	0.012
Al	0.093	0.056	0.078	0.065	0.100	0.115	0.041	0.075	0.155
Cr									
Fe ³⁺	0.019	0.024	0.018	0.074	0.070	0.091	0.058	0.023	0.041
Fe ²⁺	0.206	0.209	0.198	0.154	0.200	0.188	0.164	0.198	0.212
Mn	0.017	0.021	0.019	0.016	0.019	0.020	0.032	0.018	0.008
Mg	0.840	0.833	0.865	0.863	0.773	0.764	0.840	0.869	0.785
Ca	0.836	0.850	0.831	0.875	0.865	0.890	0.878	0.834	0.872
Na	0.032	0.034	0.028	0.023	0.046	0.034	0.030	0.024	0.022
Total	4.01	4.01	4.01	4.02	4.02	4.03	4.02	4.01	4.01

Abbreviations same as Table A2.3. Cations calculated on a 6 oxygen basis.

Table A2.4 Major element clinopyroxene compositions analysed by EMPA.

Sample ID	Maketawa cpx65_3 zone	Maketawa cpx65_4 core	Maketawa cpx67_2 rim	Maketawa cpx67_3 core	Maketawa cpx69_1 rim	Maketawa cpx69_2 zone	Maketawa cpx69_3 core	Maketawa cpx69_4 core	Maketawa cpx75_1 rim
SiO ₂	53.20	52.77	52.28	52.33	53.51	52.53	52.62	51.00	51.98
TiO ₂	0.21	0.35	0.42	0.31	0.25	0.32	0.35	0.67	0.48
Al ₂ O ₃	1.41	2.35	3.07	2.60	1.05	2.53	2.05	4.78	3.08
Cr ₂ O ₃									
Fe ₂ O ₃	-0.98	1.63	1.49	1.89	1.41	1.51	0.59	1.85	1.45
FeO	8.24	6.40	6.55	7.57	5.80	6.92	6.92	6.93	6.45
MnO	0.53	0.46	0.29	0.55	0.67	0.40	0.53	0.49	0.47
MgO	14.59	14.91	14.64	13.59	16.63	14.67	14.63	13.65	14.81
CaO	21.33	21.73	22.35	21.46	20.55	22.07	21.76	21.67	21.39
Na ₂ O	0.36	0.47	0.29	0.66	0.38	0.29	0.39	0.46	0.41
Total	98.89	101.05	101.38	100.97	100.26	101.25	99.84	101.50	100.52
Mg#	75.90	80.66	79.98	76.27	83.68	79.13	79.07	77.92	80.41
En	42.22	43.72	42.60	40.89	48.01	42.65	42.86	41.26	43.83
Fs	13.41	10.48	10.66	12.72	9.36	11.25	11.35	11.69	10.68
Wo	44.37	45.80	46.74	46.39	42.63	46.10	45.79	47.05	45.49
Si (Cations)	1.985	1.941	1.919	1.940	1.971	1.933	1.954	1.877	1.921
Ti	0.006	0.010	0.012	0.009	0.007	0.009	0.010	0.019	0.013
Al	0.062	0.102	0.133	0.114	0.046	0.110	0.090	0.207	0.134
Cr									
Fe ³⁺	-0.028	0.045	0.041	0.053	0.039	0.042	0.016	0.051	0.040
Fe ²⁺	0.258	0.196	0.200	0.234	0.178	0.212	0.215	0.212	0.199
Mn	0.017	0.014	0.009	0.017	0.021	0.013	0.017	0.015	0.015
Mg	0.812	0.818	0.801	0.751	0.913	0.805	0.810	0.749	0.816
Ca	0.853	0.856	0.879	0.853	0.811	0.870	0.866	0.854	0.847
Na	0.026	0.033	0.021	0.047	0.027	0.021	0.028	0.033	0.029
Total	3.99	4.02	4.01	4.02	4.01	4.01	4.01	4.02	4.01

Abbreviations same as Table A2.3. Cations calculated on a 6 oxygen basis.

Table A2.4 Major element clinopyroxene compositions analysed by EMPA.

Sample ID	Maketawa cpx75_2 zone	Maketawa cpx75_3 core	Maketawa cpx75_4 zone	Maketawa PA core	Maketawa PA_1 rim	Maketawa PD_1c core	Maketawa PD_1r rim	Maketawa PD_8c core	Maketawa PD_8r rim
SiO ₂	53.58	52.92	52.28	51.59	51.31	52.08	51.69	53.56	52.14
TiO ₂	0.31	0.33	0.37	0.40	0.44	0.24	0.56	0.33	0.30
Al ₂ O ₃	2.11	1.82	2.43	2.25	2.12	0.98	3.30	2.29	1.71
Cr ₂ O ₃						0.08	0.00	0.21	0.02
Fe ₂ O ₃	0.56	1.73	1.81	3.46	2.23	3.99	1.88	2.52	2.79
FeO	6.75	5.74	6.52	6.39	5.36	4.13	6.23	2.12	5.26
MnO	0.61	0.55	0.36	0.66	0.56	1.00	0.47	0.11	0.44
MgO	15.49	15.49	14.61	13.34	14.56	16.03	14.71	17.80	14.86
CaO	21.36	21.67	22.05	22.22	21.87	20.92	21.62	22.85	22.16
Na ₂ O	0.43	0.42	0.37	0.61	0.41	0.38	0.37	0.24	0.44
Total	101.22	100.67	100.80	100.93	98.86	99.84	100.82	102.03	100.13
Mg#	80.39	82.85	80.05	78.97	82.96	87.38	80.81	93.75	83.42
En	44.75	45.20	42.85	40.60	43.77	48.02	43.59	50.27	44.05
Fs	10.92	9.36	10.68	10.81	8.99	6.94	10.35	3.35	8.75
Wo	44.33	45.45	46.47	48.58	47.24	45.04	46.05	46.38	47.19
Si (Cations)	1.956	1.950	1.933	1.929	1.934	1.949	1.909	1.925	1.943
Ti	0.009	0.009	0.010	0.011	0.013	0.007	0.015	0.009	0.008
Al	0.091	0.079	0.106	0.099	0.094	0.043	0.143	0.097	0.075
Cr						0.002	0.000	0.006	0.001
Fe ³⁺	0.015	0.048	0.050	0.097	0.063	0.112	0.052	0.068	0.078
Fe ²⁺	0.206	0.176	0.201	0.198	0.168	0.129	0.192	0.064	0.164
Mn	0.019	0.017	0.011	0.021	0.018	0.032	0.015	0.003	0.014
Mg	0.843	0.851	0.805	0.744	0.818	0.894	0.809	0.954	0.826
Ca	0.836	0.856	0.873	0.890	0.883	0.839	0.855	0.880	0.885
Na	0.031	0.030	0.026	0.044	0.030	0.028	0.026	0.017	0.032
Total	4.01	4.02	4.02	4.03	4.02	4.04	4.02	4.02	4.03

Abbreviations same as Table A2.3. Cations calculated on a 6 oxygen basis.

Table A2.4 Major element clinopyroxene compositions analysed by EMPA.

Sample ID	Maketawa PD_9c core	Maketawa PD_9i zone	Maketawa PD_9r rim	Maketawa PD_16c2 core	Maketawa PE_1 core	Maketawa PE_2 rim	Maketawa PE_3 zone	Inglewood b cpx2_1 rim	Inglewood b cpx2_3 zone
SiO ₂	52.07	50.91	52.55	52.06	53.21	51.64	53.88	53.75	54.08
TiO ₂	0.26	0.49	0.32	0.43	0.32	0.53	0.32	0.22	0.24
Al ₂ O ₃	2.72	3.19	2.03	2.02	1.40	2.60	1.08	1.15	1.16
Cr ₂ O ₃	0.28	0.07	0.01	0.02					
Fe ₂ O ₃	1.76	3.59	2.07	3.94	0.53	2.56	0.71	1.25	1.07
FeO	3.51	5.04	5.74	4.98	4.43	5.86	6.78	6.23	6.79
MnO	0.13	0.51	0.55	0.49	0.24	0.33	0.64	0.95	0.96
MgO	16.64	14.53	15.10	14.28	16.70	14.02	15.23	15.67	15.73
CaO	21.98	21.82	22.04	22.81	22.43	23.06	22.28	21.63	21.56
Na ₂ O	0.22	0.42	0.36	0.54	0.16	0.33	0.35	0.36	0.32
Total	99.59	100.57	100.77	101.58	99.43	100.93	101.27	101.21	101.91
Mg#	89.42	83.71	82.42	83.65	87.05	81.11	80.05	81.81	80.55
En	48.37	43.98	44.22	42.67	47.30	41.41	43.47	45.16	44.91
Fs	5.73	8.56	9.43	8.34	7.04	9.64	10.84	10.04	10.84
Wo	45.91	47.46	46.35	48.99	45.67	48.95	45.70	44.80	44.24
Si (Cations)	1.921	1.896	1.941	1.926	1.961	1.916	1.974	1.970	1.970
Ti	0.007	0.014	0.009	0.012	0.009	0.015	0.009	0.006	0.007
Al	0.118	0.140	0.088	0.088	0.061	0.114	0.047	0.050	0.050
Cr	0.008	0.002	0.000	0.001					
Fe ³⁺	0.049	0.101	0.057	0.110	0.015	0.071	0.020	0.034	0.029
Fe ²⁺	0.108	0.157	0.177	0.154	0.137	0.181	0.207	0.190	0.206
Mn	0.004	0.016	0.017	0.015	0.007	0.010	0.020	0.029	0.030
Mg	0.915	0.807	0.832	0.788	0.917	0.776	0.832	0.856	0.854
Ca	0.869	0.871	0.872	0.904	0.886	0.917	0.874	0.849	0.841
Na	0.016	0.030	0.026	0.039	0.012	0.024	0.025	0.025	0.023
Total	4.02	4.03	4.02	4.04	4.00	4.02	4.01	4.01	4.01

Abbreviations same as Table A2.3. Cations calculated on a 6 oxygen basis.

Table A2.4 Major element clinopyroxene compositions analysed by EMPA.

Sample ID	Inglewood b cpx2_5 zone	Inglewood b cpx2_8 light core	Inglewood b cpx2_9 zone	Inglewood b cpx2_10 core	Inglewood b cpx5_1 rim	Inglewood b cpx5_2 light core	Inglewood b cpx5_4 core	Inglewood b cpx9_1 rim
SiO ₂	53.54	50.87	53.42	53.88	53.76	53.13	53.84	54.36
TiO ₂	0.31	0.53	0.33	0.24	0.34	0.34	0.29	0.20
Al ₂ O ₃	1.67	4.25	1.83	1.36	1.81	2.39	1.30	0.83
Cr ₂ O ₃								
Fe ₂ O ₃	1.55	2.90	1.45	1.58	1.19	1.53	1.07	0.68
FeO	6.84	7.12	6.78	6.13	6.86	7.67	6.74	6.52
MnO	1.02	0.60	0.81	0.87	0.81	0.70	0.65	1.08
MgO	15.39	13.23	15.25	15.88	15.32	14.46	15.67	16.07
CaO	21.22	21.81	21.63	21.57	21.64	21.17	21.68	21.45
Na ₂ O	0.40	0.46	0.37	0.37	0.41	0.56	0.34	0.31
Total	101.95	101.76	101.87	101.87	102.13	101.94	101.58	101.50
Mg#	80.10	76.94	80.10	82.26	79.96	77.14	80.60	81.50
En	44.66	40.25	44.10	45.63	44.14	42.58	44.74	45.73
Fs	11.10	12.07	10.96	9.84	11.06	12.62	10.77	10.38
Wo	44.24	47.68	44.94	44.53	44.81	44.80	44.49	43.88
Si (Cations)	1.955	1.882	1.951	1.963	1.956	1.945	1.966	1.982
Ti	0.009	0.015	0.009	0.007	0.009	0.009	0.008	0.005
Al	0.072	0.185	0.079	0.058	0.077	0.103	0.056	0.036
Cr								
Fe ³⁺	0.043	0.080	0.040	0.043	0.032	0.042	0.029	0.018
Fe ²⁺	0.208	0.219	0.206	0.186	0.208	0.234	0.205	0.198
Mn	0.031	0.019	0.025	0.027	0.025	0.022	0.020	0.033
Mg	0.838	0.730	0.831	0.863	0.831	0.789	0.853	0.873
Ca	0.830	0.864	0.846	0.842	0.843	0.830	0.848	0.838
Na	0.028	0.033	0.026	0.026	0.029	0.040	0.024	0.022
Total	4.01	4.03	4.01	4.01	4.01	4.01	4.01	4.01

Abbreviations same as Table A2.3. Cations calculated on a 6 oxygen basis.

Table A2.4 Major element clinopyroxene compositions analysed by EMPA.

Sample ID	Inglewood b cpx9_2 zone	Inglewood b cpx9_3 zone	Inglewood b cpx9_5 zone	Inglewood b cpx9_8 light zone	Inglewood b cpx9_10 core	Inglewood b cpx10_2 rim	Inglewood b cpx10_3 zone	Inglewood b cpx10_4 zone
SiO ₂	53.99	54.16	54.20	52.63	53.98	52.42	53.54	51.55
TiO ₂	0.23	0.21	0.22	0.38	0.23	0.35	0.24	0.54
Al ₂ O ₃	1.32	1.14	1.10	2.41	1.24	2.25	1.12	3.69
Cr ₂ O ₃								
Fe ₂ O ₃	0.97	1.07	0.69	1.63	1.65	2.07	1.97	2.48
FeO	7.07	6.71	6.75	7.48	6.12	6.98	6.17	7.08
MnO	0.78	0.89	0.97	0.64	0.64	0.60	1.03	0.60
MgO	15.35	15.76	15.92	14.30	15.81	14.36	15.27	13.57
CaO	22.06	21.69	21.40	22.02	21.84	22.15	22.08	22.08
Na ₂ O	0.28	0.32	0.32	0.32	0.40	0.32	0.33	0.44
Total	102.06	101.96	101.58	101.81	101.92	101.48	101.75	102.03
Mg#	79.50	80.77	80.81	77.38	82.23	78.66	81.59	77.46
En	43.66	44.90	45.39	41.69	45.28	42.02	44.16	40.64
Fs	11.26	10.69	10.78	12.18	9.79	11.40	9.97	11.83
Wo	45.08	44.41	43.83	46.13	44.94	46.58	45.88	47.53
Si (Cations)	1.966	1.971	1.975	1.934	1.966	1.934	1.963	1.898
Ti	0.006	0.006	0.006	0.011	0.006	0.010	0.007	0.015
Al	0.057	0.049	0.047	0.104	0.053	0.098	0.048	0.160
Cr								
Fe ³⁺	0.027	0.029	0.019	0.045	0.045	0.057	0.054	0.068
Fe ²⁺	0.215	0.204	0.205	0.229	0.186	0.214	0.188	0.217
Mn	0.024	0.027	0.030	0.020	0.020	0.019	0.032	0.019
Mg	0.833	0.855	0.865	0.783	0.858	0.790	0.835	0.745
Ca	0.861	0.846	0.836	0.867	0.852	0.876	0.867	0.871
Na	0.020	0.023	0.023	0.023	0.028	0.023	0.024	0.031
Total	4.01	4.01	4.01	4.02	4.02	4.02	4.02	4.02

Abbreviations same as Table A2.3. Cations calculated on a 6 oxygen basis.

Table A2.4 Major element clinopyroxene compositions analysed by EMPA.

Sample ID	Inglewood b cpx10_6 light core	Inglewood b cpx10_7 core	Inglewood b cpx15_1 rim	Inglewood b cpx15_2 zone	Inglewood b cpx15_3 zone	Inglewood b cpx15_4 zone	Inglewood b cpx15_5 core	Inglewood b cpx15_7 light core
SiO ₂	50.17	53.80	53.94	54.24	54.06	51.19	53.66	52.81
TiO ₂	0.79	0.27	0.23	0.22	0.23	0.56	0.28	0.35
Al ₂ O ₃	4.65	1.54	1.14	1.10	1.17	3.75	1.39	2.30
Cr ₂ O ₃								
Fe ₂ O ₃	2.96	1.42	1.38	1.32	1.53	2.89	1.32	2.06
FeO	7.31	6.44	6.11	6.19	6.01	7.39	7.20	7.12
MnO	0.56	0.85	0.94	0.93	0.92	0.42	0.84	0.95
MgO	12.80	15.49	15.96	16.05	16.08	13.84	15.25	14.77
CaO	21.95	21.77	21.56	21.63	21.59	21.88	21.69	20.80
Na ₂ O	0.42	0.39	0.35	0.35	0.35	0.27	0.31	0.53
Total	101.61	101.97	101.61	102.03	101.94	102.19	101.94	101.69
Mg#	75.86	81.15	82.37	82.26	82.73	77.08	79.11	78.80
En	39.21	44.59	45.76	45.78	46.00	41.10	43.74	43.85
Fs	12.48	10.36	9.80	9.87	9.61	12.22	11.55	11.80
Wo	48.32	45.05	44.44	44.35	44.39	46.68	44.72	44.36
Si (Cations)	1.864	1.960	1.969	1.971	1.967	1.886	1.961	1.940
Ti	0.022	0.007	0.006	0.006	0.006	0.016	0.008	0.010
Al	0.204	0.066	0.049	0.047	0.050	0.163	0.060	0.100
Cr								
Fe ³⁺	0.082	0.039	0.038	0.036	0.042	0.079	0.036	0.057
Fe ²⁺	0.226	0.195	0.186	0.187	0.182	0.226	0.219	0.218
Mn	0.018	0.026	0.029	0.029	0.028	0.013	0.026	0.030
Mg	0.709	0.841	0.868	0.869	0.872	0.760	0.831	0.809
Ca	0.874	0.850	0.843	0.842	0.842	0.864	0.849	0.819
Na	0.030	0.028	0.024	0.025	0.024	0.019	0.022	0.037
Total	4.03	4.01	4.01	4.01	4.01	4.03	4.01	4.02

Abbreviations same as Table A2.3. Cations calculated on a 6 oxygen basis.

Table A2.4 Major element clinopyroxene compositions analysed by EMPA.

Sample ID	Inglewood b rim	Inglewood b zone	Inglewood b cpx17_2 core	Inglewood b cpx17_3 light core	Inglewood b cpx17_4 rim	Inglewood b cpx19_1 zone	Inglewood b cpx19_2 zone	Inglewood b cpx19_5 zone	Inglewood b cpx19_6 core
SiO ₂	54.24	53.81	53.74	50.99	53.91	52.28	52.74	53.45	
TiO ₂	0.29	0.28	0.32	0.64	0.24	0.43	0.39	0.30	
Al ₂ O ₃	1.86	1.60	1.75	4.18	1.06	3.17	2.58	1.72	
Cr ₂ O ₃									
Fe ₂ O ₃	-0.49	1.23	1.64	3.17	1.23	2.45	1.84	0.89	
FeO	7.87	6.57	6.63	6.57	6.79	5.99	6.57	6.75	
MnO	0.87	0.85	0.90	0.73	0.94	0.37	0.42	0.64	
MgO	15.34	15.53	15.66	13.78	15.53	14.48	14.92	15.34	
CaO	21.22	21.54	21.27	21.58	21.86	22.46	22.19	21.47	
Na ₂ O	0.40	0.42	0.40	0.45	0.27	0.43	0.31	0.42	
Total	101.59	101.82	102.31	102.09	101.83	102.07	101.96	100.97	
Mg#	77.64	80.86	80.87	79.01	80.35	81.25	80.26	80.24	
En	43.81	44.77	45.20	41.82	44.32	42.63	43.20	44.40	
Fs	12.62	10.60	10.69	11.11	10.84	9.84	10.63	10.94	
Wo	43.57	44.63	44.10	47.07	44.84	47.53	46.17	44.66	
Si (Cations)	1.971	1.961	1.953	1.879	1.969	1.912	1.928	1.961	
Ti	0.008	0.008	0.009	0.018	0.006	0.012	0.011	0.008	
Al	0.080	0.069	0.075	0.181	0.046	0.137	0.111	0.074	
Cr									
Fe ³⁺	-0.013	0.034	0.045	0.087	0.034	0.067	0.050	0.025	
Fe ²⁺	0.239	0.200	0.201	0.201	0.207	0.182	0.200	0.207	
Mn	0.027	0.026	0.028	0.023	0.029	0.011	0.013	0.020	
Mg	0.831	0.844	0.849	0.757	0.846	0.790	0.813	0.839	
Ca	0.826	0.841	0.828	0.852	0.855	0.880	0.869	0.844	
Na	0.028	0.029	0.028	0.032	0.019	0.030	0.022	0.030	
Total	4.00	4.01	4.01	4.03	4.01	4.02	4.02	4.01	

Abbreviations same as Table A2.3. Cations calculated on a 6 oxygen basis.

Table A2.4 Major element clinopyroxene compositions analysed by EMPA.

Sample ID	Inglewood b rim	Inglewood b cpx20_3 zone	Inglewood b cpx20_4 zone	Inglewood b cpx20_5 zone	Inglewood b cpx20_6 zone	Inglewood b cpx20_7 zone	Inglewood b cpx20_8 zone	Inglewood b cpx20_9 zone
SiO ₂	53.59	53.90	53.63	52.54	53.36	52.86	53.00	53.49
TiO ₂	0.22	0.21	0.22	0.29	0.22	0.27	0.26	0.25
Al ₂ O ₃	1.92	1.12	1.05	1.85	1.07	1.60	1.44	1.12
Cr ₂ O ₃								
Fe ₂ O ₃	-1.07	0.82	1.63	2.43	1.76	1.35	2.24	1.81
FeO	8.16	7.01	6.01	6.46	5.91	7.35	5.59	5.57
MnO	0.92	0.88	0.97	0.59	0.98	0.83	0.87	0.91
MgO	14.76	15.62	15.83	14.88	15.85	14.65	15.79	15.90
CaO	20.97	21.59	21.58	22.03	21.37	21.77	21.39	21.61
Na ₂ O	0.43	0.27	0.32	0.28	0.33	0.28	0.35	0.37
Total	99.89	101.43	101.24	101.35	100.84	100.97	100.92	101.03
Mg#	76.28	79.91	82.51	80.51	82.76	78.09	83.51	83.62
En	42.88	44.55	45.64	43.38	45.93	42.59	46.07	46.03
Fs	13.33	11.20	9.68	10.50	9.57	11.95	9.10	9.01
Wo	43.79	44.25	44.69	46.13	44.50	45.46	44.83	44.96
Si (Cations)	1.977	1.972	1.968	1.939	1.966	1.955	1.954	1.965
Ti	0.006	0.006	0.006	0.008	0.006	0.008	0.007	0.007
Al	0.083	0.048	0.045	0.080	0.047	0.070	0.062	0.049
Cr								
Fe ³⁺	-0.030	0.023	0.045	0.067	0.049	0.038	0.062	0.050
Fe ²⁺	0.252	0.214	0.184	0.198	0.181	0.227	0.171	0.170
Mn	0.029	0.027	0.030	0.019	0.030	0.026	0.027	0.028
Mg	0.812	0.852	0.866	0.819	0.871	0.808	0.868	0.871
Ca	0.829	0.846	0.848	0.871	0.843	0.862	0.844	0.850
Na	0.031	0.019	0.023	0.020	0.023	0.020	0.025	0.026
Total	3.99	4.01	4.01	4.02	4.02	4.01	4.02	4.02

Abbreviations same as Table A2.3. Cations calculated on a 6 oxygen basis.

Table A2.4 Major element clinopyroxene compositions analysed by EMPA.

Sample ID	Inglewood b cpx20_10 zone	Inglewood b cpx20_14 core	Inglewood b cpx20_15 light core	Inglewood b cpx26_1 rim	Inglewood b cpx26_2 core	Inglewood b cpx34_1 rim	Inglewood b cpx34_2 zone	Inglewood b cpx34_4 zone
SiO ₂	52.06	52.19	50.18	52.11	51.64	52.54	51.92	53.35
TiO ₂	0.28	0.40	0.53	0.22	0.40	0.23	0.35	0.24
Al ₂ O ₃	1.82	2.21	3.98	1.34	2.42	1.15	2.55	1.22
Cr ₂ O ₃								
Fe ₂ O ₃	2.28	2.16	3.51	2.83	1.64	2.59	2.24	2.24
FeO	6.67	6.02	6.12	5.16	8.08	5.03	7.37	5.68
MnO	0.78	0.76	0.57	0.76	0.63	0.81	0.62	0.84
MgO	14.65	14.83	13.44	15.08	14.12	15.40	13.84	16.00
CaO	21.59	21.69	21.92	21.99	21.12	22.02	22.09	21.63
Na ₂ O	0.28	0.39	0.39	0.34	0.26	0.34	0.32	0.28
Total	100.43	100.65	100.65	99.82	100.31	100.12	101.29	101.48
Mg#	79.74	81.54	79.78	84.00	75.78	84.61	77.09	83.48
En	43.23	43.91	41.23	44.68	41.76	45.26	40.91	46.10
Fs	10.99	9.94	10.45	8.51	13.35	8.23	12.16	9.13
Wo	45.79	46.15	48.33	46.81	44.89	46.51	46.94	44.78
Si (Cations)	1.941	1.934	1.879	1.950	1.930	1.956	1.925	1.956
Ti	0.008	0.011	0.015	0.006	0.011	0.006	0.010	0.007
Al	0.080	0.096	0.176	0.059	0.107	0.051	0.111	0.053
Cr								
Fe ³⁺	0.064	0.060	0.098	0.079	0.046	0.072	0.062	0.062
Fe ²⁺	0.207	0.186	0.190	0.160	0.251	0.156	0.227	0.173
Mn	0.025	0.024	0.018	0.024	0.020	0.026	0.019	0.026
Mg	0.814	0.820	0.750	0.842	0.786	0.855	0.765	0.875
Ca	0.863	0.861	0.879	0.882	0.846	0.878	0.878	0.850
Na	0.020	0.028	0.029	0.025	0.019	0.024	0.023	0.020
Total	4.02	4.02	4.03	4.03	4.02	4.02	4.02	4.02

Abbreviations same as Table A2.3. Cations calculated on a 6 oxygen basis.

Table A2.4 Major element clinopyroxene compositions analysed by EMPA.

Sample ID	Inglewood b cpx34_5 zone	Inglewood b cpx34_6 zone	Inglewood b cpx34_7 core	Inglewood b cpx34_8 light core	Inglewood b cpx34_9 zone	Inglewood b cpx35_1 rim	Inglewood b cpx35_2 zone	Inglewood b cpx35_3 light zone
SiO ₂	52.95	53.38	52.30	48.49	51.13	53.41	53.59	52.69
TiO ₂	0.22	0.25	0.27	0.78	0.41	0.22	0.22	0.35
Al ₂ O ₃	1.44	1.25	1.41	4.37	2.48	1.23	1.10	2.06
Cr ₂ O ₃								
Fe ₂ O ₃	2.49	2.31	3.33	4.44	3.84	1.29	0.97	1.01
FeO	6.25	5.28	4.58	4.60	5.21	6.57	6.77	8.19
MnO	0.67	0.82	0.66	0.63	0.70	0.82	0.97	0.72
MgO	15.21	16.21	15.19	13.71	14.21	15.11	15.48	14.17
CaO	22.05	21.44	22.27	20.82	22.11	22.03	21.52	21.77
Na ₂ O	0.27	0.35	0.43	0.52	0.43	0.33	0.30	0.27
Total	101.55	101.30	100.43	98.36	100.52	101.01	100.92	101.24
Mg#	81.36	84.61	85.63	84.30	83.07	80.44	80.34	75.57
En	44.03	46.90	45.02	43.91	43.06	43.65	44.57	41.20
Fs	10.09	8.53	7.55	8.18	8.77	10.62	10.91	13.32
Wo	45.88	44.57	47.43	47.91	48.16	45.73	44.52	45.47
Si (Cations)	1.950	1.957	1.946	1.856	1.913	1.967	1.972	1.946
Ti	0.006	0.007	0.007	0.022	0.012	0.006	0.006	0.010
Al	0.062	0.054	0.062	0.197	0.110	0.053	0.048	0.090
Cr								
Fe ³⁺	0.069	0.064	0.093	0.126	0.107	0.036	0.027	0.028
Fe ²⁺	0.191	0.161	0.141	0.146	0.162	0.202	0.208	0.252
Mn	0.021	0.026	0.021	0.020	0.022	0.026	0.030	0.023
Mg	0.835	0.886	0.842	0.782	0.793	0.830	0.849	0.780
Ca	0.870	0.842	0.888	0.854	0.887	0.869	0.848	0.861
Na	0.020	0.025	0.031	0.039	0.031	0.024	0.021	0.020
Total	4.02	4.02	4.03	4.04	4.04	4.01	4.01	4.01

Abbreviations same as Table A2.3. Cations calculated on a 6 oxygen basis.

Table A2.4 Major element clinopyroxene compositions analysed by EMPA.

Sample ID	Inglewood b cpx35_4 light zone	Inglewood b cpx35_5 zone	Inglewood b cpx35_7 zone	Inglewood b cpx35_8 core	Inglewood b cpx35_9 zone	Inglewood b cpx37_1 rim	Inglewood b cpx37_2 zone	Inglewood b cpx37_3 light core
SiO ₂	52.03	53.74	52.27	53.26	51.93	52.07	53.79	51.64
TiO ₂	0.42	0.24	0.43	0.32	0.44	0.32	0.22	0.39
Al ₂ O ₃	2.68	1.08	2.60	1.68	2.48	1.99	1.19	2.53
Cr ₂ O ₃								
Fe ₂ O ₃	1.59	0.80	1.26	1.12	1.78	2.66	1.00	2.57
FeO	8.29	6.97	7.70	6.88	7.22	6.51	6.66	5.83
MnO	0.61	0.98	0.80	0.77	0.82	0.69	0.88	0.32
MgO	13.69	15.37	14.07	14.84	13.94	14.35	15.56	14.34
CaO	21.89	21.61	21.57	21.78	21.66	22.24	21.68	22.85
Na ₂ O	0.28	0.31	0.37	0.43	0.41	0.29	0.32	0.25
Total	101.48	101.10	101.06	101.08	100.67	101.11	101.29	100.73
Mg#	74.72	79.75	76.56	79.39	77.55	79.82	80.69	81.52
En	40.20	44.17	41.53	43.21	41.56	42.25	44.63	42.17
Fs	13.60	11.22	12.71	11.21	12.03	10.68	10.68	9.56
Wo	46.20	44.61	45.76	45.58	46.41	47.07	44.68	48.27
Si (Cations)	1.925	1.974	1.933	1.960	1.931	1.933	1.970	1.919
Ti	0.012	0.007	0.012	0.009	0.012	0.009	0.006	0.011
Al	0.117	0.047	0.113	0.073	0.109	0.087	0.051	0.111
Cr								
Fe ³⁺	0.044	0.022	0.035	0.031	0.049	0.074	0.027	0.071
Fe ²⁺	0.255	0.214	0.237	0.211	0.224	0.201	0.203	0.180
Mn	0.019	0.031	0.025	0.024	0.026	0.022	0.027	0.010
Mg	0.755	0.842	0.775	0.814	0.773	0.794	0.850	0.794
Ca	0.868	0.850	0.855	0.858	0.863	0.885	0.851	0.909
Na	0.020	0.022	0.026	0.031	0.029	0.021	0.023	0.018
Total	4.01	4.01	4.01	4.01	4.02	4.02	4.01	4.02

Abbreviations same as Table A2.3. Cations calculated on a 6 oxygen basis.

Table A2.4 Major element clinopyroxene compositions analysed by EMPA.

Sample ID	Inglewood b cpx37_4 core	Inglewood b cpx39_1 rim	Inglewood b cpx39_4 core	Inglewood b cpx39_5 light core	Inglewood b cpx41_1 zone	Inglewood b cpx41_2 rim	Inglewood b cpx41_3 core	Inglewood b 21a core
SiO ₂	51.55	52.10	53.40	50.73	52.76	53.10	51.83	52.84
TiO ₂	0.56	0.32	0.30	0.54	0.24	0.28	0.29	0.29
Al ₂ O ₃	3.05	1.56	1.60	3.13	1.25	1.55	1.47	1.36
Cr ₂ O ₃								0.00
Fe ₂ O ₃	2.38	3.00	2.07	3.55	2.50	1.93	3.32	2.57
FeO	6.14	4.80	5.90	6.08	5.24	6.14	4.94	5.39
MnO	0.57	1.07	0.93	0.77	0.81	0.88	0.77	0.56
MgO	14.34	15.44	15.51	13.79	15.87	15.31	15.11	15.97
CaO	21.81	21.45	21.90	21.65	21.38	21.42	21.72	20.96
Na ₂ O	0.42	0.38	0.35	0.44	0.35	0.44	0.39	0.41
Total	100.83	100.12	101.95	100.68	100.40	101.05	99.85	100.34
Mg#	80.71	85.23	82.48	80.30	84.45	81.70	84.60	84.09
En	42.88	46.04	44.91	42.13	46.47	44.85	45.14	46.89
Fs	10.25	7.98	9.54	10.34	8.56	10.05	8.22	8.87
Wo	46.87	45.98	45.55	47.53	44.98	45.11	46.64	44.24
Si (Cations)	1.911	1.942	1.951	1.899	1.955	1.956	1.942	1.956
Ti	0.016	0.009	0.008	0.015	0.007	0.008	0.008	0.008
Al	0.133	0.069	0.069	0.138	0.054	0.067	0.065	0.059
Cr								0.000
Fe ³⁺	0.066	0.084	0.057	0.099	0.069	0.053	0.093	0.072
Fe ²⁺	0.189	0.149	0.179	0.189	0.161	0.188	0.154	0.167
Mn	0.018	0.034	0.029	0.024	0.026	0.028	0.025	0.017
Mg	0.792	0.858	0.845	0.769	0.877	0.841	0.844	0.881
Ca	0.866	0.857	0.857	0.868	0.849	0.846	0.872	0.831
Na	0.030	0.027	0.024	0.032	0.025	0.031	0.029	0.030
Total	4.02	4.03	4.02	4.03	4.02	4.02	4.03	4.02

Abbreviations same as Table A2.3. Cations calculated on a 6 oxygen basis.

Table A2.4 Major element clinopyroxene compositions analysed by EMPA.

Sample ID	Inglewood b 21b rim	Inglewood b 22a core	Inglewood b 22b rim	Inglewood b 23a core	Inglewood b 23b zone	Inglewood b 23c rim	Inglewood b 24a core	Inglewood b 24b rim	Inglewood a cpx1_2 rim
Zone									
SiO ₂	49.55	52.89	51.93	52.46	53.52	53.22	53.48	52.75	53.12
TiO ₂	0.59	0.36	0.42	0.33	0.35	0.26	0.28	0.44	0.22
Al ₂ O ₃	4.23	1.66	2.56	1.95	0.98	1.27	1.26	2.32	1.10
Cr ₂ O ₃	0.00	0.12	0.07	0.00	0.00	0.01	0.09	0.00	
Fe ₂ O ₃	2.18	1.49	1.88	3.22	1.74	2.09	1.24	1.38	0.49
FeO	7.58	6.50	6.25	5.41	6.02	6.25	6.90	7.09	6.89
MnO	0.50	0.63	0.74	0.66	0.92	0.77	0.87	0.58	0.93
MgO	12.41	15.49	14.29	14.89	15.66	14.92	15.08	14.46	15.08
CaO	21.83	21.36	21.95	22.37	21.94	22.48	21.86	21.87	21.48
Na ₂ O	0.35	0.32	0.41	0.38	0.29	0.32	0.33	0.44	0.32
Total	99.22	100.80	100.49	101.66	101.43	101.58	101.38	101.32	99.64
Mg#	74.48	80.94	80.29	83.08	82.26	80.98	79.57	78.42	79.62
En	38.36	44.91	42.56	43.79	45.00	43.14	43.50	42.33	43.88
Fs	13.14	10.57	10.45	8.92	9.71	10.13	11.17	11.65	11.23
Wo	48.49	44.51	46.98	47.29	45.29	46.73	45.33	46.02	44.89
Si (Cations)	1.881	1.950	1.928	1.932	1.963	1.957	1.964	1.940	1.977
Ti	0.017	0.010	0.012	0.009	0.010	0.007	0.008	0.012	0.006
Al	0.189	0.072	0.112	0.085	0.042	0.055	0.054	0.101	0.048
Cr	0.000	0.003	0.002	0.000	0.000	0.000	0.002	0.000	
Fe ³⁺	0.062	0.041	0.053	0.089	0.048	0.058	0.034	0.038	0.014
Fe ²⁺	0.241	0.200	0.194	0.167	0.185	0.192	0.212	0.218	0.214
Mn	0.016	0.020	0.023	0.020	0.029	0.024	0.027	0.018	0.029
Mg	0.702	0.851	0.791	0.818	0.857	0.818	0.826	0.793	0.837
Ca	0.888	0.843	0.873	0.883	0.862	0.886	0.860	0.862	0.856
Na	0.026	0.023	0.029	0.027	0.021	0.023	0.024	0.031	0.023
Total	4.02	4.01	4.02	4.03	4.02	4.02	4.01	4.01	4.00

Abbreviations same as Table A2.3. Cations calculated on a 6 oxygen basis.

Table A2.4 Major element clinopyroxene compositions analysed by EMPA.

Sample ID	Inglewood a cpx1_3 zone	Inglewood a cpx1_4 zone	Inglewood a cpx1_5 zone	Inglewood a cpx1_6 zone	Inglewood a cpx1_7 zone	Inglewood a cpx1_8 zone	Inglewood a cpx1_9 zone	Inglewood a cpx1_10 light core
SiO ₂	53.93	53.14	53.89	53.26	53.06	51.81	53.95	51.93
TiO ₂	0.21	0.25	0.23	0.26	0.21	0.37	0.21	0.39
Al ₂ O ₃	0.94	1.43	1.08	1.42	1.15	2.45	1.00	2.54
Cr ₂ O ₃								
Fe ₂ O ₃	0.11	0.48	0.24	0.20	0.84	1.64	0.26	1.46
FeO	7.13	7.93	7.08	8.01	6.62	7.25	6.85	6.84
MnO	0.91	0.70	0.93	0.86	0.92	0.67	0.92	0.55
MgO	15.49	14.47	15.45	14.57	15.39	14.07	15.75	14.26
CaO	21.68	22.02	21.54	21.69	21.20	21.62	21.43	21.78
Na ₂ O	0.27	0.25	0.32	0.28	0.32	0.35	0.30	0.38
Total	100.67	100.65	100.76	100.55	99.71	100.23	100.68	100.12
Mg#	79.48	76.52	79.55	76.44	80.60	77.65	80.41	78.85
En	44.17	41.66	44.27	42.04	44.84	41.81	45.03	42.27
Fs	11.40	12.79	11.38	12.96	10.79	12.03	10.97	11.34
Wo	44.42	45.56	44.35	44.99	44.38	46.16	44.00	46.40
Si (Cations)	1.982	1.966	1.980	1.970	1.973	1.933	1.981	1.933
Ti	0.006	0.007	0.006	0.007	0.006	0.011	0.006	0.011
Al	0.041	0.062	0.047	0.062	0.051	0.108	0.043	0.111
Cr								
Fe ³⁺	0.003	0.013	0.007	0.006	0.024	0.046	0.007	0.041
Fe ²⁺	0.219	0.245	0.217	0.248	0.205	0.225	0.210	0.212
Mn	0.028	0.022	0.029	0.027	0.029	0.021	0.029	0.017
Mg	0.849	0.798	0.846	0.803	0.853	0.783	0.862	0.791
Ca	0.854	0.873	0.848	0.860	0.844	0.864	0.843	0.869
Na	0.019	0.018	0.023	0.020	0.023	0.025	0.021	0.028
Total	4.00	4.00	4.00	4.00	4.01	4.02	4.00	4.01

Abbreviations same as Table A2.3. Cations calculated on a 6 oxygen basis.

Table A2.4 Major element clinopyroxene compositions analysed by EMPA.

Sample ID	Inglewood a cpx1_11 core	Inglewood a cpx2_1 rim	Inglewood a cpx2_2 zone	Inglewood a cpx2_3 zone	Inglewood a cpx2_4 light zone	Inglewood a cpx2_5 core	Inglewood a cpx2_6 light core	Inglewood a cpx3_2 zone
Zone								
SiO ₂	53.58	52.87	51.61	52.23	53.11	52.89	52.66	53.89
TiO ₂	0.25	0.25	0.35	0.26	0.30	0.30	0.40	0.22
Al ₂ O ₃	1.45	1.92	1.99	1.46	1.45	1.61	2.11	1.18
Cr ₂ O ₃								
Fe ₂ O ₃	0.34	-0.60	2.09	1.89	0.54	1.13	1.23	-0.04
FeO	7.26	8.40	6.56	5.93	8.08	6.33	6.88	7.38
MnO	0.83	1.00	0.96	0.89	0.96	0.82	0.80	0.89
MgO	15.04	14.52	14.51	15.07	15.03	14.97	14.47	15.28
CaO	21.61	20.72	20.98	21.31	20.81	21.72	21.72	21.65
Na ₂ O	0.37	0.34	0.39	0.37	0.27	0.40	0.44	0.30
Total	100.74	99.42	99.43	99.42	100.55	100.17	100.72	100.75
Mg#	78.70	75.47	79.84	81.98	76.85	80.88	79.00	78.68
En	43.42	42.54	43.63	44.73	43.55	43.88	42.66	43.68
Fs	11.75	13.83	11.02	9.83	13.12	10.37	11.34	11.83
Wo	44.83	43.63	45.35	45.44	43.34	45.75	46.00	44.48
Si (Cations)	1.972	1.969	1.940	1.956	1.965	1.960	1.947	1.979
Ti	0.007	0.007	0.010	0.007	0.008	0.008	0.011	0.006
Al	0.063	0.084	0.088	0.065	0.063	0.071	0.092	0.051
Cr								
Fe ³⁺	0.009	-0.017	0.059	0.053	0.015	0.031	0.034	-0.001
Fe ²⁺	0.223	0.262	0.205	0.185	0.250	0.196	0.212	0.227
Mn	0.026	0.032	0.031	0.028	0.030	0.026	0.025	0.028
Mg	0.825	0.806	0.813	0.841	0.829	0.827	0.798	0.837
Ca	0.852	0.827	0.845	0.855	0.825	0.863	0.860	0.852
Na	0.026	0.025	0.028	0.027	0.020	0.029	0.032	0.021
Total	4.00	3.99	4.02	4.02	4.01	4.01	4.01	4.00

Abbreviations same as Table A2.3. Cations calculated on a 6 oxygen basis.

Table A2.4 Major element clinopyroxene compositions analysed by EMPA.

Sample ID	Inglewood a cpx3_3 core	Inglewood a cpx3_4 light core	Inglewood a cpx4_1 rim	Inglewood a cpx4_2 zone	Inglewood a cpx4_3 light zone	Inglewood a cpx4_4 core	Inglewood a cpx9_1 rim	Inglewood a cpx9_2 zone
Zone								
SiO ₂	53.70	53.13	53.91	52.59	51.91	53.12	53.70	53.62
TiO ₂	0.24	0.29	0.22	0.23	0.37	0.27	0.23	0.24
Al ₂ O ₃	1.26	1.65	1.01	1.16	2.32	1.44	1.15	1.32
Cr ₂ O ₃								
Fe ₂ O ₃	0.35	1.17	-0.40	1.35	0.89	0.75	-0.07	0.40
FeO	6.96	6.55	7.92	6.03	8.24	6.56	7.17	7.30
MnO	0.90	0.85	0.99	0.88	0.57	0.84	0.88	0.88
MgO	15.43	15.21	14.96	15.42	13.83	15.18	15.25	15.34
CaO	21.48	21.50	21.60	21.26	21.65	21.55	21.60	21.18
Na ₂ O	0.33	0.38	0.30	0.32	0.26	0.36	0.33	0.36
Total	100.65	100.72	100.52	99.23	100.03	100.08	100.23	100.64
Mg#	79.83	80.60	77.08	82.07	75.00	80.51	79.14	78.96
En	44.39	44.32	42.82	45.27	40.68	44.20	43.83	44.28
Fs	11.22	10.67	12.74	9.89	13.56	10.70	11.55	11.80
Wo	44.39	45.01	44.44	44.84	45.76	45.10	44.62	43.92
Si (Cations)	1.975	1.959	1.986	1.967	1.940	1.967	1.981	1.974
Ti	0.007	0.008	0.006	0.006	0.010	0.007	0.006	0.007
Al	0.055	0.072	0.044	0.051	0.102	0.063	0.050	0.057
Cr								
Fe ³⁺	0.010	0.032	-0.011	0.038	0.025	0.021	-0.002	0.011
Fe ²⁺	0.214	0.201	0.244	0.188	0.257	0.203	0.221	0.224
Mn	0.028	0.026	0.031	0.028	0.018	0.026	0.027	0.028
Mg	0.846	0.836	0.822	0.860	0.770	0.838	0.839	0.842
Ca	0.846	0.849	0.853	0.852	0.867	0.855	0.854	0.835
Na	0.024	0.027	0.021	0.023	0.019	0.026	0.023	0.026
Total	4.00	4.01	4.00	4.01	4.01	4.01	4.00	4.00

Abbreviations same as Table A2.3. Cations calculated on a 6 oxygen basis.

Table A2.4 Major element clinopyroxene compositions analysed by EMPA.

Sample ID	Inglewood a cpx9_3 light zone	Inglewood a cpx9_4 zone	Inglewood a cpx9_5 zone	Inglewood a cpx18_1 rim	Inglewood a cpx18_2 zone	Inglewood a cpx18_3 zone	Inglewood a cpx18_4 zone	Inglewood a cpx18_5 zone
SiO ₂	52.03	53.30	53.66	53.11	53.68	52.56	52.23	53.45
TiO ₂	0.40	0.28	0.26	0.23	0.23	0.31	0.35	0.23
Al ₂ O ₃	2.73	1.47	1.23	1.23	1.25	2.03	2.32	1.25
Cr ₂ O ₃								
Fe ₂ O ₃	1.06	0.47	0.36	2.02	1.88	2.34	2.85	2.22
FeO	7.95	7.03	7.16	5.25	5.84	6.61	6.60	5.56
MnO	0.50	0.81	0.79	0.84	0.82	0.55	0.55	0.91
MgO	13.97	14.90	15.17	15.98	16.01	15.02	14.77	16.18
CaO	21.86	21.79	21.71	21.44	21.56	21.78	21.70	21.20
Na ₂ O	0.27	0.36	0.34	0.37	0.35	0.29	0.33	0.36
Total	100.76	100.42	100.68	100.48	101.60	101.49	101.69	101.36
Mg#	75.85	79.08	79.08	84.50	83.07	80.30	80.07	83.90
En	40.93	43.18	43.62	46.57	46.05	43.72	43.39	46.87
Fs	13.03	11.42	11.54	8.54	9.38	10.73	10.80	8.99
Wo	46.04	45.39	44.85	44.89	44.57	45.55	45.81	44.13
Si (Cations)	1.929	1.969	1.975	1.961	1.962	1.936	1.926	1.959
Ti	0.011	0.008	0.007	0.006	0.006	0.009	0.010	0.006
Al	0.119	0.064	0.053	0.054	0.054	0.088	0.101	0.054
Cr								
Fe ³⁺	0.030	0.013	0.010	0.056	0.051	0.064	0.079	0.061
Fe ²⁺	0.246	0.217	0.220	0.161	0.178	0.202	0.202	0.170
Mn	0.016	0.025	0.025	0.026	0.025	0.017	0.017	0.028
Mg	0.772	0.820	0.833	0.880	0.872	0.825	0.812	0.884
Ca	0.868	0.862	0.856	0.848	0.844	0.859	0.857	0.833
Na	0.019	0.026	0.024	0.026	0.025	0.020	0.024	0.026
Total	4.01	4.00	4.00	4.02	4.02	4.02	4.03	4.02

Abbreviations same as Table A2.3. Cations calculated on a 6 oxygen basis.

Table A2.4 Major element clinopyroxene compositions analysed by EMPA.

Sample ID	Inglewood a cpx18_6 zone	Inglewood a cpx18_7 zone	Inglewood a cpx18_9 light core	Inglewood a cpx18_10 zone	Inglewood a cpx19_2 zone	Inglewood a cpx19_3 light zone	Inglewood a cpx19_4 zone	Inglewood a cpx19_5 light zone
SiO ₂	51.79	53.75	52.50	53.08	52.06	52.04	53.31	50.99
TiO ₂	0.43	0.24	0.36	0.25	0.30	0.38	0.24	0.53
Al ₂ O ₃	2.96	1.11	2.37	1.71	1.79	2.44	1.29	3.53
Cr ₂ O ₃								
Fe ₂ O ₃	2.70	2.02	2.52	2.43	1.22	1.29	0.50	1.65
FeO	6.82	5.70	6.69	6.75	7.35	7.88	7.37	8.18
MnO	0.52	0.91	0.52	0.98	0.65	0.51	0.84	0.47
MgO	14.69	16.33	15.12	15.21	14.13	13.78	14.85	13.27
CaO	21.46	21.24	21.54	20.40	21.90	22.19	21.73	21.81
Na ₂ O	0.29	0.34	0.30	0.59	0.28	0.26	0.31	0.27
Total	101.66	101.64	101.90	101.41	99.67	100.77	100.43	100.69
Mg#	79.45	83.70	80.21	80.17	77.48	75.76	78.24	74.38
En	43.31	46.96	44.05	45.22	41.59	40.37	42.92	39.60
Fs	11.20	9.15	10.87	11.19	12.09	12.92	11.94	13.64
Wo	45.48	43.89	45.08	43.59	46.32	46.71	45.14	46.76
Si (Cations)	1.909	1.963	1.926	1.955	1.951	1.933	1.972	1.902
Ti	0.012	0.007	0.010	0.007	0.008	0.011	0.007	0.015
Al	0.129	0.048	0.102	0.074	0.079	0.107	0.056	0.155
Cr								
Fe ³⁺	0.075	0.055	0.069	0.067	0.034	0.036	0.014	0.046
Fe ²⁺	0.209	0.173	0.204	0.207	0.229	0.244	0.228	0.254
Mn	0.016	0.028	0.016	0.031	0.020	0.016	0.026	0.015
Mg	0.807	0.889	0.827	0.835	0.789	0.763	0.819	0.738
Ca	0.848	0.831	0.847	0.805	0.879	0.883	0.861	0.871
Na	0.021	0.024	0.021	0.042	0.020	0.019	0.022	0.019
Total	4.02	4.02	4.02	4.02	4.01	4.01	4.00	4.02

Abbreviations same as Table A2.3. Cations calculated on a 6 oxygen basis.

Table A2.4 Major element clinopyroxene compositions analysed by EMPA.

Sample ID	Inglewood a cpx19_6 zone	Inglewood a cpx19_7 light zone	Inglewood a cpx21_1 rim	Inglewood a cpx21_2 zone	Inglewood a cpx21_3 light core	Inglewood a cpx21_4 core	Inglewood a cpx21_5 zone	Inglewood a cpx22_1 rim
SiO ₂	52.86	51.93	53.47	54.06	49.05	53.06	53.48	53.28
TiO ₂	0.23	0.39	0.24	0.22	1.01	0.41	0.21	0.24
Al ₂ O ₃	1.22	2.56	1.36	1.02	5.41	1.99	0.92	1.19
Cr ₂ O ₃								
Fe ₂ O ₃	1.24	1.09	2.11	1.78	4.34	2.40	2.36	2.09
FeO	6.24	7.74	5.71	5.55	6.19	5.78	5.14	5.43
MnO	0.83	0.46	0.87	0.91	0.51	0.71	0.88	0.87
MgO	15.22	13.93	15.88	16.43	12.70	15.51	16.24	15.95
CaO	21.61	22.01	21.40	21.45	21.93	21.46	21.39	21.49
Na ₂ O	0.33	0.27	0.41	0.35	0.48	0.48	0.39	0.36
Total	99.78	100.37	101.44	101.77	101.61	101.79	101.01	100.91
Mg#	81.34	76.28	83.29	84.12	78.69	82.80	84.99	84.03
En	44.45	40.88	46.10	47.01	39.81	45.41	47.10	46.34
Fs	10.20	12.71	9.25	8.87	10.78	9.43	8.32	8.81
Wo	45.35	46.41	44.65	44.12	49.41	45.16	44.58	44.86
Si (Cations)	1.967	1.932	1.959	1.968	1.830	1.941	1.966	1.961
Ti	0.006	0.011	0.007	0.006	0.028	0.011	0.006	0.007
Al	0.054	0.112	0.059	0.044	0.238	0.086	0.040	0.052
Cr								
Fe ³⁺	0.035	0.031	0.058	0.049	0.120	0.066	0.065	0.058
Fe ²⁺	0.194	0.240	0.174	0.168	0.191	0.176	0.157	0.166
Mn	0.026	0.014	0.027	0.028	0.016	0.022	0.027	0.027
Mg	0.845	0.773	0.867	0.892	0.706	0.846	0.890	0.875
Ca	0.862	0.877	0.840	0.837	0.877	0.841	0.842	0.847
Na	0.024	0.019	0.029	0.025	0.034	0.034	0.028	0.026
Total	4.01	4.01	4.02	4.02	4.04	4.02	4.02	4.02

Abbreviations same as Table A2.3. Cations calculated on a 6 oxygen basis.

Table A2.4 Major element clinopyroxene compositions analysed by EMPA.

Sample ID	Inglewood a cpx22_2 zone	Inglewood a cpx22_3 zone	Inglewood a cpx22_4 zone	Inglewood a cpx22_5 zone	Inglewood a cpx22_6 light core	Inglewood a cpx24_1 rim	Inglewood a cpx24_2 zone	Inglewood a cpx24_3 light zone
SiO ₂	51.66	53.56	51.52	53.19	52.02	53.26	53.35	52.58
TiO ₂	0.43	0.27	0.42	0.32	0.42	0.26	0.22	0.34
Al ₂ O ₃	2.92	1.27	2.96	1.84	2.96	1.40	1.19	2.07
Cr ₂ O ₃								
Fe ₂ O ₃	2.58	1.72	2.75	2.32	2.12	1.38	2.02	2.23
FeO	7.05	6.04	6.60	5.45	6.44	6.15	5.54	6.25
MnO	0.52	0.93	0.49	0.69	0.35	0.94	0.87	0.79
MgO	14.07	15.85	14.39	15.78	14.66	15.65	15.98	15.26
CaO	21.80	21.47	21.76	21.55	22.03	21.18	21.39	21.28
Na ₂ O	0.35	0.34	0.30	0.44	0.32	0.39	0.37	0.37
Total	101.38	101.45	101.19	101.58	101.33	100.60	100.94	101.17
Mg#	78.17	82.45	79.64	83.84	80.30	81.98	83.78	81.40
En	41.79	45.74	42.70	45.99	43.00	45.62	46.39	44.83
Fs	11.67	9.74	10.92	8.87	10.55	10.03	8.98	10.24
Wo	46.53	44.53	46.38	45.14	46.44	44.36	44.63	44.93
Si (Cations)	1.913	1.961	1.909	1.946	1.916	1.964	1.963	1.938
Ti	0.012	0.007	0.012	0.009	0.012	0.007	0.006	0.010
Al	0.127	0.055	0.129	0.079	0.129	0.061	0.052	0.090
Cr								
Fe ³⁺	0.071	0.047	0.076	0.063	0.058	0.038	0.056	0.062
Fe ²⁺	0.217	0.184	0.203	0.166	0.197	0.189	0.170	0.192
Mn	0.016	0.029	0.015	0.021	0.011	0.029	0.027	0.025
Mg	0.777	0.865	0.795	0.861	0.805	0.860	0.876	0.838
Ca	0.865	0.842	0.864	0.845	0.869	0.836	0.843	0.840
Na	0.025	0.024	0.022	0.031	0.023	0.028	0.027	0.027
Total	4.02	4.02	4.03	4.02	4.02	4.01	4.02	4.02

Abbreviations same as Table A2.3. Cations calculated on a 6 oxygen basis.

Table A2.4 Major element clinopyroxene compositions analysed by EMPA.

Sample ID	Inglewood a cpx24_4 zone	Inglewood a cpx24_5 light zone	Inglewood a cpx24_6 zone	Inglewood a cpx24_8 core	Inglewood a cpx35_1 rim	Inglewood a cpx35_2 zone	Inglewood a cpx35_3 zone	Inglewood a cpx35_4 zone
SiO ₂	53.27	50.68	52.68	53.56	54.21	54.09	52.84	53.80
TiO ₂	0.25	0.57	0.38	0.31	0.23	0.23	0.33	0.21
Al ₂ O ₃	1.39	3.91	2.23	1.46	1.01	1.05	2.24	1.11
Cr ₂ O ₃								
Fe ₂ O ₃	2.01	3.26	2.41	2.20	1.17	1.26	1.62	1.04
FeO	5.88	6.61	6.04	5.47	6.23	5.95	6.86	6.46
MnO	0.88	0.53	0.80	0.78	1.05	0.94	0.53	0.82
MgO	15.80	13.58	15.15	15.98	16.34	16.34	14.73	15.79
CaO	21.22	21.80	21.19	21.54	21.10	21.31	22.11	21.61
Na ₂ O	0.39	0.41	0.51	0.43	0.35	0.34	0.33	0.31
Total	101.09	101.35	101.39	101.73	101.69	101.51	101.59	101.15
Mg#	82.80	78.69	81.81	83.96	82.41	83.09	79.35	81.38
En	46.02	41.25	44.90	46.31	46.70	46.70	42.75	45.20
Fs	9.56	11.17	9.98	8.85	9.96	9.51	11.13	10.34
Wo	44.42	47.58	45.12	44.85	43.34	43.79	46.12	44.45
Si (Cations)	1.959	1.883	1.937	1.955	1.974	1.972	1.939	1.972
Ti	0.007	0.016	0.010	0.008	0.006	0.006	0.009	0.006
Al	0.060	0.171	0.097	0.063	0.043	0.045	0.097	0.048
Cr								
Fe ³⁺	0.055	0.091	0.066	0.060	0.032	0.035	0.045	0.029
Fe ²⁺	0.180	0.204	0.185	0.166	0.189	0.181	0.210	0.197
Mn	0.027	0.017	0.025	0.024	0.032	0.029	0.016	0.025
Mg	0.866	0.752	0.831	0.870	0.887	0.888	0.806	0.863
Ca	0.836	0.868	0.835	0.843	0.823	0.832	0.870	0.848
Na	0.028	0.030	0.036	0.031	0.024	0.024	0.023	0.022
Total	4.02	4.03	4.02	4.02	4.01	4.01	4.01	4.01

Abbreviations same as Table A2.3. Cations calculated on a 6 oxygen basis.

Table A2.4 Major element clinopyroxene compositions analysed by EMPA.

Sample ID	Inglewood a cpx35_5 core	Inglewood a cpx48_1 rim	Inglewood a cpx48_2 zone	Inglewood a cpx48_3 zone	Inglewood a cpx48_5 light core	Inglewood a cpx48_6 core	Inglewood a cpx51_1 rim	Inglewood a cpx51_2 zone
SiO ₂	53.31	54.73	53.30	52.53	51.63	54.27	54.16	54.64
TiO ₂	0.27	0.23	0.33	0.32	0.46	0.22	0.27	0.23
Al ₂ O ₃	1.55	1.20	1.71	2.19	2.96	1.14	1.28	1.10
Cr ₂ O ₃								
Fe ₂ O ₃	1.73	-0.76	0.43	1.32	1.93	0.19	-0.52	-0.66
FeO	6.06	8.03	8.31	7.56	7.12	7.41	8.33	7.73
MnO	0.85	0.81	0.78	0.49	0.34	0.71	0.82	0.83
MgO	15.72	15.26	14.39	14.29	14.14	14.99	14.99	15.47
CaO	21.26	21.76	21.73	22.04	21.92	22.05	21.69	21.75
Na ₂ O	0.40	0.37	0.31	0.29	0.31	0.43	0.28	0.33
Total	101.15	101.62	101.28	101.02	100.81	101.41	101.31	101.43
Mg#	82.28	77.19	75.54	77.17	78.06	78.29	76.21	78.09
En	45.72	43.09	41.50	41.60	41.76	42.84	42.52	43.66
Fs	9.84	12.74	13.44	12.31	11.74	11.88	13.27	12.25
Wo	44.44	44.17	45.06	46.09	46.51	45.28	44.21	44.10
Si (Cations)	1.957	1.988	1.961	1.942	1.916	1.983	1.980	1.988
Ti	0.008	0.006	0.009	0.009	0.013	0.006	0.007	0.006
Al	0.067	0.051	0.074	0.095	0.129	0.049	0.055	0.047
Cr								
Fe ³⁺	0.048	-0.021	0.012	0.036	0.054	0.005	-0.014	-0.018
Fe ²⁺	0.185	0.244	0.255	0.233	0.220	0.226	0.255	0.235
Mn	0.026	0.025	0.024	0.015	0.011	0.022	0.026	0.026
Mg	0.860	0.826	0.789	0.788	0.782	0.816	0.817	0.839
Ca	0.836	0.847	0.857	0.873	0.871	0.863	0.850	0.848
Na	0.028	0.026	0.022	0.021	0.022	0.030	0.020	0.023
Total	4.02	3.99	4.00	4.01	4.02	4.00	4.00	3.99

Abbreviations same as Table A2.3. Cations calculated on a 6 oxygen basis.

Table A2.4 Major element clinopyroxene compositions analysed by EMPA.

Sample ID	Inglewood a cpx51_3 zone	Inglewood a cpx51_4 zone	Inglewood a cpx51_5 core	Inglewood a cpx51_6 light core	Inglewood a cpx56_1 rim	Inglewood a cpx56_2 zone	Inglewood a cpx56_3 zone	Inglewood a cpx56_4 zone
SiO ₂	54.35	52.52	54.38	51.36	54.66	53.54	54.64	52.75
TiO ₂	0.24	0.37	0.27	0.50	0.21	0.26	0.24	0.33
Al ₂ O ₃	1.11	2.44	1.35	3.22	1.06	1.68	1.13	2.04
Cr ₂ O ₃								
Fe ₂ O ₃	-0.36	1.14	-0.28	1.94	-0.74	0.17	-0.13	0.80
FeO	7.84	7.59	7.69	6.61	7.94	8.19	7.43	8.30
MnO	0.95	0.54	0.65	0.36	0.91	0.67	0.86	0.53
MgO	15.80	14.14	15.53	14.53	15.35	14.44	15.53	14.10
CaO	20.77	22.04	21.54	21.59	21.67	21.99	21.87	22.06
Na ₂ O	0.35	0.34	0.35	0.30	0.33	0.32	0.34	0.25
Total	101.05	101.12	101.48	100.40	101.40	101.26	101.91	101.17
Mg#	78.22	76.90	78.26	79.75	77.49	75.88	78.84	75.22
En	44.98	41.31	43.97	43.07	43.39	41.46	43.86	40.75
Fs	12.52	12.41	12.21	10.93	12.61	13.18	11.77	13.43
Wo	42.50	46.28	43.82	45.99	44.01	45.37	44.38	45.82
Si (Cations)	1.985	1.938	1.979	1.908	1.990	1.966	1.982	1.948
Ti	0.006	0.010	0.008	0.014	0.006	0.007	0.007	0.009
Al	0.048	0.106	0.058	0.141	0.046	0.073	0.048	0.089
Cr								
Fe ³⁺	-0.010	0.032	-0.008	0.054	-0.020	0.005	-0.004	0.022
Fe ²⁺	0.240	0.234	0.234	0.204	0.242	0.251	0.225	0.256
Mn	0.029	0.017	0.020	0.011	0.028	0.021	0.026	0.017
Mg	0.861	0.778	0.842	0.805	0.833	0.791	0.840	0.776
Ca	0.813	0.871	0.840	0.859	0.845	0.865	0.850	0.873
Na	0.025	0.024	0.025	0.021	0.024	0.023	0.024	0.018
Total	4.00	4.01	4.00	4.02	3.99	4.00	4.00	4.01

Abbreviations same as Table A2.3. Cations calculated on a 6 oxygen basis.

Table A2.4 Major element clinopyroxene compositions analysed by EMPA.

Sample ID	Inglewood a cpx56_5 zone	Inglewood a cpx56_6 core	Inglewood a cpx56_7 zone	Inglewood a cpx56_8 zone	Inglewood a cpx56_9 zone	Inglewood a cpx57_1 rim	Inglewood a cpx57_2 zone	Inglewood a cpx57_3 zone
Zone								
SiO ₂	54.17	53.62	53.12	54.27	52.37	54.56	52.99	54.95
TiO ₂	0.21	0.24	0.26	0.29	0.41	0.22	0.33	0.27
Al ₂ O ₃	0.98	1.32	1.44	1.33	2.33	1.02	2.09	1.38
Cr ₂ O ₃								
Fe ₂ O ₃	0.53	1.22	1.71	0.06	1.43	-0.64	0.37	-1.28
FeO	6.72	6.31	6.32	7.16	7.61	8.08	8.42	8.80
MnO	0.88	0.68	0.66	0.65	0.52	0.96	0.55	0.78
MgO	15.69	15.58	15.00	15.43	14.33	15.35	14.11	15.06
CaO	21.72	21.64	22.06	22.06	21.88	21.54	22.02	21.77
Na ₂ O	0.34	0.40	0.39	0.34	0.28	0.30	0.29	0.34
Total	101.24	101.00	100.96	101.58	101.16	101.40	101.16	102.06
Mg#	80.64	81.54	80.96	79.34	77.11	77.18	74.95	75.26
En	44.74	44.95	43.63	43.71	41.77	43.40	40.72	42.24
Fs	10.74	10.18	10.26	11.38	12.40	12.83	13.61	13.88
Wo	44.52	44.87	46.11	44.91	45.83	43.76	45.67	43.88
Si (Cations)	1.980	1.968	1.959	1.975	1.935	1.989	1.952	1.987
Ti	0.006	0.007	0.007	0.008	0.011	0.006	0.009	0.007
Al	0.042	0.057	0.063	0.057	0.102	0.044	0.091	0.059
Cr								
Fe ³⁺	0.015	0.033	0.047	0.002	0.040	-0.018	0.010	-0.035
Fe ²⁺	0.205	0.193	0.194	0.218	0.234	0.247	0.259	0.267
Mn	0.027	0.021	0.021	0.020	0.016	0.030	0.017	0.024
Mg	0.855	0.852	0.825	0.837	0.789	0.834	0.775	0.812
Ca	0.851	0.851	0.872	0.860	0.866	0.841	0.869	0.843
Na	0.024	0.029	0.028	0.024	0.020	0.021	0.020	0.024
Total	4.00	4.01	4.02	4.00	4.01	3.99	4.00	3.99

Abbreviations same as Table A2.3. Cations calculated on a 6 oxygen basis.

Table A2.4 Major element clinopyroxene compositions analysed by EMPA.

Sample ID	Inglewood a cpx57_4 light zone	Inglewood a cpx57_5 zone	Inglewood a cpx57_6 light core	Inglewood a cpx57_7 core	Inglewood a cpx63_1 rim	Inglewood a cpx63_2 zone	Inglewood a cpx63_3 zone	Inglewood a cpx63_4 zone
SiO ₂	53.25	54.76	48.72	54.46	53.09	52.62	53.13	50.99
TiO ₂	0.36	0.23	0.88	0.26	0.23	0.29	0.26	0.43
Al ₂ O ₃	2.09	1.13	5.25	1.29	1.01	1.43	1.33	3.14
Cr ₂ O ₃								
Fe ₂ O ₃	-0.03	-0.88	3.80	-0.39	0.87	0.99	0.92	2.13
FeO	8.83	8.52	6.19	7.85	6.44	7.25	6.72	7.40
MnO	0.56	0.87	0.44	0.89	0.95	0.83	0.77	0.40
MgO	14.20	15.11	12.53	15.22	15.42	14.57	15.11	13.55
CaO	21.84	21.68	22.09	21.51	21.30	21.68	21.71	21.99
Na ₂ O	0.28	0.33	0.41	0.41	0.33	0.30	0.33	0.28
Total	101.38	101.76	100.31	101.52	99.63	99.94	100.27	100.29
Mg#	74.13	75.94	78.46	77.54	81.06	78.22	80.09	76.65
En	40.75	42.59	39.35	43.37	44.91	42.60	43.84	40.47
Fs	14.22	13.49	10.80	12.57	10.50	11.86	10.90	12.33
Wo	45.03	43.91	49.85	44.06	44.59	45.54	45.26	47.20
Si (Cations)	1.955	1.989	1.837	1.983	1.975	1.962	1.967	1.909
Ti	0.010	0.006	0.025	0.007	0.006	0.008	0.007	0.012
Al	0.091	0.049	0.233	0.055	0.044	0.063	0.058	0.138
Cr								
Fe ³⁺	-0.001	-0.024	0.107	-0.011	0.024	0.028	0.026	0.060
Fe ²⁺	0.271	0.259	0.193	0.239	0.200	0.225	0.207	0.230
Mn	0.017	0.027	0.014	0.027	0.030	0.026	0.024	0.013
Mg	0.777	0.819	0.704	0.826	0.855	0.810	0.834	0.756
Ca	0.859	0.844	0.892	0.839	0.849	0.866	0.861	0.882
Na	0.020	0.023	0.030	0.029	0.024	0.021	0.024	0.020
Total	4.00	3.99	4.04	4.00	4.01	4.01	4.01	4.02

Abbreviations same as Table A2.3. Cations calculated on a 6 oxygen basis.

Table A2.4 Major element clinopyroxene compositions analysed by EMPA.

Sample ID	Inglewood a cpx63_5 zone	Inglewood a cpx63_6 zone	Inglewood a cpx63_7 zone	Inglewood a cpx63_8 zone	Inglewood a cpx63_9 core	Inglewood a cpx63_10 light core	Inglewood a cpx64_1 rim	Inglewood a cpx64_2 zone
SiO ₂	53.25	50.91	53.04	51.40	52.90	52.91	52.83	53.03
TiO ₂	0.24	0.46	0.25	0.41	0.27	0.24	0.22	0.22
Al ₂ O ₃	1.15	3.46	1.28	2.50	1.32	1.23	1.03	0.95
Cr ₂ O ₃								
Fe ₂ O ₃	1.11	2.13	1.08	2.15	1.42	1.52	1.32	1.26
FeO	6.23	7.08	6.50	7.09	6.04	6.50	6.12	6.39
MnO	0.80	0.37	0.74	0.53	0.75	0.73	0.92	0.98
MgO	15.30	13.41	15.00	13.92	15.24	14.39	15.16	15.68
CaO	21.80	22.31	21.79	21.92	21.63	22.30	21.79	20.96
Na ₂ O	0.36	0.30	0.38	0.30	0.40	0.44	0.30	0.31
Total	100.26	100.42	100.05	100.20	99.97	100.27	99.70	99.78
Mg#	81.45	77.24	80.49	77.86	81.87	79.84	81.58	81.43
En	44.41	40.15	43.73	41.39	44.62	42.27	44.28	45.68
Fs	10.11	11.83	10.60	11.77	9.89	10.67	10.00	10.42
Wo	45.47	48.02	45.66	46.84	45.49	47.06	45.72	43.90
Si (Cations)	1.971	1.902	1.969	1.924	1.965	1.968	1.970	1.973
Ti	0.007	0.013	0.007	0.011	0.008	0.007	0.006	0.006
Al	0.050	0.152	0.056	0.110	0.058	0.054	0.045	0.041
Cr								
Fe ³⁺	0.031	0.060	0.030	0.060	0.039	0.042	0.037	0.035
Fe ²⁺	0.192	0.220	0.201	0.221	0.187	0.201	0.190	0.198
Mn	0.025	0.012	0.023	0.017	0.023	0.023	0.029	0.031
Mg	0.844	0.747	0.830	0.776	0.844	0.798	0.843	0.869
Ca	0.864	0.893	0.867	0.879	0.860	0.889	0.870	0.835
Na	0.026	0.022	0.027	0.022	0.029	0.032	0.022	0.022
Total	4.01	4.02	4.01	4.02	4.01	4.01	4.01	4.01

Abbreviations same as Table A2.3. Cations calculated on a 6 oxygen basis.

Table A2.4 Major element clinopyroxene compositions analysed by EMPA.

Sample ID	Inglewood a cpx64_3 light zone	Inglewood a cpx64_4 zone	Inglewood a cpx64_5 light zone	Inglewood a cpx64_6 zone	Inglewood a cpx64_7 zone	Inglewood a cpx64_8 core	Inglewood a cpx64_9 light core	Inglewood a cpx74_1 rim
SiO ₂	51.88	52.72	50.54	52.23	50.92	52.46	48.33	52.87
TiO ₂	0.29	0.25	0.43	0.25	0.37	0.25	0.98	0.23
Al ₂ O ₃	1.76	1.19	3.00	1.44	2.49	1.07	5.20	1.10
Cr ₂ O ₃								
Fe ₂ O ₃	2.01	1.83	3.00	2.37	2.70	1.95	4.23	1.65
FeO	6.90	5.72	6.51	5.68	6.48	5.47	5.54	6.04
MnO	0.74	0.82	0.44	0.79	0.58	0.79	0.55	0.97
MgO	14.33	15.31	13.57	14.88	13.79	15.40	12.82	15.44
CaO	21.65	21.83	22.18	21.84	21.94	21.60	21.61	21.45
Na ₂ O	0.30	0.32	0.29	0.38	0.33	0.34	0.46	0.31
Total	99.86	99.99	99.94	99.86	99.60	99.34	99.72	100.06
Mg#	78.81	82.74	78.91	82.45	79.26	83.44	80.66	82.06
En	42.46	44.78	40.94	44.09	41.59	45.33	40.80	45.11
Fs	11.41	9.34	10.95	9.38	10.88	8.99	9.78	9.86
Wo	46.12	45.88	48.11	46.52	47.53	45.68	49.41	45.03
Si (Cations)	1.945	1.961	1.904	1.953	1.921	1.963	1.833	1.965
Ti	0.008	0.007	0.012	0.007	0.010	0.007	0.028	0.007
Al	0.078	0.052	0.133	0.064	0.111	0.047	0.232	0.048
Cr								
Fe ³⁺	0.056	0.051	0.084	0.066	0.076	0.055	0.120	0.046
Fe ²⁺	0.215	0.177	0.204	0.176	0.203	0.171	0.174	0.187
Mn	0.023	0.026	0.014	0.025	0.019	0.025	0.018	0.030
Mg	0.801	0.849	0.762	0.829	0.776	0.860	0.725	0.856
Ca	0.870	0.870	0.895	0.875	0.886	0.866	0.878	0.854
Na	0.022	0.023	0.021	0.027	0.024	0.025	0.034	0.022
Total	4.02	4.02	4.03	4.02	4.03	4.02	4.04	4.02

Abbreviations same as Table A2.3. Cations calculated on a 6 oxygen basis.

Table A2.4 Major element clinopyroxene compositions analysed by EMPA.

Sample ID	Inglewood a cpx74_2 zone	Inglewood a cpx74_3 zone	Inglewood a cpx74_4 zone	Inglewood a cpx74_6 light core	Inglewood a cpx74_7 core	Korito cpx1_1 rim	Korito cpx1_2 zone	Korito cpx1_3 light core	Korito cpx1_4 core
SiO ₂	52.29	53.31	53.32	53.43	52.96	51.95	51.89	51.79	52.75
TiO ₂	0.30	0.23	0.18	0.14	0.31	0.29	0.28	0.42	0.32
Al ₂ O ₃	1.85	1.15	0.97	0.92	1.24	2.10	2.29	3.14	2.15
Cr ₂ O ₃									
Fe ₂ O ₃	1.70	1.06	1.30	1.26	1.81	1.91	2.48	2.60	1.85
FeO	7.01	6.79	6.44	6.98	5.84	6.41	5.62	6.02	5.41
MnO	0.65	0.93	0.66	0.76	0.65	0.49	0.38	0.41	0.45
MgO	14.35	15.43	14.70	14.75	15.85	14.28	14.50	14.01	15.37
CaO	22.03	21.35	22.56	22.02	21.44	22.29	22.69	22.70	22.30
Na ₂ O	0.29	0.30	0.37	0.39	0.31	0.33	0.30	0.40	0.34
Total	100.47	100.55	100.49	100.65	100.42	100.04	100.44	101.51	100.95
Mg#	78.57	80.24	80.33	79.07	82.94	79.96	82.22	80.68	83.57
En	42.09	44.64	42.59	42.77	45.92	42.15	42.73	41.61	44.66
Fs	11.48	10.99	10.43	11.32	9.44	10.57	9.24	9.96	8.78
Wo	46.43	44.37	46.98	45.91	44.64	47.28	48.03	48.43	46.57
Si (Cations)	1.946	1.969	1.975	1.978	1.958	1.939	1.930	1.910	1.940
Ti	0.008	0.006	0.005	0.004	0.009	0.008	0.008	0.012	0.009
Al	0.081	0.050	0.043	0.040	0.054	0.092	0.100	0.137	0.093
Cr									
Fe ³⁺	0.047	0.029	0.036	0.035	0.050	0.054	0.069	0.072	0.051
Fe ²⁺	0.217	0.209	0.199	0.215	0.180	0.199	0.174	0.185	0.166
Mn	0.020	0.029	0.021	0.024	0.020	0.015	0.012	0.013	0.014
Mg	0.796	0.850	0.812	0.814	0.874	0.795	0.804	0.771	0.842
Ca	0.878	0.845	0.895	0.873	0.849	0.891	0.904	0.897	0.878
Na	0.021	0.021	0.027	0.028	0.022	0.024	0.022	0.029	0.024
Total	4.02	4.01	4.01	4.01	4.02	4.02	4.02	4.02	4.02

Abbreviations same as Table A2.3. Cations calculated on a 6 oxygen basis.

Table A2.4 Major element clinopyroxene compositions analysed by EMPA.

Sample ID	Korito rim	Korito rim	Korito zone	Korito zone	Korito zone	Korito zone	Korito zone	Korito zone	Korito zone	Korito zone	Korito core	Korito rim
Zone	cpx18_1	cpx18_2	cpx18_3	cpx18_4	cpx18_5	cpx18_6	cpx18_7	cpx18_8	cpx18_9	cpx18_10	cpx18_11	cpx19_1
SiO ₂	52.16	53.73	53.02	53.85	52.14	53.73	52.62	53.26	52.28	52.27	52.27	52.27
TiO ₂	0.31	0.23	0.30	0.24	0.36	0.27	0.35	0.29	0.42	0.38	0.42	0.38
Al ₂ O ₃	1.90	1.11	1.64	1.12	2.54	1.25	2.41	1.55	2.29	2.62	2.29	2.62
Cr ₂ O ₃												
Fe ₂ O ₃	1.91	1.01	1.15	0.69	1.91	1.24	1.93	1.27	2.09	1.39	2.09	1.39
FeO	6.86	6.29	7.66	7.03	6.97	6.27	7.22	6.66	6.13	7.54	6.13	7.54
MnO	0.66	0.87	0.72	1.05	0.46	0.76	0.75	0.73	0.62	0.56	0.62	0.56
MgO	14.69	15.71	14.69	15.39	14.05	16.01	14.36	15.40	15.29	14.14	15.29	14.14
CaO	21.66	21.71	21.87	21.49	22.50	21.34	21.11	21.54	21.08	22.05	21.08	22.05
Na ₂ O	0.26	0.32	0.24	0.34	0.30	0.34	0.57	0.33	0.41	0.28	0.41	0.28
Total	100.41	100.97	101.29	101.20	101.23	101.22	101.32	101.04	100.61	101.24	100.61	101.24
Mg#	79.32	81.71	77.43	79.62	78.31	82.03	78.09	80.51	81.71	77.04	81.71	77.04
En	43.10	45.11	42.35	44.26	41.19	45.94	42.79	44.50	45.15	41.34	45.15	41.34
Fs	11.23	10.10	12.34	11.33	11.41	10.06	12.00	10.77	10.11	12.32	10.11	12.32
Wo	45.67	44.79	45.30	44.41	47.40	44.00	45.20	44.73	44.74	46.33	44.74	46.33
Si (Cations)	1.941	1.972	1.954	1.975	1.928	1.966	1.940	1.958	1.934	1.930	1.934	1.930
Ti	0.009	0.006	0.008	0.007	0.010	0.008	0.010	0.008	0.012	0.010	0.012	0.010
Al	0.083	0.048	0.071	0.048	0.111	0.054	0.105	0.067	0.100	0.114	0.100	0.114
Cr												
Fe ³⁺	0.053	0.028	0.032	0.019	0.053	0.034	0.053	0.035	0.058	0.038	0.058	0.038
Fe ²⁺	0.212	0.192	0.235	0.215	0.215	0.191	0.222	0.204	0.189	0.232	0.189	0.232
Mn	0.021	0.027	0.022	0.033	0.014	0.024	0.023	0.023	0.020	0.018	0.020	0.018
Mg	0.815	0.860	0.807	0.841	0.775	0.874	0.790	0.844	0.843	0.778	0.843	0.778
Ca	0.864	0.853	0.863	0.844	0.891	0.837	0.834	0.849	0.835	0.872	0.835	0.872
Na	0.019	0.023	0.017	0.024	0.022	0.024	0.041	0.023	0.030	0.020	0.030	0.020
Total	4.02	4.01	4.01	4.01	4.02	4.01	4.02	4.01	4.02	4.01	4.02	4.01

Abbreviations same as Table A2.3. Cations calculated on a 6 oxygen basis.

Table A2.4 Major element clinopyroxene compositions analysed by EMPA.

Sample ID	Korito cpx19_2 zone	Korito cpx19_3 zone	Korito cpx19_4 zone	Korito cpx19_5 zone	Korito cpx19_6 zone	Korito cpx19_7 core	Korito cpx19_8 light core	Korito cpx2_1 rim	Korito cpx2_2 light	Korito cpx2_4 core
SiO ₂	53.50	52.91	53.55	51.92	52.75	53.55	51.40	53.11	51.65	53.80
TiO ₂	0.24	0.27	0.26	0.30	0.31	0.26	0.48	0.28	0.44	0.27
Al ₂ O ₃	1.19	1.55	1.27	3.27	2.36	1.53	3.56	1.50	3.10	1.48
Cr ₂ O ₃										
Fe ₂ O ₃	1.25	1.61	1.09	2.32	1.87	1.60	2.61	1.89	2.28	1.19
FeO	6.41	6.73	6.88	5.90	7.26	6.30	6.35	5.89	7.16	6.44
MnO	0.92	0.78	0.90	0.45	0.68	0.73	0.43	0.88	0.47	0.87
MgO	15.57	14.98	15.17	14.45	14.29	15.53	13.93	15.36	13.92	15.39
CaO	21.58	21.84	21.83	22.30	21.41	21.60	22.39	21.77	22.24	21.82
Na ₂ O	0.32	0.29	0.32	0.37	0.55	0.41	0.35	0.37	0.28	0.41
Total	100.98	100.96	101.27	101.29	101.47	101.53	101.51	101.06	101.54	101.66
Mg#	81.27	79.94	79.77	81.45	77.90	81.51	79.74	82.35	77.70	81.04
En	44.91	43.50	43.71	42.79	42.37	44.91	41.51	44.79	41.07	44.39
Fs	10.35	10.92	11.09	9.74	12.02	10.19	10.55	9.60	11.79	10.39
Wo	44.74	45.59	45.20	47.47	45.61	44.90	47.94	45.61	47.15	45.22
Si (Cations)	1.967	1.954	1.967	1.912	1.943	1.959	1.898	1.956	1.909	1.964
Ti	0.007	0.008	0.007	0.008	0.009	0.007	0.013	0.008	0.012	0.007
Al	0.052	0.067	0.055	0.142	0.102	0.066	0.155	0.065	0.135	0.064
Cr										
Fe ³⁺	0.034	0.044	0.030	0.064	0.052	0.044	0.072	0.052	0.063	0.033
Fe ²⁺	0.197	0.207	0.211	0.181	0.223	0.192	0.195	0.181	0.220	0.196
Mn	0.029	0.024	0.028	0.014	0.021	0.023	0.013	0.027	0.015	0.027
Mg	0.853	0.825	0.831	0.793	0.785	0.847	0.767	0.843	0.767	0.838
Ca	0.850	0.864	0.859	0.880	0.845	0.847	0.886	0.859	0.880	0.853
Na	0.023	0.021	0.023	0.026	0.039	0.029	0.025	0.027	0.020	0.029
Total	4.01	4.01	4.01	4.02	4.02	4.01	4.02	4.02	4.02	4.01

Abbreviations same as Table A2.3. Cations calculated on a 6 oxygen basis.

Table A2.4 Major element clinopyroxene compositions analysed by EMPA.

Sample ID	Korito rim	Korito rim	Korito zone	Korito zone	Korito zone	Korito zone	Korito zone	Korito rim	Korito light core	Korito rim	Korito zone	Korito light	Korito zone
Zone	cpx20_1	cpx20_2	cpx20_3	cpx20_4	cpx20_5	cpx20_7	cpx22_1	cpx22_2	cpx22_3	cpx22_4			
SiO ₂	52.91	53.19	52.31	53.63	53.01	51.70	52.17	53.81	51.86	53.27			53.27
TiO ₂	0.25	0.23	0.34	0.23	0.29	0.43	0.33	0.24	0.39	0.28			0.28
Al ₂ O ₃	1.30	1.09	2.38	1.11	1.33	2.90	1.88	1.22	2.41	1.46			1.46
Cr ₂ O ₃													
Fe ₂ O ₃	1.83	1.26	2.01	1.19	1.64	2.58	1.90	1.11	2.03	1.32			1.32
FeO	5.64	5.89	6.66	6.17	5.94	6.79	6.11	6.39	6.99	6.32			6.32
MnO	0.88	0.92	0.51	0.85	0.75	0.62	0.82	0.84	0.53	0.71			0.71
MgO	15.46	15.51	14.27	15.45	15.66	13.84	14.79	15.33	14.12	15.24			15.24
CaO	21.67	21.70	22.35	21.91	21.39	21.51	21.65	22.18	22.19	22.05			22.05
Na ₂ O	0.36	0.34	0.36	0.37	0.36	0.57	0.36	0.34	0.27	0.33			0.33
Total	100.31	100.12	101.19	100.91	100.38	100.93	100.01	101.46	100.81	100.97			100.97
Mg#	83.08	82.49	79.32	81.74	82.51	78.52	81.26	81.10	78.34	81.17			81.17
En	45.23	45.09	41.90	44.60	45.59	41.83	43.82	44.00	41.57	44.03			44.03
Fs	9.21	9.57	10.93	9.97	9.66	11.45	10.10	10.25	11.49	10.21			10.21
Wo	45.56	45.34	47.17	45.44	44.75	46.72	46.08	45.74	46.94	45.76			45.76
Si (Cations)	1.960	1.970	1.933	1.972	1.961	1.921	1.945	1.969	1.927	1.960			1.960
Ti	0.007	0.006	0.009	0.006	0.008	0.012	0.009	0.006	0.011	0.008			0.008
Al	0.057	0.048	0.104	0.048	0.058	0.127	0.082	0.053	0.106	0.063			0.063
Cr													
Fe ³⁺	0.051	0.035	0.056	0.033	0.045	0.072	0.053	0.031	0.057	0.037			0.037
Fe ²⁺	0.174	0.182	0.205	0.189	0.183	0.210	0.190	0.195	0.216	0.194			0.194
Mn	0.028	0.029	0.016	0.027	0.024	0.020	0.026	0.026	0.017	0.022			0.022
Mg	0.854	0.856	0.786	0.847	0.863	0.766	0.822	0.836	0.782	0.836			0.836
Ca	0.860	0.861	0.885	0.863	0.848	0.856	0.865	0.870	0.883	0.869			0.869
Na	0.026	0.024	0.025	0.026	0.026	0.041	0.026	0.024	0.020	0.023			0.023
Total	4.02	4.01	4.02	4.01	4.02	4.02	4.02	4.01	4.02	4.01			4.01

Abbreviations same as Table A2.3. Cations calculated on a 6 oxygen basis.

Table A2.4 Major element clinopyroxene compositions analysed by EMPA.

Sample ID	Korito cpx22_6 core	Korito cpx3_1 rim	Korito cpx3_2 core	Korito cpx30_1 rim	Korito cpx30_2 zone	Korito cpx30_3 zone	Korito cpx30_4 core	Korito cpx34_1 rim	Korito cpx34_2 zone	Korito cpx34_3 light core
Zone										
SiO ₂	52.79	53.36	53.24	51.40	52.51	51.72	52.12	53.98	54.22	51.74
TiO ₂	0.30	0.26	0.28	0.34	0.28	0.42	0.26	0.24	0.25	0.55
Al ₂ O ₃	1.57	1.56	1.68	2.05	1.46	2.22	1.17	1.17	1.14	3.51
Cr ₂ O ₃										
Fe ₂ O ₃	1.59	0.81	1.52	4.34	3.84	4.41	0.73	0.05	0.19	1.68
FeO	6.31	7.11	6.74	5.27	4.38	4.66	6.96	7.51	7.03	7.49
MnO	0.68	0.61	0.87	0.71	0.89	0.84	0.89	0.97	0.88	0.37
MgO	14.88	14.85	14.91	15.07	15.95	14.89	14.09	15.18	15.25	13.73
CaO	22.18	22.27	21.59	21.58	21.52	21.80	21.74	21.76	22.13	22.50
Na ₂ O	0.32	0.28	0.45	0.29	0.40	0.50	0.37	0.29	0.35	0.27
Total	100.60	101.12	101.27	101.05	101.22	101.45	98.35	101.15	101.44	101.83
Mg#	80.83	78.86	79.83	83.74	86.76	85.21	78.33	78.27	79.45	76.63
En	43.31	42.64	43.61	44.98	47.12	44.93	41.93	43.33	43.46	40.27
Fs	10.27	11.43	11.02	8.73	7.19	7.80	11.60	12.03	11.24	12.28
Wo	46.41	45.93	45.38	46.29	45.69	47.27	46.48	44.65	45.31	47.44
Si (Cations)	1.954	1.962	1.958	1.915	1.939	1.917	1.973	1.978	1.979	1.903
Ti	0.008	0.007	0.008	0.010	0.008	0.012	0.007	0.007	0.007	0.015
Al	0.068	0.067	0.073	0.090	0.064	0.097	0.052	0.051	0.049	0.152
Cr										
Fe ³⁺	0.044	0.022	0.042	0.120	0.106	0.122	0.021	0.001	0.005	0.046
Fe ²⁺	0.195	0.218	0.206	0.163	0.134	0.143	0.220	0.230	0.215	0.230
Mn	0.021	0.019	0.027	0.022	0.028	0.026	0.029	0.030	0.027	0.011
Mg	0.821	0.814	0.817	0.837	0.878	0.823	0.795	0.829	0.830	0.753
Ca	0.880	0.877	0.850	0.862	0.851	0.866	0.882	0.854	0.865	0.887
Na	0.023	0.020	0.032	0.021	0.028	0.036	0.027	0.021	0.024	0.019
Total	4.01	4.01	4.01	4.04	4.04	4.04	4.01	4.00	4.00	4.02

Abbreviations same as Table A2.3. Cations calculated on a 6 oxygen basis.

Table A2.4 Major element clinopyroxene compositions analysed by EMPA.

Sample ID	Korito rim	Korito rim	Korito rim	Korito core	Korito rim	Korito zone	Korito rim	Korito core	Korito light	Korito core	Korito rim	Korito zone	Korito zone
Zone	cpx35_1	cpx35_2	cpx35_3	cpx35_3	cpx36_1	cpx36_2	cpx36_3	cpx36_4	cpx36_3	cpx36_4	cpx38_1	cpx38_2	cpx38_3
SiO ₂	51.08	52.82	53.95	53.95	53.71	53.94	53.28	53.29	53.28	53.29	52.26	53.92	53.34
TiO ₂	0.41	0.24	0.27	0.27	0.26	0.23	0.34	0.37	0.34	0.37	0.41	0.24	0.29
Al ₂ O ₃	2.86	1.16	1.21	1.21	1.13	1.14	1.81	2.13	1.81	2.13	2.93	1.28	1.96
Cr ₂ O ₃													
Fe ₂ O ₃	2.28	1.43	0.58	0.58	0.34	0.15	0.53	0.68	0.53	0.68	-0.78	0.30	0.51
FeO	7.17	6.07	6.73	6.73	7.28	7.20	8.08	7.36	8.08	7.36	9.86	6.99	7.55
MnO	0.55	0.94	0.80	0.80	1.05	0.97	0.78	0.70	0.78	0.70	0.72	0.84	0.55
MgO	13.55	15.31	15.34	15.34	15.17	15.09	14.14	15.33	14.14	15.33	13.19	15.07	14.47
CaO	22.18	21.56	22.15	22.15	21.49	21.92	22.31	21.30	22.31	21.30	21.20	22.13	22.49
Na ₂ O	0.26	0.32	0.33	0.33	0.33	0.34	0.30	0.30	0.30	0.30	0.34	0.35	0.29
Total	100.35	99.86	101.35	101.35	100.76	100.97	101.56	101.45	101.56	101.45	100.13	101.13	101.43
Mg#	77.20	81.85	80.26	80.26	78.80	78.91	75.75	78.82	75.75	78.82	70.42	79.36	77.39
En	40.46	44.76	43.79	43.79	43.72	43.27	40.75	44.10	40.75	44.10	38.84	43.19	41.51
Fs	11.95	9.93	10.77	10.77	11.76	11.57	13.04	11.85	13.04	11.85	16.32	11.23	12.13
Wo	47.60	45.31	45.44	45.44	44.52	45.16	46.21	44.05	46.21	44.05	44.84	45.58	46.36
Si (Cations)	1.913	1.966	1.973	1.973	1.977	1.980	1.957	1.948	1.957	1.948	1.944	1.975	1.955
Ti	0.012	0.007	0.007	0.007	0.007	0.006	0.009	0.010	0.009	0.010	0.011	0.007	0.008
Al	0.126	0.051	0.052	0.052	0.049	0.049	0.078	0.092	0.078	0.092	0.128	0.055	0.085
Cr													
Fe ³⁺	0.064	0.040	0.016	0.016	0.009	0.004	0.015	0.019	0.015	0.019	-0.022	0.008	0.014
Fe ²⁺	0.223	0.188	0.206	0.206	0.224	0.221	0.248	0.225	0.248	0.225	0.307	0.214	0.231
Mn	0.018	0.030	0.025	0.025	0.033	0.030	0.024	0.022	0.024	0.022	0.023	0.026	0.017
Mg	0.757	0.849	0.836	0.836	0.832	0.826	0.774	0.836	0.774	0.836	0.732	0.823	0.791
Ca	0.890	0.860	0.868	0.868	0.848	0.862	0.878	0.834	0.878	0.834	0.845	0.869	0.883
Na	0.019	0.023	0.023	0.023	0.024	0.024	0.021	0.021	0.021	0.021	0.024	0.025	0.021
Total	4.02	4.01	4.01	4.01	4.00	4.00	4.00	4.01	4.00	4.01	3.99	4.00	4.00

Abbreviations same as Table A2.3. Cations calculated on a 6 oxygen basis.

Table A2.4 Major element clinopyroxene compositions analysed by EMPA.

Sample ID	Korito cpx38_4 core	Korito cpx4_1 rim	Korito cpx4_2 core	Korito cpx42_1 rim	Korito cpx42_2 zone	Korito cpx46_1 zone	Korito cpx46_2 zone	Korito cpx46_3 zone	Korito cpx46_4 zone	Korito cpx46_6 zone
Zone										
SiO ₂	53.63	52.89	51.75	54.15	53.92	53.57	53.05	54.35	53.76	54.12
TiO ₂	0.36	0.18	0.41	0.24	0.31	0.23	0.33	0.23	0.26	0.29
Al ₂ O ₃	1.73	1.13	3.37	1.28	1.57	1.08	2.21	1.02	1.30	1.43
Cr ₂ O ₃										
Fe ₂ O ₃	0.35	1.76	2.16	-0.08	0.32	0.75	0.64	0.14	0.69	0.26
FeO	7.28	6.66	3.81	7.32	6.91	6.62	7.81	6.99	6.69	7.19
MnO	0.73	0.73	0.12	0.80	0.74	0.95	0.53	0.85	0.72	0.65
MgO	15.14	14.13	16.21	15.11	14.81	15.31	14.04	15.08	15.05	15.05
CaO	21.59	22.61	22.14	22.14	22.52	21.83	22.69	22.49	22.31	22.46
Na ₂ O	0.38	0.41	0.24	0.33	0.40	0.31	0.28	0.36	0.36	0.33
Total	101.19	100.50	100.20	101.29	101.49	100.65	101.58	101.51	101.14	101.77
Mg#	78.77	79.15	88.40	78.62	79.27	80.50	76.26	79.36	80.05	78.87
En	43.58	41.43	47.33	43.01	42.48	44.11	40.45	42.88	43.20	42.73
Fs	11.75	10.92	6.21	11.70	11.11	10.68	12.59	11.15	10.76	11.45
Wo	44.68	47.65	46.46	45.29	46.41	45.21	46.96	45.97	46.04	45.83
Si (Cations)	1.963	1.969	1.904	1.978	1.969	1.974	1.947	1.983	1.972	1.971
Ti	0.010	0.005	0.011	0.007	0.008	0.006	0.009	0.006	0.007	0.008
Al	0.075	0.049	0.146	0.055	0.068	0.047	0.096	0.044	0.056	0.061
Cr										
Fe ³⁺	0.010	0.049	0.059	-0.002	0.009	0.021	0.018	0.004	0.019	0.007
Fe ²⁺	0.223	0.207	0.117	0.224	0.211	0.204	0.239	0.213	0.205	0.219
Mn	0.023	0.023	0.004	0.025	0.023	0.030	0.017	0.026	0.022	0.020
Mg	0.826	0.784	0.889	0.823	0.806	0.841	0.769	0.820	0.823	0.817
Ca	0.847	0.901	0.873	0.866	0.881	0.862	0.892	0.879	0.877	0.876
Na	0.027	0.029	0.017	0.024	0.028	0.022	0.020	0.025	0.026	0.023
Total	4.00	4.02	4.02	4.00	4.00	4.01	4.01	4.00	4.01	4.00

Abbreviations same as Table A2.3. Cations calculated on a 6 oxygen basis.

Table A2.4 Major element clinopyroxene compositions analysed by EMPA.

Sample ID	Korito cpx46_7 zone	Korito cpx46_8 core	Korito cpx46_9 light core	Korito cpx47_1 rim	Korito cpx47_2 zone	Korito cpx47_3 zone	Korito cpx47_4 zone	Korito cpx47_5 zone	Korito cpx47_6 core	Korito cpx47_7 light core
SiO ₂	51.07	53.67	51.33	54.22	53.10	52.94	52.74	53.43	54.23	52.15
TiO ₂	0.73	0.32	0.48	0.26	0.33	0.25	0.35	0.25	0.24	0.46
Al ₂ O ₃	4.34	1.68	3.55	1.44	2.13	1.27	2.30	1.35	1.09	3.17
Cr ₂ O ₃										
Fe ₂ O ₃	1.74	0.68	2.00	-0.29	0.35	1.20	0.54	0.93	-0.05	1.29
FeO	7.35	6.68	6.63	7.62	7.82	6.37	8.47	6.74	7.46	7.62
MnO	0.41	0.64	0.33	0.80	0.53	0.84	0.46	0.75	0.78	0.42
MgO	13.00	15.27	13.49	15.00	14.17	14.77	13.66	14.65	15.08	13.45
CaO	22.69	22.05	23.01	22.05	22.58	22.20	22.54	22.43	22.27	22.91
Na ₂ O	0.38	0.36	0.29	0.35	0.27	0.34	0.27	0.38	0.30	0.31
Total	101.71	101.36	101.12	101.46	101.29	100.17	101.33	100.91	101.41	101.77
Mg#	76.00	80.31	78.46	77.82	76.37	80.56	74.22	79.53	78.29	75.95
En	38.91	43.80	40.00	42.71	40.73	43.08	39.47	42.42	42.76	39.36
Fs	12.28	10.74	10.98	12.17	12.61	10.39	13.71	10.92	11.86	12.46
Wo	48.81	45.46	49.02	45.12	46.66	46.53	46.82	46.67	45.39	48.17
Si (Cations)	1.883	1.962	1.901	1.977	1.951	1.966	1.945	1.969	1.981	1.918
Ti	0.020	0.009	0.013	0.007	0.009	0.007	0.010	0.007	0.007	0.013
Al	0.189	0.072	0.155	0.062	0.092	0.055	0.100	0.059	0.047	0.138
Cr										
Fe ³⁺	0.048	0.019	0.055	-0.008	0.010	0.033	0.015	0.026	-0.001	0.035
Fe ²⁺	0.226	0.204	0.204	0.232	0.240	0.197	0.261	0.207	0.228	0.233
Mn	0.013	0.020	0.010	0.025	0.017	0.026	0.014	0.023	0.024	0.013
Mg	0.715	0.832	0.745	0.815	0.776	0.818	0.751	0.805	0.821	0.737
Ca	0.896	0.864	0.913	0.861	0.889	0.883	0.891	0.886	0.872	0.902
Na	0.027	0.025	0.021	0.025	0.019	0.025	0.019	0.027	0.021	0.022
Total	4.02	4.01	4.02	4.00	4.00	4.01	4.01	4.01	4.00	4.01

Abbreviations same as Table A2.3. Cations calculated on a 6 oxygen basis.

Table A2.4 Major element clinopyroxene compositions analysed by EMPA.

Sample ID	Korito rim	Korito cpx5_1 zone	Korito cpx5_2 zone	Korito cpx5_3 zone	Korito cpx5_4 light	Korito cpx5_5 zone	Korito cpx5_6 core	Korito cpx53_1 zone	Korito cpx53_2 zone	Korito rim	Korito cpx56_1 rim	Korito cpx56_2 zone
Zone												
SiO ₂	52.57	53.27	52.43	52.43	50.27	52.87	52.19	53.76	50.82	52.56	52.56	53.97
TiO ₂	0.26	0.28	0.40	0.40	0.58	0.33	0.49	0.32	0.56	0.30	0.30	0.24
Al ₂ O ₃	1.35	1.42	2.00	2.00	3.90	1.58	2.77	1.43	3.81	1.89	1.89	1.11
Cr ₂ O ₃												
Fe ₂ O ₃	2.25	1.72	2.15	2.15	2.99	1.78	2.21	0.51	2.02	1.11	1.11	0.59
FeO	5.15	5.87	5.74	5.74	6.55	5.82	6.02	6.79	7.01	7.51	7.51	6.75
MnO	0.84	0.73	0.67	0.67	0.37	0.63	0.54	0.48	0.32	0.73	0.73	0.86
MgO	15.65	15.45	14.93	14.93	13.20	15.51	14.77	14.94	13.37	14.08	14.08	15.06
CaO	21.57	21.92	22.06	22.06	22.39	21.75	21.87	22.77	22.55	22.23	22.23	22.38
Na ₂ O	0.34	0.38	0.39	0.39	0.34	0.34	0.43	0.32	0.27	0.28	0.28	0.35
Total	99.98	101.03	100.74	100.74	100.59	100.61	101.28	101.32	100.73	100.68	100.68	101.31
Mg#	84.50	82.49	82.34	82.34	78.34	82.67	81.48	79.70	77.36	77.03	77.03	79.93
En	46.00	44.81	43.93	43.93	40.08	45.10	43.64	42.56	39.93	41.11	41.11	43.12
Fs	8.44	9.51	9.42	9.42	11.08	9.46	9.92	10.84	11.69	12.26	12.26	10.83
Wo	45.56	45.68	46.64	46.64	48.84	45.45	46.44	46.61	48.38	46.63	46.63	46.06
Si (Cations)	1.955	1.959	1.939	1.939	1.882	1.952	1.921	1.967	1.892	1.950	1.950	1.976
Ti	0.007	0.008	0.011	0.011	0.016	0.009	0.013	0.009	0.016	0.008	0.008	0.007
Al	0.059	0.062	0.087	0.087	0.172	0.069	0.120	0.062	0.167	0.082	0.082	0.048
Cr												
Fe ³⁺	0.063	0.047	0.059	0.059	0.084	0.049	0.061	0.014	0.056	0.031	0.031	0.016
Fe ²⁺	0.159	0.180	0.177	0.177	0.204	0.179	0.184	0.208	0.217	0.232	0.232	0.206
Mn	0.026	0.023	0.021	0.021	0.012	0.020	0.017	0.015	0.010	0.023	0.023	0.027
Mg	0.868	0.847	0.823	0.823	0.737	0.854	0.810	0.815	0.742	0.779	0.779	0.822
Ca	0.859	0.864	0.874	0.874	0.898	0.860	0.863	0.893	0.899	0.884	0.884	0.878
Na	0.025	0.027	0.028	0.028	0.024	0.024	0.030	0.023	0.020	0.020	0.020	0.025
Total	4.02	4.02	4.02	4.02	4.03	4.02	4.02	4.00	4.02	4.01	4.01	4.01

Abbreviations same as Table A2.3. Cations calculated on a 6 oxygen basis.

Table A2.4 Major element clinopyroxene compositions analysed by EMPA.

Sample ID	Korito cpx56_3 zone	Korito cpx56_4 zone	Korito cpx56_5 core	Korito cpx59_1 core	Korito cpx8_1 rim	Korito cpx8_2 zone	Korito cpx8_3 zone	Korito cpx8_4 light core	Korito cpx8_5 core	Korito cpx9_2 zone
Zone										
SiO ₂	54.34	52.15	54.15	53.76	52.86	53.41	53.26	50.78	52.49	54.39
TiO ₂	0.27	0.48	0.28	0.30	0.25	0.21	0.26	0.60	0.34	0.21
Al ₂ O ₃	1.29	3.22	1.38	1.55	1.34	1.03	1.39	3.77	1.89	1.07
Cr ₂ O ₃										
Fe ₂ O ₃	0.36	1.48	0.72	0.40	1.11	0.94	1.55	2.74	1.97	0.63
FeO	6.79	7.51	6.60	7.17	6.13	6.64	6.14	6.59	6.03	6.72
MnO	0.73	0.43	0.63	0.66	0.85	1.04	0.81	0.46	0.63	0.91
MgO	15.22	13.79	15.39	14.40	15.18	15.35	15.12	13.49	15.06	15.86
CaO	22.47	22.58	22.37	22.73	21.74	21.43	22.04	22.22	21.59	21.73
Na ₂ O	0.39	0.30	0.37	0.42	0.34	0.34	0.39	0.38	0.42	0.32
Total	101.84	101.93	101.88	101.38	99.79	100.40	100.96	101.03	100.42	101.84
Mg#	80.00	76.67	80.64	78.20	81.57	80.51	81.50	78.60	81.72	80.82
En	43.28	40.30	43.76	41.45	44.34	44.54	43.96	40.72	44.37	45.00
Fs	10.82	12.27	10.51	11.56	10.02	10.78	9.98	11.09	9.93	10.68
Wo	45.91	47.43	45.73	47.00	45.64	44.68	46.06	48.19	45.70	44.32
Si (Cations)	1.975	1.914	1.969	1.969	1.966	1.975	1.962	1.889	1.946	1.977
Ti	0.007	0.013	0.008	0.008	0.007	0.006	0.007	0.017	0.009	0.006
Al	0.055	0.139	0.059	0.067	0.059	0.045	0.060	0.165	0.082	0.046
Cr										
Fe ³⁺	0.010	0.041	0.020	0.011	0.031	0.026	0.043	0.076	0.055	0.017
Fe ²⁺	0.206	0.230	0.200	0.219	0.190	0.205	0.188	0.204	0.186	0.204
Mn	0.023	0.014	0.019	0.021	0.027	0.033	0.025	0.014	0.020	0.028
Mg	0.825	0.754	0.834	0.787	0.841	0.846	0.830	0.748	0.832	0.859
Ca	0.875	0.888	0.871	0.892	0.866	0.849	0.870	0.885	0.857	0.846
Na	0.027	0.021	0.026	0.030	0.024	0.024	0.028	0.027	0.030	0.023
Total	4.00	4.01	4.01	4.00	4.01	4.01	4.01	4.03	4.02	4.01

Abbreviations same as Table A2.3. Cations calculated on a 6 oxygen basis.

Table A2.4 Major element clinopyroxene compositions analysed by EMPA.

Sample ID	Korito cpx9_4 zone	Korito cpx9_3 light	Korito cpx9_6 core
SiO ₂	53.15	51.55	52.97
TiO ₂	0.29	0.46	0.27
Al ₂ O ₃	1.44	2.91	1.54
Cr ₂ O ₃			
Fe ₂ O ₃	1.32	1.94	1.96
FeO	6.14	7.24	5.64
MnO	0.77	0.48	0.58
MgO	15.30	13.99	15.43
CaO	21.76	21.96	21.87
Na ₂ O	0.38	0.28	0.40
Total	100.54	100.80	100.66
Mg#	81.67	77.58	83.04
En	44.52	41.38	44.98
Fs	9.99	11.96	9.19
Wo	45.49	46.66	45.83
Si (Cations)	1.962	1.916	1.955
Ti	0.008	0.013	0.008
Al	0.062	0.127	0.067
Cr			
Fe ³⁺	0.037	0.054	0.054
Fe ²⁺	0.189	0.224	0.173
Mn	0.024	0.015	0.018
Mg	0.842	0.775	0.849
Ca	0.860	0.874	0.865
Na	0.027	0.020	0.029
Total	4.01	4.02	4.02

Abbreviations same as Table A2.3. Cations calculated on a 6 oxygen basis.

Table A2.5 Major element orthopyroxene compositions analysed by EMPA.

Sample	6c	6c	6c	6c	6c	6c	6c	6c	6c	6c	6c	6c	6c	6c	6c	6c	6c	6c	6c
ID	cpx12_1	cpx12_6	cpx12_8	cpx12_9	cpx19_1	cpx19_2	cpx19_3	cpx19_4	cpx19_5	PP_2	PR_2	PV_3	PY_2						
Zone	rim	core	rim	rim	rim	rim	core	core	rim	core	core	core	core						
SiO ₂	55.91	55.58	55.71	56.17	54.95	54.17	54.46	54.00	54.86	52.15	53.43	52.38	53.24						
TiO ₂	0.17	0.23	0.19	0.21	0.16	0.15	0.22	0.24	0.17	0.19	0.20	0.21	0.28						
Al ₂ O ₃	0.81	1.11	1.23	1.14	1.04	0.73	1.50	1.61	0.78	1.58	0.90	0.97	1.52						
Cr ₂ O ₃										0.12	0.07	0.05	0.10						
Fe ₂ O ₃	0.40	0.97	0.41	0.48	-0.39	1.15	0.12	1.24	0.06	3.39	2.76	3.57	3.38						
FeO	15.14	14.49	14.89	14.59	15.70	14.34	15.55	14.75	15.35	13.33	12.16	13.09	12.17						
MnO	0.73	0.68	0.65	0.69	0.81	0.77	0.85	0.70	0.75	0.82	0.76	1.22	0.77						
MgO	27.72	27.82	27.79	28.13	26.68	26.86	26.36	26.63	26.76	26.11	27.57	26.50	27.50						
CaO	1.29	1.36	1.30	1.33	1.32	1.41	1.42	1.42	1.39	1.32	1.37	0.96	1.50						
Na ₂ O	0.02	0.04	0.01	0.05	0.02	0.03	0.02	0.02	0.03	0.03	0.06	0.01	0.01						
Total	102.18	102.28	102.18	102.78	100.29	99.60	100.51	100.61	100.16	99.06	99.28	98.97	100.48						
Mg#	76.57	77.42	76.91	77.48	75.17	77.00	75.14	76.35	75.66	77.74	80.17	78.30	80.11						
En	74.65	75.37	74.98	75.50	73.21	74.83	73.02	74.18	73.58	75.59	77.95	76.73	77.68						
Fs	22.85	21.98	22.51	21.94	24.18	22.36	24.16	22.98	23.67	21.65	19.28	21.27	19.28						
Wo	2.50	2.65	2.52	2.56	2.61	2.81	2.83	2.83	2.75	2.76	2.78	2.01	3.04						
Cations																			
Si	1.976	1.964	1.966	1.969	1.978	1.971	1.962	1.949	1.980	1.928	1.951	1.939	1.928						
Ti	0.005	0.006	0.005	0.005	0.004	0.004	0.006	0.007	0.005	0.005	0.006	0.006	0.008						
Al	0.034	0.046	0.051	0.047	0.044	0.031	0.064	0.068	0.033	0.069	0.039	0.042	0.065						
Cr										0.003	0.002	0.002	0.003						
Fe ³⁺	0.011	0.026	0.011	0.013	-0.011	0.031	0.003	0.034	0.002	0.094	0.076	0.099	0.092						
Fe ²⁺	0.447	0.427	0.439	0.427	0.473	0.435	0.468	0.444	0.463	0.412	0.371	0.405	0.368						
Mn	0.022	0.020	0.019	0.021	0.025	0.024	0.026	0.021	0.023	0.026	0.024	0.038	0.024						
Mg	1.460	1.465	1.462	1.470	1.431	1.457	1.415	1.433	1.439	1.439	1.501	1.463	1.485						
Ca	0.049	0.052	0.049	0.050	0.051	0.055	0.055	0.055	0.054	0.052	0.053	0.038	0.058						
Na	0.001	0.003	0.001	0.003	0.001	0.002	0.002	0.001	0.002	0.002	0.004	0.001	0.001						
Total	4.004	4.009	4.004	4.004	3.996	4.010	4.001	4.011	4.001	4.032	4.025	4.033	4.031						

Abbreviations same as Table A2.3. Cations calculated on a 6 oxygen basis.

Table A2.6 Major element amphibole compositions analysed by EMPA.

Sample ID	Kaupokonui A1_1	Kaupokonui A1_2	Kaupokonui A1_4	Kaupokonui A3_1	Kaupokonui A3_2
Zone	rim	zone	core	rim	zone
SiO₂	43.37	41.15	41.77	41.67	40.33
TiO₂	2.51	2.06	1.84	2.63	2.53
Al₂O₃	10.52	12.50	12.70	11.38	12.59
Fe₂O₃	5.49	7.95	2.62	6.08	5.68
FeO	6.04	4.44	7.79	5.87	7.26
MnO	0.30	0.16	0.15	0.27	0.17
MgO	14.48	14.21	14.90	14.42	13.49
CaO	11.23	11.67	13.37	11.76	12.12
Na₂O	2.03	1.93	1.98	2.02	2.06
K₂O	1.08	0.94	0.86	1.11	1.06
H₂O_{calc}	1.90	1.89	1.92	1.89	1.88
Total	98.97	98.90	99.89	99.10	99.16
Mg#	81.03	85.09	77.33	81.40	76.81
Cations					
Si	6.357	6.048	6.106	6.137	5.980
Ti	0.276	0.228	0.202	0.291	0.282
Al	1.818	2.165	2.188	1.975	2.201
Fe³⁺	0.606	0.880	0.288	0.674	0.634
Fe²⁺	0.741	0.546	0.952	0.723	0.900
Mn	0.037	0.019	0.018	0.033	0.021
Mg	3.164	3.114	3.246	3.167	2.981
Ca	1.764	1.839	2.094	1.855	1.925
Na	0.578	0.551	0.560	0.578	0.591
K	0.203	0.176	0.160	0.208	0.200
Total	15.54	15.57	15.81	15.64	15.72
P-C conditions					
T (°C)	928	983	1011	970	1002
Uncertainty	22	22	22	22	22
P (MPa)	262	432	447	329	455
Uncertainty	29	48	49	36	50
Equivalent depth (km)	9.9	16.3	16.9	12.4	17.2
ΔNNO	1.03	1.05	0.96	0.95	0.62
log fO₂	-10.35	-9.37	-9.05	-9.72	-9.51
Uncertainty	0.4	0.4	0.4	0.4	0.4
H₂O_{melt} (wt.%)	4.1	5.7	6.0	4.2	5.3
Uncertainty	0.6	0.8	0.9	0.6	0.8

Cation proportions calculated using Leake et al. (1997) on the basis of 13 cations. P-C = Physical-chemical conditions, calculated using the method of Ridolfi et al. (2010).

Table A2.6 Major element amphibole compositions analysed by EMPA.

Sample ID	Kaupokonui A3_3	Kaupokonui A3_5	Kaupokonui A4_2	Kaupokonui A4_7	Kaupokonui A5_1
Zone	core	core	rim	zone	rim
SiO₂	40.74	40.01	42.71	41.21	40.38
TiO₂	2.10	2.07	2.88	2.34	2.31
Al₂O₃	13.07	13.16	11.53	13.04	11.90
Fe₂O₃	7.94	6.41	4.21	5.50	4.52
FeO	3.80	6.37	7.67	6.93	9.75
MnO	0.13	0.23	0.27	0.22	0.30
MgO	14.80	13.51	13.78	13.17	12.09
CaO	11.92	11.98	11.45	11.52	11.88
Na₂O	2.17	2.16	2.13	2.06	1.94
K₂O	0.96	1.09	1.14	1.10	1.09
H₂O_{calc}	1.90	1.88	1.91	1.89	1.85
Total	99.55	98.88	99.70	98.98	98.03
Mg#	87.40	79.07	76.20	77.20	68.86
Cations					
Si	5.947	5.940	6.252	6.081	6.105
Ti	0.230	0.231	0.317	0.260	0.263
Al	2.248	2.303	1.988	2.267	2.120
Fe³⁺	0.873	0.717	0.464	0.611	0.514
Fe²⁺	0.464	0.791	0.939	0.856	1.233
Mn	0.016	0.029	0.034	0.028	0.039
Mg	3.221	2.990	3.006	2.898	2.726
Ca	1.865	1.906	1.796	1.822	1.925
Na	0.615	0.622	0.605	0.589	0.568
K	0.179	0.207	0.213	0.207	0.211
Total	15.66	15.73	15.61	15.62	15.70
P-C conditions					
T (°C)	1009	1011	953	985	974
Uncertainty	22	22	22	22	22
P (MPa)	487	527	335	501	405
Uncertainty	54	58	37	55	45
Equivalent depth (km)	18.4	19.9	12.7	18.9	15.3
ΔNNO	1.12	0.72	0.62	0.56	0.30
log fO₂	-8.90	-9.24	-10.32	-9.80	-10.28
Uncertainty	0.4	0.4	0.4	0.4	0.4
H₂O_{melt} (wt.%)	5.4	5.6	4.7	6.1	5.5
Uncertainty	0.8	0.8	0.7	0.9	0.8

Cation proportions calculated using Leake et al. (1997) on the basis of 13 cations. P-C = Physical-chemical conditions, calculated using the method of Ridolfi et al. (2010).

Table A2.6 Major element amphibole compositions analysed by EMPA.

Sample ID	Kaupokonui A5_3	Kaupokonui A7_1	Kaupokonui A7_2	Kaupokonui A7_3	Kaupokonui A7_4
Zone	core	core	rim	zone	core
SiO₂	40.68	41.46	40.49	40.62	41.81
TiO₂	2.17	2.93	2.52	2.90	3.12
Al₂O₃	11.85	11.12	13.00	12.42	10.86
Fe₂O₃	5.55	5.00	4.17	5.47	4.66
FeO	8.87	6.57	8.30	8.94	9.10
MnO	0.30	0.27	0.15	0.42	0.37
MgO	12.50	14.14	13.28	12.16	12.88
CaO	11.86	11.65	12.22	11.50	11.44
Na₂O	1.97	1.96	2.10	2.04	1.99
K₂O	1.16	1.09	1.14	1.31	1.37
H₂O_{calc}	1.86	1.88	1.89	1.88	1.88
Total	98.76	98.07	99.27	99.67	99.49
Mg#	71.53	79.33	74.02	70.80	71.62
Cations					
Si	6.096	6.171	6.001	6.034	6.206
Ti	0.245	0.328	0.281	0.324	0.348
Al	2.092	1.952	2.271	2.175	1.900
Fe³⁺	0.626	0.561	0.466	0.612	0.520
Fe²⁺	1.111	0.817	1.029	1.110	1.129
Mn	0.038	0.033	0.019	0.053	0.047
Mg	2.792	3.137	2.933	2.692	2.850
Ca	1.903	1.858	1.940	1.831	1.820
Na	0.571	0.565	0.604	0.588	0.573
K	0.222	0.207	0.216	0.247	0.259
Total	15.70	15.63	15.76	15.67	15.65
P-C conditions					
T (°C)	971	966	1008	980	948
Uncertainty	22	22	22	22	22
P (MPa)	389	318	503	438	295
Uncertainty	43	35	55	48	32
Equivalent depth (km)	14.7	12.0	19.0	16.5	11.2
ΔNNO	0.48	0.81	0.47	0.18	0.40
log fO₂	-10.15	-9.92	-9.57	-10.29	-10.64
Uncertainty	0.4	0.4	0.4	0.4	0.4
H₂O_{melt} (wt.%)	5.1	4.2	5.5	5.0	3.7
Uncertainty	0.8	0.6	0.8	0.8	0.5

Cation proportions calculated using Leake et al. (1997) on the basis of 13 cations. P-C = Physical-chemical conditions, calculated using the method of Ridolfi et al. (2010).

Table A2.6 Major element amphibole compositions analysed by EMPA.

Sample ID	Kaupokonui A9_3	Kaupokonui A9_4	Kaupokonui A9_5	Kaupokonui A9_6	Kaupokonui A10_1
Zone	rim	zone	zone	core	rim
SiO₂	39.81	40.47	39.66	40.50	41.06
TiO₂	2.41	3.01	2.66	2.54	2.94
Al₂O₃	13.26	11.31	12.62	11.75	11.28
Fe₂O₃	5.81	4.55	5.16	4.19	5.37
FeO	6.93	9.81	8.95	9.19	6.46
MnO	0.16	0.41	0.32	0.26	0.31
MgO	13.15	11.99	12.20	12.69	14.11
CaO	11.85	11.33	11.75	11.83	11.74
Na₂O	2.04	2.00	2.16	2.12	2.02
K₂O	1.18	1.41	1.12	1.10	1.09
H₂O_{calc}	1.87	1.85	1.86	1.86	1.88
Total	98.49	98.14	98.45	98.04	98.26
Mg#	77.18	68.55	70.86	71.11	79.58
Cations					
Si	5.937	6.123	5.969	6.105	6.113
Ti	0.270	0.343	0.301	0.288	0.330
Al	2.331	2.017	2.240	2.087	1.979
Fe³⁺	0.653	0.518	0.585	0.475	0.602
Fe²⁺	0.864	1.241	1.126	1.159	0.804
Mn	0.021	0.053	0.041	0.034	0.040
Mg	2.924	2.704	2.739	2.853	3.133
Ca	1.893	1.836	1.895	1.911	1.872
Na	0.590	0.587	0.630	0.620	0.582
K	0.225	0.272	0.216	0.211	0.207
Total	15.71	15.70	15.74	15.74	15.66
P-C conditions					
T (°C)	1012	962	998	978	976
Uncertainty	22	22	22	22	22
P (MPa)	549	349	481	386	330
Uncertainty	60	38	53	42	36
Equivalent depth (km)	20.7	13.2	18.2	14.6	12.5
ΔNNO	0.55	0.17	0.22	0.40	0.79
log fO₂	-9.40	-10.62	-9.96	-10.13	-9.78
Uncertainty	0.4	0.4	0.4	0.4	0.4
H₂O_{melt} (wt.%)	5.6	4.1	5.4	5.0	4.1
Uncertainty	0.8	0.6	0.8	0.7	0.6

Cation proportions calculated using Leake et al. (1997) on the basis of 13 cations. P-C = Physical-chemical conditions, calculated using the method of Ridolfi et al. (2010).

Table A2.6 Major element amphibole compositions analysed by EMPA.

Sample ID	Kaupokonui A10_2	Kaupokonui A10_3	Kaupokonui A10_4	Kaupokonui A11_1	Kaupokonui A11_2
Zone	zone	core	zone	rim	zone
SiO₂	41.62	41.89	41.24	41.38	41.06
TiO₂	3.09	2.74	2.65	2.85	2.85
Al₂O₃	10.79	10.79	11.33	11.66	11.56
Fe₂O₃	4.82	5.57	5.34	5.64	5.54
FeO	7.18	6.29	6.36	6.35	6.38
MnO	0.32	0.30	0.33	0.31	0.31
MgO	14.13	14.53	14.15	14.02	14.04
CaO	11.74	11.76	11.79	11.70	11.71
Na₂O	2.08	2.10	2.01	2.01	2.05
K₂O	1.09	1.07	1.03	1.06	1.07
H₂O_{calc}	1.89	1.89	1.88	1.89	1.88
Total	98.76	98.92	98.10	98.88	98.46
Mg#	77.82	80.45	79.86	79.74	79.69
Cations					
Si	6.174	6.186	6.141	6.114	6.099
Ti	0.345	0.304	0.297	0.317	0.319
Al	1.887	1.878	1.988	2.030	2.024
Fe³⁺	0.538	0.620	0.598	0.627	0.620
Fe²⁺	0.891	0.777	0.792	0.785	0.792
Mn	0.040	0.038	0.042	0.039	0.040
Mg	3.126	3.198	3.142	3.089	3.108
Ca	1.866	1.860	1.881	1.852	1.864
Na	0.599	0.602	0.581	0.576	0.591
K	0.207	0.201	0.195	0.200	0.203
Total	15.67	15.66	15.66	15.63	15.66
P-C conditions					
T (°C)	964	961	973	975	979
Uncertainty	22	22	22	22	22
P (MPa)	290	286	335	356	353
Uncertainty	32	31	37	39	39
Equivalent depth (km)	10.9	10.8	12.7	13.4	13.3
ΔNNO	0.75	0.96	0.86	0.76	0.77
log fO₂	-10.04	-9.87	-9.75	-9.81	-9.75
Uncertainty	0.4	0.4	0.4	0.4	0.4
H₂O_{melt} (wt.%)	3.7	3.7	4.5	4.6	4.4
Uncertainty	0.6	0.6	0.7	0.7	0.7

Cation proportions calculated using Leake et al. (1997) on the basis of 13 cations. P-C = Physical-chemical conditions, calculated using the method of Ridolfi et al. (2010).

Table A2.6 Major element amphibole compositions analysed by EMPA.

Sample ID	Kaupokonui A11_3	Kaupokonui A11_4	Kaupokonui A11_5	SM-6C A4_2	SM-6C A4_3	SM-6C A4_4
Zone	zone	core	core	zone	zone	zone
SiO₂	40.26	40.67	40.69	39.99	39.68	40.99
TiO₂	2.56	2.14	2.72	2.33	2.38	2.14
Al₂O₃	12.84	13.37	12.15	13.25	13.30	12.09
Fe₂O₃	6.76	7.33	4.89	7.06	8.15	7.67
FeO	5.67	4.22	7.41	5.31	4.35	4.26
MnO	0.18	0.14	0.24	0.14	0.13	0.11
MgO	13.91	14.48	13.60	13.93	13.97	14.72
CaO	11.98	11.93	11.95	11.97	11.81	11.83
Na₂O	2.03	2.03	2.00	2.09	1.99	2.03
K₂O	0.97	0.98	1.19	1.00	0.99	0.95
H₂O_{calc}	1.88	1.90	1.88	1.88	1.87	1.88
Total	99.03	99.19	98.72	98.97	98.61	98.67
Mg#	81.39	85.94	76.59	82.38	85.12	86.03
Cations						
Si	5.946	5.955	6.051	5.907	5.872	6.040
Ti	0.284	0.236	0.305	0.259	0.264	0.237
Al	2.235	2.307	2.130	2.307	2.319	2.100
Fe³⁺	0.752	0.808	0.547	0.785	0.908	0.850
Fe²⁺	0.700	0.517	0.922	0.656	0.539	0.525
Mn	0.022	0.017	0.030	0.018	0.016	0.014
Mg	3.062	3.160	3.016	3.068	3.082	3.234
Ca	1.896	1.872	1.904	1.895	1.872	1.869
Na	0.580	0.575	0.578	0.598	0.570	0.581
K	0.183	0.183	0.226	0.189	0.186	0.178
Total	15.66	15.63	15.71	15.68	15.63	15.63
P-C conditions						
T (°C)	1007	1011	992	1016	1017	988
Uncertainty	22	22	22	22	22	22
P (MPa)	478	530	411	530	539	394
Uncertainty	53	58	45	58	59	43
Equivalent depth (km)	18.1	20.0	15.5	20.0	20.4	14.9
ΔNNO	0.77	1.01	0.62	0.82	0.89	1.18
log fO₂	-9.28	-8.97	-9.68	-9.08	-9.00	-9.20
Uncertainty	0.4	0.4	0.4	0.4	0.4	0.4
H₂O_{melt} (wt.%)	5.5	5.9	4.7	5.7	5.7	4.9
Uncertainty	0.8	0.9	0.7	0.8	0.9	0.7

Cation proportions calculated using Leake et al. (1997) on the basis of 13 cations. P-C = Physical-chemical conditions, calculated using the method of Ridolfi et al. (2010).

Table A2.6 Major element amphibole compositions analysed by EMPA.

Sample ID	SM-6C A4_5	SM-6C A4_7	SM-6C A5_2	SM-6C A5_5	SM-6C A6_1	SM-6C A6_2
Zone	zone	core	rim	core	rim	zone
SiO₂	40.10	40.17	41.80	40.97	40.41	40.63
TiO₂	2.33	2.29	2.73	2.90	2.45	2.27
Al₂O₃	13.07	13.08	14.22	14.44	12.77	12.70
Fe₂O₃	6.90	6.30	0.00	0.33	7.25	7.00
FeO	5.62	5.78	10.60	11.37	4.89	4.96
MnO	0.17	0.13	0.14	0.17	0.18	0.14
MgO	13.77	13.89	13.49	12.73	14.12	14.45
CaO	11.90	11.91	13.03	12.85	11.75	12.06
Na₂O	2.07	2.16	2.21	2.31	2.08	2.08
K₂O	1.01	1.00	1.10	1.12	0.95	0.94
H₂O_{calc}	1.88	1.88	1.95	1.94	1.88	1.89
Total	98.83	98.60	101.27	101.13	98.74	99.11
Mg#	81.38	81.08	69.41	66.63	83.71	83.85
Cations						
Si	5.935	5.954	6.058	5.981	5.967	5.976
Ti	0.260	0.256	0.298	0.318	0.271	0.252
Al	2.280	2.285	2.428	2.485	2.222	2.202
Fe³⁺	0.769	0.702	0.000	0.036	0.806	0.774
Fe²⁺	0.695	0.716	1.284	1.388	0.604	0.610
Mn	0.022	0.016	0.018	0.022	0.022	0.018
Mg	3.039	3.070	2.914	2.771	3.107	3.168
Ca	1.888	1.892	2.023	2.009	1.859	1.900
Na	0.594	0.619	0.622	0.654	0.597	0.592
K	0.192	0.190	0.204	0.208	0.180	0.176
Total	15.67	15.70	15.85	15.87	15.64	15.67
P-C conditions						
T (°C)	1010	1011	1028	1035	1002	1004
Uncertainty	22	22	22	22	22	22
P (MPa)	510	514	631	684	469	456
Uncertainty	56	56	69	75	52	50
Equivalent depth (km)	19.2	19.4	23.8	25.8	17.7	17.2
ΔNNO	0.78	0.79	0.15	-0.09	0.88	0.99
log fO₂	-9.22	-9.19	-9.55	-9.67	-9.24	-9.11
Uncertainty	0.4	0.4	0.4	0.4	0.4	0.4
H₂O_{melt} (wt.%)	5.6	5.6	6.8	6.8	5.4	5.4
Uncertainty	0.8	0.8	1.0	1.0	0.8	0.9

Cation proportions calculated using Leake et al. (1997) on the basis of 13 cations. P-C = Physical-chemical conditions, calculated using the method of Ridolfi et al. (2010).

Table A2.6 Major element amphibole compositions analysed by EMPA.

Sample ID	SM-6C A6_3	SM-6C A6_4	SM-6C A7_1	SM-6C A7_2	SM-6C A7_3	SM-6C A7_4
Zone	core	zone	rim	zone	zone	zone
SiO₂	40.31	40.41	40.16	40.63	40.81	40.11
TiO₂	2.35	2.28	2.35	2.25	2.05	2.44
Al₂O₃	13.03	12.93	13.00	12.92	12.71	13.19
Fe₂O₃	6.34	6.56	6.80	7.51	7.88	5.80
FeO	5.69	5.53	5.33	4.80	4.20	6.46
MnO	0.14	0.18	0.15	0.10	0.16	0.17
MgO	13.92	14.00	14.00	14.23	14.54	13.54
CaO	11.93	11.99	11.90	11.85	11.83	11.92
Na₂O	2.08	2.03	2.09	2.05	2.10	2.13
K₂O	1.00	0.98	0.97	1.00	0.97	1.01
H₂O_{calc}	1.88	1.88	1.88	1.89	1.89	1.88
Total	98.68	98.77	98.64	99.23	99.14	98.66
Mg#	81.34	81.87	82.40	84.08	86.05	78.88
Cations						
Si	5.966	5.973	5.946	5.968	5.990	5.953
Ti	0.262	0.254	0.262	0.248	0.226	0.272
Al	2.273	2.253	2.268	2.236	2.198	2.306
Fe³⁺	0.706	0.729	0.758	0.830	0.870	0.648
Fe²⁺	0.704	0.683	0.660	0.590	0.516	0.802
Mn	0.018	0.023	0.019	0.013	0.019	0.022
Mg	3.071	3.085	3.089	3.115	3.181	2.996
Ca	1.891	1.899	1.887	1.865	1.861	1.895
Na	0.596	0.582	0.600	0.585	0.598	0.614
K	0.188	0.184	0.184	0.187	0.181	0.192
Total	15.67	15.67	15.67	15.64	15.64	15.70
P-C conditions						
T (°C)	1008	1006	1010	1002	998	1012
Uncertainty	22	22	22	22	22	22
P (MPa)	505	491	501	478	453	530
Uncertainty	56	54	55	53	50	58
Equivalent depth (km)	19.1	18.5	18.9	18.1	17.1	20.0
ΔNNO	0.80	0.85	0.84	0.95	1.10	0.63
log fO₂	-9.23	-9.21	-9.17	-9.18	-9.09	-9.33
Uncertainty	0.4	0.4	0.4	0.4	0.4	0.4
H₂O_{melt} (wt.%)	5.7	5.7	5.6	5.5	5.3	5.8
Uncertainty	0.9	0.8	0.8	0.9	0.8	0.8

Cation proportions calculated using Leake et al. (1997) on the basis of 13 cations. P-C = Physical-chemical conditions, calculated using the method of Ridolfi et al. (2010).

Table A2.6 Major element amphibole compositions analysed by EMPA.

Sample ID	SM-6C A7_5	SM-6C A7_6	SM-6C A8_1	SM-6C A8_2	SM-6C A9_1	SM-6C A9_2
Zone	zone	core	rim	core	rim	zone
SiO₂	41.87	39.51	40.73	40.48	41.58	41.34
TiO₂	2.70	2.19	2.35	2.36	2.76	2.81
Al₂O₃	11.03	13.45	13.31	13.12	14.27	14.35
Fe₂O₃	6.33	6.66	6.98	7.62	0.00	0.61
FeO	5.56	6.36	5.20	4.55	10.71	10.34
MnO	0.25	0.20	0.15	0.15	0.13	0.14
MgO	14.49	13.30	14.02	14.23	13.33	13.33
CaO	11.56	12.04	11.81	11.89	13.09	12.86
Na₂O	2.09	2.18	2.12	1.99	2.24	2.32
K₂O	0.95	0.92	1.00	0.98	1.06	1.02
H₂O_{calc}	1.89	1.87	1.90	1.89	1.95	1.94
Total	98.72	98.68	99.56	99.26	101.11	101.05
Mg#	82.30	78.85	82.79	84.80	68.94	69.69
Cations						
Si	6.175	5.881	5.962	5.939	6.045	6.008
Ti	0.300	0.245	0.259	0.261	0.302	0.307
Al	1.918	2.359	2.297	2.270	2.445	2.458
Fe³⁺	0.703	0.746	0.769	0.841	0.000	0.067
Fe²⁺	0.686	0.792	0.636	0.558	1.302	1.256
Mn	0.032	0.025	0.018	0.018	0.016	0.017
Mg	3.187	2.952	3.060	3.113	2.889	2.888
Ca	1.827	1.920	1.853	1.869	2.040	2.002
Na	0.596	0.628	0.602	0.567	0.632	0.653
K	0.178	0.176	0.186	0.183	0.196	0.188
Total	15.60	15.72	15.64	15.62	15.87	15.84
P-C conditions						
T (°C)	960	1021	1006	1008	1032	1032
Uncertainty	22	22	22	22	22	22
P (MPa)	303	571	522	502	646	659
Uncertainty	33	63	57	55	71	72
Equivalent depth (km)	11.4	21.6	19.7	19.0	24.4	24.9
ΔNNO	0.99	0.63	0.81	0.93	0.09	0.11
log fO₂	-9.85	-9.18	-9.23	-9.11	-9.54	-9.51
Uncertainty	0.4	0.4	0.4	0.4	0.4	0.4
H₂O_{melt} (wt.%)	4.3	6.1	5.8	5.7	7.0	6.9
Uncertainty	0.9	0.9	0.6	0.9	1.0	1.0

Cation proportions calculated using Leake et al. (1997) on the basis of 13 cations. P-C = Physical-chemical conditions, calculated using the method of Ridolfi et al. (2010).

Table A2.6 Major element amphibole compositions analysed by EMPA.

Sample ID	SM-6C A9_3	SM-6C A9_4	Maketawa A1_1	Maketawa A1_2	Maketawa A1_3	Maketawa A2_1
Zone	zone	core	rim	zone	core	rim
SiO₂	41.71	42.64	41.30	42.16	40.73	40.52
TiO₂	2.72	2.63	2.74	2.90	2.57	2.38
Al₂O₃	14.24	13.62	10.79	10.23	11.85	12.91
Fe₂O₃	0.09	0.00	5.19	4.18	4.96	5.70
FeO	10.76	10.48	10.53	9.84	7.77	6.80
MnO	0.12	0.12	0.58	0.62	0.28	0.17
MgO	13.35	13.74	11.64	12.78	13.28	13.45
CaO	12.97	13.08	11.41	11.72	11.82	11.90
Na₂O	2.26	2.25	1.92	2.08	2.10	2.14
K₂O	1.04	1.00	1.40	1.09	0.98	0.91
H₂O_{calc}	1.95	1.96	1.86	1.88	1.87	1.88
Total	101.22	101.53	99.37	99.47	98.19	98.78
Mg#	68.87	70.02	66.35	69.84	75.30	77.90
Cations						
Si	6.050	6.157	6.196	6.274	6.094	6.005
Ti	0.297	0.285	0.309	0.324	0.289	0.266
Al	2.435	2.318	1.908	1.794	2.089	2.255
Fe³⁺	0.010	0.000	0.586	0.468	0.559	0.636
Fe²⁺	1.306	1.266	1.321	1.225	0.972	0.843
Mn	0.014	0.015	0.074	0.079	0.035	0.022
Mg	2.888	2.958	2.605	2.836	2.962	2.973
Ca	2.016	2.024	1.834	1.868	1.895	1.890
Na	0.635	0.630	0.560	0.599	0.608	0.616
K	0.193	0.185	0.267	0.206	0.187	0.171
Total	15.84	15.84	15.66	15.67	15.69	15.68
P-C conditions						
T (°C)	1027	1012	939	936	981	1000
Uncertainty	22	22	22	22	22	22
P (MPa)	637	539	299	254	387	492
Uncertainty	70	59	33	28	43	54
Equivalent depth (km)	24.0	20.3	11.3	9.6	14.6	18.6
ΔNNO	0.12	0.25	0.16	0.39	0.58	0.62
log fO₂	-9.59	-9.71	-11.01	-10.85	-9.90	-9.52
Uncertainty	0.4	0.4	0.4	0.4	0.4	0.4
H₂O_{melt} (wt.%)	6.9	6.7	4.0	4.0	5.1	6.0
Uncertainty	1.0	1.0	0.6	0.6	0.8	0.9

Cation proportions calculated using Leake et al. (1997) on the basis of 13 cations. P-C = Physical-chemical conditions, calculated using the method of Ridolfi et al. (2010).

Table A2.6 Major element amphibole compositions analysed by EMPA.

Sample ID	Maketawa A2_2	Maketawa A4_1	Maketawa A4_2	Maketawa A4_3	Maketawa A5_1	Maketawa A5_2
Zone	zone	core	zone	zone	core	zone
SiO₂	41.41	42.26	41.94	43.83	42.02	41.07
TiO₂	2.81	2.41	2.08	2.60	2.08	1.84
Al₂O₃	11.27	12.08	12.96	10.98	13.08	13.82
Fe₂O₃	5.32	6.04	6.52	5.64	7.54	9.13
FeO	7.71	7.99	5.49	6.97	3.90	3.97
MnO	0.32	0.35	0.14	0.33	0.10	0.14
MgO	13.48	13.44	14.75	14.77	15.35	14.29
CaO	11.60	12.04	12.29	12.11	12.27	11.96
Na₂O	2.19	2.24	2.25	2.19	2.02	2.01
K₂O	1.06	0.94	0.91	0.95	1.09	1.11
H₂O_{calc}	1.88	1.93	1.94	1.96	1.94	1.92
Total	99.06	101.71	101.27	102.33	101.40	101.25
Mg#	75.71	74.99	82.74	79.07	87.51	86.52
Cations						
Si	6.144	6.113	6.032	6.254	6.009	5.910
Ti	0.313	0.262	0.225	0.278	0.224	0.199
Al	1.971	2.060	2.196	1.847	2.204	2.343
Fe³⁺	0.594	0.658	0.705	0.606	0.811	0.988
Fe²⁺	0.956	0.967	0.660	0.832	0.467	0.478
Mn	0.040	0.043	0.018	0.040	0.013	0.017
Mg	2.981	2.898	3.164	3.142	3.272	3.066
Ca	1.844	1.866	1.895	1.851	1.879	1.844
Na	0.630	0.628	0.629	0.606	0.560	0.560
K	0.201	0.174	0.166	0.174	0.200	0.204
Total	15.68	15.67	15.69	15.63	15.64	15.61
P-C conditions						
T (°C)	965	970	998	947	1001	1008
Uncertainty	22	22	22	22	22	22
P (MPa)	327	371	452	274	457	558
Uncertainty	36	41	50	30	50	61
Equivalent depth (km)	12.4	14.0	17.1	10.3	17.3	21.1
ΔNNO	0.61	0.59	0.99	0.94	1.22	1.03
log fO₂	-10.15	-10.07	-9.20	-10.12	-8.93	-8.97
Uncertainty	0.4	0.4	0.4	0.4	0.4	0.4
H₂O_{melt} (wt.%)	4.3	5.3	5.6	4.3	5.2	5.9
Uncertainty	0.6	0.8	0.8	0.6	0.8	0.9

Cation proportions calculated using Leake et al. (1997) on the basis of 13 cations. P-C = Physical-chemical conditions, calculated using the method of Ridolfi et al. (2010).

Table A2.6 Major element amphibole compositions analysed by EMPA.

Sample ID	Maketawa A5_3	Maketawa A5_4	Maketawa A6_1	Maketawa A6_2	Maketawa A7_1	Maketawa A7_2
Zone	zone	rim	core	zone	core	rim
SiO₂	41.59	43.87	43.91	43.74	40.67	42.35
TiO₂	2.22	2.59	2.42	2.52	2.39	2.64
Al₂O₃	13.25	10.63	10.82	10.36	12.12	10.47
Fe₂O₃	6.50	6.88	4.22	4.84	6.18	6.14
FeO	4.95	4.90	8.20	8.62	6.95	6.28
MnO	0.14	0.38	0.32	0.43	0.29	0.33
MgO	14.90	15.21	14.34	13.98	13.40	14.38
CaO	12.39	11.48	11.99	11.94	11.86	11.66
Na₂O	2.00	2.23	2.19	2.16	2.06	2.06
K₂O	1.06	0.89	1.09	1.11	0.97	0.94
H₂O_{calc}	1.93	1.94	1.94	1.93	1.87	1.89
Total	100.93	101.01	101.46	101.63	98.76	99.14
Mg#	84.30	84.71	75.71	74.31	77.47	80.32
Cations						
Si	5.993	6.293	6.330	6.325	6.047	6.237
Ti	0.240	0.280	0.263	0.274	0.268	0.293
Al	2.250	1.798	1.839	1.766	2.123	1.817
Fe³⁺	0.705	0.743	0.458	0.527	0.691	0.681
Fe²⁺	0.596	0.587	0.989	1.042	0.864	0.774
Mn	0.017	0.046	0.039	0.053	0.037	0.041
Mg	3.200	3.253	3.083	3.013	2.970	3.158
Ca	1.913	1.765	1.852	1.850	1.889	1.839
Na	0.558	0.621	0.613	0.605	0.595	0.589
K	0.195	0.164	0.201	0.204	0.184	0.176
Total	15.67	15.55	15.67	15.66	15.67	15.60
P-C conditions						
T (°C)	1008	936	938	930	985	945
Uncertainty	22	22	22	22	22	22
P (MPa)	488	255	270	243	407	262
Uncertainty	54	28	30	27	45	29
Equivalent depth (km)	18.4	9.6	10.2	9.2	15.4	9.9
ΔNNO	1.03	1.17	0.84	0.77	0.68	0.98
log fO₂	-9.00	-10.08	-10.36	-10.58	-9.73	-10.11
Uncertainty	0.4	0.4	0.4	0.4	0.4	0.4
H₂O_{melt} (wt.%)	5.5	4.1	4.2	3.8	5.3	4.0
Uncertainty	0.8	0.6	0.6	0.6	0.8	0.6

Cation proportions calculated using Leake et al. (1997) on the basis of 13 cations. P-C = Physical-chemical conditions, calculated using the method of Ridolfi et al. (2010).

Table A2.6 Major element amphibole compositions analysed by EMPA.

Sample ID	Maketawa A9_1	Maketawa A10_6	Maketawa A11_1	Maketawa A11_2	Maketawa A11_3	Maketawa A11_4
Zone	core	core	core	core	zone	zone
SiO₂	39.57	41.31	42.53	39.73	41.76	40.61
TiO₂	2.29	1.94	2.70	2.43	2.84	2.73
Al₂O₃	13.28	12.77	10.23	13.33	10.62	12.23
Fe₂O₃	4.79	5.87	5.48	5.99	4.34	5.47
FeO	8.83	6.33	6.89	7.16	8.60	8.16
MnO	0.16	0.15	0.39	0.29	0.37	0.35
MgO	12.32	14.19	14.12	12.85	13.44	12.92
CaO	12.06	12.18	11.52	11.82	11.75	11.85
Na₂O	2.09	2.21	2.05	2.22	2.05	2.18
K₂O	0.97	0.97	0.98	0.90	1.15	0.98
H₂O_{calc}	1.86	1.91	1.89	1.87	1.88	1.88
Total	98.22	99.82	98.78	98.59	98.79	99.35
Mg#	71.31	79.98	78.51	76.19	73.59	73.83
Cations						
Si	5.952	6.047	6.291	5.925	6.224	6.029
Ti	0.259	0.213	0.301	0.273	0.319	0.305
Al	2.354	2.204	1.783	2.343	1.866	2.139
Fe³⁺	0.542	0.646	0.610	0.672	0.486	0.612
Fe²⁺	1.111	0.775	0.852	0.893	1.072	1.013
Mn	0.020	0.018	0.049	0.037	0.047	0.044
Mg	2.762	3.096	3.114	2.858	2.986	2.859
Ca	1.943	1.911	1.825	1.889	1.876	1.884
Na	0.610	0.627	0.588	0.641	0.593	0.627
K	0.187	0.181	0.185	0.171	0.218	0.186
Total	15.74	15.72	15.60	15.70	15.69	15.70
P-C conditions						
T (°C)	1010	996	936	1012	952	987
Uncertainty	22	22	22	22	22	22
P (MPa)	567	457	250	558	281	416
Uncertainty	62	50	27	61	31	46
Equivalent depth (km)	21.4	17.3	9.4	21.1	10.6	15.7
ΔNNO	0.28	0.90	0.89	0.43	0.60	0.41
log fO₂	-9.69	-9.32	-10.35	-9.52	-10.38	-9.96
Uncertainty	0.4	0.4	0.4	0.4	0.4	0.4
H₂O_{melt} (wt.%)	6.5	5.6	3.9	6.3	3.9	5.3
Uncertainty	1.0	0.8	0.6	0.9	0.6	0.8

Cation proportions calculated using Leake et al. (1997) on the basis of 13 cations. P-C = Physical-chemical conditions, calculated using the method of Ridolfi et al. (2010).

Table A2.6 Major element amphibole compositions analysed by EMPA.

Sample ID	Maketawa A11_6	Maketawa A12_2	Maketawa A13_1	Maketawa A13_2	Maketawa A14_4	Maketawa A14_5
Zone	zone	core	rim	core	rim	zone
SiO₂	41.76	40.10	41.22	41.27	39.60	39.72
TiO₂	2.83	2.41	2.84	2.69	2.27	2.30
Al₂O₃	10.97	12.17	11.22	10.62	13.44	13.43
Fe₂O₃	5.41	4.53	4.10	4.85	5.21	5.49
FeO	7.60	9.00	8.22	10.62	7.26	6.97
MnO	0.32	0.25	0.33	0.63	0.15	0.14
MgO	13.52	12.80	13.54	11.61	13.16	13.14
CaO	11.56	12.12	11.70	11.35	12.00	11.83
Na₂O	2.07	2.22	2.25	1.93	2.18	2.11
K₂O	1.02	0.95	1.07	1.38	1.07	1.14
H₂O_{calc}	1.88	1.86	1.87	1.85	1.87	1.87
Total	98.94	98.41	98.36	98.81	98.22	98.15
Mg#	76.03	71.72	74.60	66.10	76.37	77.08
Cations						
Si	6.192	6.027	6.160	6.226	5.925	5.938
Ti	0.315	0.272	0.319	0.305	0.255	0.259
Al	1.918	2.156	1.975	1.888	2.370	2.367
Fe³⁺	0.604	0.513	0.461	0.551	0.587	0.618
Fe²⁺	0.942	1.131	1.027	1.339	0.909	0.871
Mn	0.040	0.032	0.041	0.080	0.020	0.018
Mg	2.988	2.869	3.016	2.611	2.936	2.929
Ca	1.837	1.952	1.874	1.835	1.924	1.896
Na	0.596	0.646	0.652	0.565	0.632	0.612
K	0.192	0.183	0.204	0.265	0.205	0.217
Total	15.63	15.78	15.73	15.66	15.76	15.73
P-C conditions						
T (°C)	954	994	970	935	1020	1016
Uncertainty	22	22	22	22	22	22
P (MPa)	303	426	329	290	580	578
Uncertainty	33	47	36	32	64	64
Equivalent depth (km)	11.4	16.1	12.4	11.0	21.9	21.8
ΔNNO	0.65	0.41	0.57	0.17	0.53	0.55
log fO₂	-10.28	-9.84	-10.10	-11.07	-9.29	-9.34
Uncertainty	0.4	0.4	0.4	0.4	0.4	0.4
H₂O_{melt} (wt.%)	4.4	5.4	4.2	4.0	5.9	5.9
Uncertainty	0.7	0.8	0.6	0.6	0.9	0.9

Cation proportions calculated using Leake et al. (1997) on the basis of 13 cations. P-C = Physical-chemical conditions, calculated using the method of Ridolfi et al. (2010).

Table A2.6 Major element amphibole compositions analysed by EMPA.

Sample ID	Maketawa A14_6	Maketawa A17_1	Maketawa A17_2	Inglewood b A1_1	Inglewood b A1_2
Zone	core	rim	core	rim	zone
SiO₂	39.61	41.18	39.34	42.45	41.30
TiO₂	2.07	2.82	2.38	2.95	2.78
Al₂O₃	13.60	10.96	13.33	9.70	11.45
Fe₂O₃	6.79	5.16	5.05	4.92	5.02
FeO	4.62	7.11	8.30	8.07	9.15
MnO	0.12	0.34	0.18	0.48	0.59
MgO	14.25	13.88	12.56	13.74	12.51
CaO	11.99	11.61	11.88	11.63	11.75
Na₂O	2.06	2.25	2.35	2.03	2.10
K₂O	1.16	0.99	0.96	0.94	0.99
H₂O_{calc}	1.87	1.87	1.86	1.88	1.88
Total	98.14	98.18	98.20	98.79	99.52
Mg#	84.60	77.69	72.94	75.23	70.91
Cations					
Si	5.884	6.151	5.915	6.311	6.139
Ti	0.232	0.317	0.269	0.329	0.311
Al	2.381	1.930	2.363	1.700	2.005
Fe³⁺	0.759	0.579	0.571	0.550	0.561
Fe²⁺	0.574	0.888	1.044	1.003	1.138
Mn	0.015	0.044	0.023	0.060	0.075
Mg	3.156	3.091	2.815	3.046	2.773
Ca	1.908	1.857	1.914	1.853	1.872
Na	0.592	0.651	0.686	0.585	0.604
K	0.220	0.189	0.184	0.179	0.187
Total	15.72	15.70	15.78	15.62	15.66
P-C conditions					
T (°C)	1028	967	1017	929	962
Uncertainty	22	22	22	22	22
P (MPa)	589	308	574	221	343
Uncertainty	65	34	63	24	38
Equivalent depth (km)	22.3	11.6	21.7	8.4	13.0
ΔNNO	0.96	0.73	0.31	0.73	0.31
log fO₂	-8.75	-9.99	-9.55	-10.64	-10.48
Uncertainty	0.4	0.4	0.4	0.4	0.4
H₂O_{melt} (wt.%)	5.5	4.0	6.1	3.7	5.1
Uncertainty	0.8	0.6	0.9	0.6	0.8

Cation proportions calculated using Leake et al. (1997) on the basis of 13 cations. P-C = Physical-chemical conditions, calculated using the method of Ridolfi et al. (2010).

Table A2.6 Major element amphibole compositions analysed by EMPA.

Sample ID	Inglewood b A1_3	Inglewood b A1_5	Inglewood b A1_6	Inglewood b A2_2	Inglewood b A2_3
Zone	zone	core	core	zone	rim
SiO₂	43.11	42.73	40.13	40.78	43.03
TiO₂	2.82	2.72	2.22	2.44	2.77
Al₂O₃	9.46	9.87	12.31	12.27	9.47
Fe₂O₃	6.33	6.00	6.96	4.02	4.65
FeO	6.89	7.27	7.48	9.47	8.28
MnO	0.58	0.64	0.46	0.37	0.57
MgO	13.97	13.72	12.52	12.30	13.47
CaO	11.38	11.44	11.69	11.91	11.40
Na₂O	2.00	2.05	2.15	2.09	1.94
K₂O	0.86	0.92	0.85	0.83	0.91
H₂O_{calc}	1.89	1.89	1.86	1.87	1.88
Total	99.30	99.24	98.63	98.35	98.34
Mg#	78.32	77.09	74.89	69.84	74.36
Cations					
Si	6.352	6.313	6.006	6.116	6.412
Ti	0.312	0.302	0.250	0.275	0.310
Al	1.643	1.719	2.171	2.169	1.663
Fe³⁺	0.702	0.667	0.784	0.453	0.521
Fe²⁺	0.849	0.898	0.937	1.188	1.031
Mn	0.073	0.080	0.059	0.047	0.071
Mg	3.068	3.022	2.794	2.751	2.991
Ca	1.796	1.811	1.874	1.914	1.820
Na	0.572	0.588	0.624	0.608	0.560
K	0.161	0.173	0.162	0.160	0.172
Total	15.53	15.57	15.66	15.68	15.55
P-C conditions					
T (°C)	915	924	984	978	910
Uncertainty	22	22	22	22	22
P (MPa)	204	228	436	435	210
Uncertainty	22	25	48	48	23
Equivalent depth (km)	7.7	8.6	16.5	16.4	7.9
ΔNNO	0.90	0.80	0.48	0.26	0.72
log fO₂	-10.72	-10.65	-9.93	-10.24	-10.98
Uncertainty	0.4	0.4	0.4	0.4	0.4
H₂O_{melt} (wt.%)	3.8	4.0	5.9	6.4	4.1
Uncertainty	0.6	0.6	0.9	1.0	0.6

Cation proportions calculated using Leake et al. (1997) on the basis of 13 cations. P-C = Physical-chemical conditions, calculated using the method of Ridolfi et al. (2010).

Table A2.6 Major element amphibole compositions analysed by EMPA.

Sample ID	Inglewood b A2_5	Inglewood b A2_6	Inglewood b A3_1	Inglewood b A3_2	Inglewood b A3_5
Zone	zone	core	rim	core	core
SiO₂	40.15	39.21	42.97	40.02	42.92
TiO₂	2.16	2.10	2.78	2.52	2.93
Al₂O₃	13.14	13.51	9.45	12.34	9.62
Fe₂O₃	4.82	5.57	5.26	6.00	5.82
FeO	9.72	9.89	7.81	8.69	7.59
MnO	0.34	0.35	0.57	0.38	0.57
MgO	11.58	11.08	13.64	12.19	13.55
CaO	11.81	11.81	11.42	11.80	11.31
Na₂O	2.12	2.17	1.96	2.14	1.98
K₂O	0.87	0.85	0.89	0.86	0.91
H₂O_{calc}	1.86	1.85	1.88	1.86	1.89
Total	98.57	98.40	98.62	98.80	99.09
Mg#	67.97	66.63	75.69	71.42	76.07
Cations					
Si	6.030	5.928	6.384	5.999	6.350
Ti	0.244	0.239	0.310	0.284	0.326
Al	2.326	2.408	1.654	2.180	1.678
Fe³⁺	0.545	0.633	0.588	0.677	0.648
Fe²⁺	1.221	1.251	0.970	1.090	0.940
Mn	0.043	0.044	0.072	0.048	0.072
Mg	2.591	2.497	3.021	2.723	2.987
Ca	1.900	1.912	1.818	1.896	1.792
Na	0.616	0.636	0.564	0.622	0.567
K	0.166	0.165	0.168	0.165	0.172
Total	15.68	15.71	15.55	15.68	15.53
P-C conditions					
T (°C)	990	1003	913	987	915
Uncertainty	22	22	22	22	22
P (MPa)	545	612	207	441	214
Uncertainty	60	67	23	49	24
Equivalent depth (km)	20.6	23.1	7.8	16.7	8.1
ΔNNO	0.10	-0.02	0.78	0.28	0.73
log fO₂	-10.18	-10.08	-10.88	-10.09	-10.89
Uncertainty	0.4	0.4	0.4	0.4	0.4
H₂O_{melt} (wt.%)	7.1	7.3	4.0	5.9	3.9
Uncertainty	1.1	1.1	0.6	0.9	0.6

Cation proportions calculated using Leake et al. (1997) on the basis of 13 cations. P-C = Physical-chemical conditions, calculated using the method of Ridolfi et al. (2010).

Table A2.6 Major element amphibole compositions analysed by EMPA.

Sample ID	Inglewood b A4_1	Inglewood b A4_2	Inglewood b A4_3	Inglewood b A5_1	Inglewood b A5_2
Zone	rim	core	core	rim	zone
SiO₂	42.41	43.00	41.25	42.80	42.60
TiO₂	2.85	2.89	2.49	2.80	2.65
Al₂O₃	9.74	9.58	12.11	9.87	10.07
Fe₂O₃	4.34	4.80	5.54	6.41	5.92
FeO	8.50	7.86	7.91	6.68	6.99
MnO	0.57	0.56	0.52	0.58	0.60
MgO	13.45	13.91	12.70	13.90	13.76
CaO	11.58	11.56	11.54	11.35	11.43
Na₂O	2.02	2.05	2.14	1.99	2.04
K₂O	0.93	0.90	0.88	0.92	0.84
H₂O_{calc}	1.87	1.89	1.88	1.89	1.88
Total	98.27	98.99	98.95	99.20	98.77
Mg#	73.82	75.94	74.11	78.75	77.82
Cations					
Si	6.341	6.363	6.125	6.311	6.310
Ti	0.321	0.322	0.279	0.311	0.295
Al	1.717	1.671	2.120	1.715	1.758
Fe³⁺	0.488	0.534	0.619	0.712	0.659
Fe²⁺	1.063	0.972	0.982	0.824	0.866
Mn	0.072	0.070	0.065	0.072	0.075
Mg	2.998	3.068	2.811	3.054	3.037
Ca	1.854	1.833	1.836	1.793	1.814
Na	0.585	0.589	0.616	0.569	0.586
K	0.178	0.170	0.166	0.174	0.159
Total	15.62	15.59	15.62	15.54	15.56
P-C conditions					
T (°C)	927	921	969	923	928
Uncertainty	22	22	22	22	22
P (MPa)	227	212	405	226	241
Uncertainty	25	23	45	25	26
Equivalent depth (km)	8.6	8.0	15.3	8.5	9.1
ΔNNO	0.65	0.78	0.42	0.86	0.82
log fO₂	-10.76	-10.73	-10.24	-10.61	-10.57
Uncertainty	0.4	0.4	0.4	0.4	0.4
H₂O_{melt} (wt.%)	4.0	3.8	6.0	3.9	4.4
Uncertainty	0.6	0.6	0.9	0.6	0.7

Cation proportions calculated using Leake et al. (1997) on the basis of 13 cations. P-C = Physical-chemical conditions, calculated using the method of Ridolfi et al. (2010).

Table A2.6 Major element amphibole compositions analysed by EMPA.

Sample ID	Inglewood b A5_3	Inglewood b A5_4	Inglewood b A6_1	Inglewood b A6_2	Inglewood b A7_2
Zone	core	core	rim	core	zone
SiO₂	43.35	40.42	42.98	40.20	39.26
TiO₂	2.86	2.79	2.89	2.34	2.62
Al₂O₃	9.77	12.45	9.59	12.23	12.92
Fe₂O₃	5.54	6.00	5.22	4.87	5.02
FeO	7.40	8.12	8.00	8.98	9.23
MnO	0.54	0.55	0.65	0.29	0.25
MgO	13.79	12.40	13.39	12.39	12.08
CaO	11.36	11.60	11.25	11.94	11.97
Na₂O	1.98	2.22	1.99	2.11	2.25
K₂O	0.87	0.91	0.98	0.82	0.86
H₂O_{calc}	1.90	1.88	1.88	1.86	1.85
Total	99.36	99.33	98.81	98.04	98.29
Mg#	76.87	73.14	74.90	71.09	70.00
Cations					
Si	6.376	6.009	6.380	6.057	5.923
Ti	0.316	0.312	0.323	0.265	0.297
Al	1.693	2.181	1.679	2.172	2.297
Fe³⁺	0.613	0.671	0.583	0.553	0.571
Fe²⁺	0.910	1.009	0.992	1.132	1.164
Mn	0.068	0.069	0.082	0.037	0.032
Mg	3.024	2.748	2.962	2.783	2.717
Ca	1.790	1.847	1.789	1.928	1.935
Na	0.565	0.640	0.572	0.616	0.658
K	0.164	0.172	0.185	0.157	0.165
Total	15.52	15.66	15.55	15.70	15.76
P-C conditions					
T (°C)	914	986	912	985	1009
Uncertainty	22	22	22	22	22
P (MPa)	219	442	215	436	522
Uncertainty	24	49	24	48	57
Equivalent depth (km)	8.3	16.7	8.1	16.5	19.7
ΔNNO	0.78	0.26	0.68	0.35	0.15
log fO₂	-10.85	-10.12	-10.99	-10.05	-9.86
Uncertainty	0.4	0.4	0.4	0.4	0.4
H₂O_{melt} (wt.%)	4.2	5.8	3.9	6.2	6.2
Uncertainty	0.6	0.9	0.6	0.9	0.9

Cation proportions calculated using Leake et al. (1997) on the basis of 13 cations. P-C = Physical-chemical conditions, calculated using the method of Ridolfi et al. (2010).

Table A2.6 Major element amphibole compositions analysed by EMPA.

Sample ID	Inglewood b A7_3	Inglewood b A7_4	Inglewood b A8_1	Inglewood b A8_2	Inglewood b A8_3
Zone	core	core	rim	core	core
SiO₂	39.75	42.55	43.15	39.38	43.13
TiO₂	2.67	3.12	3.10	3.16	3.11
Al₂O₃	12.50	9.64	9.53	13.16	9.72
Fe₂O₃	4.55	5.59	5.60	5.83	5.92
FeO	10.48	8.18	7.36	8.38	7.19
MnO	0.32	0.64	0.49	0.45	0.55
MgO	11.57	13.15	14.00	11.93	14.00
CaO	11.88	11.15	11.48	11.53	11.44
Na₂O	2.22	2.09	1.98	2.24	2.05
K₂O	0.90	0.95	0.87	0.89	0.91
H₂O_{calc}	1.85	1.88	1.90	1.86	1.90
Total	98.69	98.92	99.44	98.82	99.91
Mg#	66.32	74.14	77.22	71.74	77.64
Cations					
Si	5.996	6.327	6.349	5.896	6.320
Ti	0.303	0.349	0.343	0.355	0.342
Al	2.221	1.689	1.652	2.322	1.679
Fe³⁺	0.516	0.625	0.620	0.657	0.652
Fe²⁺	1.321	1.016	0.906	1.049	0.881
Mn	0.040	0.081	0.062	0.058	0.068
Mg	2.602	2.914	3.070	2.663	3.058
Ca	1.920	1.776	1.809	1.850	1.796
Na	0.651	0.601	0.564	0.649	0.583
K	0.174	0.181	0.164	0.169	0.169
Total	15.74	15.56	15.54	15.67	15.55
P-C conditions					
T (°C)	991	917	918	1008	922
Uncertainty	22	22	22	22	22
P (MPa)	469	218	207	542	215
Uncertainty	52	24	23	60	24
Equivalent depth (km)	17.7	8.2	7.8	20.5	8.1
ΔNNO	-0.01	0.56	0.80	0.01	0.79
log fO₂	-10.30	-11.02	-10.77	-10.00	-10.70
Uncertainty	0.4	0.4	0.4	0.4	0.4
H₂O_{melt} (wt.%)	6.1	3.8	3.8	6.3	3.7
Uncertainty	0.9	0.6	0.6	0.9	0.6

Cation proportions calculated using Leake et al. (1997) on the basis of 13 cations. P-C = Physical-chemical conditions, calculated using the method of Ridolfi et al. (2010).

Table A2.6 Major element amphibole compositions analysed by EMPA.

Sample ID	Inglewood b A11_1	Inglewood b A11_2	Inglewood b A11_3	Inglewood a A2_3	Inglewood a A5_1
Zone	rim	core	core	zone	rim
SiO₂	42.62	40.70	42.53	42.72	39.21
TiO₂	2.95	2.63	3.03	3.43	2.95
Al₂O₃	9.54	11.98	9.57	9.54	13.26
Fe₂O₃	4.46	6.01	5.30	2.36	3.07
FeO	8.14	7.94	7.54	10.04	11.24
MnO	0.53	0.55	0.55	0.50	0.24
MgO	13.59	12.77	13.66	13.17	11.26
CaO	11.44	11.69	11.29	11.40	11.84
Na₂O	1.97	2.28	2.02	2.25	2.40
K₂O	0.91	0.85	0.93	0.86	0.86
H₂O_{calc}	1.87	1.88	1.87	1.88	1.85
Total	98.01	99.26	98.30	98.16	98.18
Mg#	74.86	74.13	76.35	70.05	67.74
Cations					
Si	6.372	6.051	6.339	6.400	5.944
Ti	0.332	0.294	0.340	0.387	0.336
Al	1.680	2.098	1.682	1.684	2.370
Fe³⁺	0.502	0.672	0.594	0.266	0.350
Fe²⁺	1.017	0.987	0.940	1.258	1.425
Mn	0.067	0.069	0.069	0.064	0.030
Mg	3.029	2.829	3.036	2.942	2.544
Ca	1.832	1.862	1.803	1.830	1.924
Na	0.571	0.656	0.582	0.653	0.705
K	0.174	0.162	0.177	0.164	0.167
Total	15.58	15.68	15.56	15.65	15.80
P-C conditions					
T (°C)	919	979	921	921	1011
Uncertainty	22	22	22	22	22
P (MPa)	215	392	216	216	580
Uncertainty	24	43	24	24	64
Equivalent depth (km)	8.1	14.8	8.1	8.2	21.9
ΔNNO	0.70	0.41	0.73	0.35	-0.28
log fO₂	-10.83	-10.09	-10.78	-11.16	-10.23
Uncertainty	0.4	0.4	0.4	0.4	0.4
H₂O_{melt} (wt.%)	3.9	5.5	3.7	3.9	6.7
Uncertainty	0.6	0.8	0.6	0.6	1.0

Cation proportions calculated using Leake et al. (1997) on the basis of 13 cations. P-C = Physical-chemical conditions, calculated using the method of Ridolfi et al. (2010).

Table A2.6 Major element amphibole compositions analysed by EMPA.

Sample ID	Inglewood a A5_6	Inglewood a A6_1	Inglewood a A13_7	Inglewood a A7_1	Inglewood a A8_2
Zone	core	rim	core	rim	zone
SiO₂	39.52	40.81	42.45	40.02	42.14
TiO₂	2.78	3.17	3.01	2.44	2.78
Al₂O₃	13.03	11.64	10.14	11.91	9.86
Fe₂O₃	3.53	2.44	5.72	4.92	5.68
FeO	11.14	11.08	7.08	9.23	7.75
MnO	0.27	0.37	0.39	0.32	0.50
MgO	11.25	12.05	13.72	12.35	13.30
CaO	11.81	11.76	11.27	11.87	11.30
Na₂O	2.39	2.36	2.08	2.20	2.00
K₂O	0.81	0.81	0.81	0.91	0.92
H₂O_{calc}	1.85	1.87	1.88	1.85	1.86
Total	98.37	98.35	98.56	98.03	98.09
Mg#	61.85	64.28	65.96	76.79	75.42
Cations					
Si	5.979	6.148	6.294	6.049	6.307
Ti	0.316	0.360	0.336	0.278	0.313
Al	2.323	2.066	1.772	2.122	1.739
Fe³⁺	0.402	0.276	0.638	0.560	0.640
Fe²⁺	1.409	1.396	0.878	1.166	0.970
Mn	0.034	0.047	0.049	0.041	0.064
Mg	2.536	2.706	3.033	2.784	2.967
Ca	1.914	1.899	1.790	1.922	1.813
Na	0.700	0.688	0.598	0.643	0.579
K	0.156	0.156	0.153	0.176	0.177
Total	15.77	15.74	15.54	15.74	15.57
P-C conditions					
T (°C)	1001	973	930	983	924
Uncertainty	22	22	22	22	22
P (MPa)	543	375	246	406	234
Uncertainty	60	41	27	45	26
Equivalent depth (km)	20.5	14.2	9.3	15.3	8.8
ΔNNO	-0.22	-0.05	0.73	0.33	0.70
log fO₂	-10.33	-10.66	-10.62	-10.11	-10.75
Uncertainty	0.4	0.4	0.4	0.4	0.4
H₂O_{melt} (wt.%)	6.7	5.6	4.3	5.5	4.1
Uncertainty	1.0	0.8	0.7	0.8	0.6

Cation proportions calculated using Leake et al. (1997) on the basis of 13 cations. P-C = Physical-chemical conditions, calculated using the method of Ridolfi et al. (2010).

Table A2.6 Major element amphibole compositions analysed by EMPA.

Sample ID	Inglewood a A9_1	Inglewood a A9_2	Inglewood a A9_3	Inglewood a A9_4	Inglewood a A10_2
Zone	rim	core	core	zone	zone
SiO₂	43.79	43.53	40.00	40.92	41.22
TiO₂	2.73	2.72	2.30	2.32	2.50
Al₂O₃	9.46	9.52	13.49	12.63	11.28
Fe₂O₃	6.16	5.20	5.52	6.03	6.27
FeO	6.77	7.66	8.31	8.42	8.45
MnO	0.61	0.61	0.25	0.30	0.53
MgO	14.23	13.96	12.42	12.48	12.56
CaO	11.42	11.52	11.94	11.81	11.64
Na₂O	2.00	2.05	2.23	2.18	2.11
K₂O	0.89	0.88	0.89	0.85	0.89
H₂O_{calc}	1.91	1.90	1.88	1.89	1.87
Total	99.96	99.55	99.22	99.83	99.31
Mg#	78.93	76.45	72.72	72.55	72.61
Cations					
Si	6.395	6.398	5.945	6.045	6.135
Ti	0.300	0.300	0.257	0.258	0.279
Al	1.629	1.649	2.364	2.200	1.979
Fe³⁺	0.677	0.575	0.618	0.670	0.702
Fe²⁺	0.827	0.942	1.033	1.040	1.051
Mn	0.075	0.076	0.031	0.038	0.066
Mg	3.098	3.059	2.752	2.749	2.787
Ca	1.787	1.814	1.901	1.870	1.856
Na	0.565	0.584	0.643	0.624	0.610
K	0.166	0.165	0.169	0.160	0.169
Total	15.52	15.56	15.71	15.65	15.63
P-C conditions					
T (°C)	909	912	1008	981	956
Uncertainty	22	22	22	22	22
P (MPa)	200	206	575	454	331
Uncertainty	22	23	63	50	36
Equivalent depth (km)	7.5	7.8	21.7	17.2	12.5
ΔNNO	0.95	0.84	0.29	0.37	0.45
log fO₂	-10.78	-10.83	-9.71	-10.08	-10.44
Uncertainty	0.4	0.4	0.4	0.4	0.4
H₂O_{melt} (wt.%)	3.8	3.9	6.7	6.3	5.2
Uncertainty	0.6	0.6	1.0	0.9	0.8

Cation proportions calculated using Leake et al. (1997) on the basis of 13 cations. P-C = Physical-chemical conditions, calculated using the method of Ridolfi et al. (2010).

Table A2.6 Major element amphibole compositions analysed by EMPA.

Sample ID	Inglewood a A10_3	Inglewood a A10_4	Inglewood a A12_1	Inglewood a A12_2	Inglewood a A13_2
Zone	core	core	rim	core	rim
SiO₂	41.53	40.55	43.00	43.02	42.64
TiO₂	2.32	2.44	2.61	2.90	2.43
Al₂O₃	11.70	12.12	10.48	9.36	9.69
Fe₂O₃	5.38	4.96	6.07	5.38	6.00
FeO	8.86	9.63	7.35	7.55	7.04
MnO	0.43	0.37	0.55	0.62	0.47
MgO	12.67	12.24	13.63	13.84	13.95
CaO	11.89	11.97	11.53	11.50	11.49
Na₂O	2.19	2.30	2.00	1.91	2.04
K₂O	0.74	0.78	0.95	0.93	0.91
H₂O_{calc}	1.89	1.87	1.91	1.88	1.88
Total	99.60	99.23	100.08	98.89	98.53
Mg#	71.83	69.38	76.78	76.58	77.95
Cations					
Si	6.150	6.057	6.294	6.373	6.336
Ti	0.259	0.275	0.287	0.323	0.272
Al	2.043	2.134	1.809	1.634	1.696
Fe³⁺	0.600	0.557	0.668	0.599	0.671
Fe²⁺	1.097	1.203	0.900	0.935	0.874
Mn	0.054	0.047	0.068	0.078	0.060
Mg	2.798	2.727	2.975	3.058	3.091
Ca	1.886	1.915	1.808	1.825	1.829
Na	0.629	0.665	0.568	0.549	0.587
K	0.139	0.149	0.178	0.176	0.173
Total	15.65	15.73	15.55	15.55	15.59
P-C conditions					
T (°C)	962	981	930	914	922
Uncertainty	22	22	22	22	22
P (MPa)	362	413	259	201	220
Uncertainty	40	45	28	22	24
Equivalent depth (km)	13.7	15.6	9.8	7.6	8.3
ΔNNO	0.43	0.24	0.76	0.82	0.96
log fO₂	-10.35	-10.23	-10.59	-10.81	-10.54
Uncertainty	0.4	0.4	0.4	0.4	0.4
H₂O_{melt} (wt.%)	5.9	5.9	4.5	3.7	3.8
Uncertainty	0.9	0.9	0.7	0.6	0.6

Cation proportions calculated using Leake et al. (1997) on the basis of 13 cations. P-C = Physical-chemical conditions, calculated using the method of Ridolfi et al. (2010).

Table A2.6 Major element amphibole compositions analysed by EMPA.

Sample ID	Inglewood a A13_3	Inglewood a A13_4	Inglewood a A13_5	Inglewood a A13_6	Inglewood a A14_1
Zone	zone	zone	zone	zone	rim
SiO₂	43.48	41.54	41.32	41.79	43.02
TiO₂	2.58	2.65	2.73	3.00	2.71
Al₂O₃	9.59	10.53	10.90	10.58	9.61
Fe₂O₃	5.78	6.10	6.10	6.00	5.29
FeO	7.21	7.74	7.79	8.33	7.57
MnO	0.46	0.45	0.40	0.44	0.64
MgO	13.88	13.24	13.04	12.65	13.79
CaO	11.37	11.56	11.48	11.15	11.47
Na₂O	1.92	2.08	2.09	2.01	2.06
K₂O	0.86	0.91	0.93	1.04	0.85
H₂O_{calc}	1.89	1.87	1.87	1.87	1.89
Total	99.03	98.67	98.66	98.87	98.89
Mg#	77.44	75.30	74.90	73.04	77.54
Cations					
Si	6.410	6.198	6.166	6.228	6.369
Ti	0.286	0.298	0.306	0.337	0.301
Al	1.666	1.851	1.918	1.859	1.678
Fe³⁺	0.641	0.685	0.685	0.673	0.590
Fe²⁺	0.889	0.966	0.973	1.038	0.937
Mn	0.058	0.057	0.051	0.055	0.081
Mg	3.051	2.945	2.902	2.811	3.044
Ca	1.796	1.848	1.836	1.780	1.820
Na	0.549	0.601	0.605	0.580	0.590
K	0.162	0.173	0.176	0.199	0.160
Total	15.51	15.62	15.62	15.56	15.57
P-C conditions					
T (°C)	907	946	952	934	918
Uncertainty	22	22	22	22	22
P (MPa)	211	275	303	278	214
Uncertainty	23	30	33	31	24
Equivalent depth (km)	8.0	10.4	11.4	10.5	8.1
ΔNNO	0.91	0.66	0.58	0.44	0.81
log fO₂	-10.85	-10.42	-10.39	-10.83	-10.76
Uncertainty	0.4	0.4	0.4	0.4	0.4
H₂O_{melt} (wt.%)	4.2	4.4	4.6	4.4	4.1
Uncertainty	0.6	0.7	0.7	0.7	0.6

Cation proportions calculated using Leake et al. (1997) on the basis of 13 cations. P-C = Physical-chemical conditions, calculated using the method of Ridolfi et al. (2010).

Table A2.6 Major element amphibole compositions analysed by EMPA.

Sample ID	Inglewood a A14_2	Inglewood a A14_3	Inglewood a A14_4	Inglewood a A14_5	Inglewood a A14_6
Zone	zone	zone	zone	zone	zone
SiO₂	41.66	43.15	41.82	42.65	42.05
TiO₂	2.78	2.82	3.17	2.96	2.74
Al₂O₃	10.85	9.64	10.92	10.08	10.71
Fe₂O₃	4.82	5.58	5.17	4.24	5.02
FeO	8.45	7.38	8.08	8.51	7.95
MnO	0.61	0.61	0.54	0.54	0.44
MgO	12.95	13.78	13.03	13.54	13.40
CaO	11.55	11.34	11.34	11.58	11.50
Na₂O	2.14	2.02	2.11	2.14	2.16
K₂O	0.88	0.91	0.97	0.88	0.92
H₂O_{calc}	1.87	1.89	1.88	1.89	1.88
Total	98.56	99.12	99.03	99.02	98.77
Mg#	73.74	78.48	76.45	75.28	70.91
Cations					
Si	6.221	6.370	6.205	6.322	6.247
Ti	0.312	0.313	0.353	0.330	0.307
Al	1.909	1.677	1.910	1.761	1.875
Fe³⁺	0.542	0.619	0.578	0.473	0.561
Fe²⁺	1.055	0.910	1.002	1.055	0.988
Mn	0.077	0.077	0.068	0.067	0.055
Mg	2.884	3.033	2.884	2.991	2.968
Ca	1.848	1.794	1.802	1.840	1.830
Na	0.619	0.578	0.608	0.616	0.623
K	0.168	0.172	0.183	0.166	0.174
Total	15.63	15.54	15.59	15.62	15.63
P-C conditions					
T (°C)	949	915	948	932	945
Uncertainty	22	22	22	22	22
P (MPa)	299	214	299	242	285
Uncertainty	33	24	33	27	31
Equivalent depth (km)	11.3	8.1	11.3	9.1	10.7
ΔNNO	0.47	0.80	0.43	0.60	0.62
log fO₂	-10.54	-10.82	-10.60	-10.72	-10.47
Uncertainty	0.4	0.4	0.4	0.4	0.4
H₂O_{melt} (wt.%)	4.9	3.9	4.6	4.2	4.6
Uncertainty	0.7	0.6	0.7	0.6	0.7

Cation proportions calculated using Leake et al. (1997) on the basis of 13 cations. P-C = Physical-chemical conditions, calculated using the method of Ridolfi et al. (2010).

Table A2.6 Major element amphibole compositions analysed by EMPA.

Sample ID	Inglewood a A14_7	Inglewood a A14_8	Inglewood a A14_9	Inglewood a A14_10	Inglewood a A14_11
Zone	zone	zone	core	core	core
SiO₂	40.12	39.84	39.25	42.92	39.47
TiO₂	2.61	2.30	2.09	2.42	2.51
Al₂O₃	12.87	13.07	14.26	10.55	13.50
Fe₂O₃	6.32	5.71	5.93	5.25	5.72
FeO	7.60	7.75	8.57	7.94	8.71
MnO	0.49	0.35	0.32	0.55	0.51
MgO	12.55	12.63	11.83	13.56	11.90
CaO	11.68	11.88	12.03	11.70	11.82
Na₂O	2.25	2.20	2.25	2.08	2.31
K₂O	0.89	0.86	0.83	0.87	0.89
H₂O_{calc}	1.87	1.86	1.87	1.90	1.87
Total	99.25	98.46	99.25	99.74	99.21
Mg#	73.34	73.22	76.91	74.21	73.92
Cations					
Si	5.961	5.962	5.853	6.308	5.896
Ti	0.292	0.258	0.234	0.267	0.282
Al	2.253	2.306	2.507	1.828	2.377
Fe³⁺	0.707	0.643	0.666	0.581	0.642
Fe²⁺	0.944	0.970	1.069	0.976	1.087
Mn	0.062	0.044	0.040	0.069	0.064
Mg	2.780	2.817	2.631	2.972	2.651
Ca	1.859	1.904	1.921	1.843	1.892
Na	0.647	0.638	0.651	0.593	0.668
K	0.168	0.165	0.158	0.162	0.170
Total	15.67	15.71	15.73	15.60	15.73
P-C conditions					
T (°C)	998	1005	1025	933	1013
Uncertainty	22	22	22	22	22
P (MPa)	491	529	706	266	586
Uncertainty	54	58	78	29	64
Equivalent depth (km)	18.5	20.0	26.7	10.1	22.1
ΔNNO	0.33	0.40	0.14	0.73	0.09
log fO₂	-9.86	-9.67	-9.58	-10.56	-9.83
Uncertainty	0.4	0.4	0.4	0.4	0.4
H₂O_{melt} (wt.%)	6.1	6.4	7.5	4.8	6.6
Uncertainty	0.9	1.0	1.1	0.7	1.0

Cation proportions calculated using Leake et al. (1997) on the basis of 13 cations. P-C = Physical-chemical conditions, calculated using the method of Ridolfi et al. (2010).

Table A2.6 Major element amphibole compositions analysed by EMPA.

Sample ID	Inglewood a A14_12	Inglewood a A15_2	Inglewood a A15_3	Korito A1_1	Korito A1_2	Korito A1_3
Zone	zone	core	core	rim	zone	core
SiO₂	39.23	39.74	42.62	44.54	40.71	41.58
TiO₂	2.85	2.67	2.90	2.94	2.41	2.90
Al₂O₃	12.76	13.00	9.84	10.34	12.17	10.61
Fe₂O₃	6.94	6.46	5.55	1.49	4.76	3.64
FeO	7.78	7.86	6.89	11.14	9.42	9.68
MnO	0.56	0.53	0.49	0.55	0.44	0.51
MgO	12.00	12.39	14.10	13.18	12.27	12.83
CaO	11.48	11.85	11.54	12.02	11.91	11.82
Na₂O	2.23	2.17	1.93	2.05	2.17	2.09
K₂O	0.91	0.97	0.94	0.88	0.88	0.93
H₂O_{calc}	1.85	1.87	1.88	1.94	1.87	1.87
Total	98.59	99.52	98.69	101.06	99.01	98.45
Mg#	75.03	74.65	74.40	67.83	69.89	70.27
Cations						
Si	5.895	5.909	6.312	6.471	6.084	6.238
Ti	0.323	0.299	0.323	0.321	0.270	0.328
Al	2.260	2.279	1.718	1.770	2.144	1.876
Fe³⁺	0.784	0.723	0.619	0.162	0.535	0.411
Fe²⁺	0.977	0.978	0.854	1.354	1.177	1.214
Mn	0.071	0.067	0.061	0.068	0.056	0.064
Mg	2.689	2.746	3.113	2.854	2.733	2.870
Ca	1.848	1.887	1.831	1.871	1.907	1.899
Na	0.649	0.624	0.553	0.578	0.629	0.607
K	0.174	0.185	0.178	0.163	0.168	0.178
Total	15.67	15.70	15.56	15.61	15.70	15.68
P-C conditions						
T (°C)	1002	1006	929	916	978	950
Uncertainty	22	22	22	22	22	22
P (MPa)	495	509	227	245	419	285
Uncertainty	54	56	25	27	46	31
Equivalent depth (km)	18.7	19.2	8.6	9.2	15.8	10.8
ΔNNO	0.17	0.27	0.88	0.33	0.27	0.37
log fO₂	-9.96	-9.79	-10.49	-11.25	-10.24	-10.63
Uncertainty	0.4	0.4	0.4	0.4	0.4	0.4
H₂O_{melt} (wt.%)	5.9	5.9	3.8	5.2	6.0	4.6
Uncertainty	0.9	0.9	0.6	0.8	0.9	0.7

Cation proportions calculated using Leake et al. (1997) on the basis of 13 cations. P-C = Physical-chemical conditions, calculated using the method of Ridolfi et al. (2010).

Table A2.6 Major element amphibole compositions analysed by EMPA.

Sample ID	Korito A2_1	Korito A2_2	Korito A2_4	Korito A3_1	Korito A3_2	Korito A3_3	Korito A3_4
Zone	rim	rim	core	rim	zone	zone	zone
SiO₂	42.43	40.03	39.70	42.08	39.91	42.08	42.85
TiO₂	2.73	2.75	2.19	2.97	2.66	3.16	2.93
Al₂O₃	10.22	12.78	13.50	10.09	12.72	10.26	9.95
Fe₂O₃	3.62	4.62	4.94	3.40	3.74	4.80	3.63
FeO	9.25	9.49	9.80	9.15	10.44	9.16	9.40
MnO	0.50	0.44	0.38	0.57	0.46	0.54	0.43
MgO	13.34	12.13	11.71	13.25	11.59	12.76	13.29
CaO	11.86	11.99	12.11	11.73	11.84	11.38	11.65
Na₂O	2.07	2.28	2.28	2.00	2.22	2.05	2.10
K₂O	0.88	0.80	0.86	0.96	0.93	1.04	0.84
H₂O_{calc}	1.88	1.87	1.87	1.87	1.86	1.88	1.89
Total	98.78	99.17	99.34	98.09	98.37	99.12	98.96
Mg#	71.98	69.50	68.05	72.08	66.42	71.30	71.59
Cations							
Si	6.320	5.980	5.935	6.312	6.025	6.265	6.363
Ti	0.305	0.309	0.246	0.335	0.302	0.354	0.327
Al	1.793	2.251	2.378	1.785	2.263	1.801	1.741
Fe³⁺	0.406	0.519	0.556	0.384	0.425	0.538	0.405
Fe²⁺	1.153	1.185	1.226	1.148	1.318	1.140	1.168
Mn	0.063	0.055	0.048	0.073	0.059	0.069	0.054
Mg	2.961	2.701	2.610	2.964	2.608	2.833	2.942
Ca	1.893	1.919	1.940	1.886	1.914	1.816	1.854
Na	0.597	0.661	0.660	0.583	0.651	0.593	0.605
K	0.168	0.153	0.164	0.184	0.178	0.198	0.159
Total	15.66	15.73	15.76	15.65	15.74	15.61	15.62
P-C conditions							
T (°C)	937	1000	1009	938	994	933	925
Uncertainty	22	22	22	22	22	22	22
P (MPa)	253	489	587	250	497	256	235
Uncertainty	28	54	65	28	55	28	26
Equivalent depth (km)	9.6	18.5	22.2	9.4	18.8	9.7	8.9
ΔNNO	0.57	0.09	0.07	0.51	-0.05	0.38	0.52
log fO₂	-10.67	-10.06	-9.91	-10.70	-10.30	-10.92	-10.92
Uncertainty	0.4	0.4	0.4	0.4	0.4	0.4	0.4
H₂O_{melt} (wt.%)	4.5	6.3	7.0	4.2	6.4	4.1	4.4
Uncertainty	0.7	0.9	1.0	0.6	1.0	0.6	0.7

Cation proportions calculated using Leake et al. (1997) on the basis of 13 cations. P-C = Physical-chemical conditions, calculated using the method of Ridolfi et al. (2010).

Table A2.6 Major element amphibole compositions analysed by EMPA.

Sample ID	Korito A3_5	Korito A3_6	Korito A3_7	Korito A3_8	Korito A3_9	Korito A3_10	Korito A3_11
Zone	zone	zone	zone	zone	zone	zone	zone
SiO₂	40.49	41.93	41.63	42.14	42.27	40.69	42.13
TiO₂	3.15	3.05	3.09	3.04	2.84	2.98	2.84
Al₂O₃	12.08	10.64	10.82	10.31	10.44	11.52	10.41
Fe₂O₃	4.40	3.94	4.38	3.91	3.78	4.19	3.97
FeO	9.74	9.39	9.18	9.65	9.71	9.86	8.70
MnO	0.45	0.49	0.51	0.54	0.49	0.44	0.42
MgO	12.25	12.89	12.72	12.79	12.94	12.35	13.47
CaO	11.84	11.66	11.48	11.52	11.71	11.81	11.77
Na₂O	2.25	2.08	2.11	2.04	2.17	2.19	2.10
K₂O	0.90	0.94	1.02	1.13	0.91	0.97	0.87
H₂O_{calc}	1.88	1.88	1.87	1.88	1.88	1.87	1.88
Total	99.43	98.89	98.82	98.96	99.14	98.87	98.56
Mg#	69.15	71.00	71.17	70.25	70.37	69.07	73.40
Cations							
Si	6.037	6.250	6.216	6.288	6.289	6.102	6.278
Ti	0.353	0.342	0.347	0.342	0.318	0.336	0.318
Al	2.122	1.869	1.904	1.814	1.830	2.036	1.829
Fe³⁺	0.494	0.442	0.492	0.439	0.423	0.473	0.445
Fe²⁺	1.215	1.170	1.146	1.205	1.208	1.237	1.084
Mn	0.057	0.062	0.065	0.069	0.062	0.055	0.053
Mg	2.723	2.864	2.830	2.845	2.870	2.761	2.992
Ca	1.892	1.863	1.837	1.842	1.867	1.897	1.880
Na	0.651	0.600	0.611	0.590	0.626	0.637	0.608
K	0.171	0.179	0.195	0.214	0.172	0.185	0.165
Total	15.71	15.64	15.64	15.65	15.67	15.72	15.65
P-C conditions							
T (°C)	985	945	949	935	938	973	944
Uncertainty	22	22	22	22	22	22	22
P (MPa)	406	282	297	261	267	359	267
Uncertainty	45	31	33	29	29	39	29
Equivalent depth (km)	15.3	10.7	11.2	9.8	10.1	13.6	10.1
ΔNNO	0.07	0.37	0.33	0.37	0.41	0.18	0.59
log fO₂	-10.33	-10.72	-10.70	-10.89	-10.79	-10.43	-10.52
Uncertainty	0.4	0.4	0.4	0.4	0.4	0.4	0.4
H₂O_{melt} (wt.%)	5.5	4.6	4.5	4.0	4.6	5.0	4.5
Uncertainty	0.8	0.7	0.7	0.6	0.7	0.8	0.7

Cation proportions calculated using Leake et al. (1997) on the basis of 13 cations. P-C = Physical-chemical conditions, calculated using the method of Ridolfi et al. (2010).

Table A2.6 Major element amphibole compositions analysed by EMPA.

Sample ID	Korito A3_12	Korito A3_13	Korito A3_14	Korito A4_1	Korito A4_2	Korito A4_3	Korito A4_4
Zone	core	core	zone	rim	zone	zone	zone
SiO₂	40.28	41.61	40.47	43.34	41.15	43.42	42.76
TiO₂	3.20	2.77	2.94	2.91	2.72	2.44	2.94
Al₂O₃	11.84	11.40	11.97	9.54	11.68	9.87	10.06
Fe₂O₃	3.42	3.91	4.47	4.68	5.25	4.76	4.17
FeO	10.35	8.86	9.37	8.17	8.52	8.17	8.89
MnO	0.42	0.38	0.41	0.59	0.48	0.41	0.49
MgO	12.16	13.09	12.57	13.75	12.79	13.84	13.41
CaO	11.84	11.75	11.86	11.58	11.76	11.78	11.68
Na₂O	2.23	2.19	2.32	1.93	2.19	1.95	1.99
K₂O	0.99	0.91	0.95	0.94	0.83	0.86	0.98
H₂O_{calc}	1.86	1.88	1.87	1.90	1.88	1.90	1.89
Total	98.59	98.76	99.21	99.31	99.27	99.40	99.25
Mg#	67.69	72.48	70.50	75.00	72.79	75.13	72.89
Cations							
Si	6.064	6.195	6.042	6.394	6.113	6.393	6.332
Ti	0.362	0.310	0.330	0.322	0.304	0.270	0.328
Al	2.101	1.999	2.107	1.659	2.045	1.713	1.755
Fe³⁺	0.388	0.439	0.502	0.520	0.587	0.528	0.465
Fe²⁺	1.302	1.104	1.170	1.008	1.059	1.006	1.101
Mn	0.054	0.047	0.052	0.073	0.060	0.051	0.061
Mg	2.729	2.906	2.796	3.024	2.832	3.039	2.959
Ca	1.910	1.873	1.897	1.830	1.872	1.858	1.852
Na	0.650	0.632	0.672	0.552	0.632	0.555	0.572
K	0.190	0.174	0.181	0.177	0.158	0.161	0.185
Total	15.75	15.68	15.75	15.56	15.66	15.57	15.61
P-C conditions							
T (°C)	984	963	986	914	970	918	929
Uncertainty	22	22	22	22	22	22	22
P (MPa)	394	341	397	209	364	226	240
Uncertainty	43	37	44	23	40	25	26
Equivalent depth (km)	14.9	12.9	15.0	7.9	13.7	8.5	9.1
ΔNNO	0.03	0.43	0.21	0.74	0.38	0.84	0.58
log fO₂	-10.40	-10.35	-10.18	-10.89	-10.28	-10.72	-10.79
Uncertainty	0.4	0.4	0.4	0.4	0.4	0.4	0.4
H₂O_{melt} (wt.%)	5.2	5.1	5.1	3.9	5.5	4.5	4.2
Uncertainty	0.8	0.8	0.8	0.6	0.8	0.7	0.6

Cation proportions calculated using Leake et al. (1997) on the basis of 13 cations. P-C = Physical-chemical conditions, calculated using the method of Ridolfi et al. (2010).

Table A2.6 Major element amphibole compositions analysed by EMPA.

Sample ID	Korito A4_5	Korito A7_1	Korito A7_2	Korito A7_3	Korito A7_4	Korito A8_1	Korito A8_2
Zone	core	rim	zone	core	zone	rim	zone
SiO₂	43.35	43.39	43.30	40.45	43.25	42.99	40.09
TiO₂	2.80	2.74	2.80	2.20	2.82	3.02	2.47
Al₂O₃	9.29	9.57	9.66	13.42	9.83	9.72	12.63
Fe₂O₃	5.31	6.87	6.19	5.83	5.99	5.60	5.89
FeO	7.60	5.79	6.57	7.81	7.23	7.33	8.48
MnO	0.49	0.53	0.59	0.18	0.55	0.60	0.24
MgO	13.94	14.43	14.11	12.83	13.81	13.99	12.41
CaO	11.44	11.21	11.31	12.09	11.31	11.60	11.91
Na₂O	1.94	2.04	1.99	2.09	2.02	1.96	2.08
K₂O	0.91	0.90	0.92	0.94	0.97	0.93	0.92
H₂O_{calc}	1.89	1.90	1.90	1.89	1.90	1.90	1.87
Total	98.96	99.37	99.32	99.73	99.68	99.64	99.00
Mg#	76.56	81.62	79.30	74.54	77.30	77.28	72.28
Cations							
Si	6.408	6.359	6.362	5.967	6.349	6.320	5.986
Ti	0.312	0.302	0.310	0.244	0.312	0.334	0.277
Al	1.618	1.653	1.672	2.333	1.701	1.684	2.223
Fe³⁺	0.591	0.757	0.684	0.647	0.662	0.620	0.662
Fe²⁺	0.940	0.710	0.807	0.964	0.887	0.902	1.059
Mn	0.061	0.066	0.073	0.022	0.068	0.075	0.030
Mg	3.071	3.153	3.091	2.823	3.022	3.066	2.762
Ca	1.812	1.760	1.781	1.912	1.780	1.828	1.905
Na	0.557	0.581	0.566	0.598	0.576	0.560	0.603
K	0.172	0.167	0.172	0.177	0.182	0.174	0.175
Total	15.54	15.51	15.52	15.69	15.54	15.56	15.68
P-C conditions							
T (°C)	908	913	915	1004	917	925	993
Uncertainty	22	22	22	22	22	22	22
P (MPa)	197	207	213	550	222	216	470
Uncertainty	22	23	23	60	24	24	52
Equivalent depth (km)	7.4	7.8	8.0	20.8	8.4	8.2	17.7
ΔNNO	0.87	1.05	0.92	0.45	0.80	0.80	0.34
log fO₂	-10.88	-10.60	-10.70	-9.61	-10.78	-10.65	-9.93
Uncertainty	0.4	0.4	0.4	0.4	0.4	0.4	0.4
H₂O_{melt} (wt.%)	3.7	3.7	3.9	6.5	3.9	3.8	6.0
Uncertainty	0.6	0.5	0.6	1.0	0.6	0.6	0.9

Cation proportions calculated using Leake et al. (1997) on the basis of 13 cations. P-C = Physical-chemical conditions, calculated using the method of Ridolfi et al. (2010).

Table A2.6 Major element amphibole compositions analysed by EMPA.

Sample ID	Korito A8_3	Korito A8_4	Korito A8_5	Korito A8_6	Korito A8_7	Korito A8_8	Korito A8_9
Zone	zone	zone	zone	zone	zone	zone	zone
SiO₂	42.87	42.80	43.05	42.46	43.15	41.25	42.43
TiO₂	2.97	2.88	3.01	3.21	3.08	3.08	2.71
Al₂O₃	9.49	9.59	9.63	10.02	9.36	11.21	10.24
Fe₂O₃	5.11	5.17	4.51	4.94	5.80	5.44	5.57
FeO	7.55	7.78	8.50	8.28	6.90	7.66	6.59
MnO	0.63	0.56	0.56	0.50	0.43	0.39	0.36
MgO	13.93	13.84	13.70	13.59	14.31	13.46	14.36
CaO	11.59	11.68	11.68	11.59	11.41	11.69	11.61
Na₂O	1.95	1.92	1.99	2.09	2.05	2.14	2.11
K₂O	0.92	0.91	0.95	0.96	0.88	0.98	0.90
H₂O_{calc}	1.89	1.89	1.90	1.89	1.90	1.88	1.89
Total	98.88	99.02	99.48	99.54	99.27	99.18	98.76
Mg#	76.70	76.01	74.17	74.53	78.71	75.79	79.52
Cations							
Si	6.351	6.339	6.355	6.272	6.351	6.117	6.271
Ti	0.331	0.321	0.334	0.357	0.341	0.343	0.301
Al	1.657	1.674	1.676	1.744	1.623	1.959	1.785
Fe³⁺	0.570	0.576	0.501	0.549	0.642	0.607	0.620
Fe²⁺	0.935	0.964	1.050	1.023	0.849	0.950	0.815
Mn	0.079	0.070	0.070	0.062	0.054	0.050	0.045
Mg	3.077	3.056	3.014	2.994	3.139	2.974	3.163
Ca	1.839	1.853	1.848	1.835	1.799	1.857	1.839
Na	0.559	0.551	0.570	0.600	0.586	0.616	0.604
K	0.173	0.173	0.179	0.181	0.166	0.185	0.169
Total	15.57	15.58	15.60	15.62	15.55	15.66	15.61
P-C conditions							
T (°C)	922	923	922	935	925	968	941
Uncertainty	22	22	22	22	22	22	22
P (MPa)	208	213	214	236	198	322	250
Uncertainty	23	23	24	26	22	35	28
Equivalent depth (km)	7.9	8.1	8.1	8.9	7.5	12.1	9.4
ΔNNO	0.80	0.79	0.67	0.59	0.95	0.55	0.94
log fO₂	-10.70	-10.69	-10.82	-10.67	-10.50	-10.15	-10.21
Uncertainty	0.4	0.4	0.4	0.4	0.4	0.4	0.4
H₂O_{melt} (wt.%)	3.7	3.8	3.8	3.8	3.5	4.4	4.0
Uncertainty	0.6	0.6	0.6	0.6	0.5	0.7	0.6

Cation proportions calculated using Leake et al. (1997) on the basis of 13 cations. P-C = Physical-chemical conditions, calculated using the method of Ridolfi et al. (2010).

Table A2.6 Major element amphibole compositions analysed by EMPA.

Sample ID	Korito A8_10	Korito A8_11	Korito A9_2	Korito A9_3	Korito A9_4	Korito A10_1	Korito A10_2
Zone	core	core	zone	zone	core	rim	core
SiO₂	39.30	40.43	43.60	42.74	41.32	40.48	40.26
TiO₂	2.69	2.25	2.58	3.03	2.27	2.40	2.11
Al₂O₃	13.48	12.68	12.31	10.12	11.99	12.79	12.96
Fe₂O₃	5.92	5.44	3.85	5.92	6.29	5.81	7.37
FeO	8.17	7.21	9.49	6.91	7.50	8.77	7.61
MnO	0.35	0.21	0.49	0.42	0.35	0.30	0.35
MgO	12.24	13.55	12.86	14.07	13.20	12.17	12.31
CaO	11.84	12.06	11.81	11.48	11.71	11.93	11.85
Na₂O	2.20	2.26	2.18	2.08	2.19	2.04	2.02
K₂O	1.01	0.97	0.91	0.87	1.05	0.81	0.84
H₂O_{calc}	1.87	1.88	1.95	1.90	1.89	1.88	1.87
Total	99.08	98.95	102.03	99.55	99.76	99.36	99.56
Mg#	72.77	77.01	70.73	78.40	75.81	71.20	74.24
Cations							
Si	5.870	6.001	6.266	6.277	6.094	6.017	5.969
Ti	0.302	0.251	0.279	0.335	0.251	0.268	0.235
Al	2.373	2.219	2.085	1.752	2.084	2.240	2.265
Fe³⁺	0.666	0.608	0.417	0.654	0.699	0.650	0.823
Fe²⁺	1.020	0.895	1.140	0.849	0.926	1.090	0.944
Mn	0.044	0.026	0.060	0.053	0.044	0.038	0.044
Mg	2.726	2.999	2.754	3.081	2.902	2.697	2.721
Ca	1.895	1.917	1.818	1.807	1.851	1.900	1.882
Na	0.636	0.650	0.607	0.593	0.625	0.587	0.582
K	0.193	0.184	0.166	0.163	0.198	0.153	0.159
Total	15.72	15.75	15.59	15.56	15.67	15.64	15.62
P-C conditions							
T (°C)	1018	1002	950	933	972	987	990
Uncertainty	22	22	22	22	22	22	22
P (MPa)	582	467	385	239	385	481	499
Uncertainty	64	51	42	26	42	53	55
Equivalent depth (km)	22.0	17.6	14.5	9.0	14.5	18.2	18.8
ΔNNO	0.19	0.66	0.29	0.81	0.63	0.27	0.43
log fO₂	-9.67	-9.47	-10.67	-10.49	-9.99	-10.09	-9.87
Uncertainty	0.4	0.4	0.4	0.4	0.4	0.4	0.4
H₂O_{melt} (wt.%)	6.2	5.5	6.3	4.0	5.1	6.7	6.6
Uncertainty	0.9	0.8	1.0	0.6	0.8	1.0	1.0

Cation proportions calculated using Leake et al. (1997) on the basis of 13 cations. P-C = Physical-chemical conditions, calculated using the method of Ridolfi et al. (2010).

Table A2.6 Major element amphibole compositions analysed by EMPA.

Sample ID	Korito A11_2	Korito A12_1	Korito A12_2	Korito A12_3	Korito A12_4	Korito A14_1	Korito A14_5
Zone	core	rim	zone	zone	core	rim	core
SiO₂	40.27	42.53	41.95	40.33	41.09	43.14	41.51
TiO₂	2.20	2.61	2.40	2.09	1.90	2.54	1.95
Al₂O₃	12.50	10.05	11.08	13.18	12.28	9.80	11.89
Fe₂O₃	5.92	5.96	5.82	5.42	6.35	6.08	6.61
FeO	8.30	7.01	7.47	9.15	7.68	6.67	6.97
MnO	0.31	0.59	0.50	0.31	0.27	0.61	0.26
MgO	12.50	13.71	13.40	12.17	12.94	14.15	13.30
CaO	11.97	11.38	11.69	12.07	11.91	11.47	11.81
Na₂O	2.05	1.99	2.08	2.25	2.12	2.05	2.01
K₂O	0.86	0.98	0.85	0.86	0.80	0.91	0.79
H₂O_{calc}	1.86	1.88	1.88	1.88	1.88	1.89	1.88
Total	98.72	98.70	99.12	99.71	99.21	99.30	98.99
Mg#	72.87	77.72	76.19	70.34	75.02	79.09	77.28
Cations							
Si	6.023	6.309	6.209	5.986	6.091	6.347	6.142
Ti	0.247	0.292	0.268	0.234	0.212	0.281	0.217
Al	2.202	1.758	1.932	2.306	2.145	1.699	2.074
Fe³⁺	0.666	0.666	0.648	0.606	0.708	0.673	0.736
Fe²⁺	1.037	0.870	0.924	1.136	0.952	0.821	0.863
Mn	0.039	0.074	0.062	0.039	0.034	0.075	0.033
Mg	2.786	3.033	2.957	2.694	2.858	3.104	2.935
Ca	1.918	1.809	1.855	1.919	1.891	1.809	1.873
Na	0.594	0.573	0.597	0.646	0.609	0.584	0.576
K	0.163	0.186	0.161	0.164	0.151	0.170	0.149
Total	15.67	15.57	15.61	15.73	15.65	15.56	15.60
P-C conditions							
T (°C)	988	927	951	998	974	921	964
Uncertainty	22	22	22	22	22	22	22
P (MPa)	456	241	309	529	420	221	379
Uncertainty	50	26	34	58	46	24	42
Equivalent depth (km)	17.2	9.1	11.7	20.0	15.9	8.3	14.3
ΔNNO	0.43	0.83	0.70	0.26	0.63	0.96	0.78
log fO₂	-9.92	-10.56	-10.28	-9.91	-9.93	-10.55	-9.97
Uncertainty	0.4	0.4	0.4	0.4	0.4	0.4	0.4
H₂O_{melt} (wt.%)	6.2	4.1	5.1	6.7	6.2	3.9	6.0
Uncertainty	0.9	0.6	0.8	1.0	0.9	0.6	0.9

Cation proportions calculated using Leake et al. (1997) on the basis of 13 cations. P-C = Physical-chemical conditions, calculated using the method of Ridolfi et al. (2010).

Table A2.6 Major element amphibole compositions analysed by EMPA.

Sample ID	Korito A14_6	Korito A14_7	Korito A14_8	Korito A15_1	Korito A15_2	Korito A16_1
Zone	zone	zone	zone	rim	zone	rim
SiO₂	40.95	41.80	40.97	43.62	43.12	43.95
TiO₂	1.97	1.98	2.09	2.52	2.41	2.89
Al₂O₃	12.53	11.56	12.22	9.34	9.93	9.43
Fe₂O₃	6.41	6.44	5.70	6.96	5.21	2.68
FeO	7.27	7.01	7.93	6.18	7.52	9.93
MnO	0.25	0.27	0.34	0.64	0.50	0.64
MgO	13.12	13.58	12.96	14.18	14.01	13.21
CaO	12.00	11.93	11.93	11.24	11.71	11.19
Na₂O	2.07	2.03	2.18	1.96	2.02	2.20
K₂O	0.80	0.76	0.79	0.92	0.89	1.13
H₂O_{calc}	1.88	1.89	1.88	1.90	1.89	1.90
Total	99.25	99.25	98.98	99.44	99.21	99.15
Mg#	76.28	77.55	74.44	80.34	76.86	70.32
Cations						
Si	6.058	6.168	6.089	6.400	6.358	6.508
Ti	0.219	0.219	0.233	0.278	0.268	0.322
Al	2.185	2.011	2.141	1.616	1.726	1.646
Fe³⁺	0.714	0.715	0.637	0.768	0.578	0.298
Fe²⁺	0.900	0.865	0.986	0.759	0.927	1.230
Mn	0.031	0.034	0.043	0.079	0.063	0.080
Mg	2.893	2.988	2.871	3.101	3.080	2.915
Ca	1.902	1.887	1.900	1.767	1.850	1.775
Na	0.593	0.581	0.628	0.556	0.576	0.631
K	0.150	0.144	0.150	0.172	0.167	0.214
Total	15.64	15.61	15.68	15.49	15.59	15.62
P-C conditions						
T (°C)	983	960	978	903	924	899
Uncertainty	22	22	22	22	22	22
P (MPa)	445	346	417	196	230	205
Uncertainty	49	38	46	22	25	23
Equivalent depth (km)	16.8	13.1	15.8	7.4	8.7	7.7
ΔNNO	0.66	0.85	0.57	1.05	0.91	0.50
log fO₂	-9.77	-9.98	-9.94	-10.78	-10.55	-11.40
Uncertainty	0.4	0.4	0.4	0.4	0.4	0.4
H₂O_{melt} (wt.%)	6.3	5.7	6.1	3.7	4.2	3.6
Uncertainty	0.9	0.9	0.9	0.6	0.6	0.4

Cation proportions calculated using Leake et al. (1997) on the basis of 13 cations. P-C = Physical-chemical conditions, calculated using the method of Ridolfi et al. (2010).

Table A2.6 Major element amphibole compositions analysed by EMPA.

Sample ID	Korito A16_2	Korito A16_3	Korito A16_4	Korito A16_5	Korito A16_6	Korito A16_7
Zone	zone	zone	zone	zone	zone	zone
SiO₂	40.36	42.41	40.87	42.17	41.52	39.79
TiO₂	2.77	2.98	2.99	3.10	3.50	2.75
Al₂O₃	12.08	9.98	11.38	10.49	11.15	13.52
Fe₂O₃	3.55	3.05	3.58	3.52	3.49	5.16
FeO	10.53	9.59	10.59	9.65	8.21	8.00
MnO	0.36	0.56	0.56	0.44	0.34	0.28
MgO	11.91	13.14	11.95	13.01	13.75	12.52
CaO	11.88	11.68	11.66	11.58	11.68	11.70
Na₂O	2.13	2.01	2.17	2.15	2.31	2.35
K₂O	0.97	0.95	1.06	1.07	0.92	0.86
H₂O_{calc}	1.86	1.87	1.86	1.88	1.89	1.88
Total	98.39	98.23	98.66	99.07	98.76	98.80
Mg#	66.85	70.94	66.79	70.62	74.90	73.62
Cations						
Si	6.087	6.354	6.152	6.277	6.163	5.927
Ti	0.314	0.335	0.338	0.347	0.390	0.308
Al	2.147	1.761	2.018	1.839	1.951	2.373
Fe³⁺	0.403	0.344	0.406	0.394	0.389	0.578
Fe²⁺	1.327	1.202	1.333	1.201	1.020	0.996
Mn	0.045	0.071	0.071	0.056	0.043	0.035
Mg	2.677	2.934	2.681	2.886	3.043	2.781
Ca	1.920	1.875	1.880	1.847	1.857	1.868
Na	0.623	0.585	0.633	0.622	0.665	0.679
K	0.186	0.182	0.203	0.203	0.175	0.163
Total	15.73	15.64	15.72	15.67	15.70	15.71
P-C conditions						
T (°C)	981	930	964	942	972	1014
Uncertainty	22	22	22	22	22	22
P (MPa)	421	242	350	271	318	583
Uncertainty	46	27	38	30	35	64
Equivalent depth (km)	15.9	9.1	13.2	10.2	12.0	22.0
ΔNNO	0.06	0.47	0.06	0.38	0.44	0.20
log fO₂	-10.41	-10.87	-10.71	-10.77	-10.20	-9.71
Uncertainty	0.4	0.4	0.4	0.4	0.4	0.4
H₂O_{melt} (wt.%)	5.8	4.3	5.0	4.1	4.3	6.5
Uncertainty	0.9	0.6	0.7	0.6	0.6	1.0

Cation proportions calculated using Leake et al. (1997) on the basis of 13 cations. P-C = Physical-chemical conditions, calculated using the method of Ridolfi et al. (2010).

Table A2.6 Major element amphibole compositions analysed by EMPA.

Sample ID	Korito A16_8	Korito A16_9	Korito A16_10	Korito A16_11	Korito A16_12
Zone	zone	zone	core	core	zone
SiO₂	42.45	41.15	41.79	39.23	42.00
TiO₂	3.18	3.31	3.18	2.94	3.04
Al₂O₃	10.22	11.14	10.99	13.50	10.48
Fe₂O₃	2.53	3.03	3.84	4.66	3.65
FeO	9.58	9.99	9.37	9.44	9.35
MnO	0.38	0.43	0.42	0.38	0.39
MgO	13.57	12.73	13.02	11.85	13.15
CaO	11.81	11.74	11.71	11.77	11.66
Na₂O	2.14	2.26	2.23	2.32	2.06
K₂O	1.00	0.96	0.94	1.11	1.12
H₂O_{calc}	1.89	1.87	1.89	1.87	1.88
Total	98.76	98.60	99.37	99.06	98.78
Mg#	71.64	69.44	71.25	69.11	71.48
Cations					
Si	6.317	6.167	6.200	5.880	6.265
Ti	0.356	0.373	0.354	0.331	0.341
Al	1.792	1.968	1.921	2.384	1.843
Fe³⁺	0.284	0.342	0.429	0.526	0.410
Fe²⁺	1.192	1.252	1.162	1.183	1.167
Mn	0.048	0.055	0.053	0.049	0.050
Mg	3.011	2.844	2.880	2.647	2.925
Ca	1.884	1.885	1.861	1.890	1.863
Na	0.619	0.657	0.640	0.674	0.596
K	0.190	0.183	0.178	0.212	0.213
Total	15.69	15.73	15.68	15.78	15.67
P-C conditions					
T (°C)	942	967	957	1019	944
Uncertainty	22	22	22	22	22
P (MPa)	253	325	304	592	272
Uncertainty	28	36	33	65	30
Equivalent depth (km)	9.5	12.3	11.5	22.4	10.3
ΔNNO	0.49	0.18	0.33	-0.05	0.45
log fO₂	-10.65	-10.54	-10.56	-9.89	-10.65
Uncertainty	0.4	0.4	0.4	0.4	0.4
H₂O_{melt} (wt.%)	4.0	4.6	4.6	6.0	4.0
Uncertainty	0.6	0.7	0.7	0.9	0.6

Cation proportions calculated using Leake et al. (1997) on the basis of 13 cations. P-C = Physical-chemical conditions, calculated using the method of Ridolfi et al. (2010).

Table A2.7 EMPA data for Fe-Ti oxides.

Sample ID	Zone	popn/host	kaupokonui M1	kaupokonui M2_1	kaupokonui M2_2	kaupokonui M3_1	kaupokonui M3_2	kaupokonui M4_1	kaupokonui M4_2	kaupokonui M4_3	kaupokonui M5_1
			core small	core mid	rim mid	core large	rim large	core large	rim large	rim large	core large
	SiO ₂		0.05	0.05	0.03	0.05	0.07	0.06	0.08	0.09	0.05
	TiO ₂		6.21	6.37	6.23	6.26	6.06	6.32	6.21	6.20	6.46
	Al ₂ O ₃		3.16	3.13	3.25	3.37	3.42	3.12	3.21	3.21	3.22
	Fe ₂ O ₃		55.21	55.36	55.37	55.31	55.30	54.96	55.32	54.91	55.98
	FeO		32.54	32.27	32.17	32.27	31.79	32.40	32.57	32.37	32.60
	MnO		0.73	0.71	0.73	0.70	0.69	0.71	0.60	0.68	0.69
	MgO		2.85	3.20	3.13	3.18	3.30	2.89	3.00	2.95	3.31
	CaO		0.00	0.00	0.00	0.00	0.00	0.12	0.00	0.01	0.00
	Cr ₂ O ₃										
	Total		100.74	101.07	100.91	101.14	100.64	100.59	100.99	100.44	102.31
	Ti#		6.36	6.53	6.40	6.42	6.27	6.49	6.36	6.39	6.55
	Xusp		0.17	0.17	0.17	0.17	0.17	0.17	0.17	0.17	0.17
	Cations										
	Si		0.002	0.002	0.001	0.002	0.003	0.002	0.003	0.003	0.002
	Ti		0.171	0.174	0.171	0.171	0.166	0.174	0.170	0.171	0.174
	Al		0.136	0.134	0.139	0.144	0.147	0.135	0.138	0.138	0.136
	Cr										
	Fe ⁺³		1.519	1.514	1.517	1.510	1.516	1.513	1.516	1.513	1.511
	Fe ⁺²		0.995	0.981	0.979	0.979	0.968	0.991	0.992	0.991	0.978
	Mn		0.023	0.022	0.022	0.022	0.021	0.022	0.019	0.021	0.021
	Mg		0.155	0.173	0.170	0.172	0.179	0.158	0.163	0.161	0.177
	Ca		0.000	0.000	0.000	0.000	0.000	0.005	0.000	0.001	0.000

Abbreviations same as Table A2.3. Population relates to either host crystals or size groups for groundmass oxides: large ~ 100 μm; mid ~ 50 μm; small ~ 10 μm. Cation proportions calculated using Lepage (2003).

Table A2.7 EMPA data for Fe-Ti oxides.

Sample ID	Zone	popn/host	Kaupokonui M5_2 rim large	Kaupokonui M5_3 rim large	Kaupokonui M6_1 rim large	Kaupokonui M6_2 core large	Kaupokonui M6_3 rim large	Kaupokonui M6_4 core small	Kaupokonui M7_1 core small	Kaupokonui M8_1 core small	Kaupokonui M8_2 core small
SiO ₂			0.07	0.06	0.08	0.04	0.07	0.13	0.11	0.10	0.10
TiO ₂			6.21	6.29	6.16	6.16	6.06	5.90	5.75	5.82	5.78
Al ₂ O ₃			3.55	3.40	3.68	3.60	3.84	3.62	3.68	3.44	3.47
Fe ₂ O ₃			55.46	55.94	55.59	56.82	55.35	55.85	55.01	54.95	54.93
FeO			32.29	32.58	32.48	31.60	32.28	32.06	31.31	31.32	31.41
MnO			0.65	0.68	0.62	0.56	0.58	0.59	0.59	0.70	0.63
MgO			3.27	3.24	3.23	3.09	3.26	3.33	3.37	3.28	3.22
CaO			0.00	0.00	0.00	1.26	0.00	0.00	0.02	0.00	0.00
Cr ₂ O ₃											
Total			101.48	102.20	101.84	103.12	101.42	101.48	99.83	99.61	99.52
Ti#			6.36	6.39	6.29	6.27	6.22	6.06	6.02	6.09	6.04
Xusp			0.17	0.17	0.17	0.16	0.17	0.16	0.16	0.16	0.16
Cations											
Si			0.002	0.002	0.003	0.002	0.002	0.005	0.004	0.004	0.004
Ti			0.169	0.170	0.167	0.164	0.164	0.160	0.158	0.161	0.160
Al			0.151	0.144	0.156	0.151	0.163	0.154	0.159	0.149	0.151
Cr											
Fe ⁺³			1.507	1.511	1.505	1.518	1.503	1.517	1.516	1.521	1.522
Fe ⁺²			0.975	0.978	0.977	0.938	0.974	0.967	0.959	0.963	0.967
Mn			0.020	0.021	0.019	0.017	0.018	0.018	0.018	0.022	0.020
Mg			0.176	0.173	0.173	0.163	0.175	0.179	0.184	0.180	0.177
Ca			0.000	0.000	0.000	0.048	0.000	0.000	0.001	0.000	0.000

Abbreviations same as Table A2.3. Population relates to either host crystals or size groups for groundmass oxides: large ~ 100 μm; mid ~ 50 μm; small ~ 10 μm. Cation proportions calculated using LePage (2003).

Table A2.7 EMPA data for Fe-Ti oxides.

Sample ID	Zone	popn/host	Kaupokonui M9		Kaupokonui M10_1		Kaupokonui M10_2		Kaupokonui M10_3		Kaupokonui M11_1		Kaupokonui M11_2		Kaupokonui M11_3		Kaupokonui M12_1		Kaupokonui M13_1		
			core small	core small	core small	core small	core mid	core small	core small	core rim small	core small	core small	core small	core small	core small	core small	core small	core small	core small	core cpx	
SiO ₂			0.08	0.08	0.08	0.09	0.07	0.07	0.08	0.08	0.08	0.06	0.06	0.08	0.07	0.07	0.07	0.07	0.07	0.07	
TiO ₂			6.08	5.89	6.09	6.09	6.15	6.15	6.15	6.15	5.98	6.05	6.05	5.94	6.28	6.31	6.31	6.28	6.31	6.31	
Al ₂ O ₃			3.59	3.40	3.32	3.32	3.45	3.45	3.45	3.41	3.41	3.34	3.34	3.40	2.85	2.85	2.85	2.85	3.23	3.23	
Fe ₂ O ₃			55.22	54.50	55.19	55.19	54.99	54.99	54.99	55.31	55.31	55.39	55.39	54.95	54.64	54.64	54.64	54.64	55.55	55.55	
FeO			32.03	31.58	32.32	32.32	32.71	32.71	32.71	32.14	32.14	32.18	32.18	31.86	32.66	32.66	32.66	32.66	31.95	31.95	
MnO			0.67	0.74	0.64	0.64	0.63	0.63	0.63	0.69	0.69	0.67	0.67	0.66	0.73	0.73	0.73	0.73	0.83	0.83	
MgO			3.25	3.02	3.00	3.00	2.83	2.83	2.83	3.03	3.03	3.05	3.05	3.06	2.61	2.61	2.61	2.61	3.28	3.28	
CaO			0.00	0.00	0.00	0.00	0.00	0.00	0.00	0.00	0.00	0.00	0.00	0.01	0.00	0.00	0.00	0.00	0.16	0.16	
Cr ₂ O ₃																					
Total			100.92	99.21	100.64	100.64	100.83	100.83	100.83	100.65	100.65	100.75	100.75	99.96	99.84	99.84	99.84	99.84	101.50	101.50	
Ti#			6.27	6.17	6.26	6.26	6.31	6.31	6.31	6.17	6.17	6.22	6.22	6.17	6.46	6.46	6.46	6.46	6.47	6.47	
Xusp			0.17	0.17	0.17	0.17	0.17	0.17	0.17	0.17	0.17	0.17	0.17	0.17	0.18	0.18	0.18	0.18	0.17	0.17	
Cations																					
Si			0.003	0.003	0.003	0.003	0.002	0.002	0.002	0.003	0.003	0.002	0.002	0.003	0.003	0.003	0.003	0.003	0.003	0.003	
Ti			0.166	0.164	0.167	0.167	0.169	0.169	0.169	0.164	0.164	0.166	0.166	0.164	0.175	0.175	0.175	0.175	0.171	0.171	
Al			0.154	0.148	0.143	0.143	0.148	0.148	0.148	0.147	0.147	0.144	0.144	0.147	0.124	0.124	0.124	0.124	0.137	0.137	
Cr			1.509	1.518	1.517	1.517	1.509	1.509	1.509	1.519	1.519	1.520	1.520	1.519	1.521	1.521	1.521	1.521	1.511	1.511	
Fe ⁺³			0.972	0.977	0.987	0.987	0.998	0.998	0.998	0.981	0.981	0.981	0.981	0.979	1.010	1.010	1.010	1.010	0.966	0.966	
Fe ⁺²			0.020	0.023	0.020	0.020	0.019	0.019	0.019	0.021	0.021	0.021	0.021	0.020	0.023	0.023	0.023	0.023	0.025	0.025	
Mn			0.176	0.166	0.163	0.163	0.154	0.154	0.154	0.165	0.165	0.166	0.166	0.168	0.144	0.144	0.144	0.144	0.177	0.177	
Mg			0.000	0.000	0.000	0.000	0.000	0.000	0.000	0.000	0.000	0.000	0.000	0.001	0.000	0.000	0.000	0.000	0.006	0.006	
Ca																					

Abbreviations same as Table A2.3. Population relates to either host crystals or size groups for groundmass oxides: large ~ 100 μ m; mid ~ 50 μ m; small ~ 10 μ m. Cation proportions calculated using Lepage (2003).

Table A2.7 EMPA data for Fe-Ti oxides.

Sample ID	Zone	Kaupokonui M13_2		Kaupokonui M14_1		Kaupokonui M14_2		Kaupokonui M15_1		Kaupokonui M15_2		Kaupokonui M15_3		Kaupokonui M16_1		Kaupokonui M17_1		Kaupokonui M19	
		core	cpx	core	cpx	core	cpx	core	cpx	core	cpx	core	cpx	core	plag	core	amph	core	amph
	popn/host																		
	SiO ₂	0.07	0.08	0.07	0.06	0.07	0.06	0.07	0.06	0.07	0.07	0.07	0.07	0.05	0.12	0.08	0.12	0.08	0.08
	TiO ₂	6.03	6.27	6.09	6.26	6.09	6.26	6.24	6.24	6.24	6.24	6.36	6.53	6.53	5.92	6.01	5.92	6.01	6.01
	Al ₂ O ₃	3.50	3.16	3.38	3.12	3.38	3.12	3.08	3.08	3.08	3.04	3.04	3.05	3.05	3.58	3.33	3.58	3.33	3.33
	Fe ₂ O ₃	55.89	55.08	54.69	55.45	54.69	55.45	54.84	54.84	54.84	55.21	55.21	55.64	55.64	54.32	53.90	54.32	53.90	53.90
	FeO	32.24	32.38	31.85	32.70	31.85	32.70	32.12	32.12	32.12	32.64	32.64	33.38	33.38	31.16	30.84	31.16	30.84	30.84
	MnO	0.66	0.71	0.64	0.68	0.64	0.68	0.67	0.67	0.67	0.76	0.76	0.75	0.75	0.63	0.66	0.63	0.66	0.66
	MgO	3.23	3.06	3.18	2.92	3.18	2.92	3.04	3.04	3.04	2.93	2.93	2.79	2.79	3.15	2.99	3.15	2.99	2.99
	CaO	0.02	0.00	0.03	0.00	0.03	0.00	0.08	0.08	0.08	0.05	0.05	0.00	0.00	0.39	0.64	0.39	0.64	0.64
	Cr ₂ O ₃	0.13	0.17	0.16	0.15	0.16	0.15	0.14	0.14	0.14	0.20	0.20	0.12	0.12	0.04	0.12	0.04	0.12	0.12
	Total	101.76	100.91	100.09	101.33	100.09	101.33	100.29	100.29	100.29	101.25	101.25	102.32	102.32	99.32	98.57	99.32	98.57	98.57
	Ti#	6.17	6.44	6.33	6.38	6.33	6.38	6.45	6.45	6.45	6.50	6.50	6.58	6.58	6.23	6.37	6.23	6.37	6.37
	Xusp	0.17	0.17	0.17	0.17	0.17	0.17	0.17	0.17	0.17	0.17	0.17	0.18	0.18	0.16	0.17	0.16	0.17	0.17
	Cations																		
	Si	0.002	0.003	0.003	0.002	0.003	0.002	0.003	0.002	0.003	0.002	0.002	0.002	0.002	0.004	0.003	0.004	0.003	0.003
	Ti	0.164	0.172	0.168	0.171	0.168	0.171	0.172	0.171	0.172	0.174	0.174	0.177	0.177	0.164	0.168	0.164	0.168	0.168
	Al	0.149	0.136	0.146	0.133	0.146	0.133	0.133	0.133	0.133	0.130	0.130	0.130	0.130	0.156	0.146	0.156	0.146	0.146
	Cr	0.004	0.005	0.005	0.004	0.005	0.004	0.004	0.004	0.004	0.006	0.006	0.004	0.004	0.001	0.003	0.001	0.003	0.003
	Fe ⁺³	1.516	1.510	1.508	1.516	1.508	1.516	1.513	1.513	1.513	1.511	1.511	1.509	1.509	1.506	1.508	1.506	1.508	1.508
	Fe ⁺²	0.972	0.987	0.976	0.994	0.976	0.994	0.985	0.985	0.985	0.993	0.993	1.006	1.006	0.960	0.959	0.960	0.959	0.959
	Mn	0.020	0.022	0.020	0.021	0.020	0.021	0.021	0.021	0.021	0.023	0.023	0.023	0.023	0.020	0.021	0.020	0.021	0.021
	Mg	0.173	0.166	0.174	0.158	0.174	0.158	0.166	0.166	0.166	0.159	0.159	0.150	0.150	0.173	0.166	0.173	0.166	0.166
	Ca	0.001	0.000	0.001	0.000	0.001	0.000	0.003	0.003	0.003	0.002	0.002	0.000	0.000	0.015	0.026	0.015	0.026	0.026

Abbreviations same as Table A2.3. Population relates to either host crystals or size groups for groundmass oxides: large ~ 100 μm; mid ~ 50 μm; small ~ 10 μm. Cation proportions calculated using LePage (2003).

Table A2.7 EMPA data for Fe-Ti oxides.

Sample ID	Zone	popn/host	Kaupokonui M20	Kaupokonui M21_1	Kaupokonui M21_2	Kaupokonui M22_1	Kaupokonui M22_2	Kaupokonui M23	Kaupokonui M24	SM-6C M1_1	SM-6C M1_2	SM-6C M1_3
			core large	core large	core large	core mid	core small	core small	core small	core large	core small	core small
	SiO ₂		0.06	0.05	0.03	0.04	0.09	0.11	0.09	0.08	0.09	0.08
	TiO ₂		6.09	6.29	6.25	6.16	6.03	5.90	5.94	9.11	8.78	8.82
	Al ₂ O ₃		3.39	3.01	3.15	3.22	3.25	3.40	3.35	3.57	3.84	3.68
	Fe ₂ O ₃		55.85	55.93	55.55	56.02	55.20	55.70	55.38	0.14	0.10	0.13
	FeO		32.63	32.90	32.71	32.41	32.10	32.07	32.29	49.57	48.78	48.99
	MnO		0.68	0.75	0.70	0.77	0.77	0.67	0.67	34.34	33.61	33.59
	MgO		3.02	2.89	2.91	3.10	3.01	3.16	2.96	0.66	0.62	0.62
	CaO		0.00	0.00	0.00	0.00	0.00	0.00	0.00	3.60	3.61	3.63
	Cr ₂ O ₃		0.14	0.16	0.17	0.16	0.14	0.12	0.11	0.03	0.03	0.06
	Total		101.87	101.99	101.48	101.86	100.58	101.13	100.79	101.10	99.45	99.59
	Ti#		6.20	6.37	6.37	6.27	6.22	6.06	6.11	9.40	9.25	9.27
	Xusp		0.17	0.17	0.17	0.17	0.17	0.16	0.17	0.25	0.25	0.25
Cations												
	Si		0.002	0.002	0.001	0.001	0.003	0.004	0.003	0.003	0.003	0.003
	Ti		0.165	0.171	0.171	0.167	0.166	0.161	0.163	0.247	0.242	0.242
	Al		0.144	0.128	0.135	0.137	0.140	0.145	0.144	0.151	0.165	0.158
	Cr		0.004	0.004	0.005	0.005	0.004	0.004	0.003	0.004	0.003	0.004
	Fe ⁺³		1.517	1.521	1.517	1.522	1.518	1.521	1.520	1.345	1.342	1.347
	Fe ⁺²		0.985	0.994	0.993	0.978	0.981	0.973	0.985	1.035	1.028	1.026
	Mn		0.021	0.023	0.022	0.024	0.024	0.020	0.021	0.020	0.019	0.019
	Mg		0.162	0.156	0.157	0.167	0.164	0.171	0.161	0.193	0.197	0.198
	Ca		0.000	0.000	0.000	0.000	0.000	0.000	0.000	0.001	0.001	0.002

Abbreviations same as Table A2.3. Population relates to either host crystals or size groups for groundmass oxides: large ~ 100 μm; mid ~ 50 μm; small ~ 10 μm. Cation proportions calculated using Lepage (2003).

Table A2.7 EMPA data for Fe-Ti oxides.

Sample ID	Zone	popn/host	SM-6C M2	SM-6C M3_1	SM-6C M3_2	SM-6C M4	SM-6C M5_1	SM-6C M5_2	SM-6C M5_3	SM-6C M5_4	SM-6C M6	SM-6C M7	SM-6C M8	SM-6C M9_1	SM-6C M9_2
			core large	core large	core mid	core large	core large	core large	core large	rim large	core mid	core small	core small	core small	core small
SiO ₂			0.06	0.05	0.08	0.19	0.05	0.07	0.09	0.09	0.07	0.11	0.12	0.08	0.09
TiO ₂			9.14	9.19	9.13	9.22	6.46	6.40	6.43	6.39	9.11	9.23	5.21	8.89	8.35
Al ₂ O ₃			3.60	3.72	3.69	3.75	5.16	5.33	5.45	5.32	3.70	3.51	5.24	3.69	3.62
Fe ₂ O ₃			0.13	0.12	0.18	0.16	0.17	0.16	0.10	0.13	0.15	0.14	0.14	0.15	0.15
FeO			48.70	48.99	48.44	47.68	52.37	51.95	52.21	51.65	49.37	48.06	53.81	48.92	49.86
MnO			34.16	34.36	34.02	32.44	32.48	32.26	32.56	32.40	34.50	34.13	30.02	33.83	32.68
MgO			0.67	0.69	0.63	0.65	0.42	0.48	0.47	0.38	0.63	0.62	0.43	0.64	0.60
CaO			3.41	3.54	3.60	3.36	3.44	3.44	3.44	3.35	3.54	3.50	4.00	3.58	3.89
Cr ₂ O ₃			0.13	0.00	0.01	1.64	0.00	0.00	0.00	0.00	0.00	0.01	0.05	0.01	0.05
Total			100.00	100.65	99.78	99.09	100.55	100.09	100.74	99.71	101.09	99.31	99.02	99.79	99.28
Ti#			9.54	9.53	9.57	9.91	6.81	6.79	6.78	6.79	9.41	9.69	5.64	9.32	8.83
Xusp			0.26	0.26	0.26	0.26	0.19	0.19	0.19	0.19	0.26	0.26	0.15	0.25	0.23
Cations															
Si			0.002	0.002	0.003	0.007	0.002	0.002	0.003	0.003	0.003	0.004	0.004	0.003	0.003
Ti			0.251	0.250	0.250	0.254	0.175	0.174	0.174	0.175	0.247	0.255	0.143	0.244	0.230
Al			0.155	0.159	0.159	0.162	0.219	0.227	0.231	0.228	0.157	0.152	0.225	0.159	0.156
Cr			0.004	0.003	0.005	0.004	0.005	0.005	0.003	0.004	0.004	0.004	0.004	0.004	0.004
Fe ⁺³			1.336	1.334	1.330	1.313	1.421	1.415	1.412	1.413	1.339	1.327	1.476	1.343	1.373
Fe ⁺²			1.042	1.040	1.038	0.993	0.980	0.976	0.979	0.985	1.040	1.047	0.915	1.032	1.000
Mn			0.021	0.021	0.019	0.020	0.013	0.015	0.014	0.012	0.019	0.019	0.013	0.020	0.019
Mg			0.186	0.191	0.196	0.183	0.185	0.186	0.184	0.182	0.190	0.192	0.217	0.195	0.212
Ca			0.005	0.000	0.000	0.064	0.000	0.000	0.000	0.000	0.000	0.000	0.002	0.000	0.002

Abbreviations same as Table A2.3. Population relates to either host crystals or size groups for groundmass oxides: large ~ 100 μm; mid ~ 50 μm; small ~ 10 μm. Cation proportions calculated using Lepage (2003).

Table A2.7 EMPA data for Fe-Ti oxides.

Sample ID	Zone	popn/host	SM-6C M9_3		SM-6C M10		SM-6C M11		SM-6C M12_1		SM-6C M13_1		SM-6C M13_2		SM-6C M13_3		SM-6C M13_4		SM-6C M13_5		SM-6C M14		SM-6C M15_1		SM-6C M15_2		SM-6C M15_3			
			core small	core small	core small	core mid	core amph	core amph	core amph	core amph	core amph	core cpx	core cpx	core amph	core amph	core cpx	core amph	core amph	core cpx	core amph	core cpx	core rim	core rim	core rim	core rim	core rim	core rim	core rim	core rim	core rim
SiO ₂			0.13	0.08	0.16	0.06	0.07	0.07	0.14	0.12	0.07	0.07	0.07	0.08	0.08	0.12	0.07	0.07	0.08	0.08	0.09	0.09	0.09	0.09	0.09	0.09	0.08	0.08	0.10	
TiO ₂			7.96	8.98	5.89	9.63	6.80	6.80	6.54	6.34	6.80	6.80	6.54	9.09	9.09	6.34	8.95	8.95	9.09	9.09	9.09	6.14	6.14	6.14	9.32	9.32	9.02	9.02	9.20	
Al ₂ O ₃			3.70	3.78	4.65	2.98	5.17	5.17	4.60	4.83	5.17	5.17	4.60	3.69	3.69	4.83	3.73	3.73	3.69	3.69	3.69	5.71	5.71	5.71	3.36	3.36	3.39	3.39	3.29	
Fe ₂ O ₃			0.16	0.14	0.11	0.17	0.24	0.24	0.10	0.12	0.24	0.24	0.10	0.09	0.09	0.12	0.16	0.16	0.09	0.09	0.09	0.20	0.20	0.20	0.13	0.13	0.13	0.13	0.12	
FeO			50.05	48.84	52.61	47.94	51.14	51.14	51.94	51.64	51.14	51.14	51.94	48.96	48.96	51.64	48.79	48.79	48.96	48.96	48.96	51.74	51.74	51.74	47.91	47.91	47.66	47.66	48.07	
MnO			32.11	33.99	30.48	35.29	32.27	32.27	31.72	31.11	32.27	32.27	31.72	33.60	33.60	31.11	33.47	33.47	33.60	33.60	33.60	31.45	31.45	31.45	33.70	33.70	33.32	33.32	33.69	
MgO			0.53	0.61	0.44	0.68	0.40	0.40	0.61	0.52	0.40	0.40	0.61	0.65	0.65	0.52	0.62	0.62	0.65	0.65	0.65	0.40	0.40	0.40	0.69	0.69	0.73	0.73	0.77	
CaO			3.98	3.60	3.91	2.92	3.63	3.63	3.33	3.50	3.63	3.63	3.33	3.91	3.91	3.50	3.81	3.81	3.91	3.91	3.91	3.82	3.82	3.82	3.69	3.69	3.49	3.49	3.55	
Cr ₂ O ₃			0.06	0.01	0.05	0.02	0.00	0.00	0.37	0.38	0.00	0.00	0.37	0.00	0.00	0.38	0.03	0.03	0.00	0.00	0.00	0.00	0.00	0.00	0.00	0.02	0.02	0.00	0.00	
Total			98.69	100.02	98.31	99.70	99.72	99.72	99.36	98.56	99.72	99.72	99.36	100.06	100.06	98.56	99.61	99.61	100.06	100.06	99.56	99.56	99.56	99.56	98.90	98.90	97.84	97.84	98.78	
Ti#			8.49	9.39	6.37	9.94	7.25	7.25	6.97	6.85	7.25	7.25	6.97	9.53	9.53	6.85	9.43	9.43	9.53	9.53	6.62	6.62	6.62	9.84	9.84	9.63	9.63	9.71		
Xusp			0.22	0.26	0.17	0.27	0.20	0.20	0.19	0.19	0.20	0.20	0.25	0.25	0.19	0.25	0.25	0.25	0.25	0.25	0.19	0.19	0.19	0.26	0.26	0.26	0.26	0.26	0.26	
Cations																														
Si			0.005	0.003	0.006	0.002	0.002	0.002	0.005	0.004	0.002	0.002	0.003	0.003	0.004	0.002	0.002	0.002	0.003	0.003	0.003	0.003	0.003	0.003	0.003	0.003	0.003	0.003	0.004	0.004
Ti			0.220	0.246	0.163	0.267	0.186	0.186	0.180	0.175	0.186	0.186	0.180	0.248	0.248	0.175	0.246	0.246	0.248	0.248	0.167	0.167	0.167	0.258	0.258	0.253	0.253	0.256	0.256	
Al			0.160	0.162	0.202	0.129	0.221	0.221	0.198	0.209	0.221	0.221	0.198	0.158	0.158	0.209	0.160	0.160	0.158	0.158	0.243	0.243	0.243	0.146	0.146	0.149	0.149	0.143	0.143	
Cr			0.005	0.004	0.003	0.005	0.007	0.007	0.003	0.004	0.007	0.007	0.003	0.003	0.003	0.004	0.004	0.004	0.003	0.003	0.006	0.006	0.006	0.004	0.004	0.004	0.004	0.003	0.003	
Fe ⁺³			1.385	1.337	1.457	1.328	1.396	1.396	1.429	1.428	1.396	1.396	1.429	1.337	1.337	1.428	1.339	1.339	1.337	1.337	1.409	1.409	1.409	1.327	1.327	1.336	1.336	1.335	1.335	
Fe ⁺²			0.988	1.034	0.938	1.087	0.979	0.979	0.970	0.956	0.979	0.979	0.970	1.020	1.020	0.956	1.021	1.021	1.020	1.020	0.952	0.952	0.952	1.037	1.037	1.038	1.038	1.040	1.040	
Mn			0.017	0.019	0.014	0.021	0.012	0.012	0.019	0.016	0.012	0.012	0.019	0.020	0.020	0.016	0.019	0.019	0.020	0.020	0.012	0.012	0.012	0.022	0.022	0.023	0.023	0.024	0.024	
Mg			0.218	0.195	0.215	0.160	0.196	0.196	0.182	0.192	0.196	0.182	0.182	0.211	0.211	0.192	0.207	0.207	0.211	0.211	0.206	0.206	0.206	0.203	0.203	0.194	0.194	0.195	0.195	
Ca			0.002	0.000	0.002	0.001	0.000	0.000	0.015	0.015	0.000	0.000	0.015	0.000	0.000	0.015	0.001	0.001	0.000	0.000	0.000	0.000	0.000	0.000	0.000	0.001	0.001	0.000	0.000	

Abbreviations same as Table A2.3. Population relates to either host crystals or size groups for groundmass oxides: large ~ 100 μm; mid ~ 50 μm; small ~ 10 μm. Cation proportions calculated using Lepage (2003).

Table A2.7 EMPA data for Fe-Ti oxides.

Sample ID	SM-6C M15_4		SM-6C M15_5		SM-6C M16_1		SM-6C M16_2		Maketawa M1_1		Maketawa M2_1		Maketawa M2_2		Maketawa M3		Maketawa M4_1		Maketawa M4_2		Maketawa M4_3		
	core	cpx	core	cpx	core	cpx	rim	mid	core	large	core	large	core	large	core	mid	core	large	core	mid	core	mid	
Zone																							
popn/host																							
SiO ₂	0.08	0.07	0.07	0.12	0.09	0.12	0.12	0.12	0.12	0.05	0.05	0.08	0.08	0.07	0.07	0.03	0.03	0.03	0.03	0.07	0.07	0.05	
TiO ₂	9.18	8.75	8.75	8.03	8.95	6.18	6.18	6.18	6.18	6.39	6.39	6.46	6.46	6.43	6.43	6.48	6.48	6.48	6.48	6.36	6.36	6.45	
Al ₂ O ₃	3.39	3.32	3.32	3.52	3.68	2.79	2.79	2.79	2.79	2.80	2.80	2.81	2.81	2.87	2.87	2.92	2.92	2.92	2.92	2.91	2.91	2.95	
Fe ₂ O ₃	0.11	0.14	0.14	0.76	0.17	0.16	0.16	0.16	0.16	0.12	0.12	0.14	0.14	0.11	0.11	0.14	0.14	0.14	0.14	0.09	0.09	0.18	
FeO	47.77	48.55	48.55	49.20	47.91	53.87	53.87	53.87	53.87	54.98	54.98	54.25	54.25	54.14	54.14	54.93	54.93	54.93	54.93	53.90	53.90	54.29	
MnO	33.47	32.62	32.62	31.51	33.30	32.22	32.22	32.22	32.22	32.72	32.72	32.78	32.78	32.56	32.56	32.88	32.88	32.88	32.88	32.39	32.39	32.75	
MgO	0.73	0.67	0.67	0.61	0.63	0.78	0.78	0.78	0.78	0.83	0.83	0.82	0.82	0.84	0.84	0.89	0.89	0.89	0.89	0.81	0.81	0.82	
CaO	3.53	3.76	3.76	4.21	3.52	2.61	2.61	2.61	2.61	2.71	2.71	2.61	2.61	2.67	2.67	2.68	2.68	2.68	2.68	2.60	2.60	2.65	
Cr ₂ O ₃	0.10	0.12	0.12	0.05	0.27	0.01	0.01	0.01	0.01	0.00	0.00	0.00	0.00	0.00	0.00	0.00	0.00	0.00	0.08	0.08	0.00		
Total	98.36	97.99	97.99	98.02	98.52	98.74	98.74	98.74	98.74	100.60	100.60	99.94	99.94	99.68	99.68	100.94	100.94	100.94	100.94	99.20	99.20	100.14	
Ti#	9.75	9.35	9.35	8.71	9.54	6.45	6.45	6.45	6.45	6.54	6.54	6.65	6.65	6.64	6.64	6.61	6.61	6.61	6.61	6.61	6.61	6.63	
Xusp	0.26	0.25	0.25	0.23	0.26	0.18	0.18	0.18	0.18	0.18	0.18	0.18	0.18	0.18	0.18	0.18	0.18	0.18	0.18	0.18	0.18	0.18	
Cations																							
Si	0.003	0.003	0.003	0.004	0.003	0.004	0.004	0.004	0.004	0.002	0.002	0.003	0.003	0.003	0.003	0.001	0.001	0.001	0.001	0.002	0.002	0.002	
Ti	0.256	0.244	0.244	0.223	0.249	0.174	0.174	0.174	0.174	0.176	0.176	0.180	0.180	0.179	0.179	0.178	0.178	0.178	0.178	0.178	0.178	0.179	
Al	0.148	0.145	0.145	0.153	0.160	0.123	0.123	0.123	0.123	0.121	0.121	0.122	0.122	0.125	0.125	0.126	0.126	0.126	0.126	0.128	0.128	0.128	
Cr	0.003	0.004	0.004	0.022	0.005	0.005	0.005	0.005	0.005	0.004	0.004	0.004	0.004	0.003	0.003	0.004	0.004	0.004	0.004	0.003	0.003	0.005	
Fe ⁺³	1.331	1.357	1.357	1.369	1.331	1.516	1.516	1.516	1.516	1.519	1.519	1.509	1.509	1.508	1.508	1.512	1.512	1.512	1.512	1.509	1.509	1.506	
Fe ⁺²	1.037	1.013	1.013	0.974	1.028	1.008	1.008	1.008	1.008	1.004	1.004	1.013	1.013	1.008	1.008	1.006	1.006	1.006	1.006	1.008	1.008	1.009	
Mn	0.023	0.021	0.021	0.019	0.020	0.025	0.025	0.025	0.025	0.026	0.026	0.026	0.026	0.026	0.026	0.028	0.028	0.028	0.028	0.025	0.025	0.025	
Mg	0.195	0.208	0.208	0.232	0.194	0.146	0.146	0.146	0.146	0.148	0.148	0.144	0.144	0.147	0.147	0.146	0.146	0.146	0.146	0.144	0.144	0.146	
Ca	0.004	0.005	0.005	0.002	0.011	0.000	0.000	0.000	0.000	0.000	0.000	0.000	0.000	0.000	0.000	0.000	0.000	0.000	0.003	0.003	0.000	0.000	

Abbreviations same as Table A2.3. Population relates to either host crystals or size groups for groundmass oxides: large ~ 100 μm; mid ~ 50 μm; small ~ 10 μm. Cation proportions calculated using Lepage (2003).

Table A2.7 EMPA data for Fe-Ti oxides.

Sample ID	Maketawa M4_4		M5_1		M5_2		M6		M7_1		M7_2		M7_3		M7_4		M7_5		M7_6		
	Zone	popn/host	core small	core mid	core mid	core mid	core large	core mid	core mid	core mid	core small	core mid	core small	core mid	core mid	core mid	core mid	core mid	core small	core small	
SiO ₂	0.25		0.26	0.05	0.05	0.05	0.05	0.07	0.13	0.11	0.13	0.11	0.09	0.09	0.09	0.09	0.09	0.09	0.08	0.08	
TiO ₂	6.01		6.47	6.45	6.45	6.35	6.42	5.06	5.06	5.05	5.06	5.05	6.55	6.55	6.55	6.55	6.55	6.55	6.33	6.33	
Al ₂ O ₃	2.71		2.83	2.86	2.86	2.88	3.06	4.75	4.75	5.26	4.75	5.26	3.05	3.05	3.05	3.05	3.05	3.05	3.03	3.03	
Fe ₂ O ₃	0.10		0.14	0.14	0.14	0.13	0.18	0.14	0.14	0.13	0.14	0.13	0.17	0.17	0.17	0.17	0.17	0.17	0.15	0.15	
FeO	45.94		52.78	54.00	54.00	54.37	54.25	54.08	54.08	54.36	54.08	54.36	53.87	53.87	53.87	53.87	53.87	53.87	54.52	54.52	
MnO	29.10		32.44	32.81	32.81	32.34	32.47	30.78	30.78	31.09	30.78	31.09	32.62	32.62	32.62	32.62	32.62	32.62	32.50	32.50	
MgO	0.65		0.79	0.76	0.76	0.72	0.84	0.39	0.39	0.41	0.39	0.41	0.76	0.76	0.76	0.76	0.76	0.76	0.79	0.79	
CaO	2.05		2.59	2.54	2.54	2.82	2.82	3.25	3.25	3.33	3.25	3.33	2.83	2.83	2.83	2.83	2.83	2.83	2.80	2.80	
Cr ₂ O ₃	0.50		0.16	0.00	0.00	0.00	0.00	0.16	0.16	0.11	0.16	0.11	0.02	0.02	0.02	0.02	0.02	0.02	0.01	0.01	
Total	87.30		98.45	99.61	99.61	99.67	100.10	98.74	98.74	99.86	98.74	99.86	99.97	99.97	99.97	99.97	99.97	99.97	100.20	100.20	
Ti#	7.13		6.79	6.65	6.65	6.56	6.63	5.42	5.42	5.38	5.42	5.38	6.78	6.78	6.78	6.78	6.78	6.78	6.52	6.52	
Xusp	0.20		0.19	0.18	0.18	0.18	0.18	0.18	0.15	0.15	0.15	0.15	0.18	0.18	0.18	0.18	0.18	0.24	0.18	0.18	
Cations																					
Si	0.011		0.010	0.002	0.002	0.002	0.002	0.002	0.005	0.004	0.005	0.004	0.003	0.003	0.003	0.003	0.003	0.003	0.003	0.003	
Ti	0.191		0.182	0.180	0.180	0.177	0.178	0.140	0.140	0.138	0.140	0.138	0.182	0.182	0.182	0.182	0.182	0.179	0.175	0.175	
Al	0.135		0.125	0.125	0.125	0.126	0.133	0.206	0.206	0.225	0.206	0.225	0.132	0.132	0.132	0.132	0.134	0.134	0.131	0.131	
Cr	0.003		0.004	0.004	0.004	0.004	0.005	0.004	0.004	0.004	0.004	0.004	0.005	0.005	0.005	0.005	0.003	0.003	0.004	0.004	
Fe ⁺³	1.459		1.487	1.507	1.507	1.513	1.502	1.499	1.499	1.487	1.499	1.487	1.493	1.493	1.493	1.493	1.499	1.499	1.509	1.509	
Fe ⁺²	1.027		1.016	1.018	1.018	1.000	0.999	0.948	0.948	0.945	0.948	0.945	1.005	1.005	1.005	1.005	1.060	1.060	0.999	0.999	
Mn	0.023		0.025	0.024	0.024	0.022	0.026	0.012	0.012	0.013	0.012	0.013	0.024	0.024	0.024	0.024	0.020	0.020	0.025	0.025	
Mg	0.129		0.145	0.140	0.140	0.156	0.155	0.179	0.179	0.180	0.179	0.180	0.156	0.156	0.156	0.156	0.114	0.114	0.154	0.154	
Ca	0.022		0.006	0.000	0.000	0.000	0.000	0.006	0.006	0.004	0.006	0.004	0.001	0.001	0.001	0.001	0.263	0.263	0.000	0.000	

Abbreviations same as Table A2.3. Population relates to either host crystals or size groups for groundmass oxides: large ~ 100 μm; mid ~ 50 μm; small ~ 10 μm. Cation proportions calculated using Lepage (2003).

Table A2.7 EMPA data for Fe-Ti oxides.

Sample ID	Maketawa M8_1	Maketawa M8_2	Maketawa M9	Maketawa M10_1	Maketawa M10_2	Maketawa M10_3	Maketawa M11	Maketawa M12	Maketawa M13_1	Maketawa M14
Zone	core small	core small	core small	core small	core small	core small	core small	core small	core amph	core amph
popn/host	small	small	small	small	small	small	small	small	amph	amph
SiO ₂	0.06	1.22	0.10	0.07	0.08	0.05	0.07	0.06	0.24	0.10
TiO ₂	6.27	5.90	7.63	6.31	6.37	6.40	6.51	6.20	6.00	6.24
Al ₂ O ₃	2.90	2.77	1.55	2.85	2.86	2.94	3.10	3.02	2.83	2.79
Fe ₂ O ₃	0.11	0.09	0.12	0.15	0.18	0.15	0.25	0.11	0.14	0.11
FeO	54.34	51.43	52.41	54.62	54.53	54.54	53.84	53.17	52.59	54.88
MnO	32.24	31.35	34.43	32.50	32.56	32.62	31.83	31.46	31.52	32.38
MgO	0.91	0.73	1.56	0.82	0.90	0.83	0.72	0.77	0.77	0.77
CaO	2.66	2.58	1.50	2.71	2.70	2.72	3.27	2.88	2.25	2.74
Cr ₂ O ₃	0.05	1.55	0.00	0.00	0.00	0.00	0.00	0.01	0.61	0.09
Total	99.54	97.61	99.29	100.02	100.18	100.25	99.60	97.70	96.96	100.09
Ti#	6.50	6.40	7.76	6.50	6.56	6.58	6.79	6.57	6.41	6.42
Xusp	0.18	0.17	0.21	0.18	0.18	0.18	0.18	0.18	0.17	0.17
Cations										
Si	0.002	0.046	0.004	0.002	0.003	0.002	0.003	0.002	0.009	0.004
Ti	0.175	0.166	0.216	0.175	0.177	0.177	0.180	0.176	0.172	0.173
Al	0.127	0.122	0.069	0.124	0.124	0.127	0.135	0.134	0.127	0.121
Cr	0.003	0.003	0.004	0.004	0.005	0.004	0.007	0.003	0.004	0.003
Fe ⁺³	1.516	1.451	1.487	1.517	1.511	1.510	1.492	1.507	1.507	1.522
Fe ⁺²	1.000	0.983	1.086	1.003	1.003	1.004	0.980	0.991	1.003	0.998
Mn	0.029	0.023	0.050	0.026	0.028	0.026	0.023	0.025	0.025	0.024
Mg	0.147	0.144	0.084	0.149	0.149	0.149	0.180	0.162	0.128	0.150
Ca	0.002	0.062	0.000	0.000	0.000	0.000	0.000	0.001	0.025	0.004

Abbreviations same as Table A2.3. Population relates to either host crystals or size groups for groundmass oxides: large ~ 100 μm; mid ~ 50 μm; small ~ 10 μm. Cation proportions calculated using Lepage (2003).

Table A2.7 EMPA data for Fe-Ti oxides.

Sample ID	Maketawa M15_1		Maketawa M15_2		Maketawa M15_3		Maketawa M16_1		Maketawa M17_1		Maketawa M17_3		Ingleswood b M1		Ingleswood b M2_1		Ingleswood b M2_3		Ingleswood b M3_1		
	Zone	core	cpx	core	cpx	core	cpx	core	cpx	core	cpx	core	small	core	mid	core	mid	core	large		
popn/host																					
SiO ₂		0.06	0.06	0.06	0.09	0.09	0.09	0.09	0.06	0.16	0.16	0.07	0.07	0.03	0.03	0.03	0.03	0.02	0.02	0.02	
TiO ₂		6.39	6.16	6.22	6.22	6.22	6.26	6.42	6.42	6.08	6.08	7.20	7.20	7.24	7.24	7.24	7.24	7.27	7.27	7.27	
Al ₂ O ₃		2.85	2.84	2.94	2.94	2.94	3.36	2.93	2.93	3.41	3.41	2.01	2.01	1.93	1.93	1.93	1.93	1.99	1.99	1.99	
Fe ₂ O ₃		0.15	0.12	0.15	0.15	0.15	0.17	0.12	0.12	0.09	0.09	53.48	53.48	51.37	51.37	51.37	51.37	54.13	54.13	54.13	
FeO		54.77	54.47	54.78	54.78	54.78	50.71	53.84	53.84	53.94	53.94	33.95	33.95	32.97	32.97	32.97	32.97	34.19	34.19	34.19	
MnO		32.60	31.98	32.37	32.37	32.37	29.50	32.26	32.26	32.25	32.25	1.26	1.26	1.20	1.20	1.20	1.20	1.28	1.28	1.28	
MgO		0.79	0.78	0.79	0.79	0.79	0.65	0.77	0.77	0.78	0.78	1.90	1.90	1.90	1.90	1.90	1.90	1.90	1.90	1.90	
CaO		2.76	2.72	2.74	2.74	2.74	3.21	2.77	2.77	2.74	2.74	0.00	0.00	0.00	0.00	0.00	0.00	0.00	0.00	0.00	
Cr ₂ O ₃		0.03	0.13	0.10	0.10	0.10	0.66	0.04	0.04	0.08	0.08	99.87	99.87	96.65	96.65	96.65	96.65	100.77	100.77	100.77	
Total		100.39	99.26	100.18	100.18	100.18	94.59	99.21	99.21	99.52	99.52	7.31	7.31	7.60	7.60	7.60	7.60	7.31	7.31	7.31	
Ti#		6.56	6.40	6.41	6.41	6.41	6.97	6.68	6.68	6.34	6.34	0.20	0.20	0.21	0.21	0.21	0.21	0.20	0.20	0.20	
Xusp		0.18	0.17	0.17	0.17	0.17	0.18	0.18	0.18	0.17	0.17										
Cations																					
Si		0.002	0.002	0.003	0.003	0.003	0.003	0.002	0.002	0.006	0.006	0.003	0.003	0.001	0.001	0.001	0.001	0.001	0.001	0.001	
Ti		0.177	0.172	0.172	0.172	0.172	0.182	0.180	0.180	0.169	0.169	0.202	0.202	0.210	0.210	0.210	0.210	0.202	0.202	0.202	
Al		0.123	0.125	0.127	0.127	0.127	0.153	0.128	0.128	0.149	0.149	0.088	0.088	0.088	0.081	0.081	0.088	0.087	0.087	0.087	
Cr		0.004	0.003	0.004	0.004	0.004	0.005	0.003	0.003	0.003	0.003	1.502	1.502	1.490	1.491	1.491	1.490	1.507	1.507	1.507	
Fe ⁺³		1.515	1.523	1.517	1.517	1.517	1.472	1.505	1.505	1.499	1.499	1.059	1.059	1.063	1.077	1.077	1.063	1.058	1.058	1.058	
Fe ⁺²		1.002	0.994	0.996	0.996	0.996	0.952	1.002	1.002	0.996	0.996	0.040	0.040	0.039	0.036	0.036	0.039	0.040	0.040	0.040	
Mn		0.025	0.025	0.025	0.025	0.025	0.021	0.024	0.024	0.024	0.024	0.106	0.106	0.109	0.102	0.102	0.109	0.105	0.105	0.105	
Mg		0.151	0.151	0.150	0.150	0.150	0.185	0.153	0.153	0.151	0.151	0.000	0.000	0.000	0.000	0.000	0.000	0.000	0.000	0.000	
Ca		0.001	0.005	0.004	0.004	0.004	0.027	0.002	0.002	0.003	0.003										

Abbreviations same as Table A2.3. Population relates to either host crystals or size groups for groundmass oxides: large ~ 100 μm; mid ~ 50 μm; small ~ 10 μm. Cation proportions calculated using Lepage (2003).

Table A2.7 EMPA data for Fe-Ti oxides.

Sample ID	Inglewood b	Inglewood b	Inglewood b	Inglewood b	Inglewood b	Inglewood b	Inglewood b	Inglewood b	Inglewood b	Inglewood b	Inglewood b	Inglewood b
Zone	M3_2	M3_3	M4_1	M4_2	M4_3	M4_4	M4_5	M5_1	M5_2			
popn/host	rim large	core large	core large	rim large	core large	core large	rim large	core large	rim large	core large	rim large	
SiO ₂	0.04	0.07	0.02	0.02	0.04	0.05	0.07	0.26	0.02	0.26	0.07	0.02
TiO ₂	7.30	7.19	7.41	7.26	7.13	7.42	7.23	6.99	7.34	6.99	7.23	7.34
Al ₂ O ₃	1.83	1.97	2.07	1.96	1.98	1.96	1.96	2.08	2.10	2.08	1.96	2.10
Fe ₂ O ₃												
FeO	53.98	54.02	53.42	53.25	53.91	53.79	54.11	53.70	53.71	53.70	54.11	53.71
MnO	33.93	33.87	34.28	34.19	33.78	34.30	33.93	33.88	34.19	33.88	33.93	34.19
MgO	1.42	1.43	1.22	1.09	1.35	1.38	1.37	1.18	1.32	1.18	1.37	1.32
CaO	1.93	1.94	1.89	1.76	1.92	1.87	2.00	2.09	1.90	2.09	2.00	1.90
Cr ₂ O ₃	0.00	0.02	0.00	0.00	0.00	0.01	0.01	0.00	0.00	0.00	0.01	0.00
Total	100.43	100.50	100.31	99.52	100.10	100.78	100.67	100.18	100.58	100.18	100.67	100.58
Ti#	7.37	7.27	7.49	7.36	7.23	7.47	7.30	7.11	7.41	7.11	7.30	7.41
Xusp	0.20	0.20	0.21	0.20	0.20	0.20	0.20	0.19	0.20	0.19	0.20	0.20
Cations												
Si	0.002	0.003	0.001	0.001	0.001	0.002	0.002	0.009	0.001	0.009	0.002	0.001
Ti	0.204	0.201	0.207	0.205	0.200	0.206	0.201	0.195	0.205	0.195	0.201	0.205
Al	0.080	0.086	0.091	0.086	0.087	0.086	0.085	0.091	0.092	0.091	0.085	0.092
Cr												
Fe ⁺³	1.509	1.508	1.493	1.503	1.511	1.498	1.507	1.500	1.497	1.500	1.507	1.497
Fe ⁺²	1.054	1.050	1.065	1.072	1.052	1.061	1.050	1.052	1.059	1.052	1.050	1.059
Mn	0.045	0.045	0.038	0.035	0.042	0.043	0.043	0.037	0.041	0.037	0.043	0.041
Mg	0.107	0.107	0.104	0.098	0.107	0.103	0.110	0.116	0.105	0.116	0.110	0.105
Ca	0.000	0.001	0.000	0.000	0.000	0.000	0.000	0.000	0.000	0.000	0.000	0.000

Abbreviations same as Table A2.3. Population relates to either host crystals or size groups for groundmass oxides: large ~ 100 μm; mid ~ 50 μm; small ~ 10 μm. Cation proportions calculated using LePage (2003).

Table A2.7 EMPA data for Fe-Ti oxides.

Sample ID	Inglewood b		Inglewood b		Inglewood b		Inglewood b		Inglewood b		Inglewood b		Inglewood b		Inglewood b			
	M6	M7_2	M9	M10	M11	M12	M13	M14	M15	M6	M7_2	M9	M10	M11	M12	M13	M14	M15
Zone	core	core	core	core	core	core	core	core	core	core	core	core	core	core	core	core	core	core
popn/host	small	small	large	mid	mid	large	mid	large	mid	mid	large	mid	large	mid	large	mid	large	small
SiO ₂	0.08	0.06	0.03	0.06	0.05	0.03	0.08	0.06	0.08	0.03	0.06	0.08	0.06	0.08	0.03	0.08	0.06	0.08
TiO ₂	7.11	5.87	7.28	7.30	7.37	7.38	7.32	7.50	7.32	7.38	7.50	7.32	7.50	7.32	7.38	7.32	7.50	5.38
Al ₂ O ₃	2.01	2.54	2.09	2.18	2.06	1.98	2.04	2.03	2.04	1.98	2.03	2.04	2.03	2.04	1.98	2.04	2.03	4.08
Fe ₂ O ₃	53.42	54.80	53.68	52.91	53.29	53.04	52.50	52.81	52.50	53.04	52.81	52.50	52.81	52.50	53.04	52.50	52.81	54.24
MnO	33.50	32.31	34.18	34.21	34.48	34.09	33.87	34.59	33.87	34.09	34.59	33.87	34.59	33.87	34.09	33.87	34.59	32.53
MgO	1.31	1.13	1.25	1.28	1.26	1.24	1.33	1.27	1.33	1.24	1.27	1.33	1.27	1.33	1.24	1.33	1.27	0.83
CaO	2.03	2.05	1.89	1.79	1.73	1.85	1.81	1.68	1.81	1.85	1.68	1.81	1.68	1.81	1.85	1.81	1.68	2.15
Cr ₂ O ₃	0.00	0.04	0.00	0.00	0.00	0.00	0.00	0.01	0.00	0.00	0.00	0.00	0.01	0.00	0.00	0.00	0.01	0.00
Total	99.46	98.80	100.47	99.83	100.34	99.71	99.03	100.05	99.03	99.71	100.05	99.03	100.05	99.03	99.71	99.03	100.05	99.42
Ti#	7.27	6.08	7.35	7.43	7.44	7.51	7.51	7.59	7.51	7.51	7.59	7.51	7.59	7.51	7.51	7.51	7.59	5.62
Xusp	0.20	0.17	0.20	0.21	0.21	0.21	0.21	0.21	0.21	0.21	0.21	0.21	0.21	0.21	0.21	0.21	0.21	0.16
Cations																		
Si	0.003	0.002	0.001	0.002	0.002	0.001	0.002	0.002	0.002	0.002	0.001	0.002	0.002	0.002	0.001	0.002	0.002	0.003
Ti	0.200	0.166	0.203	0.205	0.206	0.208	0.207	0.210	0.207	0.208	0.208	0.207	0.210	0.206	0.208	0.207	0.210	0.150
Al	0.089	0.112	0.091	0.096	0.090	0.087	0.091	0.089	0.091	0.090	0.087	0.091	0.089	0.090	0.087	0.091	0.089	0.178
Cr			0.002	0.003	0.003	0.003	0.002	0.003	0.003	0.003	0.003	0.002	0.003	0.003	0.003	0.002	0.003	0.004
Fe ⁺³	1.505	1.551	1.498	1.486	1.491	1.493	1.487	1.482	1.487	1.493	1.482	1.487	1.482	1.491	1.493	1.487	1.482	1.512
Fe ⁺²	1.049	1.016	1.060	1.068	1.072	1.066	1.066	1.079	1.066	1.066	1.066	1.066	1.079	1.072	1.066	1.066	1.079	1.008
Mn	0.042	0.036	0.039	0.040	0.040	0.039	0.042	0.040	0.040	0.039	0.039	0.042	0.040	0.040	0.039	0.042	0.040	0.026
Mg	0.113	0.115	0.105	0.099	0.096	0.103	0.102	0.093	0.096	0.103	0.103	0.102	0.093	0.096	0.103	0.102	0.093	0.119
Ca	0.000	0.002	0.000	0.000	0.000	0.000	0.000	0.000	0.000	0.000	0.000	0.000	0.000	0.000	0.000	0.000	0.000	0.000

Abbreviations same as Table A2.3. Population relates to either host crystals or size groups for groundmass oxides: large ~ 100 μm; mid ~ 50 μm; small ~ 10 μm. Cation proportions calculated using LePage (2003).

Table A2.7 EMPA data for Fe-Ti oxides.

Sample ID	Inglewood b		Inglewood b		Inglewood b		Inglewood b		Inglewood b		Inglewood b		Inglewood b		
	M16	M17	M18_1	M18_2	M19	M20	M21_1	M22	M23	core	small	mid	core	amph	
Zone	core	core	core	core	core	core	core	core	core	core	core	core	core	core	
popn/host	small	small	mid	mid	mid	small	amph	amph	amph	amph	small	amph	amph	cpx	
SiO ₂	0.45	0.05	0.10	0.06	0.06	0.08	0.20	0.08	0.08	0.04	0.08	0.20	0.08	0.04	
TiO ₂	5.76	7.20	6.95	6.99	7.18	6.89	7.10	6.24	6.24	7.40	6.89	7.10	6.24	7.40	
Al ₂ O ₃	2.29	1.98	2.12	2.23	2.04	2.28	1.98	2.63	2.63	2.09	2.28	1.98	2.63	2.09	
Fe ₂ O ₃	0.05	0.08	0.14	0.06	0.11	0.08	0.11	0.10	0.10	0.11	0.08	0.11	0.10	0.11	
FeO	53.26	53.98	52.81	53.23	53.01	53.56	51.09	53.24	53.24	52.19	53.56	51.09	53.24	52.19	
MnO	31.65	34.07	33.25	33.47	33.65	33.43	31.84	32.57	32.57	33.75	33.43	31.84	32.57	33.75	
MgO	1.18	1.37	1.23	1.26	1.25	1.25	1.21	0.85	0.85	1.26	1.25	1.21	0.85	1.26	
CaO	2.03	1.86	2.00	1.98	1.96	2.04	1.98	1.98	1.98	1.88	2.04	1.98	1.98	1.88	
Cr ₂ O ₃	0.45	0.00	0.00	0.00	0.00	0.00	0.86	0.25	0.25	0.02	0.00	0.86	0.25	0.02	
Total	97.13	100.60	98.61	99.29	99.26	99.62	96.37	97.95	97.95	98.74	99.62	96.37	97.95	98.74	
Ti#	6.11	7.27	7.19	7.18	7.36	7.06	7.58	6.52	6.52	7.62	7.06	7.58	6.52	7.62	
Xusp	0.16	0.20	0.20	0.20	0.20	0.19	0.20	0.18	0.18	0.21	0.19	0.20	0.18	0.21	
Cations															
Si	0.017	0.002	0.004	0.002	0.002	0.003	0.008	0.003	0.003	0.001	0.003	0.008	0.003	0.001	
Ti	0.165	0.201	0.197	0.197	0.203	0.193	0.206	0.178	0.178	0.210	0.193	0.206	0.178	0.210	
Al	0.103	0.087	0.094	0.098	0.090	0.100	0.090	0.118	0.118	0.093	0.100	0.090	0.118	0.093	
Cr	0.001	0.002	0.004	0.002	0.003	0.002	0.003	0.003	0.003	0.003	0.002	0.003	0.003	0.003	
Fe ⁺³	1.530	1.506	1.499	1.501	1.497	1.504	1.480	1.518	1.518	1.481	1.504	1.480	1.518	1.481	
Fe ⁺²	1.010	1.056	1.049	1.049	1.056	1.043	1.025	1.032	1.032	1.065	1.043	1.025	1.032	1.065	
Mn	0.038	0.043	0.039	0.040	0.040	0.040	0.039	0.027	0.027	0.040	0.040	0.039	0.027	0.040	
Mg	0.116	0.103	0.112	0.110	0.110	0.114	0.113	0.112	0.112	0.106	0.114	0.113	0.112	0.106	
Ca	0.018	0.000	0.000	0.000	0.000	0.000	0.036	0.010	0.010	0.001	0.000	0.036	0.010	0.001	

Abbreviations same as Table A2.3. Population relates to either host crystals or size groups for groundmass oxides: large ~ 100 μm; mid ~ 50 μm; small ~ 10 μm. Cation proportions calculated using LePage (2003).

Table A2.7 EMPA data for Fe-Ti oxides.

Sample ID	Inglewood b		Inglewood b		Inglewood b		Inglewood b		Inglewood b		Inglewood a		Inglewood a		Inglewood a		
	M24_2	M24_3	M24_4	M24_5	M25	M1_1	M1_2	M1_3	M1_4	core	amph	core	amph	core	amph	core	amph
Zone	core	core	core	core	core	core	core	core	core	core	core	core	core	core	core	core	core
popn/host	amph	amph	amph	amph	cpx	amph	amph	amph	amph	amph	amph	amph	amph	amph	amph	amph	amph
SiO ₂	4.44	0.06	1.53	0.07	0.10	0.06	0.06	0.06	0.06	0.06	0.06	0.06	0.03	0.03	0.03	0.03	0.03
TiO ₂	6.61	6.89	5.70	5.85	6.91	7.38	7.28	7.21	7.36	7.28	7.28	7.21	7.21	7.21	7.21	7.21	7.36
Al ₂ O ₃	2.38	2.18	2.08	2.10	2.07	1.94	2.05	1.94	1.91	2.05	2.05	1.94	1.94	1.94	1.94	1.91	1.91
Fe ₂ O ₃	0.18	0.19	0.14	0.13	0.09	54.48	53.75	54.70	54.22	53.75	53.75	54.70	54.70	54.70	54.70	54.22	54.22
FeO	41.21	52.94	50.47	53.96	53.03	34.06	33.88	33.87	34.24	33.88	33.88	33.87	33.87	33.87	33.87	34.24	34.24
MnO	34.78	33.58	32.08	32.06	33.15	1.29	1.35	1.32	1.23	1.29	1.35	1.32	1.32	1.32	1.23	1.23	1.23
MgO	0.91	0.92	0.91	0.93	1.23	2.20	1.99	2.15	2.01	2.20	1.99	2.15	2.15	2.15	2.01	2.01	2.01
CaO	3.06	1.86	2.16	1.79	1.88	0.00	0.05	0.00	0.00	0.00	0.05	0.00	0.00	0.00	0.00	0.00	0.00
Cr ₂ O ₃	1.28	0.13	1.01	0.24	0.23	101.42	100.42	101.23	101.01	101.42	100.42	101.23	101.23	101.23	101.01	101.01	101.01
Total	94.84	98.75	96.09	97.14	98.69	7.40	7.38	7.24	7.39	7.40	7.38	7.24	7.24	7.24	7.39	7.39	7.39
Ti#	7.64	7.09	6.21	6.12	7.14	0.20	0.20	0.19	0.20	0.20	0.20	0.19	0.19	0.19	0.20	0.20	0.20
Xusp	0.22	0.20	0.17	0.17	0.19												
Cations																	
Si	0.168	0.002	0.059	0.003	0.004	0.002	0.002	0.001	0.001	0.002	0.002	0.001	0.001	0.001	0.001	0.001	0.001
Ti	0.188	0.195	0.164	0.169	0.196	0.204	0.203	0.200	0.204	0.204	0.203	0.200	0.200	0.200	0.204	0.204	0.204
Al	0.106	0.097	0.094	0.095	0.092	0.084	0.090	0.084	0.083	0.084	0.090	0.084	0.084	0.084	0.083	0.083	0.083
Cr	0.005	0.006	0.004	0.004	0.003												
Fe ⁺³	1.175	1.502	1.456	1.558	1.505	1.504	1.500	1.514	1.506	1.504	1.500	1.514	1.514	1.506	1.506	1.506	1.506
Fe ⁺²	1.102	1.059	1.028	1.029	1.046	1.045	1.051	1.042	1.057	1.045	1.051	1.042	1.042	1.057	1.057	1.057	1.057
Mn	0.029	0.029	0.030	0.030	0.039	0.040	0.042	0.041	0.038	0.040	0.042	0.041	0.041	0.038	0.038	0.038	0.038
Mg	0.173	0.105	0.124	0.102	0.106	0.120	0.110	0.118	0.110	0.120	0.110	0.118	0.118	0.110	0.110	0.110	0.110
Ca	0.052	0.005	0.041	0.010	0.009	0.000	0.002	0.000	0.000	0.000	0.002	0.000	0.000	0.000	0.000	0.000	0.000

Abbreviations same as Table A2.3. Population relates to either host crystals or size groups for groundmass oxides: large ~ 100 μm; mid ~ 50 μm; small ~ 10 μm. Cation proportions calculated using LePage (2003).

Table A2.7 EMPA data for Fe-Ti oxides.

Sample ID	Inglewood a		Inglewood a		Inglewood a		Inglewood a		Inglewood a		Inglewood a		Inglewood a		
	M1_5	M1_6	M2_1	M3_1	M3_2	M5_1	M6_1	M6_2	M6_3	M1_5	M1_6	M2_1	M3_1	M3_2	
Zone	core	core	core	core	core	core	core	core	core	core	core	core	core	core	
popn/host	amph	amph	large	mid	mid	large	mid	mid	mid	large	mid	mid	mid	mid	
SiO ₂	0.04	0.04	0.02	0.03	0.05	0.04	0.04	0.07	0.05	0.04	0.04	0.04	0.07	0.05	
TiO ₂	6.79	7.28	7.20	7.33	7.28	7.27	7.41	7.25	7.33	7.27	7.41	7.41	7.25	7.33	
Al ₂ O ₃	1.95	1.85	1.97	1.89	1.93	1.90	1.85	1.96	1.97	1.90	1.85	1.85	1.96	1.97	
Fe ₂ O ₃															
FeO	55.29	54.60	54.06	54.13	54.35	54.18	53.98	53.72	53.39	54.18	53.98	53.98	53.72	53.39	
MnO	33.99	34.10	34.08	33.91	33.92	33.82	33.99	33.75	33.91	33.82	33.99	33.99	33.75	33.91	
MgO	1.07	1.31	1.24	1.29	1.31	1.38	1.27	1.21	1.23	1.38	1.27	1.27	1.21	1.23	
CaO	1.95	2.04	1.90	2.09	2.09	2.06	2.09	2.12	1.98	2.06	2.09	2.09	2.12	1.98	
Cr ₂ O ₃	0.00	0.00	0.00	0.01	0.03	0.00	0.00	0.00	0.00	0.00	0.00	0.00	0.00	0.00	
Total	101.08	101.21	100.47	100.68	100.96	100.63	100.62	100.08	99.85	100.63	100.62	100.62	100.08	99.85	
Ti#	6.80	7.30	7.26	7.39	7.32	7.34	7.47	7.36	7.44	7.34	7.47	7.47	7.36	7.44	
Xusp	0.19	0.20	0.20	0.20	0.20	0.20	0.20	0.20	0.20	0.20	0.20	0.20	0.20	0.20	
Cations															
Si	0.001	0.001	0.001	0.001	0.002	0.002	0.001	0.002	0.002	0.002	0.001	0.001	0.002	0.002	
Ti	0.188	0.202	0.201	0.204	0.202	0.202	0.206	0.203	0.206	0.202	0.206	0.206	0.203	0.206	
Al	0.085	0.080	0.086	0.083	0.084	0.083	0.081	0.086	0.086	0.083	0.081	0.081	0.086	0.086	
Cr															
Fe ⁺³	1.535	1.513	1.510	1.507	1.509	1.510	1.504	1.503	1.499	1.510	1.504	1.504	1.503	1.499	
Fe ⁺²	1.049	1.050	1.058	1.049	1.046	1.047	1.053	1.050	1.058	1.047	1.053	1.053	1.050	1.058	
Mn	0.033	0.041	0.039	0.041	0.041	0.043	0.040	0.038	0.039	0.043	0.040	0.040	0.038	0.039	
Mg	0.107	0.112	0.105	0.115	0.115	0.114	0.115	0.118	0.110	0.114	0.115	0.115	0.118	0.110	
Ca	0.000	0.000	0.000	0.000	0.001	0.000	0.000	0.000	0.000	0.000	0.000	0.000	0.000	0.000	

Abbreviations same as Table A2.3. Population relates to either host crystals or size groups for groundmass oxides: large ~ 100 μm; mid ~ 50 μm; small ~ 10 μm. Cation proportions calculated using Lepage (2003).

Table A2.7 EMPA data for Fe-Ti oxides.

Sample ID	Inglewood a		Inglewood a		Inglewood a		Inglewood a		Inglewood a		Inglewood a		Inglewood a	
	M7_1	M7_2	M8_1	M9_1	M9_2	M9_3	M11_1	M11_2	M11_3	core small	core small	core mid	core large	core large
Zone	core small	core small	core small	core small	core small	core small	core mid	core large	core large					
popn/host	0.05	0.36	0.07	0.05	0.08	0.06	0.03	0.07	0.03					
SiO ₂	7.17	7.18	6.94	7.32	7.47	7.42	7.34	7.51	7.44					
TiO ₂	1.93	2.01	1.85	1.93	2.03	1.97	1.83	2.06	1.99					
Al ₂ O ₃	54.05	54.85	54.47	53.14	52.56	53.37	54.13	53.77	54.25					
FeO	33.94	32.58	33.72	34.03	33.86	34.01	33.83	34.26	34.12					
MnO	1.19	1.23	1.20	1.27	1.30	1.27	1.33	1.32	1.42					
MgO	1.99	1.98	1.98	1.81	1.99	2.02	2.10	2.08	2.08					
CaO	0.00	1.96	0.00	0.01	0.00	0.00	0.00	0.00	0.01					
Cr ₂ O ₃	100.31	102.14	100.22	99.56	99.29	100.11	100.60	101.06	101.35					
Total	7.25	7.31	7.02	7.44	7.65	7.52	7.41	7.56	7.47					
Ti#	0.20	0.18	0.19	0.20	0.21	0.20	0.20	0.21	0.20					
Xusp														
Cations														
Si	0.002	0.013	0.002	0.002	0.003	0.002	0.001	0.002	0.001					0.001
Ti	0.201	0.196	0.194	0.206	0.211	0.208	0.205	0.208	0.206					0.206
Al	0.084	0.086	0.081	0.085	0.090	0.086	0.080	0.089	0.086					0.086
Cr														
Fe ⁺³	1.511	1.496	1.525	1.498	1.483	1.494	1.509	1.490	1.500					
Fe ⁺²	1.055	0.988	1.049	1.066	1.061	1.058	1.048	1.055	1.048					
Mn	0.037	0.038	0.038	0.040	0.041	0.040	0.042	0.041	0.044					
Mg	0.110	0.107	0.110	0.101	0.111	0.112	0.116	0.114	0.114					
Ca	0.000	0.076	0.000	0.000	0.000	0.000	0.000	0.000	0.000					0.000

Abbreviations same as Table A2.3. Population relates to either host crystals or size groups for groundmass oxides: large ~ 100 μm; mid ~ 50 μm; small ~ 10 μm. Cation proportions calculated using Lepage (2003).

Table A2.7 EMPA data for Fe-Ti oxides.

Sample ID	Inglewood a M11_4 rim large	Inglewood a M11_5 rim large	Inglewood a M12_1 rim large	Inglewood a M12_2 core large	Inglewood a M13_1 core amph	Inglewood a M13_2 core amph	Inglewood a M13_4 core amph	Inglewood a M15_1 core amph	Inglewood a M15_2 core amph
Zone									
popn/host									
SiO ₂	0.09	0.09	0.00	0.06	0.07	0.08	0.87	0.02	0.07
TiO ₂	7.13	7.39	7.30	7.52	7.12	6.79	4.34	34.65	6.54
Al ₂ O ₃	2.00	1.91	1.89	2.06	1.85	1.95	2.16	0.27	2.15
Fe ₂ O ₃									
FeO	52.22	53.35	54.11	53.72	54.40	55.18	38.76	0.36	55.35
MnO	33.17	34.18	33.75	34.48	33.80	33.47	24.17	57.14	33.16
MgO	1.35	1.25	1.25	1.28	1.45	1.38	1.06	0.85	1.15
CaO	1.90	1.92	2.13	1.97	1.96	2.09	1.97	2.61	2.16
Cr ₂ O ₃	0.02	0.00	0.00	0.00	0.00	0.03	0.08	0.07	0.12
Total	97.89	100.09	100.44	101.09	100.64	100.98	73.41	95.96	100.69
Ti#	7.41	7.49	7.38	7.55	7.18	6.85	6.20	35.17	6.62
Xusp	0.20	0.20	0.20	0.21	0.19	0.18	0.17	1.00	0.18
Cations									
Si	0.004	0.003	0.000	0.002	0.003	0.003	0.044	0.001	0.002
Ti	0.204	0.207	0.204	0.208	0.198	0.189	0.163	0.988	0.182
Al	0.090	0.084	0.083	0.090	0.081	0.085	0.127	0.012	0.094
Cr									
Fe ⁺³	1.495	1.495	1.510	1.489	1.517	1.532	1.459	0.010	1.538
Fe ⁺²	1.055	1.065	1.047	1.063	1.047	1.033	1.011	1.811	1.024
Mn	0.044	0.039	0.039	0.040	0.045	0.043	0.045	0.027	0.036
Mg	0.108	0.106	0.118	0.108	0.108	0.115	0.147	0.147	0.119
Ca	0.001	0.000	0.000	0.000	0.000	0.001	0.004	0.003	0.005

Abbreviations same as Table A2.3. Population relates to either host crystals or size groups for groundmass oxides: large ~ 100 μm; mid ~ 50 μm; small ~ 10 μm. Cation proportions calculated using Lepage (2003).

Table A2.7 EMPA data for Fe-Ti oxides.

Sample ID	Inglewood a M15_3	Inglewood a M15_4	Inglewood a M16_1	Inglewood a M16_2	Inglewood a M16_3	Inglewood a M16_4	Inglewood a M16_6	Inglewood a M17_1	Inglewood a M17_2
Zone	core	rim	core	core	core	core	core	rim	core
popn/host	amph	amph	amph	amph	amph	amph	amph	cpx	cpx
SiO ₂	0.07	0.05	7.82	0.08	0.03	0.03	0.06	0.04	0.07
TiO ₂	7.18	7.07	6.19	7.15	7.28	7.29	7.07	7.17	7.09
Al ₂ O ₃	1.85	1.95	3.51	1.93	1.98	1.99	1.90	1.94	1.96
Fe ₂ O ₃									
FeO	54.79	54.97	39.16	54.50	54.74	56.64	55.15	54.37	54.74
MnO	33.81	33.90	45.05	34.09	34.07	34.53	33.70	33.59	33.56
MgO	1.43	1.29	0.86	1.24	1.37	1.41	1.48	1.43	1.50
CaO	2.12	2.09	0.68	1.94	2.08	2.15	2.07	2.11	2.15
Cr ₂ O ₃	0.00	0.00	2.17	0.10	0.02	0.22	0.11	0.03	0.01
Total	101.26	101.32	105.43	101.03	101.58	104.26	101.53	100.69	101.08
Ti#	7.21	7.09	6.48	7.18	7.29	7.12	7.10	7.25	7.15
Xusp	0.19	0.19	0.25	0.20	0.20	0.19	0.19	0.19	0.19
Cations									
Si	0.003	0.002	0.267	0.003	0.001	0.001	0.002	0.002	0.003
Ti	0.199	0.196	0.159	0.198	0.201	0.196	0.195	0.200	0.196
Al	0.080	0.084	0.141	0.084	0.086	0.084	0.082	0.085	0.085
Cr									
Fe ⁺³	1.517	1.521	1.007	1.513	1.510	1.522	1.523	1.513	1.517
Fe ⁺²	1.040	1.043	1.287	1.052	1.045	1.031	1.034	1.039	1.034
Mn	0.045	0.040	0.025	0.039	0.043	0.043	0.046	0.045	0.047
Mg	0.116	0.115	0.035	0.107	0.114	0.115	0.113	0.116	0.118
Ca	0.000	0.000	0.079	0.004	0.001	0.008	0.004	0.001	0.000

Abbreviations same as Table A2.3. Population relates to either host crystals or size groups for groundmass oxides: large ~ 100 μm; mid ~ 50 μm; small ~ 10 μm. Cation proportions calculated using Lepage (2003).

Table A2.7 EMPA data for Fe-Ti oxides.

Sample ID	Inglewood a		Inglewood a		Inglewood a		Inglewood a		Inglewood a		Inglewood a		Inglewood a	
	M17_5	M17_6	M18_3	M19_1	M19_2	M20	M21	M22	M23	rim	core	core	core	core
Zone	cpx	cpx	cpx	large	large	large	large	large	small	core	core	core	core	core
popn/host														
SiO ₂	0.06	0.05	0.07	0.06	0.06	0.04	0.05	0.09	0.05	0.05	0.09	0.05	0.09	0.05
TiO ₂	6.98	7.23	6.16	7.12	7.15	7.40	7.27	7.11	7.11	7.27	7.11	7.11	7.11	6.87
Al ₂ O ₃	1.99	2.00	1.84	2.02	2.02	1.97	2.00	2.02	2.02	2.00	2.02	2.02	2.02	1.86
Fe ₂ O ₃	54.74	55.08	42.86	0.14	0.11	0.09	0.05	0.11	0.11	0.05	0.11	0.11	0.11	0.09
FeO	33.62	33.90	26.81	54.21	54.14	53.27	54.15	53.81	53.81	54.15	53.81	53.81	53.81	55.27
MnO	1.43	1.44	1.18	34.04	34.01	34.00	34.10	33.94	33.69	34.10	33.94	33.94	33.94	33.69
MgO	2.03	2.17	1.97	1.29	1.31	1.33	1.33	1.27	1.36	1.33	1.27	1.27	1.27	1.36
CaO	0.04	0.07	0.23	1.95	1.96	1.88	1.98	1.94	2.03	1.98	1.94	1.94	1.94	2.03
Cr ₂ O ₃	100.89	101.93	81.12	0.00	0.00	0.09	0.00	0.00	0.00	0.00	0.00	0.00	0.00	0.00
Total	7.04	7.23	7.82	100.83	100.76	100.05	100.92	100.28	101.22	100.92	100.28	100.28	100.28	101.22
Ti#	0.19	0.19	0.21	0.20	0.20	0.21	0.20	0.20	0.19	0.20	0.20	0.20	0.20	0.19
Xusp	0.002	0.002	0.003	0.002	0.002	0.001	0.002	0.003	0.002	0.002	0.003	0.002	0.003	0.002
Cations														
Si	0.194	0.199	0.212	0.198	0.199	0.207	0.202	0.199	0.190	0.202	0.199	0.199	0.199	0.190
Ti	0.087	0.086	0.099	0.088	0.088	0.086	0.087	0.089	0.081	0.087	0.089	0.087	0.089	0.081
Al	1.521	1.513	1.472	1.508	1.507	1.493	1.504	1.504	1.532	1.504	1.504	1.504	1.504	1.532
Fe ⁺³	1.038	1.035	1.023	1.052	1.052	1.059	1.053	1.054	1.038	1.053	1.054	1.054	1.054	1.038
Fe ⁺²	0.045	0.044	0.046	0.040	0.041	0.042	0.042	0.040	0.042	0.042	0.040	0.042	0.040	0.042
Mn	0.112	0.118	0.134	0.108	0.108	0.104	0.109	0.108	0.112	0.109	0.108	0.108	0.108	0.112
Mg	0.002	0.003	0.011	0.000	0.000	0.003	0.000	0.000	0.000	0.000	0.000	0.000	0.000	0.000
Ca														

Abbreviations same as Table A2.3. Population relates to either host crystals or size groups for groundmass oxides: large ~ 100 μm; mid ~ 50 μm; small ~ 10 μm. Cation proportions calculated using LePage (2003).

Table A2.7 EMPA data for Fe-Ti oxides.

Sample ID	Inglewood a	Korito M1_1		Korito M1_2		Korito M2_1		Korito M2_2		Korito M3_1		Korito M4_1		Korito M4_2		Korito M4_3		Korito M4_4		Korito M4_5		Korito M4_6		Korito M4_7			
		core	mid	core	mid	core	mid	core	mid	core	mid	core	mid	core	rim	large	core	large	core	large	core	mid	core	mid	core	small	core
Zone																											
popn/host																											
SiO ₂	0.12	0.02	7.17	7.00	0.06	0.05	7.09	7.24	0.05	7.24	7.24	0.05	7.31	7.11	7.37	7.41	7.37	7.41	7.41	7.37	7.41	6.97	6.99	6.85	6.85	6.85	
TiO ₂	7.08	2.14	2.14	2.14	2.14	2.05	2.05	2.09	2.04	2.04	2.04	2.13	2.13	2.08	2.14	2.13	2.14	2.13	2.13	2.14	2.07	2.07	2.05	2.09	2.09	2.09	
Al ₂ O ₃	0.10	0.11	0.11	0.11	0.11	0.11	0.11	0.14	0.08	0.08	0.08	0.11	0.11	0.06	0.07	0.12	0.07	0.12	0.12	0.07	0.08	0.08	0.10	0.09	0.09	0.09	
Fe ₂ O ₃	53.51	54.82	54.82	53.80	53.80	55.30	55.30	54.78	54.66	54.66	54.66	54.03	54.03	54.50	54.87	54.39	54.87	54.39	54.39	54.87	54.72	54.72	54.13	54.10	54.10	54.10	
MnO	33.65	34.19	34.19	33.65	33.65	34.34	34.34	34.26	34.29	34.29	34.29	33.93	33.93	33.97	34.43	34.29	34.43	34.29	34.29	34.43	33.61	33.61	33.37	33.24	33.24	33.24	
MgO	1.25	1.33	1.33	1.17	1.17	1.22	1.22	1.35	1.27	1.27	1.27	1.38	1.38	1.27	1.38	1.40	1.38	1.40	1.40	1.38	1.27	1.27	1.32	1.30	1.30	1.30	
CaO	1.99	2.04	2.04	2.02	2.02	2.06	2.06	2.08	2.04	2.04	2.04	2.13	2.13	2.07	2.11	2.10	2.11	2.10	2.10	2.11	2.18	2.18	2.14	2.12	2.12	2.12	
Cr ₂ O ₃	0.05	0.00	0.00	0.05	0.05	0.00	0.00	0.00	0.00	0.00	0.00	0.00	0.00	0.00	0.00	0.00	0.00	0.00	0.00	0.00	0.01	0.01	0.00	0.00	0.00	0.00	
Total	99.72	101.81	101.81	99.98	99.98	102.21	102.21	101.98	101.67	101.67	101.67	101.06	101.06	101.10	102.42	101.88	102.42	101.88	101.88	102.42	100.95	100.95	100.13	99.86	99.86	99.86	
Ti#	7.22	7.17	7.17	7.12	7.12	7.05	7.05	7.23	7.24	7.24	7.24	7.38	7.38	7.15	7.33	7.41	7.33	7.41	7.41	7.33	7.04	7.04	7.12	6.99	6.99	6.99	
Xusp	0.20	0.20	0.20	0.19	0.19	0.19	0.19	0.20	0.20	0.20	0.20	0.20	0.20	0.19	0.20	0.20	0.20	0.20	0.20	0.20	0.19	0.19	0.19	0.19	0.19	0.19	
Cations																											
Si	0.004	0.001	0.001	0.002	0.002	0.002	0.002	0.002	0.002	0.002	0.002	0.002	0.002	0.002	0.002	0.001	0.002	0.001	0.001	0.002	0.002	0.002	0.001	0.003	0.003	0.003	
Ti	0.199	0.197	0.197	0.196	0.196	0.194	0.194	0.199	0.200	0.200	0.200	0.202	0.202	0.197	0.202	0.204	0.202	0.204	0.204	0.202	0.193	0.193	0.195	0.192	0.192	0.192	
Al	0.086	0.092	0.092	0.094	0.094	0.088	0.088	0.090	0.088	0.088	0.088	0.092	0.092	0.090	0.092	0.092	0.092	0.092	0.092	0.092	0.090	0.090	0.090	0.092	0.092	0.092	
Cr	0.003	0.003	0.003	0.003	0.003	0.003	0.003	0.004	0.002	0.002	0.002	0.003	0.003	0.002	0.002	0.003	0.002	0.003	0.003	0.002	0.002	0.002	0.003	0.003	0.003	0.003	
Fe ⁺³	1.504	1.509	1.509	1.507	1.507	1.517	1.517	1.505	1.507	1.507	1.507	1.496	1.496	1.510	1.500	1.495	1.500	1.495	1.495	1.500	1.517	1.517	1.514	1.517	1.517	1.517	
Fe ⁺²	1.051	1.046	1.046	1.047	1.047	1.046	1.046	1.046	1.050	1.050	1.050	1.044	1.044	1.046	1.046	1.047	1.046	1.047	1.047	1.046	1.036	1.036	1.037	1.036	1.036	1.036	
Mn	0.040	0.041	0.041	0.037	0.037	0.038	0.038	0.042	0.039	0.039	0.039	0.043	0.043	0.040	0.043	0.043	0.043	0.043	0.043	0.043	0.040	0.040	0.042	0.041	0.041	0.041	
Mg	0.111	0.111	0.111	0.112	0.112	0.112	0.112	0.113	0.112	0.112	0.112	0.117	0.117	0.113	0.114	0.115	0.114	0.115	0.115	0.114	0.120	0.120	0.118	0.118	0.118	0.118	
Ca	0.002	0.000	0.000	0.002	0.002	0.000	0.000	0.000	0.000	0.000	0.000	0.000	0.000	0.000	0.000	0.000	0.000	0.000	0.000	0.000	0.000	0.000	0.000	0.000	0.000	0.000	

Abbreviations same as Table A2.3. Population relates to either host crystals or size groups for groundmass oxides: large ~ 100 μm; mid ~ 50 μm; small ~ 10 μm. Cation proportions calculated using Lepage (2003).

Table A2.7 EMPA data for Fe-Ti oxides.

Sample ID	Zone	popn/host	Korito M4_8	Korito M5	Korito M6	Korito M7	Korito M8	Korito M9_1	Korito M9_2	Korito M10	Korito M11	Korito M12	Korito M13	Korito M14	Korito M15
			core mid	core mid	core mid	core small	core small	core small	core small	core small	core small	core small	core small	core small	core small
SiO ₂			0.04	0.03	0.05	0.08	0.08	0.08	0.10	0.12	0.07	0.10	0.05	0.06	0.06
TiO ₂			7.01	7.44	7.23	7.00	7.10	6.91	6.89	7.08	7.12	6.75	7.72	6.98	7.30
Al ₂ O ₃			2.12	2.04	2.07	2.09	2.06	2.13	2.12	2.09	2.07	2.05	2.30	2.09	2.51
Fe ₂ O ₃			0.11	0.12	0.09	0.16	0.14	0.09	0.10	0.09	0.08	0.10	0.10	0.12	0.12
FeO			54.74	54.28	53.93	54.22	54.30	53.73	54.49	54.81	53.63	54.28	53.87	55.00	37.16
MnO			33.80	34.52	33.80	33.87	33.94	33.42	33.69	34.42	33.64	33.06	35.29	34.00	36.94
MgO			1.31	1.23	1.35	1.18	1.28	1.23	1.18	1.19	1.23	1.34	0.98	1.24	0.92
CaO			2.10	2.03	2.10	2.05	2.07	2.05	2.14	2.00	2.08	2.14	2.03	2.09	4.66
Cr ₂ O ₃			0.00	0.00	0.00	0.00	0.00	0.02	0.00	0.00	0.00	0.05	0.00	0.00	1.91
Total			101.23	101.69	100.63	100.65	100.97	99.66	100.71	101.80	99.93	99.86	102.34	101.57	98.59
Ti#			7.05	7.43	7.33	7.08	7.16	7.06	6.97	7.06	7.26	6.90	7.66	6.99	8.53
Xusp			0.19	0.20	0.20	0.19	0.19	0.19	0.19	0.19	0.20	0.19	0.21	0.19	0.25
Cations															
Si			0.001	0.001	0.002	0.003	0.003	0.003	0.004	0.004	0.002	0.004	0.002	0.002	0.252
Ti			0.194	0.205	0.201	0.195	0.197	0.194	0.191	0.195	0.200	0.189	0.211	0.192	0.196
Al			0.092	0.088	0.090	0.091	0.090	0.094	0.092	0.090	0.091	0.090	0.098	0.090	0.105
Cr			0.003	0.003	0.003	0.005	0.004	0.003	0.003	0.003	0.002	0.003	0.003	0.003	0.003
Fe ⁺³			1.515	1.496	1.501	1.509	1.506	1.510	1.514	1.509	1.503	1.522	1.473	1.517	0.996
Fe ⁺²			1.039	1.057	1.045	1.047	1.046	1.043	1.041	1.053	1.048	1.030	1.073	1.042	1.100
Mn			0.041	0.038	0.042	0.037	0.040	0.039	0.037	0.037	0.039	0.042	0.030	0.038	0.028
Mg			0.115	0.111	0.116	0.113	0.114	0.114	0.118	0.109	0.116	0.119	0.110	0.114	0.247
Ca			0.000	0.000	0.000	0.000	0.000	0.001	0.000	0.000	0.000	0.002	0.000	0.000	0.073

Abbreviations same as Table A2.3. Population relates to either host crystals or size groups for groundmass oxides: large ~ 100 μm; mid ~ 50 μm; small ~ 10 μm. Cation proportions calculated using Lepage (2003).

Table A2.7 EMPA data for Fe-Ti oxides.

Sample ID	Zone	popn/host	Korito M16_1		Korito M16_2		Korito M16_3		Korito M16_4		Korito M16_5		Korito M16_6		Korito M17		Korito M18_1		Korito M18_2		Korito M18_3		Korito M19_1	
			core	cpx	core	cpx	core	cpx	core	cpx	core	cpx	core	cpx	core	cpx	core	plag	core	plag	core	plag	core	plag
SiO ₂			0.06	0.04	0.04	0.03	0.03	0.02	0.02	0.06	0.06	0.07	0.07	0.16	0.05	0.07	0.06	0.06	0.06	0.06	0.06	0.06	0.02	0.02
TiO ₂			7.18	7.23	7.31	7.39	7.39	7.39	7.39	7.03	7.03	6.99	6.99	6.48	7.37	7.28	6.89	7.35	7.35	7.35	7.35	7.35	7.35	7.35
Al ₂ O ₃			2.02	2.09	2.03	2.26	2.26	2.26	2.26	2.06	2.06	2.12	2.12	1.66	2.19	2.08	2.11	1.88	1.88	1.88	1.88	1.88	1.88	1.88
Fe ₂ O ₃			0.17	0.15	0.15	0.12	0.12	0.12	0.12	0.11	0.11	0.11	0.11	0.11	0.14	0.16	0.15	0.15	0.15	0.15	0.15	0.15	0.15	0.15
FeO			54.85	54.79	54.65	54.48	54.48	54.48	54.48	54.41	54.41	54.38	54.38	53.41	54.61	54.02	54.99	54.72	54.72	54.72	54.72	54.72	54.72	54.72
MnO			34.22	33.99	34.18	34.69	34.69	34.69	34.69	33.59	33.59	33.68	33.68	34.30	34.40	33.94	33.76	34.17	34.17	34.17	34.17	34.17	34.17	34.17
MgO			1.29	1.34	1.31	1.01	1.01	1.01	1.01	1.23	1.23	1.21	1.21	1.23	1.22	1.28	1.32	1.30	1.30	1.30	1.30	1.30	1.30	1.30
CaO			2.07	2.20	2.11	2.13	2.13	2.13	2.13	2.12	2.12	2.07	2.07	0.99	2.19	2.10	2.09	2.14	2.14	2.14	2.14	2.14	2.14	2.14
Cr ₂ O ₃			0.02	0.01	0.03	0.00	0.00	0.00	0.00	0.13	0.13	0.12	0.12	0.00	0.00	0.10	0.00	0.00	0.00	0.00	0.00	0.00	0.00	0.00
Total			101.88	101.84	101.78	102.11	102.11	102.11	102.11	100.74	100.74	100.74	100.74	98.34	102.17	101.03	101.37	101.73	101.73	101.73	101.73	101.73	101.73	101.73
Ti#			7.17	7.24	7.31	7.36	7.36	7.36	7.36	7.12	7.12	7.07	7.07	6.61	7.35	7.35	6.93	7.35	7.35	7.35	7.35	7.35	7.35	7.35
Xusp			0.19	0.20	0.20	0.20	0.20	0.20	0.20	0.19	0.19	0.19	0.19	0.19	0.20	0.20	0.19	0.20	0.20	0.20	0.20	0.20	0.20	0.20
Cations																								
Si			0.002	0.001	0.001	0.001	0.001	0.001	0.001	0.002	0.002	0.003	0.003	0.006	0.002	0.003	0.002	0.001	0.001	0.001	0.001	0.001	0.001	0.001
Ti			0.197	0.199	0.201	0.203	0.203	0.203	0.203	0.195	0.195	0.194	0.194	0.186	0.202	0.202	0.190	0.202	0.202	0.202	0.202	0.202	0.202	0.202
Al			0.087	0.090	0.087	0.097	0.097	0.097	0.097	0.090	0.090	0.092	0.092	0.075	0.094	0.090	0.091	0.081	0.081	0.081	0.081	0.081	0.081	0.081
Cr			0.005	0.004	0.004	0.003	0.003	0.003	0.003	0.003	0.003	0.003	0.003	0.003	0.004	0.005	0.004	0.004	0.004	0.004	0.004	0.004	0.004	0.004
Fe ⁺³			1.509	1.506	1.504	1.493	1.493	1.493	1.493	1.512	1.512	1.511	1.511	1.537	1.495	1.497	1.520	1.508	1.508	1.508	1.508	1.508	1.508	1.508
Fe ⁺²			1.046	1.038	1.045	1.057	1.057	1.057	1.057	1.037	1.037	1.040	1.040	1.096	1.047	1.045	1.037	1.046	1.046	1.046	1.046	1.046	1.046	1.046
Mn			0.040	0.041	0.041	0.031	0.031	0.031	0.031	0.039	0.039	0.038	0.038	0.040	0.038	0.040	0.041	0.040	0.040	0.040	0.040	0.040	0.040	0.040
Mg			0.113	0.120	0.115	0.116	0.116	0.116	0.116	0.117	0.117	0.114	0.114	0.057	0.119	0.115	0.115	0.117	0.117	0.117	0.117	0.117	0.117	0.117
Ca			0.001	0.001	0.001	0.000	0.000	0.000	0.000	0.005	0.005	0.005	0.005	0.000	0.000	0.004	0.000	0.000	0.000	0.000	0.000	0.000	0.000	0.000

Abbreviations same as Table A2.3. Population relates to either host crystals or size groups for groundmass oxides: large ~ 100 μm; mid ~ 50 μm; small ~ 10 μm. Ca:ton proportions calculated using Lepage (2003).

APPENDIX 3:

TRACE ELEMENT DATA

Table A3.1 Glass trace element data

Table A3.2 Plagioclase trace element data

Table A3.3 Clinopyroxene trace element data

Table A3.4 Amphibole trace element data

Table A3.1 Trace element concentrations of glass analysed by solution ICP-MS.

wt%	Kaupokonui	SM-6C	Maketawa	Inglewood b	Inglewood a	Korito
SiO₂ EMPA *	67.32	61.69	68.74	71.55	72.79	72.34
CaO	2.72	5.09	2.28	1.84	1.41	1.61
ppm						
Li	30.0	30.0	24.5	32.9	20.6	24.2
Sc	3.28	9.45	2.69	1.24	1.06	1.49
Ti	2378	5322	2187	1987	1296	1731
V	56.2	128.2	43.8	19.6	12.3	18.0
Co	5.09	10.4	3.73	1.66	1.12	1.43
Cu	76.0	147.6	55.0	57.6	14.8	21.5
Zn	51.0	80.5	49.6	26.4	28.0	21.7
Ga	17.3	26.6	16.1	16.6	11.5	13.7
Rb	108	102	77.9	101	66.9	76.7
Sr	324	531	283	239	176	194
Y	14.6	26.8	14.0	17.3	12.1	16.2
Zr	190	255	178	251	154	182
Nb	6.20	9.94	5.87	7.43	4.80	5.87
Mo	2.39	2.88	1.85	2.87	1.80	1.43
Cs	6.64	6.38	5.05	6.66	4.44	4.86
Ba	1171	1288	983	1140	752	887
La	21.6	25.9	17.6	21.0	14.4	18.3
Ce	40.8	55.1	34.1	41.4	29.0	38.6
Pr	4.55	6.81	3.94	4.83	3.32	4.52
Nd	16.6	27.6	14.7	17.8	12.5	17.6
Sm	3.04	5.90	2.87	3.36	2.37	3.45
Eu	0.873	1.63	0.861	0.869	0.623	0.838
Gd	2.90	5.72	2.70	3.17	2.20	3.13
Tb	0.394	0.809	0.380	0.435	0.317	0.441
Dy	2.35	4.82	2.28	2.67	1.93	2.64
Ho	0.484	0.973	0.474	0.568	0.401	0.544
Er	1.49	2.85	1.43	1.78	1.23	1.64
Tm	0.233	0.414	0.216	0.270	0.193	0.264
Yb	1.62	2.84	1.56	1.99	1.43	1.79
Lu	0.253	0.429	0.243	0.320	0.223	0.278
Hf	4.65	6.78	4.40	6.23	3.85	4.43
Ta	0.431	0.653	0.409	0.552	0.329	0.391
W	1.10	1.24	0.81	1.01	0.655	0.763
Pb	32.0	41.1	25.7	36.1	23.5	26.8
Th	11.3	13.4	9.37	12.7	8.12	9.58
U	2.95	3.09	2.21	2.94	2.03	2.36

* Average SiO₂ content for each sample from EMPA.

Table A3.2 Trace element concentrations in plagioclase crystals analysed by LA-ICP-MS.

Sample ID	Zone	8b	9b	9c	10a	10b	10c	11a	11b	13a
		core	core	sieved	rim	zone	sieved	rim	core	rim
EMPA ID		P8_7	P9_11	P9_4	P10_2	P10_5	P10_10	P11_1	P11_5	P13_2
An		41.85	57.07	67.55	52.87	62.81	57.53	58.40	66.52	51.12
CaO (wt%)		8.36	11.49	13.51	10.59	12.99	11.50	11.80	13.58	10.38
Li		17.2	11.9	12.6	16.9	20.6	10.7	23.9	18.1	16.1
Mg		163.018	549.903	338.623	373.578	335.215	217.124	339.092	389.914	319.099
Mg		176.652	553.961	405.435	358.760	318.821	208.180	332.043	419.406	341.920
Mg		170	552	372	366	327	213	336	405	331
Rb		BDL	6.22	BDL	BDL	1.51	BDL	BDL	1.15	0.62
Sr		1368	1510	1481	1778	1362	1154	1650	1522	1527
Y		0.376	0.598	BDL	BDL	0.730	BDL	BDL	BDL	0.170
Cs		BDL	0.300	BDL	BDL	BDL	BDL	BDL	BDL	BDL
Ba		580	436	322	804	310	191	422	409	491
La		6.19	4.70	3.76	6.31	4.75	2.42	4.61	4.86	4.85
Ce		9.06	7.13	4.05	10.1	7.83	4.48	7.13	6.53	7.27
Pr		0.716	0.670	0.398	0.647	0.889	0.330	0.466	0.551	0.557
Nd		2.35	1.97	2.51	2.40	2.82	1.12	1.56	2.19	1.93
Eu		0.925	0.731	0.697	0.845	0.581	0.354	0.588	0.799	0.678
Pb		8.24	5.58	4.15	6.82	4.81	3.85	5.08	6.84	5.43

Conc. in ppm unless otherwise stated. EMPA ID = major element data point and associated trace element data. Ca value used for normalisation and key atomic % shown. BDL= below detection limit. ID designates crystal and spot.

Table A3.2 Trace element concentrations in plagioclase crystals analysed by LA-ICP-MS.

Sample ID	Zone	13b	13c	13d	15b	17a	17b	20a	20c	21a
EMPA ID		P13_4	P13_5	P13_6	P15_7	P17_1	P17_4	P20_1	P20_4	P21_1
An		59.41	51.25	48.36	55.59	50.22	52.40	55.07	40.18	48.02
CaO (wt%)		12.14	10.45	9.90	11.66	9.82	10.21	11.08	8.11	9.81
Li		9.01	8.77	12.1	13.7	8.75	8.20	23.7	8.12	18.5
Mg		362.782	281.408	489.531	326.324	254.857	348.058	344.894	219.362	320.544
Mg		340.202	297.366	483.771	308.154	268.063	351.394	382.731	209.834	347.856
Mg		351	289	487	317	261	350	364	215	334
Rb		BDL	0.74	10.67	BDL	BDL	BDL	BDL	BDL	BDL
Sr		1759	1805	1647	1655	1251	1773	1743	1432	1488
Y		BDL	0.160	0.884	BDL	BDL	BDL	BDL	BDL	BDL
Cs		BDL	BDL	0.538	BDL	BDL	BDL	BDL	BDL	BDL
Ba		567	663	754	573	307	701	610	629	473
La		5.63	6.47	8.61	6.47	3.26	7.02	6.88	5.73	4.52
Ce		8.61	9.94	14.2	8.63	4.80	9.42	9.02	8.01	6.75
Pr		0.655	0.725	1.390	0.639	0.398	0.830	0.642	0.706	0.500
Nd		2.19	2.28	3.83	1.51	1.30	2.40	2.28	2.59	1.66
Eu		0.806	0.875	1.339	0.796	0.438	1.074	0.904	0.992	0.580
Pb		6.64	7.12	9.83	7.48	3.66	7.32	6.88	6.55	4.86

Conc. in ppm unless otherwise stated. EMPA ID = major element data point and associated trace element data. Ca value used for normalisation and key atomic % shown. BDL= below detection limit. ID designates crystal and spot.

Table A3.2 Trace element concentrations in plagioclase crystals analysed by LA-ICP-MS.

Sample ID	SM-6C 1a rim	SM-6C 1b zone	SM-6C 1c core	SM-6C 5a rim	SM-6C 5c sieved	SM-6C 10b D	SM-6C 11a rim	SM-6C 11b zone	SM-6C 12 core
EMPA ID	P1_2	P1_5	P1_6	P5_1	P5_3	P10_1	P11_1	P11_2	P12_2
An	50.76	60.00	64.94	53.04	59.80	89.01	50.89	59.17	55.43
CaO (wt%)	9.98	12.00	13.06	10.64	11.96	18.06	10.10	11.79	10.88
Li	5.36	3.59	8.63	14.3	6.53	3.19	5.01	5.69	9.65
Mg	537.620	397.737	535.103	474.785	533.907	353.600	466.718	558.548	489.906
Mg	518.739	379.405	468.361	403.270	548.590	412.694	507.588	627.544	454.843
Mg	528	389	502	439	541	383	487	593	472
Rb	0.69	BDL	BDL	0.66	0.72	BDL	BDL	0.54	BDL
Sr	1461	1396	1738	1407	1625	1291	1441	1425	1377
Y	0.322	0.438	BDL	BDL	0.406	BDL	0.768	0.310	0.257
Cs	BDL	BDL	BDL	BDL	BDL	BDL	BDL	BDL	BDL
Ba	601	356	509	586	523	81.1	555	437	498
La	5.46	4.29	6.01	4.66	4.47	1.09	5.20	3.94	5.45
Ce	8.46	7.52	10.2	8.12	7.25	2.29	9.29	5.98	7.29
Pr	0.705	0.653	0.757	0.600	0.549	0.213	0.688	0.595	0.707
Nd	2.31	2.82	2.60	2.60	2.55	0.578	3.39	1.94	1.81
Eu	0.919	0.664	1.15	0.841	0.725	0.360	1.07	0.717	1.11
Pb	4.72	5.20	8.87	5.23	4.36	0.75	4.46	3.55	4.57

Conc. in ppm unless otherwise stated. EMPA ID = major element data point and associated trace element data. Ca value used for normalisation and key atomic % shown. BDL= below detection limit. ID designates crystal and spot.

Table A3.2 Trace element concentrations in plagioclase crystals analysed by LA-ICP-MS.

Sample ID	SM-6C 15b	SM-6C 16a	SM-6C 16c	SM-6C 16d	Maketawa 1a	Maketawa 2a	Maketawa 2b	Maketawa 3a	Maketawa 3b
Zone	core	rim	sieved	core	core	rim	core	rim	core
EMPA ID	P15_5	P16_1	P16_4	P16_8	P1_2	P2_2	P2_5	P3_1	P3_5
An	62.43	54.46	49.35	52.74	71.12	45.37	60.73	48.46	50.29
CaO (wt%)	12.29	10.83	9.86	10.58	14.35	9.06	12.31	9.63	9.94
Li	6.33	6.71	5.33	8.65	10.7	9.89	8.73	9.11	7.00
Mg	562.852	476.545	372.999	321.802	490.031	337.870	388.034	267.011	305.995
Mg	576.933	492.568	368.493	339.941	515.317	348.447	354.078	244.524	288.523
Mg	570	485	371	331	503	343	371	256	297
Rb	BDL	BDL	0.60	BDL	BDL	BDL	BDL	BDL	BDL
Sr	1507	1458	1261	1257	1799	1629	2176	1707	1801
Y	0.222	0.376	0.340	0.620	BDL	BDL	BDL	BDL	BDL
Cs	BDL	BDL	BDL	BDL	BDL	BDL	BDL	BDL	BDL
Ba	455	409	302	269	187	840	578	512	621
La	3.95	4.22	3.85	4.11	1.90	7.17	4.95	5.65	5.77
Ce	5.89	5.89	5.95	6.46	3.41	10.1	5.77	6.84	8.29
Pr	0.542	0.547	0.553	0.591	0.193	0.810	0.540	0.527	0.646
Nd	1.63	2.14	1.81	2.16	1.15	2.32	1.40	1.63	2.10
Eu	0.899	0.661	0.630	0.743	0.249	1.19	0.766	0.645	0.776
Pb	3.36	3.96	4.89	4.86	1.96	6.10	6.01	4.99	5.09

Conc. in ppm unless otherwise stated. EMPA ID = major element data point and associated trace element data. Ca value used for normalisation and key atomic % shown. BDL= below detection limit. ID designates crystal and spot.

Table A3.2 Trace element concentrations in plagioclase crystals analysed by LA-ICP-MS.

Sample ID	Maketawa	Maketawa	Maketawa	Maketawa	Maketawa	Maketawa	Maketawa	Maketawa	Maketawa	Maketawa
Zone	5a	5b	6a	6b	6c	6e	7	8a	8b	
	rim	zone	rim	core	zone	rim	core	rim	sieved	
EMPA ID	P5_1	P5_2	P6_1	P6_4	P6_2	P6_10	P7_2	P8_1	P8_4	
An	51.54	66.80	48.20	64.44	68.54	57.74	61.87	53.59	52.35	
CaO (wt%)	10.25	13.29	9.68	12.91	13.70	11.59	12.16	10.71	10.46	
Li	12.4	8.36	18.2	6.72	14.3	22.2	17.4	10.9	12.8	
Mg	338.447	339.071	373.654	411.828	351.210	380.569	348.775	371.880	176.520	
Mg	351.301	309.634	372.217	416.065	325.207	353.635	303.581	344.298	169.875	
Mg	345	324	373	414	338	367	326	358	173	
Rb	BDL	BDL	0.554	2.19	BDL	BDL	BDL	BDL	BDL	
Sr	1873	1700	1497	1683	1548	1815	1642	1484	1552	
Y	BDL	BDL	BDL	BDL	0.604	BDL	BDL	BDL	BDL	
Cs	BDL	BDL	BDL	0.132	BDL	BDL	BDL	BDL	BDL	
Ba	617	327	416	340	214	660	370	353	676	
La	5.71	3.13	4.26	2.69	3.27	5.75	3.04	3.13	6.61	
Ce	8.38	4.21	6.18	4.92	4.97	9.13	4.74	4.94	8.54	
Pr	0.625	0.312	0.488	0.386	0.483	0.646	0.500	0.330	0.787	
Nd	2.60	1.06	1.49	1.63	2.07	2.19	1.53	1.26	1.88	
Eu	0.837	0.414	0.778	0.495	0.560	0.932	0.553	0.619	1.28	
Pb	4.69	4.07	3.87	5.09	3.32	6.05	4.12	3.21	7.58	

Conc. in ppm unless otherwise stated. EMPA ID = major element data point and associated trace element data. Ca value used for normalisation and key atomic % shown. BDL= below detection limit. ID designates crystal and spot.

Table A3.2 Trace element concentrations in plagioclase crystals analysed by LA-ICP-MS.

Sample ID	Maketawa		Maketawa		Inglewood b		Inglewood b		Inglewood b		Inglewood b		Inglewood b					
	10a	rim	10c	core	1b	core	3	core	4a	rim	4b	sieved	4e	core	5a	zone	5c	core
EMPA ID	P10_1		P10_4		P1_7		P3_7		P4_1		P4_7		P4_12		P5_2		P5_12	
An	53.06		70.30		67.69		45.60		46.65		49.35		84.60		65.72		43.57	
CaO (wt%)	10.49		14.18		13.69		8.97		9.26		9.93		17.20		13.10		8.56	
Li	8.72		4.21		6.55		10.0		12.6		9.11		3.39		9.07		8.83	
Mg	310.605		229.279		325.122		208.977		243.513		237.933		182.182		687.319		174.471	
Mg	295.579		191.696		341.991		215.236		219.059		228.503		194.928		687.526		178.473	
Mg	303		210		334		212		231		233		189		687		176	
Rb	0.427		BDL		BDL		0.57		BDL		BDL		BDL		BDL		1.00	
Sr	1581		1209		1571		1401		1401		1327		1252		1792		1171	
Y	BDL		BDL		0.134		0.273		BDL		BDL		BDL		0.162		BDL	
Cs	BDL		BDL		BDL		BDL		BDL		BDL		BDL		BDL		BDL	
Ba	393		214		222		647		750		548		72.0		340		317	
La	3.31		1.87		2.52		6.18		5.63		5.45		0.76		2.43		2.68	
Ce	5.19		2.72		3.96		8.30		9.43		9.65		1.46		3.73		5.44	
Pr	0.442		0.275		0.338		0.695		1.09		0.850		0.133		0.307		0.382	
Nd	1.75		0.78		1.25		2.22		3.41		3.55		0.63		1.38		1.35	
Eu	0.572		0.223		0.537		1.05		1.33		0.967		0.209		0.572		0.743	
Pb	4.31		3.20		3.93		8.08		10.7		7.94		1.37		2.52		6.40	

Conc. in ppm unless otherwise stated. EMPA ID = major element data point and associated trace element data. Ca value used for normalisation and key atomic % shown. BDL= below detection limit. ID designates crystal and spot.

Table A3.2 Trace element concentrations in plagioclase crystals analysed by LA-ICP-MS.

Sample ID	Inglewood b	Inglewood b	Inglewood b	Inglewood b	Inglewood b	Inglewood b	Inglewood b	Inglewood b	Inglewood b	Inglewood b	Inglewood b	Inglewood b
Zone	9a	9b	9c	13b	13c	14a	14b	14c	14d			
	rim	zone	core	zone	core	rim	core	rim	core			core
EMPA ID	P9_1	P9_2	P9_4	P13_4	P13_5	P14_2	P14_4	P14_6	P14_10			
An	43.08	59.28	42.44	67.19	86.94	44.33	44.88	44.18	50.06			
CaO (wt%)	8.69	12.06	8.59	13.41	17.71	8.85	8.81	8.66	9.88			
Li	12.6	6.74	9.96	7.30	5.92	9.85	14.2	8.51	11.0			
Mg	286.826	287.248	204.882	261.218	379.111	237.339	238.055	213.285	261.174			
Mg	281.107	298.713	212.704	272.145	414.436	244.895	218.422	210.757	256.246			
Mg	284	293	209	267	397	241	228	212	259			
Rb	BDL	0.284	0.857	BDL	BDL	0.769	BDL	0.779	0.734			
Sr	1382	1521	1416	1653	1875	1403	1386	1438	1586			
Y	BDL	0.303	BDL	0.163	0.140	BDL	BDL	0.190	0.214			
Cs	BDL	BDL	BDL	BDL	BDL	BDL	BDL	BDL	BDL			
Ba	619	351	706	246	189	677	723	664	691			
La	6.42	2.94	6.33	2.75	2.20	5.68	6.20	5.16	6.01			
Ce	8.27	5.02	8.85	4.19	3.78	8.57	9.78	8.19	8.81			
Pr	0.752	0.436	0.653	0.436	0.403	0.704	0.682	0.630	0.766			
Nd	1.75	1.56	2.01	1.36	1.22	2.03	2.72	1.55	2.13			
Eu	0.861	0.624	1.15	0.661	0.492	0.891	1.26	1.02	1.10			
Pb	7.48	4.32	9.16	4.60	2.51	9.09	8.18	7.43	7.60			

Conc. in ppm unless otherwise stated. EMPA ID = major element data point and associated trace element data. Ca value used for normalisation and key atomic % shown. BDL= below detection limit. ID designates crystal and spot.

Table A3.2 Trace element concentrations in plagioclase crystals analysed by LA-ICP-MS.

Sample ID	Inglewood b	Inglewood b	Inglewood b	Inglewood b	Inglewood a	Inglewood a	Inglewood a	Inglewood a	Inglewood a	Inglewood a
Zone	17a	17b	21a	21b	1a	1b	1c	8a	8c	8c
	rim	zone	zone	sieved	rim	zone	core	rim	sieved	sieved
EMPA ID	P17_2	P17_5	P21_2	P21_3	P1_3	P1_4	P1_9	P8_1	P8_4	
An	47.88	43.94	43.09	71.58	39.57	43.11	82.49	42.77	50.79	
CaO (wt%)	9.63	8.61	8.55	14.41	7.99	8.75	16.61	8.70	10.44	
Li	9.63	16.5	8.81	5.53	7.16	8.51	3.84	8.40	6.52	
Mg	218.493	194.589	208.815	369.920	191.993	209.849	221.653	190.628	166.758	
Mg	224.513	215.589	226.567	405.255	184.820	203.913	198.734	180.328	167.253	
Mg	222	205	218	388	188	207	210	185	167	
Rb	0.673	0.580	0.611	0.846	0.630	0.559	BDL	0.554	BDL	
Sr	1537	1359	1319	1788	1211	1386	1588	1277	1274	
Y	BDL	0.173	0.170	BDL	0.263	0.182	BDL	0.133	BDL	
Cs	BDL	BDL	BDL	BDL	BDL	BDL	BDL	BDL	BDL	
Ba	652	658	626	253	561	596	152	541	353	
La	5.66	6.03	5.59	2.34	5.53	5.12	1.49	4.97	3.93	
Ce	7.98	7.92	8.36	4.10	7.49	7.42	2.21	7.15	6.53	
Pr	0.532	0.634	0.685	0.384	0.596	0.613	0.185	0.498	0.377	
Nd	2.04	1.95	2.21	1.61	2.12	1.89	0.84	1.66	2.49	
Eu	0.883	1.042	0.941	0.358	0.786	0.859	0.250	0.878	0.697	
Pb	6.51	7.22	6.77	3.40	6.16	6.44	2.93	6.76	4.87	

Conc. in ppm unless otherwise stated. EMPA ID = major element data point and associated trace element data. Ca value used for normalisation and key atomic % shown. BDL= below detection limit. ID designates crystal and spot.

Table A3.2 Trace element concentrations in plagioclase crystals analysed by LA-ICP-MS.

Sample ID	Inglewood a	Inglewood a	Inglewood a	Inglewood a	Inglewood a	Inglewood a	Inglewood a	Inglewood a	Inglewood a	Inglewood a	Inglewood a
Zone	12a	12c	19a	19c	19d	21b	21c	22a	22b	21a	22c
	rim	sieved	rim	zone	core	sieved	core	rim	zone	core	rim
EMPA ID	P12_1	P12_7	P19_2	P19_6	P19_7	P21_3	P21_5	P22_1	P22_3		
An	45.58	48.34	42.55	73.22	84.34	43.11	39.05	44.47	44.42		
CaO (wt%)	8.99	9.64	8.68	14.73	17.43	8.60	7.85	8.95	9.12		
Li	6.61	9.03	9.38	6.56	2.82	7.31	7.82	11.0	8.90		
Mg	191.322	234.293	192.156	291.960	233.548	144.189	175.294	199.526	206.635		
Mg	191.447	232.965	186.522	266.417	219.401	150.304	184.758	228.251	205.795		
Mg	191	234	189	279	226	147	180	214	206		
Rb	BDL	BDL	0.468	BDL	BDL	BDL	0.376	0.84	1.19		
Sr	1405	1357	1363	1622	1485	1208	1246	1489	1388		
Y	BDL	0.386	0.197	BDL	BDL	BDL	0.191	0.168	0.331		
Cs	BDL	BDL	BDL	BDL	BDL	BDL	BDL	BDL	BDL		
Ba	537	714	540	199	95.3	369	553	796	632		
La	5.01	6.28	5.34	2.52	1.61	4.06	4.59	6.37	5.67		
Ce	6.80	9.96	8.43	3.28	2.36	5.14	6.82	9.13	8.09		
Pr	0.538	0.859	0.653	0.350	0.306	0.323	0.645	0.737	0.639		
Nd	1.21	2.00	2.08	1.20	1.35	1.33	1.96	1.97	2.12		
Eu	0.768	0.995	0.906	0.576	0.385	0.659	0.902	1.14	0.887		
Pb	6.22	9.07	7.09	4.23	1.97	5.99	6.12	9.01	7.10		

Conc. in ppm unless otherwise stated. EMPA ID = major element data point and associated trace element data. Ca value used for normalisation and key atomic % shown. BDL= below detection limit. ID designates crystal and spot.

Table A3.2 Trace element concentrations in plagioclase crystals analysed by LA-ICP-MS.

Sample ID	Inglewood a		Inglewood a		Inglewood a		Inglewood a		Inglewood a		Inglewood a		Korito					
	22c	zone	22d	zone	22e	core	22f	core	22g	rim	24a	rim	24b	zone	2b	sieved	2c	sieved
EMPA ID	P22_3		P22_3		P22_5		P22_5		P22_1		P24_1		P24_1		P2_2		P2_3	
An	44.42		44.42		65.72		65.72		44.47		42.43		42.43		77.00		81.97	
CaO (wt%)	9.12		9.12		13.12		13.12		8.95		8.73		8.73		15.49		16.70	
Li	8.05		8.18		7.30		4.52		9.97		9.59		7.80		8.58		6.46	
Mg	202.318		191.354		211.321		266.247		200.128		200.503		195.914		293.354		141.467	
Mg	189.311		232.082		204.524		255.293		220.050		209.072		199.119		320.333		157.976	
Mg	196		212		208		261		210		205		198		307		150	
Rb	0.48		BDL		BDL		2.76		BDL		0.65		0.75		BDL		BDL	
Sr	1378		1398		1528		1458		1458		1420		1422		1675		1240	
Y	0.166		BDL		BDL		0.998		BDL		0.131		0.164		BDL		BDL	
Cs	BDL		BDL		BDL		0.306		BDL		BDL		BDL		BDL		BDL	
Ba	493		490		231		224		634		631		667		173		135	
La	4.91		5.55		2.53		3.78		6.43		5.70		5.71		3.20		2.37	
Ce	6.80		7.54		3.79		6.63		8.99		7.70		7.68		5.22		6.80	
Pr	0.608		0.639		0.340		0.645		0.784		0.615		0.622		0.462		0.478	
Nd	1.57		1.22		1.23		2.09		2.17		1.85		2.01		2.36		1.56	
Eu	0.803		0.895		0.598		0.545		0.937		1.10		1.02		0.562		0.420	
Pb	5.91		4.75		3.51		4.17		7.18		7.23		7.05		2.93		5.90	

Conc. in ppm unless otherwise stated. EMPA ID = major element data point and associated trace element data. Ca value used for normalisation and key atomic % shown. BDL= below detection limit. ID designates crystal and spot.

Table A3.2 Trace element concentrations in plagioclase crystals analysed by LA-ICP-MS.

Sample ID	Zone	Korito 3c	Korito 6a	Korito 6b	Korito 6d	Korito 6e	Korito 7a	Korito 7b	Korito 14b	Korito 14d
		core	rim	zone	sieved	sieved	rim	core	zone	core
EMPA ID		P3_9	P6_2	P6_5	P6_7	P6_7	P7_1	P7_4	P14_4	P14_10
An		75.58	68.32	40.96	45.55	45.55	42.40	67.35	41.17	49.85
CaO (wt%)		15.36	13.97	8.43	9.03	9.03	8.45	13.59	8.44	10.27
Li		5.62	7.04	14.5	7.68	8.50	15.1	11.8	9.57	8.31
Mg		412.291	412.216	190.021	155.130	547.854	185.160	293.508	230.019	241.096
Mg		427.004	439.105	213.188	153.547	585.083	184.048	280.266	235.767	257.898
Mg		420	426	202	154	566	185	287	233	249
Rb		BDL	BDL	BDL	BDL	4.30	BDL	BDL	BDL	0.486
Sr		1776	1503	1411	1128	1045	1312	1902	1516	1567
Y		BDL	0.424	BDL	BDL	1.442	BDL	BDL	BDL	BDL
Cs		BDL	BDL	BDL	BDL	0.545	BDL	BDL	BDL	BDL
Ba		211	165	670	385	370	561	376	723	538
La		2.10	2.26	5.60	4.21	4.45	5.68	4.18	5.84	5.16
Ce		3.33	4.41	6.99	6.94	7.20	7.56	6.73	8.71	7.74
Pr		0.319	0.445	0.513	0.518	0.802	0.527	0.582	0.661	0.657
Nd		1.14	1.67	1.04	1.51	3.43	1.54	2.05	1.67	1.90
Eu		0.494	0.488	0.904	0.609	0.636	0.910	0.819	0.931	0.893
Pb		2.13	2.57	7.43	5.02	6.38	6.67	5.37	8.08	7.26

Conc. in ppm unless otherwise stated. EMPA ID = major element data point and associated trace element data. Ca value used for normalisation and key atomic % shown. BDL= below detection limit. ID designates crystal and spot.

Table A3.2 Trace element concentrations in plagioclase crystals analysed by LA-ICP-MS.

Sample ID	Zone	Korito 15a	Korito 15b	Korito 15c	Korito 19	Korito 21a	Korito 21c	Korito 24
EMPA ID		P15_2	P15_5	P15_9	P19_6	P21_1	P21_5	P24_3
An		43.93	43.71	78.74	74.20	43.00	85.20	62.11
CaO (wt%)		8.89	8.95	16.07	14.66	8.76	17.34	12.68
Li		8.04	9.54	3.03	6.40	9.21	2.65	7.36
Mg		212.905	200.544	221.565	370.212	250.434	337.406	212.863
Mg		214.368	180.867	218.073	399.447	263.581	356.330	214.108
Mg		214	191	220	385	257	347	213
Rb		0.665	0.825	BDL	2.686	BDL	BDL	0.202
Sr		1331	1448	1659	1434	1667	1327	1676
Y		0.212	0.160	BDL	0.766	BDL	0.135	BDL
Cs		BDL	BDL	BDL	0.160	BDL	BDL	BDL
Ba		521	706	165	226	848	79.1	217
La		4.74	5.72	1.92	2.74	7.10	1.33	3.16
Ce		6.79	8.07	4.40	5.29	9.04	1.94	4.93
Pr		0.549	0.676	0.225	0.544	0.711	0.197	0.468
Nd		1.89	2.01	1.44	1.93	2.76	0.74	1.94
Eu		0.897	1.05	0.443	0.596	1.116	0.271	0.635
Pb		6.03	7.26	4.91	4.67	7.81	1.28	3.67

Conc. in ppm unless otherwise stated. EMPA ID = major element data point and associated trace element data. Ca value used for normalisation and key atomic % shown. BDL= below detection limit. ID designates crystal and spot.

Table A3.3 Trace element concentrations in clinopyroxene crystals analysed by LA-ICP-MS. Abbreviations same as Table A3.2.

Sample ID	Zone	EMPA ID	CaO (wt%)	Mg#	Mn (wt%)	4a	4b	4c	4e	4g	8c	8d	22a	22b	22c
						rims	zone	zone	zone	core	core	dark rim	rim	zone	zone
						cpx4_2	cpx4_3	cpx4_3	cpx4_7	cpx4_11	cpx8_3	cpx8_9	cpx22_1	cpx22_2	cpx22_2
						20.78	20.90	20.90	21.93	20.93	21.56	21.20	20.72	21.47	21.47
						78.54	81.66	81.66	87.95	82.66	83.12	88.18	82.86	85.80	85.80
						0.694	0.703	0.614	0.156	0.408	0.544	0.155	0.609	0.528	0.503
Li						9.59	10.2	9.03	8.68	10.0	7.79	3.15	5.22	5.88	5.99
Sc						103	97.0	91.4	96.4	99.1	48.3	123	70.5	67.6	65.4
Ti						1830	1642	1810	1327	3056	2265	1610	1481	1687	1724
V						156	119	129	84.9	212	178	146	114	125	121
Cr						BDL	BDL	BDL	2693	BDL	BDL	385	BDL	BDL	BDL
Ni						6.16	5.60	8.71	164	19.0	8.16	133	8.64	10.2	9.56
Cu						2.56	0.80	3.81	4.00	3.99	7.18	4.49	1.16	1.67	1.15
Zn						102	85.0	90.3	32.6	65.3	92.6	21.4	72.7	73.7	68.4
Sr						31.8	30.1	36.5	45.3	41.6	46.7	36.6	33.9	38.4	43.5
Y						65.3	74.8	53.6	8.1	41.3	35.8	14.0	53.5	41.0	40.8
Zr						62.4	49.5	38.9	5.1	43.6	69.9	12.3	42.6	44.7	45.8
La						6.13	8.96	5.05	0.76	4.03	5.23	0.86	6.32	5.02	6.52
Ce						26.5	36.1	23.1	3.3	17.8	19.9	2.8	24.5	19.4	22.6
Pr						5.81	6.97	4.56	0.60	3.35	3.93	0.65	4.79	3.55	4.32
Nd						35.0	35.5	26.0	4.2	21.8	19.5	4.5	27.4	21.5	24.7
Sm						11.3	13.8	10.1	2.13	7.77	5.89	1.29	8.04	6.48	9.09
Eu						1.73	2.20	2.08	0.58	1.81	1.39	0.63	2.08	1.75	1.59
Gd						13.0	13.0	10.5	1.25	8.00	6.57	2.37	9.44	7.57	7.51
Tb						1.85	2.34	1.59	0.233	1.31	0.96	0.26	1.57	1.33	1.38
Dy						13.8	15.1	10.4	1.12	8.76	5.93	2.38	10.2	8.94	8.13
Ho						3.00	3.27	1.88	0.244	1.58	1.21	0.67	2.17	1.37	1.33
Er						8.07	7.78	6.23	0.769	4.13	4.12	1.35	5.45	4.35	3.79
Tm						1.06	1.18	0.558	0.134	0.629	0.539	0.137	0.605	0.538	0.552
Yb						6.70	8.67	4.42	0.609	3.58	3.47	1.01	4.86	3.75	3.66
Lu						0.800	1.12	0.835	0.179	0.597	0.550	0.175	1.06	0.523	0.690
Hf						2.66	2.50	1.47	0.236	2.15	2.80	0.349	2.07	2.57	1.73

Table A3.3 Trace element concentrations in clinopyroxene crystals analysed by LA-ICP-MS. Abbreviations same as Table A3.2.

Sample ID	Zone	EMPA ID	CaO (wt%)	Mg#	Mn (wt%)	22g	27a	27b	27e	27f	27h	33a	33b	33c	33d
						core	rim	zone	zone	zone	core	dark rim	zone	core	core
						cpx22_6	cpx27_1	cpx27_5	cpx27_7	cpx27_6	cpx27_9	cpx33_1	cpx33_7	cpx33_7	cpx33_9
						21.89	21.69	21.52	21.74	21.16	21.93	21.71	20.56	20.56	21.99
						84.40	83.91	88.97	84.23	79.37	84.39	86.60	78.14	78.14	81.05
						0.539	0.315	0.154	0.561	0.630	0.505	0.452	0.891	0.856	0.661
Li						7.56	5.53	4.91	7.83	5.96	6.96	10.4	14.0	12.4	9.95
Sc						92.1	57.0	98.8	81.3	80.5	72.6	67.1	55.2	57.6	50.6
Ti						1928	2346	1647	1574	1356	2155	2166	2556	2635	2119
V						141	192	147	139	115	153	192	212	205	119
Cr						BDL	BDL	115.0	BDL	BDL	BDL	26.4	BDL	BDL	BDL
Ni						5.65	7.36	126	9.30	4.48	5.21	74.2	17.0	19.9	5.66
Cu						2.81	3.45	3.90	3.91	4.02	3.40	3.67	6.12	5.88	3.54
Zn						75.9	53.8	23.9	82.3	84.9	81.5	76.6	154	130	84.7
Sr						41.8	41.9	37.3	35.3	35.8	46.1	55.5	52.8	52.3	41.3
Y						50.8	24.1	11.2	45.1	44.0	42.4	29.5	50.6	53.3	44.3
Zr						59.7	62.0	10.2	43.6	40.5	59.3	45.1	70.5	70.3	40.4
La						5.95	2.30	0.62	4.74	4.63	5.91	3.21	4.44	5.30	3.92
Ce						26.0	11.0	3.2	20.8	21.6	24.2	16.4	22.1	24.2	17.7
Pr						5.03	1.91	0.58	3.75	4.34	4.52	2.71	4.14	4.05	3.73
Nd						29.4	11.8	3.5	23.1	23.6	25.6	16.4	23.5	24.9	21.6
Sm						9.23	4.80	1.26	7.40	8.04	8.16	5.11	7.01	6.30	8.10
Eu						1.95	1.28	0.49	1.70	1.90	1.89	1.73	1.86	1.89	1.75
Gd						7.85	4.25	2.81	6.73	7.23	8.32	5.86	7.59	8.04	8.40
Tb						1.64	0.79	0.15	1.58	1.22	1.32	0.98	1.36	1.16	1.35
Dy						10.9	5.23	2.74	8.08	9.07	8.46	5.13	8.43	8.44	7.94
Ho						1.87	1.09	0.42	2.01	1.50	1.61	1.05	1.83	1.69	1.53
Er						5.04	1.92	0.89	4.53	5.45	4.82	3.26	5.30	5.56	5.26
Tm						0.798	0.357	0.235	0.631	0.606	0.522	0.377	0.641	0.714	0.864
Yb						4.56	1.35	0.86	4.52	3.08	4.12	2.73	5.06	5.25	3.32
Lu						0.743	0.469	0.107	0.561	0.800	0.641	0.357	0.596	0.748	0.713
Hf						1.82	3.15	0.244	2.24	1.75	2.87	1.52	2.63	2.47	1.86

Table A3.3 Trace element concentrations in clinopyroxene crystals analysed by LA-ICP-MS. Abbreviations same as Table A3.2.

Sample ID	Kaupokonui	Kaupokonui	Kaupokonui	Kaupokonui	Kaupokonui	Kaupokonui	Kaupokonui	Kaupokonui	Kaupokonui	Kaupokonui	Kaupokonui	Kaupokonui	Kaupokonui	Kaupokonui
Zone	33e	33f	64c	64d	64e	64g	64h	66a	66e	66f	zone	rim	zone	core
EMPA ID	cpx33_7	cpx33_9	cpx64_6	cpx64_6	cpx64_7	cpx64_9	cpx64_6	cpx66_4	cpx66_10	cpx66_12				
CaO (wt%)	20.56	21.99	22.05	22.05	21.05	21.08	22.05	22.16	22.36	21.91				
Mg#	78.14	81.05	84.39	84.39	82.36	82.96	84.39	81.81	79.50	83.43				
Mn (wt%)	0.605	0.698	0.622	0.535	0.639	0.623	0.607	0.580	0.642	0.551				
Li	10.9	9.47	6.41	7.49	9.32	8.98	7.09	7.28	6.76	7.18				
Sc	55.5	52.5	80.7	94.0	56.0	57.6	88.0	124	103	48.4				
Ti	2504	1835	1464	1700	2391	2452	1603	1412	1182	1675				
V	168	115	116	124	147	150	120	145	156	126				
Cr	BDL	BDL	BDL	BDL	BDL	BDL	BDL	BDL	BDL	BDL				
Ni	10.8	5.71	4.88	4.05	10.7	10.5	5.93	6.10	6.13	4.06				
Cu	5.44	2.13	2.16	1.50	2.47	2.97	2.96	1.35	2.63	1.32				
Zn	104	103	86.9	76.1	103	102	82.8	92.0	102	76.6				
Sr	42.3	37.0	34.5	38.7	39.4	43.7	37.0	33.1	28.8	41.9				
Y	42.4	43.7	47.8	45.0	47.3	47.2	51.4	46.4	36.4	33.6				
Zr	56.0	36.7	45.4	45.4	49.1	65.4	45.6	48.7	34.5	42.7				
La	4.41	4.06	5.70	4.67	3.82	4.28	5.64	5.36	5.14	4.79				
Ce	20.9	19.8	23.2	22.0	18.3	20.5	23.3	23.1	21.3	20.0				
Pr	4.10	3.76	4.46	4.47	3.66	4.03	4.62	4.52	4.09	3.74				
Nd	22.8	20.4	25.1	23.5	21.2	25.7	24.7	26.2	21.8	20.0				
Sm	6.38	8.70	8.67	7.80	7.63	8.21	10.27	8.88	7.59	6.63				
Eu	1.74	1.72	1.96	1.83	1.70	2.37	2.20	1.71	1.29	1.34				
Gd	5.72	7.34	8.92	7.94	7.88	7.48	9.36	9.29	7.08	7.38				
Tb	1.52	1.34	1.45	1.53	1.26	1.16	1.59	1.60	1.13	1.14				
Dy	7.60	8.42	9.58	8.66	9.62	9.11	9.65	9.41	7.05	7.61				
Ho	1.54	1.23	2.03	1.79	1.66	1.79	2.01	1.89	1.34	1.42				
Er	4.77	5.18	5.76	6.34	6.08	6.01	5.72	5.58	4.46	4.68				
Tm	0.567	0.846	0.708	0.514	0.670	0.911	0.856	0.659	0.486	0.539				
Yb	3.56	5.06	4.71	3.73	4.74	4.26	3.83	4.38	3.54	2.80				
Lu	0.626	0.813	0.614	0.494	0.666	0.628	0.516	0.696	0.621	0.449				
Hf	3.54	2.08	1.92	1.76	2.28	1.89	2.32	2.28	1.88	1.90				

Table A3.3 Trace element concentrations in clinopyroxene crystals analysed by LA-ICP-MS. Abbreviations same as Table A3.2.

Sample ID	Kaupokonui	Kaupokonui	Kaupokonui	Kaupokonui	Kaupokonui	Kaupokonui	SM-6C	SM-6C	SM-6C	SM-6C	SM-6C	SM-6C	SM-6C	SM-6C	SM-6C	SM-6C	SM-6C		
Zone																			
EMPA ID																			
CaO (wt%)																			
Mg#																			
Mn (wt%)																			
Li	6.21	6.48	6.43	0.566	0.629	0.636	0.534	0.428	0.428	0.567	0.567	0.567	0.686	0.697	0.724	0.705	0.589	0.535	0.701
Sc	98.3	81.8	106	6.43	6.48	6.21	5.92	6.36	6.36	6.73	6.73	6.73	7.13	6.43	4.17	6.04	5.62	6.53	6.51
Ti	1316	1330	1547	106	1330	1316	92.7	86.4	86.4	63.1	63.1	63.1	61.6	47.6	49.4	47.9	58.9	84.3	52.3
V	171	174	150	1547	174	171	1509	2525	2525	2411	2411	2411	2487	2058	1606	1995	2347	2719	2011
Cr	BDL	BDL	BDL	BDL	BDL	BDL	BDL	BDL	BDL	BDL	BDL	BDL	BDL	BDL	BDL	BDL	BDL	BDL	BDL
Ni	4.93	5.00	7.63	7.63	5.00	4.93	7.95	17.7	17.7	9.81	9.81	9.81	6.80	8.78	12.3	7.79	10.2	16.3	8.22
Cu	2.13	3.36	1.47	1.47	3.36	2.13	1.29	2.65	2.65	3.14	3.14	3.14	4.05	6.44	3.92	2.50	3.90	5.83	3.13
Zn	100	101	85.9	85.9	101	100	83.7	60.4	60.4	93.8	93.8	93.8	106	109	95.0	104	77.5	83.7	108
Sr	29.1	29.2	35.8	35.8	29.2	29.1	37.0	41.3	41.3	40.5	40.5	40.5	38.7	36.4	34.4	37.8	37.8	47.2	38.0
Y	34.0	35.1	44.7	44.7	35.1	34.0	43.6	36.6	36.6	38.0	38.0	38.0	50.6	38.5	44.0	39.4	50.4	47.7	45.8
Zr	38.8	42.8	49.2	49.2	42.8	38.8	46.0	31.8	31.8	54.6	54.6	54.6	59.1	61.0	40.8	65.2	44.7	37.1	62.8
La	6.28	5.76	5.39	5.39	6.28	6.28	5.09	2.78	2.78	3.87	3.87	3.87	4.72	4.28	4.43	4.23	4.19	4.00	3.98
Ce	22.9	23.1	22.1	22.1	22.9	22.9	22.6	13.9	13.9	17.6	17.6	17.6	21.4	15.9	18.3	17.7	19.1	18.3	19.7
Pr	3.99	4.15	4.37	4.37	4.15	3.99	4.31	2.69	2.69	3.33	3.33	3.33	3.82	3.49	3.92	3.58	3.68	3.73	3.97
Nd	19.6	21.7	23.3	23.3	19.6	19.6	24.6	17.5	17.5	20.5	20.5	20.5	24.9	18.5	22.3	20.2	23.8	21.0	21.0
Sm	6.70	6.01	8.71	8.71	6.70	6.70	8.46	5.69	5.69	6.44	6.44	6.44	8.13	5.69	6.57	6.73	7.75	8.31	6.67
Eu	1.05	1.25	1.74	1.74	1.05	1.05	1.68	1.60	1.60	1.85	1.85	1.85	1.73	1.12	1.60	1.30	1.79	1.93	1.25
Gd	6.46	5.75	8.60	8.60	6.46	6.46	8.99	8.31	8.31	6.37	6.37	6.37	10.0	6.59	6.54	6.78	7.21	7.97	8.90
Tb	0.86	1.12	1.52	1.52	0.86	0.86	1.40	1.37	1.37	1.15	1.15	1.15	1.32	1.20	1.10	1.24	1.53	1.42	1.30
Dy	6.18	6.86	8.92	8.92	6.18	6.18	8.73	6.76	6.76	7.73	7.73	7.73	11.1	6.91	8.95	6.68	10.4	9.09	7.65
Ho	1.39	1.25	1.74	1.74	1.39	1.39	1.69	1.29	1.29	1.34	1.34	1.34	1.92	1.28	2.13	1.41	1.79	1.83	1.67
Er	4.36	4.05	4.91	4.91	4.36	4.36	4.98	3.79	3.79	4.93	4.93	4.93	6.38	3.46	4.97	3.83	5.08	4.82	5.35
Tm	0.488	0.479	0.539	0.539	0.488	0.488	0.668	0.517	0.517	0.526	0.526	0.526	0.781	0.506	0.672	0.554	0.791	0.711	0.756
Yb	3.30	3.70	4.78	4.78	3.30	3.30	4.25	3.88	3.88	4.12	4.12	4.12	3.94	3.61	4.49	4.26	5.06	4.09	5.45
Lu	0.696	0.767	0.566	0.566	0.696	0.696	0.681	0.466	0.466	0.567	0.567	0.567	0.909	0.491	0.569	0.441	0.851	0.538	0.487
Hf	2.31	2.30	2.24	2.24	2.31	2.31	1.90	1.33	1.33	1.94	1.94	1.94	2.58	3.11	1.73	3.22	3.08	1.53	2.99

Table A3.3 Trace element concentrations in clinopyroxene crystals analysed by LA-ICP-MS. Abbreviations same as Table A3.2.

Sample ID	SM-6C	SM-6C	SM-6C	SM-6C	SM-6C	SM-6C	SM-6C	SM-6C	SM-6C	SM-6C	SM-6C	SM-6C	SM-6C	SM-6C	SM-6C	SM-6C	SM-6C	SM-6C
Zone	16c	16d	20a	20d	29c	29h	29j	29k	31a	31c	31f	33b	33c	33e	33f	33g	33h	33i
EMPA ID	core	zone	rim	core	rim	zone	zone	core	core	zone	rim	core	zone	rim	rim	core	zone	rim
CaO (wt%)	cpx16_7	cpx16_7	cpx20_1	cpx20_5	cpx29_2	cpx29_3	cpx29_3	cpx29_4	cpx31_4	cpx31_2	cpx31_1	cpx33_3	cpx33_2	cpx33_2	cpx31_1	cpx33_3	cpx33_2	cpx33_2
Mg#	20.82	20.82	19.97	21.70	20.35	20.80	20.80	21.72	20.66	21.24	20.95	21.50	21.34	21.34	20.95	21.50	21.34	21.34
Mn (wt%)	76.54	76.54	79.30	76.86	77.46	81.93	81.93	78.68	81.06	81.45	81.68	81.97	82.74	82.74	81.68	81.97	82.74	82.74
Li	0.652	0.454	0.354	0.713	0.404	0.402	0.442	0.539	0.572	0.622	0.446	0.410	0.389	0.441	0.446	0.410	0.389	0.441
Sc	4.54	5.78	5.77	5.54	5.15	5.36	5.20	4.78	4.61	6.16	5.81	5.60	5.40	5.79	5.81	5.60	5.40	5.79
Ti	45.5	86.5	93.9	60.0	87.9	109	69.6	60.1	69.6	95.3	81.1	100	90.9	83.6	81.1	100	90.9	83.6
V	1752	2830	2392	2605	2707	3969	2516	2359	1811	1728	2531	3984	3766	3036	2531	3984	3766	3036
Cr	97	178	163	147	175	236	165	186	169	179	171	236	231	189	171	236	231	189
Ni	BDL	BDL	51.0	BDL	BDL	BDL	BDL	BDL	BDL	BDL	BDL	BDL	BDL	BDL	BDL	BDL	BDL	BDL
Cu	6.52	12.6	21.6	5.13	13.3	13.1	16.2	18.9	12.3	14.2	14.0	13.8	13.3	12.8	14.0	13.8	13.3	12.8
Zn	6.76	5.47	3.76	3.15	3.75	4.16	3.57	3.06	3.99	3.51	4.01	4.19	3.61	4.68	4.01	4.19	3.61	4.68
Sr	84.9	65.9	52.1	107	56.2	58.8	66.6	79.7	80.0	96.1	67.3	62.0	59.1	63.1	67.3	62.0	59.1	63.1
Y	36.9	42.2	43.0	37.8	41.2	50.6	44.8	47.4	43.2	28.3	40.7	47.7	49.6	43.1	40.7	47.7	49.6	43.1
Zr	44.1	45.9	29.5	53.7	39.0	64.0	38.5	36.9	38.0	59.4	45.8	48.8	44.3	55.2	45.8	48.8	44.3	55.2
La	42.1	39.1	31.9	61.0	35.0	59.6	45.6	62.8	49.2	65.5	34.9	49.9	42.5	46.3	34.9	49.9	42.5	46.3
Ce	4.40	3.90	2.11	4.43	3.14	5.68	3.39	4.53	4.86	5.83	3.47	3.94	4.19	4.63	3.47	3.94	4.19	4.63
Pr	18.6	17.7	11.3	22.2	12.0	21.4	14.7	17.8	20.0	24.1	15.6	16.9	16.9	18.9	15.6	16.9	16.9	18.9
Nd	3.85	3.18	2.18	4.34	2.48	4.50	3.16	3.37	3.95	4.83	3.27	3.50	3.67	4.00	3.27	3.50	3.67	4.00
Sm	22.9	21.9	14.4	24.4	16.3	29.5	16.4	19.7	19.1	26.4	20.6	23.1	21.9	23.9	20.6	23.1	21.9	23.9
Eu	7.06	8.54	5.17	8.32	6.02	11.2	6.33	6.14	6.23	8.75	7.55	6.85	7.34	8.58	7.55	6.85	7.34	8.58
Gd	1.48	1.66	1.63	1.74	1.47	2.43	1.42	1.42	1.42	1.86	1.61	1.94	1.93	1.83	1.61	1.94	1.93	1.83
Tb	8.50	9.04	6.77	9.19	7.73	11.63	5.73	6.70	6.28	9.55	8.57	9.29	8.71	9.93	8.57	9.29	8.71	9.93
Dy	1.28	1.24	0.82	1.65	1.26	1.67	1.00	0.951	1.01	1.63	1.32	1.62	1.44	1.71	1.32	1.62	1.44	1.71
Ho	8.71	9.56	6.05	10.0	7.89	11.8	7.01	7.04	7.77	10.9	8.86	10.3	8.92	9.17	8.86	10.3	8.92	9.17
Er	1.37	1.93	1.07	2.02	1.53	2.32	1.22	1.40	1.50	2.17	1.64	2.01	1.70	1.98	1.64	2.01	1.70	1.98
Tm	5.95	5.02	3.25	6.24	4.11	6.80	3.32	4.05	4.32	6.98	5.15	5.31	4.65	4.90	5.15	5.31	4.65	4.90
Yb	0.628	0.669	0.438	0.873	0.588	0.862	0.602	0.585	0.596	0.957	0.590	0.642	0.594	0.673	0.590	0.642	0.594	0.673
Lu	3.47	3.76	1.86	5.18	3.06	5.38	3.66	3.92	3.74	5.86	3.53	4.38	3.31	4.93	3.53	4.38	3.31	4.93
Hf	0.572	0.431	0.278	0.986	0.605	0.769	0.368	0.456	0.667	0.957	0.647	0.657	0.642	0.813	0.647	0.657	0.642	0.813
	2.04	1.46	1.23	3.15	1.38	2.78	1.61	2.23	2.27	2.57	1.74	2.16	1.71	1.90	1.74	2.16	1.71	1.90

Table A3.3 Trace element concentrations in clinopyroxene crystals analysed by LA-ICP-MS. Abbreviations same as Table A3.2.

Sample ID	Maketawa Zone	Maketawa 8a	Maketawa 8b	Maketawa 8c	Maketawa 9c	Maketawa 9d	Maketawa 9e	Maketawa 9g	Maketawa 10b	Maketawa 10c	Maketawa 17b	Maketawa 17c	Maketawa 17e
EMPA ID	cpx8_1	cpx8_4	cpx8_10	cpx9_5	cpx9_6	cpx9_6	cpx9_8	cpx9_11	cpx10_6	cpx10_7	cpx17_3	cpx17_4	cpx17_10
CaO (wt%)	20.81	21.89	22.21	22.30	22.65	22.65	21.41	22.03	21.66	22.00	22.70	22.40	22.15
Mg#	82.50	80.82	79.15	82.07	79.04	79.04	80.40	83.12	80.58	74.37	80.88	84.00	82.98
Mn (wt%)	0.485	0.947	0.402	0.697	0.640	0.640	0.927	0.757	0.528	0.672	1.057	0.606	0.917
Li	4.24	5.88	8.25	4.35	4.83	4.83	7.07	4.30	5.56	6.58	5.30	5.76	6.18
Sc	49.3	59.0	67.8	86.3	92.1	92.1	35.3	75.7	52.9	41.0	114	114	42.0
Ti	1635	1434	2613	1432	1212	1212	1518	1672	1848	1459	825	1487	2115
V	114	79	179	113	118	118	69	144	120	142	99	111	105
Cr	BDL	BDL	BDL	BDL	10.6	10.6	BDL	BDL	BDL	BDL	BDL	BDL	BDL
Ni	15.3	4.74	10.7	17.1	13.3	13.3	3.39	9.69	14.4	7.78	10.4	12.8	0.91
Cu	5.25	3.62	4.52	2.35	1.04	1.04	4.35	5.49	0.12	0.95	6.65	1.47	2.45
Zn	66.1	111	55.7	98.4	100	100	106	110	81.8	133	109	84.1	115
Sr	42.0	30.2	48.0	32.1	25.7	25.7	30.1	36.6	40.3	29.7	12.0	29.2	32.6
Y	30.9	60.7	27.8	46.6	34.6	34.6	56.4	50.0	33.3	26.4	59.5	48.5	61.6
Zr	41.0	42.7	47.7	41.5	38.3	38.3	36.8	46.1	40.0	37.7	21.7	41.3	55.6
La	4.19	5.24	2.11	6.11	4.47	4.47	7.04	4.98	4.10	3.79	7.19	5.17	6.13
Ce	14.6	22.3	9.3	22.2	18.7	18.7	30.8	21.2	16.9	16.8	32.1	20.6	25.8
Pr	2.80	4.77	1.70	4.10	3.65	3.65	5.57	4.20	2.79	3.04	6.07	4.01	5.42
Nd	14.4	24.6	12.4	25.6	20.9	20.9	32.2	25.8	20.8	16.8	32.5	23.4	31.8
Sm	5.27	6.11	5.28	8.45	6.09	6.09	9.04	6.72	4.81	4.54	9.64	8.83	9.69
Eu	1.38	2.03	1.34	1.78	1.32	1.32	2.14	0.96	1.28	0.93	1.36	1.96	2.55
Gd	5.41	10.2	6.80	9.95	7.65	7.65	11.3	11.8	6.99	5.58	14.8	10.1	11.2
Tb	0.924	1.59	0.734	1.48	1.01	1.01	1.88	1.70	0.865	0.710	2.00	1.19	1.97
Dy	5.96	9.43	5.14	10.1	7.37	7.37	15.4	11.3	6.56	5.64	10.3	10.2	12.9
Ho	1.12	2.43	1.04	2.04	1.41	1.41	2.57	2.25	1.51	1.24	2.47	1.75	2.56
Er	3.94	5.88	2.77	5.38	3.71	3.71	6.84	5.16	3.55	3.07	6.19	5.30	7.14
Tm	0.630	0.998	0.316	0.774	0.544	0.544	0.920	0.855	0.486	0.352	0.435	0.768	0.896
Yb	2.95	5.75	2.01	4.79	3.22	3.22	4.82	4.88	2.91	3.46	5.84	4.54	5.95
Lu	0.289	1.03	0.234	0.786	0.618	0.618	1.00	0.793	0.217	0.623	0.857	0.717	0.948
Hf	1.33	1.01	3.04	1.62	1.88	1.88	1.82	1.75	1.88	2.11	1.16	1.09	2.67

Table A3.3 Trace element concentrations in clinopyroxene crystals analysed by LA-ICP-MS. Abbreviations same as Table A3.2.

Sample ID	Inglewood b	Inglewood b	Inglewood b	Inglewood b	Inglewood b	Inglewood b	Inglewood b	Inglewood b	Inglewood b	Inglewood b	Inglewood b	Inglewood b	Inglewood b	Inglewood b	Inglewood b
Zone	2g	10a	19a	19b	19d	19f	19g	20a	20b	20d	zone	rim	zone	zone	zone
EMPA ID	cpx2_1	cpx10_2	cpx19_1	cpx19_5	cpx19_2	cpx19_5	cpx19_2	cpx20_2	cpx20_4	cpx20_5	cpx19_2	cpx20_2	cpx20_4	cpx20_5	
CaO (wt%)	21.63	22.15	21.86	22.19	22.46	22.19	22.46	20.97	21.58	22.03	22.46	20.97	21.58	22.03	
Mg#	81.81	78.68	80.36	80.28	81.28	80.28	81.28	76.29	82.52	80.54	81.28	76.29	82.52	80.54	
Mn (wt%)	0.645	0.626	0.922	0.677	0.358	0.754	0.383	0.826	0.862	0.690	0.383	0.826	0.862	0.690	
Li	8.59	5.49	6.60	7.23	7.47	6.82	8.11	6.55	7.81	8.28	8.11	6.55	7.81	8.28	
Sc	42.5	43.2	35.3	45.0	51.4	50.4	51.7	39.9	42.0	54.7	51.7	39.9	42.0	54.7	
Ti	2077	2317	1416	1688	2765	1707	1831	1371	1431	1767	1831	1371	1431	1767	
V	105	136	68.9	104	183	96.9	147	70.6	74.2	114	147	70.6	74.2	114	
Cr	BDL	BDL	BDL	BDL	13.5	BDL	BDL	BDL	BDL	BDL	BDL	BDL	BDL	BDL	
Ni	2.95	0.867	2.12	7.27	15.24	5.99	9.31	0.391	2.39	6.68	9.31	0.391	2.39	6.68	
Cu	0.967	1.19	0.626	0.642	0.581	1.53	2.68	2.76	0.644	BDL	2.68	2.76	0.644	BDL	
Zn	103	100	121	97.7	70.1	97.4	73.8	120	126	105	73.8	120	126	105	
Sr	39.1	39.0	35.3	42.1	50.8	40.1	46.6	31.6	32.4	36.9	46.6	31.6	32.4	36.9	
Y	38.3	35.8	47.1	38.5	16.2	44.3	16.6	49.8	53.4	43.5	16.6	49.8	53.4	43.5	
Zr	56.9	74.1	34.2	33.4	32.5	38.2	27.7	37.8	40.1	50.0	27.7	37.8	40.1	50.0	
La	3.46	3.47	4.99	4.74	2.15	4.81	2.16	4.24	5.48	3.64	2.16	4.24	5.48	3.64	
Ce	15.1	13.8	22.0	20.4	9.4	18.8	8.6	17.3	23.0	15.3	8.6	17.3	23.0	15.3	
Pr	2.77	2.72	4.11	3.72	1.78	3.84	1.67	3.65	4.30	3.06	1.67	3.65	4.30	3.06	
Nd	18.9	17.8	25.0	20.9	10.4	21.8	8.3	19.5	27.6	21.1	8.3	19.5	27.6	21.1	
Sm	6.45	5.60	6.94	6.59	3.25	6.29	2.32	7.95	8.14	6.06	2.32	7.95	8.14	6.06	
Eu	2.01	1.72	1.82	1.85	1.05	1.87	1.06	0.84	1.69	1.41	1.06	0.84	1.69	1.41	
Gd	6.81	5.97	7.52	7.18	3.06	9.22	4.09	8.21	9.83	6.80	4.09	8.21	9.83	6.80	
Tb	1.57	1.20	1.34	1.13	0.51	1.51	0.61	1.33	1.47	1.07	0.61	1.33	1.47	1.07	
Dy	7.57	5.88	8.48	7.61	3.40	8.22	3.08	9.87	9.62	8.38	3.08	9.87	9.62	8.38	
Ho	1.76	1.46	1.50	1.52	0.613	1.34	0.596	1.92	2.02	2.00	0.596	1.92	2.02	2.00	
Er	4.38	3.00	4.56	4.22	1.58	4.16	1.34	5.20	6.07	5.10	1.34	5.20	6.07	5.10	
Tm	0.578	0.475	0.586	0.524	0.230	0.780	0.192	0.642	0.813	0.532	0.192	0.642	0.813	0.532	
Yb	4.50	4.92	5.42	4.35	1.38	4.66	1.31	5.36	5.13	4.32	1.31	5.36	5.13	4.32	
Lu	0.786	0.614	0.816	0.602	0.235	0.707	0.196	0.798	0.881	0.776	0.196	0.798	0.881	0.776	
Hf	3.37	4.46	2.22	1.59	1.09	1.50	1.35	2.00	2.04	2.62	1.35	2.00	2.04	2.62	

Table A3.3 Trace element concentrations in clinopyroxene crystals analysed by LA-ICP-MS. Abbreviations same as Table A3.2.

Sample ID	Inglewood b	Inglewood b	Inglewood b	Inglewood b	Inglewood b	Inglewood b	Inglewood b	Inglewood b	Inglewood b	Inglewood b	Inglewood b
Zone	20e	20h	26c	34a	34c	34d	34g	35a	35c	35e	
EMPA ID	cpx20_6	cpx20_8	cpx26_1	cpx34_1	cpx34_6	cpx34_6	cpx34_7	cpx35_2	cpx35_5	cpx35_7	
CaO (wt%)	21.37	21.39	21.99	22.02	21.44	21.44	22.27	21.52	21.61	21.57	
Mg#	82.78	83.53	77.85	84.64	84.64	84.64	85.69	80.34	79.75	76.57	
Mn (wt%)	0.848	0.875	0.843	0.690	0.894	0.913	0.669	0.875	0.799	0.939	
Li	9.27	7.86	6.81	7.78	7.88	7.22	6.06	8.85	8.34	7.91	
Sc	42.3	45.3	44.0	37.3	47.3	44.7	58.7	43.2	39.8	45.1	
Ti	1812	2282	1955	1755	1859	1601	2156	1435	1455	2148	
V	84.9	98.3	87.7	98.2	90.6	77.7	126	80.0	79.7	94.3	
Cr	BDL	BDL	BDL	BDL	BDL	BDL	15.9	BDL	BDL	BDL	
Ni	1.96	2.86	2.47	0.69	4.10	2.42	6.52	2.32	2.45	2.13	
Cu	0.90	BDL	1.21	BDL	2.06	3.52	1.09	4.30	0.973	0.692	
Zn	124	117	117	111	120	116	108	132	112	120	
Sr	33.4	35.3	37.4	38.3	34.7	32.1	40.1	32.3	33.6	35.1	
Y	61.1	78.7	60.4	35.5	65.4	60.3	52.1	55.6	39.6	71.8	
Zr	71.0	88.8	63.6	49.2	63.1	50.3	50.8	41.9	43.0	79.7	
La	4.45	7.09	5.75	4.47	5.84	5.33	5.35	4.49	4.13	6.99	
Ce	19.2	28.9	22.6	14.7	25.0	21.8	21.3	19.6	16.6	28.8	
Pr	4.39	5.58	4.98	3.14	5.00	4.58	4.13	4.47	3.66	5.23	
Nd	27.1	38.9	30.1	19.6	30.1	27.9	23.2	23.0	22.6	31.9	
Sm	9.51	12.7	12.8	6.83	12.6	9.69	9.12	8.31	7.77	12.20	
Eu	1.45	2.46	2.37	1.46	1.97	1.67	1.62	1.69	1.50	2.26	
Gd	11.0	14.2	10.0	7.41	10.86	10.29	8.75	9.68	7.19	11.54	
Tb	1.75	2.26	1.88	1.22	1.83	1.62	1.29	1.25	0.95	2.10	
Dy	10.9	14.5	11.1	6.62	11.8	10.7	9.62	9.95	8.71	12.9	
Ho	2.32	3.19	1.80	1.26	2.34	2.18	1.87	1.87	1.51	2.52	
Er	6.09	8.98	7.04	4.05	7.65	6.88	5.66	6.76	3.69	6.59	
Tm	0.855	1.18	1.11	0.600	0.977	1.05	0.754	0.988	0.646	1.01	
Yb	5.88	7.29	5.15	3.74	6.81	6.69	5.11	5.40	3.45	6.71	
Lu	0.918	1.21	0.910	0.729	1.08	0.969	0.971	1.01	0.278	1.12	
Hf	4.02	4.73	3.41	2.30	3.43	2.31	2.85	1.70	2.03	4.36	

Table A3.3 Trace element concentrations in clinopyroxene crystals analysed by LA-ICP-MS. Abbreviations same as Table A3.2.

Sample ID	Inglewood b	Inglewood b	Inglewood b	Inglewood b	Inglewood b	Inglewood b	Inglewood b	Inglewood b	Inglewood b	Inglewood b	Inglewood b	Inglewood a
Zone	35g	37b	37e	37f	37g	41b	41c	41e	41f	41a	rim	rim
EMPA ID	cpx35_9	cpx37_2	light core	core	cp37_2	cp37_1	cp37_2	cp37_1	cp37_2	cp37_1	cp37_2	cp37_1
CaO (wt%)	21.66	21.68	22.85	21.81	21.68	21.38	21.42	21.38	21.42	21.38	21.42	21.48
Mg#	77.57	80.69	81.56	80.74	80.69	79.16	77.68	79.16	77.68	79.16	77.68	79.62
Mn (wt%)	0.867	0.890	0.366	0.438	0.914	0.663	0.636	0.944	0.676	0.899	0.676	0.899
Li	7.02	7.50	8.06	7.41	7.18	7.90	5.13	8.04	8.15	8.32	8.15	8.32
Sc	48.8	39.1	63.9	56.1	39.3	47.2	43.4	39.7	43.5	37.3	43.5	37.3
Ti	2090	1411	2532	2460	1471	1789	1518	1465	1383	1419	1383	1419
V	97.3	73.0	162	150	73.1	106	116	75.0	93.1	72.7	93.1	72.7
Cr	BDL	BDL	BDL	BDL	BDL	BDL	BDL	BDL	BDL	BDL	BDL	BDL
Ni	3.39	2.38	3.50	3.94	4.10	6.39	8.10	2.88	7.65	1.60	7.65	1.60
Cu	BDL	1.22	0.537	1.76	BDL	BDL	0.799	BDL	BDL	BDL	BDL	BDL
Zn	116	130.6	74.4	70.0	120	87.6	99.1	125.6	103	125	103	125
Sr	36.2	32.5	49.3	47.9	36.0	36.7	35.1	32.3	34.5	34.9	34.5	34.9
Y	61.1	49.0	20.8	27.2	50.5	40.6	32.9	56.1	37.1	49.6	37.1	49.6
Zr	67.3	36.7	42.4	40.8	36.8	39.0	42.9	39.3	35.0	40.3	35.0	40.3
La	6.06	4.69	1.89	2.71	4.89	4.00	4.31	4.97	3.32	4.91	3.32	4.91
Ce	25.3	20.5	8.1	11.1	20.5	17.6	18.3	22.0	16.7	20.9	16.7	20.9
Pr	5.00	4.36	1.73	2.20	4.55	3.46	3.42	5.04	3.78	4.38	3.78	4.38
Nd	30.3	24.9	10.6	13.4	22.8	18.4	19.0	27.7	18.5	26.1	18.5	26.1
Sm	9.39	8.53	3.71	4.89	8.12	5.90	4.63	8.91	6.32	6.32	6.32	6.32
Eu	2.29	1.82	1.12	1.26	1.49	1.45	1.20	1.77	1.54	1.89	1.54	1.89
Gd	11.26	9.24	4.35	4.44	7.56	9.54	6.22	12.5	6.58	11.2	6.58	11.2
Tb	1.76	1.52	0.76	1.05	1.63	1.29	0.76	1.86	1.10	1.28	1.10	1.28
Dy	11.1	9.37	4.62	5.12	9.22	8.20	6.50	9.25	6.57	10.5	6.57	10.5
Ho	2.33	1.87	0.777	1.02	1.35	1.54	1.08	1.84	1.18	2.15	1.18	2.15
Er	7.10	5.40	2.68	2.47	6.45	4.18	3.66	6.24	3.99	5.76	3.99	5.76
Tm	1.02	0.742	0.256	0.495	0.792	0.712	0.622	0.914	0.825	0.610	0.825	0.610
Yb	6.39	5.27	1.62	2.19	4.87	4.28	3.33	4.88	2.93	4.66	2.93	4.66
Lu	0.883	0.803	0.303	0.481	0.737	0.631	0.548	1.033	0.392	0.656	0.392	0.656
Hf	3.34	1.62	2.36	1.87	1.35	1.69	2.32	1.44	1.55	1.54	1.55	1.54

Table A3.3 Trace element concentrations in clinopyroxene crystals analysed by LA-ICP-MS. Abbreviations same as Table A3.2.

Sample ID	Inglewood a zone	Inglewood a cpx1_7	Inglewood a cpx1_9	Inglewood a zone	Inglewood a cpx1_11	Inglewood a cpx1_3	Inglewood a rim	Inglewood a cpx18_1	Inglewood a cpx18_2	Inglewood a zone	Inglewood a cpx18_7	Inglewood a light core	Inglewood a rim	Inglewood a light zone	Inglewood a zone
Zone	1c	1d	1e	1f	18a	18b	18f	18g	19a	19c	19d	19e	19f	19g	19h
EMPA ID	zone	zone	core	zone	rim	zone	zone	light core	rim	light zone	zone	light core	rim	light zone	zone
CaO (wt%)	cpx1_7	cpx1_9	cpx1_11	cpx1_3	cpx18_1	cpx18_2	cpx18_7	cpx18_9	cpx19_2	cpx19_7	cpx19_6	cpx18_9	cpx19_2	cpx19_7	cpx19_6
Mg#	21.20	21.43	21.61	21.68	21.44	21.56	21.24	21.54	21.90	22.01	21.61	21.54	21.90	22.01	21.61
Mn (wt%)	80.61	80.41	78.70	79.48	84.53	83.09	83.72	80.24	77.49	76.29	81.35	80.24	77.49	76.29	81.35
Li	0.924	1.06	0.963	0.866	0.822	0.966	0.809	0.597	0.614	0.512	0.915	0.597	0.614	0.512	0.915
Sc	8.13	8.45	7.67	9.42	7.28	7.01	9.08	8.68	9.06	9.28	6.96	8.68	9.06	9.28	6.96
Ti	38.8	48.0	45.2	35.6	37.9	38.4	52.4	50.6	41.8	52.8	44.8	50.6	41.8	52.8	44.8
V	1536	1821	1992	1469	1442	1445	2061	2200	2270	2368	1593	2200	2270	2368	1593
Cr	81.7	95.2	101	75.6	75.6	75.0	132	131	127	130	81.5	131	127	130	81.5
Ni	BDL	BDL	BDL	BDL	BDL	BDL	BDL	BDL	BDL	BDL	BDL	BDL	BDL	BDL	BDL
Cu	2.86	4.56	1.68	1.71	3.11	1.71	3.65	1.20	1.39	1.40	3.13	1.20	1.39	1.40	3.13
Zn	0.43	BDL	BDL	1.30	BDL	0.33	0.54	2.30	1.18	1.31	BDL	2.30	1.18	1.31	BDL
Sr	130	119	126	112	106	117	102	85.0	89.1	77.7	109	85.0	89.1	77.7	109
Y	39.0	37.6	42.9	32.8	36.6	32.8	36.9	43.9	42.7	45.3	35.2	43.9	42.7	45.3	35.2
Zr	60.0	74.0	62.5	49.6	39.3	57.9	56.5	47.4	36.9	35.9	58.5	47.4	36.9	35.9	58.5
La	53.4	59.1	60.9	39.2	38.3	42.6	94.1	79.5	65.4	60.2	45.8	79.5	65.4	60.2	45.8
Ce	5.61	6.16	5.65	4.11	4.69	5.94	4.52	5.75	2.91	2.72	5.35	5.75	2.91	2.72	5.35
Pr	24.1	26.9	24.7	20.0	17.3	22.6	19.0	20.4	12.6	11.0	22.7	20.4	12.6	11.0	22.7
Nd	5.00	5.54	4.94	3.95	3.39	4.86	3.77	4.31	2.63	2.74	4.58	4.31	2.63	2.74	4.58
Sm	29.1	33.2	28.5	23.3	21.4	26.8	23.7	24.0	17.2	17.6	28.2	24.0	17.2	17.6	28.2
Eu	10.4	12.2	11.9	6.97	7.65	9.28	7.43	8.09	5.42	6.64	7.46	8.09	5.42	6.64	7.46
Gd	1.87	2.34	2.20	1.61	1.62	1.88	1.95	2.19	1.58	1.77	1.45	2.19	1.58	1.77	1.45
Tb	10.8	9.27	9.83	11.4	6.93	10.4	10.4	9.08	6.93	6.79	10.5	9.08	6.93	6.79	10.5
Dy	1.65	2.14	1.95	1.65	1.07	1.69	1.87	1.54	1.02	1.24	1.82	1.54	1.02	1.24	1.82
Ho	10.6	14.9	13.6	13.0	7.55	10.1	9.00	8.77	7.46	6.90	10.1	8.77	7.46	6.90	10.1
Er	1.90	2.62	2.36	2.13	1.40	1.96	1.83	1.79	1.16	1.18	2.29	1.79	1.16	1.18	2.29
Tm	4.55	7.50	7.57	6.74	4.09	6.34	6.18	5.32	4.44	3.82	6.15	5.32	4.44	3.82	6.15
Yb	0.921	1.071	0.713	0.587	0.555	0.856	1.001	0.658	0.599	0.537	0.905	0.658	0.599	0.537	0.905
Lu	6.19	7.47	6.91	4.48	4.26	6.34	5.74	4.05	4.14	3.26	5.64	4.05	4.14	3.26	5.64
Hf	0.798	1.12	1.39	0.910	0.725	0.841	1.12	0.577	0.512	0.526	0.917	0.577	0.512	0.526	0.917
	2.58	2.23	2.38	2.50	1.97	2.09	4.93	5.21	2.58	2.78	2.38	5.21	2.58	2.78	2.38

Table A3.3 Trace element concentrations in clinopyroxene crystals analysed by LA-ICP-MS. Abbreviations same as Table A3.2.

Sample ID	Inglewood a	Inglewood a	Inglewood a	Inglewood a	Inglewood a	Inglewood a	Inglewood a	Inglewood a	Inglewood a	Inglewood a	Inglewood a	Inglewood a	Inglewood a	Inglewood a
Zone														
EMPA ID	cpx35_1	cpx35_3	cpx35_4	cpx51_3	cpx51_5	light core	rim	zone	zone	zone	zone	zone	zone	core
CaO (wt%)	21.10	22.11	21.61	20.77	21.54	21.59	21.54	21.54	21.54	21.54	21.54	21.84	21.68	21.51
Mg#	82.42	79.36	81.38	78.22	78.26	79.77	77.18	78.26	77.18	77.18	74.13	74.13	75.95	77.54
Mn (wt%)	0.758	0.512	0.972	0.873	0.774	0.496	0.971	0.583	0.971	0.971	0.729	0.729	0.899	0.845
Li	7.62	8.12	7.09	8.23	8.56	7.99	8.06	8.75	8.06	8.06	8.66	8.66	8.46	7.05
Sc	35.2	45.5	40.6	38.7	49.9	60.4	38.3	46.9	38.3	38.3	53.8	53.8	45.3	44.5
Ti	1636	2200	1461	1382	1704	2590	1436	2122	1436	1436	1662	1662	1862	2267
V	92.8	141	71.0	71.4	87.0	150	69.0	138	69.0	69.0	124	124	93.0	109
Cr	BDL	BDL	BDL	BDL	BDL	BDL	BDL	BDL	BDL	BDL	BDL	BDL	BDL	BDL
Ni	0.42	1.59	3.58	2.75	11.6	5.67	1.29	10.7	1.29	1.29	4.74	4.74	3.10	4.66
Cu	0.11	1.86	0.12	1.43	1.30	3.20	BDL	0.17	BDL	BDL	2.29	2.29	0.21	0.09
Zn	116	85.6	120	128	110	78.0	118	96.8	118	118	105	105	113	110
Sr	39.8	50.0	32.6	34.2	46.7	43.2	32.4	49.1	32.4	32.4	35.5	35.5	33.8	40.2
Y	40.7	32.7	62.6	53.3	43.8	38.9	58.2	39.4	58.2	58.2	42.2	42.2	66.1	67.4
Zr	45.2	57.4	41.1	38.4	44.3	60.2	42.5	53.7	42.5	42.5	46.6	46.6	59.2	74.6
La	3.95	11.1	5.49	4.52	4.82	3.38	5.07	3.19	5.07	5.07	4.05	4.05	6.23	6.80
Ce	16.1	29.2	24.3	20.4	18.9	14.1	23.2	14.5	23.2	23.2	16.3	16.3	26.1	30.5
Pr	3.35	4.82	5.04	4.05	3.81	2.82	5.01	3.11	5.01	5.01	3.08	3.08	5.52	6.09
Nd	21.5	25.9	30.3	23.0	23.1	16.0	29.1	19.1	29.1	29.1	19.7	19.7	32.2	35.4
Sm	5.79	6.70	10.2	6.63	7.25	6.36	9.51	5.02	9.51	9.51	6.54	6.54	10.9	11.1
Eu	1.94	2.18	1.96	1.69	1.87	1.72	2.27	1.73	2.27	2.27	1.31	1.31	2.31	2.78
Gd	7.83	6.44	10.9	9.75	8.61	8.34	10.1	7.29	10.1	10.1	6.65	6.65	12.3	12.7
Tb	1.23	1.15	2.08	1.62	1.29	1.14	2.05	1.09	2.05	2.05	1.11	1.11	1.89	2.25
Dy	8.77	7.51	12.5	10.2	8.65	6.70	10.6	7.29	10.6	10.6	6.97	6.97	12.6	13.1
Ho	1.50	1.50	2.53	2.31	1.73	1.58	2.32	1.29	2.32	2.32	1.24	1.24	2.50	2.68
Er	4.82	3.63	8.71	5.18	4.15	3.79	8.22	3.53	8.22	8.22	4.52	4.52	7.42	6.62
Tm	0.416	0.454	1.138	0.872	0.748	0.446	0.629	0.585	0.629	0.629	0.458	0.458	0.885	0.723
Yb	3.10	2.17	7.69	5.73	3.47	3.77	6.08	3.70	6.08	6.08	2.91	2.91	6.33	6.16
Lu	0.633	0.494	1.47	1.09	0.795	0.563	0.854	0.482	0.854	0.854	0.362	0.362	0.714	0.991
Hf	2.00	2.65	1.77	1.73	1.99	4.03	1.53	3.41	1.53	1.53	1.85	1.85	2.68	4.15

Table A3.3 Trace element concentrations in clinopyroxene crystals analysed by LA-ICP-MS. Abbreviations same as Table A3.2.

Sample ID	Inglewood a	Inglewood a	Inglewood a	Inglewood a	Inglewood a	Korito	Korito	Korito	Korito	Korito	Korito	Korito	Korito	Korito	Korito	Korito	Korito
Zone	63b	63d	63e	63f	63g	1c	1d	1e	4d	4e	5c	9a	9f				
EMPA ID	cpx63_6	cpx63_5	cpx63_6	cpx63_9	cpx63_10	core	light core	light zone	rim	core	zone	core	zone				
CaO (wt%)	22.31	21.80	22.31	21.63	22.30	cpx1_2	cpx1_4	cpx1_3	cpx4_1	cpx4_2	cpx5_3	cpx9_6	cpx9_3				
Mg#	77.26	81.46	77.26	81.88	79.86	82.26	83.59	80.72	79.16	88.42	82.37	83.06	81.68				
Mn (wt%)	0.986	0.545	0.637	0.737	0.790	0.383	0.503	0.404	0.629	0.128	0.719	0.628	0.859				
Li	7.49	10.5	8.44	7.00	6.49	7.72	5.30	7.09	5.87	7.31	8.33	8.12	7.34				
Sc	40.2	57.0	42.9	55.2	54.9	52.1	71.1	52.8	60.7	142	42.6	46.2	43.6				
Ti	1336	2546	2082	1688	1518	1765	2247	2895	919	4820	1743	1364	1548				
V	75.3	142	116	117	123	159	136	190	117	270	120	135	102				
Cr	BDL	BDL	BDL	BDL	BDL	92.1	200	19.0	35.8	2790	BDL	BDL	BDL				
Ni	2.83	1.16	2.43	7.50	5.40	26.9	25.2	14.0	50.1	137	8.99	20.8	6.52				
Cu	2.48	BDL	0.44	BDL	1.77	0.744	0.751	1.69	0.895	1.09	1.16	0.279	0.250				
Zn	135	82.9	88.1	98.1	108	73.7	73.9	77.5	98.1	22.5	111	110	111				
Sr	39.3	39.8	44.6	33.9	32.7	47.5	44.2	56.2	30.6	53.8	41.7	34.8	33.9				
Y	64.0	40.0	33.1	57.9	48.2	14.2	34.9	22.5	30.9	14.1	38.8	28.0	54.6				
Zr	40.1	82.5	48.2	50.9	51.5	23.3	44.8	43.5	27.4	33.8	38.7	37.7	45.4				
La	7.15	3.28	3.14	5.32	5.05	1.94	3.31	2.33	4.04	2.12	4.26	3.72	5.81				
Ce	29.6	16.5	12.9	24.5	23.3	8.5	15.0	11.2	17.5	8.2	21.1	19.7	26.0				
Pr	5.52	2.87	2.77	4.59	4.20	1.55	2.76	2.13	3.36	1.54	3.98	3.37	4.84				
Nd	30.1	19.0	18.3	25.0	25.8	9.3	18.2	12.0	17.1	8.8	22.0	15.9	23.8				
Sm	9.47	6.90	5.61	9.50	7.98	2.48	4.68	4.50	5.81	2.88	7.26	4.74	8.04				
Eu	2.19	1.71	1.67	1.83	1.58	0.79	1.31	1.00	0.86	0.79	1.67	1.22	1.77				
Gd	10.4	10.1	6.27	9.76	9.20	2.88	6.50	3.60	4.44	2.84	7.27	4.59	9.83				
Tb	1.71	1.01	0.98	1.70	1.21	0.48	1.34	0.62	0.90	0.45	1.18	0.89	1.34				
Dy	11.9	11.2	8.06	10.2	10.0	2.71	6.45	4.34	5.19	3.01	7.29	5.05	9.56				
Ho	1.97	1.92	1.27	2.37	2.12	0.60	1.27	0.86	1.17	0.56	1.61	0.90	1.81				
Er	5.53	5.11	4.39	7.42	5.67	1.38	4.33	2.15	3.51	1.32	4.22	3.16	6.73				
Tm	0.911	1.022	0.552	0.846	0.836	0.185	0.438	0.446	0.372	0.188	0.520	0.385	0.900				
Yb	6.61	3.45	2.93	5.57	4.60	1.41	3.36	2.17	3.56	1.31	3.60	2.76	5.60				
Lu	0.869	0.410	0.565	0.971	0.893	0.215	0.619	0.320	0.449	0.086	0.556	0.387	0.757				
Hf	2.09	5.59	2.85	2.55	2.22	1.16	2.21	1.62	1.66	1.88	1.78	1.48	2.19				

Table A3.3 Trace element concentrations in clinopyroxene crystals analysed by LA-ICP-MS. Abbreviations same as Table A3.2.

Sample	Korito	Korito	Korito	Korito	Korito	Korito	Korito	Korito	Korito	Korito	Korito	Korito	Korito	Korito	Korito	Korito	Korito	Korito	Korito	
ID	18a	18c	18d	18e	20a	20c	20d	20e	20i	20j	20o	20p	22b	22d						
Zone	core	zone	zone	rim	zone	zone	zone	zone	zone	zone	light core	light core	core	zone						
EMPA ID	cpx18_9	cpx18_6	cpx18_7	cpx18_4	cpx20_2	cpx20_4	cpx20_4	cpx20_4	cpx20_5	cpx20_5	cpx20_7	cpx20_7	cpx22_6	cpx22_4						
CaO (wt%)	21.08	21.34	21.11	21.49	21.70	21.91	21.91	21.91	21.39	21.39	21.51	21.51	22.18	22.05						
Mg#	81.73	82.04	78.11	79.62	82.49	81.74	81.74	81.74	82.53	82.53	78.55	78.55	80.84	81.18						
Mn (wt%)	0.755	0.754	0.777	0.895	0.632	0.682	0.680	0.751	0.476	0.694	0.555	0.876	0.704	0.818						
Li	9.55	9.25	8.87	7.47	9.20	8.20	7.27	7.41	7.74	7.66	7.91	7.68	7.13	7.61						
Sc	45.4	43.8	43.7	36.3	50.3	53.2	48.1	48.4	46.0	43.0	49.0	36.3	51.2	50.8						
Ti	1870	1721	1816	1490	2396	1902	1962	1742	2518	1585	1730	1302	1629	1548						
V	153	136	137	89.4	168	118	109	117	149	106	123	75.2	100	102						
Cr	17.1	BDL	BDL	BDL	BDL	BDL	BDL	BDL	BDL	BDL	BDL	BDL	BDL	BDL						
Ni	10.9	10.4	10.3	4.28	8.50	8.33	9.93	9.54	4.51	6.94	5.81	4.28	8.48	5.57						
Cu	1.37	1.27	1.23	0.593	0.826	1.83	1.10	1.13	1.75	1.00	2.05	0.567	1.28	1.11						
Zn	116	123	112	114	100	93.9	93.2	98.5	73.4	93.9	85.9	109	101	106						
Sr	38.4	35.6	39.7	34.6	39.7	47.2	45.6	40.1	44.2	38.6	46.4	32.6	41.0	34.9						
Y	45.0	44.3	44.8	49.8	36.9	41.4	36.9	43.0	26.2	35.4	23.1	42.5	45.3	49.3						
Zr	57.7	49.1	51.5	41.4	55.2	50.0	41.9	41.8	42.9	38.3	43.8	33.4	40.1	43.7						
La	4.42	4.54	4.30	5.10	3.66	3.83	3.72	4.45	2.21	3.58	2.45	4.68	5.21	4.54						
Ce	20.9	20.5	20.9	22.6	18.5	18.5	17.2	20.1	10.4	17.2	11.2	19.9	20.5	20.9						
Pr	4.06	3.85	3.97	4.53	3.94	3.61	3.20	3.81	2.27	3.53	2.19	4.24	4.22	4.27						
Nd	23.0	22.3	22.3	26.1	20.5	21.2	20.9	22.3	13.6	18.8	12.8	23.5	23.9	24.3						
Sm	7.02	5.96	6.82	7.63	5.52	6.62	5.52	7.82	3.92	6.53	4.37	6.39	7.68	9.28						
Eu	1.59	1.43	1.63	1.72	1.65	1.53	1.48	1.62	1.18	1.49	1.19	1.61	1.70	1.66						
Gd	7.66	7.57	8.01	9.01	6.68	7.34	7.15	7.91	5.81	7.66	4.67	8.33	8.63	7.99						
Tb	1.34	1.11	1.33	1.50	1.27	1.22	1.08	1.28	0.81	1.21	0.80	1.39	1.39	1.28						
Dy	9.17	8.27	8.71	9.21	9.31	7.79	8.44	9.00	5.81	7.82	5.10	9.17	8.66	8.91						
Ho	1.81	1.45	1.77	1.86	1.48	1.30	1.40	1.47	1.08	1.20	0.90	1.60	1.82	1.80						
Er	5.59	4.51	5.05	5.69	3.77	4.52	4.48	4.80	2.58	4.03	2.60	4.93	5.43	5.56						
Tm	0.783	0.542	0.671	0.772	0.566	0.648	0.572	0.613	0.323	0.627	0.379	0.789	0.705	0.738						
Yb	4.68	4.41	4.50	4.88	3.87	3.99	3.28	4.07	2.55	3.96	2.85	4.81	4.47	5.14						
Lu	0.770	0.581	0.733	0.777	0.693	0.581	0.591	0.582	0.374	0.547	0.355	0.850	0.747	0.985						
Hf	2.42	2.14	2.17	1.67	2.39	2.40	2.76	1.85	2.04	1.69	2.26	1.84	2.03	1.78						

Table A3.3 Trace element concentrations in clinopyroxene crystals analysed by LA-ICP-MS. Abbreviations same as Table A3.2.

Sample	Korito	Korito	Korito	Korito	Korito	Korito	Korito	Korito	Korito
ID	22f	38c	38g	38i	38i	38i	38i	46b	46f
Zone	zone	core	zone	zone	rim	zone	rim	zone	zone
EMPA ID	cpx22_2	cpx38_4	cpx38_4	cpx38_3	cpx38_2	cpx38_2	cpx38_2	cpx46_2	cpx46_4
CaO (wt%)	22.18	21.59	21.59	22.49	22.13	22.69	22.13	22.69	22.31
Mg#	81.11	78.77	78.77	77.39	79.36	76.26	79.36	76.26	80.05
Mn (wt%)	0.942	0.711	0.626	0.929	0.957	0.546	0.957	0.546	0.895
Li	6.85	7.10	8.60	8.59	8.96	8.05	8.96	8.05	7.03
Sc	40.3	49.8	45.0	36.3	36.1	45.2	36.1	45.2	42.0
Ti	1483	1864	1931	1631	1461	1826	1461	1826	1468
V	88.1	122	139	88.3	80.6	115	80.6	115	81.7
Cr	BDL	BDL	BDL	BDL	BDL	BDL	BDL	BDL	BDL
Ni	4.40	7.55	5.27	4.88	1.66	0.716	1.66	0.716	5.38
Cu	1.10	1.48	1.26	0.330	1.75	0.765	1.75	0.765	1.80
Zn	116	97.0	93.8	126	120	85.6	120	85.6	104
Sr	34.9	39.0	42.2	39.4	35.2	44.6	35.2	44.6	33.9
Y	53.9	42.7	30.0	53.3	51.4	25.8	51.4	25.8	49.4
Zr	43.9	43.0	55.8	55.0	48.2	41.3	48.2	41.3	38.6
La	4.94	4.04	2.84	5.64	4.42	2.38	4.42	2.38	4.71
Ce	22.6	19.7	12.6	23.8	20.9	10.6	20.9	10.6	20.3
Pr	4.53	3.71	2.66	4.50	4.34	2.30	4.34	2.30	4.00
Nd	27.3	20.9	15.2	28.0	26.1	13.2	26.1	13.2	23.4
Sm	8.22	7.71	5.27	8.22	8.92	4.50	8.92	4.50	8.17
Eu	1.73	1.59	1.23	2.13	1.68	1.12	1.68	1.12	1.87
Gd	8.93	7.99	6.14	9.93	10.4	5.61	10.4	5.61	8.10
Tb	1.41	1.13	0.99	1.61	1.67	0.95	1.67	0.95	1.49
Dy	9.07	6.98	6.13	10.87	9.31	4.97	9.31	4.97	9.91
Ho	1.94	1.69	1.06	2.04	1.85	1.09	1.85	1.09	1.79
Er	5.93	4.47	3.03	5.20	5.58	3.03	5.58	3.03	4.70
Tm	0.829	0.422	0.415	0.770	0.604	0.519	0.604	0.519	0.760
Yb	5.67	4.47	3.00	5.04	4.43	2.14	4.43	2.14	5.35
Lu	0.824	0.612	0.391	0.660	0.794	0.475	0.794	0.475	0.788
Hf	1.59	1.98	2.81	2.58	2.26	2.13	2.26	2.13	1.96

Table A3.4 Trace element concentrations in amphibole crystals analysed by LA-ICP-MS.
Abbreviations same as Table A3.2.

Sample	Kaupokonui	Kaupokonui	Kaupokonui	Kaupokonui	Kaupokonui
ID	A3a	A3b	A5b	A7a	A7b
zone	rim	core	core	rim	core
EMPA ID	A3_2	A3_3	A5_3	A7_2	A7_4
CaO	12.12	11.92	11.86	12.22	11.44
Mg#	76.81	87.40	79.33	74.02	71.62
Mn (wt%)	0.161	0.134	0.254	0.195	0.417
Li	3.33	3.14	3.24	4.13	4.13
Sc	84.5	92.9	68.8	90.4	103.8
Ti	14632	12712	13394	14090	18812
V	602	563	504	562	530
Cr	24.1	65.4	46.6	7.4	8.6
Ni	107	169	38.3	43.3	24.7
Zn	78.6	56.7	114	94.2	157
Rb	4.12	4.03	4.05	4.30	4.60
Sr	327	325	216	349	157
Y	25.8	20.6	47.6	31.2	129
Zr	62.4	47.4	118	82.0	136
Nb	3.04	1.86	5.95	4.12	16.9
Ba	308	254	262	316	353
La	3.88	2.82	9.53	4.37	22.1
Ce	14.9	10.8	35.1	14.6	83.8
Pr	2.85	2.34	6.25	3.24	15.5
Nd	13.3	11.4	34.5	17.3	85.0
Sm	5.20	3.26	8.57	5.43	24.5
Eu	1.35	1.38	2.45	1.53	5.73
Gd	4.95	5.45	8.74	6.22	22.5
Tb	0.591	0.779	1.45	0.929	4.21
Dy	6.60	5.11	9.98	6.07	25.59
Ho	1.19	0.739	1.48	1.25	4.95
Er	2.91	1.88	4.91	3.85	12.5
Tm	0.164	0.374	0.713	0.432	1.73
Yb	2.08	0.978	4.01	2.01	11.3
Lu	0.273	0.224	0.333	0.321	0.959
Hf	2.89	2.55	4.85	4.25	6.67
Ta	BDL	0.145	0.300	0.213	0.359
Pb	2.09	1.22	1.67	0.631	2.54

**Where EMPA analyses were invalid, data from a similar crystal (on the basis of texture and backscatter intensity) were substituted.*

Table A3.4 Trace element concentrations in amphibole crystals analysed by LA-ICP-MS.
Abbreviations same as Table A3.2.

Sample ID	Kaupokonui A9d rim	Kaupokonui A9e zone	Kaupokonui A9f core	Kaupokonui A11a rim	Kaupokonui A11b core
EMPA ID	A9_2	A9_4	A9_6	A11_1	A11_4
CaO	11.89	11.33	11.83	11.70	11.93
Mg#	81.70	68.55	71.11	79.74	85.94
Mn (wt%)	0.125	0.333	0.216	0.137	0.133
Li	4.67	3.88	4.76	4.10	3.50
Sc	81.1	45.9	62.4	80.1	78.4
Ti	12764	15867	15422	13471	12538
V	556	495	664	512	543
Cr	216.0	BDL	15.6	13.8	26.9
Ni	169	20.3	17.3	123	160
Zn	66.4	150	107	58.9	47.5
Rb	5.24	4.42	4.87	4.13	3.58
Sr	331	218	328	328	317
Y	20.5	47.6	29.6	26.3	24.2
Zr	46.7	88.0	65.1	75.9	52.1
Nb	1.80	9.99	3.88	3.31	2.45
Ba	309	376	339	284	276
La	3.54	10.0	4.60	3.92	2.47
Ce	11.9	40.0	18.8	15.6	11.3
Pr	2.90	7.04	3.43	2.61	2.07
Nd	12.3	36.0	19.0	13.4	12.3
Sm	2.95	10.1	6.80	3.71	3.08
Eu	1.46	2.60	1.52	1.19	1.80
Gd	6.18	11.9	5.98	3.92	5.58
Tb	0.586	1.54	0.823	0.746	0.542
Dy	4.27	10.0	6.26	6.06	3.19
Ho	0.581	1.93	1.23	1.03	0.74
Er	1.90	5.06	3.27	3.25	3.49
Tm	0.204	0.916	0.368	0.214	0.245
Yb	1.22	4.74	2.89	2.12	2.20
Lu	0.213	0.635	0.334	0.205	0.248
Hf	2.33	3.57	3.06	4.40	1.82
Ta	0.201	0.427	0.233	0.333	0.076
Pb	1.53	2.40	1.97	1.19	0.557

**Where EMPA analyses were invalid, data from a similar crystal (on the basis of texture and backscatter intensity) were substituted.*

Table A3.4 Trace element concentrations in amphibole crystals analysed by LA-ICP-MS. Abbreviations same as Table A3.2.

Sample	SM-6C	SM-6C	SM-6C	SM-6C	SM-6C	SM-6C	SM-6C
ID	A1f	A3a	A3g	A3h	A3d	A3j	A5d
zone	core	rim	zone	zone	zone	core	rim
EMPA ID	A7_1*	A7_1*	A7_5*	A7_5*	A7_4*	A7_6*	A5_2
CaO	11.90	11.90	11.56	11.56	11.92	12.04	13.03
Mg#	82.40	82.40	82.30	82.30	78.88	78.85	69.41
Mn (wt%)	0.160	0.141	0.142	0.134	0.159	0.215	0.151
Li	1.63	1.84	1.93	1.30	1.35	1.71	2.29
Sc	60.0	80.6	79.8	82.7	72.5	78.1	86.8
Ti	14929	15160	15381	15322	15669	17323	16020
V	532	570	610	584	579	475	613
Cr	8.70	38.1	26.1	30.8	15.2	9.44	39.1
Ni	33.9	52.0	53.7	70.8	42.6	43.7	47.4
Zn	68.3	68.4	66.5	63.9	72.0	93.0	72.8
Rb	3.15	3.01	4.02	4.48	3.64	3.43	2.61
Sr	276	322	342	352	289	282	346
Y	25.4	22.4	20.8	20.0	25.1	61.0	23.9
Zr	35.1	34.3	35.2	33.6	35.9	58.1	34.6
Nb	3.53	2.33	1.88	2.29	2.55	8.15	2.47
Ba	283	317	295	312	284	284	285
La	3.65	2.91	2.96	2.53	3.51	5.93	3.22
Ce	14.6	13.0	12.6	12.2	14.9	30.6	11.6
Pr	2.77	2.41	2.32	2.06	2.51	6.06	1.99
Nd	15.4	14.1	15.1	13.8	14.9	40.0	12.7
Sm	3.38	4.08	3.82	4.95	4.35	8.68	3.81
Eu	1.30	1.92	1.37	1.40	1.92	2.49	1.34
Gd	4.67	6.18	4.28	6.04	5.21	13.9	4.53
Tb	0.910	0.840	0.621	0.734	0.779	1.76	0.666
Dy	3.97	4.45	2.99	3.49	5.52	11.3	5.54
Ho	0.807	0.687	0.459	0.837	1.17	2.45	0.914
Er	2.25	2.22	2.06	2.11	3.03	5.69	1.90
Tm	0.413	0.286	0.204	0.264	0.237	0.743	0.350
Yb	2.08	1.80	1.27	1.55	1.91	5.32	1.46
Lu	0.228	0.220	0.322	0.219	0.208	0.703	0.331
Hf	1.68	1.91	1.39	1.64	1.04	3.00	1.91
Ta	0.135	0.076	0.162	0.207	0.316	0.280	0.127
Pb	1.34	1.08	0.801	1.57	1.42	0.862	0.653

*Where EMPA analyses were invalid, data from a similar crystal (on the basis of texture and backscatter intensity) were substituted.

Table A3.4 Trace element concentrations in amphibole crystals analysed by LA-ICP-MS.
Abbreviations same as Table A3.2.

Sample	SM-6C	SM-6C	SM-6C	SM-6C	SM-6C	SM-6C	SM-6C
ID	A5e	A6b	A6d	A7a	A7b	A7c	A7d
zone	core	rim	core	rim	zone	zone	core
EMPA ID	A5_5	A6_1	A6_3	A7_1	A7_4	A7_5	A7_6
CaO	12.85	11.75	11.93	11.90	11.92	11.56	12.04
Mg#	66.63	83.71	81.34	82.40	78.88	82.30	78.85
Mn (wt%)	0.177	0.155	0.140	0.141	0.162	0.269	0.210
Li	3.48	2.20	1.51	1.29	1.98	1.84	1.67
Sc	75.1	85.8	88.1	83.3	79.0	83.2	59.2
Ti	16401	16051	14986	15487	16734	18577	14663
V	632	610	571	592	614	502	594
Cr	16.4	9.47	40.4	24.1	15.1	BDL	3.88
Ni	25.3	44.5	55.9	64.4	54.2	41.7	35.2
Zn	72.2	59.9	61.4	70.1	75.1	100	91.1
Rb	8.33	3.19	2.83	4.58	4.42	3.38	3.85
Sr	396	336	338	351	359	256	296
Y	27.9	27.1	22.8	20.2	24.7	68.5	27.5
Zr	59.3	39.7	36.4	35.5	36.5	81.1	44.2
Nb	3.68	2.83	2.40	1.67	3.29	11.80	2.72
Ba	397	301	281	343	330	443	361
La	4.78	3.02	2.21	2.48	3.32	11.19	4.49
Ce	18.5	12.7	10.7	12.3	13.7	49.6	17.7
Pr	3.02	2.24	2.60	2.06	2.38	7.84	3.53
Nd	17.0	17.3	13.3	13.8	14.2	48.3	19.0
Sm	6.32	4.72	3.85	3.31	4.05	14.38	5.28
Eu	1.79	1.27	1.40	1.68	1.74	3.26	1.47
Gd	5.19	6.58	5.31	5.77	5.31	15.17	5.67
Tb	0.910	0.925	1.04	0.743	1.06	2.25	0.937
Dy	5.38	5.13	4.04	4.58	6.11	17.6	5.08
Ho	0.908	0.867	0.578	0.754	0.785	2.393	0.917
Er	1.73	2.25	1.92	2.07	2.12	7.59	2.21
Tm	0.141	0.274	0.110	0.117	0.222	0.755	0.331
Yb	2.26	1.89	0.79	1.97	1.37	5.26	2.06
Lu	0.491	0.205	0.237	0.272	0.280	0.424	0.270
Hf	2.33	1.30	1.72	1.30	1.78	3.39	2.31
Ta	0.356	0.203	0.263	0.240	0.080	0.534	0.040
Pb	3.95	0.908	1.13	0.918	0.767	1.36	1.26

**Where EMPA analyses were invalid, data from a similar crystal (on the basis of texture and backscatter intensity) were substituted.*

Table A3.4 Trace element concentrations in amphibole crystals analysed by LA-ICP-MS.
Abbreviations same as Table A3.2.

Sample ID	SM-6C A9a	Maketawa A1a	Maketawa A1c	Maketawa A1d	Maketawa A1f	Maketawa A4a
zone	core	rim	zone	zone	core	zone
EMPA ID	A9_4	A1_1	A1_2	A1_2	A1_3	A4_2
CaO	13.08	11.41	11.72	11.72	11.82	12.29
Mg#	70.02	66.35	69.84	69.84	75.30	82.74
Mn (wt%)	0.161	0.361	0.584	0.592	0.569	0.166
Li	2.39	3.53	6.04	4.97	4.64	3.37
Sc	93.9	64.6	42.9	35.5	51.9	77.7
Ti	17139	16853	17362	16364	17509	13752
V	635	413	391	366	319	497
Cr	41.5	15.4	BDL	BDL	6.44	19.0
Ni	61.1	25.2	29.2	17.7	9.27	176
Zn	69.1	140	244	235	215	68.8
Rb	4.37	3.25	4.09	4.45	2.82	4.05
Sr	377	207	105	103	119	316
Y	26.8	69.9	129	120	141	26.9
Zr	35.6	111	127	130	160	54.7
Nb	2.72	11.1	23.6	23.1	23.1	2.47
Ba	310	353	312	320	313	234
La	3.03	13.0	22.6	19.1	22.4	3.43
Ce	12.4	48.8	85.4	81.2	84.4	13.3
Pr	2.71	9.51	15.7	14.2	16.1	2.38
Nd	12.0	46.2	78.7	73.1	87.4	14.9
Sm	6.18	12.3	24.6	21.4	25.3	4.52
Eu	1.94	3.51	4.74	4.54	5.65	1.98
Gd	5.66	15.8	23.2	22.0	30.3	6.44
Tb	1.09	2.01	3.71	3.08	3.87	0.920
Dy	5.83	13.1	23.7	23.7	27.7	6.16
Ho	0.900	2.82	4.13	4.37	5.68	1.17
Er	2.25	7.16	12.1	11.2	14.4	2.78
Tm	0.288	0.847	1.74	1.73	1.90	0.241
Yb	1.73	4.65	11.2	11.0	12.3	2.30
Lu	0.196	0.87	1.25	1.49	1.79	0.19
Hf	1.28	5.29	5.60	4.70	7.08	2.70
Ta	0.255	0.508	0.726	0.566	0.691	0.051
Pb	1.25	2.07	2.05	2.52	1.94	0.662

**Where EMPA analyses were invalid, data from a similar crystal (on the basis of texture and backscatter intensity) were substituted.*

Table A3.4 Trace element concentrations in amphibole crystals analysed by LA-ICP-MS. Abbreviations same as Table A3.2.

Sample ID	Maketawa A9a	Maketawa A9b	Maketawa A10a	Maketawa A11c	Maketawa A11d
zone	rim	core	core	zone	core
EMPA ID	A9_2	A9_1	A10_6	A11_3	A11_1
CaO	11.62	12.06	12.18	11.75	11.52
Mg#	78.54	71.31	79.98	73.59	78.51
Mn (wt%)	0.366	0.384	0.178	0.408	0.347
Li	3.85	3.32	4.02	4.00	3.97
Sc	79.4	88.1	65.4	71.3	65.5
Ti	17617	18537	13196	18089	16360
V	429	451	498	451	477
Cr	2.86	9.64	9.37	25.5	22.7
Ni	28.1	33.2	145	43.3	48.8
Zn	125	148	79.3	166	151
Rb	8.22	2.88	4.23	2.90	3.07
Sr	229	221	394	215	291
Y	94.8	99.0	27.3	85.1	62.2
Zr	148	140	59.8	129	104
Nb	14.9	17.2	2.70	13.8	8.89
Ba	447	415	340	383	370
La	16.9	16.7	4.56	15.6	10.1
Ce	55.9	61.7	17.7	58.3	35.7
Pr	10.4	10.5	2.84	9.66	6.37
Nd	56.2	68.5	17.3	59.8	38.4
Sm	15.5	17.4	7.20	13.3	14.0
Eu	4.38	4.29	1.47	5.86	3.78
Gd	18.1	21.2	6.56	17.6	14.7
Tb	3.03	3.19	0.788	3.26	1.96
Dy	17.3	19.9	5.93	19.2	11.7
Ho	3.29	3.55	0.752	3.04	1.98
Er	10.4	10.2	2.12	6.73	6.50
Tm	1.65	1.07	0.448	1.06	0.595
Yb	7.82	8.77	3.27	7.26	5.99
Lu	1.13	1.43	0.21	0.84	0.43
Hf	7.09	5.59	1.96	4.80	4.69
Ta	0.735	0.659	0.028	0.533	0.345
Pb	2.74	1.59	1.19	2.55	2.01

**Where EMPA analyses were invalid, data from a similar crystal (on the basis of texture and backscatter intensity) were substituted.*

Table A3.4 Trace element concentrations in amphibole crystals analysed by LA-ICP-MS.
Abbreviations same as Table A3.2.

Sample	Maketawa	Maketawa	Inglewood b	Inglewood b	Inglewood b
ID	A13a	A13d	A1b	A1c	A1d
zone	rim	core	rim	core	zone
EMPA ID	A13_1	A13_2	A1_5	A1_6	A1_6
CaO	11.70	11.35	11.44	11.69	11.69
Mg#	74.60	66.10	77.09	74.89	74.89
Mn (wt%)	0.377	0.571	0.660	0.596	0.633
Li	4.15	3.55	8.27	5.64	6.80
Sc	78.3	32.5	55.3	51.3	49.3
Ti	19085	16581	17068	16121	16335
V	459	361	292	331	348
Cr	3.21	BDL	BDL	BDL	14.3
Ni	27.4	15.2	7.69	13.7	14.3
Zn	141	211	226	210	209
Rb	2.76	3.89	2.91	3.84	3.16
Sr	251	112	168	139	145
Y	87.8	114	150	122	117
Zr	132.5	141	141	136	133
Nb	12.6	19.6	20.4	16.4	16.6
Ba	414	382	415	370	349
La	13.9	19.4	22.3	19.8	19.5
Ce	52.3	70.5	94.1	79.1	75.3
Pr	9.91	13.9	17.1	15.2	13.7
Nd	56.0	71.2	95.4	84.8	72.7
Sm	19.2	20.5	26.1	23.9	20.5
Eu	3.49	3.95	5.81	5.27	5.16
Gd	20.3	22.2	29.8	21.7	22.6
Tb	3.05	3.46	4.77	3.34	3.08
Dy	16.7	19.0	32.1	24.4	22.7
Ho	2.71	4.05	6.67	4.69	5.21
Er	11.2	11.1	16.1	12.7	12.6
Tm	0.89	1.70	1.99	1.57	1.35
Yb	7.86	10.4	13.7	12.6	13.0
Lu	1.20	1.41	2.29	1.37	1.31
Hf	4.41	5.33	6.17	6.56	6.55
Ta	0.966	0.621	0.646	0.743	0.337
Pb	2.13	1.85	2.98	3.70	3.16

**Where EMPA analyses were invalid, data from a similar crystal (on the basis of texture and backscatter intensity) were substituted.*

Table A3.4 Trace element concentrations in amphibole crystals analysed by LA-ICP-MS.
Abbreviations same as Table A3.2.

Sample	Inglewood b	Inglewood b	Inglewood b	Inglewood b	Inglewood b
ID	A2a	A3	A8	A10a	A10b
zone	rim	core	core	rim	zone
EMPA ID	A2_3	A3_5	A8_3	A1_5*	A1_5*
CaO	11.40	11.31	11.44	11.44	11.44
Mg#	74.36	76.07	77.64	77.09	77.09
Mn (wt%)	0.672	0.568	0.595	0.534	0.485
Li	5.34	5.83	5.86	3.82	5.31
Sc	51.3	51.0	46.9	45.6	67.4
Ti	17677	15824	16011	15465	19299
V	306	315	300	286	411
Cr	2.11	BDL	11.0	3.32	9.66
Ni	9.57	2.18	3.99	11.6	31.1
Zn	220	208	194	174	168
Rb	3.04	2.59	2.86	1.98	2.95
Sr	165	178	155	153	216
Y	148	116	112	106	107
Zr	147	112	123	101	125
Nb	16.5	15.5	14.9	13.6	17.1
Ba	394	342	307	311	371
La	22.4	17.2	17.7	17.2	16.2
Ce	95.2	73.3	70.6	73.0	67.2
Pr	16.2	13.5	13.9	13.4	11.0
Nd	94.8	68.6	68.7	76.0	72.1
Sm	24.6	17.1	21.8	21.5	21.8
Eu	6.08	4.79	4.98	5.78	4.95
Gd	24.3	17.7	24.4	24.8	24.8
Tb	4.32	3.72	3.59	3.08	3.34
Dy	27.2	22.2	22.9	24.2	24.4
Ho	5.73	5.09	4.36	3.97	4.16
Er	16.4	13.0	13.1	13.2	11.8
Tm	2.23	1.83	1.47	1.51	1.50
Yb	12.3	9.99	12.5	9.92	9.58
Lu	1.96	1.27	1.57	1.70	1.15
Hf	7.28	6.30	5.02	5.81	4.39
Ta	0.524	0.581	0.516	0.737	0.550
Pb	1.89	2.40	2.59	1.64	1.95

**Where EMPA analyses were invalid, data from a similar crystal (on the basis of texture and backscatter intensity) were substituted.*

Table A3.4 Trace element concentrations in amphibole crystals analysed by LA-ICP-MS.
Abbreviations same as Table A3.2.

Sample	Inglewood b	Inglewood a	Inglewood a	Inglewood a	Inglewood a
ID	A11b	A9a	A9b	A10a	A10b
zone	core	core	light core	rim	core
EMPA ID	A11_2	A9_2	A9_3	A10_1	A10_4
CaO	11.69	11.52	11.94	11.28	11.97
Mg#	74.13	76.45	72.72	74.88	69.38
Mn (wt%)	0.454	0.567	0.636	0.540	0.365
Li	5.18	5.52	6.20	4.31	4.31
Sc	42.0	51.5	59.9	53.2	59.6
Ti	14358	15625	17455	16827	14290
V	308	303	310	302	449
Cr	BDL	9.20	BDL	BDL	2.12
Ni	3.15	4.25	2.48	9.15	15.8
Zn	176	193	213	190	138
Rb	3.15	3.41	2.66	2.56	3.30
Sr	308	167	159	187	261
Y	59.1	123	139	117	51.7
Zr	87.2	129	140	135	83.0
Nb	6.62	13.9	16.9	13.6	4.39
Ba	296	336	351	372	220
La	8.11	17.2	20.8	17.5	6.72
Ce	37.6	73.2	86.9	70.6	25.4
Pr	7.33	13.5	15.3	12.2	4.93
Nd	38.9	73.3	84.8	71.9	32.6
Sm	13.8	24.7	23.9	23.1	8.42
Eu	3.26	4.84	5.32	5.06	3.18
Gd	14.8	23.2	27.7	23.3	12.2
Tb	1.98	3.66	4.22	3.43	1.54
Dy	11.8	22.9	28.2	20.0	9.68
Ho	2.41	4.69	5.48	4.36	2.04
Er	5.83	13.9	17.0	12.7	6.21
Tm	0.74	1.71	1.43	1.79	0.542
Yb	5.34	13.0	13.5	10.5	4.53
Lu	0.81	1.47	1.81	1.42	0.629
Hf	4.29	5.80	6.21	5.41	4.27
Ta	0.327	0.578	0.833	0.746	0.174
Pb	2.05	2.31	2.33	2.17	2.12

**Where EMPA analyses were invalid, data from a similar crystal (on the basis of texture and backscatter intensity) were substituted.*

Table A3.4 Trace element concentrations in amphibole crystals analysed by LA-ICP-MS.
Abbreviations same as Table A3.2.

Sample	Inglewood a	Inglewood a	Korito	Korito	Korito
ID	A13a	A13b	A3B	A3C	A3D
zone	zone	core	zone	zone	zone
EMPA ID	A13_5	A13_7	A3_2	A3_7	A3_11
CaO	11.48	11.27	11.84	11.48	11.77
Mg#	74.90	77.54	66.42	71.17	73.40
Mn (wt%)	0.498	0.414	0.519	0.433	0.401
Li	4.64	4.30	5.27	4.93	4.11
Sc	63.9	68.6	72.0	58.1	70.6
Ti	17962	18311	19737	17279	18987
V	371	400	415	391	401
Cr	9.08	2.64	11.6	BDL	5.97
Ni	30.1	31.3	24.7	28.5	27.6
Zn	186	152	174	166	139
Rb	3.10	2.94	2.71	3.43	2.46
Sr	160	209	192	177	193
Y	108	96.8	111	79.9	128
Zr	134	132	126	113	126
Nb	15.3	13.5	14.8	12.7	16.5
Ba	361	304	356	285	339
La	16.6	13.6	16.8	11.8	18.3
Ce	68.7	54.6	62.6	48.4	70.2
Pr	12.1	10.4	11.4	9.81	12.7
Nd	67.9	58.4	63.7	48.8	77.3
Sm	21.3	19.9	19.8	15.3	22.8
Eu	4.15	4.15	4.46	3.61	5.44
Gd	23.7	21.2	21.0	12.2	22.9
Tb	3.19	3.27	3.41	2.80	3.63
Dy	19.8	19.5	21.0	15.3	22.4
Ho	3.69	3.45	4.03	3.49	4.30
Er	12.8	11.4	10.7	8.05	13.7
Tm	1.85	1.41	1.68	0.970	1.78
Yb	11.3	9.49	9.29	6.87	8.74
Lu	1.17	1.31	1.22	0.955	1.34
Hf	4.99	4.31	5.90	4.69	5.90
Ta	0.514	0.809	0.547	0.427	0.557
Pb	1.89	1.51	2.54	1.43	1.52

**Where EMPA analyses were invalid, data from a similar crystal (on the basis of texture and backscatter intensity) were substituted.*

Table A3.4 Trace element concentrations in amphibole crystals analysed by LA-ICP-MS.
Abbreviations same as Table A3.2.

Sample	Korito	Korito	Korito	Korito	Korito	Korito
ID	A3E	A3F	A3G	A7A	A11a	A12B
zone	core	zone	zone	rim	core	zone
EMPA ID	A3_13	A3_6	A3_10	A7_2	A11_2	A12_3
CaO	11.75	11.66	11.81	11.31	11.97	12.07
Mg#	72.48	71.00	69.07	79.30	72.87	70.34
Mn (wt%)	0.209	0.427	0.379	0.279	0.320	0.330
Li	3.29	5.25	5.14	4.25	5.27	3.85
Sc	65.4	65.8	66.9	55.1	48.6	57.9
Ti	14652	17713	16346	13176	13216	13318
V	541	375	462	359	349	337
Cr	1.32	4.46	3.85	BDL	11.4	BDL
Ni	35.1	22.6	24.8	BDL	BDL	BDL
Zn	90.9	171	155	109	141	144
Rb	3.17	2.32	3.65	3.89	2.66	2.79
Sr	323	202	288	304	292	333
Y	32.1	93.5	50.7	43.0	49.0	49.6
Zr	51.5	125	102	56.2	67.2	80.1
Nb	3.57	12.3	6.63	4.71	2.74	5.57
Ba	243	318	256	278	247	293
La	4.78	13.1	6.86	5.93	6.06	6.12
Ce	18.6	54.8	26.6	23.3	25.3	25.9
Pr	2.68	10.6	5.55	4.32	5.19	4.98
Nd	18.1	60.5	27.6	29.7	32.5	29.3
Sm	5.76	18.2	9.90	8.00	11.3	8.71
Eu	2.20	3.71	2.82	2.03	3.05	2.92
Gd	6.85	19.8	10.6	9.27	10.1	12.8
Tb	1.03	2.84	1.50	1.49	1.38	1.74
Dy	5.77	16.8	10.3	8.31	10.0	9.54
Ho	1.11	3.36	2.04	1.73	1.76	1.92
Er	2.69	9.47	5.27	4.82	5.70	6.04
Tm	0.335	1.23	0.698	0.613	0.596	0.582
Yb	1.74	7.71	3.40	3.76	4.82	2.62
Lu	0.286	1.20	0.740	0.446	0.656	0.514
Hf	1.24	5.88	5.36	2.25	2.86	3.39
Ta	0.072	0.535	0.275	0.292	0.207	0.132
Pb	3.51	1.96	1.57	1.71	1.64	1.55

**Where EMPA analyses were invalid, data from a similar crystal (on the basis of texture and backscatter intensity) were substituted.*

Table A3.4 Trace element concentrations in amphibole crystals analysed by LA-ICP-MS. Abbreviations same as Table A3.2.

Sample	Korito	Korito	Korito
ID	A12C	A14A	A14D
zone	core	rim	core
EMPA ID	A12_4	A14_1	A14_5
CaO	11.91	11.47	11.81
Mg#	75.02	79.09	77.28
Mn (wt%)	0.264	0.462	0.254
Li	4.10	4.27	4.70
Sc	53.3	51.7	55.3
Ti	12093	15069	12391
V	319	281	343
Cr	BDL	BDL	BDL
Ni	BDL	4.32	3.54
Zn	109	157	108
Rb	2.66	2.30	2.77
Sr	315	216	283
Y	37.9	101	42.9
Zr	67.2	111	62.2
Nb	3.28	9.81	2.27
Ba	237	267	221
La	4.58	12.4	4.95
Ce	16.8	50.3	21.3
Pr	3.58	9.81	4.24
Nd	21.8	59.1	27.9
Sm	7.65	18.9	8.66
Eu	2.29	3.85	2.83
Gd	8.23	20.4	11.9
Tb	1.09	3.14	1.46
Dy	6.75	19.1	8.74
Ho	1.48	4.01	1.88
Er	3.10	10.8	4.84
Tm	0.502	1.26	0.470
Yb	3.34	8.17	2.34
Lu	0.607	1.05	0.420
Hf	3.93	6.33	3.23
Ta	0.172	0.503	0.138
Pb	0.72	1.77	1.15

**Where EMPA analyses were invalid, data from a similar crystal (on the basis of texture and backscatter intensity) were substituted.*

APPENDIX 4: DIFFUSION MODELLING IMAGES AND PROFILES

Table A4.1 Diffusion ages calculated for each zone in this study

A compilation of the BSE images used for modelling and the profile that was modelled

Table A4.1 Diffusion ages calculated for each zone used in this study. Errors are based on $\pm 40^\circ$ C error.

<i>Kaupokonui</i>	Age	Minimum	Maximum
Rims			
cpx2a3	0.30	0.08	1.20
cpx5a1	0.39	0.11	1.55
cpx17a1	0.34	0.09	1.36
cpx23a1	0.24	0.07	0.96
cpx24a1	0.38	0.10	1.50
cpx30a1	2.25	0.62	8.90
cpx31a1	1.02	0.28	4.02
cpx32a2	0.70	0.19	2.78
cpx40a1	0.91	0.25	3.60
Dark rims			
cpx1a2	0.63	0.17	2.50
cpx11a2	0.25	0.07	1.00
cpx21a2	0.71	0.20	2.81
cpx26a1	0.22	0.06	0.86
cpx33a8	0.60	0.17	2.38
cpx35a2	0.42	0.11	1.64
cpx46a1	0.22	0.06	0.86
Outer oscillatory zones			
cpx6a1	0.12	0.03	0.49
cpx7a3	0.43	0.12	1.71
cpx21a5	1.40	0.39	5.53
cpx22a3	0.17	0.05	0.69
cpx24a2	0.48	0.13	1.91
cpx47a1	0.62	0.17	2.46
cpx52a1	0.52	0.14	2.06
cpx52a2	0.14	0.04	0.53
cpx60a1	0.25	0.07	0.98
cpx61a1	0.51	0.14	2.03
Inner oscillatory zones			
cpx10b1	0.15	0.04	0.60
cpx10b3	0.58	0.16	2.30
cpx10b4	1.02	0.28	4.02
cpx24a5	0.38	0.11	1.51
cpx31a3	2.23	0.62	8.81
cpx36a1	1.30	0.36	5.14
cpx43a2	0.62	0.17	2.47
cpx47a5	0.30	0.08	1.17
cpx51a2	0.57	0.16	2.27
cpx51a4	0.52	0.14	2.04
cpx55a4	0.58	0.16	2.31

Table A4.1 Diffusion ages calculated for each zone used in this study. Errors are based on $\pm 40^\circ$ C error.

<i>Maketawa</i>	Age	Minimum	Maximum
Rims			
cpx6a1	0.45	0.11	2.05
cpx9b2	0.53	0.13	2.44
cpx14b1	1.67	0.41	7.63
cpx23b1	0.38	0.09	1.74
cpx26a1	1.16	0.28	5.28
cpx32b1	0.74	0.18	3.37
cpx50a1	0.73	0.18	3.33
cpx51a2	0.53	0.13	2.40
cpx71b1	0.30	0.07	1.36
Inner zones			
cpx6a2	0.58	0.14	2.65
cpx14b2	4.50	1.09	20.57
cpx25b1	1.22	0.30	5.57
cpx35b1	1.81	0.44	8.28
cpx46a1	1.64	0.40	7.51
cpx51a1	1.71	0.42	7.81
Cores			
cpx14b3	2.84	0.69	12.96
cpx32b2	3.60	0.88	16.47
cpx35b2	7.55	1.83	34.51
cpx65a1	0.87	0.21	3.99

Table A4.1 Diffusion ages calculated for each zone used in this study. Errors are based on $\pm 40^\circ$ C error.

<i>Inglewood b</i>	Age	Minimum	Maximum
Rims			
cpx8a2	2.91	0.64	14.75
cpx24b1	3.93	0.87	19.95
cpx29b2	1.62	0.36	8.21
Outer oscillatory zones			
cpx2a1	1.45	0.32	7.33
cpx7b1	2.20	0.49	11.17
cpx9b2	3.96	0.88	20.09
cpx10a5	1.74	0.39	8.84
cpx12b2	2.41	0.53	12.23
cpx13b2	2.57	0.57	13.05
cpx15b2	2.18	0.48	11.06
cpx21a1	3.15	0.70	16.00
cpx24b2	3.34	0.74	16.96
cpx25a1	2.32	0.51	11.77
cpx28b2	1.71	0.38	8.68
cpx34a1	1.60	0.35	8.12
cpx39a1	1.83	0.40	9.29
Inner oscillatory zones			
cpx2a3	1.86	0.41	9.42
cpx8a3	11.90	2.63	60.38
cpx9b3	5.18	1.15	26.29
cpx9b4	14.94	3.30	75.79
cpx10a9	2.04	0.45	10.36
cpx11a1	2.83	0.63	14.34
cpx15b3	2.70	0.60	13.68
cpx21a2	7.76	1.72	39.39
cpx28b3	7.05	1.56	35.75
cpx29b3	8.12	1.79	41.18
cpx33a1	2.06	0.46	10.46

Table A4.1 Diffusion ages calculated for each zone used in this study. Errors are based on $\pm 40^\circ$ C error.

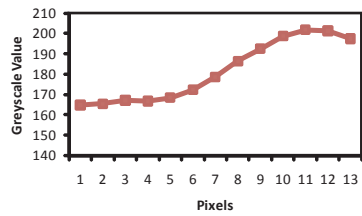
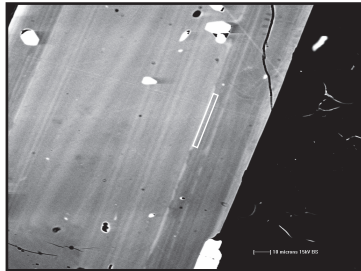
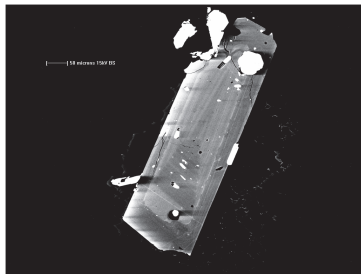
<i>Inglewood a</i>	Age	Minimum	Maximum
Rims			
cpx1b3	3.42	0.79	16.40
cpx5a2	0.68	0.16	3.25
cpx30b1	3.87	0.90	18.56
cpx39a1	1.37	0.32	6.55
cpx44a1	2.18	0.50	10.45
cpx54a1	3.93	0.91	18.86
Minor zones			
cpx5a4	0.76	0.18	3.65
cpx31a3	1.62	0.38	7.78
cpx33b1	0.64	0.15	3.05
cpx58a1	1.09	0.25	5.22
Second zone from rim			
cpx33b2	1.43	0.33	6.85
cpx48a2	1.94	0.45	9.30
cpx56b1	1.43	0.33	6.87
cpx66a1	1.93	0.45	9.29
cpx69b1	2.82	0.65	13.55
Inner zones			
cpx21a1	2.74	0.64	13.17
cpx30b2	2.14	0.50	10.26
cpx31a4	2.17	0.50	10.42
cpx35b1	2.79	0.65	13.40
cpx63c2	3.37	0.78	16.18
cpx68b2	5.90	1.37	28.32
cpx73a2	3.55	0.82	17.07
cpx74a1	3.01	0.70	14.45
cpx111a1	3.03	0.70	14.55
cpx112a2	3.07	0.71	14.74

Table A4.1 Diffusion ages calculated for each zone used in this study. Errors are based on $\pm 40^\circ$ C error.

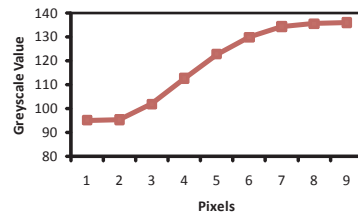
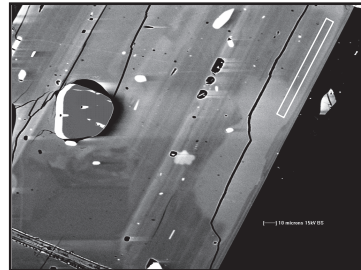
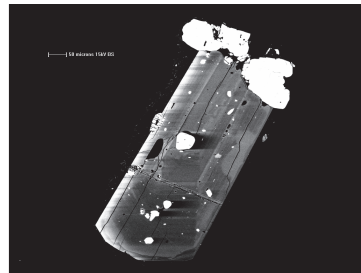
<i>Korito</i>	Age	Minimum	Maximum
Rims			
cpx4b3	0.82	0.20	3.70
cpx12a1	0.37	0.09	1.70
cpx18b1	0.66	0.16	2.98
cpx19a1	0.61	0.15	2.77
cpx28b1	1.21	0.29	5.46
cpx30a1b	0.60	0.15	2.72
cpx38b1	0.46	0.11	2.07
cpx39b1	1.10	0.27	4.97
cpx44a1	2.46	0.60	11.15
cpx46a1	0.57	0.14	2.60
Second zone from rim			
cpx8a1	3.66	0.89	16.61
cpx14a1	2.75	0.67	12.46
cpx18b4	8.87	2.16	40.20
cpx34a1b	5.20	1.27	23.55
Third zone from rim			
cpx7b1	0.79	0.19	3.58
cpx9a1	0.36	0.09	1.65
cpx17a2b	0.95	0.23	4.31
cpx18b3	3.00	0.73	13.61
cpx19a4	2.04	0.50	9.26
cpx20b1	0.85	0.21	3.87
Inner zones			
cpx10a1	2.89	0.71	13.10
cpx17a6	2.96	0.72	13.43
cpx19a3	2.23	0.54	10.12
cpx20b2	3.39	0.83	15.36
cpx28b3	2.23	0.54	10.10
cpx46a2	2.50	0.61	11.33

Kaupokonui-Rims

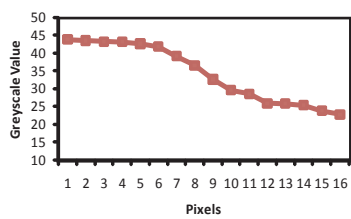
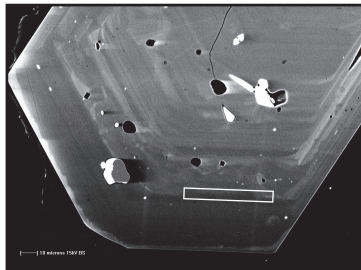
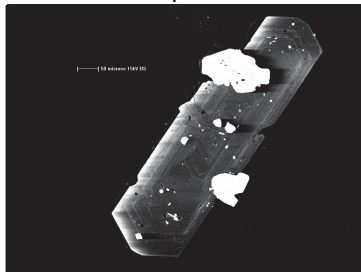
cpx2a3



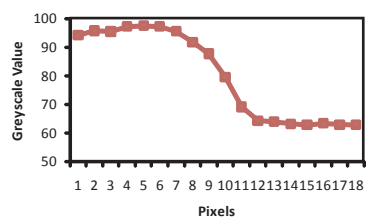
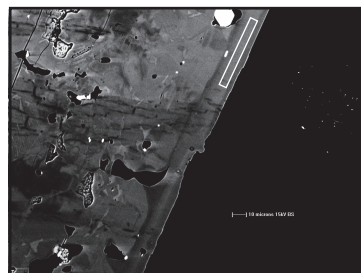
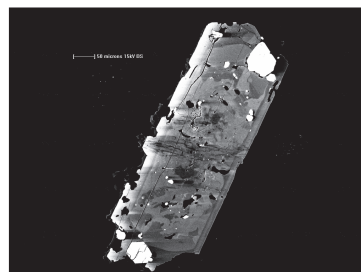
cpx5a1



cpx17a1

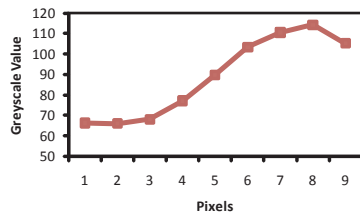
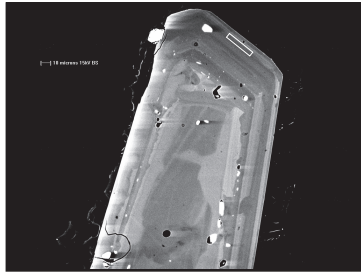


cpx23a1

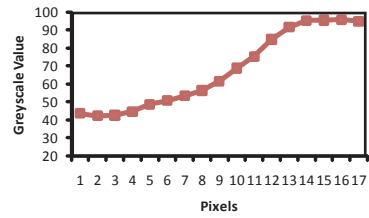
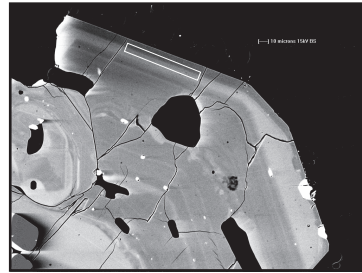
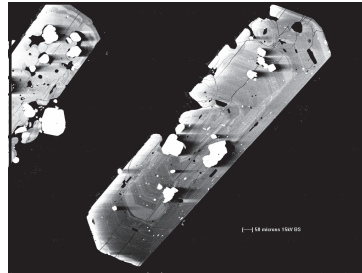


Kaupokonui-Rims

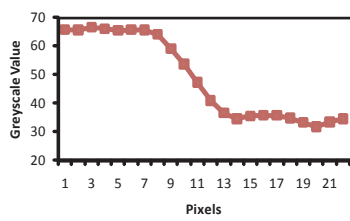
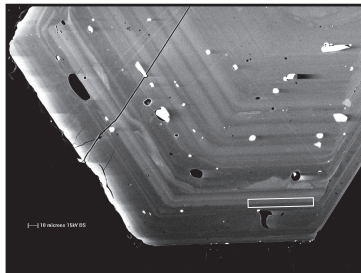
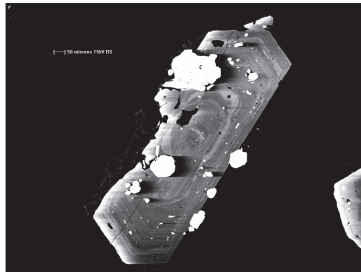
cpx24a1



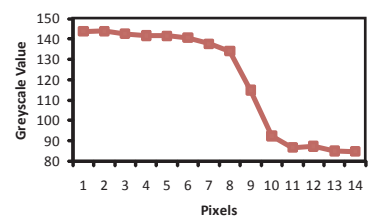
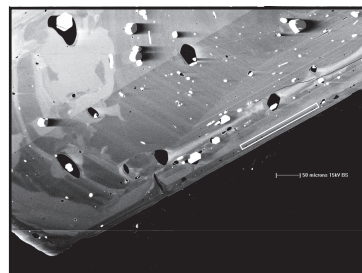
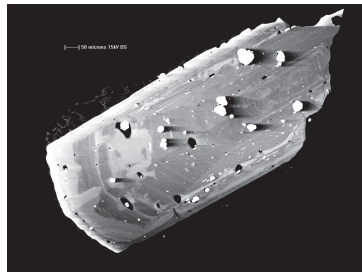
cpx30a1



cpx31a1

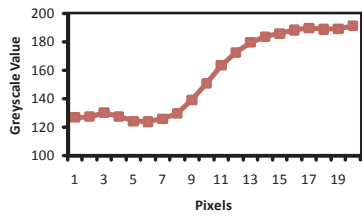
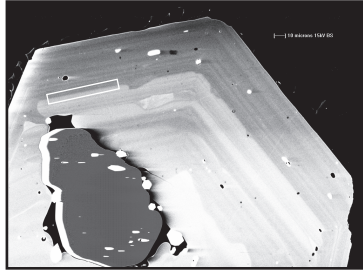


cpx32a2



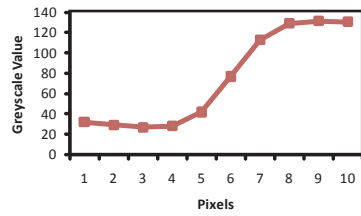
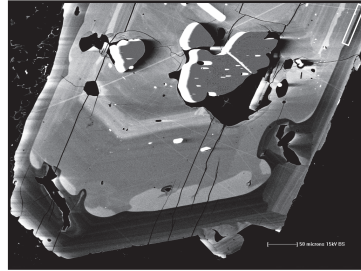
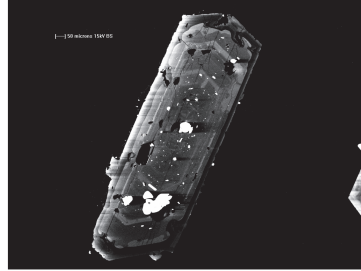
Kaupokonui-Rims

cpx40a1

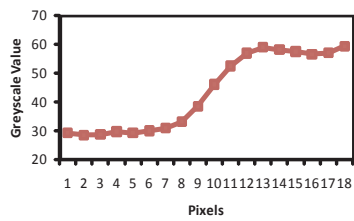
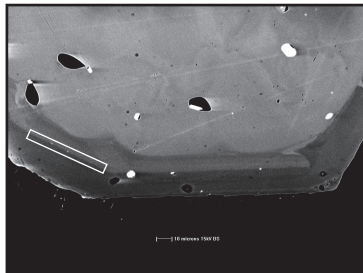
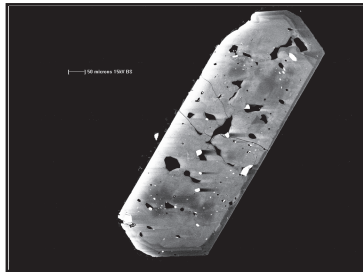


Kaupokonui-Dark rims

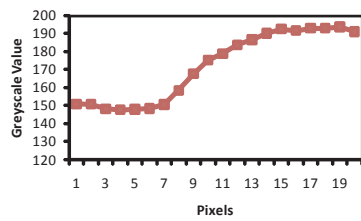
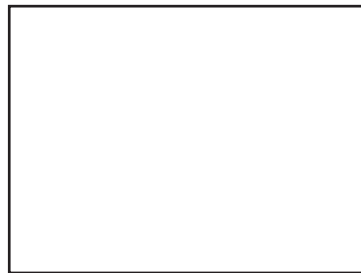
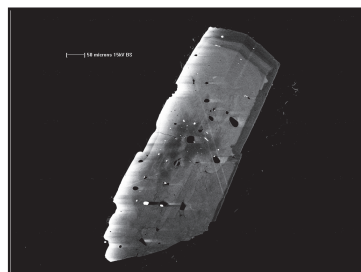
cpx1a2



cpx11a2

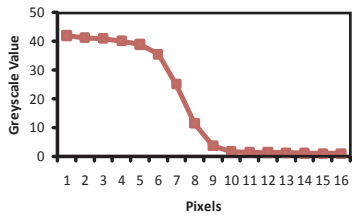
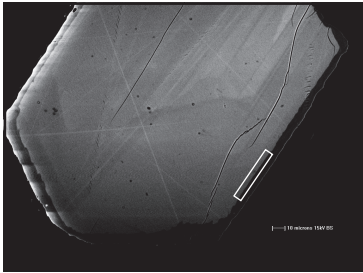
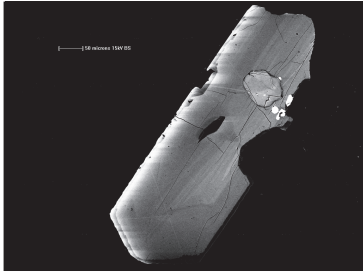


cpx21a2

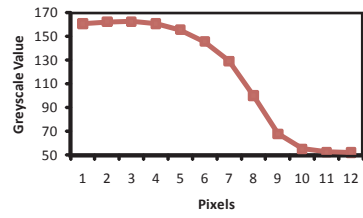
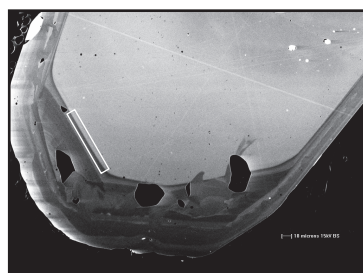
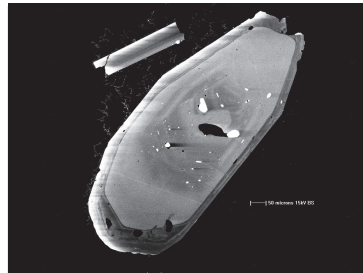


Kaupokonui-Dark rims

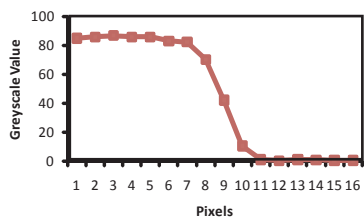
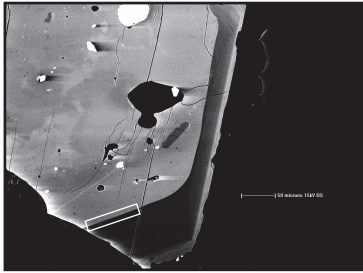
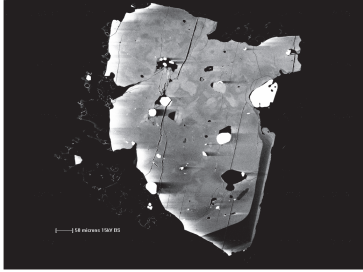
cpx26a1



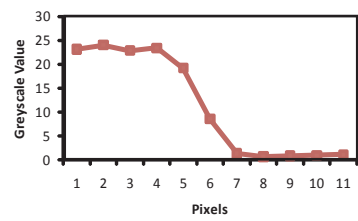
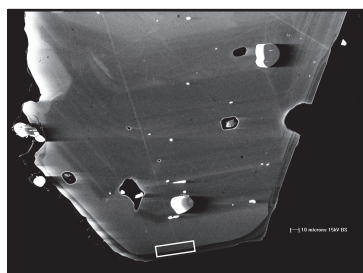
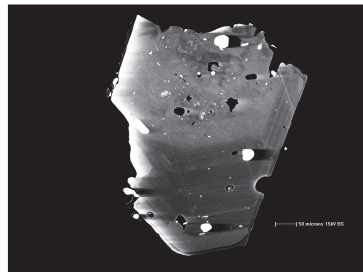
cpx33a8



cpx35a2

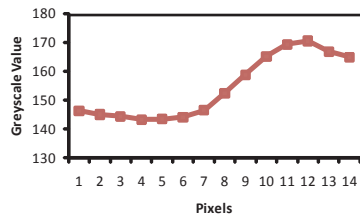
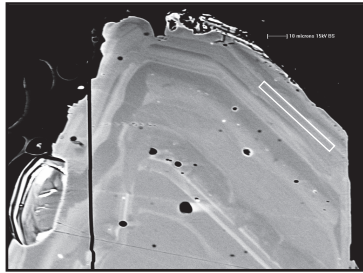
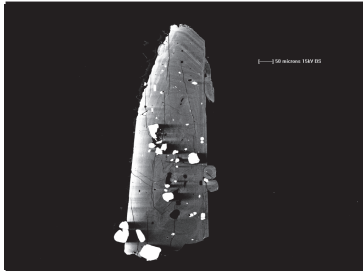


cpx46a1

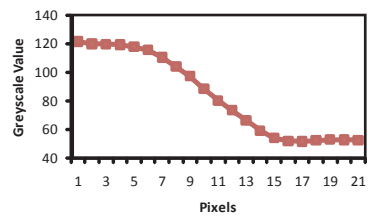
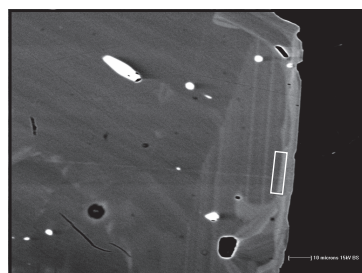
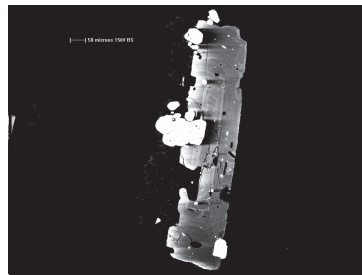


Kaupokonui-Outer oscillatory zones

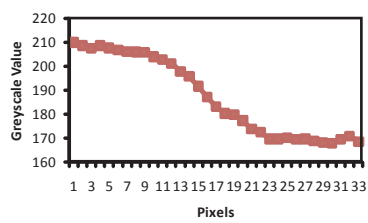
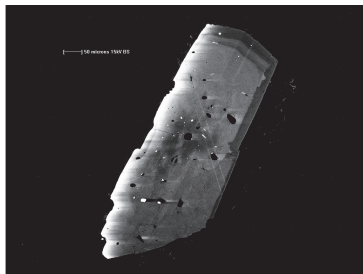
cpx6a1



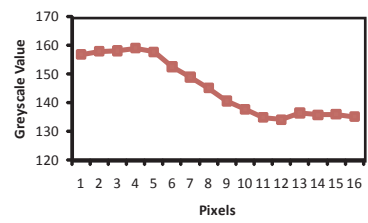
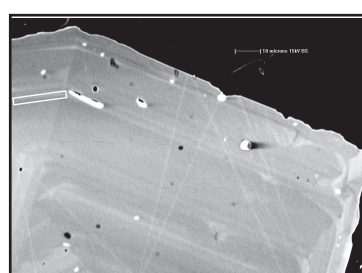
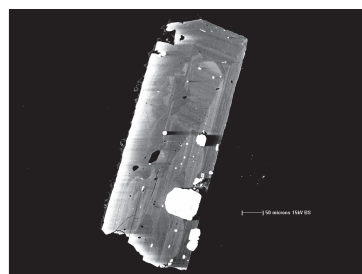
cpx7a3



cpx21a5

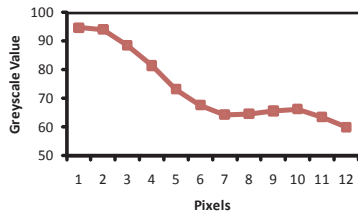
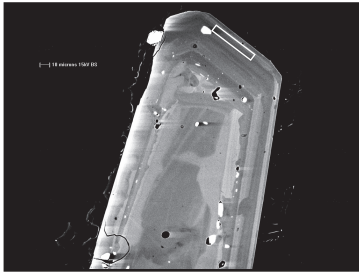
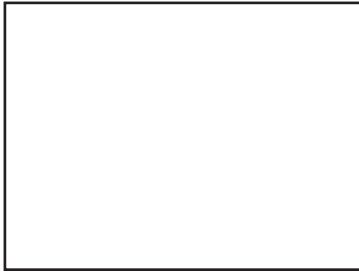


cpx22a3

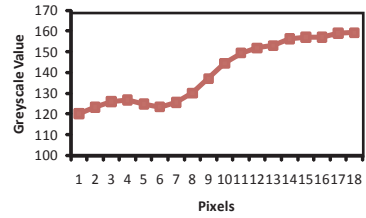
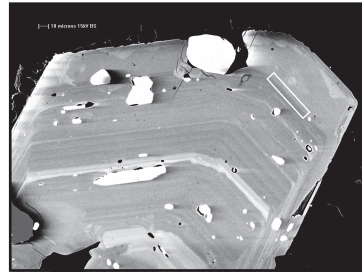
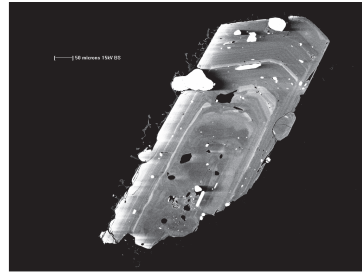


Kaupokonui-Outer oscillatory zones

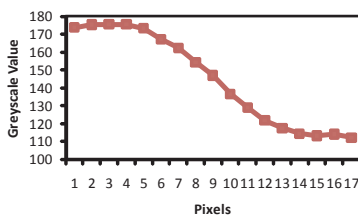
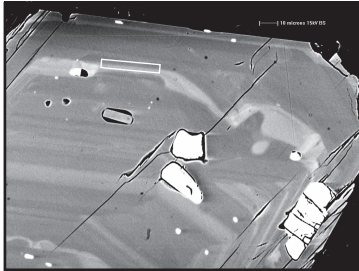
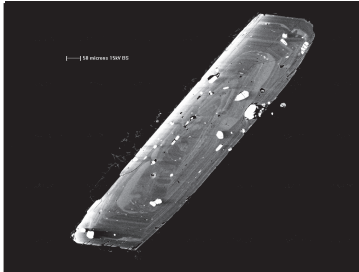
cpx24a2



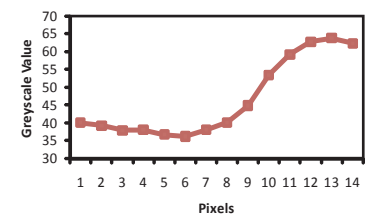
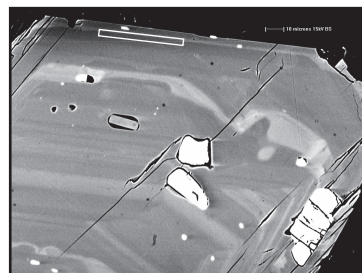
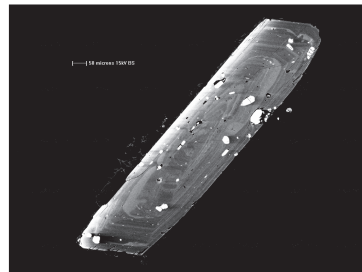
cpx47a1



cpx52a1

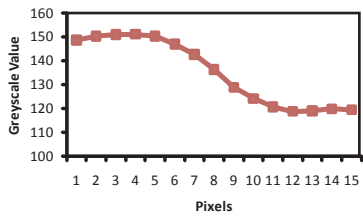
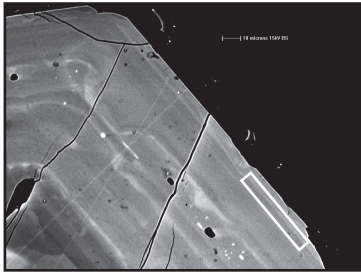
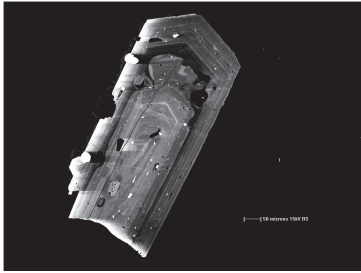


cpx52a2

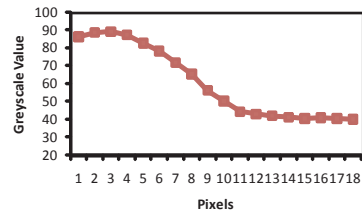
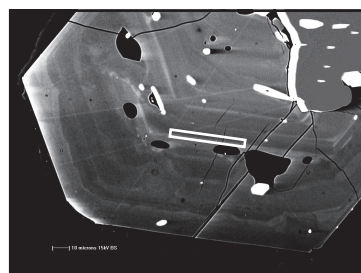


Kaupokonui-Outer oscillatory zones

cpx60a1

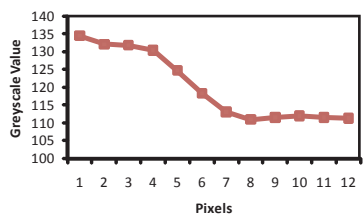
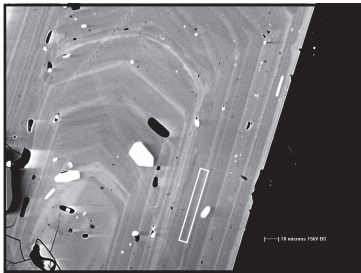
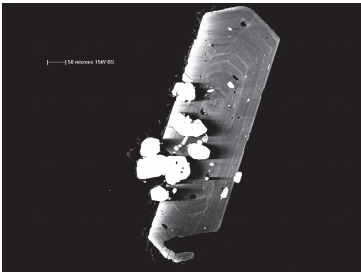


cpx61a1

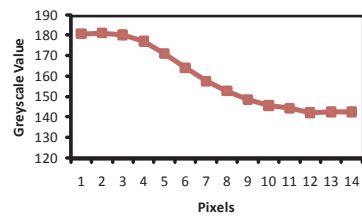
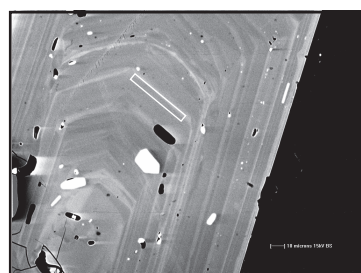
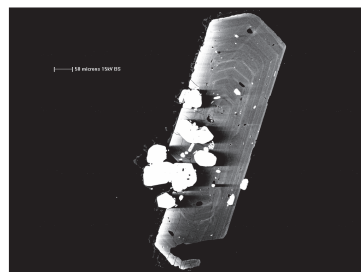


Kaupokonui-Inner oscillatory zones

cpx10b1

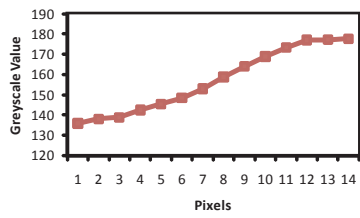
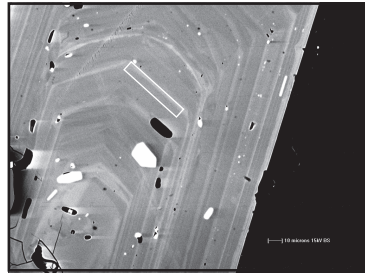
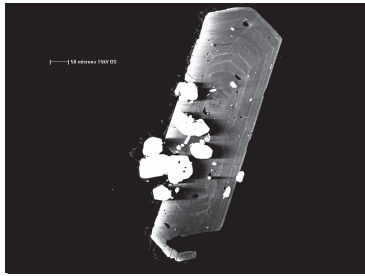


cpx10b3

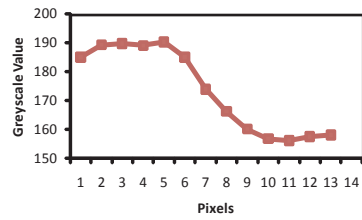
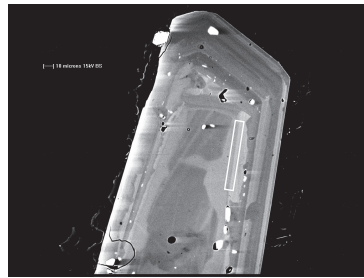


Kaupokonui- Inner oscillatory zones

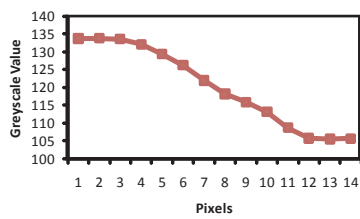
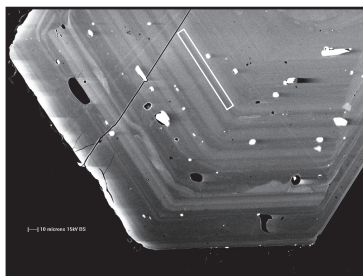
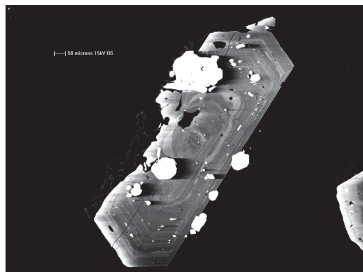
cpx10b4



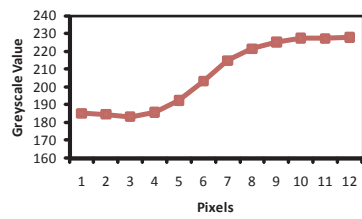
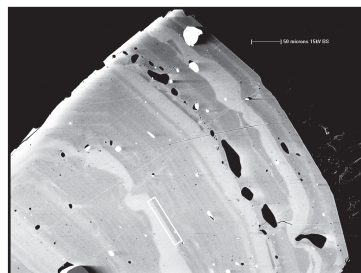
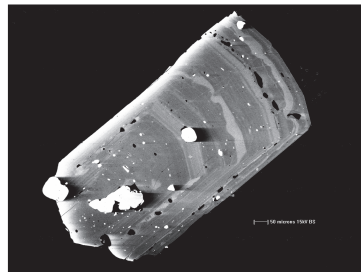
cpx24a5



cpx31a3

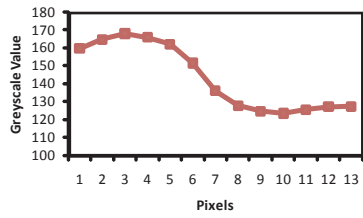
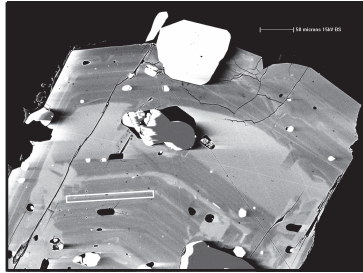
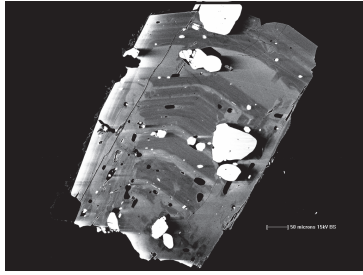


cpx36a1

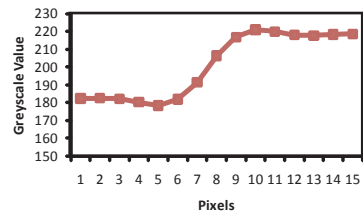
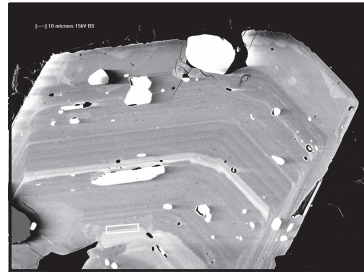
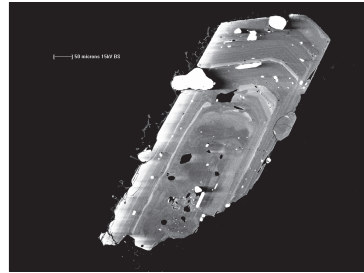


Kaupokonui- Inner oscillatory zones

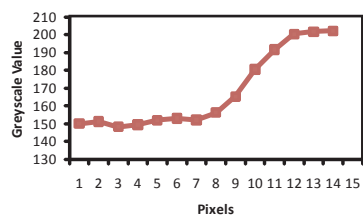
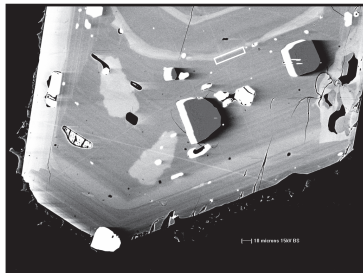
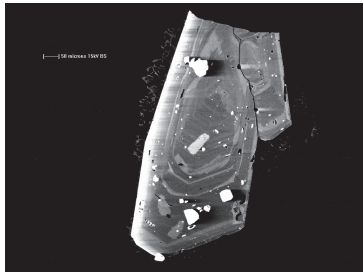
cpx43a2



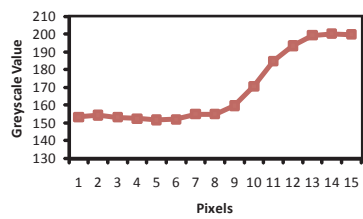
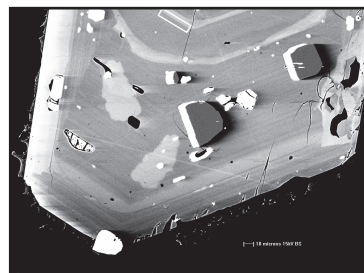
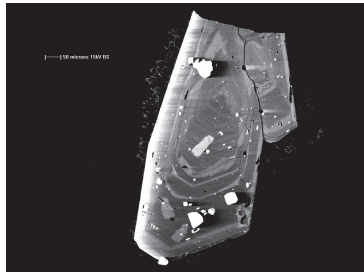
cpx47a5



cpx51a2

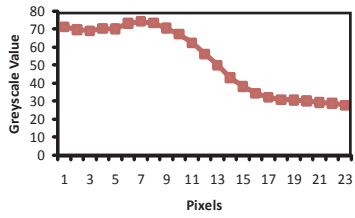
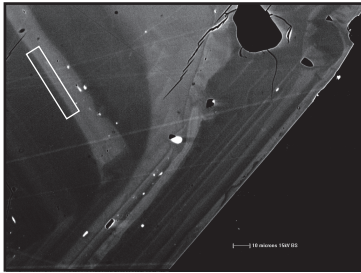
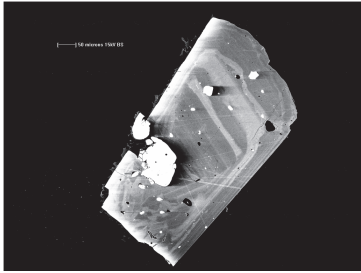


cpx51a4



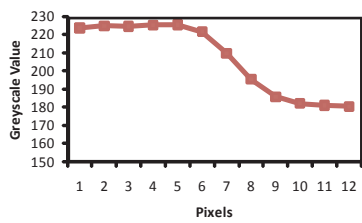
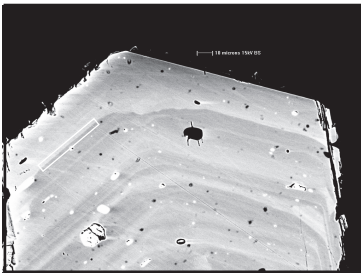
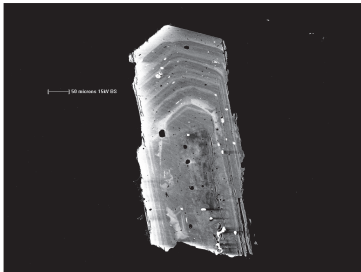
Kaupokonui- Inner oscillatory zones

cpx55a4

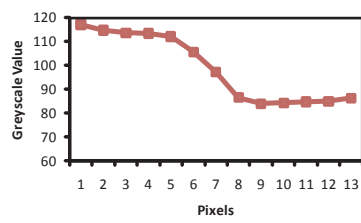
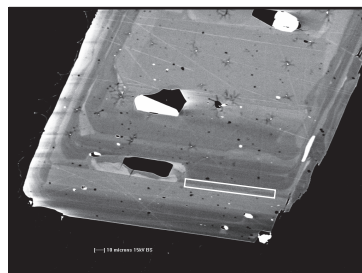


Maketawa-Rims

cpx6a1

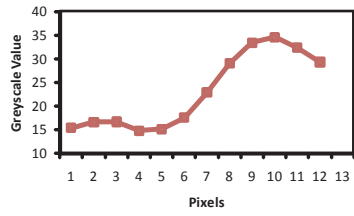
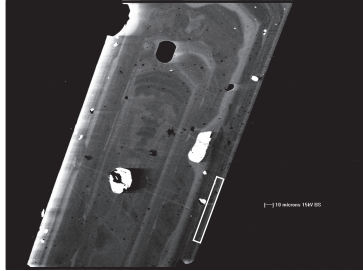
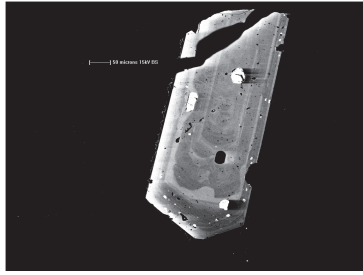


cpx9b2

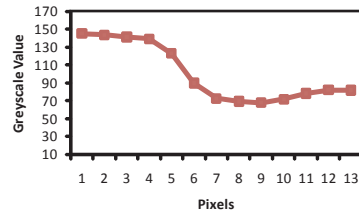
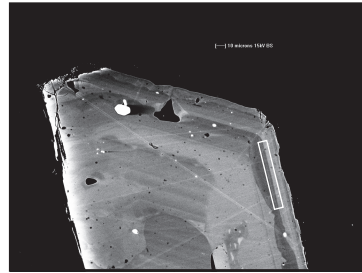
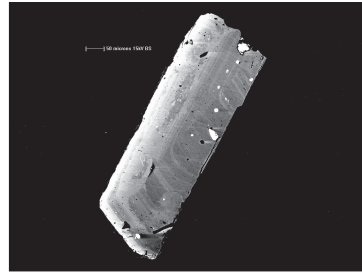


Maketawa-Rims

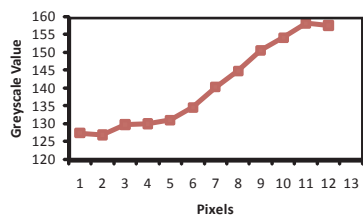
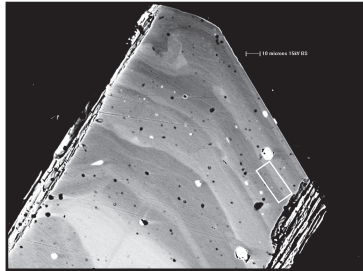
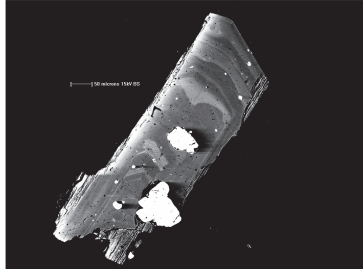
cpx14b1



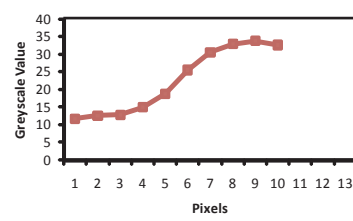
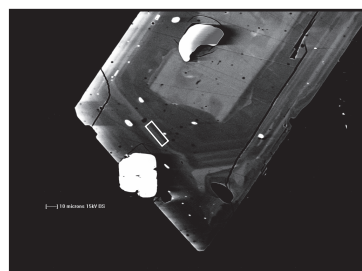
cpx23b1



cpx26a1

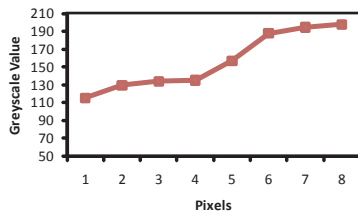
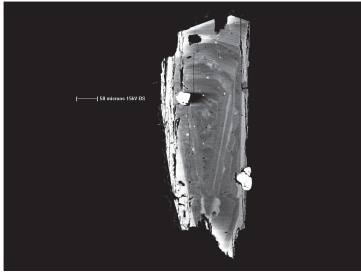


cpx32b1

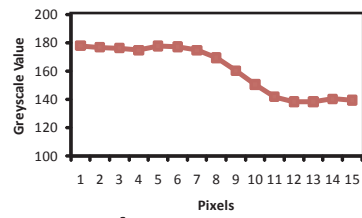
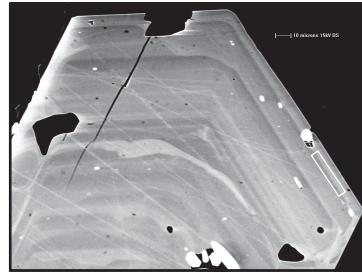
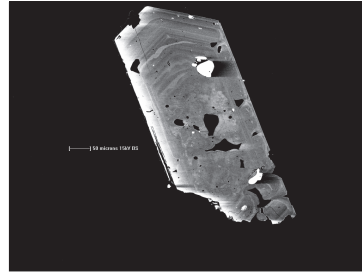


Maketawa-Rims

cpx50a1

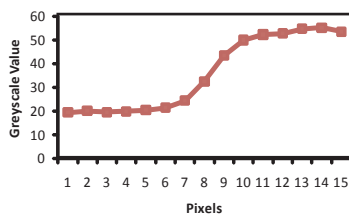
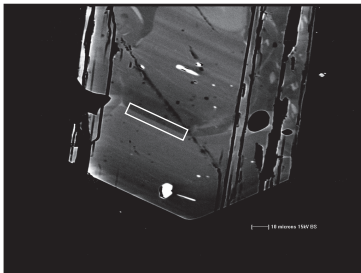
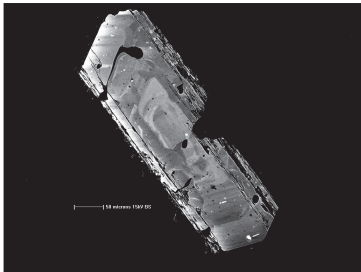


cpx51a2

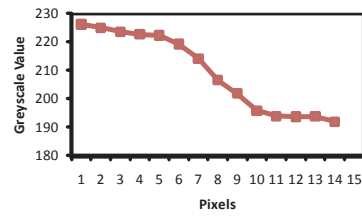
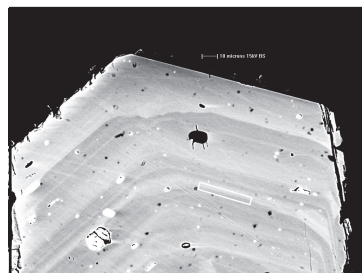
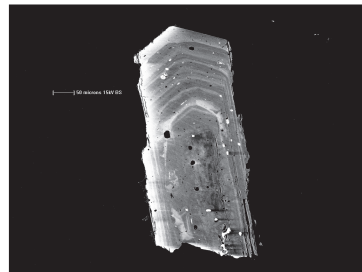


Maketawa-Inner zones

cpx71b1

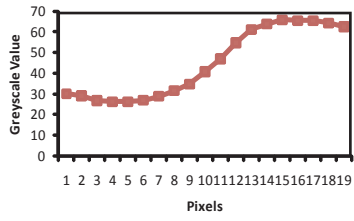
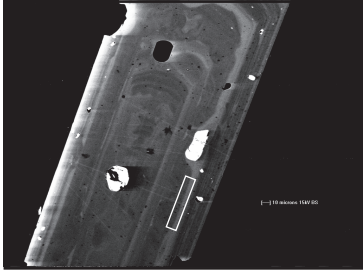
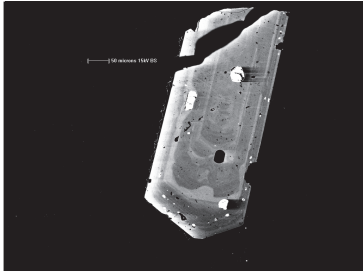


cpx6a2

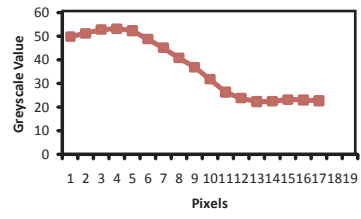
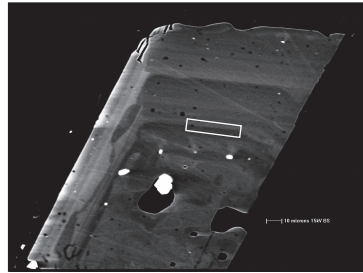


Maketawa-Inner zones

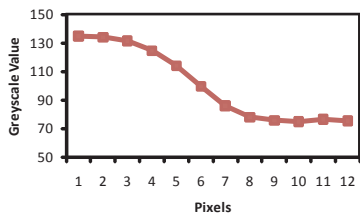
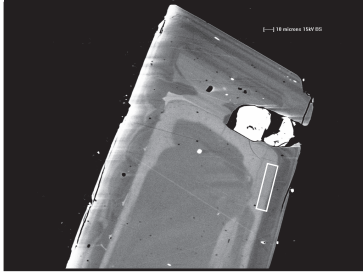
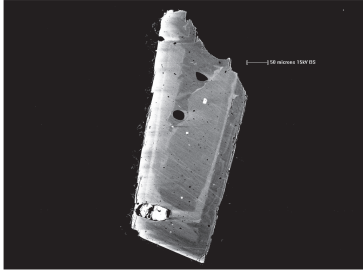
cpx14b2



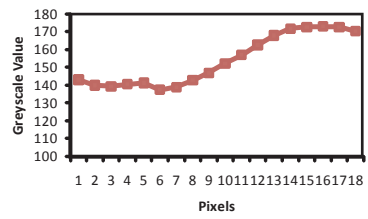
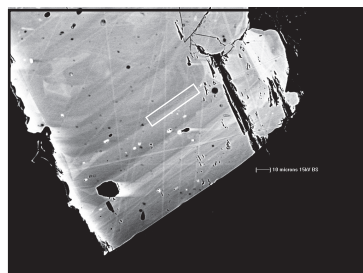
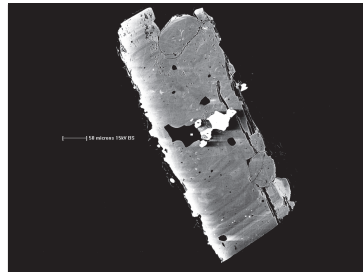
cpx25b1



cpx35b1

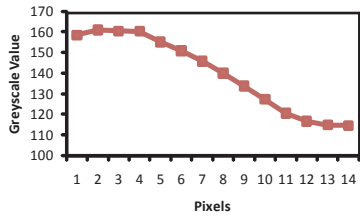
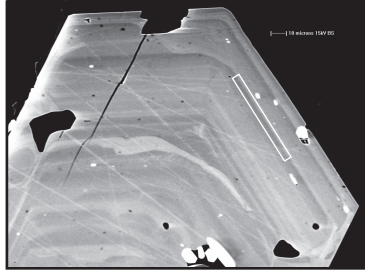
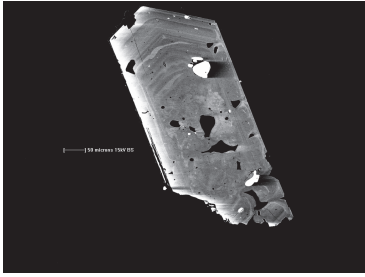


cpx46a1



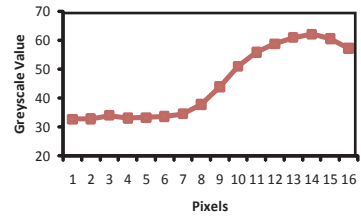
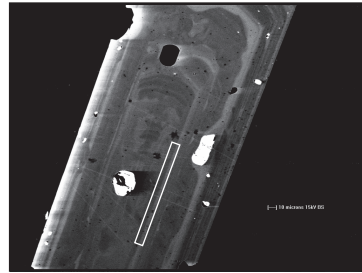
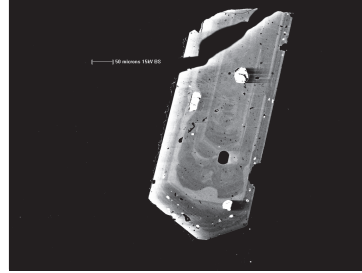
Maketawa-Inner zones

cpx51a1

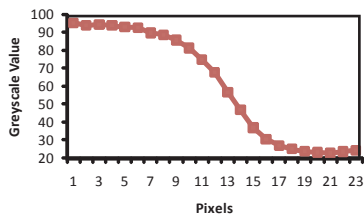
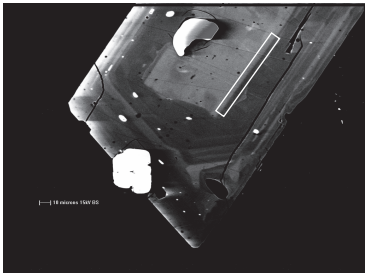


Maketawa-Cores

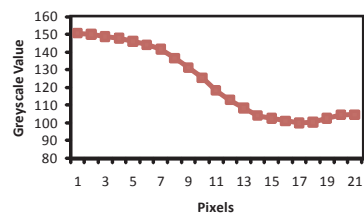
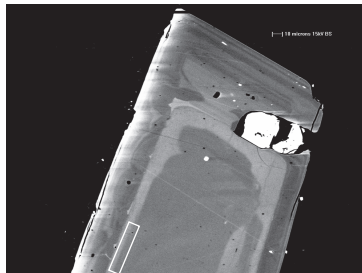
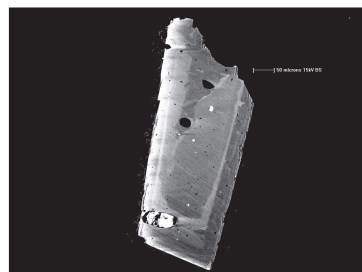
cpx14b3



cpx32b2

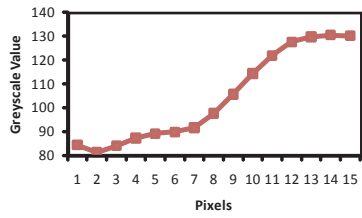
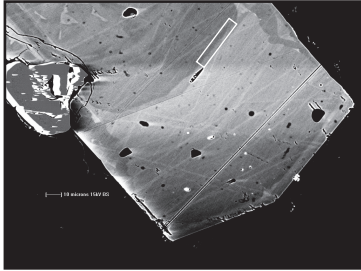


cpx35b2



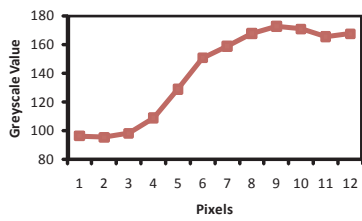
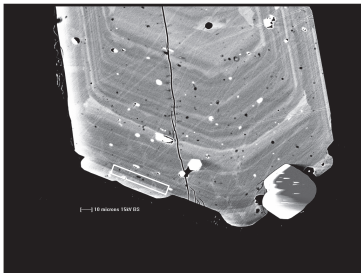
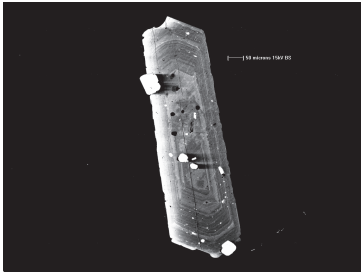
Maketawa-Cores

cpx65a1

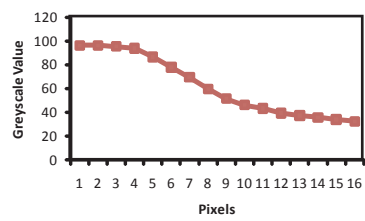
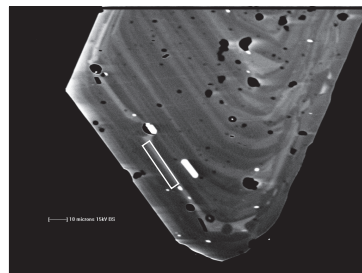
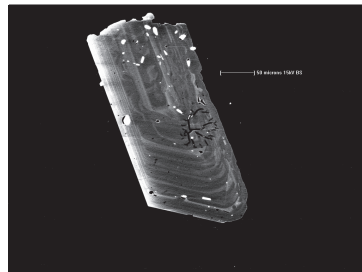


Inglewood b-Rims

cpx8a1

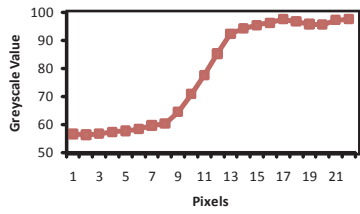
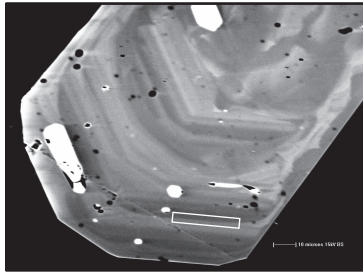
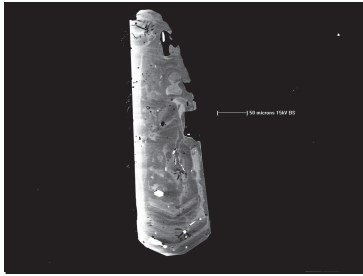


cpx24b1



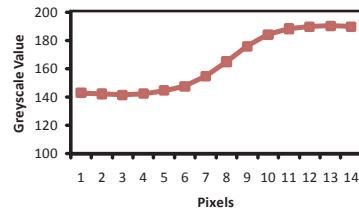
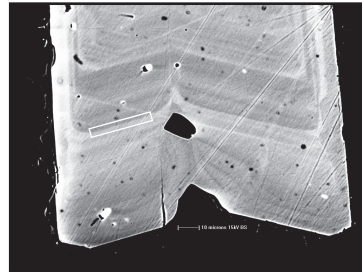
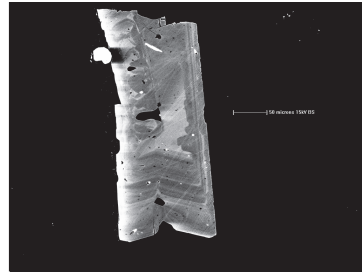
Inglewood b-Rims

cpx29b2

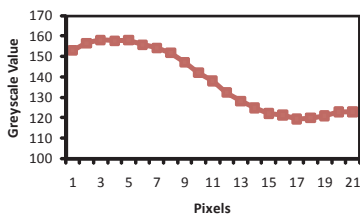
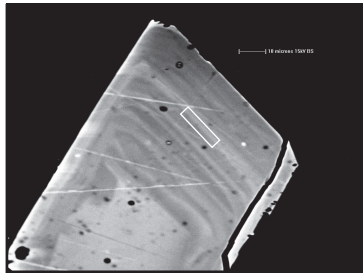
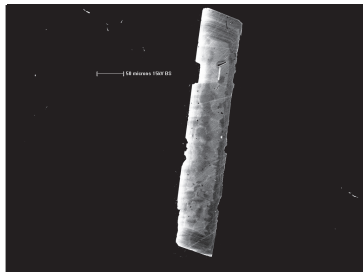


Inglewood b-Outer oscillatory zones

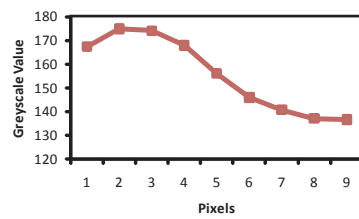
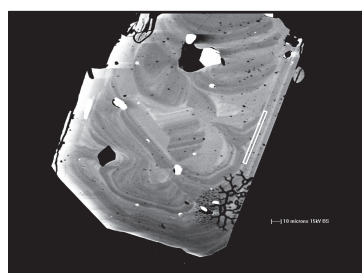
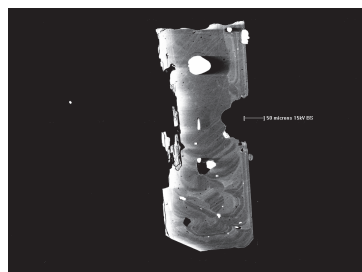
cpx2a1



cpx7b1

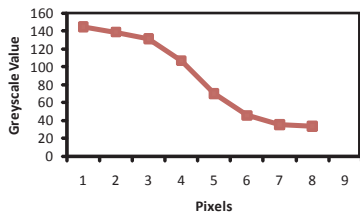
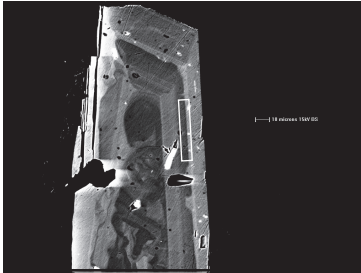
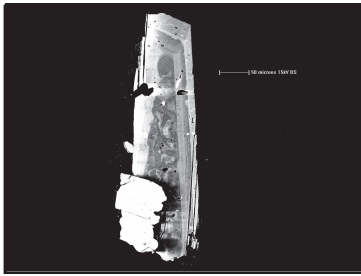


cpx9b2

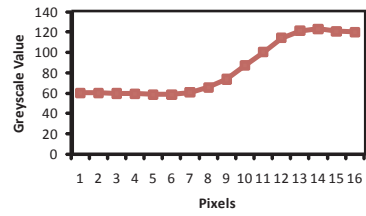
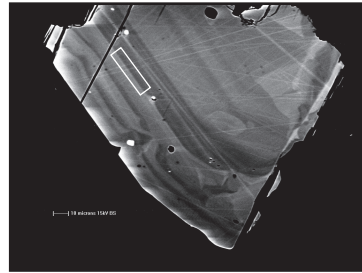
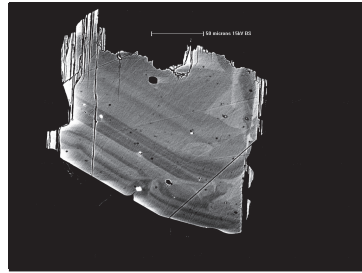


Inglewood b-Outer oscillatory zones

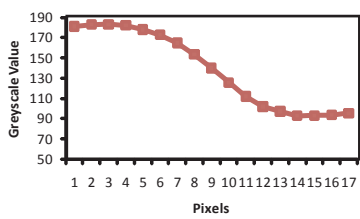
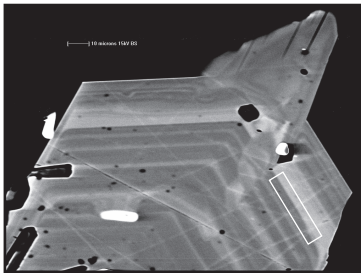
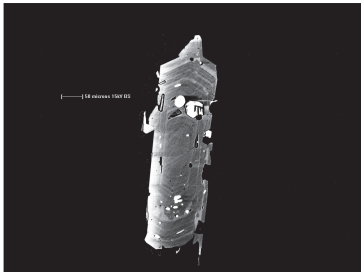
cpx10a5



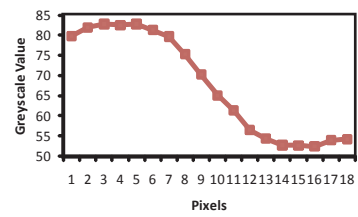
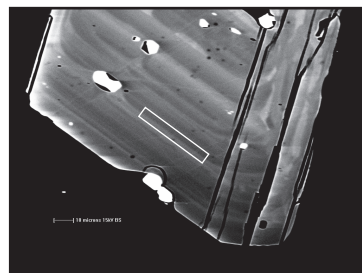
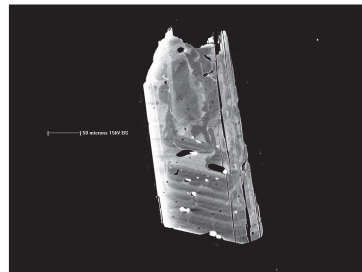
cpx12b2



cpx13b2

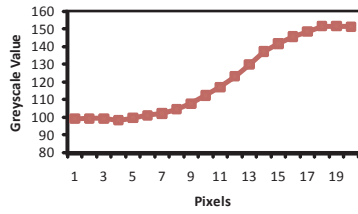
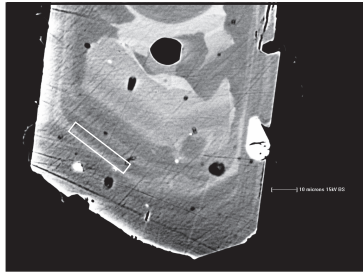
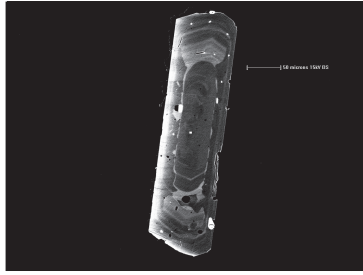


cpx15b2

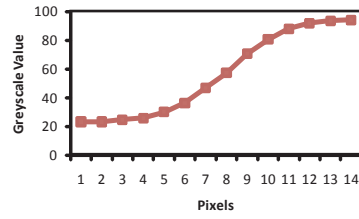
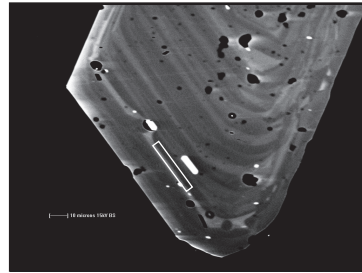
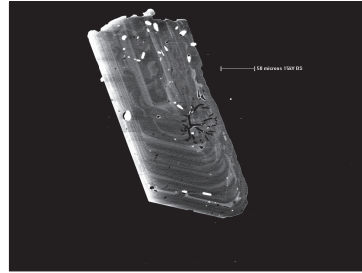


Inglewood b-Outer oscillatory zones

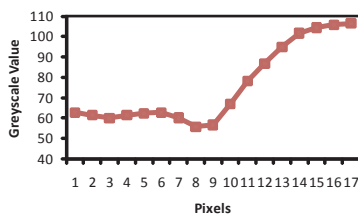
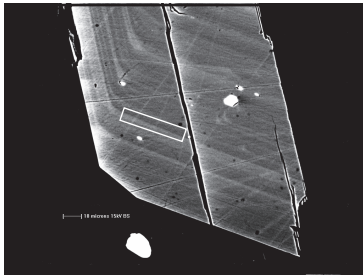
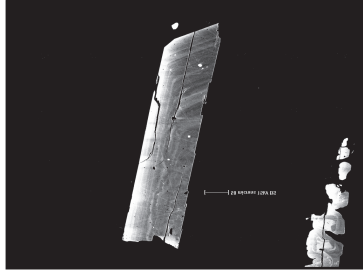
cpx21a1



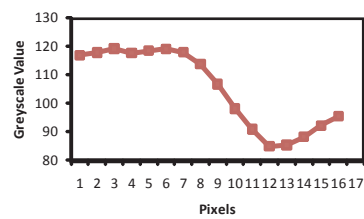
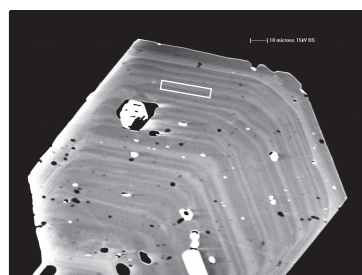
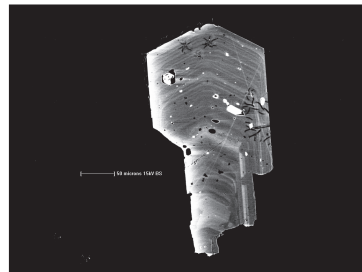
cpx24b2



cpx25a1

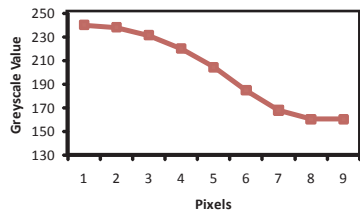
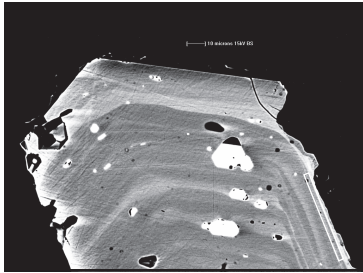
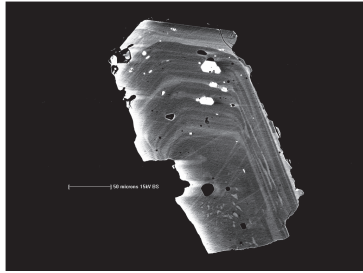


cpx28b2

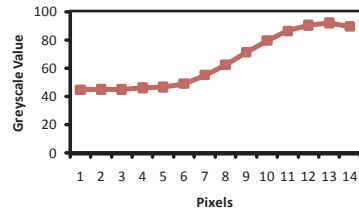
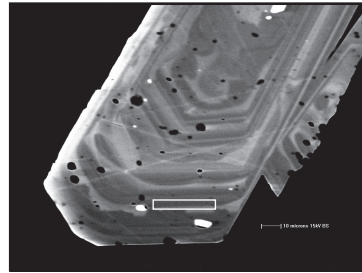
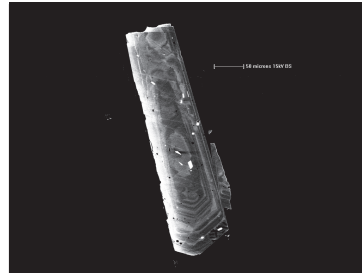


Inglewood b-Outer oscillatory zones

cpx34a1

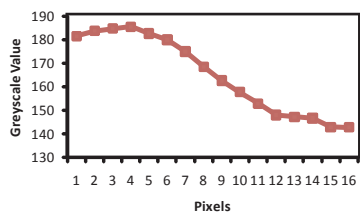
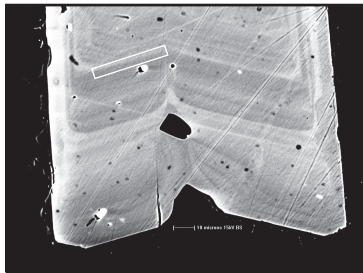
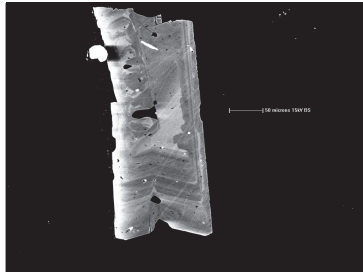


cpx39a1

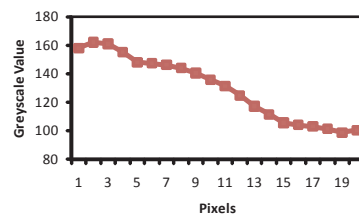
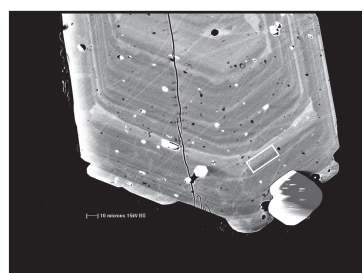
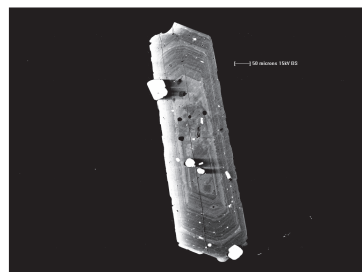


Inglewood b-Inner oscillatory zones

cpx2a3

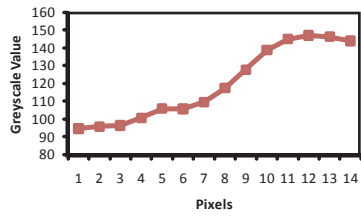
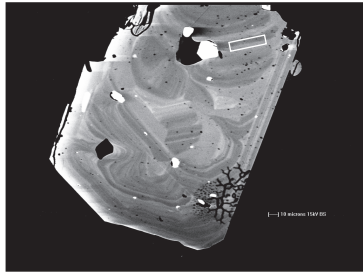
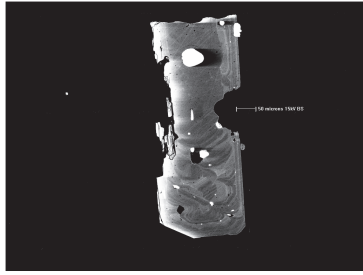


cpx8a3

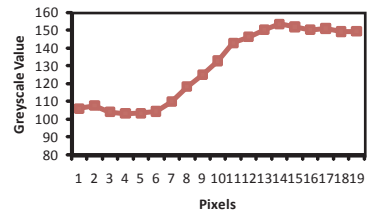
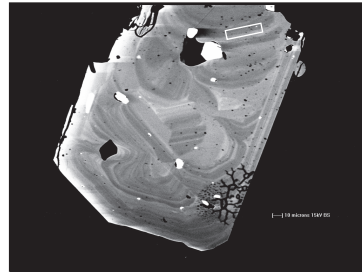
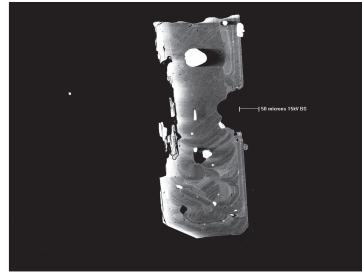


Inglewood b-Inner oscillatory zones

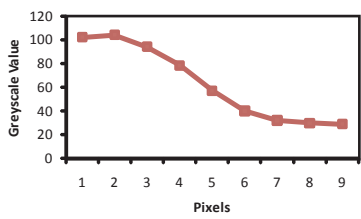
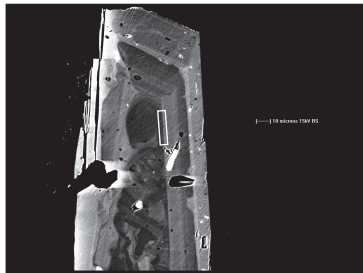
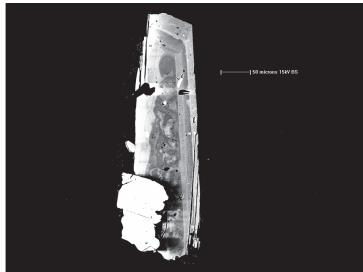
cpx9b3



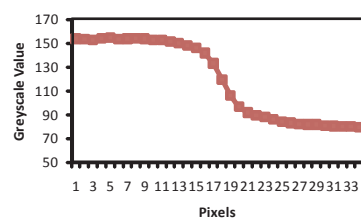
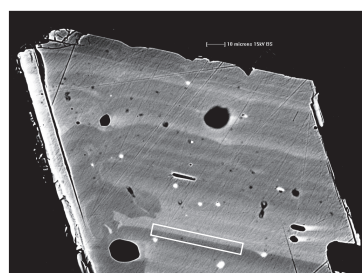
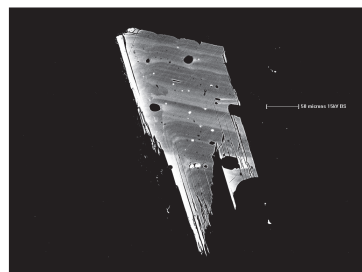
cpx9b4



cpx10a9

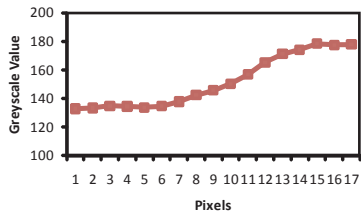
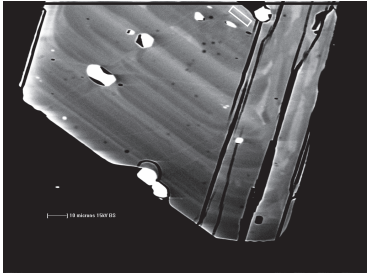
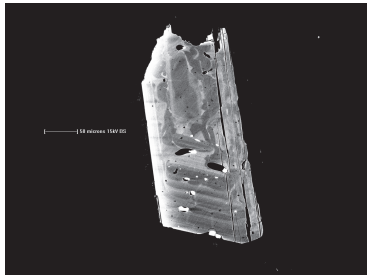


cpx11a1

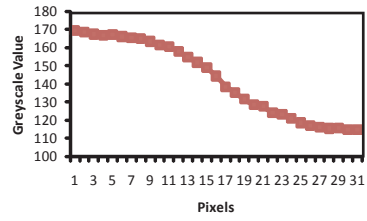
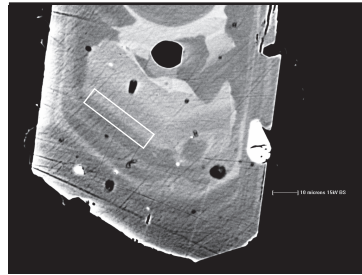
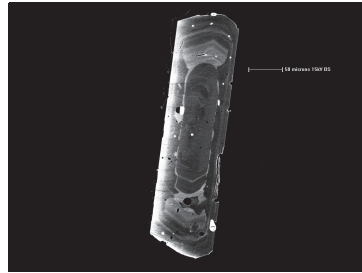


Inglewood b-Inner oscillatory zones

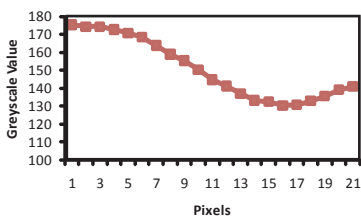
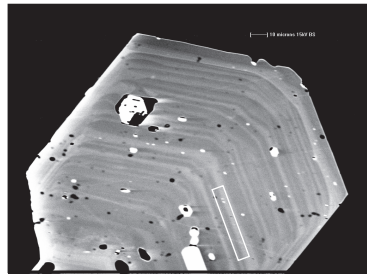
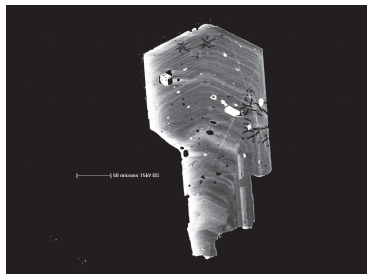
cpx15b3



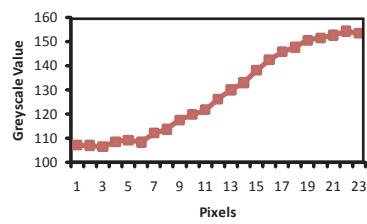
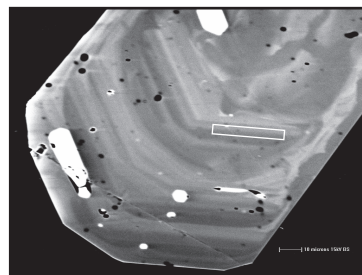
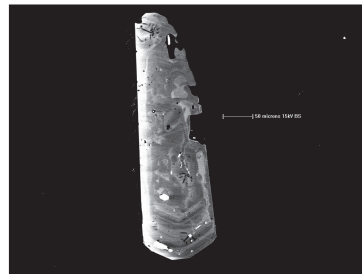
cpx21a2



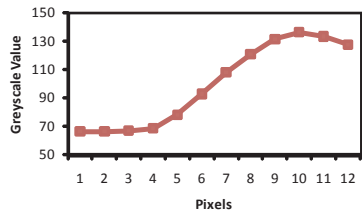
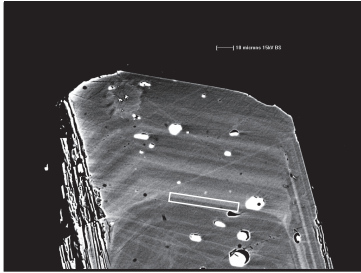
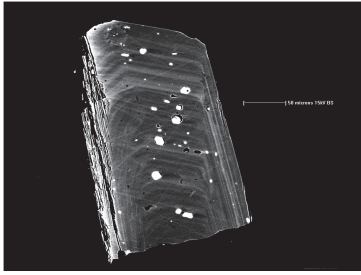
cpx28b3



cpx29b3

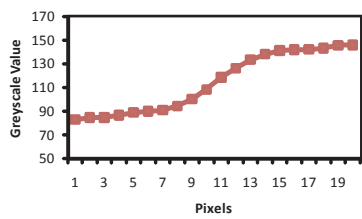
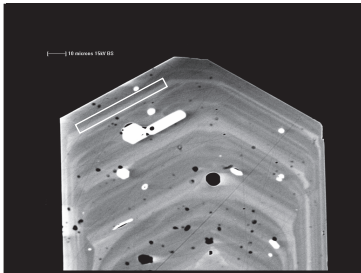
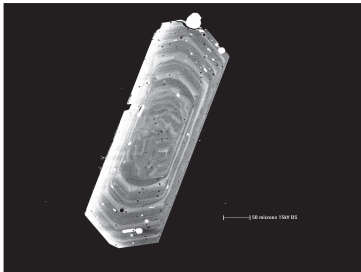


Inglewood *b*-Inner oscillatory zones
cpx33a1

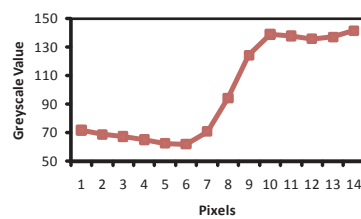
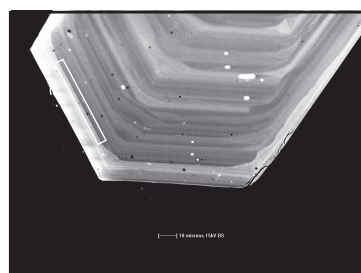
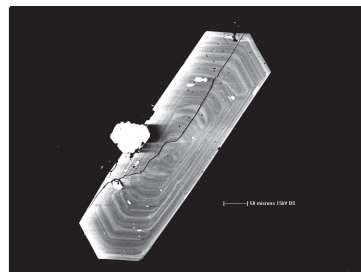


Inglewood *a*-Rims

cpx1b3

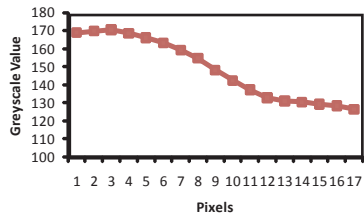
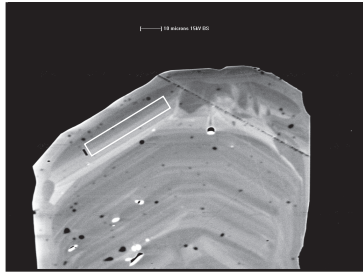


cpx5a2

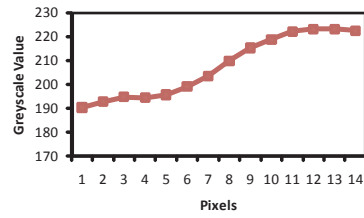
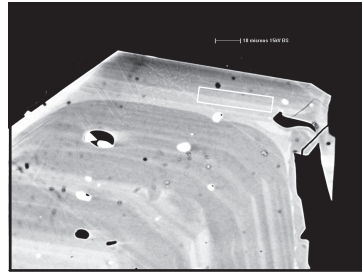
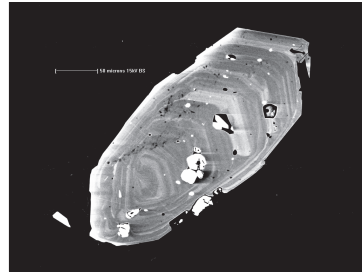


Inglewood *a*-Rims

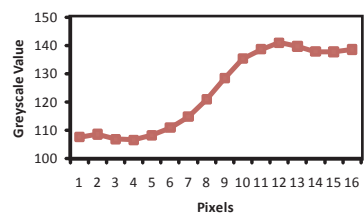
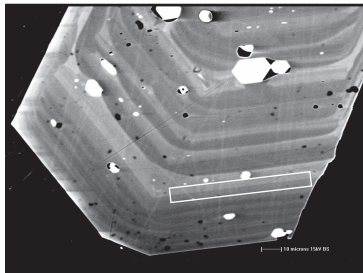
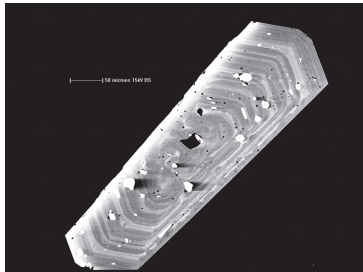
cpx30b1



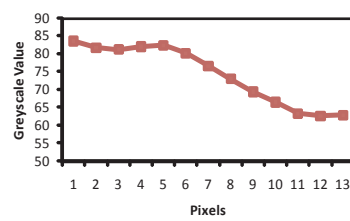
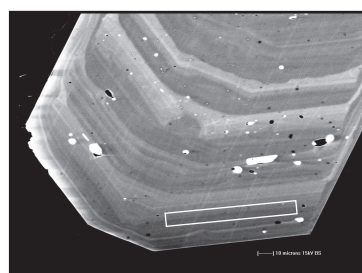
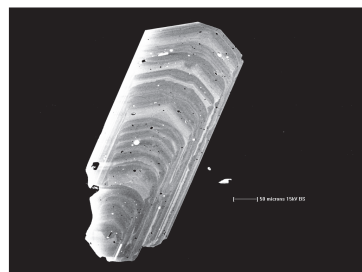
cpx39a1



cpx44a1

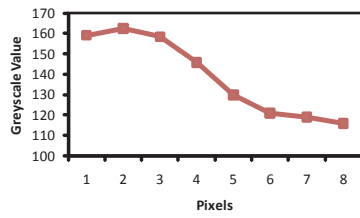
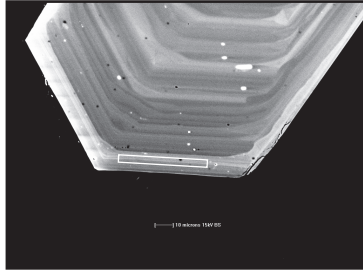
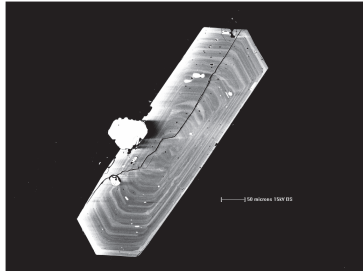


cpx54a1

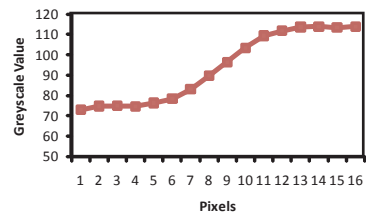
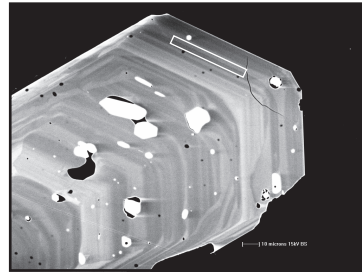
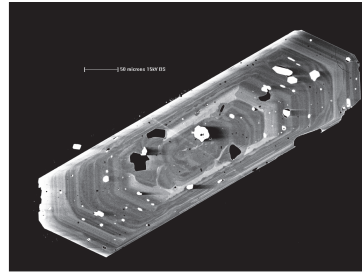


Inglewood *a*-Minor zones

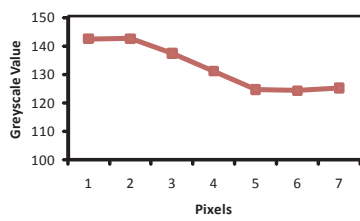
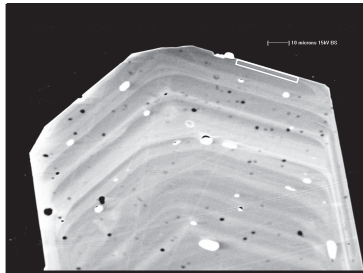
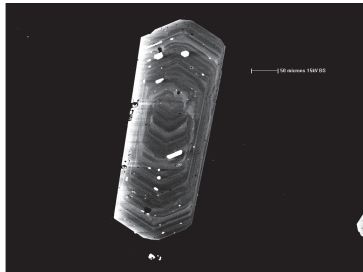
cpx5a4



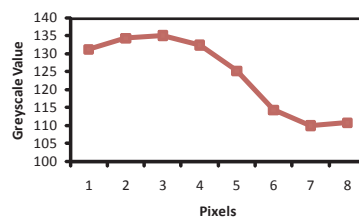
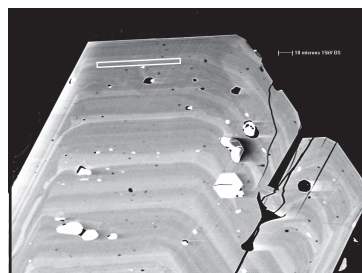
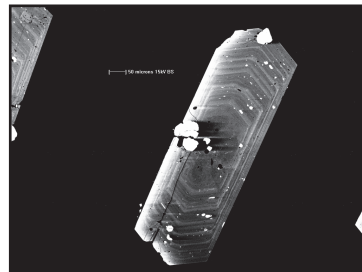
cpx31a3



cpx33b1

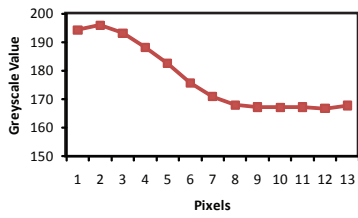
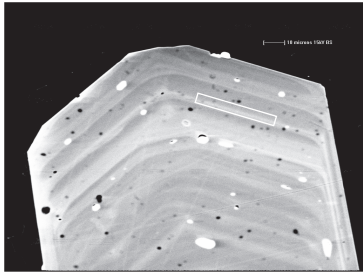
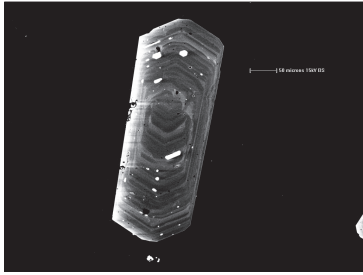


cpx58a1

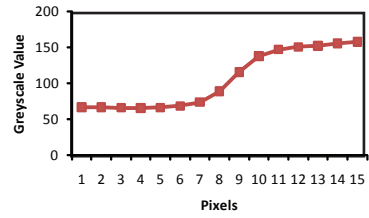
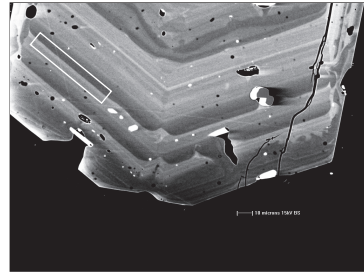
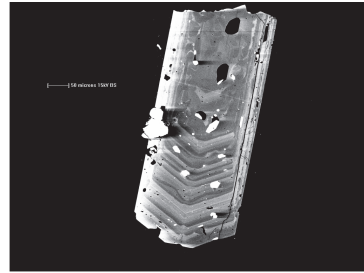


Inglewood a-Second zone from rim

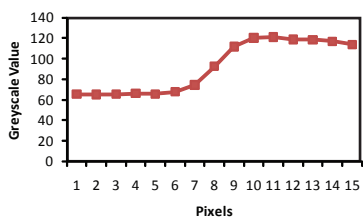
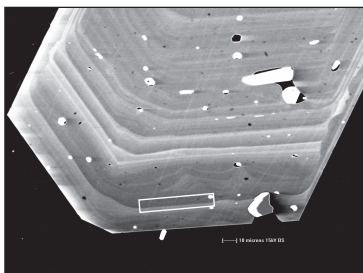
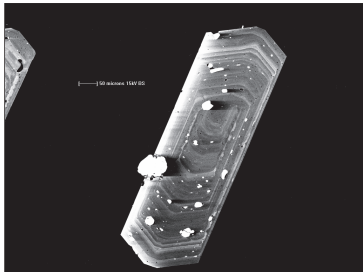
cpx33b2



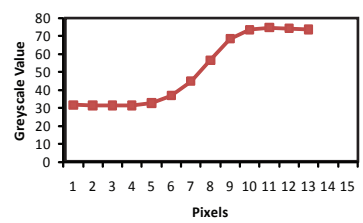
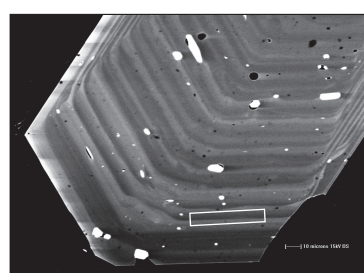
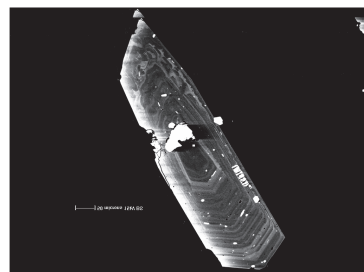
cpx48a2



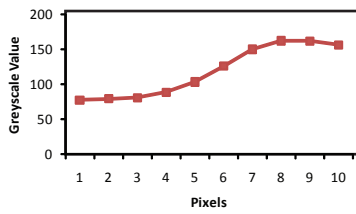
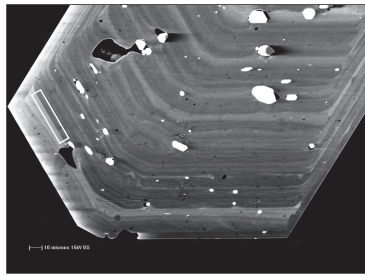
cpx56b1



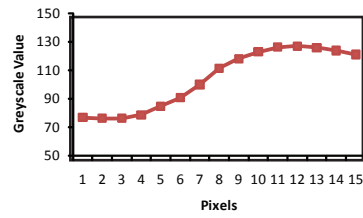
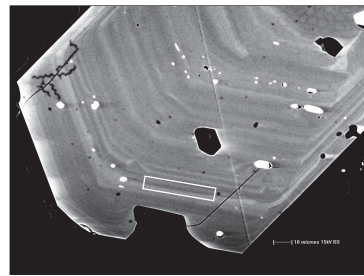
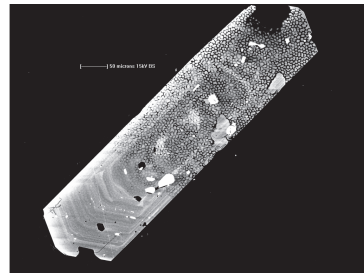
cpx66a1



Inglewood a-Second zone from rim
cpx69b1

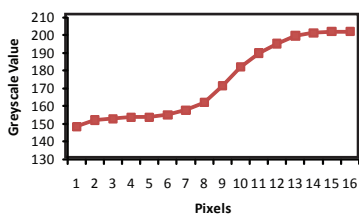
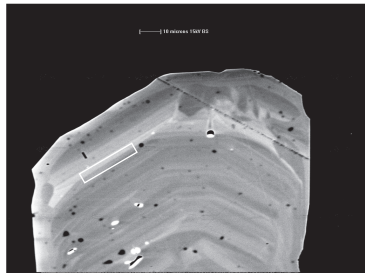
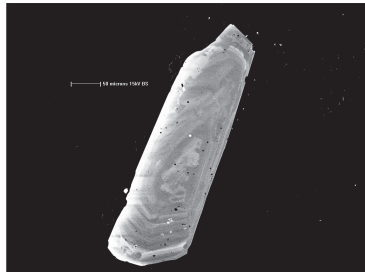


Inner zones
cpx21a1

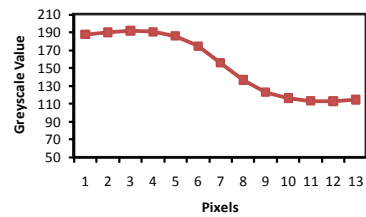
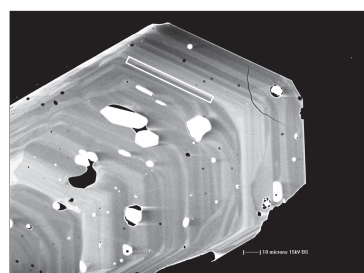
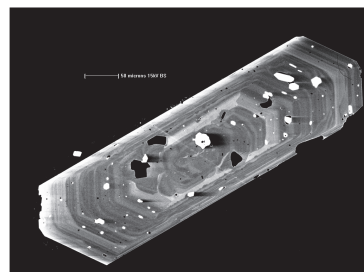


Inglewood a-Inner zones

cpx30b2

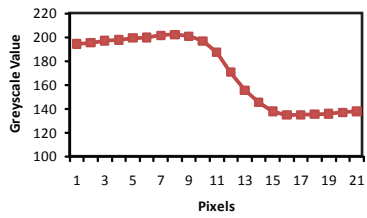
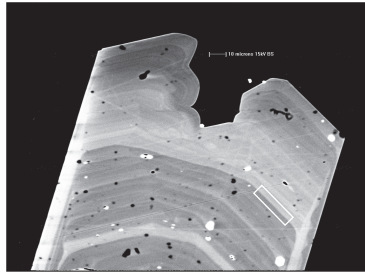
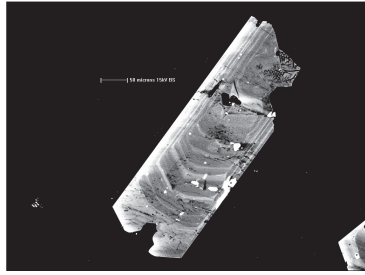


cpx31a4

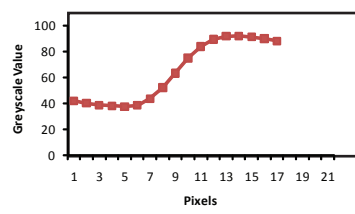
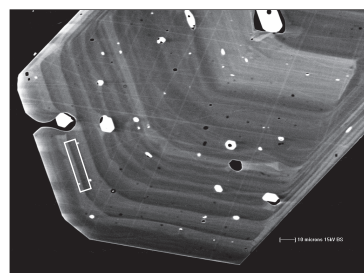
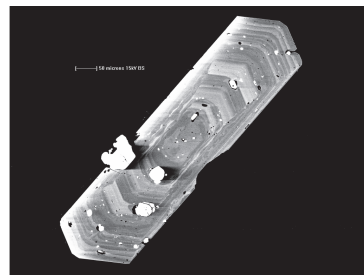


Inglewood α -Inner zone

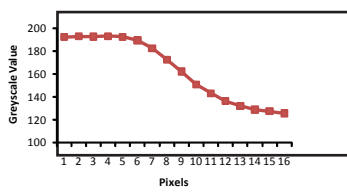
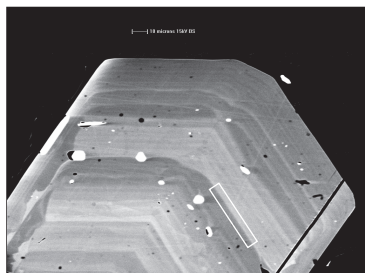
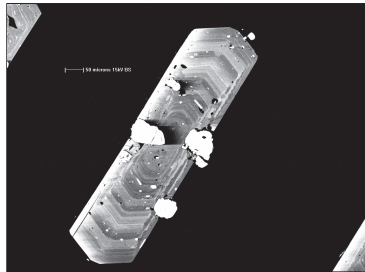
cpx35b1



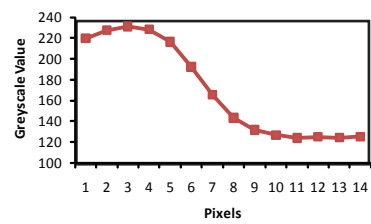
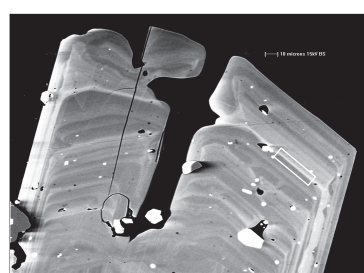
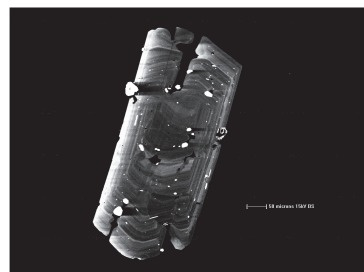
cpx63c2



cpx68b2

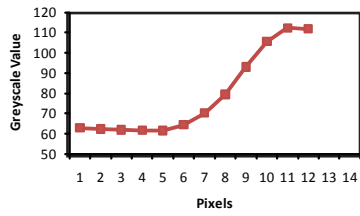
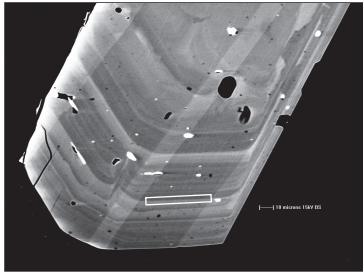
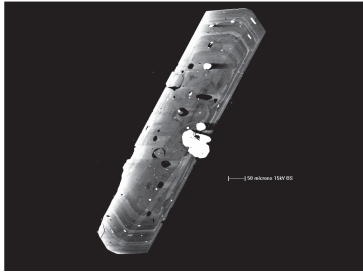


cpx73a2

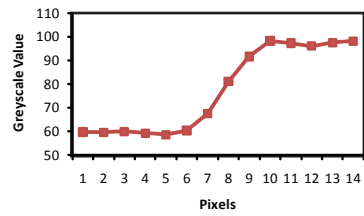
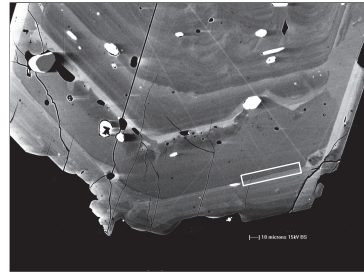
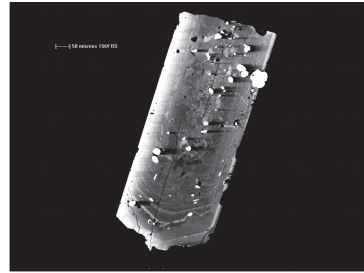


Inglewood a-Inner zones

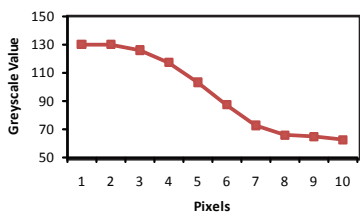
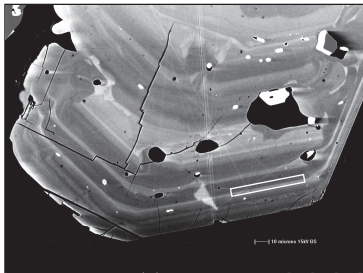
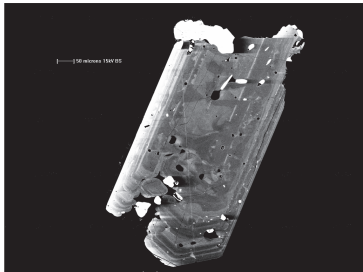
cpx74a1



cpx111a1

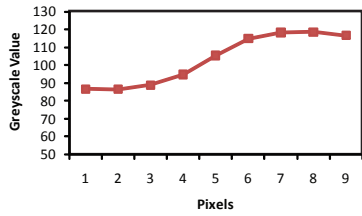
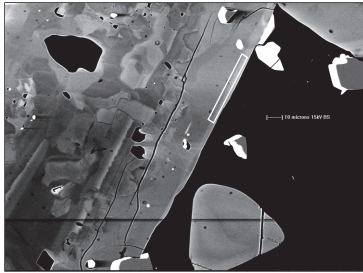
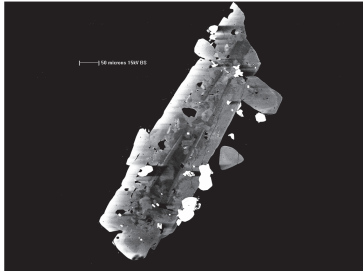


cpx112a2

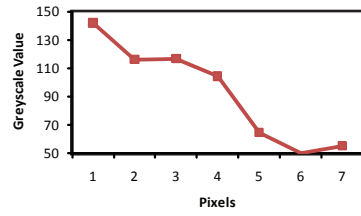
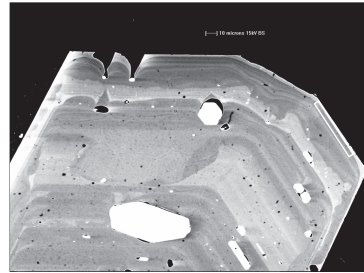
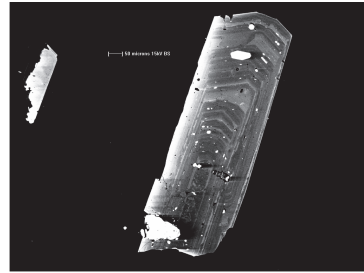


Korito-Rims

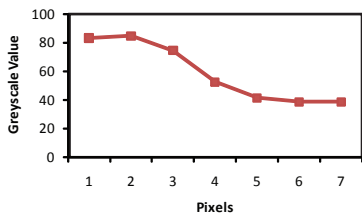
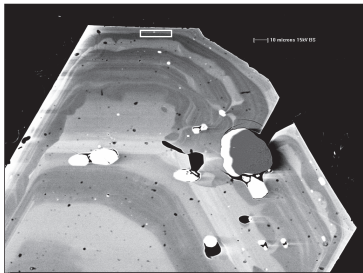
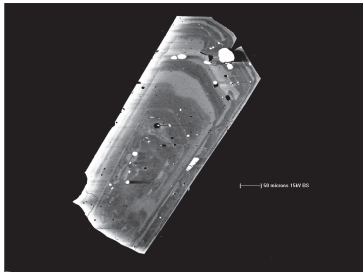
cpx4b3



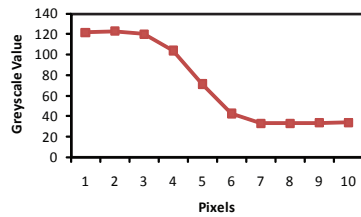
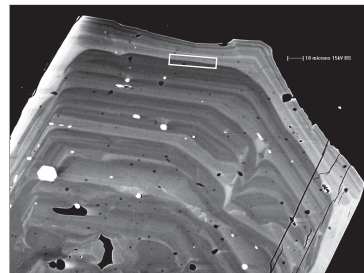
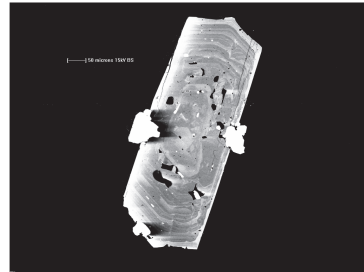
cpx12a1



cpx18b1

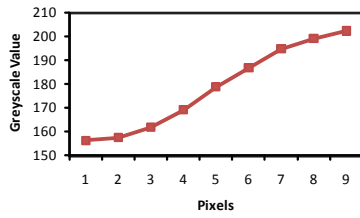
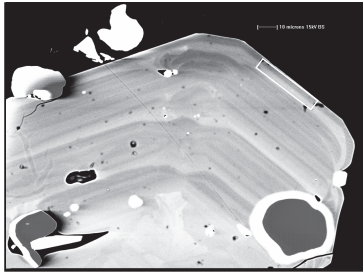
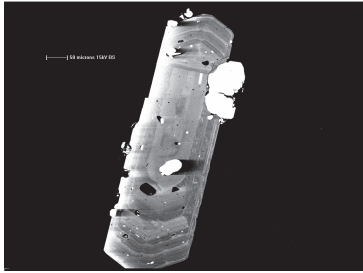


cpx19a1

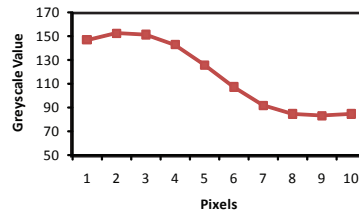
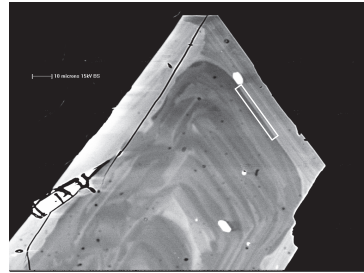
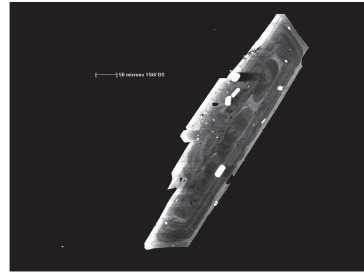


Korito-Rims

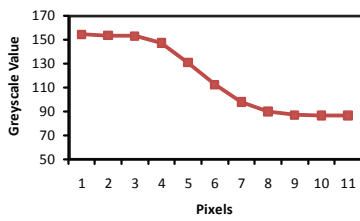
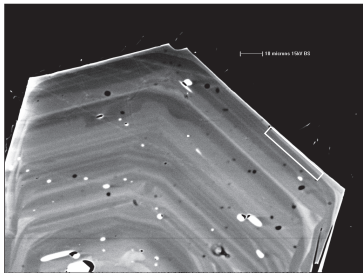
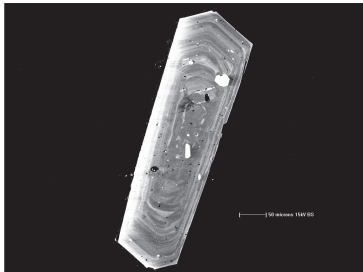
cpx28b1



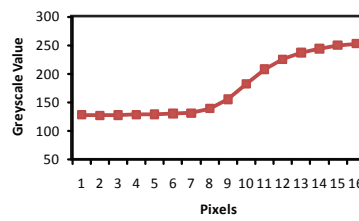
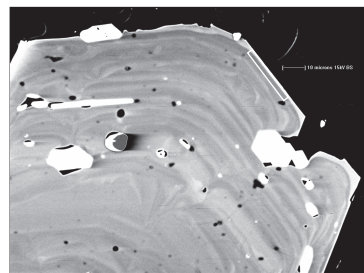
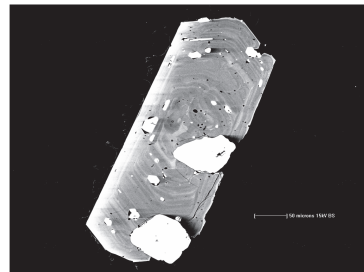
cpx30a1b



cpx38b1

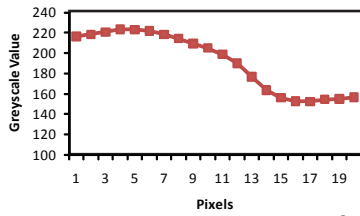
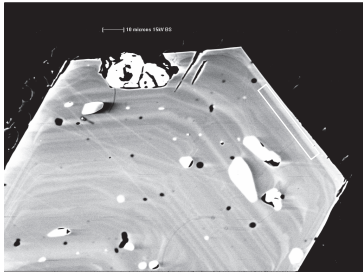
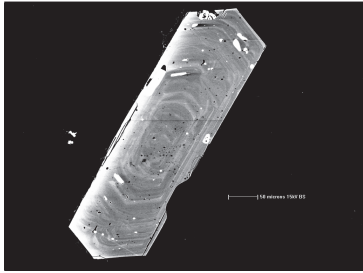


cpx39b1

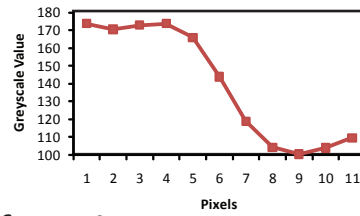
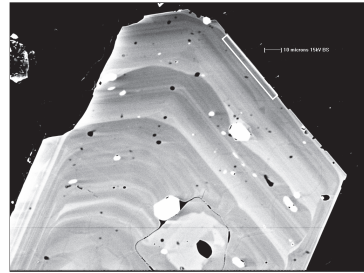
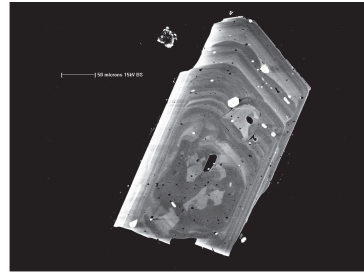


Korito-Rims

cpx44a1

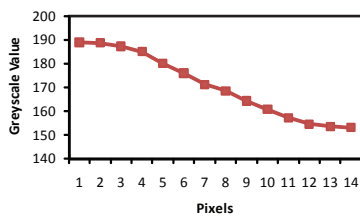
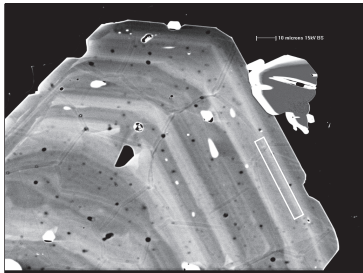
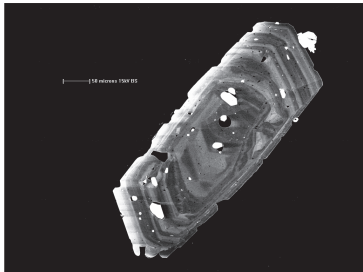


cpx46a1

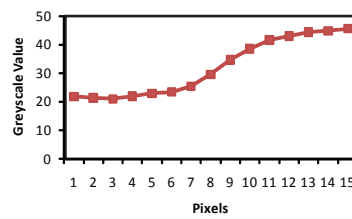
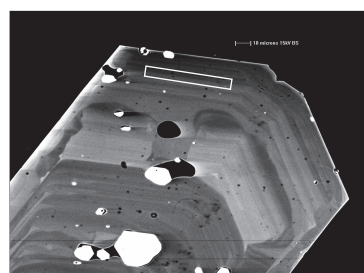


Korito-Second zone from rim

cpx8a1

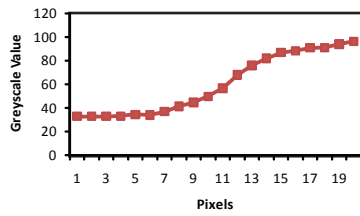
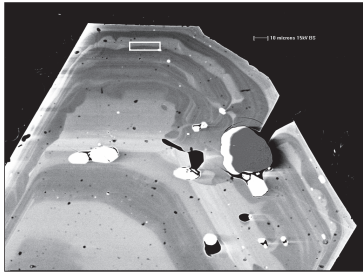
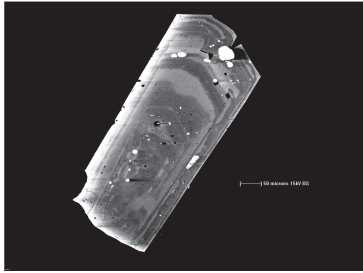


cpx14a1

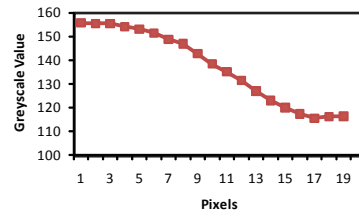
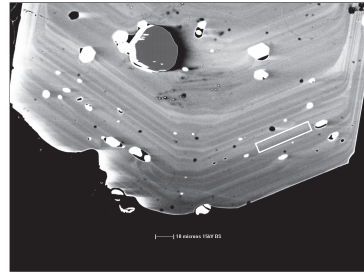
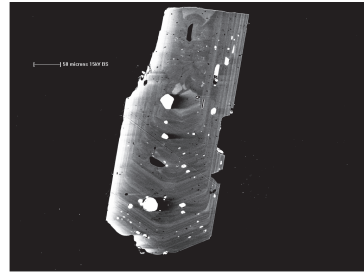


Korito-Second zone from rim

cpx18b4

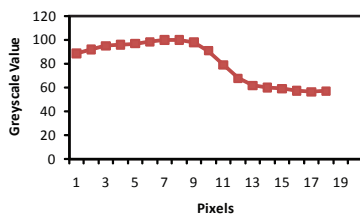
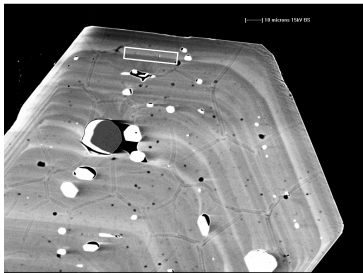
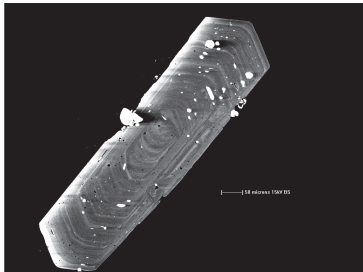


cpx34a1b

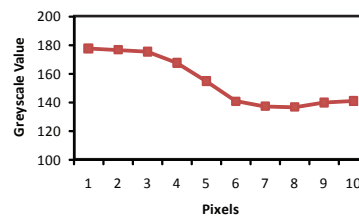
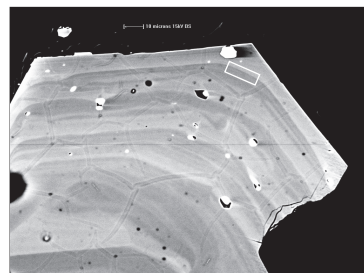
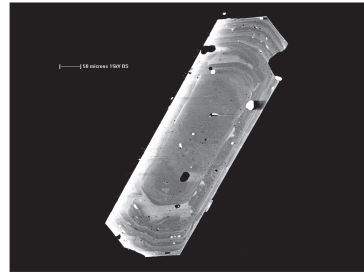


Korito-Thrid zone from rim

cpx7b1

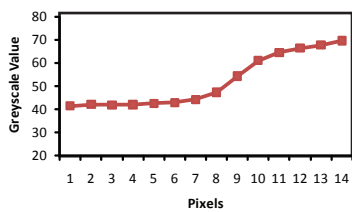
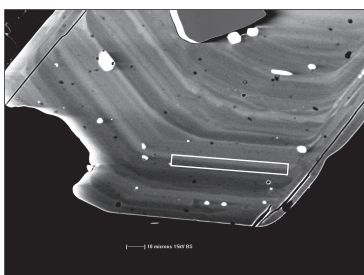
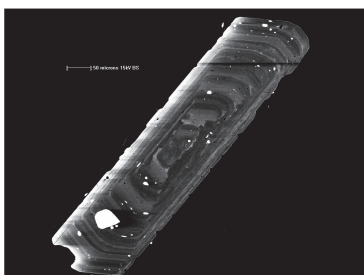


cpx9a1

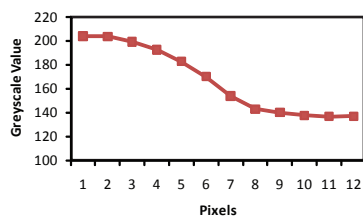
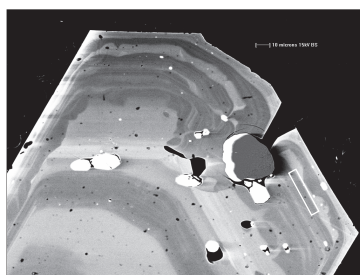
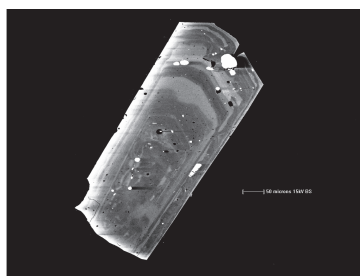


Korito-Third zone from rim

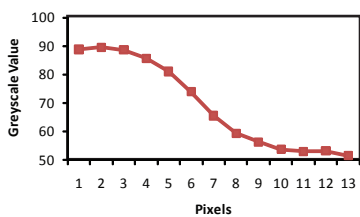
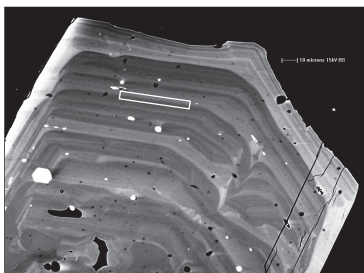
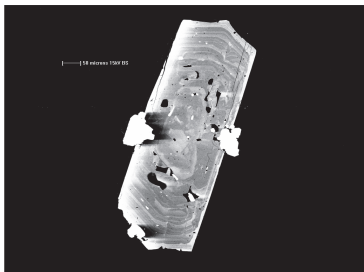
cpx17a2b



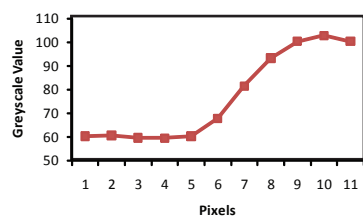
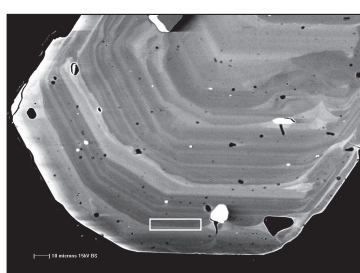
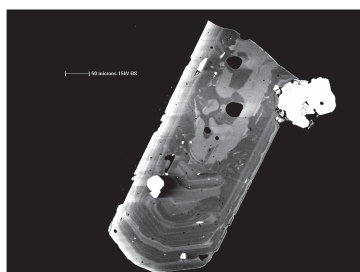
cpx18b3



cpx19a4

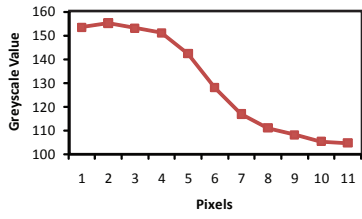
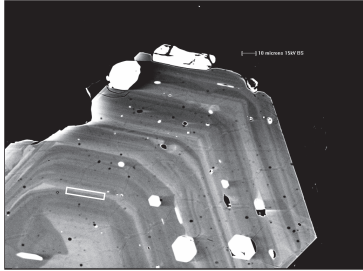
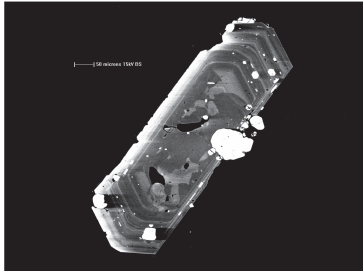


cpx20b1

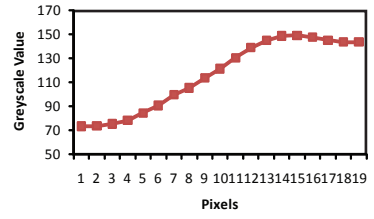
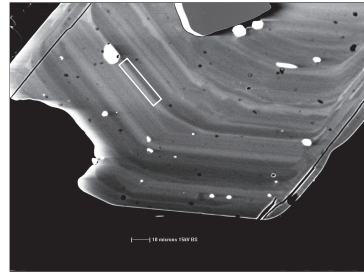
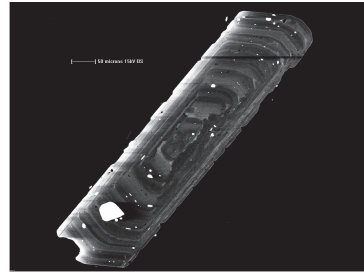


Korito-Inner zones

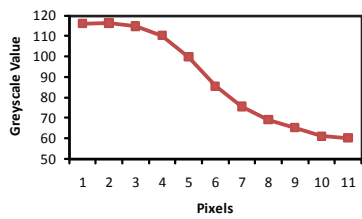
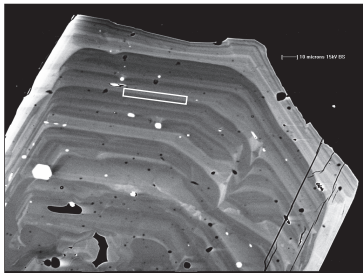
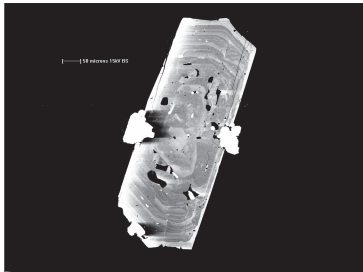
cpx10a1



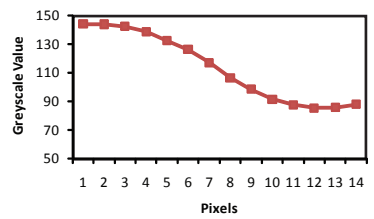
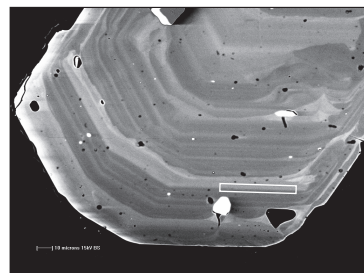
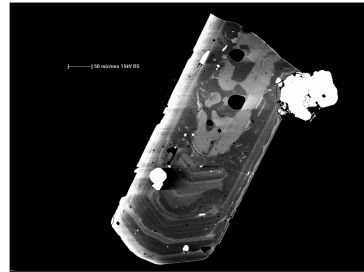
cpx17a6



cpx19a3

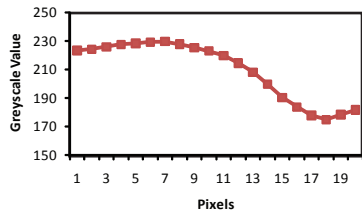
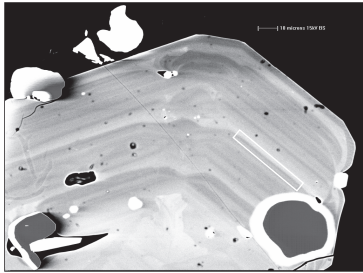
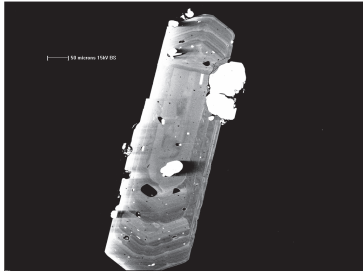


cpx20b2



Korito-Inner zones

cpx28b3



cpx46a2

